

Urethane Chemistry and Applications

Urethane Chemistry and Applications

Kenneth N. Edwards, EDITOR

Kenneth N. Edwards Enterprises

ASSOCIATE EDITORS

**Wilson F. Gum, James E. Johnson,
Fredrick E. Bailey, Jr., Ralph S. Graff,
Wolfgang G. Glasser, Daniel Klemperer,
and Kurt C. Frisch**

Based on a symposium sponsored
by the Macromolecular Secretariat,
at the Second Chemical Congress
of the North American Continent
(180th ACS National Meeting),
Las Vegas, Nevada,
August 24–29, 1980.

A C S S Y M P O S I U M S E R I E S **172**

AMERICAN CHEMICAL SOCIETY

WASHINGTON, D. C. 1981



Library of Congress CIP Data

Urethane chemistry and applications.
(ACS symposium series, ISSN 0097-6156; 172)

Includes bibliographies and index.

1. Urethanes—Congresses.

I. Edwards, Kenneth N. II. American Chemical Society, Macromolecular Secretariat. III. Chemical Congress of the North American Continent. IV. Series.

TP1180.P8U75 668.4'239 81-15070
ISBN 0-8412-0664-3 AACR2
ASCMC 8 172 1-589 1981

Copyright © 1981

American Chemical Society

All Rights Reserved. The appearance of the code at the bottom of the first page of each article in this volume indicates the copyright owner's consent that reprographic copies of the article may be made for personal or internal use or for the personal or internal use of specific clients. This consent is given on the condition, however, that the copier pay the stated per copy fee through the Copyright Clearance Center, Inc. for copying beyond that permitted by Sections 107 or 108 of the U.S. Copyright Law. This consent does not extend to copying or transmission by any means—graphic or electronic—for any other purpose, such as for general distribution, for advertising or promotional purposes, for creating new collective work, for resale, or for information storage and retrieval systems.

The citation of trade names and/or names of manufacturers in this publication is not to be construed as an endorsement or as approval by ACS of the commercial products or services referenced herein; nor should the mere reference herein to any drawing, specification, chemical process, or other data be regarded as a license or as a conveyance of any right or permission, to the holder, reader, or any other person or corporation, to manufacture, reproduce, use, or sell any patented invention or copyrighted work that may in any way be related thereto.

PRINTED IN THE UNITED STATES OF AMERICA

**American Chemical
Society Library**

1155 16th St. N. W.

In Urethane Chemistry and Applications; Edwards, K., et al.;
ACS Symposium Series; American Chemical Society: Washington, DC, 1981.

Washington, D. C. 20038

ACS Symposium Series

M. Joan Comstock, *Series Editor*

Advisory Board

David L. Allara	James P. Lodge
Kenneth B. Bischoff	Marvin Margoshes
Donald D. Dollberg	Leon Petrakis
Robert E. Feeney	Theodore Provder
Jack Halpern	F. Sherwood Rowland
Brian M. Harney	Dennis Schuetzle
W. Jeffrey Howe	Davis L. Temple, Jr.
James D. Idol, Jr.	Gunter Zweig

FOREWORD

The ACS SYMPOSIUM SERIES was founded in 1974 to provide a medium for publishing symposia quickly in book form. The format of the Series parallels that of the continuing ADVANCES IN CHEMISTRY SERIES except that in order to save time the papers are not typeset but are reproduced as they are submitted by the authors in camera-ready form. Papers are reviewed under the supervision of the Editors with the assistance of the Series Advisory Board and are selected to maintain the integrity of the symposia; however, verbatim reproductions of previously published papers are not accepted. Both reviews and reports of research are acceptable since symposia may embrace both types of presentation.

PREFACE

Although the diisocyanate polyaddition process was discovered by O. Bayer at the end of the 1930s, it was not until after the Second World War that some of the commercial possibilities became apparent. Since that time, the urethane and related reactions have resulted in a tremendous growth of varied industries covering all areas of macromolecules.

In 1979 the Macromolecular Secretariat of the American Chemical Society agreed that a symposium on Urethane Chemistry and Applications was of broad and current interest and that such a symposium met the requirements of being topical to all of the member divisions of the Secretariat. As a result, this symposium was scheduled for 1980, and a group of specialists representing each of the member ACS Divisions, as well as the Division of Chemical Marketing and Economics, was recruited. These individuals subsequently became the associate editors of this book.

The editors selected the papers presented in their respective fields to provide as good an insight as possible into the chemistry and marketing of isocyanates, using original research rather than tutorial papers. In this regard they succeeded admirably.

To all the editors and authors whose hard work made the Symposium a success, I would like to say "Thank You" for a job well done.

KENNETH N. EDWARDS
Kenneth N. Edwards Enterprises
Glendale, California 91206

June 8, 1981

Worldwide Polyurethane Markets

PETER J. MANNO

The Upjohn Company, Polymer Chemicals Division, P.O. Box 685, La Porte, TX 77571

Discussing any worldwide topic is an awesome task at best and fraught with many pitfalls. Political and social and economic differences combine to not only confuse the current situation; but, also obscure the future outlook as well. The next decade will be shaped by many of the familiar economic, social and political factors widely discussed in the media. Some of the key problems that will affect many of the countries of the world include:

- Energy
- Inflation
- Economic Instability
- Protectionism
- Economic Nationalism
- International Balance of Payments
- Political Instability

To properly assess the impact of these factors would be far beyond the scope of this paper. Nevertheless, a good market researcher enjoys facing up to the challenge, and I shall endeavor to forecast the 1990 worldwide polyurethane markets.

Let me caution you that a market study is basically a current snapshot of the market and its outlook, and the future will probably differ from projections. How close it comes to the actual situation is a measure of the market researcher's ability.

Worldwide Demand

Polyurethane products historically have proven to be one of the most versatile plastic materials available. The wide range of physical properties from supersoft flexible foam; to tough elastomers; and to long wearing coatings has resulted in many end use applications. As a result, the 1980's will begin with a worldwide demand approaching 6,652 million pounds (3 million t),

0097-6156/81/0172-0009\$05.00/0
© 1981 American Chemical Society

as shown in Table I. The traditional volume leader among the polyurethane products continues to be flexible foam, principally used for furniture and transportation applications. Despite the slowdown in the U. S. construction, the worldwide demand for energy-saving rigid foam insulation should continue strong. Elastomer demand is centered in shoe sole and auto applications. The balance of polyurethane demand is rounded out by a variety of polyurethane products including adhesives, sealants, fibers, and coatings.

The U. S./Canada and West European regions are the volume leaders accounting for 35% and 33% of the 1980 total respectively. The highly industrialized countries in these regions have long recognized the excellent cost/performance benefits of polyurethane products. In addition, strong consumer demand for furniture, bedding, autos, and insulation has been a significant factor in the growth of polyurethane products for these applications. The Japan/Far East demand will reach 889 million pounds in 1980, as consumer demand continues to increase steadily for polyurethane-containing products. The Middle East/Africa/East European region is slowly developing as a polyurethane market, but is severely constrained by economic and political problems.

The future worldwide demand for polyurethanes will depend on the net result of a series of key impetus and constraint factors:

Demand Impetus

- Conservation of energy
- Replacement of natural materials
- Productivity and economics
- Safety and Health
- Aesthetics

Demand Constraints

- World economic situation
- Increased costs and prices
- Some market saturation
- Governmental restrictions

The impact of these factors will vary from country to country and it is difficult to quantify. However, the net effect will be an overall 7.0% annual growth in polyurethane demand to a 13,051 million pound level in 1990 as shown in Table I. The relative ranking of the country grouping will remain the same as in 1980. A discussion of the polyurethane growth prospects for various country groupings will be detailed in the following sections of this paper.

United States/Canada

The United States finally succumbed to spiralling inflation and interest rates during the first quarter of 1980, and the long heralded recession was upon us. As a result, many estimates of 1980 demand will result in growth rates to 1990 that are unrealistically high. Thus, some caution should be exercised in interpreting the ten year growth rates.

The Canadian economic activity is showing signs of following the U.S. pattern despite a reasonably good year in 1979. With 70% of the Canadian chemical exports destined for the U.S. markets, a mid-1980 recession seems quite probable. This close linking of the two economies will probably continue through this next decade.

Both the U.S. and Canadian demand for polyurethanes will continue to escalate during the "Eighties", despite the temporary setback this year, and will total 2,350 million pounds as shown in Table II. The performance of polyurethane products has resulted in penetration of a number of key markets, particularly transportation and construction. Despite soaring raw materials costs, polyurethane will continue to make headway as energy conservation requirements and recognize its superior insulation properties. Smaller more fuel-efficient automobiles will use liberal amounts of polyurethane elastomers in a variety of lightweight exterior body and styling applications. New uses of polyurethanes will add additional demand that could propel U.S./Canada 1990 usage to levels well in excess of the 4,850 million pounds forecasted.

U.S./Canada Markets. Flexible foam will continue to dominate the polyurethane end uses. Its superior cushioning properties will maintain an almost 100% penetration of furniture and transportation markets. Furniture demand for flexible foam will follow consumer demand for upholstered furniture. Some steady growth is expected for bedding applications, but will probably not exceed 30% of the mattress units by 1990.

Transportation markets have historically been a major user of polyurethane products. Molded flexible foam cushioning provides superior seating and significant reductions in assembly labor costs. This demand will experience some decrease early in the 80's as autos become smaller but should recover later in the decade.

Flexible polyurethane foam carpet underlay is used as either prime or rebonded foam. The polyurethane foam offers superior cushioning and is particularly attractive for contract installations or premium carpets. The prime foam usage should increase steadily to about 310 million pounds in 1990. The demand for rebonded foam carpet underlay depends on the availability of scrap foam and will probably not exceed 300 million pounds annually.

Rigid foam uses will average a 11.2% annual increase and reach 1,608 million pounds by 1990. Most of the impetus will come from the insulation use of rigid foam for building and construction.

Building and construction use of polyurethane products will increase at a record pace during the 1980's. The slow down in residential housing starts in 1980 will have a temporary effect on the increasing demand for polyurethane foam residential sheathing. The return to normal housing starts (about 1981-1982) should further accelerate the demand. Commercial roofing applications have made significant use of polyurethane rigid foam panels for the typical asphalt built-up roof construction. The asphalt-free, single-ply membrane roofing may well use thicker layers (3 inch or more) of insulation to maximize energy conservation and be ideally suited for polyurethane foam. Residential sheathing will probably be the fastest growing market as consumers attempt to offset rising fuel and energy costs by increasing the amount and efficiency of their residential insulation.

Polyurethane rigid foam insulation also can be applied as a spray system to a variety of surfaces. Retro-fitting commercial roofs as well as insulation of tanks and pipes has had increasing acceptance. The next decade will require even further conservation of energy in all manufacturing facilities, and provide an ideal market for sprayed rigid foam insulation. By the end of this decade, the demand for spray systems could readily double the current level.

Polyurethane elastomer demand will more than double in volume during the 1980's and easily reach 552 million pounds. Over 60% will be for transportation use as U.S. auto manufacturers work to meet federal fuel economy and bumper damage standards. The use of polyurethane elastomers for transportation markets has received increasing attention from the auto industry. The need for improved fuel economy to meet government standards has focused on lightweight materials, and polyurethane elastomers have been a prime candidate. Their excellent physical properties have been utilized in flexible bumper fascia, as well as more rigid trim and decorative body parts. Recent development of glass-filled polyurethane elastomers composition are being tested for auto fenders, doors, and trunk lids. Widespread use of polyurethane elastomer external body components could readily add an additional 100 million pounds to this total.

Polyurethane elastomer shoe soles have received wide acceptance for women's fashion shoes as well as a variety of sports footwear. The lightweight microcellular shoe soles have permitted wide styling flexibility in women's shoes. Fine details simulating wood, cork, leather, and hand-stitching can be readily reproduced. New style sports shoes incorporate multi-color and multi-density soles. Other polyurethane elastomers will find ready use in high performance applications utilizing their superior wear, corrosion and abrasion resistance properties.

The coatings/adhesives and sealants category will post the highest growth rate and average 11.5% annually. Polyurethane coatings (in particular high solids paints for autos) and the emerging use of polyurethane binder adhesives (e.g. foundry cores, and woodchip particleboard) could develop substantial market demand. Polyurethane's value as an adhesive or binder continues to enjoy excellent acceptance by the foundry industry. Their use as binders for sand cores used in metal casting provides a fast, low-energy consuming technology. More recently, isocyanates have been used as binders for woodchip particleboard, or formed as a bonded woodchip core between thin wood veneers. The isocyanate containing products offer an excellent weather-resistant particleboard, as well as a manufacturing process that is formaldehyde-free and consumes less energy.

Latin America

Latin America is usually defined to include Mexico, The Caribbean, Central and South America. This market region includes about 370 million inhabitants. The individual countries represent a wide range of political, social, and economical scenarios. High inflation rates and large trade balance deficits are prevalent in many of the countries. Limited infrastructure (e.g. highways, public utilities, etc.) has seriously hampered their economic growth. However, strong raw material positions (e.g. petroleum, metal ores, etc.) have enhanced export income and helped improve the national GNP and levels of industrialization. For example, three major oil fields have been discovered in Mexico within the past few years, and Venezuela's oil-based economy is well known.

With a few exceptions, the polyurethane markets in Latin America are in their early stages of development and offer a significant potential demand over the next decade. The current polyurethane demand is centered in Argentina, Brazil, Mexico, and Venezuela, representing 85% of the total demand of 448 million pounds expected in 1980 as shown in Table III.

Argentina continues to experience the severe inflationary problems that have curtailed growth during recent years. General Motors closed its auto assembly plant and consumer prices continue to rise rapidly. A steady improvement is expected over the next decade as inflation appears to be coming under control; auto production stabilizes, and consumer demand strengthens in furniture/bedding markets.

Brazil is to be the volume leader in urethane demand, reflecting strong flexible foam demand, principally for automotive, furniture, and bedding uses. An expected modest decrease in inflation rate and strong auto production will give impetus to this growth through the eighties.

TABLE I
WORLDWIDE POLYURETHANE DEMAND OUTLOOK (MMLBS)

	1980	1985	1990	80/90 %/Yr.
U.S./Canada	<u>2350</u>	<u>3541</u>	<u>4850</u>	7.5
Latin America	448	645	940	7.7
W. Europe	2200	2949	3946	6.0
Middle East/Africa/ E. Europe	765	1064	1565	7.4
Japan/Far East	889	1236	1750	7.0
Total	<u>6652</u>	<u>9435</u>	<u>13051</u>	7.0

TABLE II
U.S./CANADA POLYURETHANE DEMAND (MMLBS)

	1980	1985	1990	80/90 %/Yr.
Flexible Foam	<u>1364</u>	<u>1756</u>	<u>2000</u>	3.9
Rigid Foam	555	1022	1608	11.2
Elastomers	199	329	552	10.7
Others	<u>232</u>	<u>434</u>	<u>690</u>	11.5
Total	<u>2350</u>	<u>3541</u>	<u>4850</u>	7.5

TABLE III
LATIN AMERICAN POLYURETHANE DEMAND (MMLBS)

	1980	1985	1990	80/90 %/Yr.
Flexible Foam	<u>306</u>	<u>427</u>	<u>610</u>	7.2
Rigid Foam	63	111	180	11.1
Elastomers	62	78	100	4.9
Others	<u>17</u>	<u>29</u>	<u>50</u>	11.4
Total	<u>448</u>	<u>645</u>	<u>940</u>	7.7

Mexican urethane demand has been constrained by raw materials costs. Flexible foam markets will show some strength in the 80's, reflecting a steady auto production and moderate increases for furniture and bedding uses. Rigid foam applications are still in the early stages of market development; but, commercial/industrial insulation uses are increasing well. Mexico leads Latin America in urethane elastomer usage, paced by its demand for shoe sole applications.

Venezuela is emerging as a strong Latin American market for urethanes. A strong consumer demand and significant exports to Andean Pact countries have provided much of the growth. Continued increases in auto production, furniture/bedding, and some insulation markets should give further impetus to polyurethane demand.

Latin American Markets. Flexible polyurethane foam for premium as well as inexpensive mattresses has been the major growth market in most Latin American countries, and often represented 50% of the flexible demand. Growth prospects to 1990 are good as consumers upgrade some of their previous purchases, and increased market penetration is realized in some countries (e.g. Mexico) that have considerable potential. Furniture demand for flexible polyurethane foam is relatively modest compared to bedding end uses. Styling trends and the proliferation of small furniture producers have not opted for flexible urethane foam cushioning. Upholstered furniture demand will continue to be constrained by low consumer income, as well as small artisan production facilities.

Building and construction use of polyurethane markedly trails the volume and variety of applications prevalent in North America. The use of rigid foam for insulating commercial and residential buildings is in its early stages of development. There are only about a half a dozen manufacturers of continuous polyurethane laminate panels in Latin America. The utilization of rigid foam insulation has experienced limited success for refrigeration uses, both domestic and commercial. The outlook to 1990 is not particularly encouraging. Considerable government incentives will be required to stimulate the construction industry to utilize rigid foam in public housing. Industry awareness of energy costs may provide some incentives for commercial usage of high-efficiency polyurethane insulation. In addition, the traditional building materials (e.g. stone, bricks, etc.) do not lend themselves to replacement or simultaneous usage with polyurethane foam insulation.

The transportation industry has many of the worldwide auto producers represented in seven Latin American countries. Brazil is the volume leader (over 1 million autos and trucks in 1979), followed by Mexico, Argentina, and Venezuela. These auto producers are rapidly adopting the concept of molded polyurethane foam seating including the superior cushioning of high resiliency foams. The pressure for increased fuel economy via weight re-

duction experienced by U.S. auto producers is not present in Latin American markets. Consequently, the RIM elastomer technology is just beginning to get attention and some auto producers are considering some applications.

The balance of the polyurethane end uses comprises a myriad of applications, including domestic refrigeration, shoes, carpet underlay, fibers, foundry core binders, etc. that used polyurethane products. Latin American refrigerator manufacturers are rapidly converting from fiber-glass to rigid polyurethane foam insulation. As consumer demand for these appliances increases, the urethane demand should follow. Polyurethane elastomers for shoe sole have had a dramatic growth in certain Latin American countries with significant exports to their northern neighbors. Barring any major styling changes, Mexico could well lead Latin America to a strong worldwide polyurethane elastomer shoe sole market position.

Polyurethane adhesives or binders are finding acceptance by the Latin American foundry industry. Growth over the next few years should be substantial.

Europe/Middle East/Africa

The European region consists of Western Europe, Eastern Europe and the Middle East/Africa nations.

Western Europe is defined geographically as:

- Benelux
 - Belgium, Netherlands, Luxembourg
- France
- Italy
- Nordic Countries
 - Norway, Sweden, Finland, Denmark, Iceland
- United Kingdom
- West Germany
- Other European
 - Austria, Switzerland, Spain, Portugal, Greece, Yugoslavia

This region includes about 360 million inhabitants. Economic trade organizations (e.g. EEC, EFTA) lend some stability; but the wide spectrum of political and social ideology among the individual countries causes periodic problems. The OPEC crude oil price increases, international currency fluctuations, and steadily increasing inflation rates affected most of the countries. The 1980 business recession being experienced by the U.S. could well portend similar problems for these countries within the next few years.

The Eastern European countries include: USSR, East Germany, Poland, Hungary, Bulgaria, Rumania, Czechoslovakia, and Albania. These countries consist of about 400 million inhabitants. These socialistic countries have state-controlled economies that only recently are beginning to swing towards the manufacture of consumer items. The USSR is probably the largest volume consumer of polyurethane products, followed closely by East Germany. Finally, Hungary, Czechoslovakia and Poland form a second tier of consumers about half of the level for the USSR and East Germany.

The Middle East and Africa region consists of:

•Middle East

- Turkey, Syria, Lebanon, Jordan, Israel, Cyprus, Kuwait, Iran, Iraq, Saudi Arabia, Egypt

•Africa

- all of continental Africa, except Egypt

The region contains about 640 million inhabitants. The Middle East countries are rich in petroleum and offer the prospect of being a principal source of petrochemicals over the next decade. Many of the countries in the Middle East and Africa are just beginning to develop markets for polyurethanes. Egypt, South Africa, and Turkey are the current leaders in polyurethane usage.

The Europe/Middle East/Africa polyurethane demand is summarized in Tables IV and V. The overall polyurethane demand for Western Europe is expected to reach about 2,200 million pounds in 1980. West Germany alone will account for 25% of the total, followed by Italy (20%), France (13%) and the United Kingdom (9%). Based on current growth expectations, overall demand should increase about 6.0% annually, and reach the 4,000 million pound level by 1990. The Middle East, Africa, and Eastern European countries will represent a combined total demand of 765 million pounds in 1980. Despite the well known social, political, and economic problems for many of these countries. The Middle East/Africa/E. Europe could reach a 1,565 million pound polyurethane demand by 1990.

Europe/Middle East/Africa Markets. Flexible foam end uses account for the bulk of the polyurethane demand, principally for transportation, furniture and bedding applications. The excellent cushioning properties, lightweight, and ease of installation of polyurethane flexible foam is well recognized. A principle user of flexible foam is the West European auto industry that produced 15.5 million units (about 4.1 million from E. Europe) in 1979. The average auto uses 10 kg. to 15 kg. of flexible foam and semi-flexible foam, primarily for cushioning and safety padding. Molded auto seats are now widely used with full depth, HR (high resiliency) flexible urethane foam which is steadily replacing the traditional "bench" or foam topper pad types of con-

struction. The HR foam uses ranges from a high level of acceptance in Scandinavia to moderate usage in Italy and West Germany and finally, to limited applications in France. Furniture demand for flexible polyurethane foam has been a slow developing market. Styling trends differ among the various countries, and many of the low volume furniture manufacturers still use traditional cushioning materials.

The future growth prospects will be related to the new residential construction and level of personal income available in the various countries.

Bedding use of flexible polyurethane foam for premium as well as inexpensive mattresses has been a major growth market and represent close to 50% of the flexible foam demand. The polyurethane foam mattresses are available in a range of densities and product qualities despite moderate promotional efforts by mattress producers. Growth prospects for the next decade are good. Some consumers will upgrade the quality of their previous mattress purchases, and a strong demand will continue for the low-priced units in certain areas, e.g. the Middle East and Africa.

Rigid polyurethane foam applications are centered in building and construction, refrigerated transport and domestic appliances. The building and construction markets include residential and non-residential construction, commercial refrigeration and industrial insulation, e.g. tanks and pipes. West Germany is the European leader in this market. Thermal insulation use of polyurethane foam for building and construction applications are well accepted. Both polyurethane and polyisocyanurate foams are used to provide excellent thermal insulation, combined with low moisture vapor permeability, high strength/weight ratio in composites (panels), dimensional stability, and economy of production by continuous processes. There are about 18 to 20 manufacturers of continuous PUR laminate panels in this region. West Germany has approved a regulation that all residential buildings constructed after June, 1979 must use DIN 4102 B-2 class foam insulation for roofs and walls. This trend toward more severe fire ratings is likely to be followed in the other European countries. A polyisocyanurate foam insulated steel deck roofing panel has passed French fire tests and qualifies for reduced fire insurance premiums.

Industrial usage includes a variety of tank, vessel, and piping insulation. The PIR foams are often preferred, because of their higher continuous service temperature (150°C). Cut and preshaped slabstock is used for many industrial plant piping applications. The foam spraying of tanks and pipelines is getting considerable attention in the Middle East and African markets. There is also interest in using polyurethane foam for the insulation of LNG tankers. These ships use high-density rigid foam (up to 100 kg/m^3) and require significant quantities per tanker. Countries with well established ship building industries are vying for this market.

Movement of perishable food products by refrigerated transport from the Southern European agricultural nations to the Northern European countries has become a well-developed transport business. Low temperature insulation of transportation equipment such as refrigerated trucks utilizes the lightweight and superior insulation properties of rigid polyurethane foam. Metal-faced polyurethane foam panels as well as cut slabstock foam are used to insulate the vehicles and containers.

Appliance manufacturers use rigid polyurethane foam as insulation for refrigerators and freezers. The foam provides excellent insulation, is lightweight, and is easy to install. Refrigerator demand continues strong, matching the increased standard of living in many European countries and reflecting significant export markets. Consumer demand for both domestic and export markets should remain strong to 1990.

The polyurethane elastomer demand will receive its impetus from automotive and footwear applications. Uses of polyurethane elastomers for autos is centered in a variety of solid and microcellular applications, ranging from small exterior trim strips to full-sized auto bumpers. The use of Reaction Injection Molding (RIM) processing is gaining increasing interest for the production of large surface area and thin cross section polyurethane elastomer parts. In contrast to their U.S. counterparts, the European auto makers do not have the same pressure to reduce auto weight, improve fuel economy, and meet low damage auto bumper standards. Their interest is primarily for export models to meet U.S. standards and utilization of the styling flexibility offered by RIM polyurethane elastomers. Consequently, there is a modest trend toward the use of RIM bumpers and future consideration of reinforced RIM components (e.g. glass-fiber reinforced RIM polyurethane elastomer auto fender).

The footwear industry uses polyurethane as microcellular elastomer for shoe soles; thermoplastic elastomers for ski boots, coatings for shoe uppers, and adhesives. The microcellular elastomer shoe soles have been used for over 10 years. The polyurethane shoe sole offers lightweight and flexibility in styling. Fine detail simulating wood, cork, leather, and handstitching can be readily reproduced. New style sport shoes have been developed to incorporate multi-colors and multi-density soles. As a result, these shoe soles are used in women's high-fashion shoes, work shoes, and a variety of leisure and sport shoes. The current demand for polyurethane shoe soles is for continued steady growth and demand. There has been a continued shift of the shoe sole market to the Middle East and Eastern European areas.

The use of polyurethane as a binder has found two interesting applications: foundry cores and woodchip particleboard. The foundry industry has recognized the value of polyurethane adhesive binders to bind sand foundry cores for metal casting. This application is increasing steadily. The use of isocyanate binders for woodchip particleboard is receiving significant attention. The

coated woodchip can be pressed into a particleboard or formed as a bonded woodchip core between thin wood veneers. The isocyanate-containing products offer superior weathering and moisture-resistant properties. Developmental program underway, could provide some sizable markets within the next few years.

Japan/Far East

The Japan/Far East region is geographically defined to include Japan, Australia, New Zealand, Korea, Taiwan, Philippines, India, Peoples Republic of China, and the rest of Southeast Asia. This region includes about 2,400 million inhabitants. The countries represent a wide range of political beliefs and economic levels of development. Japan, with its highly industrialized economy and international export program, is the principle economic force in the region. Korea and Taiwan are rapidly growing economies that are competing with Japan for export markets. Most of the Southeast Asian countries are in early or agrarian stages of economic development.

Japan is the principle supplier of both polyurethane and raw material products throughout the region. They represent over 60% of the 1980 polyurethane demand of 990 million pounds listed in Table VI. Korea and Taiwan are developing significant polyurethane demand, much of it destined for export markets. Australia and New Zealand are steadily developing their domestic polyurethane markets. Finally, the other countries (with a few exceptions) are in the preliminary stages of using polyurethane products.

Japan/Far East Markets. The flexible foam demand is centered primarily in transportation, furniture, and bedding markets. The transportation industry will use polyurethane flexible foam mostly for automotive seating and safety padding. Full-depth molded foam seating is replacing the traditional "bench" or foam topper pad type of construction. The transportation industry is a key factor in the Japanese economy, with 1979 production exceeding 10 million vehicles and over half being exported to the U.S. While the demand for both flexible and semi-flexible foam will remain strong over the next decade, the worldwide business slowdown, plus increased U.S. production of small-sized autos, may well reduce demand over the near term.

The furniture and bedding industry use of polyurethane flexible foam for mattresses, pads, and cushioning is a fairly stable market. Furniture manufactured with polyurethane flexible foam offers excellent cushioning properties and reduced assembly labor. Polyurethane foam mattresses are an ideal use for flexible foam. The lightweight and comfort of these foam units has received ready acceptance by consumers.

The polyurethane rigid foam usage will total about 223 million pounds in 1980 and is expected to increase to about 551 million pounds in 1990. Building and construction and domestic appliance applications account for the bulk of the usage. Construction

TABLE IV
WESTERN EUROPE POLYURETHANE DEMAND (MMLBS)

	1980	1985	1990	80/90 %/Yr.
Flexible Foam	<u>1393</u>	<u>1682</u>	<u>2175</u>	4.6
Rigid Foam	495	810	1136	8.7
Elastomers	157	237	345	8.2
Others	155	220	290	6.5
Total	<u>2200</u>	<u>2949</u>	<u>3946</u>	6.0

TABLE V
MIDDLE EAST/AFRICA/E. EUROPE POLYURETHANE DEMAND (MMLBS)

	1980	1985	1990	80/90 %/Yr.
Flexible Foam	<u>422</u>	<u>599</u>	<u>775</u>	6.2
Rigid Foam	190	273	480	9.7
Elastomers	141	178	288	7.4
Others	12	14	22	6.2
Total	<u>765</u>	<u>1064</u>	<u>1565</u>	7.4

TABLE VI
JAPAN/FAR EAST POLYURETHANE DEMAND (MMLBS)

	1980	1985	1990	80/90 %/Yr.
Flexible Foam	<u>493</u>	<u>631</u>	<u>800</u>	5.0
Rigid Foam	223	348	551	9.5
Elastomers	63	112	206	12.6
Others	<u>110</u>	<u>145</u>	<u>193</u>	5.8
Total	<u>889</u>	<u>1236</u>	<u>1750</u>	7.0

applications include insulation for roof, wall, and industrial uses, e.g. tanks and pipes. The development of the Australian Northwest Shelf oil and gas fields will provide a substantial market demand for polyurethane foam insulation that could approach multi-thousand ton levels.

The Japanese building and construction uses of polyurethane products have been rather limited. The insulation value of rigid polyurethane foam has found some acceptance for commercial and industrial use. However, the potentially large-volume residential market remains elusive, despite the Japanese government's offer to provide low-interest loans for energy-saving insulation. Some progress has occurred in the manufacture of polyurethane continuous laminate panels, and four producers are now involved in providing panels for cold storage and agricultural buildings.

The use of polyurethane elastomers for automotive bumpers and body parts is a rapidly growing transportation market. Japanese auto manufacturers have been using RIM processing to produce large surface area and thin cross-section elastomer parts. Toyota introduced a RIM bumper in 1977 and is currently using RIM bumpers on 8 auto models. Some RIM bumpers incorporate an energy-absorbing microcellular foam insert to meet the U.S. auto bumper standards. Mitsubishi Motors has RIM bumpers on two models (Gallant Sigma and Lancer). Nissan Motors is also using RIM bumpers on the Datsun 280ZX.

The Australian auto industry shares the concern of its U.S. counterparts to reduce auto weight and improve fuel economy. A good example is the Ford Falcon XD that is 116 kg. lighter than the previous equivalent model. Part of the weight reduction comes from the use of impact energy-absorbing front and rear bumpers made from RIM molded polyurethane elastomers. The RIM bumpers use about 12 kg. of polyurethane and are attached to a support beam of high-strength glass-reinforced polyester. If other auto producers begin developing similar design, the Australian RIM usage could reach significant levels within the next few years.

Of the many other end uses for polyurethane products, shoe soles and synthetic leather should be mentioned. The polyurethane shoe sole usage reached a peak demand in 1973 before styling trends and competition from other synthetic materials resulted in market erosion. The expected demand will be centered in women's fashion, sports, and recreational shoes for both domestic and export markets.

The polyurethane leather demand provides both a domestic and export market. There are 6 Japanese producers of poromeric leather who will supply about 15 million square meters of leather in 1980 for shoes (about 50%), clothing, and a variety of other products (luggage, cases, gloves, belts, etc.). There is some synthetic leather production in Korea and Taiwan.

An interesting use of polyurethane elastomers is an application being evaluated by the Japanese railroad. The elastomer is applied to the side and bottom surfaces of a concrete railroad tie and serves as a sound absorbing medium for sections of the

track going through residential areas or over concrete bridges. Over 60,000 ties will be coated with elastomer (25 mm thickness) in 1980, and represents over 4 million pounds of elastomer.

The Peoples Republic of China (PRC) is embarked on an ambitious program of economic and industrial growth, directed to overcome many years of political and social upheavals. The PRC has had to scale down its original plans and is focusing on a slower, more balance and selective development program. The initial emphasis will be on agriculture and light industries, to supply consumer needs and encourage exports. The polyurethane sector has not been neglected. A 22 million pound isocyanate plant is scheduled for completion in late 1981, with a capacity of producing crude and pure methylene diphenyl diisocyanate (MDI). While some of this production will be used domestically, the bulk is destined for export markets in Southeast Asia.

The PRC markets for polyurethanes are centered in a range of applications from conventional flexible cushioning and rigid foam insulation to more sophisticated uses, such as shoe soles, synthetic leather and gymnasium playing surfaces. While statistics are not readily available, the PRC consumes about 10 million pounds of rigid foam and 8 million pounds of flexible foam annually. Recent plans to build a 3 million m² per year poromeric polyurethane synthetic leather plant should give impetus to polyurethane demand in 1982/83.

RECEIVED June 1, 1981.

Polyurethane Foam in Furnishings Markets

R. C. SNYDER

The Dow Chemical Company, Organic Chemicals Department, Midland, MI 48640

Industry Structure

The furnishings market for flexible urethane foam can be divided into three major segments: furniture, bedding, and carpet underlayment. These markets are supplied flexible foam by a larger number of firms known as the flexible slab foam industry which convert liquid chemicals to large foam buns made on a continuous conveyor. An infinite variety of cushion shapes are fabricated from the large foam buns.

Although on the order of 90% of the foam volume used by the furnishings industry is made by the flexible slab foam industry, molded flexible foam is also used for some commercial furniture and mattresses. Most of the molded foam is used by the auto industry.

The flexible slab foam industry is characterized by a large number of individual firms which frequently have multi-site foam production and fabricating locations. These are located around the major furniture manufacturing centers of the U.S. and the other major metropolitan markets for serving the bedding and carpet underlayment markets.

The Total Market

The furnishings industries account for about 60% of the almost 1.4 billion pound production of flexible urethane in 1979. About 60% of the furnishings volume is used by the furniture industry while mattresses and carpet underlay about equally divide the remainder.

The consumption of polyurethane foam has matured since 1973. Rapid growth occurred through 1973 due to penetration and/or replacement of rubber and spring cushions in upholstered furniture, other seating including auto and transportation, and bedding applications.

0097-6156/81/0172-0025\$05.00/0

© 1981 American Chemical Society

Beginning with the period of the 1974-75 recession, flexible urethane foam appears to be experiencing the more mature segment of its life cycle. Over the span of 13 years, flexible urethane foam has experienced a compounded growth rate of 11% per year (Figure 1). Economic cycles impacted the growth twice during this period: 1970-71 and 1974-75. The peak-to-peak growth rate over the five-year period 1973 to 1978 was 3.8% per year (Figure 2). Growth had continued during the period but at a moderate rate as flexible polyurethane foam has built volume 1) in carpet underlay at the expense of sponge rubber, and 2) because of the popular waterbed which uses foam for a dual structural and cushion purpose.

Foam volume in 1980 will continue the decline begun in 1979 in response to the decreased level of economic activity. Auto, truck, and recreational vehicle production declines contributed to the 1979 foam volume drop. The large production worker layoffs in these and related industries in early 1980 caused a reduction in consumer purchasing power and impacted overall consumer psychology, thus the fall-off in home furnishings demand in 1980.

Expectations are for a 12% decline in flexible foam production in 1980. The total peak-to-valley decline over the three-year period 1978-80 is forecast at 15%. This compares with a 15.5% decline over the two-year period of 1974-75.

Flexible Urethane Foam

	<u>1977</u>	<u>1978</u>	<u>1979</u>	<u>1980</u>	<u>1981F</u>	<u>1982F</u>	<u>1983F</u>	<u>1984F</u>
Billion lbs	1.35	1.42	1.38	1.21	1.30	1.41	1.51	1.60
% Change	+9	+5	-2.5	-12	+7	+9	+7	+6

The peak-to-peak (1978-84) growth rate expected during the current business cycle is only 2% per year even though the last four years will be in the 7-9% per year range (Figure 3). The utilization of flexible urethane foam is believed to be in the mature phase of its life cycle; thus the growth outlook is dependent on the level of consumer spending for durable goods during the growth years coming out of the current recession (1982-84).

The Furniture Segment

Demographic data suggests that 1975 to 1985 should be a strong period for home furnishings sales. The age group 18-34 will increase by 28% during this ten-year period. The Conference Board predicts that the number of households with heads under 35 will reach an unprecedented 35% of total households by 1985. Home furnishings buying should be stimulated by this rate of household formation by people in their prime buying age.

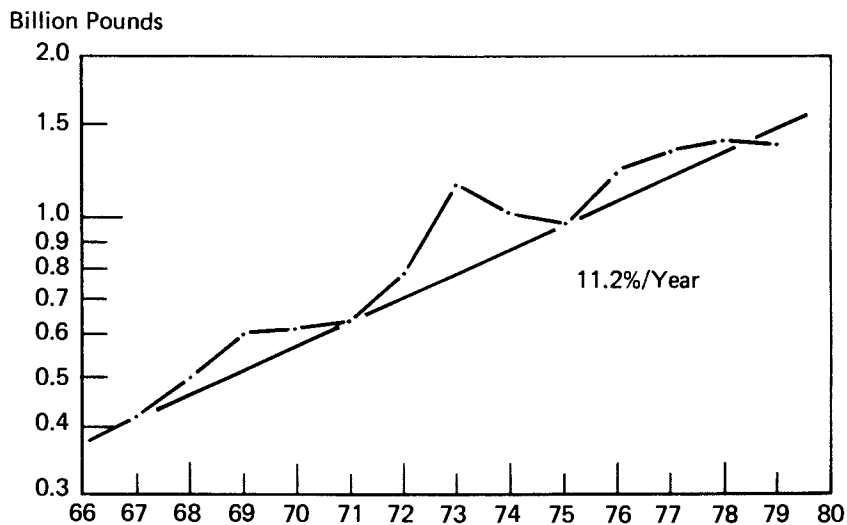


Figure 1. Compound growth rate of polyether flexible urethane foam.

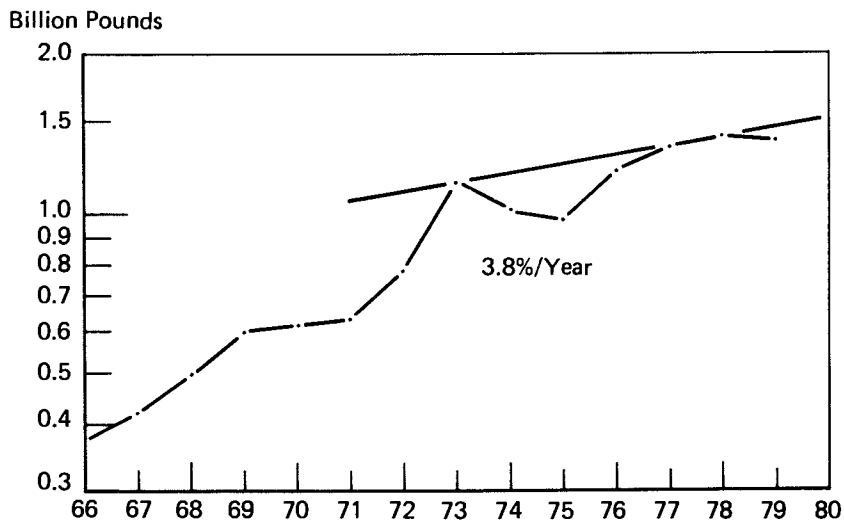


Figure 2. Peak-to-peak growth rate of polyether flexible urethane foam.

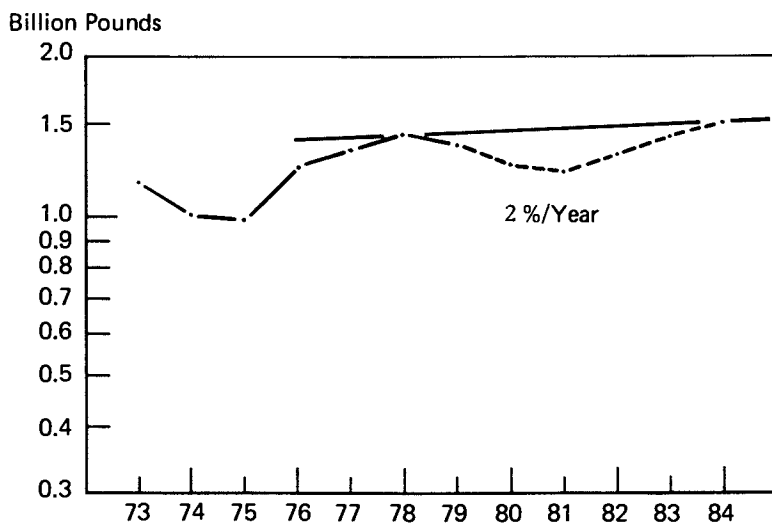


Figure 3. Projected peak-to-peak growth rate of polyether flexible urethane foam.

Flexible urethane foam for furniture applications is the largest single end use accounting for an estimated 37% last year. Consumption of foam in furniture was estimated to be flat last year and is expected to decline in 1980. This should be followed by strong growth years in 1981-83 which we are estimating at 7-9% per year (see below).

Foam Consumption: Furniture

	<u>1977</u>	<u>1978</u>	<u>1979</u>	<u>1980</u>	<u>1981</u>	<u>1982</u>	<u>1983</u>	<u>1984</u>
Million lbs	486	505	496	458	496	540	576	604
% Change		+4	-2	-8	+8	+9	+7	+5

This forecast assumes that the furniture segment is fully penetrated by flexible urethane foam. Style changes may impact cushion dimensions somewhat, but are considered an insignificant factor in the forecast. Flammability issues remain unsettled; however, this forecast assumes technology development will continue to keep urethane foam in the forefront as the best choice for cushioning applications.

The Bedding Segment

Data on the bedding industry is incomplete for 1979. Foam mattress production appeared to have declined relative to 1978 but overall adult mattress shipments were probably up around 2%. The penetration of the adult mattress market by foam core units appears to have slowed in 1979. The available industry data indicates foam core is about 17-18% of the adult mattress market and innerspring units comprising the remainder.

Foam Consumption: Bedding

	<u>1977</u>	<u>1978</u>	<u>1979</u>	<u>1980</u>	<u>1981</u>	<u>1982</u>	<u>1983</u>	<u>1984</u>
Million lbs	155	160	157	150	158	166	173	178
% Change		+3	-2	-6	+5	+5	+4	+3

The growth in waterbed production has had a positive impact on urethane foam demand. Boarder or dam components made from a firm, high density flexible urethane foam has bouyed foam consumption in bedding despite foams lack of growth in other bedding applications, i.e. foam cores and topper pads.

About 30% of the foam used by the bedding industry is used to upholster adult innerspring mattresses. Quilted covers backed with a thin layer of urethane foam contributes to the plush upholstered look. Foam topper pads cover the innersprings and provide comfort to the sleeper.

The topper pad application for urethane receives strong competition from garneted cotton felt pads. The mattress industry continuously evaluates the relative cost and consumer acceptance of the two alternative padding materials. Utilization of flexible urethane foam and the relative share of the available topper pad volume appears to cycle with the competitive price pressures perceived to exist in the retail mattress market. When mattress prices weaken due to slack demand, mattress manufacturers appear willing to cut costs at the expense of consumer comfort and consequently shift a higher ratio of production to cotton felt.

During 1976 and 1977 cotton linters for felting enjoyed a low rate of price escalation relative to urethane raw materials (Figure 4). However, in the last two years, the price of linters has moved up rapidly to the same range of urethane raw materials.

3/80 Price Index (1975=100)

Cotton linters	189%
Flexible foam polyol	162%
TDI	182%

The cotton linters situation is likely to continue to follow its historical cyclical price pattern; therefore, over the five-year forecast period it is not expected that either alternative topper pad material will gain a secure position relative to the other.

Carpet Underlay

The consumption of prime flexible urethane foam in carpet underlay is estimated at 147M lbs in 1979. Additionally, 24M lbs of foaming bonding agent is used in manufacturing bonded urethane scrap underlay. The total consumption of virgin urethane material is estimated at 171M lbs. Scrap urethane foam consumed in bonded underlay is not included in this underlay volume to avoid double counting. Scrap generated in the processing of urethane foam for each of the applications previously described is included with the foam for that application.

Prime urethane underlay continues to grow at the expense of waffle sponge rubber and fiber pad. Since 1977 prime urethane underlay has grown from 19% of shipments to 34% while rubber sponge has declined from 34% to 22%. This erosion of rubber's position is expected to continue during the forecast period.

Foam Consumption: Carpet Underlay

	<u>1977</u>	<u>1978</u>	<u>1979</u>	<u>1980</u>	<u>1981</u>	<u>1982</u>	<u>1983</u>	<u>1984</u>
Million lbs	114	140	171	155	165	184	200	210
% Change		+23	+22	-9	+6	+11	+9	+5

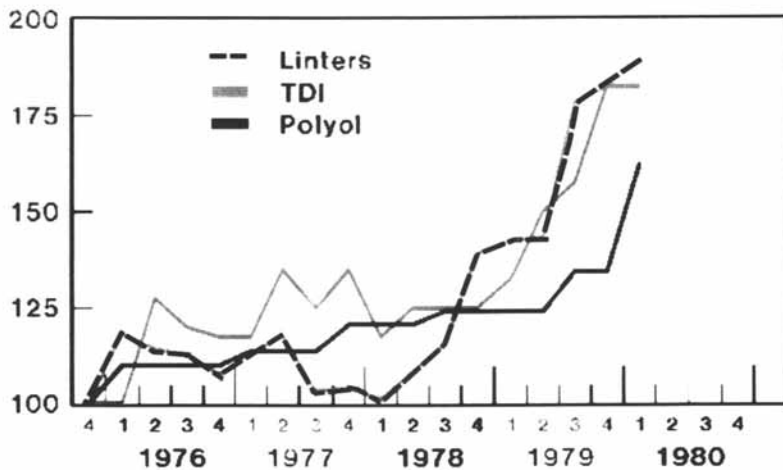


Figure 4. Cotton linters vs. urethane intermediates. Price index (12/1975 = 100).

Summary

The furnishings market for flexible urethane foam will rebound from the current economic downturn with strong growth in the 1982-84 period. The first volume upturn is expected in those portions of the market that are related to new housing starts which will revive in late 1980 and early 1981 due to improved interest rates and mortgage money availability. The major foam volume, however, is dependent on the replacement market in furnishings which will not show significant improvement until unemployment rates and consumer psychology improves. The timing of the turn-around and the magnitude of the upturn will depend on future economic policy and the impact on the level of spending by consumers for durable goods.

	Flexible Urethane Foam					
	<u>Pounds, Billions</u>					
	<u>1979</u>	<u>1980</u>	<u>1981</u>	<u>1982</u>	<u>1983</u>	<u>1984</u>
<u>All Uses</u>	1.38	1.21	1.30	1.41	1.51	1.60
<u>Furniture</u>	0.50	0.46	0.50	0.54	0.58	0.60
<u>Bedding</u>	0.16	0.15	0.16	0.17	0.17	0.18
<u>Underlay</u>	0.17	0.16	0.17	0.18	0.20	0.21
% Furnishings	60	63	63	63	63	62

RECEIVED June 1, 1981.

Automotive Uses for Polyurethanes

DONALD G. LEIS

Silicones and Urethane Intermediates Division—Section K1487,
Union Carbide Corporation, Old Ridgebury Road, Danbury, CT 06817

The automobile has become an integral part of the American economy and way of life. This dependence on the automobile has been reinforced by the decline of the core of many American cities which has resulted in a dispersal of traditional city functions to the suburbs. Suburban residential communities, offices, plants and shopping centers could not exist without the automobile.

As a result, for the majority of American people, there is no viable short term alternative for personal transportation without incurring very major population shifts and economic dislocations.

During the past 25 years, while this move to suburbia was taking place, the number of licensed cars in the United States has been increasing at an average annual rate of 4.3%, while domestic car production had been increasing at an average annual rate of 1.6%. (Table I)

The extent of the dependence of the American people upon the automobile is gained from the following statistics.

The U.S. Department of Transportation has estimated that by 1978 (Table 2), there were an estimated 154 million licensed vehicles and 142 million licensed drivers with an average of 1.09 vehicles per driver. Of the total vehicles, 76% or 117 million were automobiles and 71% of the licensed drivers owned cars.

In 1978 (Table 3), motor vehicles travelled 1.54 trillion miles with an average of nearly 10,000 miles per vehicle and consumed an estimated 277 billion gallons of fuel which represented nearly 40% of the total domestic petroleum usage.

During the 1970's, with the formation of the OPEC cartel, a major change occurred in the price structure of crude petroleum and as a result the price of gasoline. The extent of this change is shown in Figure I.

The initial price increase was followed by four years of relative price stability. However, this was followed by a rapid escalation of price which started in 1979. With the removal

TABLE 1

LICENSED VEHICLES AND CAR PRODUCTIONGROWTH RATE - 1953 - 1978

	<u>ANNUAL GROWTH RATE, %</u>
LICENSED CARS	4.3
CAR PRODUCTION	1.6

TABLE 2

MOTOR VEHICLE STATISTICS1978

TOTAL LICENSED VEHICLES	154 MILLION
TOTAL LICENSED DRIVERS	142 MILLION
TOTAL PASSENGER CARS	117 MILLION

SOURCE: DOT

TABLE 3

MOTOR VEHICLE STATISTICS1978

TOTAL VEHICLE, MILES	1.54 TRILLION
TOTAL FUEL USAGE, GALLONS	277 BILLION
PETROLEUM USAGE	~ 40%

SOURCE: DOT

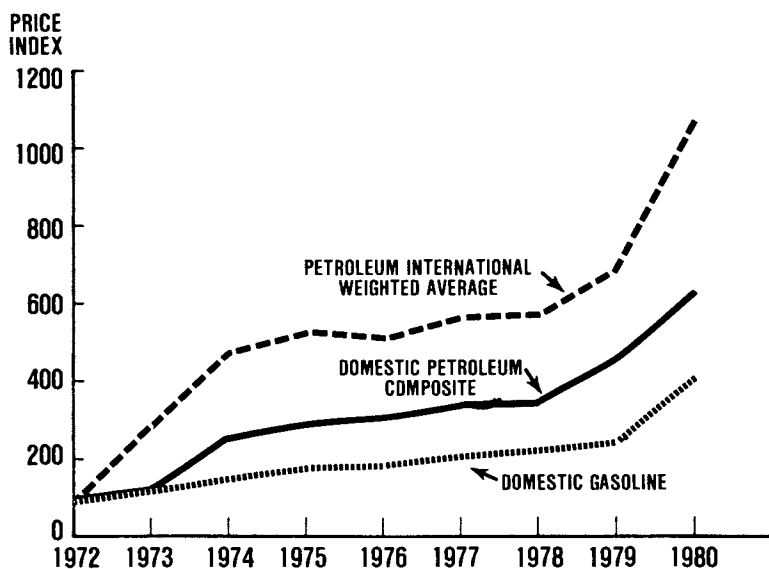


Figure 1. Petroleum and gasoline 1972–1980 price index (1972 = 100).

of price controls on domestic petroleum, the price should reach that of the international market.

The extent of the price escalation in 1979 is shown in the fact that in the 15 month period January 1979 to March 1980, the weighted average international price for petroleum increased from \$13.77 per barrel to \$29.65 per barrel.

In the past eight years, while the international price of petroleum has increased 957%, the domestic composite price has increased 540% and the price of gasoline increased 300%. Because the highest rate of increase occurred in the past year, the effect has been a sharp market trend from large to small cars and in the American Buyer's requirement for a new car.

As a result of this changed market environment, there now exists in the United States a large fleet of over 100 million cars, many of which were built in an era of relatively cheap and available gasoline, which are now rapidly being obsoleted in terms of fuel efficiency.

This need can be met only by a new generation of cars, designed and engineered for a market environment similar to that which exists in Japan and Western Europe, where gasoline has always been relatively expensive.

The situation is similar to that which occurred when the large, heavy, powerful cars of the 1920's were replaced by the small, simple cars of the 1930's to meet the needs of a population emerging from the great depression.

The Present Market

During the past two decades the use of all plastics has increased significantly in the American automobile industry. Urethanes of all types have played an important role in this growth. Thus, as shown in Figure 2, the average use of plastics has grown from an estimated 20 pounds per car in 1960 to a level of 204 pounds per car in 1979. During this period the average use of urethanes increased from four pounds per car to 43 pounds per car.

The first significant use of a urethane in the automotive industry was the 1957 model year with the use of cut urethane flexible foam topper pads for automotive seating in several cars. These topper pads replaced non-woven cotton padding.

The use of urethane foams and elastomers has grown rapidly (Figure 3), with urethane foam growing from an average of 4 pounds per car in 1960 to an average of 35 pounds per car in 1979 and with urethane elastomers growing from 0.5 pound per car in 1969 to 8 pounds per car in 1979. In 1977 (Figure 4), urethane was the major plastic used in the American car by one major manufacturer.

The growth of urethane foam was accelerated in 1972 with the development of high resilience flexible urethane foam for automotive deep foam seating. One of the first significant uses

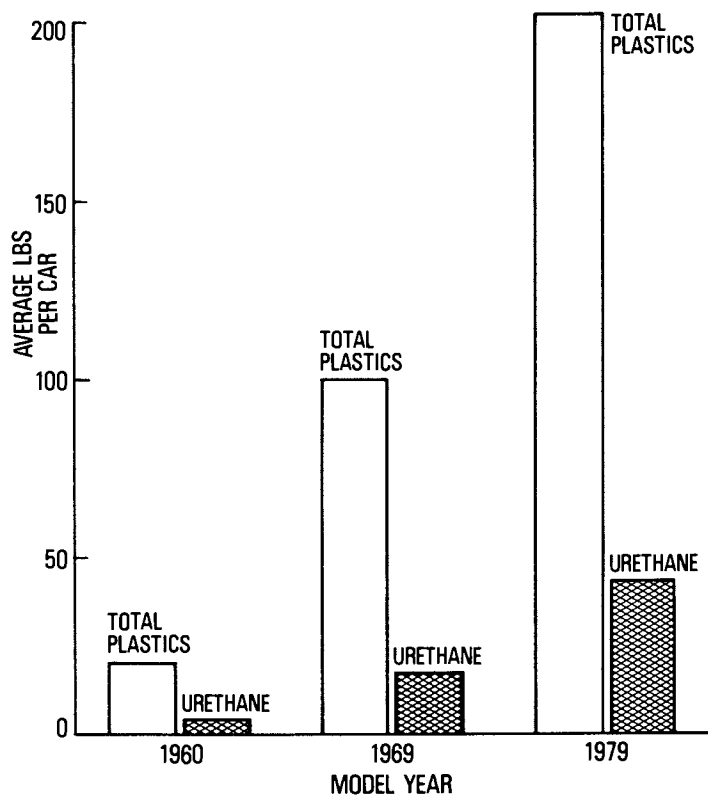


Figure 2. Automotive use of plastics and urethanes 1960-1979.

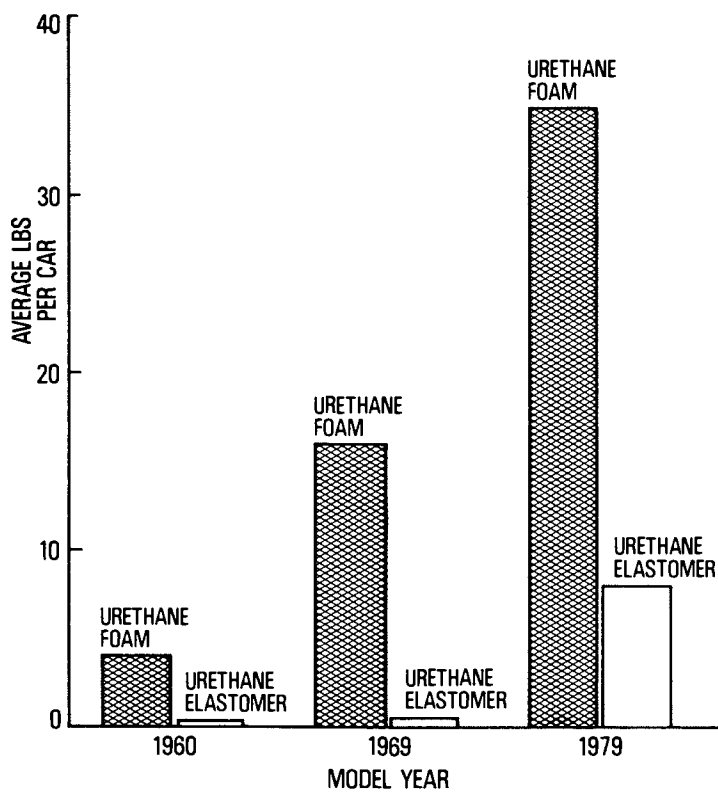


Figure 3. Automotive use of urethane foam and elastomers 1960–1979.

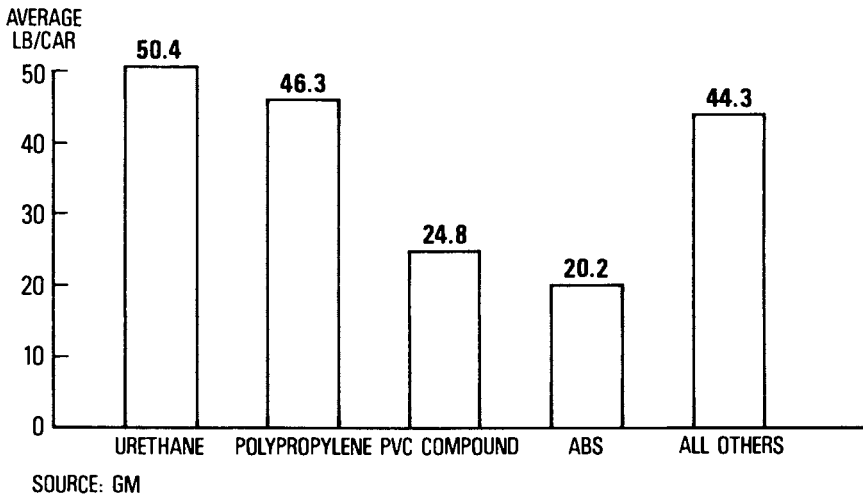


Figure 4. Average plastics use per car in 1977 model year.

of a urethane elastomer occurred in 1973 with the injection molded thermoplastic urethane for sight shields and fender extenders. The use of urethane elastomers increased rapidly after the introduction of RIM molded urethane fascias in the 1975 model year.

In the 1979 model year (Table 4), the use of urethane foam and elastomers averaged 43 pounds per car. Of this 35 pounds was urethane foam. This breaks down to 24 pounds per car of molded foam for seating, 6 pounds of molded foam for other applications, 4.7 pounds of slabstock for upholstery and trim and 0.3 pounds for energy managing bumpers.

The average of 8 pounds per car of urethane elastomer was composed of 1.3 pounds of TPU, 4.8 pounds of RIM thermoset elastomer and 1.9 pounds of cast thermoset urethane.

Future Market

Over the past several years, responsible spokesmen have projected significantly greater use of all types of plastics in the American car by 1985. Some of these projections have been: (Table 5)

<u>DATE</u>	<u>SOURCE</u>	<u>LB/CAR</u>
2/8/78	R. W. Garrity Ford	350
2/8/78	W. Maki GM	350
6/20/79	J. Tuttle GM	255-350
12/4/79	J. Degnon Ford	285-350

Thus, the average use of plastics in 1985 is projected to be 51 to 146 pounds per car higher than current use.

The design of the smaller, lighter, more fuel efficient cars of the future will result in significant changes in the various materials used in the car. A major manufacturer (Table 6) has projected the following composition of the average automobile in 1987 compared to the typical 1978 automobile.

The car of the 1980's will have a significantly lower content of iron, steel and lead but a significantly higher content of aluminum and plastics.

The plastic content of the car is projected to increase from 5.4 to 9.1 percent of the car in the period 1978 to 1985.

Historically, the bulk of urethanes and other plastics have been for interior seating and trim and for mechanical and electrical parts. With its first use in 1970, SMC was the major plastic used on the outside of the car. The promulgation of the Motor Vehicle Safety Standard 215, the bumper standard, resulted in an increase in the external uses of urethanes and other plastics. This resulted in the use of various types of elastomers for bumper sight shields, fender extenders and fascia.

Most of the future growth of the use of plastic for auto-

TABLE 4
AUTOMOTIVE USE OF URETHANE FOAMS
AND ELASTOMERS
1979 MODEL YEAR

	<u>AVERAGE LB/CAR</u>
<u>URETHANE FOAM</u>	
MOLDED SEATING	24.02
MOLDED OTHER	5.97
SLABSTOCK	4.73
ENERGY MANAGING	0.30
<u>TOTAL</u>	<u>35.02</u>
<u>URETHANE ELASTOMER</u>	
T P U	1.30
RIM THERMOSET	4.85
CAST THERMOSET	1.89
R R I M	-
<u>TOTAL</u>	<u>8.04</u>
<u>GRAND TOTAL</u>	<u>43.06</u>

TABLE 5
PROJECTED USE OF PLASTICS IN THE
AUTOMOTIVE INDUSTRY

<u>1985 MODEL YEAR</u>			
<u>DATE</u>	<u>SOURCE</u>		<u>AVERAGE LB/CAR</u>
2/8/78	R. W. GARRITY	FORD	350
2/8/78	W. MAKI	GM	350
6/20/79	J. TUTTLE	GM	255-350
12/4/79	J. DEGNAN	FORD	285-350

TABLE 6
COMPOSITION OF THE AMERICAN AUTOMOBILE

<u>MATERIAL</u>	<u>LB/CAR</u>		<u>%</u>	
	<u>1978</u>	<u>1987</u>	<u>1978</u>	<u>1987</u>
IRON	625	293	17.9	10.4
STEEL	2,066	1,687	59.0	59.9
ALUMINUM	121	180	3.5	6.4
LEAD	22	22	0.6	0.8
RUBBER	99	81	2.8	2.9
GLASS	95	79	2.7	2.8
ZINC	18	9	0.5	0.3
PLASTICS	189	255	5.4	9.1
OTHER	264	210	7.6	7.4
<u>TOTAL</u>	<u>3,499</u>	<u>2,816</u>	<u>100.0</u>	<u>100.0</u>

SOURCE: GM

motives applications is expected to be external with composite plastics replacing sheet metal for the body skin.

A recent report by the Arthur Anderson Co., has projected an increase in the use of composites from 60 pounds per car in 1980 to an estimated 200 pounds in 1990. (Table 7). During this period the use of composites would increase from 5% of the external body panels in 1980 to 25% in 1990.

Future Urethane Use

With the smaller and lighter cars of the future, the amount of urethane foam used for seating and interior trim will decrease. The use of energy managing urethane foam for bumper applications will increase as the use of soft bumpers and flexible fascia increase. The use of urethane foam for all applications is projected to drop about 7% by 1985 model year.

The use of urethane elastomers will grow as the use of soft bumpers and fascia increase. Most of this growth will be RIM thermoset elastomers. The use of 4.8 pounds per car should grow to 15.3 pounds per car by 1985.

The development of reinforced RIM urethane materials is expected to contribute to the future automotive use of urethane materials in external body panels.

This process, in which a high modulus urethane elastomer is reinforced by milled glass fibers is currently commercially used in a three piece air spoiler used on the 1980 Pontiac Sunbird. The first use of reinforced RIM urethane front fenders is scheduled for use on a 1981 model car.

The use of RRIM for external body panels is expected to increase rapidly with the potential use of an average of 4 pounds per car by 1985.

This material has a number of advantages for external body applications. (Table 8)

1. Weight is one-half that of steel; therefore, a front fender with a weight of 9.4 pounds in steel weighs 4.4 pounds in RRIM.
2. These parts show the good painting characteristics of a urethane.
3. The RIM process makes possible molding of very complex shapes.
4. A RRIM fender will resist minor denting.

However, at this state of development of this technology, there are several disadvantages. These are:

TABLE 7
AUTOMOTIVE USE OF COMPOSITE PLASTICS

<u>MODEL YEAR</u>	<u>1980</u>	<u>1985</u>	<u>1990</u>
COMPOSITES, LB/CAR	60	100	200
COMPOSITES, % OF BODY PANELS	5	10	25

SOURCE: A. ANDERSON CO.

TABLE 8
REINFORCED RIM URETHANE

ADVANTAGES

- . LOW WEIGHT
- . PAINTABLE SURFACE
- . CAPABLE OF COMPLEX PARTS
- . RESISTS MINOR DENTING

DISADVANTAGES

- . OFF-LINE PAINTING
- . COEFFICIENT OF LINEAR EXPANSION
- . PRODUCTIVITY

1. At present, off-line painting is required. However, with the industry moving to lower paint bake temperatures on-line painting should become feasible.
2. The coefficient of linear expansion which is greater than that of steel should be compensated by proper design and fastening techniques.
3. Productivity of the process is still low by automotive industry standards. Process improvement is needed before RRIM can be extensively used in automotive applications.

Automotive uses of urethane foams and elastomers for the 1985 model year are estimated to be over 54 pounds per car divided between urethane foam and elastomer as follows: (Table 9)

The use of molded seating will be 22 pounds per car, a drop of 2 pounds. Other molded foam will be 4.78 for a decrease of about 1 pound per car. The use of slabstock for upholstery and trim will be marginally lower at 4.22 pounds per car while energy managing foam could be about 1.8 pounds for a total of 32.78 pounds per car.

The use of urethane elastomers should markedly increase from 8 to nearly 22 pounds per car. The use of TPU and cast elastomers is projected to decrease marginally while RIM urethane elastomer increases four-fold. With the successful use of RRIM composite urethane automotive use is projected to be 4 pounds per car. Thus, the use of all types of urethane elastomer should increase from 8 pounds in 1979 to a projected use of nearly 22 pounds per car in 1985.

Based on the production of 8.45 million cars in the 1979 model year and the projected production of 8.4 million cars in 1985, the total automotive market for urethane materials (Table 10) is estimated to increase from 364 million pounds in 1979 to 459.7 million pounds in 1985.

The market for urethane foam is expected to drop by 20 million pounds in 1985 reflecting the impact of smaller cars.

The market for urethane elastomers of all types is projected to increase by nearly 116 million pounds as a result of increased use for external body parts.

The major increase will be the increased use of RIM urethane thermoset elastomer for flexible fascia and bumpers and reinforced RIM urethane materials for fenders and other body parts.

TABLE 9

AUTOMOTIVE URETHANES PROJECTED USE

<u>MODEL YEAR</u>	<u>AVERAGE LB/CAR</u>	
	<u>1979</u>	<u>1985</u>
<u>URETHANE FOAM</u>		
MOLDED SEATING	24.02	22.00
MOLDED OTHER	5.97	4.78
SLABSTOCK	4.73	4.22
ENERGY MANAGING	0.30	1.78
<u>TOTAL</u>	<u>35.02</u>	<u>32.78</u>
<u>URETHANE ELASTOMERS</u>		
T P U	1.30	1.00
RIM THERMOSET	4.85	15.33
OTHER THERMOSET	1.89	0.73
R R I M	-	4.00
<u>TOTAL</u>	<u>8.04</u>	<u>21.89</u>
<u>GRAND TOTAL</u>	<u>43.06</u>	<u>54.67</u>

TABLE 10

AUTOMOTIVE URETHANES TOTAL MARKET

<u>MODEL YEAR</u>	<u>1979</u>	<u>1985</u>
PRODUCTION, MILLION	8.45	8.40
<u>URETHANE FOAM</u>	<u>MILLION POUNDS</u>	
MOLDED SEATING	203.0	185.0
MOLDED OTHER	50.6	40.3
SLABSTOCK	40.0	35.2
ENERGY MANAGING	2.4	15.2
<u>TOTAL</u>	<u>296.0</u>	<u>275.7</u>
<u>URETHANE ELASTOMERS</u>		
T P U	11.0	8.4
RIM THERMOSET	41.0	128.5
OTHER THERMOSET	16.1	13.4
R R I M	-	33.7
<u>TOTAL</u>	<u>68.1</u>	<u>184.0</u>
<u>GRAND TOTAL</u>	<u>364.1</u>	<u>459.7</u>

**American Chemical
Society Library
1155 16th St. N. W.**

Conclusion

Urethane materials are expected to remain one of the major plastics used in the American automobile through the 1980's. With the coming revolution in car design that is required to meet the changed market environment, the American automobile companies are faced with a formidable challenge and will require the support of the Chemical Industry in developing improved products and processes so that this challenge can be met.

RECEIVED June 1, 1981.

Insulation Markets for Isocyanurates and Polyurethanes

E. H. FUHS

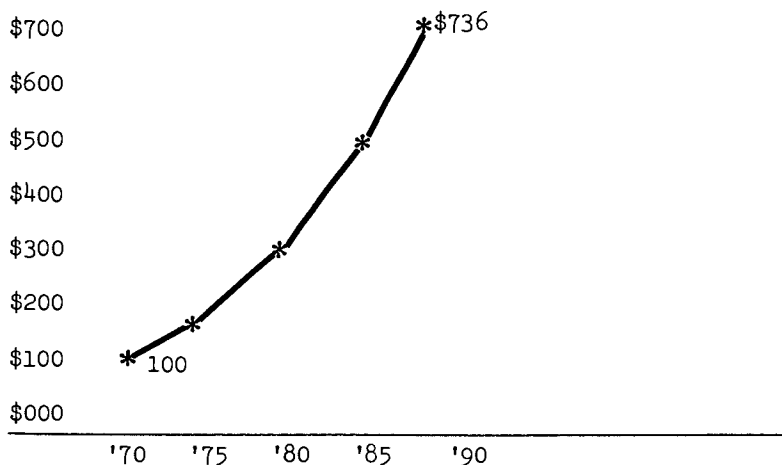
Insulation Products, Celotex Corporation, Tampa, FL 33607

The decade of the 1980s offers practically limitless market potential for polyurethanes and isocyanurates. Attesting to that statement are the increased demands for more efficient ways to insulate and thereby conserve energy, as well as proposed government programs such as the Department of Energy's Residential Conservation Service (R.C.S.) program and Building Energy Performance Standards (B.E.P.S.).

Consumer demands in this regard are not to be taken lightly inasmuch as energy-consciousness is not a fad mentality. It is a "pocketbook" issue that will be with us on a long-term basis.

Research released by Data Resources Incorporated related to a Consumer Energy Index indicates that a monthly heating bill of \$100 in 1970 will average \$736 by 1990 if no energy-saving action is taken.

Exhibit I
Consumer Energy Index - Average Monthly Heating Cost
 1970 - 1990



0097-0001/0172-0049\$05.00/0
 © 1981 American Chemical Society

Further manifestations of this increasing energy-consciousness include dramatic changes in insulation-buying patterns. Insulation retailers tell us that they are now selling insulation longer in the spring...earlier in the fall and through the summer. As a matter of fact, the peaks and valleys that we used to experience in the sale of insulation products have begun to level out.

Essentially, the broad marketplace is being impacted by the clamor of an increasingly energy-conscious public whose cries for relief and assistance have prompted governmental agencies to develop and propose legislation and standards designed to protect and satisfy. We are all aware of the additional factors that have a role in this scenario: dwindling domestic energy resources, the heavy reliance on foreign sources of energy and related imbalance of trade, and others.

As a country we find ourselves aggressively pursuing new sources of energy and at the same time taking the necessary steps to maximize utilization of existing and emerging energy supplies.

While it would be foolhardy for me to imply or suggest that isocyanurates and polyurethanes offer this country the solutions to its multi-faceted energy-related problems, I strongly believe that they represent the most cost-effective way to meet the challenges present within the shelter insulation markets of the 80s.

Insulation Markets

The insulation markets holding tremendous potential for penetration during the current decade include: commercial, industrial (retrofit and new construction), residential (retrofit and new construction) farm buildings and metal buildings.

On closer examination of the individual market segments described previously, I would suggest the following as realistic estimates of market potential through 1985:

Commercial/Industrial Segment. Defined as the commercial, manufacturing, educational and public building group, this segment includes retrofit and new construction opportunities.

Exhibit II

Commercial/Industrial

Retrofit:	1980 - 6,300,000,000 sq. ft.
	1985 - 4,500,000,000 sq. ft.
New Construction:	1980 - 519,000,000 sq. ft.
(excluding roofs)	1985 - 513,000,000 sq. ft.

In the retrofit or re-insulation area, the current potential is approaching 6.3 billion square feet. By the middle of the decade, that potential will have diminished to 4.5 billion square feet because many buildings will have undergone retrofitting and new buildings will have incorporated more efficient standards.

With regard to new construction, the potential in 1980 for penetration is 519,000,000 square feet of insulation material excluding roofs. We predict thicker material will be used as energy costs increase and most of this construction will be in foam plastic insulations. While urethane penetration is slight in the commercial area today -- with the exception of roof insulation -- its impact in this area could equal 50% of the market by 1985 as recognition of its high R-value with a thinner profile gains in recognition.

Certain emerging industrial applications for rigid board insulation, such as petrochemical tanks, pre-dryers used in lumber processing and solar collectors, are not reflected in terms of market potential in this presentation. As of this date, no source exists that can readily identify the size of this segment in terms of re-insulations or new construction activities. This situation will undoubtedly change, and I am certain that data, when available, will have an additional, favorable impact on the overall insulation market.

Residential Segment. The penetration potential within this segment again is divided into retrofit and new construction categories. In terms of retrofit potential, we project a 1980 potential of 1.6 billion square feet with gradual increases to 1985 where the potential will be 1.75 billion square feet. This market segment includes insulating undercourse for residing applications and underlayment for do-it-yourself or remodeling contractors in interior applications under wallboard or paneling.

Exhibit III

Residential

Retrofit:	1980 - 1,600,000,000 sq. ft.
	1985 - 1,750,000,000 sq. ft.
New Construction:	1980 - 2,116,000,000 sq. ft.
	1985 - 3,330,000,000 sq. ft.
Vaulted Ceilings:	1980 - 600,000,000 sq. ft.
	1985 - 714,000,000 sq. ft.

When we speak of residential construction that includes sheathing and the sub-category of vaulted ceilings. Sheathing potential will grow through the first half of the decade from 2,116,000,000 square feet to 3,330,000,000 square feet. The substantial increase will make this segment the largest -- by far -- of all. That tremendous growth reflects foam insulations function as the remedy to "Thermal Short Circuits" of the framing utilized in most of this type construction.

Farm Building Segment. The farm building segment consists of two basic types of construction: pre-engineered metal frame and wood post frame. Both metal frame and wood frame construction are usually covered with configured metal roofing and siding. These structures are most often used for animal confinement and machine storage.

The market potential for insulation in farm buildings is estimated at 257,000,000 square feet at present. By 1985, that potential will have increased to 277,000,000 square feet.

Metal Building Segment. The present market potential for insulation materials is 293,000,000 square feet. We estimate that potential to increase to 459,000,000 square feet through the next four years due to anticipated reductions in site and construction costs plus the increasing speed of construction. Metal buildings will become an increasingly viable alternative to conventional construction.

Cumulative Market Potential. Having defined market potential by segment, the cumulative impact, both now and through the middle of the 1980s offers significant opportunities. At present, the total potential within the defined insulation markets equals 11,685,000 square feet. As we approach the middle of the decade this potential will be 11,543,000,000.

Exhibit IV

Cumulative Market Potential

1980 - 11,685,000,000 sq. ft.

1985 - 11,543,000,000 sq. ft.

Plus

Full Commercial/Industrial

Market, Roof Insulation and

Emerging Applications

Please note that those figures do not reflect roof insulation, which this year represents a potential of more than 3 billion board feet of one-inch fiberboard equivalent to 1.25 billion board feet of one-inch urethane. By mid-decade, we anticipate the market to grow to 4 billion board feet or 1.66 billion board feet of one-inch urethane.

While the potential is evident, there are factors which will have an impact on the successful penetration within the marketplace.

Market Impact Factors. As I had indicated earlier in this presentation, the federal government will influence insulation markets during the 1980s to a greater degree than at any other time in the history of the industry. The agency responsible for this development is the Department of Energy and its Residential Conservation Service (R.C.S.) program and Building Energy Performance Standards (B.E.P.S.).

In addition, the new Minimum Property Standards announced by the Department of Housing and Urban Development in 1979 are generally anticipated to be the norm for all residential construction. While the new FHA standards apply directly to federally-financed housing, they have begun to filter down to the local level. This movement has been slow, but steady and past history dictates that the new standards will eventually be manifest in most local housing codes nationally.

Residential Conservation Service (R.C.S.) Program. The Department of Energy's Residential Conservation Service (R.C.S.) program mentioned previously is geared to the residential retrofit or re-insulation market. Under the aegis of the program, public utilities nationally will be required to perform energy audits at the request of individual customers. Upon completion of the audits, the utilities must provide the consumer with lists of approved products and contractors capable of undertaking the recommended re-insulation task. Additionally, the utilities must be in a position to arrange consumer financing for the retrofit, if necessary.

As part of the R.C.S. program, specifications for approved insulation products will be provided to the utilities. That same data will be used by the Internal Revenue Service with regard to its tax rebate program, should it continue.

Building Energy Performance Standards (B.E.P.S.). While the scope of the R.C.S. program is limited to residential retrofits or re-insulations on an "as requested" basis by consumers in concert with their local utilities, the Building Energy Performance Standards are much broader. The standards relate to residential and non-residential construction. According to the standards, which are to go into effect in August of 1981, new structures will be limited to the number of

British Thermal Units (BTU's) used on an annual basis per square foot by type of building. The standards applicable to a given structure are maximums.

The Department of Energy has estimated that the new standards will result in 42% increase in the market for insulation materials. DOE further predicts that the lion's share of that increase will go to foam sheathing in residential applications over the near term.

I should point out that the proposed Building Energy Performance Standards have come under heavy fire on several fronts. For example, the National Association of Homebuilders is bitterly opposed and has requested a two-year delay so that a pilot program can be implemented to test the standards under actual conditions. The National Association of Home Manufacturers opposes BEPS in their present form as being overly complex and unenforceable. The American Institute of Architects, National Institute of Building Sciences, Building Official Code Administrators and others favor the performance standard approach, but all want the existing standards tempered to a degree or gradually implemented.

This discussion notwithstanding, I firmly believe BEPS will become a fact of life within the next two years. They may be altered, but they will most definitely come to be.

While governmental activity is anticipated to favorably impact the insulation market in this decade, there are a number of potential limiting factors relative to overall penetration. Primary among these factors are inadequate "k" factor reporting, flammability, toxicity and the influence of these factors upon insurance underwriters and code authorities.

"K" Factor Reporting. The outlook I have presented so far is most favorable, but there are also some factors in the marketplace which may tend to reduce the public's acceptance of isocyanurates and polyurethanes. These challenges can be effectively overcome, but it is important to analyze them. They spring from consumer and industry misunderstandings which can be remedied by effective information programs. One problem is the so-called "numbers game" involving "k" factors. Some manufacturers, in order to gain the best possible "k Factor" for their products, conduct testing under conditions that aren't likely to occur in the real world. They may establish their "k Factors" on tests done at low mean temperatures, aware their performance will be better this way. Or they may incorporate reflective air space into their test assemblies, even though that air space isn't likely to be found in actual applications.

The solution is simple: consistent testing methods must be required, with severe penalties for cheaters. When customers are able to compare apples and apples, informed decisions follow. The Federal Trade Commission's pending Home Insulation

Regulation, which my company has supported, would be a partial solution. While affecting only the residential market, it would set the precedent of establishing consistent testing and reporting methods for various insulation materials. The obvious superiority of polyurethanes and isocyanurates will thus be demonstrated.

Flammability. The flammability issue is another area where consistent testing methods can demonstrate that certain plastic products can perform with predictable safety. In the early 70s, there were some admittedly regrettable problems with plastic insulations. A regulatory scramble followed, punishing all of the industry for the abuses of a few. The public became somewhat distrustful, a problem that has taken years to overcome.

However, there are polyurethanes and isocyanurates on the market that have demonstrated their superior fire performance. Our Thermax is one such product. We developed it and patented the process. We have a team of trained specialists working with legislative and regulatory bodies to demonstrate how it complies with their codes. Other manufacturers appear to be doing the same thing. It will take this kind of education effort by our industry to prove that today's polyurethanes and isocyanurates can overcome the flammability problems of their predecessors.

Toxicity. Still another problem is toxicity. There has been much speculation about the toxic gases produced when polyurethanes and isocyanurates burn. However, technology hasn't come up with a test or series of tests to measure which burning materials pose a greater threat to life-safety than others. Our own tests show that more lethal hydrogen cyanide gas is produced when nylon carpet burns than when foam plastic insulation materials are ignited. So, while I concede that this is an unresolved challenge, it is being studied in scores of private and publicly-funded laboratories around the country.

The 1980s: A Decade of Challenge and Opportunity. From this discussion, I hope each of you can see and appreciate that we are in a decade that will offer us significant challenges and opportunities.

The challenges come from those factors that have the potential to limit penetration of insulation markets, while the opportunities for growth reside in most every segment of the marketplace.

I personally look forward to the 80s. I hope each of you share in that feeling.

RECEIVED April 30, 1981.

Urethane Binders and Adhesives

ROBERT J. SCHAFER and WOLFGANG A. OPLESCH

Ashland Chemical Company, P.O. Box 2219, Columbus, OH 43216

Urethane binders and adhesives represented about 5% (120 million pounds) of total U.S. urethane use in 1979, Table I.

Table I. U.S. Urethane Use 1979

Flexible Foam	1400MM lbs.
Rigid Foam	555
Elastomers	190
Surface Coatings	85
Adhesives & Sealants	<u>140</u>
	2370

Manufacturer sales in the U.S. adhesives industry are rapidly approaching 2 billion dollars per year. The industry already consumes more polymers than the industrial coating industry - 1,350 million pounds compared to 1,250 million pounds in 1978. About 1.4 billion pounds of film forming polymers, resin and additives were used by the adhesives industry in 1979.

Growth of the U.S. adhesives industry is expected to be about 8% per year during the 1980's. Howard Ellerhorst, Jr., President of Chemical Marketing Services in Cincinnati predicted 8% per year growth during the 1980's in his presentation to the Chemical Marketing Research Association Conference in November 1979. Stanford Research Institute of Menlo Park, California, predicted use of specialty adhesives and sealants would grow at 8% per year from 1978 through 1983. In mid-1979 Business Communications Company of Stamford, Connecticut, predicted a 7% per year growth for adhesives during the time period 1975-1985.

The value and projections for synthetic adhesives by major application is shown in Table II.

0097-6156/81/0172-0057\$05.00/0

© 1981 American Chemical Society

Table II. Value and Projections for Synthetic Adhesives
By Major Application
(In Millions of Dollars)

<u>Market</u>	<u>1979</u>	<u>1985</u>	<u>Avg. Annual Growth Rate, %/Yr. 1979-1985</u>
Paper and converting paperboard	\$ 580	\$ 835	6.3%
Book binding, gummed products, labels, business forms, tape	130	187	6.2
Metal bonding, foundry, assembly	150	190	4.0
Transportation	220	295	5.0
Construction	867	1,430	8.7
Textile, apparel, shoes	180	257	6.0
Electrical/electronic	124	208	9.0
Furniture	320	420	4.0
Retail, resale	90	130	6.3
Specialty: space, medical, florist sport equip., miscellaneous	95	140	6.7
Caulk and sealant	<u>342</u>	<u>558</u>	<u>8.5</u>
Total	\$3,098	\$4,650	70.7%

Source: Business Communications Co., Published in Adhesives Age, July 1979, p. 41.

Of these markets, the only significant impact of urethane has been on the foundry adhesives market where urethanes have captured about one-third of the 150 million dollar market. Urethane adhesive use in the United States in 1979 is shown in Table III.

Table III. U.S. Urethane Adhesive Use

<u>Market</u>	<u>1979</u>	<u>Average Annual Growth Rate, %/Yr. 1980-1985</u>
Foundry Sand	75MM lbs.	8-10%
Rebonded Carpet Underlay	25	-
Construction	5	20+%
Transportation	5	20+%
Shoe	5	-
Other (Textiles, Tapes,..)	<u>5</u>	<u>-</u>
Total	120	8-10%

The bonding of foundry sand is by far the most significant use at 75 million pounds per year. The rebonding of foam for carpet underlay is a distant second at 25 million pounds per year. Construction, transportation, shoe bonding and other uses each total about 5 million pounds a year. The total use is 120 million pounds per year. The rest of this paper will concentrate on three market segments: foundry sand, construction and transportation. The foundry sand bonding industry will be covered because of its significance and the construction and transportation industries because of the seeming potential for growth in these particular industries. The growth rates projected are my own and are based on a variety of sources.

Foundry Binders

Urethane adhesives were introduced to the foundry industry in 1965 by ADM Chemicals, which is now part of Ashland Chemical Company. The product was an immediate success, and within two years more than 10 million pounds of urethane adhesive was being sold into the U.S. foundry industry. Ashland Chemical introduced a second urethane adhesive to the industry in 1968 and a third in 1970. These unique products were highly successful. On a worldwide basis, growth rate for the use of urethane adhesives by the foundry industry has averaged 20% per year over the period 1970 to 1980. Over 125 million pounds of urethane adhesives were used by the foundry industry throughout the world in 1979. U.S. use in 1979 was about 75 million pounds. The foundry industry uses urethane adhesives to bond sand. Typically, one to two percent adhesive is used in combination with a clean, dry sand. The resin-sand mixture is shaped into a core or mold and cured. A core forms the internal passageways in a casting such as the passageways from the carburetor to the cylinders in the intake manifold of an automobile engine. A mold is used to form the external shape of a casting. After the metal is poured into the mold and around the core, the binder must break down so that the casting can be separated from the mold and core. In theory, after the binder has decomposed, the sand should be free-flowing and easy to separate from the casting. Although the binder's usefulness is essentially spent after one use, the sand can usually be rebonded with additional adhesive to make subsequent castings. Small cores for pneumatic valves may weigh as little as an ounce and large cores for castings such as stationary turbines, might weigh more than 10,000 pounds. Molds can weigh as little as 10 pounds and as much as 100,000 pounds.

Two of the three binder systems used by the foundry industry are two-component, room-temperature curing adhesives. All systems use polymeric MDI as the isocyanate component. All of the cross-linkable components are polyols. The first polyol introduced into the industry was an alkyd oil resin consisting of linseed oil, pentaerythritol and isophthalic acid. The system

is designed so that there is an excess of hydroxyl groups to react with the isocyanate. The second and third products introduced to the foundry industry were based on phenolic resins as the polyol. The commercial system incorporates a preferred, unique phenolic resin. This resin is based on phenol and formaldehyde, contains a predominance of ortho-ortho linkages, a high percentage of ether linkages between the benzene rings, and is capped on both ends by methylol groups. This resin is the subject of U.S. Patent 3,485,797 dated December 23, 1969. These polyols have no counterparts in the rest of the urethane industry.

Two unique processes based upon novel curing mechanisms have been developed for the phenolic polyols. In the first process the cure is internally catalyzed, that is, the catalyst is mixed with the polyol, isocyanate and sand components. The catalyst, however, is unique and provides the advantageous feature of this system which is the long delay after the components are mixed and quick cure once the curing starts, as shown in Figure 1. The figure also illustrates the effect of catalyst type on time to work with the mix (WT) and on time when the core can be handled or stripped (ST). This innovative feature has allowed the foundry industry to increase their core manufacturing productivity by as much as 50-100% of what is achievable with any other core binder system.

The second process involves a three-component room-temperature curing adhesive. A unique method was devised for curing phenolic polyols based on the fact that sand, even when packed to maximum density, is very porous. As a result, a gas catalyst can be blown through the core. Using this phenomenon, a novel process was developed wherein the sand and resin components are mixed, formed into the desired shape and then cured by blowing a mixture of a tertiary amine gas and an inert carrier gas through the core. Typically, triethylamine, dimethylethylamine or trimethylamine are used as a curing gas and the carrier gas is either air, nitrogen or carbon dioxide. A schematic of this process is shown in Figure 2. Several advantages accrued from the development of these urethane adhesives are shown in Table IV.

Table IV. Advantages of Urethane Adhesives
As Used to Bond Foundry Sands

- Improved Sand Flowability
- Increased Productivity
- Room Temperature Cure
- Lower Energy Consumption
- Less Expensive Tooling
- Less Tool Wear
- Easier Control of Fumes During Core Making
- Excellent Shakeout in Iron and Steel

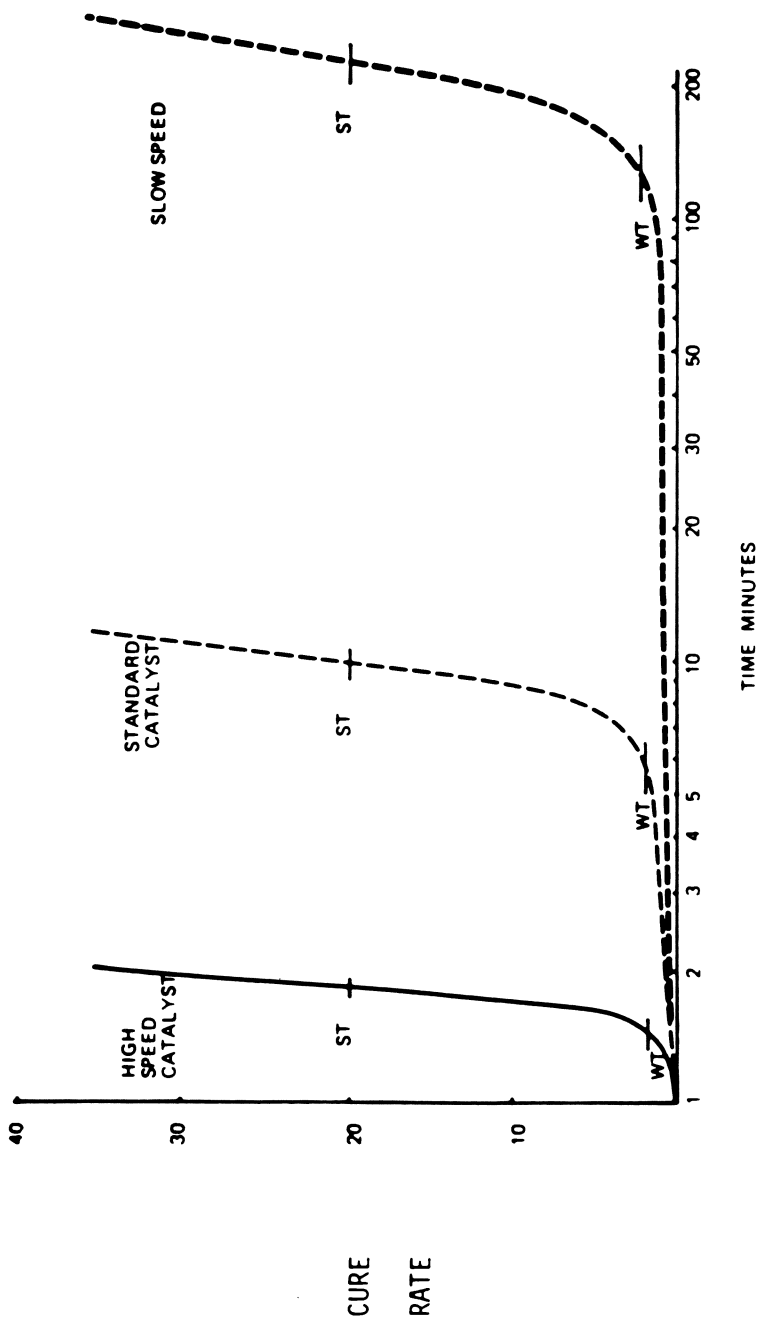


Figure 1. Effect of catalyst type on compressive strength build-up for urethane binders.

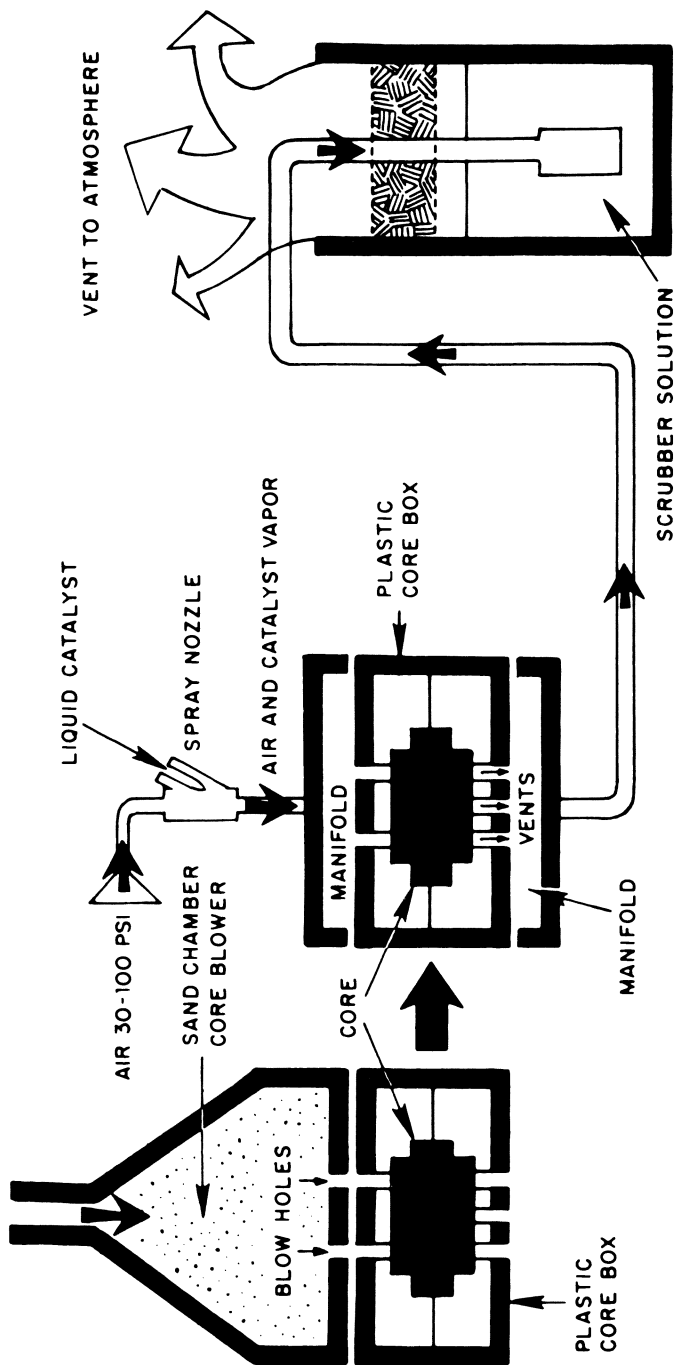


Figure 2. Schematic of equipment for cold box process.

Improved sand flowability resulted from the oil nature of the urethane adhesives. Increased productivity was achieved because of the unique curing characteristics of the urethane adhesives. In the gas cure process, cure sufficient for removal of a core from a core box can be achieved in as little time as a few seconds. Prior to the development of the gas cure or cold box process as it is sometimes called, cores for high production use had normally been cured at temperatures of about 300 to 400°F. By the cold box process cores are cured quickly at room temperature. Several advantages accrued from this fact. Less energy was used because the core boxes did not have to be heated. Less expensive plastic tooling could be used instead of the iron or steel tooling required when temperatures of 400+ are experienced. Lack of heat and improved sand flowability allowed for lower blow pressures and thus low sand velocity when the sand was blown into the core box, resulting in less tool wear. Control of formaldehyde and sometimes phenol fumes from alternate adhesives for core making are a continual problem. In the cold box process, although amine gas fumes must be controlled, they are easier to control. Finally, the urethane adhesives provided excellent shakeout when the cores and molds were used to cast iron and steel. Shakeout is related to the breakdown of the binder system and the ease of separation of the core or mold sand from the casting.

Two factors of concern to the foundry industry in the 80's will be better methods for controlling smoke and fumes and better shakeout for aluminum castings, Table V.

Table V. Opportunities for Improvement of Urethane Adhesives As Used to Bond Foundry Sands

- Better Methods to Control Smoke Generated During Casting
- Better Shakeout from Aluminum Castings

Control of smoke and fumes in foundries has always been a concern as organic materials have been used in cores and molds for centuries. However, recent public and government attention have brought these matters into focus. Urethane adhesives have not been singled out for special attention, but like the many other organic materials used in cores and molds, urethane adhesives create smoke and fumes as hot metal is poured into a mold, during the time the metal is cooling, during the shakeout process and during subsequent cooling and clean-up of the sand for reuse. Many improvements have been made in foundries, especially through the use of better ventilation. Control of smoke and fumes will be an important challenge of the foundry industry in the 80's and improvements through better adhesive technology will constitute an opportunity for better urethane adhesives.

Core shakeout is often difficult from aluminum castings. Aluminum is cast at a much lower temperature than iron or steel, 1400°F versus 2500 to 3000°F, and aluminum has a heat content much lower than iron or steel. As a result, the cores or molds are heated to a much lower temperature and the temperatures are not always sufficient to adequately break down the adhesive. This problem will be even more significant in the future as more and more aluminum castings are used by the automobile industry. About 25% of the foundry adhesives are used to make cores and molds for automotive castings. A very significant change is taking place in the automotive casting industry, based on the need for reducing auto weight, Table VI.

Table VI. Change in Automotive Castings*

<u>Year</u>	<u>Casting Wt.-Avg. Car</u>	
	<u>Aluminum</u>	<u>Ferrous</u>
1979	70 lbs.	600 lbs.
1985	120	400
1990	150	250

* Data from Arthur Anderson Co. as reported in Chemical Week, 8/15/79, p. 19.

The significance of the change on the use of urethane adhesives could be even greater than would be indicated by the figures shown as the castings that are changing over from ferrous to aluminum are those that are heavily cored. This is especially true of engine blocks, heads and intake manifolds. What is needed are adhesives with better shakeout characteristics at the low casting temperatures of aluminum. There is an opportunity to develop better urethane adhesives for casting aluminum.

The foundry industry is expected to have an annual growth rate of 5 to 6% through the next five years. During this time there is opportunity for additional penetration of urethane adhesives in the core binder area. In the automotive area, which constitutes about 25% of the foundry industry potential, about 20% of the cores are made using urethane adhesives. Planned and future conversions to urethane adhesives should increase the percentage of automotive cores made using urethanes from the current 20% to 40% within the next five years. Pipe shops which currently use very little urethane adhesive are now converting to urethanes. Finally, the farm implement industry, which is currently a heavy user of urethane adhesives, is planning significant expansion. As a result, I expect an annual growth in the use of urethane adhesives in the U.S. of 8-10% over the next five years.

Construction Adhesives

It is estimated that the U.S. construction industry currently uses about 5 million pounds of urethane adhesives. In spite of the current slow-down, the average annual projected housing demand in the United States for the period 1980-1989 is expected to be 2.5 million units according to E. Dickerhoof, T.C. Marcin, and C.G. Caril of the U.S. Forest Products Laboratory. See Table VII.

Table VII. Average Annual Projected Housing Demand in the United States by Census Region and Type of Unit for the Period 1980-89*

Region	Housing Type				
	Total	Total			Mobile
	All Housing Types	Slg. Family Units	Multi-Family Units	Single-Family Units	Home Shipments
(In Millions of Units)					
Northeast	0.32	0.29	0.17	0.12	0.03
North Central	0.49	0.43	0.33	0.10	0.06
South	1.05	0.90	0.73	0.17	0.15
West	0.63	0.54	0.40	0.14	0.09
Total U.S.	2.49	2.16	1.63	0.53	0.33

* Based on data developed at the U.S. Forestry Products Lab., Published in Plywood & Panel, April 1980, p.21.

At the same time, significant changes are taking place in the composition of wood structural composite board. These same authors, writing in Forest Industries, April 1980, stated "In the last two years, plans to build approximately 12 new plants to produce some type of wood structural composite board have been reported. Several of these announced plants are under construction or completed, and at least a dozen or more are reportedly being considered. More than half of these plants will produce waferboard."

"Waferboard is a structural board made of wood wafers cut to predetermined dimensions randomly distributed and bonded with phenolic adhesives." It is estimated that by 1981, 80 million pounds of adhesives on a solid basis will be used in waferboard and other types of particleboard bonding. Currently either solid or liquid phenolic resins are being used in these applications. Formaldehyde and phenol fumes and phenol formaldehyde powder dust,

when powders are used, are continuing to be a problem. It is almost certain there will be ever-increasing pressures on the industry to control these dusts and fumes. Recently it has been shown that isocyanate binders can be used to replace phenolic binders. The binder is essentially 100% polymeric isocyanate and bonds are formed by reaction with moisture in the wood as well as with hydroxyl groups in the cellulose, hemicellulose, lignon, and other products in the wood surface. In any event, according to industry sources, good chemical bonds are achieved at binder levels as low as 5%. Advantages claimed for isocyanate versus phenolic adhesives in bonding particleboard are shown in Table VIII.

Table VIII. Advantages Claimed for Isocyanate vs. Phenolic Adhesives in Bonding Particle Board

- No formaldehyde release
- Shorter press cycles
- Improved hydrolysis resistance
- Less binder required
- Ability to use higher moisture content furnish
- No residual binder odor
- Use of RF heating if desired
- Long binder storage life ≈6 months

Overall, it is claimed that all expenses considered urethane adhesives are cheaper to use than phenolic adhesives.

Obviously, this is an excellent potential opportunity for isocyanates. One of the obstacles that will have to be overcome is the resistance of the powder users to convert to liquids since different types of coating equipment are required. In any event, the isocyanate manufacturing companies are working diligently to prove the advantages of their product.

A second type of urethane adhesive is currently being introduced to the U.S. construction industry. The adhesive was originally developed in Japan. The system is two component. The isocyanate component is a modified polymeric MDI. The cross-linkable component contains water with water-soluble or water-emulsifiable resins. The adhesive produces strong, water-resistant bonds and has shown promise as a possible lower cost substitute for resorcinol formaldehyde resins in the adhesion of laminated beams. The product is now being used in Japan to bond wood and various other porous substrates at the rate of about 10 million pounds per year. The first U.S. application of the product has been the bonding of wood doors. The opportunities for products of this type should be excellent in view of the ever-increasing governmental pressures on solvents.

Transportation Industry

Urethane structural adhesives have been very popular for bonding of plastics to plastics and plastics to metal by the transportation industry. As an example, more than 90% of the bonds in Fords' experimental graphite car were urethane adhesives rather than rivets or welds. Urethane structural adhesives have been used by the transportation industry since 1969. It is estimated that 5 million pounds of urethane structural adhesives were used in the transportation industry in the United States in 1979. Some of the advantages of urethane adhesives as used by the transportation industry are shown in Table IX.

Table IX. Advantages of Urethane Adhesives
as Used by Transportation Industry

- Versatile
- Easy to use
- Produce good durable bonds
- Cost effective

Versatility is a valuable asset. Urethanes can be used to bond a variety of plastics to plastics and plastics to metal. They also can be used with little precleaning of surfaces to be bonded. They produce good durable bonds and overall they are cost effective. Some authorities are predicting growth of 300 to 400% in the next 5 years in the use of structural adhesives by the transportation industry. With the rush of the automobile companies to convert to plastics because of energy requirements, it is not unlikely that this will occur.

In summary, urethane binders and adhesives represented about 5% (120 million pounds) of total U.S. urethane use in 1979. Some of the key factors which should influence the use of urethane adhesives in the 80's are shown in Table X.

Table X. Key Factors Which Should Influence the
Use of Urethane Adhesives in the 80's

<u>Factors</u>	<u>Foun- dry</u>	<u>Construc- tion</u>	<u>Trans- portation</u>
Auto conversion from ferrous to aluminum castings	●		
Increased use of particleboard by construction industry		●	
Regulation of solvents		●	●
Control of worker exposure to hazardous chemicals	●	●	●
Auto conversion to more plastics			●
Increased cost of energy	●	●	●
Increased cost of labor	●	●	●
New Urethane Adhesive Technology	●	●	●

Automotive conversion from ferrous to aluminum castings, control of worker exposure to hazardous chemicals, the increased cost of energy, the increased cost of labor, and new urethane adhesive technology will all influence the use of urethane adhesives by the foundry industry. Adhesive use in the construction industry will be influenced by the increased use of particle board, the regulation of solvents, the control of worker exposure to hazardous chemicals, the increased cost of energy and labor, and the development of new urethane adhesive technology. The transportation industry should be affected by the regulation of solvents, the control of worker exposure to hazardous chemicals, the automotive conversion to more plastics, the increased cost of energy and labor, and the development of new technology. As a result, it is anticipated that the growth rate for urethane adhesives should be at least as good as the 8% predicted for specialty adhesives. Foundry binders led the growth in the 70's with 75 million pounds used in 1979 and growth should continue in this industry at an 8-10% rate for the next five years. Although the base of use in the construction and transportation industries is rather low at 5 million pounds each in 1979, the opportunities for growth are significant and growth rates of 20% or greater are expected over the next 5 years.

Certainly the opportunity for growth, at least in certain segments of the industry, is very good. More than likely there are areas of opportunity that have not yet been identified or discussed in this paper. One such area might be adhesives for the tire industry. It is known that some work has been done in this area. Certainly, there is a great opportunity for new technology.

RECEIVED June 1, 1981.

Metal Replacement Opportunities for Urethane Systems

SIDNEY H. METZGER, JR.

Polyurethane Division, Mobay Chemical Corporation, Pittsburgh, PA 15205

For the past fifteen years polyurethanes have played an important role in the automotive industry. Up until 1975 that role was confined primarily to flexible foam for automotive seating and semi-rigid filler foam for instrument panels. The combined market for these two applications came to over 400 M lbs. in 1979. In 1975, with the introduction of reaction injection molded (RIM) polyurethane elastomeric fascia for the Chevrolet Monza 2+2 and the corresponding Buick Skyhawk and Oldsmobile Starfire, a significant new automotive market opened up for polyurethanes. For the first time polyurethanes were making a major inroad into replacing external metal in automobiles. RIM elastomeric fascia were developed to meet damageability regulations. It was not long, however, before it became necessary to lower the weight of automobiles in order to reduce gasoline consumption. This drive to lower weight has spawned many new developments, the primary purpose of which is to replace steel for external body panels. Two of the most important of these developments are reinforced RIM (RRIM) and polyurethane-based SMC (PUR-SMC).

RIM Fascia

The impetus for developing the RIM process for producing elastomeric fascia parts was furnished by the requirements of the Motor Vehicle Safety Standard 215, which went into effect in 1973. This regulation required that the front and rear ends of automobiles had to withstand a 5 mph. impact without impairment of functional parts. A more stringent regulation, Standard 581, which came into effect for all bumpers made after September 1, 1979, required that the bumper withstand the 5 mph. impact with no more than a 3/8" dent in the bumper itself.

RIM polyurethane elastomers are a natural to meet the regulations. The process is highly suitable for producing complicated large, thin fascia to cover the entire front end

0097-6156/81/0172-0069\$05.00/0
© 1981 American Chemical Society

of an automobile. A Class A surface is obtained which can be easily painted. The painted elastomers will withstand a 5 mph. impact at -20 F without damage and retain sufficient stiffness at the elevated temperatures encountered in hot climates.

Although the initial impetus for RIM development was government regulations, it soon became apparent that the RIM technology offered significant advantages in styling and weight savings. The styling freedom offered is apparent in such automobiles as the Pontiac Firebird, Ford Mustang, Plymouth Horizon TC3 and Dodge Mirada, all of which have full front fascia. Additionally, the possibility exists of completely changing the looks of a car by simply restyling the front and rear RIM fascia covering.

All the above factors taken together - damageability resistance, styling freedom, and weight savings - have led to a very rapid rise in the RIM polyurethane fascia and bumper cover market. Table I historically summarizes the market from 1977 to 1980.

It should be noted that the 1980 figures do not take into consideration the deep recession in which the automotive industry presently finds itself. Actual numbers for 1980 are about 60-70% of those shown.

The future for RIM in the automotive industry looks very bright. The model year 1981 will see the introduction of polyurethane fascia on the Oldsmobile Cutlass A-special, the Pontiac Grand Prix, the New Chrysler Imperial Y-body, Plymouth and Dodge K-body and the Oldsmobile Omega X-body. It can be projected with some confidence that by 1985 at least 70% of all U.S. cars will incorporate some form of RIM polyurethane elastomer on the front and/or rear, representing a consumption of at least 100 M lbs. of raw material. The high volume use of RIM elastomers by the automotive industry has a significant impact on the polyurethane raw material market. The major ingredients are shown in Table II. Additionally, there are usually small amounts of blowing agent and a tin catalyst in the system.

At the present time most fascia are about 0.125" - 0.150" thick and are manufactured employing a RIM elastomer with a nominal room temperature flexural modulus of 172 MPa. But, the trend in the automotive industry is to go to thinner fascia produced with the RIM elastomers with 345 MPa nominal flexural modulus. In Table III are shown the average usage of the major components of both the 172 MPa and 345 MPa RIM systems. These average values are the best estimate based on known formulations currently being used in production.

Based on the formulations in Table III (neglecting blowing agent and catalyst) and the projected total RIM fascia market through 1985, Figure I can be drawn to show the impact of the RIM market on polyol, isocyanate (pure MDI)* and extender.

TABLE I
 RIM - BUMPERS AND FISCIA MARKET

Model Year	1977		1978		1979		1980(1)	
	lbs./ Car (000)	M Lbs	lbs./ Car (000)	M Lbs	lbs./ Car (000)	M Lbs	lbs./ Car (000)	M Lbs
Chevy Monza 2+2	30	2.34	30	40.0	30	1.2	30	40
Buick Skyhawk	30	0.78	30	24.6	30	0.74	30	24
Old's Starfire	14	0.28	14	17.4	-	0.24	-	-
Corvette	14	0.56	14	47.7	14	0.67	14	50
Pontiac Firebird	25	3.43	25	187.0	25	4.68	25	195
Chevrolet Camaro			25	272.0	25	6.80	25	265
Chevrolet Monte Carlo			18	388	18	6.98	18	388
Pontiac LeMans			20	136	20	2.72	20	150
Ford Mustang					21	6.93	21	330
Ford Capri					18	1.98	18	110
Dodge Omni 024					22	1.65	22	75
Plymouth Horizon TC3					22	1.65	22	75
Chrysler New Yorker					8	0.40	8	50
Pontiac Phoenix (80)					18	0.45	18	25
Mercury Cougar XR-7								150
Ford T-Bird					20	6.00	20	300
Dodge Mirada					21	1.16	21	55
Old's Sporty Omega					16	0.08	16	5
Chevy "B" Body					3	1.80	3	600
Total Units	302		1113		1777		2887	
Total Pounds	7.40		24.0		37.2		48.90	

(1) Does not take into consideration the recessionary period in 1980.

TABLE II

MAJOR INGREDIENTS OF RIM ELASTOMERIC
POLYURETHANES FOR FASCIA APPLICATIONS

FLEXIBLE BACKBONE	<ol style="list-style-type: none"> 1. Polyether polyols made with propylene oxide and "capped" with ethylene oxide. 2. Graft polyols made from grafting polyacrylonitrile onto the basic polyether (also ethylene oxide - "capped").
ISOCYANATE	<ol style="list-style-type: none"> 1. Quasi-prepolymer of MDI prepared by reacting small quantities of polyols with MDI. 2. Carbodiimide - modified MDI
EXTENDERS	<ol style="list-style-type: none"> 1. 1, 4 - butanediol 2. Ethylene glycol 3. Aromatic diamines

TABLE III

AVERAGE USAGE OF MAJOR COMPONENTS
OF RIM FASCIA POLYURETHANE SYSTEMS

Basis: 100 lbs. of final polymer

172 MPa flexural modulus

Avg. ratio = 68 isocyanate/100 polyol blend

Polyol = 50.3 lb.

Extender = 9.2

Isocyanate = 40.5

345 MPa flexural modulus

Avg. ratio = 73 isocyanate/100 polyol blend

Polyol = 45.9 lb.

Extender = 11.9

Isocyanate = 42.2

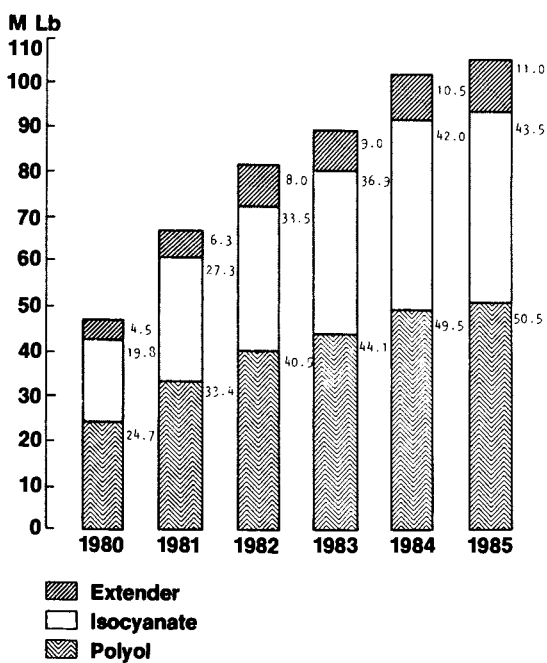


Figure 1. Projected RIM fascia market divided into major components.

*(Although an MDI quasi-prepolymer is used, for simplification it will be treated as pure MDI. Quasi-prepolymers are about 85-90% pure MDI. Carbodiimide - modified MDI's are prepared from pure MDI.) Beginning in 1981 the total RIM market was based on 9 M cars being produced through 1983, then 9.5 M cars in 1984 and 1985. Of the total RIM fascia systems, the calculated division of products is based on 10% of the 345 MPa system in 1980 and an incremental increase of 10% in the succeeding years. Average fascia weight was taken at 16 lbs. per car. These estimates provide a good picture of market impact on polyol, pure MDI and extender to be expected from the RIM fascia market for the U.S. automotive industry.

RRIM

The necessity to lower the weight of automobiles in order to meet the 1985 government CAFE requirements of 27.5 mpg. has spawned the development of high modulus RIM polyurethanes and reinforced RIM (RRIM) to replace metal in fenders, door panels, trunk lids, etc. The RRIM polyurethanes are well suited for the external body panel application where structural requirements are at a minimum. In addition to significantly lighter weight in comparison to steel, the RRIM panels eliminate corrosion problems and improve resistance to damage.

In cooperation with the automotive companies, physical properties and basic performance guidelines for RRIM body panels, such as fenders and door panels, are now being defined. The following general guidelines have been established to date:

1. Sufficient stiffness to resist air currents under driving conditions and to resist excessive deformation when leaned upon. Part support design will play a role.
2. Low enough coefficient of linear thermal expansion to allow practical mating with metal and to insure no change in shape during hot/cold cycles.
3. Ultimately, sufficient resistance to sag and distortion at on-line paint temperatures to allow on-line painting with the part mounted on the auto. At present shooting for 163°C, but future paint cure temperatures will come down. For initial fenders, automotive is willing to paint off-line.
4. Sufficient impact resistance to resist damage from minor parking lot collisions, to resist damage due to door opening dents and to be shatter-resistant at average impact speeds.
5. Appearance of painted parts to match exterior sheet metal and to retain gloss.

The primary purposes of adding reinforcement are to increase stiffness, improve sag resistance at 163°C and lower

the coefficient of linear thermal expansion. Knowing that increased stiffness lowers impact resistance, one of the questions that must be answered is what is the best compromise for exterior panel applications?

The properties and performance of reinforced RIM polyurethanes are to a large degree dependent upon the properties and performance of the basic high modulus RIM elastomers. The road to success is to develop a stiff polymer with relatively high impact resistance and a flat response of modulus and impact resistance to changes in temperature. This property combination normally results in low sag at 163°C and good low temperature impact properties. Systems presently being reinforced and evaluated for exterior automotive panels yield unfilled elastomers in a flex modulus range of approximately 345-1035 MPa at 25°C.

Studies of the effects of various types of fiber and particulate fillers have shown that milled glass fibers are in the near term the most suitable means to achieve part stiffness and the required reduction in the coefficient of linear thermal expansion to allow practical mating of RIM polyurethane panels with steel.

The effect of physical properties of RIM urethane systems through reinforcement with milled glass fibers and mica flakes has been studied in some detail⁽¹⁾. It was found that in the urethane systems investigated the effects of milled glass fiber or mica flake reinforcement on coefficient of linear thermal expansion, flexural modulus, percent elongation, and notched Izod impact are practically independent of the urethane matrix. Milled glass fibers orient during the molding, resulting in anisotropic behavior in the physical properties of the molded parts.

The best combination of physical properties for basic high modulus systems has been accomplished through the use of an amine extender in combination with a quasi-prepolymer modification of MDI. These systems are designated Bayflex® 110 types. The resultant physical properties of these RIM polymers are exceptional, and parts can be demolded in as little as 15 seconds with excellent green strength. Tables IV and V provide the physical properties both unfilled and filled of the amine-extended 345 and 483 MPa systems, respectively. The flat response of modulus to temperature (-30°C/65°C flex modulus factor), combined with the high elongation and excellent impact resistance of these systems, is carried over to the glass filled systems.

Where the part to be molded is a large thin part (0.100") with a very long flow path for the entering reacting system, the very fast amine-extended systems are sometimes too fast, making it difficult to properly fill the mold. For such parts a modified aromatic amine-extended system has been developed which is an excellent compromise between physical properties

TABLE IV

PHYSICAL PROPERTIES OF GLASS-FILLED BAYFLEX 110-50

	<u>Unfilled</u>	25% Glass ¹	
		<u> </u> ²	<u>⊥</u> ³
Specific gravity	1.04	1.28	1.28
Tensile Str., MPa	26.2	30.3	21.4
Elongation, %	280	45	100
Flexural Modulus, MPa			
RT	365	1626	826
- 30°C	827	2944	1543
+ 65°C	241	1280	554
- 30°C/+ 65°C Factor	3.4	2.3	2.8
Heat Sag, mm			
1 hr @ 250°F	5.1	0.5	1.5
1/2 hr @ 325°F	10.2	3	5.7
Hardness, Shore D	61	66	66
Impact Strength, Notched Izod, J/m	581	208	165
Tear Str., Die C, kN/m	110	142	130
CLTE, $\alpha \times 10^{-6}/^{\circ}\text{C}$	180	39	136

-
1. Mixture of P-117B and 731 OCF $\frac{1}{16}$ " milled glass fiber
 2. Parallel to flow direction
 3. Perpendicular to flow direction

TABLE V

BAYFLEX 110-70

	Unfilled	20% 1/16" OCF 731 Glass	
			⊥
Density, pcf.	64.3	79.6	79.6
Tensile, MPa	30.8	31.7	24.1
Elongation, %	220	30	140
Flexural Modulus, MPa			
RT	482	1685	847
- 30°C	849	3044	1926
+ 65°C	321	1122	593
- 30°/65° Flex Mod Factor	2.6	2.7	3.2
Heat Sag, mm			
1 hr @ 250°F	2.5	1.3	2.5
1/2 hr @ 325°F	9.1	2.8	7.6
Hardness, Shore D	63	75	75
Impact Strength, Notched Izod, J/m	463	133	101
Tear Str., Die C, kN/m	100	126	111
Coeff of Linear Thermal Expansion,			
x 10 ⁻⁶ /°C	147.0	46.7	131.7
x 10 ⁻⁶ /°F	81.7	25.9	73.2

and improved flowability. The basic physical properties of this system both unfilled and filled are shown in Table VI.

Many of the same basic raw materials shown in Table II for RIM fascia systems are also used in high modulus systems. Additionally, however, polyether polyols "filled" with dispersions of polyureas are used⁽²⁾. These are the so-called PHD polyols developed by Bayer AG, the PHD being an abbreviation for Polyharnstoff-Dispersion. These polyols provide the same "filler" effect as the graft polyols (Table II) for increasing the modulus of the polymer without increasing the amount of extender.

For most of the classical-extended types, a higher functionality MDI type isocyanate is used, the composition of which is a mix of polymeric and monomeric MDI.

At this point in time in the development of RRIM technology, it is difficult to predict the future market and the resultant impact on the polyurethane raw material market. RRIM polyurethanes will be able to compete for external body panels such as fenders, door panels, deck lids and possibly hoods. At the present time RRIM has the inside track for the material of choice for front fender applications. By the end of 1980 or the beginning of 1981, several thousand Oldsmobile Sport Omegas will be equipped with RRIM polyurethane front fenders for thorough in-the-field testing. Once these fenders are found suitable, it is quite likely that several car models will be equipped with front fenders manufactured from RRIM polyurethanes. First automobiles equipped with such fenders will probably be the 1983 model year, and a decent guess would be about 0.5 M cars. By the 1985 model year we could be seeing in the range of 2 M cars with RRIM polyurethane fenders. Each front fender should weigh approximately 5 lbs., which would add up to about 10 lbs. of RRIM per automobile. A breakdown of major component usage for both amine-extended and classical-extended systems is shown in Table VII (blowing agent and catalyst excluded). Based on the above assumptions, a bar graph (Figure 2) can be drawn showing the market potential of the major components of the RRIM system. For the estimate it was assumed that the market would be shared 50-50 by the amine-extended types and the classical-extended types. Again, for simplification all MDI types are treated as pure MDI.

RRIM fenders have an excellent chance of succeeding, the only question mark being timing. It is possible that because of the necessity to meet the 27.5 miles per gallon CAFE regulations, the scramble to lower weight, will be accelerated, which could lead to a lot more RRIM than the 20 M lbs. shown in 1985.

Based on the tremendous momentum that has built in the polyurethane industry for development of RRIM technology, it can be confidently expected that significant improvements

TABLE VI
 PHYSICAL PROPERTIES OF THE GLASS FILLED⁽¹⁾
 BAYFLEX 103/E-512 SYSTEM

Property	<u>Unfilled</u>	<u> </u>	<u>⊥</u>
Specific Gravity	1.04	1.17	1.17
Tensile Str., MPa	28.30	37.20	30.30
Ultimate Elongation, %	130.00	20.00	20.00
Flexural Modulus, MPa			
RT	646.00	1634.00	929.00
-30°C	1234.00	2708.00	1672.00
+65°C	413.00	1111.00	539.00
Flexural Modulus Factor (-30°/65°C)	3.00	2.44	3.10
Heat Sag, mm			
1 hr @ 250°F	4.00	0.50	1.70
1/2 hr @ 325°F	14.00	2.20	4.80
Notched Izod Impact	352.00	164.00	157.00
Die C Tear Str., kN/m	122.00	108.00	97.00
Shore D Hardness	67.00	70.00	70.00
CLTE, $\alpha \times 10^{-6}/^{\circ}\text{C}$			
20 \longrightarrow -40°	--	43.00	89.30
20 \longrightarrow 66°	--	32.70	85.20
20 \longrightarrow 121°	--	32.20	89.40

1. 20% 1/16" 731 milled glass fibers in the final polymer

TABLE VII
 AVERAGE USAGE OF MAJOR COMPONENTS
 OF HIGH MODULUS RIM ELASTOMERS

Basis:	100 lb. Final Polymer	100 lb. Final Polymer with 25% glass
<u>Amine-extender types</u>		
Polyol, lb.	48.4	36.3
Extender, lb.	14.5	10.9
MDI-type isocyanate, lb.	37.1	27.8
<u>Classical-extended types</u>		
Polyol, lb.	38.3	28.7
Extender, lb.	10.1	7.6
Higher Functionality MDI type	51.6	38.7

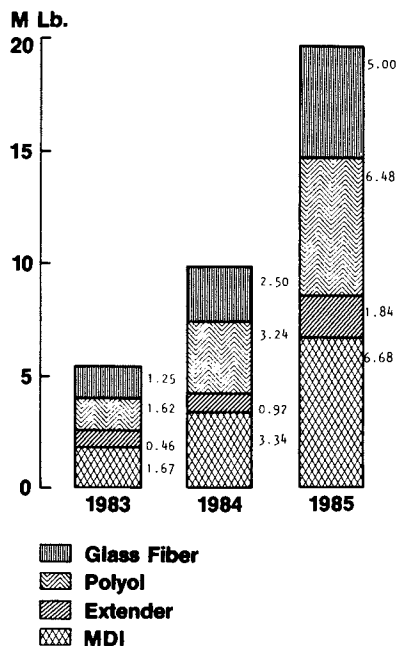


Figure 2. Projected RRIM market for automotive front fenders divided into major components. Basis: RRIM polyurethane containing 25% glass fiber; weight of each fender = 5 lbs.

in the overall technology, both in the polymer properties and processing, will be effected at a very rapid pace. With such improvements RRIM polyurethanes will become more and more capable of competing with steel in body panels, and we can expect accelerated testing by the automotive industry of RRIM door panels and trunk lids, in addition to fenders.

Polyurethane SMC (PUR-SMC)

One of the new technologies that has been developed as a result of the large market potential for the replacement of steel by lighter weight plastics is a PUR-SMC (Baypreg) developed by Bayer, AG in Leverkusen, West Germany. In this new development, polyurethane chemistry has been adapted to the existing processing technology of unsaturated polyester SMC (UP-SMC). The basic design of the equipment used in the manufacture of resin mats can remain unchanged; only the metering and mixing configurations for the unsaturated polyester chemicals must be changed to accommodate the polyurethane technology. Compression molding of the mats is accomplished by the hot press process in the same steel tools as used for UP-SMC. Good demoldability is possible without using any external mold release. One distinct advantage of PUR-SMC over UP-SMC is that the resin mat requires no maturation period after manufacture and is stable for many days at room temperature.

The properties of PUR-SMC lie between those of RRIM and UP-SMC (Table VIII). As can be seen, the properties of this particular PUR-SMC lie closer to UP-SMC than RRIM. The advantages of PUR-SMC over UP-SMC are more elasticity, higher elongation and improved impact resistance.

PUR-SMC is only in its infancy. One can be sure that, given the tremendous versatility of polyurethane chemistry, there will be developed a variety of PUR-SMC products. The material represented by the physical properties in Table VIII has been used in Europe to produce prototype motorcycle fenders and prototype front and rear bumpers for the Porsche 924. The improved impact over UP-SMC was clearly shown through comparison of the impact resistance of the Porsche bumpers made with both PUR-SMC and UP-SMC.

The development of PUR-SMC technology will lead to further possibilities for the replacement of steel in automobiles, as well as the replacement of some UP-SMC use where better impact resistance is desired. As more elastic, lower modulus PUR-SMC's are developed and higher and higher modulus RIM systems are developed, competition for the same application can be foreseen, especially external body panels for automobiles. It is too early for market predictions for PUR-SMC, but with successful developments a meaningful penetration into replacement for steel in automobiles can be foreseen by the late 1980's.

TABLE VIII
 PHYSICAL PROPERTIES OF PU-SMC (BAYPREG)
 COMPARED TO COMPETITIVE MATERIALS

Property	<u>UP-SMC</u> (1)	<u>PU-SMC</u> (1)	<u>RRIM</u> (2)	<u>Steel</u>	<u>Alu.</u>
Specific Gravity, g/cc	1.70	1.70	1.25	7.28	2.75
Flexural E Modulus, MPa	10,000- 15,000	5,000	2,300	210,000	74,000
Elongation, %	2	6	23	-	-
Tensile, MPa	120	120	48	320	230
Coeff, Linear Therm. Expansion x 10 ⁻⁶ , mm/mm/°C	30	20	35 ⁽³⁾	10-12	24
Shrinkage, %	0.01	0.05	0.15	-	-
Impact Strength at -30°C, KJ/m ²	80	100	-	-	-

-
1. 30% glass
 2. 25% glass
 3. Measured parallel to flow

Market Impact

How will this new market of polyurethane replacement for steel in automobiles impact the total supply position of the polyurethane industry for monomeric MDI and polyethers? Table IX shows the MDI supply/demand picture through 1985, where MDI here is the total of polymeric and monomeric MDI.

Based on the numbers in Figures 1 and 2, by 1985 RIM and RRIM will require approximately 50 M lbs. of monomeric MDI, which is about one-third of the monomeric MDI supply in 1985 (Table IX; based on 20-25% of 85% nameplate capacity, excluding ARCO capacity, = 137-171 M lbs. monomeric MDI). This will leave about 100 M lbs. of monomeric MDI for cast elastomers, thermoplastic polyurethanes, shoe soles, semi-rigid foams, and some adhesives and sealants, a monomeric MDI supply which should be more than sufficient for these applications. As RRIM grows, a need for capacity expansion can be seen in the late 1980's. No effects on the market will be seen from PUR-SMC until after 1985, and at the present time meaningful projections are impossible.

Table X is a summary of the polyurethane industry polyol supply. With a nameplate capacity of 2.5 billion lbs. and today's market hovering around 1.5 billion lbs., no supply problem is anticipated through 1985. The combined RIM and RRIM 1985 polyol market of about 57 M lbs. hardly makes a dent in the tremendous industry capacity.

Overall, the polyurethane raw material supply capacity appears to be adequate to meet the needs of an expanded RIM and RRIM market for replacement of steel in automobiles, at least through 1985. Should it become apparent that market demands will outstrip monomeric MDI supply capability in the late 1980's, then undoubtedly expansions of capacity will be forthcoming.

By 1985, it has been predicted that interior applications for plastics will amount to 108 lb./car and exterior applications for plastics, to 154 lb./car, giving a total of 262 lb./car (excluding under the hood applications) (3). Of the exterior applications it can be expected that the combined RIM and RRIM markets for steel replacement will amount to approximately 7% of the total and 12% of the exterior applications.

Non-Automotive Applications

Up to now practically all development and marketing efforts have been directed toward automotive applications. But, the spin-off into non-automotive applications could be equally as important. How fast this spin-off occurs is a function of

TABLE IX
MDI SUPPLY/DEMAND

<u>Producer Capacity</u>	<u>1980</u>	<u>1981</u>	<u>1982</u>	<u>1983</u>	<u>1984</u>	<u>1985</u>
Mobay	200	250	300	—————>		
Upjohn	250	280	—————>			
Rubicon	100	—————>				
BASF	-	-	100	150	—————>	
ARCO	<u>-</u>	<u>-</u>	<u>50</u>	<u>150</u>	—————>	
Total ⁽¹⁾	550	630	830	980	980	980
85% of Nameplate	468	535	705	833	833	833
90% of Nameplate	495	567	747	882	882	882
<u>Demand</u>						
Domestic	390	430	490	560	620	680
Export	<u>90</u>	<u>90</u>	<u>60</u>	<u>40</u>	<u>40</u>	<u>40</u>
Total	480	520	550	600	660	720
Excess Capacity/ Shortfall-at 85% of Nameplate	(12)	15	55	233	173	113
-at 90% of Nameplate	15	47	197	282	222	162

(1) Includes both polymeric and monomeric MDI. The monomeric MDI equals 20-25% of total MDI production (excluding ARCO who will not be producing monomeric MDI).

TABLE X
INDUSTRY POLYOL SUPPLY

<u>Producer</u>	<u>Nameplate Capacity (\bar{M} lb.)</u>
BASF Wyandotte	425
E. R. Carpenter	200
Dow Chemical	475
Mobay	250
Olin Corporation	250
Jefferson Chemical	100
Union Carbide	600
Other	<u>195</u>
TOTAL	2,495

how much effort industry can and is willing to direct toward the non-automotive market.

Most of the potential applications foreseen will utilize either high modulus RIM elastomers or RRIM elastomers. Some present applications utilizing high modulus RIM are:

1. Motorcycle boots
2. Ski boots
3. Snowmobile belly pans
4. Sanitary troughs for farm use
5. Golf carts

Potential applications are:

1. Agricultural machinery
2. Farm equipment such as watering and feed troughs, hoppers, grain dispensers and animal sanitary drainage systems
3. Abrasion resistant liners for coal chutes and grain hoppers
4. Lawn and garden equipment, including tractor parts, utility carts, spreaders and lawn mower housings.

The development of non-automotive RIM and RRIM applications will be slow unless considerably more effort is expended in this direction by the polyurethane industry. It has been predicted that by 1983 the non-automotive RIM and RRIM polyurethane elastomers will be approximately $6 \bar{M}$ lbs. (4).

Literature Cited

1. McGregor, D. J.; Parker, R. A. Controlling the Physical Properties of RIM Urethanes with Non-Organic Reinforcement, Paper No. 790166, Society of Automotive Engineers Congress and Exposition, Detroit, Michigan, Feb. 26 - Mar. 2, 1979.
2. Phillips, B. A.; Taylor, R. P. PHD Polyols for RIM Applications, paper presented at Rubber Division, American Chemical Society Meeting, Atlanta, Georgia, Mar. 27-30, 1979.
3. "Detroit's Weighting Game", Plastics World, May 1977, p. 38.
4. "New RIM Technology for the Non-Automotive User", Modern Plastics, Mar. 1980, p. 50.

RECEIVED June 1, 1981.

Health Considerations for Isocyanates

RICHARD HENDERSON

Health Sciences and Toxicologic Research, Olin Corporation, New Haven, CT 06511

Isocyanates were discovered by Wurtz in 1849 and their uses in polyurethane began in 1937. The isocyanates and abbreviations that will be used in this presentation are shown in Table I.

Abbreviations of Isocyanates

Table I

Toluene diisocyanate	TDI
Diphenylmethane diisocyanate	MDI
Hexamethylene diisocyanate	HDI, HMDI
Napthalene diisocyanate	NDI
Isophorene diisocyanate	IPDI
Dicyclohexylethane 4,4-diisocyanate	----

There were 650,000 metric tons of TDI and 450,000 metric tons of MDI produced in 1978, not including production in countries having central economic planning (Table II). These two isocyanates constitute the largest volume; the other isocyanates were produced in much smaller quantities.

Production of Isocyanates - 1978

(1000 metric tons)

Table II

TDI	650
MDI	450

Polyurethanes are the major products in which isocyanates are used. The percent of total polyurethanes in different uses is given in Table III.

0097-6156/81/0172-0087\$05.00/0
© 1981 American Chemical Society

Uses of PolyurethanesTable III

<u>Use</u>	<u>Percent</u>
Furniture and mattresses	40
Automotive	20
Building construction	11
Refrigeration	6
Shoes	4
Textiles	6
Coatings	5
Other	8

It is estimated that there are more than 200,000 workers engaged in the production and uses of isocyanates. The isocyanates are used for their reactivity as crosslinking agents. Considering their reactivity, it is a tribute to the industry that research has enabled the establishment of safe work practices and safe levels of exposure.

Even though uses of isocyanates in polyurethanes started in 1937, it was not until 1951 that the first occupational health problems associated with isocyanates appeared in the medical literature. There have been many more cases of effects of excessive exposure to isocyanates reported in the 1950's than in the 1970's. Greater care is now taken to explain potential adverse effects from excessive exposure and to adequately control exposures. Fuchs *et al.* (1) published observations on an asthmatic syndrome in seven out of nine persons exposed to TDI. In 1953, Reinl (2) reported cases of respiratory problems in 17 workers exposed to TDI and/or other isocyanates; 13 of these cases were severe and death of one was attributed to occupational exposures.

There were many other reports (3-10) published in the 1950's of similar cases of occupational health problems, primarily respiratory, in workers exposed to isocyanates in manufacture of polyurethane foams and polyisocyanate-based lacquers and glues. One additional fatality was reported (6). Elkins (11) in 1962 reviewed the published occupational health problems attributed to TDI and identified 222 cases in the literature through 1960. The concentrations of isocyanates involved in most of the cases and the possible exposures to other respiratory irritants were not usually reliably determined. It is possible that the concentrations of isocyanates to which workers may have been exposed occasionally in the 1950's and early 1960's may have been above presently accepted allowable limits.

Examples of concentrations to which workers were reportedly exposed are shown in Table IV.

Reported Concentrations of IsocyanatesTable IV

<u>Type of Operation</u>	<u>TDI Concentration (ug/m³)</u>	<u>Reference</u>
Spray	6400	Gandevia (12)
TDI distillation	140	Williamson (13)
TDI production	14-40*	Weill <u>et al.</u> (15)

*Depending on job category

In evaluating any data on concentrations to which persons may have been exposed, it must be remembered that analytical methods require time for sampling; and the longer the sampling time, the greater the possibility of short term peak concentrations being averaged out and missed. Such short term peak concentrations may be of great significance in terms of respiratory irritant effects.

Bunge et al. (14) found a mean concentration of 0.0197 ppm of different isocyanates (TDI, MDI, and NDI) in the work environment of a polyurethane plastics laboratory. The concentrations of the different isocyanates are not specified in their paper.

The allowable exposure limits (TLV) for TDI in major industrial countries was 0.14 mg/m³ at the time of the studies referred to above.

The fact that these concentrations have been measured does not mean that occupational exposures occur; persons may use respiratory protection equipped to prevent exposure. All persons who have excessive occupational exposure to isocyanates may experience primary irritant effects in the respiratory tract depending on the extent of excessive exposure. Brief accidental exposures to concentrations of isocyanates tenfold or more above the TLV may cause short term respiratory irritation with recovery 24-48 hours following cessation of exposure. Continuing repeated workday exposures several-fold higher than the TLV can cause chronic respiratory irritation. All individuals will not suffer the same degree of respiratory irritation from excessive exposures due to individual biochemical and physiological differences. Studies have shown that on the order of five percent of persons who have had an occupational exposure to TDI develop a bronchial asthmatic type of response to subsequent exposures that are below concentrations causing any detectable primary irritation.

Persons who have developed a bronchial asthmatic reactivity to one isocyanate may show bronchial asthmatic reactivity to other isocyanates according to studies reported by O'Brien et al. (16).

The mechanism for the development of the bronchial asthmatic reactivity from exposure to isocyanates has not been clearly defined, although there has been and continues to be considerable research on this effect. Bruchner (17), Scheel (18), Nava et

al. (19), Butcher *et al.* (20), Taylor (21), Porter *et al.* (22), Karol *et al.* (23), are among the research workers who have investigated the mechanism of bronchial asthmatic response. Only in cases that have developed an extreme sensitivity as demonstrated by bronchial asthmatic response to a few minutes exposure to concentrations of isocyanate on the order of 25 ug/m^3 has there been a demonstration of a circulating antibody that will react with a human serum albumin-toluene monoisocyanate antigen. Research is continuing to define the mechanism or mechanisms of the bronchial asthmatic response that some persons develop from exposures to isocyanates.

Of particular interest is one case reported by Butcher (24) that appears to suggest that the bronchial asthmatic reactivity to TDI may be reversible. Original challenge exposure of 25 ug/m^3 of TDI for 15 minutes to confirm clinically observed reactivity resulted in significant decline in lung function. After the person had been removed from occupational exposure for six months, there was no decline in lung function following a controlled challenge exposure.

The primary respiratory irritancy and bronchial asthmatic reactivity discussed above are generally accepted as occupational health problems that can occur from excessive exposure to isocyanates either as vapor or as inhalable particles in workplace air. If spilled or splashed on the skin or in the eyes, the isocyanates can cause irritation.

Nava *et al.* (19) have reported a case of eczematous dermatitis from TDI. Karol *et al.* (23) reported finding tolyl-specific antibodies in serum of two persons who displayed skin reactions when exposed to TDI. Rothe (25) described 12 cases of contact eczema in workers exposed to MDI or partially polymerized MDI and four similar cases in workers exposed to IPDI.

As with many other chemicals, there have been some reports (26-29) of psychological problems in workers having potential exposure to isocyanates and other chemicals in polyurethane production operations. It is not possible to determine a cause-effect relationship to a particular chemical exposure nor a level of exposure from the published reports. These reports on psychological problems are mentioned here for completeness in reviewing the literature on occupational health aspects in the uses of isocyanates and not because great importance is placed on this aspect.

The present Occupational Safety and Health Administration legal limit for exposure to TDI and MDI is 0.02 ppm (0.14 mg/m^3 for TDI and 0.2 mg/m^3 for MDI). These are ceiling values. In order to operate within this ceiling limit, the time-weighted average concentration will be below 0.02 ppm. Thus, operations that are meeting the present legal limit probably would have little or no difficulty meeting the 0.005 ppm 10 hour time-weighted average limit proposed by the National Institute for Occupational Safety and Health.

The five year prospective study of employees in a TDI plant conducted by Weill et al. (15) included preplacement and periodic respiratory function and immunologic evaluations as well as measurements of exposures using continuous personnel monitors. The cost of this study was over \$750,000. A two-year inhalation carcinogenicity study of TDI using rats and mice is costing over \$400,000. Individual producers of TDI have done experimental animal toxicology and employee health evaluations.

In summary, the major potential occupational health problem from excessive exposure to isocyanates is primary respiratory irritation. A fraction of workers exposed may develop a bronchial asthmatic reaction to isocyanates and there appears to be some cross reactivity. The most extensive study, including preexposure baseline respiratory function measurements, has provided data indicating that keeping exposures to TDI below 0.02 ppm (0.14 ug/m³) appears to prevent decrement in respiratory function. There are less data on exposures and respiratory function of workers using other isocyanates. Isocyanates such as MDI are less volatile than TDI. There is less potential for exposure to vapors of the lower volatility isocyanates, but exposures to vapor and to particulates can occur and exposures to all isocyanates do need to be controlled in order to protect workers.

Literature Cited

1. Fuchs, S.; Valade, P. Clinical and experimental study of several cases of intoxication by Desmodur T (toluene diisocyanate 1-2-4 and 1-2-6). Arch Mal Prof, 1951, 12, 191-96.
2. Reinl, W. Diseases in the manufacture of polyurethane based plastics. Zentralbl Arbeitsmed Arbeitsschutz, 1953, 3, 102-07.
3. Schur, E. Injury from Desmodur lacquers--irritating gas or allergy? Med Klin, 1959, 54, 168-70.
4. Reinl, W. Occupational asthma and similar illnesses and their insurance coverage. Zentralbl Arbeitsmed Arbeitsschutz, 1955, 5, 33-37.
5. Ganz, H.; Mager, E. Injuries to health by Molotpren foam material. Zentralbl Arbeitsmed Arbeitsschutz, 1954, 4, 42-44.
6. Schuermann, D. Injuries to health caused by modern varnishes and foam materials. Dtsch Med Wochenschr, 1955, 80, 1661-63.
7. Woodbury, J. W. Asthmatic syndrome following exposure to tolylene diisocyanate. Ind Med Surg, 1956, 25, 540-43.
8. Johnstone, R. T. Toluene 2,4-diisocyanate--Clinical features. Ind Med Surg, 1957, 26, 33-34.
9. Sands, F. W.; Boffardi, G.; James, K. E.; Lundy, W.; Walsh, W. S. Toluene diisocyanate--engineering and medical control of exposures in polyurethane foam manufacturing. Am Ind Hyg Assoc J, 1957, 18, 331-34.
10. Walworth, H. T.; Virchow, W. E. Industrial hygiene experiences with toluene diisocyanate. Am Ind Hyg Assoc J, 1959, 20, 205-10.
11. Etkins, H. B.; McCarl, G. W.; Brugsch, H. G.; Fahy, J. P.

- Massachusetts experience with toluene diisocyanate. Am Ind Hyg Assoc J. 23:265-72, 1962.
12. Gandevia, G. Studies of ventilatory capacity and histamine response during exposure to isocyanate vapour in polyurethane foam manufacture. Br J Ind Med 20:204-09, 1963.
13. Williamson, K. S. Studies of diisocyanate workers (1). Trans Assoc Ind Med Off 14:81-88, 1964.
14. Bunge, W., Ehrlicher, H., Kimmerle, G. Medical aspects of work with surface coating systems using the spraying technique. Z Arbeitsmed Arbeitsschutz Prophylaxe 4 (Special Ed.): 1-46, 1977.
15. Weill, H., Salvaggio, J., Ziskind, M., Jones, R. N., Diem, J., Butcher, B., Carr, J., Glindmeyer, H., Dharmarajan, V. Annual Report--Respiratory and Immunologic Evaluation of Isocyanate Exposure in a New Manufacturing Plant. Unpublished report submitted to NIOSH by Tulane University School of Medicine, New Orleans, LA, April 1978, 27 pp.
16. Weill, H., Diem, J. E., Dharmarajan, V., Glindmeyer, H., Jones, R., Carr, J., O'Neil, C., Salvaggio, J. Final Report--Respiratory and Immunologic Evaluation of Isocyanate Exposure in a New Manufacturing Plant. Unpublished report submitted to NIOSH by Tulane University School of Medicine, New Orleans, LA, September, 1979., 52 pp.
17. O'Brien, I. M., Harries, M. G., Burge, P. S., Pepys, J., Diisocyanate induced asthma--reactions to TDI, MDI, HDI, and histamine. Clin All 1979, Vol. 9, pp. 1-6.
18. Bruckner, H. D., Avery, S. B., Stetson, D. M., Dodson, V. N., Ronayne, J. J. Clinical and immunologic appraisal of workers exposed to isocyanates. Arch Environ Health 16:619-25, 1968.
19. Scheel, L. D., Killens, R., Josephson, A. Immunochemical aspects of toluene diisocyanate (TDI) toxicity. Am Ind Hyg Assoc J. 25:179-84, 1964.
20. Nava, C., Arbosti, G., Briatico-Vangosa, G., Cirila, A. M., Marchisio, M., Zedda, S. Pathology produced by isocyanates--methods of immunological investigation. Ric Clin Lab 5:135-45, 1975.
21. Butcher, B. T., Savaggio, J. E., Weill, H., Ziskind, M. M. Toluene diisocyanate (TDI) pulmonary disease--immunologic and inhalation challenge studies. J Allergy Clin Immunol 58:89-100, 1976.
22. Taylor, G. Immune responses to tolylene diisocyanate (TDI) exposure in man. Proc R Soc Med 63:379-80, 1970.
23. Porter, C. V., Higgins, R. L., Scheel, L. D. A retrospective study of physiologic and immunologic changes in workers exposed to toluene diisocyanate. Am Ind Hyg Assoc J 36:159-68, 1975.
24. Karol, M. H., Ioset, H. H., Alarie, Y. C. Toly-specific IgE antibodies in workers with hypersensitivity to toluene diisocyanate. Am Ind Hyg Assoc J 39:454-58, 1978.

25. Butcher, B. Six-Month Progress Report to International Isocyanate Institute: Study of TDI Asthma. June 30, 1979.
26. Rothe, A. Occupational skin diseases caused by polyurethane chemicals. Derufs-Dermatosen 24:7-24, 1976.
27. Mastromatteo, E. Recent occupational health experiences in Ontario. J Occup Med 7:502-11, 1965.
28. Le Quesne, P. M., Axford, A. T., McKerrow, C. B., Jones, A. P. Neurological complications after a single severe exposure to toluene diisocyanate. Br J Ind Med 33:73-78, 1976.
29. Axford, A. T., McKerrow, C. B., Jones, A. P., Le Quesne, P. M. Accidental exposure to isocyanate fumes in a group of firement. Br J Ind Med 3:65-71, 1976.
30. Filatova, V. S., Babochkina, M. S., Jurando, T. B. Problems of industrial hygiene and the state of health of workers in diisocyanate production plants. Gig Tr Prof Zabol 6:25-31, 1962.

RECEIVED June 1, 1981.

Fluorocarbons—Energy Extenders of Polyurethane Foams

DAVID C. FARISS and FREDERICK E. HENOCH

Petrochemicals Department—Freon Products Laboratory,
E. I. du Pont De Nemours & Co., Inc., Wilmington, DE 19898

"Energy efficiency" has very quickly become more than just buzz words in the United States. Americans aren't just talking about it anymore. The nation is doing something about it daily at home, at work and at play.

For many, energy efficiency and energy conservation are a recent phenomenon. But that is not the case for the polyurethane business. This industry has been conscious of the nation's need for energy conservation, and has been doing something about it, for far longer than the average citizen has been aware.

The key work that gets business going and keeps it going is savings: in heat loss or heat gain; in weight; in fabrication cost; in product lifetimes; in usable space; and savings in labor.

Our standard of living and the cost of it is dependent to a significant extent on the availability of flexible and rigid polyurethane foams.

What kind of stakes are involved? A 1979 "Outlook" annual market survey by the Upjohn Company indicates that the total United States market for polyurethanes would be 2,444 million pounds including 1,450 million pounds for flexible foam, 615 million for rigid foam and 379 million for elastomers, coatings and adhesives.

A Rand Corporation research study for the Environmental Protection Agency ("Economic Implications of Regulating CFC Emissions from Non-Aerosol Applications" R-2524-EPA) estimated that in 1979 some 590 million pounds of flexible polyurethane foam and 489 million pounds of rigid polyurethane foam were produced using chlorofluorocarbons (CFCs) as the blowing agents. Rand estimated that about 100 million pounds of CFC was used to produce these foams, including 40 million pounds for flexible foam and 60 million pounds for rigid foams.

Before fluorocarbon compounds were discovered by Thomas Midgley in 1928 and introduced by Du Pont to the refrigeration market in the 1930's, refrigerants then in use were either quite

0097-6156/81/0172-0095\$05.00/0
© 1981 American Chemical Society

toxic and/or flammable. Fluorocarbons found a very receptive market, because of their high efficiency, low toxicity and non-flammability. In the ensuing years, fluorocarbons have found a growing number of applications because of their unique combination of physical properties and attractive safety features.

In many applications, fluorocarbons are used because of their superior thermodynamic properties. Such is the case with polyurethane and polystyrene insulating foams. Two main fluorocarbons used for foams are chlorofluorocarbon 11 and chlorofluorocarbon 12.

CFC 11 and CFC 12. These play an important, energy-efficient role in the formation of the uniform cellular structure of rigid insulating foam. But this advantage is small compared with the insulating value of the fluorocarbon which is trapped in the interior cells of the foam. Polyurethane and extruded polystyrene foams have "R" values two to three times higher than loose fiberglass and about twice as high as fiberglass batts. Even if rigid insulation foams could somehow be made with air or carbon dioxide in the cells, insulation effectiveness would be reduced by more than half. Fluorocarbons are the difference in making plastic foams the best energy savers in the insulation marketplace.

Thermally efficient foam plastics are essential in the design and operation of large and small refrigerators, freezers, coolers and transportation equipment. Without the efficiency of fluorocarbon-containing foams, internal space and capacity would be lost. Also bulkier, more energy-inefficient refrigeration units would be needed. Large industrial storage tanks such as fuel oil and liquid natural gas tanks rely on sprayed-on rigid polyurethane foams which can be blown only with CFCs. There is no other practical way known today to insulate these tanks.

Not only are rigid polyurethane insulating foams energy efficient, they are durable as well. Du Pont recently completed an accelerated aging study to determine the length of time that the fluorocarbon remains in the insulation. The study found that one-half of the fluorocarbon remained in a one-inch thick piece of rigid polyurethane insulation after more than 80 years, and the half-life of fluorocarbon in a two-inch slab of polystyrene insulation is estimated at 75 years.

There also are numerous advantages chlorofluorocarbons offer structural plastic designers and molders. As the transportation and construction industries become more energy-minded, more of those structural components are being shifted to plastic from metal. The optimal material of construction frequently is cellular plastics. Reduced weight and lower costs of most cellular plastic parts are possible without sacrificing the necessary strength and other attributes.

Furthermore, the use of chlorofluorocarbons in injection molding and reaction injection molding has resulted in more uniform cellular structure, reduced weight per unit, better

surface finish, fewer rejects and, in some cases, shorter molding cycle times. Molding technology is on the move to meet the new market needs, and chlorofluorocarbon blowing agents could be an important part of the new process innovation.

However, there are clouds on the regulatory horizon. There are individuals and institutions who sincerely believe that valid reasons exist to establish government regulations to limit or even eliminate many CFC blown plastic foam products. Since 1974, CFCs and particularly CFC 11 and CFC 12 have been under scrutiny by scientists, environmentalists, and government agencies because of a theory -- based on a computer model -- that these compounds threaten to deplete the ozone layer in the stratosphere.

The international scientific community is far from unanimous in its interpretation of the theory's validity. Many of the so-called "real world" atmospheric measurements remain in conflict with the predictions of the depletion theory. In addition, analysis of actual ozone measurements taken during the last 20 years has shown no depletion of the ozone layer.

Government and industry are funding research to determine conclusively whether ozone depletion actually has -- or even will -- occur. These programs include measurement of the stability of CFCs in the atmosphere, investigation of the chemical reactions which may be occurring in the atmosphere, and further analysis of actual ozone measurements.

At this time, six years after the allegations were first raised, the threat of any ozone depletion is as theoretical as the depletion theory itself.

C. N. Masten, director of Du Pont's FREON® Products Division, noted recently in a public statement:

"It makes scientific and economic sense to postpone regulatory decisions until there is an international resolution of the critical scientific uncertainties in the ozone depletion theory. Even if the theory should eventually be proved correct, a five-year delay in further U.S. regulatory action to allow needed scientific research would result only in ozone depletion of less than one-third of one percent."

The conclusion is that the risk of waiting is minimal, but the risk of damage from precipitous federal regulatory action could be enormous.

Nevertheless, the Environmental Protection Agency recently announced that it plans to propose limiting U.S. production of CFCs for nonaerosol uses. However, no other major industrialized nation followed the EPA's lead in banning CFCs as aerosol propellants in 1978. Since ozone depletion, should it occur, would be a global problem, it would seem to make sense to obtain international agreement rather than rushing off to establish another regulatory action which would place added economic burden on the U.S. industry and consumer.

A recent study conducted by Battelle Laboratories in Columbus, Ohio, ("Energy Consequences of Chlorofluorocarbon Regulation") concluded that a total ban of CFCs would cause a net energy penalty of 9.5 billion gallons of fuel equivalent in the tenth year of the ban and a cumulative total of 49.8 billion gallons for the first decade following the ban. The study shows that nine billion gallons of fuel will:

- Fuel 12 million average cars for one year (about 10% of all cars on the road in the United States).
- Supply enough energy for 11 cities the size of Toledo (population about 500,000) for one year.
- Save 18 times the fuel value that "gasohol" is expected to provide by 1985.
- Provide the energy equivalent to 45% of current annual oil production of Alaska's North Slope, 38% of oil imports from Iran in 1978 or 9.5% of total U.S. crude oil imports in 1978.

The conclusion is startling: a ban on the use of CFCs would seriously aggravate already serious energy problems in the U.S.A.

The Battelle study also shows how much energy could be wasted if CFCs were not available for use in insulating foams:

ENERGY PENALTIES ASSOCIATED WITH THE ELIMINATION OF
CFCs IN INSULATING FOAMS

(Millions of gallons of fuel equivalent)

	<u>1981</u>	<u>1990</u>	<u>Decade</u>
Commercial Construction	106	1565	7010
Residential Construction	8	126	610
Industrial Construction	4	52	260
Refrigeration	68	833	4420
Tanks & Pipes	30	393	2040
Transportation Equipment	<u>1</u>	<u>10</u>	<u>60</u>
TOTAL	217	2979	14403

CFCs truly are extenders that provide the ultimate in energy efficiency of urethane foams. Their availability at reasonable cost in the future may depend upon how effectively Americans respond to the threat of proposed regulations by our government.

There is a potential conflict between national needs for energy conservation and an environmental concern based on an unverified theory. The energy-conserving contributions of CFC-containing plastic foam insulation are consistent with the goals of the U.S. Department of Energy. The Environmental Protection Agency has served advance notice of its intention to limit CFC production to save the environment. We all must carefully watch for the resolution of this significant conflict in the near future.

RECEIVED June 1, 1981.

Future Impact of Reduced Fire Hazards on Urethane Foam

JOHN G. SCHUHMAN

Urethane Chemicals TS&D, The Dow Chemical Company, Freeport, TX 77541

Today science is judged equally for its perceived technical merit and social effect. In reality, however, negative effects are easily measured while positive effects normally are not noted or recordable. For example, society has begun to label urethane foams as a fire hazard. Proper management of this fire issue may be one of the most influential factors in future urethane technology and market opportunities.

Variables that must be considered in assessing fire risk in upholstered furnishings will be examined in this paper. Standards that have been established will be summarized and future standards and testing will be discussed.

Background

Entering the '80s the fire problem is well defined. We know the extent to which furniture and sleeping products are involved in fires, but have not been able to specifically identify the role of urethane foam involvement. Unmodified urethane foam can be ignited by open flames and burn rapidly. Modified urethane foams, however, are more ignition resistant. Most importantly, overall fire risk involves three important elements: 1) the material ignited, 2) occupancy, and 3) the ignition source. Variance in these three interrelated factors will influence potential fire risk (Figure 1).

Apart from these technical considerations, of course, fire risk is an emotional issue. Measuring the value of human life and the social effects of fire are highly abstract and remain the most difficult hurdles in establishing fire risk criteria. This paper will attempt only to describe the technical variables of assessing fire risk.

Knowing the technical elements illustrated in Figure 1, a fire hazard expert can reconstruct a fire event. The overall fire problem then is assessed by the number and magnitude of those individual fire events. For example, residential fires accounted for 95% of all structural civilian fatalities in 1977. About one-quarter of that group started with furniture and 18%

0097-6156/81/0172-0101\$05.00/0
© 1981 American Chemical Society

with sleeping products. In furniture-related fires, cigarette ignitions caused ten times as many fatalities as small open flame ignitions. For mattresses, the ratio is 5:1. Clearly, cigarette-related accidents are preeminent in fire fatalities classified "residential" occupancy.

In evaluating fire statistics, it is important to recognize that these numbers are extrapolated from only a few recorded actual cases. For instance, the Consumer Product Safety Commission (CPSC) report on upholstered furniture flammability shows a total of only three fatalities recorded for upholstered furniture fires initiated from open-flame sources for the states of California and Ohio in 1977. A single multi-fatality fire could dramatically change those numbers as happened in 1976. That year only one fire was coded as originating from a match or lighter.

The urethane industry has a keen interest in all this activity because a lot of flexible urethane foam goes into upholstered furniture and bedding made today. A very high percentage of urethane foam goes into products where strong codes are now in place. About 70% of the fires are ignited and more than 95% of the fatalities occur in the residential market which represents 83% of the total volume. Most authorities relate this high fatality profile to the lack of public awareness of fire hazards (Figure 2).

The following two limited studies dispute the assumptions that half these upholstered furniture related fire deaths involved urethane foam. These studies also reflect the significance of analyzing the fire problem from a composite perspective rather than by simply evaluating the components individually.

One federal study reports 185 random incidents in which upholstered furniture was the first item to ignite. In that study the National Bureau of Standards Textile Chemists coded the composition of inner layer substrates. Seven percent were coded as urethane and 13% were combinations of cellulosic and urethane materials.

The report also shows only 50% of the outer fabrics weighed more than 20 oz. per yard while 95% weighed 12 oz. per yard. Approximately 90% of the fabrics were cellulosic. In addition, nearly 90% of the furniture incidents were coded "cigarette ignited." The prominent roles of cigarette ignition and cellulosic fabric in fatal scenarios is apparent in this study.

In a second study, only about 6% of the fires recorded started in occupied patient rooms where urethane foam might be a contributor to fire spread. According to the study of fires in 75 Massachusetts hospitals, 11% were in unoccupied areas where urethane foams could not be ruled out. However, 41% of the fires started in areas where urethane foam would not normally be present. In this case, upholstered furniture with urethane components probably did not play a significant role in this institutional fire setting.

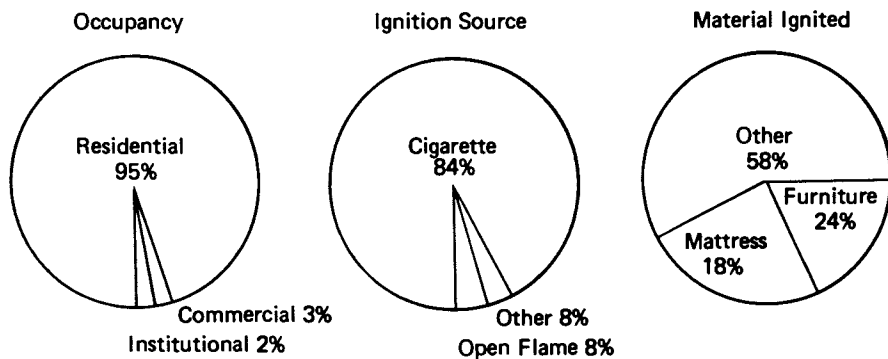


Figure 1. *Interrelated flammability considerations.*

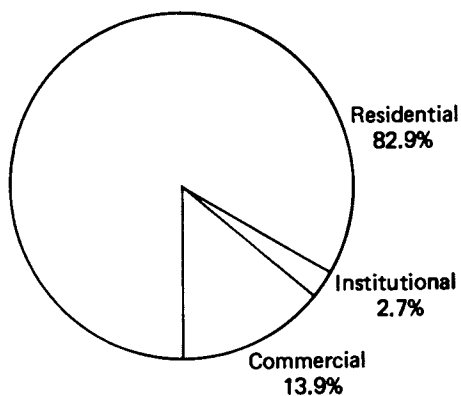


Figure 2. *The 1978 occupancy percentages/use of urethane foam.*

These studies and additional data suggest that generic banning of urethane foam will not solve the problem since the variables are numerous and complex. Tools to assess component, composite and overall system performance will be needed. Based on these criteria some urethane materials will be accepted while others will not be marketed. Developing reliable assessment criteria has progressed significantly and will continue to do so during the '80s.

A detailed consideration of the following key variables in risk assessment will help to set the stage for discussion of future standards work.

Variables: Ignition Source

A cigarette ignition test requirement for mattresses has existed since 1973 in the U.S. The CPSC has studied the effectiveness of that test and confirmed a definite reduction in fatalities attributed to cigarette ignited fires over the four-year existence of the standard. Mattresses containing flexible urethane foam meet the requirements of this cigarette ignition test (Figure 3).

This rapid statistical response in reducing mattress smoldering fire losses is gratifying. Yet there is controversy about whether the improvements were caused by the standard or by public education. "Learn Not to Burn" and other educational programs developed by the National Fire Protection Association and the Society of the Plastics Industry (SPI) seem to have been instrumental in increasing public awareness of fire hazards. These should be recognized as effective tools to help the general public prevent and respond to fires.

The other type of ignition source considered in setting standards is the open flame. To date the federal government has not taken action to set standards to reduce the risk of open flame ignition. However, industry has demonstrated it can establish effective fire testing and standards in lieu of federal codes.

This has also been accomplished in cigarette smoldering standards. The Upholstered Furniture Action Council (UFAC) designed its own proposal establishing a national industry voluntary program of furniture construction standards. Thus, industry has produced upholstered furniture that is more resistant to cigarette ignition than in the past. The progress of this UFAC program suggests that the CPSC will have no reason to regulate because industry will have accomplished and exceeded the federal objectives.

At the state level, California has been the leader in handling the fire problem. This state requires all flexible urethane foams used in furniture to be flame retardant (i.e., to pass a vertical open flame test and smolder resistant screening as set forth in the test requirement of the California Bureau of

Home Furnishings Bulletin 117). This state has been successful in acting on the fire problem primarily because California is required by state law to take that specific approach toward flame resistance unlike the CPSC which is under general Congressional order to reduce fire deaths and losses.

In summary, cigarette smoldering and open flame are the two types of ignition considered in assessing fire risk. Federal cigarette standards are in place for the mattress industry. Industry has been the leader in cigarette ignition testing for furniture. An effective open flame standard has not been accepted, but industry and state governments are working toward that goal.

Variables: Occupancy

Three primary occupancy classifications are used in fire risk assessment: residential, institutional and commercial. The Urethane Division of the SPI recently conducted an examination of all major areas in which flexible urethane foams are used. In June, 1979 they reported:

"Combustibility performance standards for products in which flexible polyurethane foams, or other combustible material are used should vary according to types of occupancies and certain other end use conditions."

This means that performance standards for certain high risk areas (such as penal and medical institutions, places of public assembly and mass transportation) should be different than those for residential or private transportation.

In high risk areas a greater chance of open flame ignition exists whether accidental or intentional. Other problems in these areas include limited mobility and high ratios of occupancy.

Non-residential fire incidences may be few but they are often significant in severity and are highly visible events. They represent a major thrust for future standard research.

Variables: Construction and Fabric

The furniture industry is also adapting to address the problems presented by fabric and construction in the fire risk of upholstered furniture. Specifically they are trying to improve cigarette smoldering resistance in furniture.

The dilemma of the furniture industry is the overwhelming customer appeal of cellulosic fabrics, though these fabrics represent significant fire risk around carelessly handled cigarettes. In comparison, most common synthetic fabrics are poorly rated in customer appeal even though they may be a solution to the cigarette ignition problem.

Many furniture manufacturers have chosen to retain cellulosic fabrics and meet UFAC standards by changing construction design. Upholstered furniture construction can be complex. Some design requirements dictate different seating and back constructions. Block forms are predominantly urethane foam construction; quilted or designed backs are upholstered by a fiberpacking technique. Reducing fire hazard potential in block urethane seat cushions would mean a significant construction adaptation for the furniture industry. The quilted or designed back construction, on the other hand, would require a simple component replacement.

Unfortunately, because upholstered furniture manufacturers are wood and upholstery specialists, they regard foam to be the least important. The conventional cushion construction used precut foam with a fabric covering. Some manufacturers choose to add a garnetted fiberfil between the foam and fabric covering for a plush look and feel. Some foamers reproduce this by adhering two grades of foam into one item. A third type of construction uses woven fabrics or solid foams as barriers to reduce open flame combustion of furniture and mattresses used in the commercial or institutional markets (Figure 4).

The mattress market history provides an interesting view of one industry's response to the forced introduction of a flammability standard. The message of adaptation, rather than complete change, is perhaps a preview of the future for the furniture industry. Whatever the combination of fabric and construction, industry recognizes the importance of these variables in the overall assessment of fire risk and has adapted manufacturing to reduce fire hazards.

Future Testing, Standards and Industry Action

Fire codes or standards have governed urethane business for some time and have played a prominent role in the creation of building codes. Unfortunately, fire statistics currently are based on a minimum number of collected fire cases which become the base for regulatory activity that impacts industry and consumers.

At first, property protection was the key concern to those studying fire hazards. However, during the past decade an emphasis shift has refocused attention to the non-structural and personal life safety parameters of fire. Many technical codes and standards reflect this significant progress of the past decade (Figure 5). This chart in 1989 would show further changes in future flammability standards.

An analysis of the impact of some of the current standards reflects a trend which may continue through the '80s. For instance, the federal cigarette ignition standard imposed on the mattress industry in 1973 resulted in little change in the penetration of full foam mattresses into a dominantly innerspring

Change in bed-related fire/burn fatalities, 1974-1978 -28%
 Change in number of fire/burn fatalities in private dwellings, 1974-1978 +17%
 Change in number of fire/burn fatalities, 1974-1978 -13%

Source: Consumer Product Safety Commission Report dated 1980.

Figure 3. Effectiveness of FF4-72 federal cigarette mattress standard (enforced December 1973).

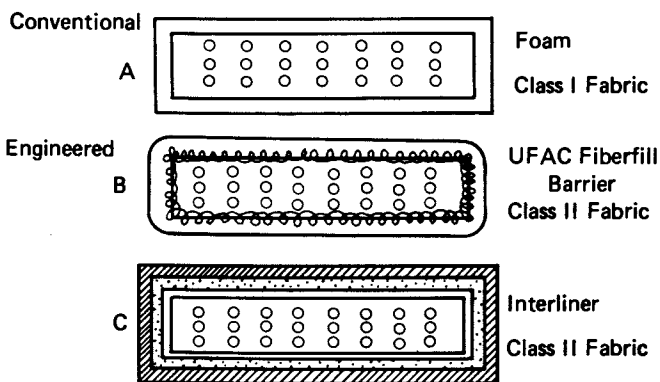


Figure 4. Construction options.

	Residential	Commercial	Institutional
Mattress	FF 4 - 72 (Cigarette Mattress Test)	None	E - 162
Furniture	UFAC / Cal. 117 (Cigarette Ignition Test)	E - 162 (Radiant Panel Test)	None
Automotive	MV 302 (Horizontal Open Flame Test)	MV 302	Imminent
Carpet	FF 2 - 71 (Pill Test)	FF 2 - 71 E - 648 (Radiant Panel Flooring Test)	

Future Standards: Commercial Furniture – Rate of Heat Release (RHR) Test Smolder
 Institutional Mattress – RHR Test Open Flame
 Residential Furniture/Mattress – To Be Announced

Figure 5. Flammability standards.

economy. It did, however, result in a quilt replacement and a 50% switch to urethane foam toppers. Innersprings, however, remain unchallenged in the residential bedding market.

By contrast institutional and prison mattress markets have special needs best met by a urethane core type mattress. These include the need for repeated sanitizing and reduced handling weight. In prisons, mattresses must be designed to control hidden contraband as well. While this market volume is only five million pounds per year, it demands open-flame resistant foam. It is a very visible market and regulations developed for this market will potentially impact the residential sector.

As we enter the '80s, several future flammability standards are in initial stages of development. Industry has been considering more strict performance standards for residential use, some specialists believe all foam components should pass Cal. 117 vertical open flame testing requirements. Others, including CPSC and UFAC representatives, believe final composition performance must be the bottom line in setting standards. However, long-term composite testing and open-flame testing will be stressed in the industry. Fire growth rates will be the basis for performance standards in the institution and commercial applications.

There will be two parallel thrusts based on composite and component solutions. The composite thrust will be the initial area of concentrated tests and standards. This emphasis will be succeeded by a series of component or product related solutions like the UFAC labeling and interliner approaches (Figure 6).

Though the standards at destination I have been established for component foam testing, they will become secondary to the national industry voluntary controls as outlined in the UFAC program.

In the next two steps the residential upholstered furniture questions should be resolved. The second destination is an appropriate open flame composite assessment test along with an improved UFAC cigarette resistance test. The third destination will be development of a foam that meets UFAC labeling test requirements and replaces their construction approach.

Finally, urethane foams will have a flammability performance permitting their general use in non-residential occupancies. These would include high risk mattress and later furniture uses.

Some difficulty has arisen in determining appropriate tests for setting these standards. Cigarette smoldering ignition tests are predictable because the ignition sequence can be reasonably defined. Fine tuning is needed, but fire experts are relaxed with today's cigarette ignition testing as basically realistic.

By contrast, the possible ignition scenarios are so broad for open or diffused flame, fires, that many different tests have been derived. Though each of these tests has merit, no

single method has gained universal acceptance. Consequently, an established British furniture standard has been recognized for its varied ignition source resistance and is the proposed European Common Market standard. This concept was used in the prison mattress program at the California Bureau of Home Furnishings and the Metro Bus Project at the National Bureau of Standards.

In summary, reducing fire hazard -- not passing tests -- is our industry's goal. We must be alert to the status and changes in our nation's fire experience. We are doing this cooperatively through industry groups like the Urethane Division of SPI.

Business Impact

The era of composite solutions will be 1980-83 (Figure 7). Changes will occur in foam use but no dramatic change in present urethane foam fire property mix is expected during this period. In setting standards for the industry, UFAC's voluntary program will gain national prominence. The California standard will change in importance from foam control to become the catalyst for fabric improvement.

UFAC's labeling program does not call for a unique fire performing foam unless UFAC quality is available. That quality will not be commercially achieved during this three-year period, thus we do not look for a significant shift in the fire performance mix of the urethane foam sold.

During this period, use of cellulosic upholstery fabrics could be reduced to a 50% market share to retain as much engineered construction as possible. In accordance with UFAC criteria, construction will be employed to meet UFAC standards. However, there may be a higher value placed on urethane foams for use with synthetic upholstery fabrics. Commercial and institutional markets will choose "C" type constructions or specialized combustion resistant foam but market impact will be minor.

The era of component solutions for the residential fire problem should begin about 1984. In the furniture market both foam and fabric will meet UFAC requirements in order to pass smoldering tests. During this stage a dramatic change should take place in the fire performance property mix of foams sold into the furniture industry. Creative technology will achieve cost effective foams that control smoldering and demonstrate open flame resistance as defined by Cal. 117. The upholstered furniture industry will then revert back to conventional constructions and pay a premium price for foam.

Concurrently the fabric industry will announce a similar achievement for cellulosic upholstery fabrics. These will be treated for a class "A" rating without property penalty. While the class "A" heavyweight cotton upholstery fabric represents a

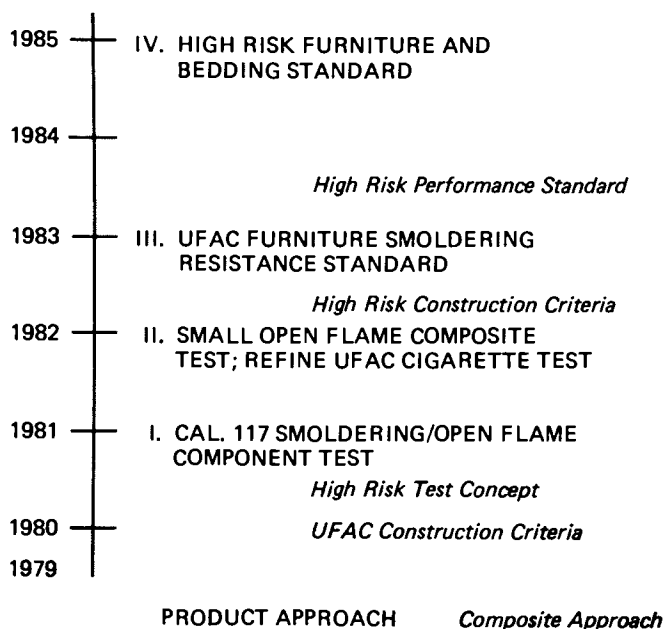


Figure 6. Flammability standards and action during the 1980's.

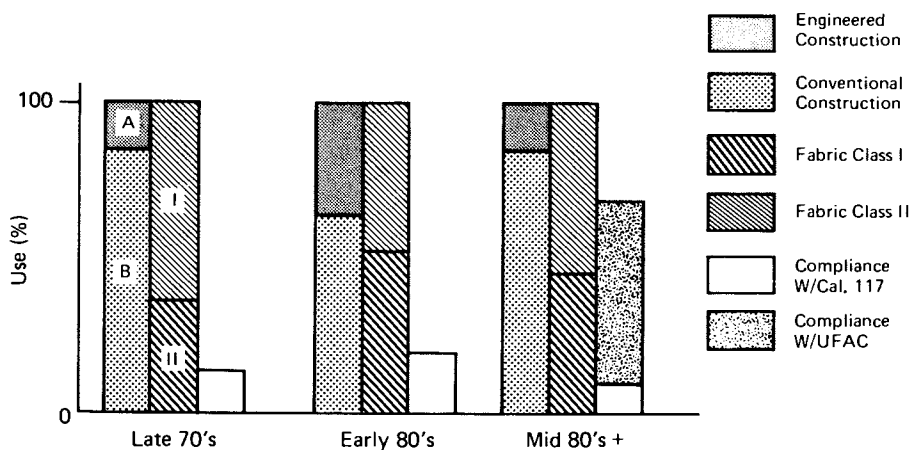


Figure 7. Market changes due to flammability concern: residential upholstered furniture.

UFAC smoldering solution, it also is the most practical open-flame ignition solution for the upholstered furniture market.

By 1986, the impact on urethane foam will be a conversion to about 40% UFAC grade foam for the furniture industry. An estimated 70% of the upholstery fabrics will be cotton. Sixty percent of that will be UFAC "A" grade. Individually, furniture manufacturers will choose either or both solutions but it will be common to revert back to conventional construction.

Not only will an individual product risk performance be questioned, but its role in the overall environment will be brought into focus. This era of the late '80s, therefore, may be called the era of environmental or system solutions as differentiated from component or composite solutions.

We have an opportunity to shape and mold the future, and to benefit society by our struggle with assessing fire hazard. It is a challenge the urethane industry has already begun to meet.

Summary

This paper recognizes the presence of a fire-risk in many products, as well as components. Fire risk was described by statistics for products that contain urethane foams. Those products can be related to fire fatalities, ignition source, or occupancy factors. The federal data collected about frequency and consequences of our nation's fire losses cannot tell us which, or how many, of these products did contain urethane foam. Our available data in that area cannot give a persuasive description of the situation.

The paper presents evidence to show that the urethane isocyanate industry is doing something to minimize fire risk associated with its materials. The framework of codes and standards now in place should lead to a future reduction of fire losses. Still, we are not sure we have fully resolved the question of "how to" assess fire risk. But, as an industry we are working on that and our route is in place.

For the urethane industry, the immediate future will be affected only by a slight decrease in the volume of foam used by the furniture industry with no change in present combustion performance mix.

This is the result of the furniture industry's option for construction adaptation, rather than component change.

Component solutions in foam and fabric will characterize 1983 to 1986. Foam will reclaim its market position and a significant portion of foam sold will be highly resistant to smoldering. Fortunately, the best open flame solution will be a by-product of this activity.

The late '80s will find the urethane market affected by the rougher problems of managing more severe open-flame fire situations. The institutional market size involved will be small, but will have a subtle effect on the residential market for urethane foams.

We must communicate to all users of urethane foam accurate fire risk information. SPI's bulletin, "Using Flexible Urethane Foams Safely" and other safety documents are valuable only as they are read and understood. This is a critical task.

Foam will burn. Though we make it more ignition resistant or slower in fire growth, the real test is in the finished product's performance. Today's urethane foam finished products are improving our quality of life and will have an even more positive impact on reducing fire hazard in the future.

RECEIVED April 30, 1981.

The Effects of Regulatory Actions on the Marketing of Rigid Polyurethane Foam Insulation

ROBERT G. PILMER

CPR Division, The Upjohn Company, Torrance, CA 90503

It is estimated that 615 million pounds of rigid polyurethane foam were made during 1979⁽¹⁾. The market for these foamed plastics has been growing at an annual 15 percent rate for the last few years. It is projected that similar growth may resume in future years. The construction market is the key to future growth, as the greatest share of rigid polyurethane foam is used in thermal insulation applications.

The rate of building construction has been down for some while due to high interest rates and the scarcity of funds. This condition is expected to improve gradually. The consumption of rigid polyurethane foams as thermal insulation can be expected to increase with the renewed building activity.

Regulations in various stages of adoption require energy conservation in the design of new buildings. The installation of thermal insulation is one of the means of meeting these proposed energy conservation standards. The Federal Department of Energy has a proposal out for comment called Energy Performance Standards for New Buildings⁽²⁾. The state of California has also moved in this direction⁽³⁾. As standards of this sort are introduced, the demand for thermal insulation for new construction should increase sharply. Because of their high thermal resistance, chlorofluorocarbon (CFC) blown rigid polyurethane foams may gain a greater share of this market in the future.

Thermal insulation materials are rated by their resistance to heat flow. This is generally stated as the "R" value. The greater the R value, the better the insulation. Let us consider insulation sufficient to give an R of 19. In conventional 2 x 4 stud construction, sufficient thicknesses of some types of insulating materials cannot be emplaced in the nominal 3-5/8 inch space available to yield an R-19 rating. On the other hand, this level of thermal resistance can be achieved easily within this space when it is filled with a rigid CFC blown polyurethane foam. In addition, rigid polyurethane foams sprayed-in-place effectively seal the structure against air infiltration, a benefit derived from few other types of insulation.

0097-6156/81/0172-0113\$05.00/0

© 1981 American Chemical Society

Like most materials that have become a significant item of commerce, rigid polyurethane foams have become regulated. When a regulation is first introduced, it inhibits the sales of the affected materials, and the experience with rigid polyurethane foams has been no exception. What follows is a description of the actions of four different types of organizations that will affect the future sales of rigid polyurethane foams.

The Model Building Codes

Approximately 55 percent of the sales of rigid polyurethane foams has been in the construction market in recent years. This has not always been so. The uses and qualities of materials used in construction are regulated by the local building codes. Generally, the local governing body adopts one of the model building codes^(4,5,6). Three organizations presently write these model codes: The International Conference of Building Officials (ICBO), Building Officials and Code Administrators (BOCA), and The Southern Building Code Congress (SBCC). Each organization provides a means for building officials, architects, engineers, etc. to meet with their peers, exchange ideas, and act to regulate building construction in a uniform manner.

Rigid polyurethane foams were not considered distinctive in the way they burn and were regulated, along with all other building materials, solely on the basis of flame spread*. (*References to flame spread or numerical flame spread ratings throughout this paper are not intended to reflect hazards presented by these or any other materials under actual fire conditions.) The surface burning characteristics (flame spread rating) of construction materials is determined by a procedure called a tunnel test. For most applications a maximum flame spread rating of 75 or 200 was considered suitable. In the late 1960's, rigid polyurethane foams able to meet these flame spread requirements were finding their way into more and more construction applications. Because of their high insulation efficiency, architects and builders were becoming increasingly interested in polyurethane foams. It was not clear to either the polyurethane industry or to the construction industry that foamed plastics could present an unacceptable fire risk if left exposed in an interior application, and no special precautions for installation were recommended. As a consequence, some foamed plastics were installed on the insides of buildings and left exposed or given only a coat of ordinary paint. In light of today's knowledge, these were misapplications of the product.

In 1974, the Federal Trade Commission brought it forcibly to the attention of 26 manufacturers of foamed plastics, raw material suppliers, and The Society of the Plastics Industry that, among other things, the tunnel test did not correctly evaluate the actual fire hazards of these materials. The building codes responded accordingly, and the first code language

specifically addressing foamed plastics was introduced. As often happens, the resulting regulatory actions were not inclusive and are probably excessive. At best, it must be stated that there are inequities in the present building codes. Here briefly are the key points in the building codes of today.

1. All foamed plastics shall be covered by a thermal barrier with the ignition inhibiting characteristics of 1/2 inch gypsum wall board (15-minute finish rating).
2. The foamed plastic, when tested in the thicknesses intended for use, shall have a flame spread rating no greater than 75 and a smoke developed rating of no greater than 450.
3. Each building code has a list of specific conditions and requirements for the use of foamed plastics. Typically, these cover trim, masonry construction, cold storage buildings, metal faced building units, roofing applications, doors and exterior sheathing.
4. Alternate materials or conditions of use may be permitted if diversified tests establish that the intent of the code has been satisfied.

These regulations, although conservative, are attainable. The effect of these building codes has been to inhibit the sales of rigid polyurethane foams. Conversely, competing thermal insulation materials have benefitted from the restrictions placed on foamed plastics. However, I fear that had not these regulations been put into effect, incidents involving the misapplication of rigid foamed plastics might be occurring with alarming frequency. The news media have been known to pick up on a series of incidents and prepare an expose. A series of such articles has appeared in The Los Angeles Times. The articles were critical of the combustible nature of flexible polyurethane foams. Statements made in these articles have been interpreted by some as applying equally to rigid foams. This includes some of the less knowledgeable building officials. The bad press for flexible polyurethane foams has effected the perception of rigid polyurethane foams. Frankly, I would rather have a restrictive regulation than a bad press.

Where the building codes have been enforced, rigid polyurethane foams have established a remarkably good fire-loss record. I feel that we are regarded with far less suspicion today than we were four or five years ago and that acceptance has contributed greatly to the increased sales of the past few years.

I would like to cite an example of a manufacturer who has taken note of the building codes and created a new product in response. In dry, windy weather, fire can jump from building to

building by burning brands being blown from roof to roof. This has placed the wood shingle manufacturers in a difficult position. The fire experience for wood shake roofing, with the current trend towards building houses closer and closer together, has been gradually getting worse. The county of Los Angeles recently acted by banning untreated wood shingles for roofs.

This particular manufacturer created a composite panel consisting of a glass-fiber reinforced plastic outer shell backed with a rigid polyurethane foam. The product looks like a cluster of hand split wood shakes. When installed, the panels interlock and look exactly like a shake shingle roof to the casual observer. These panels have been tested and qualify as a Class A built-up roof covering. In addition, they provide a much greater resistance to the transmission of heat than wood shake shingles. The panels are fast and easy to install and quite durable.

In the future, I anticipate greater acceptance of rigid polyurethane foams in construction applications, and with the greater acceptance will come growth. I would also anticipate that the inequities in the building codes will be dealt with. Whether these changes will take the form of greater restrictions on competing materials or less restrictions on rigid polyurethane foams, I cannot predict. Either event will be beneficial to the growth of the rigid polyurethane foam market. Lastly, innovative ways of using rigid polyurethane foams, such as the roof panels I have discussed, will surely occur. These new applications will also add to the growth.

The Insurance Services Office

There is a second type of organization which has had an influence on the properties of materials used in building construction. That organization is the insurance carrier. If the carrier who insures a building disapproves of a material used in its construction, or the manner in which the material is used, it can impose a substantial disincentive to its use by increasing the insurance premiums on the building. Such an occurrence has taken place with the Insurance Services Office (ISO) in the preparation of their Commercial Fire Rating Schedule⁽⁷⁾. They have reached a conclusion in their rating factors for foamed plastics which simply does not correlate with the facts. In their judgment, less property damage is likely to occur using exposed 25 flame spread foam (30 percent increase in rating factor) than with a 75 flame spread foam installed behind a 15 minute thermal barrier (50 percent increase in rating factor). It is most difficult to understand how they reached this conclusion. Certainly the Federal Trade Commission, the code writing organizations, and the foamed plastics industry would disagree. In my experience, a low flame-spread rating for a rigid polyurethane foam when left exposed does not produce a lower level of life safety hazard or expected damage level than

that which can be expected from a product with a somewhat higher flame spread rating but installed behind an ignition-inhibiting thermal barrier. Fortunately, most people will follow the building codes and will install an ignition barrier over the foamed plastic. This rating schedule does not, in my judgment, fairly evaluate the differences in performance between products with different flame spreads. These differences are much smaller than the rating schedule would have you believe. Secondly, this rating schedule penalizes foamed plastic insulation covered with a thermal barrier disproportionately to other types of insulations.

I continue to receive calls from our field sales representatives in which their customers have run afoul of ISO. In several recent contacts, the insurance rater insisted on 25 flame spread foam in a roof in spite of the fact that the foam we proposed to offer is classified by the Underwriters Laboratories as a component in a Class A built-up roof covering and the 25 flame spread rated foam chosen has not been rated in roofing. The extra cost for a 25 flame spread rated foam often causes the buyer to think twice and reconsider the use of a polyurethane foam. The requirement for a 25 flame spread foam in roofing seems particularly inappropriate since unregulated asphalt, tar, and roofing felts would be permitted and at no penalty whatsoever.

The ISO rating schedule is used mostly by the insurance companies who write policies on small industrial buildings. Large factories are insured by organizations such as Factory Mutual, and homes are insured by companies who, to this point, don't care what type of insulation is used in the construction of the house.

If organizations, such as the Society of the Plastics Industry, and the individual members of the foamed plastics industry can persuade ISO to examine their loss record more critically, I feel confident that a fairer rating schedule will be forthcoming. When this takes place, increased sales of rigid polyurethane foams should result.

R-Value Representations

As noted previously, thermal insulation materials are sold on the basis of R-values. The higher the R-value, the better the insulation. Regulations to insure that accurate representations are made about the efficiency of thermal insulation materials are appearing in many places around the country. Such a regulation is in effect in the state of Ohio⁽⁸⁾. The Federal Trade Commission has promulgated such a rule to be in effect nationwide. However, congressional action prevented the implementation of this regulation from last August until this June. The state of California also has adopted a similar rule, but it was enjoined by a California court action. The principal motivation for these

regulations is to see that the consumer has accurate information upon which to make a decision when he selects insulation for his home. One of the key features of each of these regulatory actions is that all statements about the thermal resistance of a product (R-value) must be backed up with substantiating test data. In each case, where a regulation has been challenged in court, the matter of the substantiating test data is at issue. As example, a rigid polyurethane insulation manufacturer may not make the statement that 5-1/2 inches of his product has an R-value of 34 unless he has tested samples 5-1/2 inches thick and the product, indeed, had an R-value of 34. That sounds fair enough. But, test instruments that will accomodate samples of this thickness are extremely scarce. Rigid polyurethane foams are quite efficient insulators, so great thickness is not required to achieve large R-values. In the case of the less efficient insulation materials, R-value of 34 can be achieved only with thicknesses far greater than can be accomodated by any test instrument. Therein lies the battle.

The FTC trade regulation rule will now go into effect September 29, 1980 except full thickness testing will not be required. When the National Bureau of Standards has thick calibration standards available, the FTC expects to implement the full thickness testing requirement of the trade regulation rule. The new NBS reference standards should be available January 1, 1981. Similarly, after a one-year delay, the California Energy Commission is moving ahead to put their insulation standards into effect. Additional hearings were conducted Wednesday, August 27, 1980. The litigation, which was the cause of the suspension, has been terminated.

Rigid polyurethane foams have a special problem when it comes to making a fair statement about their R-values. Essentially, all of these products are expanded with chlorofluorocarbon 11 (CFC-11), which is trichlorofluoromethane. At the time of formation, all of these materials have essentially the same R-value of about 7.5 to 8.0 per inch of thickness. At one time, that is how these products were marketed. The initial thermal resistance, however, changes with time. Where the foamed plastic is exposed to air, the air migrates into the cells, diluting the chlorofluorocarbon gas. The thermal resistance decreases when this takes place. This is a slow process and may go on for years. To the extent that the foam is sandwiched between air impervious skins, the process is all but halted.

Recall that the building codes do not permit foamed plastics to be left exposed in any construction application. Hence, there are always facings in close proximity to the foamed insulation. To the extent that the facings are impermeable and are tightly attached, air intrusion is halted. On the other hand, some surfacing materials, such as asphalt and asphalt-impregnated felts which might be placed over the foam in a roofing application, are semipermeable and air can enter into the foam.

In other installations, there might be a gap between the foam and the required thermal barrier, thus permitting air intrusion. The phenomenon of decreasing R-value has presented the industry with a dilemma. What is the proper statement to make about the thermal resistance of one's rigid polyurethane foam insulation? The lower the R-value statement you make, the less competitive your product will be. In the past, it has been difficult to advertise the aged R-values when your competition advertises only the initial R-values.

All regulatory bodies are in agreement. You cannot represent your product based upon its initial performance. Representative samples of the product must be aged prior to testing. There is substantial unanimity as to the aging conditions. Chlorofluorocarbon-expanded foams must be aged either 90 days at 140°F or two years at room temperature before testing. Promotional statements may only be made based upon the results of such testing. When these rules are enforced, that will end this debate.

What effect the reporting of lower R-values for rigid polyurethane foams will have is not clear. The values will still be better than for any other type of insulation. One would have to presume that these products would look less attractive and, therefore, sales might suffer. However, other insulation materials will also be impacted by these regulations. Loose fill materials settle, and may also look less attractive. The regulatory agencies have taken note of this and require that tests be performed on these materials in the settled condition. Rigid polyurethane foams, of course, do not settle. To the extent that urea-formaldehyde foams shrink creating voids, they, too, will be required to advertise what really happens to the thermal resistance of their products. Rigid polyurethane foams do not shrink in this manner. Some types of insulation materials do not give linear increases in thermal resistance with increasing thickness. This too, must be accurately reported according to the regulations. Rigid polyurethane foams, on the other hand, improve in performance above a straight line relationship. It is my belief that this reflects the effect of fewer torn and broken cells in thicker foams. In the thinner cross sections, the torn and broken cells allow greater amounts of the chlorofluorocarbon blowing agent to escape and the optimum thermal resistance is not realized.

It is difficult to project, at this point, how all of these changes in the reporting of product R-values will ultimately affect polyurethane foam sales. I do not expect any big surprises. I expect only small shifts in market position. It should be expected that those products sold with air-impermeable faces attached will show the strongest sales performance.

EPA vs. Chlorofluorocarbon Blown Foams

To this date, the Environmental Protection Agency (EPA) has restricted the use of chlorofluorocarbons (CFCs) only when used as aerosol propellants, and not when used as blowing agents as they are in the manufacture of foamed plastics. I am sure you are all aware that the EPA intends to expand its regulations on the uses of chlorofluorocarbons. At this point, it appears that this agency will act to limit the manufacture and sale of CFCs to that of the year 1979 and no more. The EPA is also considering reducing this maximum in future years. The effect of this action could be quite severe. Market forces will, no doubt, drive up the price people are willing to pay for CFCs. Hopefully, other materials will become available to replace CFCs in many applications. There are apparently alternatives to CFCs in some products, such as flexible polyurethane foams. Vapor degreasing operations may also find acceptable alternate materials. Certainly, with a fixed or diminishing supply of CFCs, those materials which are most cost effective will best be able to afford the increased cost. In mechanical refrigeration uses of CFCs, where the refrigerant is vital and adds but a small amount of the cost of the total product, it is hard to conceive of a price which is prohibitive. In rigid polyurethane foams, the impact of a price increase in CFCs will be more strongly felt. CFCs constitute a significant portion of the total product (12-18 percent). In those applications where the rigid polyurethane foam is no longer cost effective, a switch to other insulation materials will surely take place. Such an application might be where the difference in performance of a CFC-expanded polyurethane and some competitive types of insulation is small. There are other applications where rigid polyurethane foams are most cost effective and a price increase in the CFC component of the foam will have little, if any, impact. An example of such an application might be where the rigid polyurethane foam permits a savings of space and/or weight due to its combination of thermal and structural properties. The differences in thermal performance between CFC expanded rigid polyurethane foams and other types of insulation materials are greatest where impermeable facings are applied over the foam.

Summary

There are other regulatory agencies whose actions have had some effect on the cost of making polyurethane foams. OSHA, for example, has established an upper limit of 0.02 ppm of isocyanate vapors in the atmosphere that workers breathe. This limit has been in existence for several years and is not expected to change in the future. With the current raw materials in use today, this threshold limit is easily met with simple ventilation equipment.

You will note that three of the regulatory activities discussed here are directed toward construction applications -- the building codes, insurance ratings, and insulation efficiency

statements. There is also a substantial market outside of the construction industry. This market is not impacted by these three regulatory activities, but will be impacted by a limitation on the amount of chlorofluorocarbons that may be produced. It is typified by the transportation insulation market -- e.g., trucks, trailers, and railroad cars. In these applications, the rigid polyurethane foam is valued not only as an insulation material but also as a structural component. Glass fiber insulation and loose fill insulation lose some of their insulation efficiency due to settling and compaction that occurs from the continual bumping and pounding of the road. Rigid polyurethane foams are not affected in this way. Rigid polyurethane foams are particularly valued in this way of application since the amount of space which must be devoted to insulation can be reduced. The exterior dimensions of these vehicles are fixed by statute and, therefore, thinner insulation permits a greater interior productive capacity. However, this market is much smaller than the construction market, and polyurethane foams have fairly well saturated this market.

The greatest potential for future growth lies in the sales of rigid polyurethane foams into the construction market. It is my strong belief that as building officials come to understand foamed plastics better, and as the manufacturers of foamed plastics come to understand the building codes, the codes will become less and less of a hinderance to the sale of rigid polyurethane foams. I would expect a similar scenario with insurance rates. I am less optimistic about the effect of EPA's proposal to reduce the amount of chlorofluorocarbons available. Our product is already relatively high priced. Further increases in price will, no doubt, have a significant effect on some segments of sales. Where rigid polyurethane foams can be sold as the insulation material with a plus, the future is bright. Where rigid polyurethane foams must compete only as straight insulation, the future is more uncertain.

What does the future hold? For the innovative and those who learn to live with the regulations, sales should be good. I believe it will be worth the effort.

Literature Cited

1. Urethane '79 - The Americas, B-7366, The Upjohn Company, Polymer Chemicals Division, 1979.
2. "Energy Performance Standards for New Buildings," Federal Register, Department of Energy, November 28, 1979.
3. "Energy Conservation Standards for New Residential and Non-Residential Buildings," California Energy Commission 127B:01, December 6, 1978.
4. Uniform Building Code, 1979 Edition, International Conference of Building Officials.
5. Basic Building Codes, 1978 Edition, Building Officials and Code Administrators (BOCA).

6. Standard Building Code, 1979 Edition, Southern Building Code Congress International, Inc.
7. "Commercial Fire Rating Schedule", Insurance Service Office, April, 1978.
8. Ohio Insulation Rule, Substantive Rule 109:4-3-14, effective December 7, 1978.

RECEIVED June 1, 1981.

A Reaction Sequence Model for Flexible Urethane Foam

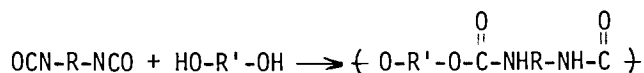
F. E. BAILEY, JR. and F. E. CRITCHFIELD

Research and Development Department, Silicones and Urethane Intermediates Division, Union Carbide Corporation, South Charleston, WV 25303

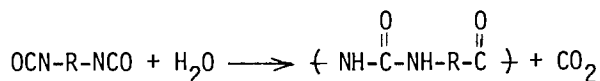
In the process of making free-rise, water-blown flexible urethane foam, a mixture of relatively low molecular weight components is transformed in a matter of minutes into the controlled, highly "engineered," supramolecular architecture of foam. The foam produced meets specifications for bedding, seating, carpet padding - applications for which there are particular physical property criteria. This process is fascinating because it is one of the few instances in industrial polymer chemistry in which rapid polymerization occurs in such a controlled way that a defined supramolecular architecture is simultaneously achieved.

The very familiar, open-cell foam structure of a flexible urethane is shown in the scanning electron micrograph of a section of foam in Figure 1. The structure is that of a system of regular dodecahedra with open-faced pentagonal cell boundaries. The problem addressed in this work is the sorting out of the sequence of chemical reactions which occurs in the foaming process and defining the timing of these reactions which leads to stable foam of desired properties.

In elementary descriptions of the making of urethane foam, a set of two reactions is often given: the reaction of a polyol and a diisocyanate to yield a polyurethane:



and the reaction of diisocyanate with water to yield disubstituted ureas (polyureas) and carbon dioxide:



The sum of these reactions is described as leading to block

0097-6156/81/0172-0127\$05.00/0
© 1981 American Chemical Society

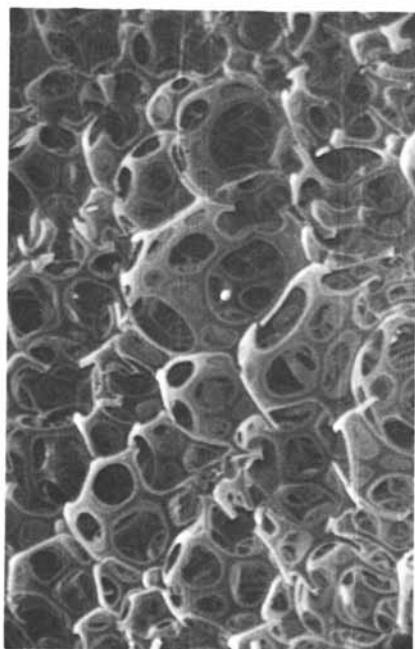
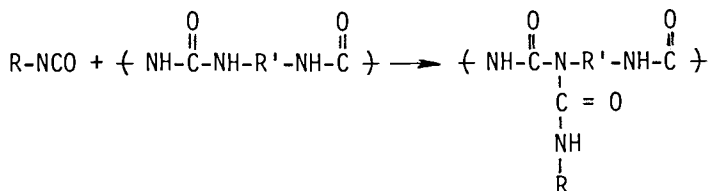


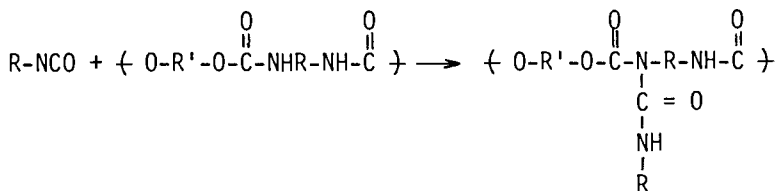
Figure 1. Scanning electron micrograph of a section of water-blown, HR urethane foam.

urethane-urea polymer of the (AB)_n type, blown into foam by the generated carbon dioxide. The first reaction yielding urethane from a polyol with functionality greater than two is referred to as the "gelling reaction" leading to the three dimensional urethane network while the second, "blowing reaction," is considered also to contribute to "gel" primarily through association of highly polar species, the polyureas, in the polymer phase of the foam.

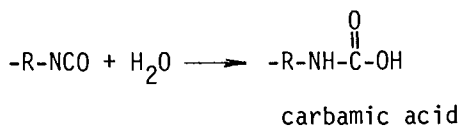
It has also been noted that in these polymerizations, some further degrees of crosslinking can occur due to post reaction of isocyanate with already formed ureas or urethane. Isocyanate can react with substituted ureas to form biuret:

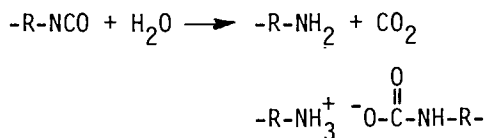


or with urethane to form allophanate:



Conceptually, there are severe problems in accepting the simple view of these simultaneously occurring reactions when the regular architecture of foam is observed. Further, evidence has been presented recently (1) for the presence of other species during foaming particularly at the early stages of reaction (2, 3). Infrared analysis of foam shortly after mixing shows only very low concentrations of the polymer species, urethane and disubstituted urea, but significant concentrations of carbamic acid and arylamine carbamates, due to hydrolysis of isocyanate:





arylamine carbamate

Carbamic acid, an intermediate in the hydrolysis, is an apparently persistent species in the reaction forming measurable concentrations of carbamate salts. Later in the reaction sequence these carbamic acid species are converted to polyureas:



Further, water in concentrations measurable by such classic techniques as Karl Fischer titration can be found in the foaming system, Figure 2. During the first minute of foaming, the reaction of water appears to follow first order kinetics.

In this paper, instrumental means are used to obtain a physical description of the rise of urethane foam and cell opening. Infrared analysis is used to identify the chemical species present in reacting foam and to determine the order and relative rates of reaction of these species. From these data, a reaction sequence model is deduced for the process of making stable, water-blown urethane foam.

Experimental

In the work described, three urethane formulations have been principally used. These formulations which produce "good," representative foam were selected for convenience in laboratory manipulation. With water levels of 2.5 phr, these formulations given in Table I permit a convenient quantity of polyol to be handled to produce one or two-gallon volumes of 2.0 to 2.6 lb per cu ft foam. The studies have covered the range of water contents from 1.5 to 4.5 phr water while centering on the mid-range without loss of generality in developing the reaction model.

A standard mixing procedure (2, 3) for laboratory formulations has been used. This procedure is one which has evolved in the laboratories empirically over the years to permit making or small scale, laboratory foams which closely approximate foams from the same formulations made on foam machines. The procedure involves intensive mixing in a baffled one-quart container for 60 seconds prior to pouring into an open topped one or two-gallon container. An electric timer which records total mixing time signals end-of-mixing by turning on the instrumented measuring system. This end-of-mixing is taken as time "zero" for kinetic and rise profile measurements.

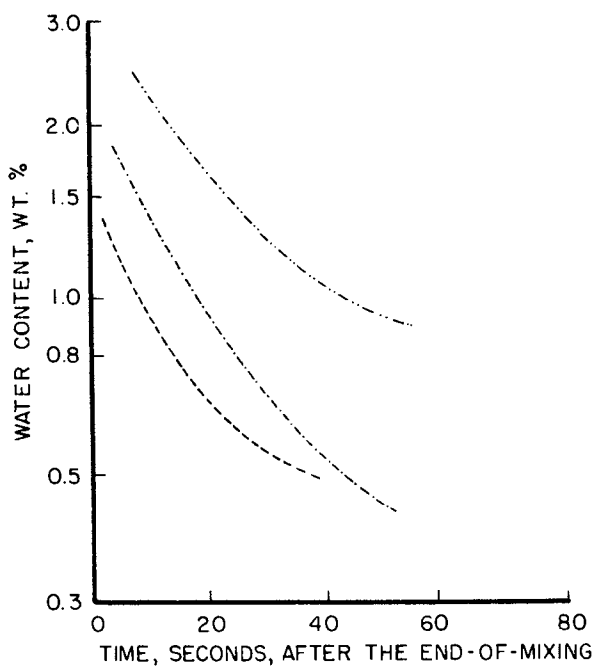


Figure 2. Disappearance of water as a function of time during the first minute after the end-of-mixing: HR Formulation at 105 index. Key: ---, 2.0 phr water; - · - ·, 2.5 phr water; - · · -, 3.0 phr water.

TABLE I
WATER-BLOWN, FLEXIBLE URETHANE FOAM FORMULATIONS

<u>Formulation "A"</u>	<u>Formulation "B"</u>	<u>Formulation "B"</u>
Polyether Polyol (1)	100 phr	Polyether Polyol (3)
Surfactant (2)	1.0	Surfactant (4)
Water	2.5	Surfactant (5)
Amine Catalyst, A-1	0.12	Water
Stannous Octoate	0.2	Amine Catalyst, A-1
TDI (105 Index)	34.28	Stannous Octoate
		TDI (105 Index)
		100 phr
		1.0
		2.5
		0.1
		0.05
		31.11
		Polyether Polyol (3)
		Polymer Polyol (4)
		Surfactant (5)
		Water
		Amine Catalyst, A-1
		Dibutyltin Dilaurate
		Triethylenediamine
		SF58 Isocyanate
		(105 Index)
		60 phr
		40
		1.5
		2.5
		0.1
		0.02
		0.3
		33.03

Foam Properties

<u>"A"</u>	<u>"B"</u>	<u>"HR"</u>
Density	2.1 lb/cu ft	2.5 lb/cu ft
Air Porosity	63.2 ft ³ /min/ft ²	54.5 lb/min/ft ²
Tensile strength	12.2 psi	15.5 psi
Elongation	230%	160%

- (1) A Polyether "Triol" with a Hydroxyl Number of 47.
- (2) Silicone Surfactant, L-6202.
- (3) A High Molecular Weight, Ethylene Oxide Capped Polyether Polyol with a Hydroxyl Number of 34.
- (4) Polymer Polyol, 20% Solids, with a Hydroxyl Number of 28.
- (5) Silicone Surfactant, L-5303.

Foam Rise Profile. At the end-of-mixing, formulations are poured into a one or two-gallon open-topped container and free rise foaming is measured. The rise profile and rate of foam rise has been measured with a Fluidyne System (4, 5). Foam rise and rate of rise as functions of time after the end-of-mixing are received as graphical output from the Fluidyne System.

Foaming Pressure. Using the same foam measuring system (4, 5), a "foaming pressure" can also be determined. It is possible to measure "foaming pressure" with a small transducer placed at the side, near the bottom, of the container in which foam is poured and allowed to expand in free-rise. This "foaming pressure" in free-rise can be recorded as a function of time if desired. Formally, it is possible then to calculate a "foam viscosity" knowing "foam pressure" and rate-of-rise. While this calculation leads to a quantity with the units of viscosity, it must be remembered that the foam is a multiphase system, one phase of which is an expanding gas; and, that the rising foam is not flowing as a liquid but is a system in anisotropic expansion. In any case, the "foaming pressure" in free-rise foams is of the order of 0.02 psig in a system with a rise-rate of about four inches per minute (3, 6).

"Gel Profile." During foam rise, the initially froth-like foam develops some mechanical integrity. This mechanical integrity or "gel" has been measured in a number of ways and described in terms of a "gel profile" in parallel with "rise profile" (7). One method of determining a "gel profile" of a rising foam is using a "BB" drop test in which "BB's" are dropped, from a height of one inch above a rising foam, in a line across the foam surface. Later, the position of "BB's" in the foam is determined. This method generates an intuitively appealing, usually symmetric curve reflecting the position of the "BB's" in the foam (location of the "BB" from the bottom of the foam as a percent of the foam height plotted as a function of the time at which the "BB" was dropped). While on close inspection such a "gel profile" is difficult to interpret since only the final position of the "BB" is measured (it is not known whether the "BB" reached this position by descending ever more slowly into a "gelling" structure or by being buoyed upward by an expanding foam), "gel profile" does correspond to the very real circumstance of the development of a measurable mechanical strength in the foam and provides some measure of the development of structure within the reacting foam.

Cell-Opening. An important parameter in the formation of flexible foam is the time of cell-opening. In the formation of foam, Figure 1, the regular dodecahedra with open-faced pentagonal cell boundaries arise from gas cells expanding as spheres in the reacting foam (8). These cells begin to achieve a closest packing geometry with thinning walls developing in areas of

closest contact as liquid phase drains into the interstices. Rupture of the thin cell walls or "windows" produces the open-cell foam. Since cell-opening will lead to a path for the evolution of carbon dioxide from the rising foam, carbon dioxide evolution as a function of time has been used to follow the cell-opening process.

Initially, to measure carbon dioxide evolution, a mixed formulation was poured into a container which was covered and through which a carrier gas, nitrogen, was passed over the rising foam. The carrier gas was then sparged into lime water. The time was noted when a cloud point was observed due to carbon dioxide. It was found that this cloud point was reproducible. In order to measure cell opening more accurately, a simple infrared technique was adopted. The carrier gas was passed through an infrared gas cell in a Perkin-Elmer Model 281B Infrared Spectrophotometer set at 2320 cm^{-1} and absorbance measured as a function of time after the end-of-mixing.

Infrared Analysis. Infrared analysis has been used to identify the chemical species present in reacting foam and to determine the order and relative rates of reaction of these species. For these measurements, a Foxboro/Wilks Model 80 Computing Infrared Analyzer and a Perkin-Elmer Model 281B Infrared Spectrophotometer have been used. Infrared absorption band assignments in the carbonyl region are summarized in Table II (1, 2, 3, 9-17). In Figure 3, a portion of the infrared spectrum of a water-blown urethane foam is shown. Absorbances can be identified due to isocyanate at 2270 cm^{-1} , urethane at 1730 cm^{-1} , biuret at 1670 cm^{-1} , diarylurea at 1645 cm^{-1} and aromatic carbon-carbon at 1605 cm^{-1} . Independently, infrared absorbances due to carbamic acid and arylamine carbamates have been established in biochemical systems (10). Recently, information concerning competing absorbances due to non-hydrogen bonded (soluble) polyureas has been developed (15, 16, 17). General agreement, however, is that precipitated disubstituted urea shows an infrared absorbance at 1645 cm^{-1} . For infrared analysis, a sample of foam is taken with a small spatula very shortly after pouring from the rising foam, spread on the salt plate of a thermostated infrared cell and covered. The sample can either be quenched on a cold salt plate or held at a reaction temperature. The chemical reactions occurring (3) can be followed isothermally. For these measurements, a reaction temperature (18) must be selected which will allow the measurements to be related to the reaction sequences occurring in the free-rise foam under approximately adiabatic conditions. This temperature has been determined by inserting a fine-size, highly responsive thermocouple through the side of the reaction container to a point in the center, about three inches from the bottom of the reacting foam. Omega subminiature thermocouples (SC PSS-020G-6, copper-constantan) and BLH HT Microminiature thermocouples (TCC-ES 200, copper-constantan) have been used.

TABLE II
INFRARED ABSORPTION BAND ASSIGNMENTS

Isocyanate	2270 cm^{-1}
Urethane	1730
Carbamic Acid	1710
Allophanate	1710
Arylamine Carbamate	1670
Biuret	1660-1680
Diarylurea	1645
Aromatic Carbon-Carbon	1605

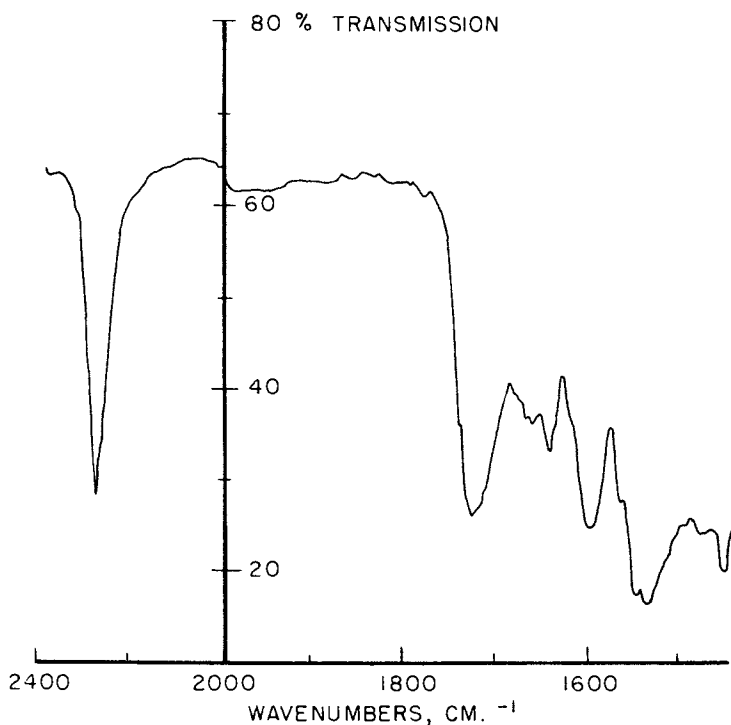


Figure 3. Infrared spectrum of a water-blown polyether polyol polyurethane.

Results and Discussion

Physical Description of Foam Rise. In Figures 4, 5 and 6, the rise profile, rate of foam rise and "gel profiles" for the three formulations "A," "B" and "HR" are summarized. The results for formulations "A" and "B" are similar. The maximum rate of foam rise occurs between 20 and 40 seconds after the end-of-mixing and full rise is achieved in about three minutes. Structure which develops within the rising foam and is measured by "gel profile" occurs after the maximum rate-of-rise and is generally complete before full rise height is achieved. The major difference observed in the case of formulation "HR", Figure 6, is in the shape and timing of the "gel profile," in comparison, the "gel profile" for "HR" begins to rise later, rises more abruptly but is complete at about the same time.

For these formulations, the maximum "foam pressure" (3, 6) of 0.02-0.03 psig is observed at about the same time as the maximum foam rate-of-rise, ca. four inches per minute. It is formally possible to calculate a "foam viscosity" which, after appropriate factors are multiplied to adjust dimensions, will be of the order of 10^4 cps at the time of 30 to 60 seconds after the end-of-mixing. During this time, the foams will have reached 30 to 60 percent of final rise height. Without further analysis of the complexities, it is possible to say that the very low foaming pressure in free-rise, flexible foam coupled with the rapid rise-rate intuitively supports the calculation of a relatively low liquid phase viscosity, about the same as that of the starting polyol at this stage of the foaming process.

Cell-Opening. In the earlier experiments using a cloud point detector, a surge in carbon dioxide evolution was observed reproducibly at a point in the foaming process at which there was a change in shape, an inflexion, in the rate-of-rise curve. In Figure 7, the rate of foam rise is shown as a function of time for Formulation "B." After the maximum rise rate at about 50 seconds, the rate of foam rise decreases rapidly. At 90 seconds, there is an inflexion after which there is a less rapid decline in rise-rate. This point of inflexion corresponds closely to the time the cloud point would be observed.

It should be noted that the shape of the rate-of-rise curve after the maximum rise-rate can be associated with familiar but unwanted situations also related to cell-opening. If after the maximum rate-of-rise, the rise-rate falls sharply to zero as a result of cell-opening, foam collapse is catastrophic. If the decline in rise-rate to zero is sharp without inflexion and without appreciable cell-opening, foam shrinkage is severe.

In Figure 8, the evolution of carbon dioxide from formulation "B" during foaming is shown measured by infrared absorbance at

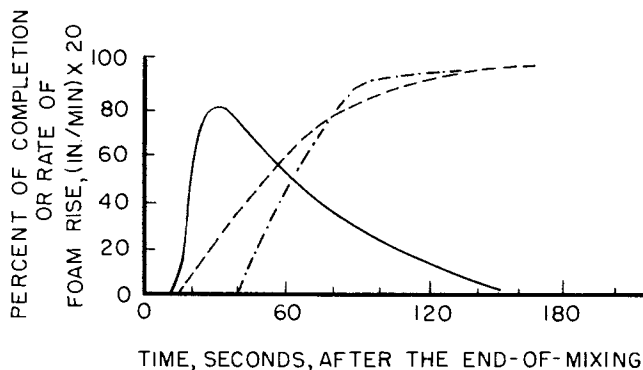


Figure 4. Rise and "gel" profiles, Formulation A. Key: —, rise rate; ---, rise profile; - · - ·, "gel" profile.

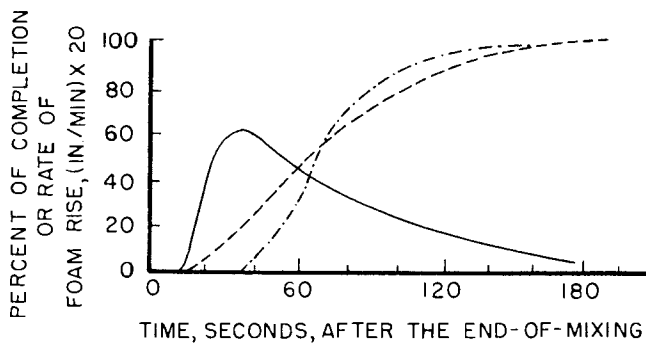


Figure 5. Rise and "gel" profiles, Formulation B. Key: —, rise rate; ---, rise profile; - · - ·, "gel" profile.

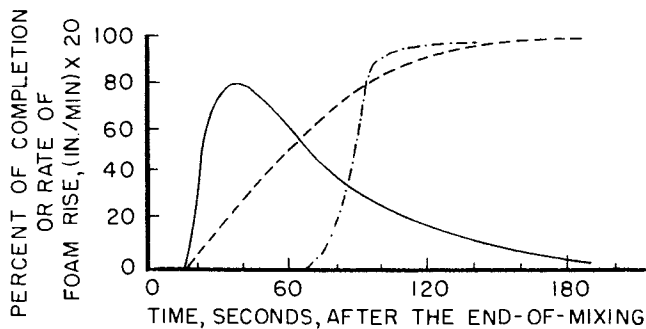


Figure 6. Rise and "gel" profiles, Formulation HR. Key: —, rise rate; ---, rise profile; - · - ·, "gel" profile.

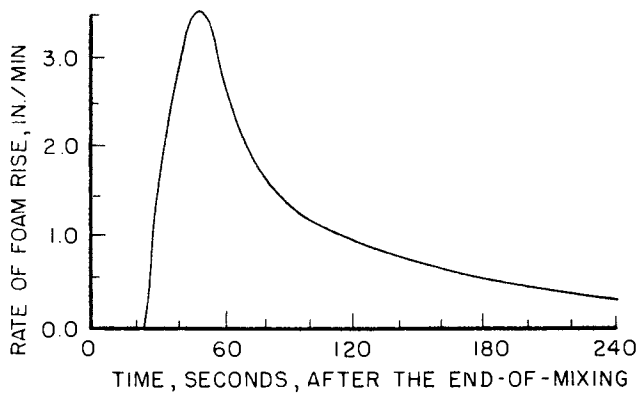


Figure 7. Rate of foam rise, Formulation B.

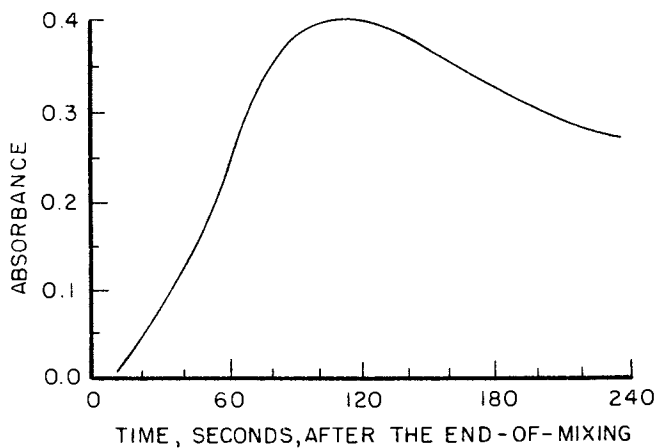


Figure 8. Evolution of carbon dioxide from reacting foam, Formulation B, measured by infrared absorbance at 2320 cm^{-1} .

2320 cm^{-1} of the carrier gas passed over the rising foam. A maximum in absorbance is measured at about 90 seconds corresponding closely to the inflexion in the rate-of-rise curve, Figure 7.

In Figure 9, the rate of evolution of carbon dioxide from formulation "A" is compared with the rise and "gel profiles" for this formulation. A maximum in cell-opening is measured before full rise height is achieved and at the time of an inflexion in the rise-rate curve. This maximum in the rate of cell-opening happens while the processes measured by "gel profile" are occurring.

In Figure 10, this comparison of rate-of-rise and carbon dioxide evolution is shown for "HR" foam. Again a close correspondence is found between a maximum in the rate of evolution of carbon dioxide and an inflexion in the rate-of-rise curve.

This discussion of the cell-opening has been limited to the first two or three minutes after the end-of-mixing. It is clear from these data that carbon dioxide evolution continues and accelerates after these early times of reaction. In Figure 11, the evolution of carbon dioxide from rising, reacting formulations "A" and "HR" is shown for a more extended time. Two maxima are found. The first has been discussed in terms of the inflexion observed in the rise-rate curve. The second maxima, close to the times of full rise of foam, correspond to the times usually taken as cell opening (1) when in large scale foaming larger bubbles erupt from the surface or when there is a very noticeable gas evolution.

From these observations of carbon dioxide evolution from rising, reacting foam, it is clear that there are very broad distributions of cell-opening times. Further, cell-opening appears to be separately associated with two characteristics of the physical rise of foam. First, there is a surge in cell opening at the time when there is an inflexion in the rate-of-rise curve. Later, there is a second maximum near the completion of foam rise. After these maxima, the rate of evolution declines sharply in the case of formulation "A." With high resiliency formulations, significant quantities of carbon dioxide are evolved for an extended time. This difference may be associated with the typically incomplete cell-opening in "HR" foams.

The continuous evolution of carbon dioxide from water-blown foam from the earliest times of reaction is a mechanism for significant heat loss from free-rise foam, the magnitude of which will depend on the scale of foaming. This observation offers an explanation for the departure from adiabaticity, lower than expected maximum reaction temperature, in smaller scale foaming.

Infrared Measurements. In Figure 12, the infrared spectra of two foam formulations are shown which have been quenched on cold salt plates 20-30 seconds after the end-of-mixing. The first formulation is "A"; the second, a similar formulation also at 105 isocyanate index but with 4 phr water. In each, the strong

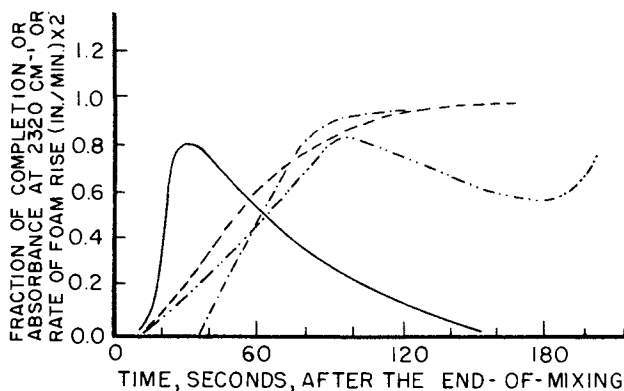


Figure 9. Comparison of the rise profile and "gel" profile of Formulation A with the evolution of carbon dioxide measured by infrared absorbance at 2320 cm^{-1} . Key: —, rate of rise; ---, rise profile; - · - ·, "gel" profile; · · · ·, carbon dioxide evolution.

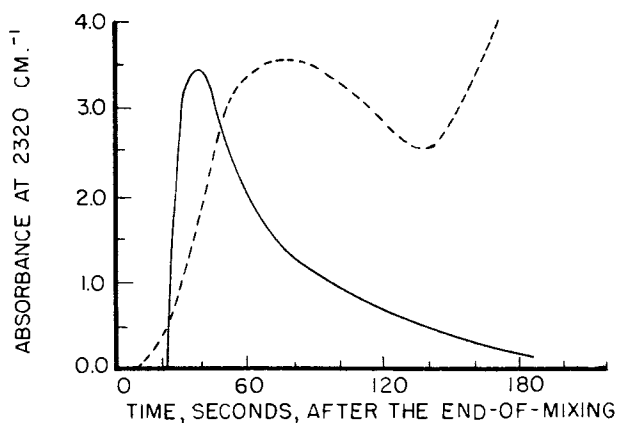


Figure 10. Comparison of the rate of foam rise and evolution of carbon dioxide of Formulation HR. Key: —, rate of foam rise; ---, evolution of carbon dioxide.

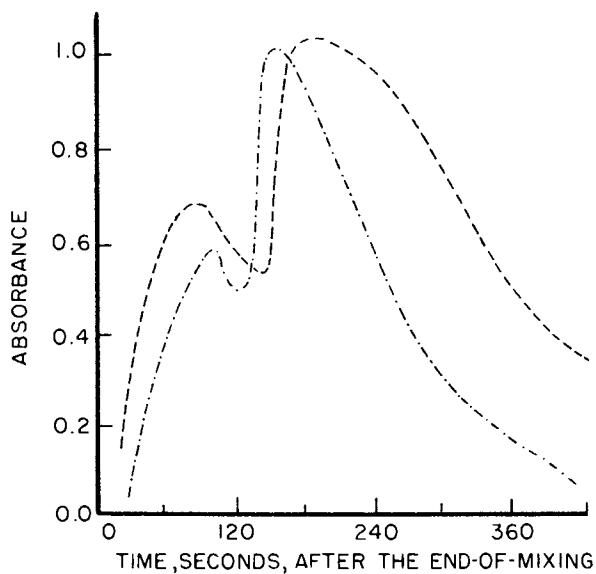


Figure 11. Evolution of carbon dioxide from reacting water-blown urethane foam measured by infrared absorbance. Key: - · - ·, Formulation A; ---, Formulation HR.

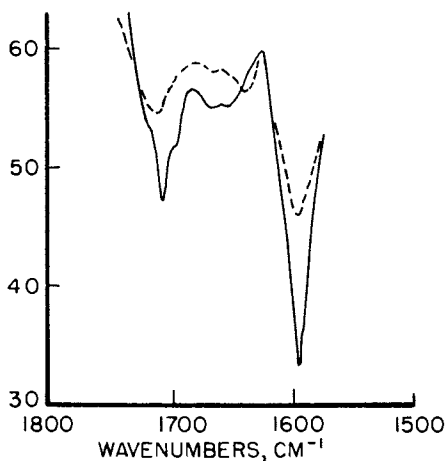


Figure 12. Infrared spectra of two formulations, quenched on cold salt plates. Key: ---, Formulation A, 30 s after the end-of-mixing; —, Formulation A but with four parts water, 20 s after the end-of-mixing.

absorbance at 1710 cm^{-1} typical of carbamic acid is observed. In the high water formulation, weak absorbance in the 1660-1680 region assigned to arylamine carbamate is observed. In Figure 13, these same formulations have been held at 120°C for 30 minutes. The absorbances have changed. Absorbances at 1730 cm^{-1} due to urethane and at 1645 cm^{-1} due to diarylurea have developed.

The transient species, carbamic acid and arylamine carbamate, are present early in the foaming reactions. The absorbance assigned to arylamine carbamate at 1670 cm^{-1} is too weak to interfere significantly with the measurement of the absorbance at 1645 cm^{-1} used to follow the rate of formation of diarylurea in the reacting foams. The absorbance at 1645 cm^{-1} is observed 30-40 seconds after the end-of-mixing, close to the time of maximum rate-of-rise. The absorbance at 1710 cm^{-1} is significant at times less than two minutes. For such early times of reaction, a high resolution infrared spectrophotometer is required. The post reaction species, allophanate and biuret, do not interfere with measurements centering on the earlier stages of the foaming process and when formulations are not of high isocyanate index (3).

In Figures 14, 15, and 16 absorbances due to urethane and substituted urea are given relative to aromatic carbon-carbon, which is constant for any one formulation, as functions of time for formulations "A," "B," and "HR" at 120°C . The general features are that the concentration of urea increases rapidly with time reaching an apparently limiting value after three to five minutes. Urethane concentration increases more slowly than urea over the first eight to ten minutes of reaction after which it continues to increase monotonously for 30 minutes and longer. It is important to note that the early increase in concentration of urea is faster in the "HR" formulation than in either "A" or "B."

In Figure 17, the absorbance due to substituted ureas at 1645 cm^{-1} for the three formulations at early times of reaction are given as functions of time. These data are compared with the rise profile, gel profile and cell-opening times previously discussed, Figures 4-10. Concentrations of ureas are measurable from about the time of the peak rate of foam rise and achieve an apparently limiting value after about four minutes, about the time foam rise is complete. "Gel profile" appears to monitor structural developments in the foams which are occurring at the same time as the increase in urea concentration. In the "HR" formulation, onset of "gel" is delayed. This delay in onset of "gel" in high resiliency foams has often been observed (1, 7). No such delay, however, is observed in formation of diarylurea. While no direct measurement is yet available, it is taken that "gel profile" measures association of the polyureas into domains. In "HR" foams this domain formation is delayed, permitting larger, more completely aligned polyurea domains and accounting for the principal property characteristics which distinguish high resiliency foam (3).

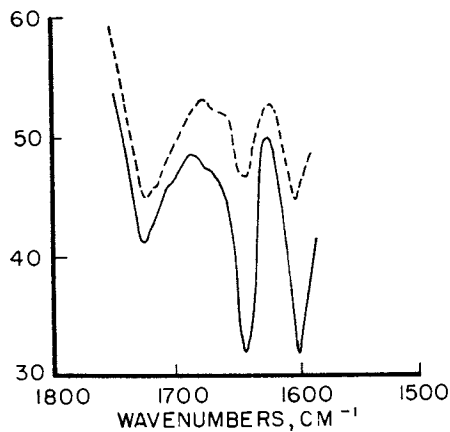


Figure 13. Infrared spectra of two formulations at 120°C. Key: —, Formulation A after 30 min; ---, Formulation A but with four parts water after 25 min.

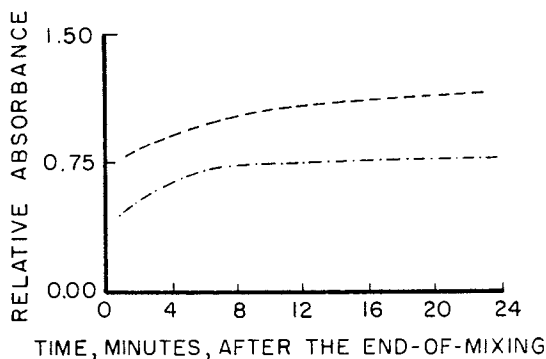


Figure 14. Relative absorbance due to urethane (---) and ureas (-·-·) as a function of time for Formulation A.

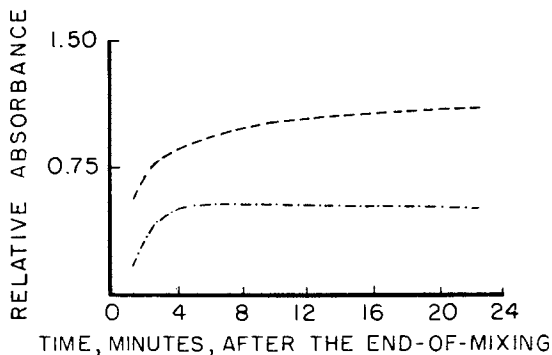


Figure 15. Relative absorbance due to urethane (---) and ureas (-·-·) as a function of time for Formulation B.

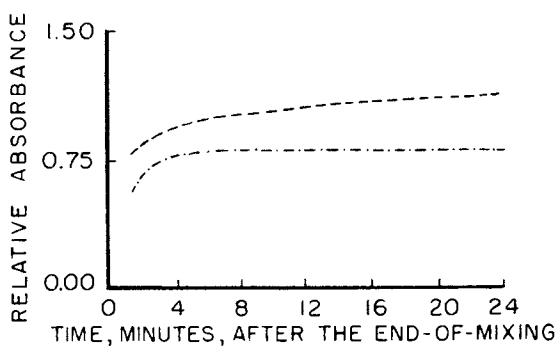


Figure 16. Relative absorbance due to urethane (—) and ureas (- - -) as a function of time for Formulation HR.

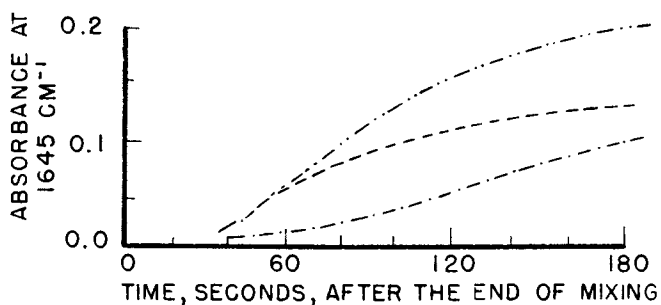


Figure 17. Absorbance due to substituted ureas at 1645 cm^{-1} as a function of time for three formulations: A (---); B (- · - ·); HR (- · · -).

Conclusions

The objective of these studies has been to develop a reaction sequence model for flexible urethane foam which would account for the physical stages in the foaming process evident from foam rise measurements. In Figure 18, a generalized rise profile and "gel profile" is used to summarize the reaction sequence model.

In the earliest stage of foaming, the rising foam is a froth-like multiphase system of expanding gas cells surrounded by liquid phase which contains out-of-phase carbamic acid and arylamine carbamates which tend to stabilize the foam. At about the time disubstituted urea can be measured by infrared in the foam, the system achieves its maximum rate-of-rise. These highly polar species begin to "thicken" the system retarding the rate-of-rise.

As the gas cells expand and begin to pack in the multiphase structure, the regions of closest packing of the cells thin as the still relatively low molecular weight liquid phase drains into the interstices. Rise-rate drops sharply. At this point, there is an initial surge in the rupture rate of the membranes separating the gas cells which permits a relaxing of the foam resulting in an inflexion in the descending rate-of-rise curve. A principally physical gel develops in the liquid phase as the highly polar urea groups aggregate into polyurea domains. Finally, as the foam achieves full rise, urethane network formation becomes the predominant chemical reaction and the foam develops a true, longer-range bulk modulus.

This sequence model of chemical reactions clearly emphasizes the delicate balance required between the urea and urethane reactions in order to achieve the optimum foam structure and properties. The desired supramolecular architecture of foam develops before the principal molecular weight building reactions predominate. Liquid flows and phase development occur while viscosities are still relatively low. The urethane forming reactions then proceed at rates which are reasonable in the light of currently postulated mechanisms (19) crosslinking the system. The timing of this crosslinking is critical relative to the formation of polyureas in order to obtain the stable foam with good bulk modulus.

Abstract. Infrared analysis of reacting foams has been used to determine the sequence of chemical reactions that occurs in the foaming process and to relate this sequence of reactions to the stages evident in the formation of foam measured by rate-of-rise techniques. A reaction sequence model has been developed in which at the earliest stage of foaming, out-of-phase carbamic acid and carbamic acid salts, formed by hydrolysis of isocyanate, are the main species present tending to stabilize the froth-like foam. These species are in turn converted into polyureas. In the latter stages of the reaction sequence, urethane formation becomes predominant as the foam develops substantial bulk modulus

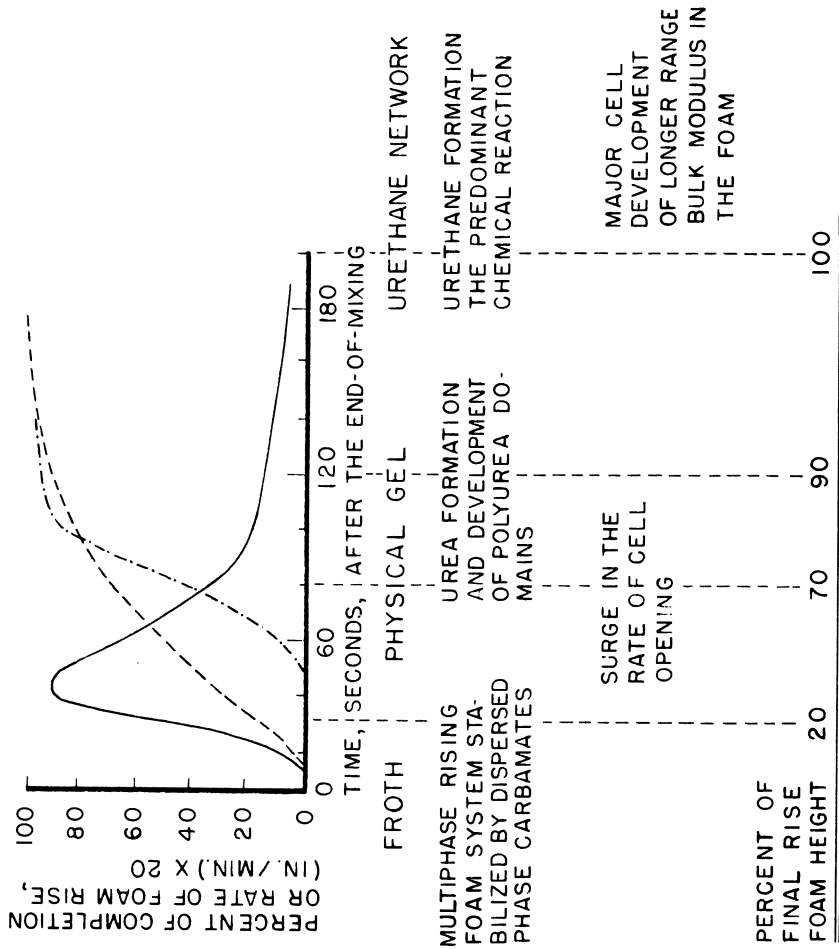


Figure 18. General summary of rise and "gel" profiles indicating the stages evident in the physical formation of foam and the sequence of chemical reactions occurring.

with growth of polymer molecular weight. This sequence of chemical reactions permits polymerization and molecular architecture to be achieved simultaneously to produce useful structures from these very fast reactions.

Literature Cited

1. Rossmly, G. R.; Kollmeier, H. J.; Liddy, W.; Shator, H. and Wiemann, M.; J. Cellular Plastics, 1977, 13, 26.
2. Bailey, Jr., F. E. and Critchfield, F. E.; Polymer Preprints, 1980, 21 No. 2, p. 296.
3. Bailey, Jr., F. E. and Critchfield, F. E., J. Cellular Plastics (submitted for publication).
4. Jennings, R.; J. Cellular Plastics, 1969, 5, 1.
5. Fluidyne Instrumentation, Oakland, California.
6. Van Thuyne, A. and Zeeger, B.; J. Cellular Plastics, 1978, 14, 150.
7. Rowton, R. L.; J. Cellular Plastics, 1980, 16, 27.
8. Kanner B. and Prokai, B.; Advances in "Urethane Science and Technology" Vol. 2, Technomic Publishing Company, Westport, 1973; p. 221.
9. Merten, R.; Lauer, D. and Dahm, M.; J. Cellular Plastics, 1968, 7, 252.
10. Johnson, S. L. and Morrison, D. L.; J. Amer. Chem. Soc., 1972, 94, 1323.
11. Hocker, J. and Born, L.; J. Polymer Sci. Polymer Letters Ed., 1979, 17, 723.
12. Senick, G. A. and MacKnight, W. J.; Macromolecules, 1980, 13, 106.
13. Paik Sung, C. S.; Wu, C. B. and Wu, C. S.; Macromolecules, 1980, 13, 111.
14. Paik Sung, C. S.; Smith, T. W. and Suny, N. H.; Macromolecules, 1980, 13, 117.
15. Rossmly, G.; Kollmeier, H. J.; Liddy, W.; Shator, H.; Wiemann, M.; "Cellular and Non-cellular Polyurethanes," International Conference, Strasbourg, France, June 9-13, 1980; p. 633, Urethane Division of the S.P.I.
16. Hauptman, G.; Dörmer, K.-H.; Hocker, H. and Pfisterer, G.; "Cellular and Non-cellular Polyurethanes," International Conference, Strasbourg, France, June 9-13, 1980; p. 617, Urethane Division of the S.P.I.
17. Zharkov, V. V.; Kopusov, L. I. and Petrov, E. A.; "Cellular and Non-cellular Polyurethanes," International Conference, Strasbourg, France, June 9-13, 1980; p. 657, Urethane Division of the S.P.I.
18. Rossmly, G.; Lidy, W.; Schator, H.; Wiemann, M. and Kollmeier; J. Cellular Plastics, 1977, 15, 276.
19. Gia, Huynh ba; Jerome, R. and Teyssie, Ph; Polymer Preprints, 1980, 21 No. 2, p. 307.

RECEIVED May 14, 1981.

**American Chemical
Society Library
1155 16th St. N. W.**

Urethane Block Polymers

Kinetics of Formation and Phase Development

S. L. HAGER, T. B. MacRURY, R. M. GERKIN, and F. E. CRITCHFIELD

Union Carbide Corporation, South Charleston, WV 25303

Polyurethane elastomers are normally prepared by reacting an aromatic diisocyanate with a mixture composed of a low molecular weight "extender" diol and a higher molecular weight (≥ 1000) macroglycol. This leads to a multiblock copolymer consisting of alternating macroglycol soft segments and diol extended isocyanate hard segments. These segments often separate into "soft" and "hard" phases.

Polymerization in such systems is based on the reaction of isocyanate with hydroxyl groups to form the urethane linkage. Organometallic compounds (especially organotin) are often used to catalyze this reaction in commercial applications such as Reaction Injection Molding. Formation of elastomers with good mechanical properties is dependent on both reaction kinetics and development of two phase morphology.

Most studies of the kinetics of the isocyanate-hydroxyl reaction have been done in systems composed of monofunctional reactants in various solvents (1,2). Even in these ideal systems, which have little resemblance to the more complicated polyurethane formulations, the reaction mechanism and kinetics are not well understood especially for the catalyzed reaction. This coupled with the added complexities encountered in polyurethane systems requires empirical determination of kinetic data if conversion during polymerization is to be predicted. A few kinetic studies on simple polyurethane systems have been reported (3,4). Infrared spectroscopy was used to measure reaction rates in low catalyst formulations (3) while adiabatic temperature rise methods have been used to study fast systems (3,4,5).

Separation of hard and soft phases during polymerization is a complexity that may occur in very incompatible systems. Tirrell *et. al.* (6) have predicted the effect this might have on the polymerization reaction. Experimental evidence for phase separation during polymerization has been limited to observation of turbidity development during the reaction (7,8). Several investigators (9,10) have studied phase

0097-6156/81/0172-0149\$05.00/0
© 1981 American Chemical Society

separation on longer time scales in the final polymer.

In this work, we describe an automated differential scanning calorimetric (DSC) technique that can be used to measure polymerization kinetics for formation of urethane block polymers. The same technique is also used to measure phase separation during formation of polyurethane elastomers and the effect that separation has on the polymerization. The elastomer formulations consisted of modified liquid *p,p'*-diphenylmethyl diisocyanate (MDI), 1,4-butanediol and an (oxypropylene-oxyethylene) macroglycol for the soft segment.

Experimental

The chemicals used in this work are all commercial products and were used as received except as noted. A polyoxypropylene-polyoxyethylene polyol (30% oxyethylene cap-Union Carbide Corporation experimental Polyol 12-56) was used to provide the soft segment. This capping gave a primary hydroxyl content of $\sim 83\%$. The polyether had a number average molecular weight of 2000 and a functionality very close to 2.0. It was free of moisture and acid ($<0.05\%$). Dissolved gases were removed just prior to use by stripping under vacuum for about 30 minutes. Anhydrous butanediol (GAF Corporation) was used as the extender. This was stored over 5A molecular sieve prior to use. Modified liquid MDI (Upjohn Isonate 143L) was used as the diisocyanate. The modified MDI, which contains 5-9% of MDI adducts, had an equivalent weight of 144. It was used instead of pure crystalline MDI so that reactant mixing could be carried out at low temperatures (10-25°C) where the urethane reaction rate is slow. Dibutyltin dilaurate (M&T chemicals) was used as the catalyst.

Reaction mixtures were prepared by weighing together or by combining preweighed amounts of the reactants at room temperature or slightly below. The formulations contained approximately equal equivalents of free isocyanate and hydroxyl. The ratio of hard to soft segment content was controlled by varying the relative amounts of extender and macroglycol in the formulation. Catalyst, when used, was contained in the macroglycol. Little reaction occurred during this formulating stage because the diisocyanate did not dissolve rapidly in the macroglycol and extender but stayed as a separate liquid phase until agitated. After weighing the reactants, they were rapidly mixed and sampled either into a DSC cup and into a precooled DSC cell for immediate analysis or into liquid nitrogen to quench the reaction for later analysis. In some runs the mixture was cast into a mold and specimens were removed and quenched in liquid nitrogen as the reaction proceeded. This "hand-casting" technique for preparing polyurethane elastomers has been described elsewhere (11).

A duPont 990 Thermal Analyzer with Model 910 DSC cell base

was used for measuring thermal changes in the reaction mixture. The cell base was enclosed in a glove box purged with dry nitrogen so that very cold specimens could be transferred to DSC cups and to the DSC cell without moisture pick-up. DSC scans were made from low temperatures (-70°C) by heating at $10^{\circ}\text{C}/\text{min}$ in a dry nitrogen atmosphere. Indium was used to calibrate the temperature scale and heat flow response. The temperature scale was also corrected for the thermal lag of the specimen behind the temperature measured by the instrument. The Thermal Analyzer was interfaced directly to a Digital Equipment Corporation PDP 1134 minicomputer (12). This computer performed real time data collection during the run and did the subsequent data analysis and plotting. The data analysis included transformations of the data contained in the exothermic reaction peak to provide information about kinetic parameters.

Results and Discussion

Kinetic Analysis of DSC Data. The reaction of isocyanate with hydroxyl groups is highly exothermic and appears as a strong exothermic peak in the DSC heating curves (Figure 1). This peak can be extracted from the overall DSC curve by subtracting a specific heat baseline from reaction onset to completion. A linear change in specific heat with temperature was assumed. This procedure yields a plot of the heat generation rate as a function of temperature which can be integrated on a time base to give the total heat generated also as a function of temperature (Figure 2). If we assume a constant heat of reaction independent of conversion and no significant interferences from side reactions then this data is readily converted to fractional reaction rate and fraction remaining as a function of temperature. These data can then be fit to various kinetic models. The assumptions made in converting the DSC peak to reaction data are essentially the same as those used in studies by the adiabatic temperature rise method (3,4,5). Richter *et. al.* (3) have discussed these in some detail and have concluded that they should not introduce a significant error. Phase separation and gelation are two additional factors that may alter the reaction rate. Indeed, the discontinuity seen (Figures 1,2) in the DSC reaction peak for a typical polyurethane formulation (47.8% hard segment content) is attributed to phase separation (discussed later). This often limits the kinetic analysis of data from systems containing butanediol extender to low conversion ($<60\%$). Additionally, the kinetic analysis may be complicated by reactivity differences between the hydroxyl groups on the macroglycol and those on the extender. This complication was neglected for the extended system studied here because of the low percentage ($\sim 20\%$) of total hydroxyl content contributed by the macroglycol.

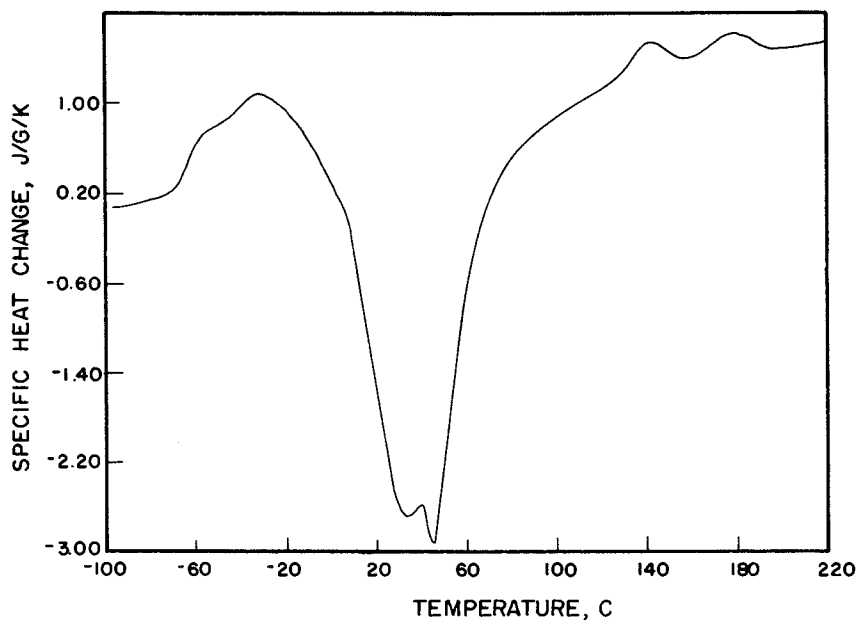


Figure 1. DSC curve of urethane reaction formulation (extended), 18 mg specimen heated at 10°C/min in nitrogen.

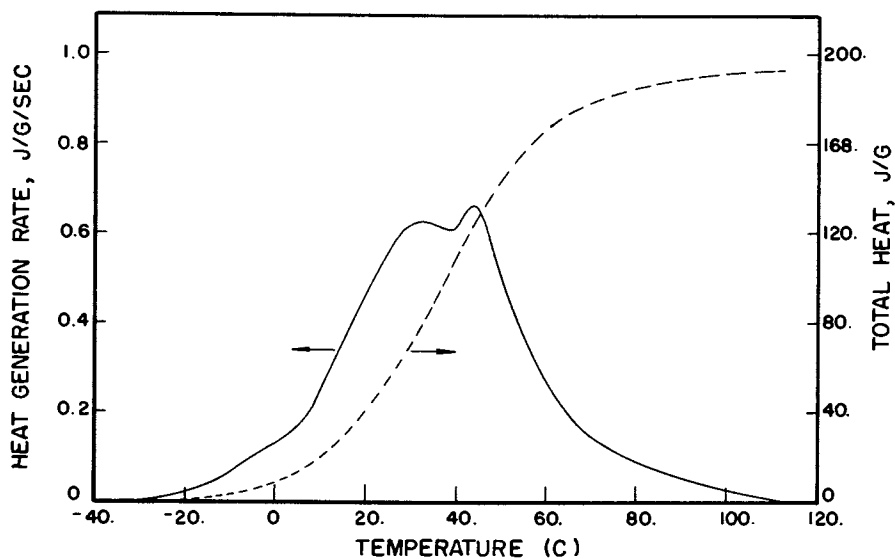
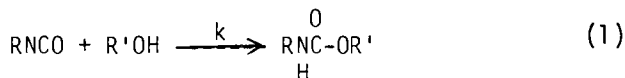


Figure 2. Exothermic reaction peak and integral after peak isolation from DSC curve (Figure 1).

In its simplest form the urethane reaction is depicted by:



An n th order rate equation is normally used (3,4,5) in fitting the reaction data for both catalyzed and uncatalyzed reactions

$$- \frac{d[\text{C}]}{dt} = k [\text{C}]^n \quad (2)$$

where $[\text{C}]$ is the concentration of isocyanate or hydroxyl groups and n is an empirically determined reaction order.

Incorporating the Arrhenius expression for k and converting to fractional reaction rate ($F = [\text{C}]/[\text{C}_0]$), we obtain

$$R(F) = - \frac{dF/dt}{F^n} = A [\text{C}_0]^{n-1} \exp(-E/RT) \quad (3)$$

For catalyzed systems the apparent k and A values in equations 2 and 3 will be dependent on catalyst concentration. This dependence has also been fit with an n th order expression (3)

$$k = k_c [\text{CAT}]^{n_c} \quad A = A_c [\text{CAT}]^{n_c} \quad (4)$$

where k_c is the rate constant and A_c is the pre-exponential factor for the catalyzed reaction.

If equation 3 is to be used in fitting reaction data then a reasonably straight line should be obtained for some value of n when $\log(R(F))$ is plotted vs $1/T$. A graphical approach similar to that described by Hauser and Field (13) was employed to determine n . The order was incrementally varied and the n value giving the "best" straight line selected to fit the data (Figure 3). In some cases where this method did not reveal a clear order preference, isothermal reaction studies were also run by DSC. Here the heat generation rate was measured vs time at constant temperature to yield a plot (after computer transformation) of \log reaction rate vs \log fraction left (Figure 4). The slope of this line can then be taken as the reaction order for fitting the dynamic heating data. Isothermal studies were limited to low temperatures and low catalyst levels so that excessive temperature rise did not occur in the specimen during the measurement.

Polymerization Kinetics. DSC reaction studies were performed on catalyzed and uncatalyzed formulations containing diisocyanate (modified MDI) and polyether macroglycol (ethylene oxide capped polyoxypropylene) or containing diisocyanate, macroglycol and butanediol. Figures 1-4 demonstrate the procedure for extracting kinetic data from the DSC reaction profile and provide a typical example for a catalyzed (0.5 mM dibutyltin dilaurate) formulation containing 52.2% macroglycol,

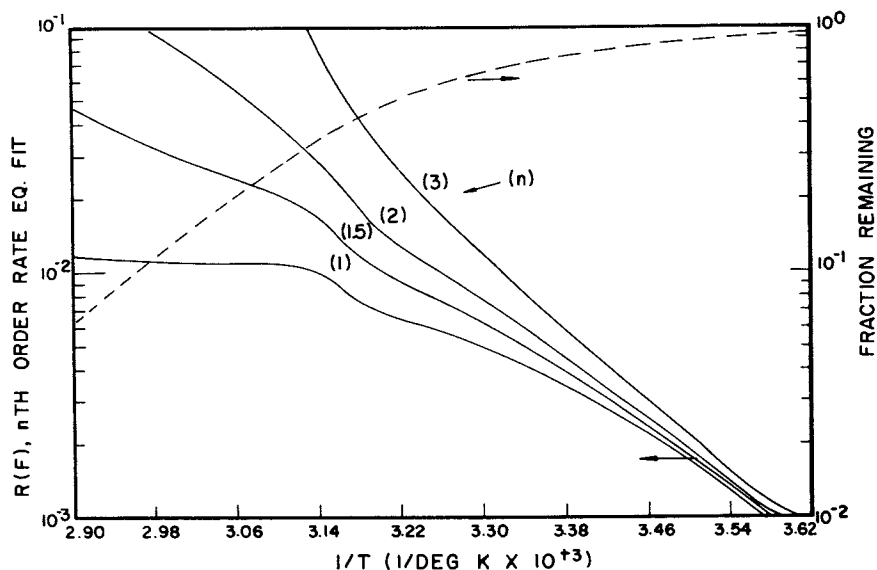


Figure 3. The $R(F)$ function (see test) obtained by computer reduction of reaction data in Figure 2 assuming reaction orders of 1.0, 1.5, 2.0, and 3.0.

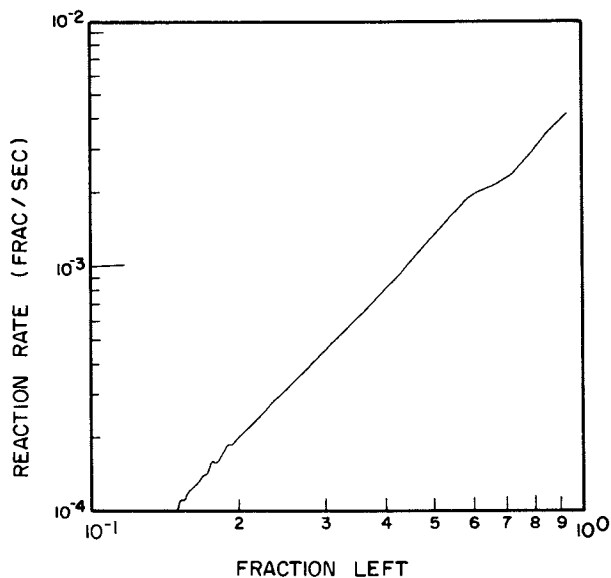


Figure 4. Log fractional reaction rate vs. log unreacted fraction taken from isothermal DSC measurement of heat released during urethane polymerization (extended formulation); 32°C.

38.6% diisocyanate and 9.2% BDO. This ratio of macroglycol/diisocyanate/BDO was used for most of this study and will be referred to as the extended formulation. Uncatalyzed systems give a substantially broader and higher temperature exothermic peak. For example the first reaction peak occurs at 35°C with 0.5 mM catalyst compared to ~70°C without catalyst. Higher catalyst levels reduce the peak to still lower temperatures. Systems without the BDO extender (86.6% macroglycol, 13.4% diisocyanate, unextended formulation) yield smaller reaction peaks at slightly higher temperatures (39°C for system with 0.57 mM catalyst). This is due to the lower concentration of reactive groups in the stoichiometric mixture. No discontinuity or second peak is seen in the unextended formulation. For the extended formulation the reaction of BDO with isocyanate accounts for almost 80% of the total heat released with the remaining 20% coming from the macroglycol-isocyanate reaction.

Table I summarizes the kinetic parameters extracted from the DSC data for these formulations. The reaction in the uncatalyzed systems gave a poor fit to an n th order reaction model especially above 50% reacted. This may be due to autocatalysis by carbamate groups (1,2) as they form or complexities due to minor impurities in these systems. Second order kinetics provided a reasonably good fit to the early portion (<50%) of the reaction and were used to obtain the apparent pre-exponential factors (A) and activation energies (E) shown in Table I. Relatively small values of E and A were obtained in both the extended and unextended formulations without catalyst.

A second order reaction model gave a good fit to the polymerization reaction in both the catalyzed formulations. In the case of the extended system, this was also confirmed by isothermal measurements at 32°C (Figure 4). The slope of the plot of log reaction rate vs log fraction remaining was 2.1 before the discontinuity and ~2 afterwards. This implies that second order kinetics are still followed after the discontinuity which occurs between 55 and 60% reacted.

The activation energy and pre-exponential factors for the catalyzed reactions were significantly higher than for the uncatalyzed ones (Table I). This causes the exothermic peak in the DSC heating curve to be much sharper than that obtained without catalyst. In spite of their higher activation energies, the catalyzed reactions occur much faster due to the very large increase in the pre-exponential factors. Adiabatic temperature rise studies of polyurethane kinetics have shown similar changes in E and A with catalysis (5). The presence of extender seems to decrease A and possibly E although the effect is substantially less than that of the catalyst.

Table I
Kinetic Parameters for Polymerization of
Extended (48% Hard Segment) and
Unextended Urethane Formulations

<u>System</u>	<u>N</u> ^a	<u>N</u> _c ^b	<u>A</u> (1/M·s)	<u>E</u> (kJ/M)
Uncatalyzed-Unextended	2 ^c	-	5 × 10 ⁴	50
Uncatalyzed-Extended	2 ^c	-	5 × 10 ³	41
Catalyzed-Unextended	2	1.1	1.7 × 10 ¹³	69
Catalyzed-Extended	2	0.65	3.5 × 10 ¹⁰	64
Est. Std. Dev. ^d	-	+0.1	e	+3

- a. Concentration dependence on active groups.
 b. Catalyst concentration dependence.
 c. Poor fit to nth order model.
 d. Catalyzed systems.
 e. Standard deviation of $\sim \pm 0.3$ in log (A).

Catalyst concentration dependences in the two systems were obtained by making measurements at several catalyst levels between 0.1 and 2mM. A dependence of 1.1 was found for the unextended system by performing a least squares fit of the log *k* vs log [Cat] data (Figure 5). The rate constants were calculated using the A and E values from fitting the DSC data and subtracting the rate constant predicted for the uncatalyzed reaction. This correction was less than 20% except at very low catalyst levels (<0.2 mM). The value of 1.1 is within experimental uncertainty of 1.0, which is the value predicted by most reaction models involving catalyst complexation with one or both of the reactants as the initial step in the reaction scheme (1,2). The extended formulation yields a catalyst concentration dependence of 0.65, which is significantly below that of the unextended system. Catalyst dependences between 0.5 and 1.0 have been observed in other urethane systems (3) and have been attributed to a preactivation step for the catalyst, possibly ionization, prior to complexation. Although this data is consistent with such a pathway, the complexities involved in the extended system dissuade against reaching any definitive conclusions concerning the reaction mechanism based solely on these measurements. Similarly, the A and E values that have been obtained are parameters for fitting the reaction data. Their significance in terms of kinetic theories is open to question.

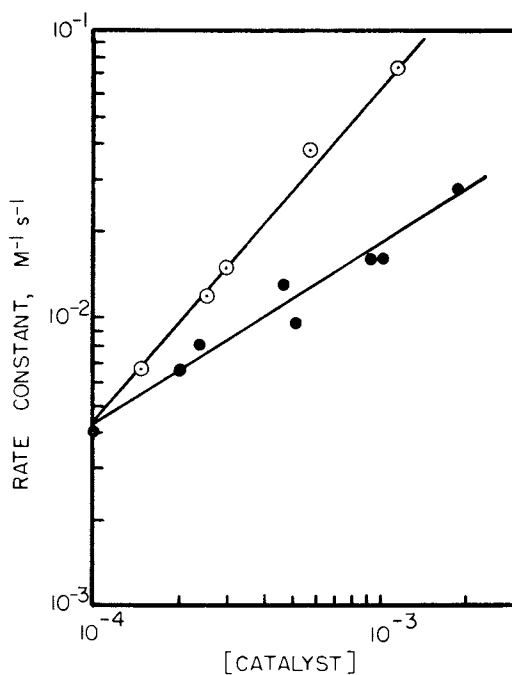


Figure 5. Catalyst dependence of rate constants (50°C) for polymerization of extended (●) and unextended (○) formulations.

These data do, however, provide the information needed to approximately predict the rate constant as a function of temperature and catalyst level. Assuming the catalyzed and uncatalyzed rate constants are additive we obtain for the BDO extended system

$$k(\text{M}^{-1}\text{s}^{-1}) = 5.1 \times 10^3 \exp(-4900/T) + 3.5 \times 10^{10} [\text{CAT}]^{0.65} \exp(-7660/T). \quad (5)$$

The first term in this expression represents the contribution from the uncatalyzed reaction and the second term, that from the catalyzed reaction. At typical reaction temperatures (above 25°C), the catalyzed reaction dominates even at very low catalyst levels (0.1 mM) because of the much larger pre-exponential factor. Equation 5 can be used to provide rate constants which could reasonably predict conversion vs time at a given temperature up to at least 60% reacted. The accuracy of the prediction will decrease above about 75°C since this requires extrapolation outside the temperature range in which the fitting was done. Also use of the rate constants at high conversion are likely to be less satisfactory due to the discontinuity observed in the reaction profile for the extended formulation at 55 to 60% reacted and a variety of other factors (side reactions, gelation) that are likely to become important especially above 90% reacted.

Phase Development During Polymerization. Polyether based polyurethanes are known to phase separate faster than those based on polyester soft segments. Indeed, formulations like those used in this work become opaque during the polymerization indicating that domain superstructures (14) have formed. Development of this opacity has been used (7,8) to indicate phase separation during the polymerization although questions arise as to whether formation of small domains that do not scatter visible light occur before this.

The discontinuity in the DSC reaction peak that leads to the second maximum is believed to be caused by the onset of phase separation. Visual observations of specimens (extended formulation) during DSC scans revealed that the first indication of opacity occurs slightly (within ~3°C) after the onset of this discontinuity. Small samples and slow heating (5°C/min) were used when making these observations to reduce the time lag between thermal changes in the sample and detection by the DSC.

The source of the increased rate of heat generation may be due to physical and/or chemical changes. Spontaneous separation of the hard and soft phases could release energy and produce a second peak. The observed magnitude of the change, ~10 J/g, is larger than would be expected from phase separation unless the hard segments crystallize as well. One

or more endothermic peaks, that may represent melting of crystalline hard segments formed during the polymerization, have been detected by DSC after the exothermic reaction peak (Figure 1). However, these do not always occur whereas the reaction discontinuity is highly reproducible. Another explanation is that phase separation leads to an increase in the reaction rate. This could occur if the material that separates is predominantly reacted thus concentrating the unreacted components in the remaining phase. An example of this would be separation of reacted hard segment leaving behind a phase consisting of unreacted components and reacted soft segments. A definite choice between these hypotheses is not possible based on this data.

To confirm that phase separation begins in the extended formulation at about 60% reacted, studies were made of changes in the low temperature glass relaxation during the course of the polymerization. This was done by removing specimens during reaction molding and quenching in liquid nitrogen to freeze the reaction and morphological state. These were then transferred cold ($< -40^{\circ}\text{C}$) to DSC sample pans and then into the DSC (see Experimental Section). Figure 6 shows the change in the glass relaxation as a function of conversion for the partially reacted mixtures (to avoid confusion, curves I-III were not plotted through the exothermic peak). Early in the reaction a single sharp glass relaxation is observed due to the amorphous mixture. This relaxation shifts to higher temperatures as the reaction proceeds probably due to the increase in molecular weight. At higher conversions, the transition broadens and finally shows evidence of splitting into two distinct parts at about 99% reacted (240 seconds in the mold at $\sim 100^{\circ}\text{C}$). The lower temperature region resembles the soft segment relaxation after post-cure of the polymer for 16 hours at 100°C . The higher temperature portion may be either a glass relaxation for a loosely formed hard phase or possibly a melting transition for this phase. No substantive transition is observed in this temperature range after post-cure, instead a distinct hard segment melting peak is seen at 184°C (not shown) with an apparent heat of fusion of 13.4 Joules per gram of sample (28 Joules per gram of hard segment).

Much of the broadening in the glass relaxation that occurs during the polymerization is likely due to the early stages of phase separation. After separation has begun, the onset temperature of this transition should indicate the most separated soft segments while the completion temperature should indicate the most separated hard segments. These two temperatures are found to increase at about the same rate up to approximately 60% reacted (Figure 7), which is to be expected if we are measuring the onset and completion of a one phase system. After 60% reacted, however, the onset temperature peaks and drops while the completion temperature continues to

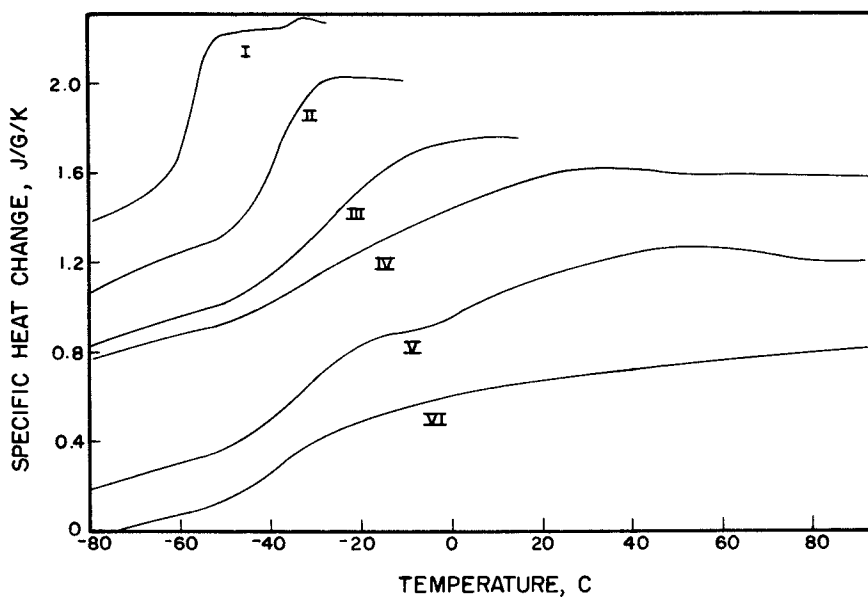


Figure 6. Low-temperature glass relaxation for reaction specimens taken from mold and quenched in liquid nitrogen at various times during the polymerization. Key: I, 1% reacted at 17 s; II, 54% reacted at 40 s; III, 84% reacted at 45 s; IV, 95% reacted at 60 s; V, 99% reacted at 240 s; VI, post-cured 16 h at 140°C.

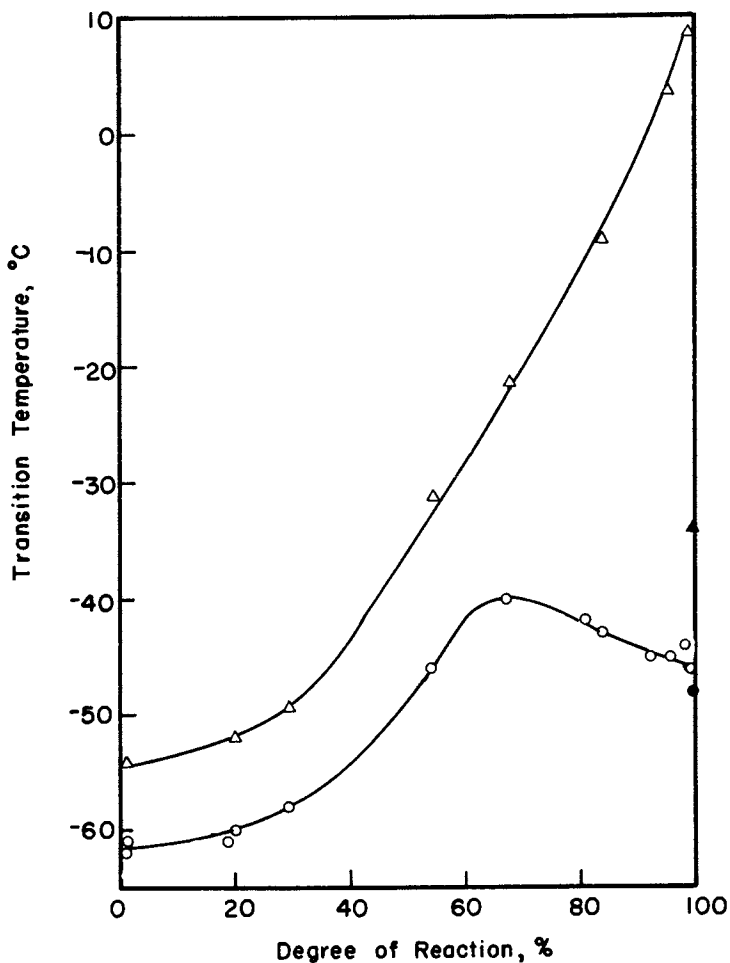


Figure 7. Change in onset (O) and completion (Δ) of low-temperature transition for specimen removed from mold and quenched at various degrees of reaction; solid points are for post-cured specimen (see Figure 6).

increase rapidly with conversion. The point where these two temperatures separate rapidly is very near 60% reacted; which is essentially the same as the point of occurrence of the discontinuity in the reaction peak (\sim 57% reacted). This combined with the opacity observations is strong evidence that the discontinuity in the DSC curve is caused by phase separation.

The sharpness of the DSC discontinuity makes this a good means of identifying accurately the point during the reaction at which phase separation begins. From the continuous integral of the reaction peak (Figure 2) we can determine the total amount of heat released during the reaction in the DSC and the amount before and after separation. Measurements on systems in which reaction prior to loading into the DSC was minimized by using low catalyst levels and low temperature mixing yielded an apparent heat of reaction of 85 kJ/eq. Calorimetric measurements (15) have given values in the range 82-105 kJ/eq for the reaction of various isocyanates with n-butyl alcohol. The degree of reaction when phase separation occurs in the urethane formulations was calculated using

$$\alpha = \frac{\Delta H_T - \Delta H_U}{\Delta H_T} \quad (6)$$

where ΔH_T is the total heat of reaction expected based on the initial concentration of -OH or -NCO assuming 85 kJ/eq as the heat of reaction and ΔH_U is the measured reaction heat released after separation taken from the DSC reaction data. The first detectable deviation from the reaction profile was taken as the onset of separation. This procedure can be used for samples that are partially reacted when loaded into the DSC since it is not necessary to measure the total heat of reaction.

The degree of reaction at phase separation was determined by this method for a series of formulations based on BDO, modified MDI, and the polyether macroglycol in which the soft segment content was varied. Stoichiometry was maintained by changing the relative amounts of BDO and macroglycol and the catalyst level was kept constant (0.3 mM) to maintain roughly the same reaction temperature (Table II, Figure 8). (NOTE: Measurements at different catalyst levels have not shown a significant dependence of separation on temperature.) Phase separation occurred earlier in the reaction as the soft segment level was decreased from 73% ($\alpha=1.0$) to 28% ($\alpha=0.45$). At still lower soft segment levels separation appeared to occur later in the reaction; however, it was difficult to drive the reaction to completion due to reduced mobility in these rigid, high hard segment systems.

By decreasing the soft segment content we are increasing the length of the hard segments that exist at a particular degree of reaction. Table II lists the number and weight

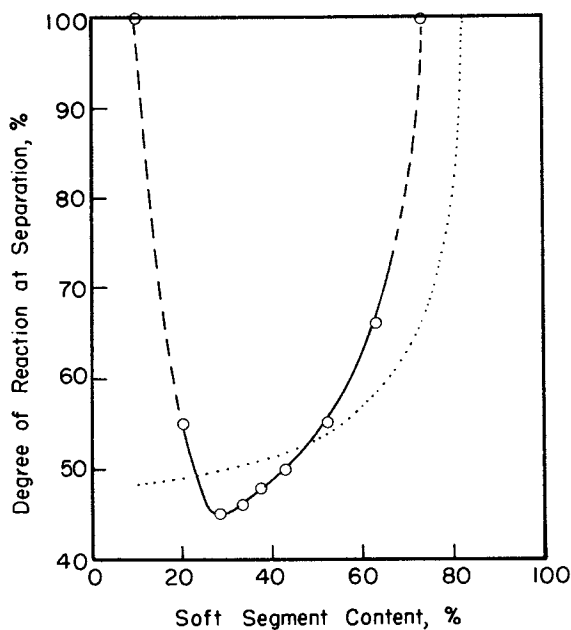


Figure 8. Effect of soft segment content on point of phase separation during polyurethane polymerization as indicated by discontinuity in DSC reaction profile. Dotted line shows theoretical prediction assuming separation at constant number-average sequence length (1.3) of hard segments (see text).

average sequence lengths calculated at the time of phase separation by applying equations developed by Lopez-Serrano *et al.* (16) and making several assumptions. These equations are

$$\bar{N}_n = \frac{1}{1 - r_1 q_1^2} \quad (7)$$

$$\bar{N}_w = \frac{1 + r_1 q_1^2}{1 - r_1 q_1^2} \quad (8)$$

where in our case \bar{N}_n is the number average length of isocyanate-BDO units, \bar{N}_w is the weight average length of these, r_1 is the initial ratio of BDO concentration to isocyanate and q_1 is the fractional conversion of BDO at the point of phase separation. These equations assume a first order concentration dependence on the -NCO and -OH and equal reactivity at both ends of the molecules. The reader is referred to reference 16 for a derivation and complete discussion of these equations. If we assume that the hydroxyls on BDO react at the same rate as those on the macroglycol then q_1 is equal to ∞ and \bar{N}_n and \bar{N}_w are readily calculated from the experimental data.

Table II

Fraction of Functional Groups Reacted At Phase Separation (∞) Plus Calculated Number Average and Weight Average Hard Segment Sequence Lengths at Separation As a Function of Soft Segment Content.

Soft Segment Content (%)	∞	\bar{N}_n	\bar{N}_w
10	1.0	-	-
20	0.55	1.40	1.81
28	0.45	1.23	1.46
33	0.46	1.24	1.47
37.5	0.48	1.26	1.51
43	0.50	1.27	1.54
52.2	0.57	1.35	1.69
63	0.66	1.35	1.69
73	1.0	-	-

Based on these equations and assumptions, phase separation is found to occur at \bar{N}_n of 1.23 to 1.40 and \bar{N}_w of 1.46 to

1.81 over the soft segment range from 28-63% (Table II). This indicates that very short hard segments, probably containing only two isocyanate molecules, can phase separate. Also it appears that phase separation occurs at about the same hard segment length in these systems. The dotted line in Figure 8 shows the predicted curve if phase separation always occurred at $\bar{N}_n = 1.3$. Excluding the very low soft segment formulations, the experimental data give a curve similar to the predicted curve except for a steeper rise with increasing soft segment content. This deviation could be due, at least in part, to the dynamic nature of the DSC measurement which may delay separation by different amounts in these formulations depending on the rate of separation. Also, the kinetic data (previously discussed) imply that the reaction rate of hydroxyl on macroglycol is slightly different from that of the extender and this would alter the segment molecular-weight development.

Recent light transmission measurements by Castro *et. al.* (8) on systems similar to those studied here have yielded similar results. Using opacity development as an indicator, they find that phase separation occurs at N_n equal to ~ 1.3 .

Conclusions

Differential scanning calorimetry can be used to measure both reaction kinetics and phase separation during the polyurethane polymerization. Automated data reduction greatly facilitates the measurement. Using these methods kinetic expressions were developed for predicting rate constants as a function of temperature and catalyst level for a polyether based polyurethane. Phase separation was detected by DSC during the polymerization by measuring broadening of the low temperature glass relaxation. The onset of this broadening was found to correlate with development of opacity in the reacting mixtures and with a distinct discontinuity in the DSC reaction peak. This discontinuity coupled with the integrated reaction peak offers an excellent means for rapidly measuring phase separation. Decreasing soft segment content (70 \rightarrow 30%) causes phase separation to occur at a lower degree of reaction. Estimates of sequence lengths reveal that separation occurs at roughly equal hard segment length over a wide compositional range and that very short lengths, probably only two MDI units long, are likely to separate.

Acknowledgements

The authors wish to acknowledge the laboratory assistance of G. S. Cook and R. L. Rollins, and useful technical discussion with K. L. Hoy, C. W. Macosko, R. E. Camargo, and E. L. Thomas.

References

1. S. L. Reegen and K. C. Frisch in "Advances in Urethane Science and Technology", K. C. Firsch and S. L. Reegen, eds., Vol. 1, pp 1-30, 1971.
2. A. Farkos and G. A. Mills in "Advances in Catalysis", D. D. Elex, P. W. Selwood and P. B. Weise, eds., Vol. 13, pp. 393-446, Academic Press, New York, 1962.
3. E. B. Richter and C. W. Macosko, *Polym. Eng. and Sci.*, 18, 1012 (1978).
4. E. Broyer, C. W. Macosko, F. E. Critchfield and L. F. Lawler, *ibid.*, 18, 382 (1978).
5. E. C. Steinle, unpublished work.
6. M. Tirrell, L. J. Lee and C. W. Macosko in "Polymerization Reactors and Processes", pp 150-179, ACS Press, Washington, D. C. (1979).
7. R. M. Gerkin, unpublished work.
8. J. M. Castro, F. Lopez-Serrano, R. F. Camargo, C. W. Macosko and M. Tierrell, submitted to *J. Appl. Polym. Sci.*
9. cf. S. L. Cooper, R. W. Seymour and J. C. West in "Encyclopedia of Polym. Sci. & Tech.", Supp. Vol. 1, H. F. Mark and N. M. Bikales, eds., p. 521, 1976.
10. G. L. Wilkes and R. Wildnauer, *J. Appl. Physics*, 46, (1975).
11. R. J. Zdrahala, R. M. Gerkin, S. L. Hager and F. E. Critchfield, *J. Appl. Polym. Sci.*, 24, 2041 (1979).
12. S. L. Hager, *Thermochimica Acta*, 26, 149 (1978).
13. H. M. Hauser and J. E. Field, *Thermochimica Acta*, 27, 1 (1978).
14. Y-J. P. Chang and G. L. Wilkes, *J. Polym. Sci.: Polym. Phys. Ed.* 13, 455 (1975).
15. E. G. Lovering and K. J. Laidler, *Can. J. of Chem.*, 40, 26 (1962).
16. F. Lopez-Serrano, J. M. Castro, C. M. Macosko and M. Tirrell, *Polymer*, 21, 263 (1980).

RECEIVED April 30, 1981.

Flow Mechanics of Polyurethane Foam Formation

J. T. LINDT and W. KOSTRZEWSKI

Department of Metallurgical and Materials Engineering, University of Pittsburgh,
Pittsburgh, PA 15261

The foam architecture is resulted from a complex interaction between the physico-chemical and operating parameters characterizing a given processing situation. While considerable attention has been devoted to the chemistry and, to a somewhat lesser extent, to the morphology of polyurethanes, only a severely limited amount of information is available on flow phenomena occurring during the foam formation. As a result, rational methods for neither rheological characterization nor scale-up have been developed. Large scale experiments are often required to analyze and solve processing problems.

The inability to analyze flow-related material defects is a serious drawback; shear and normal stresses associated with the foaming process can be responsible for a variety of defects such as cell structure irregularities, large voids, excessive curvature or even splitting of the foam-free surface, local density gradients and leakages from molds.

Presently, an exploratory attempt is made to examine, in phenomenological terms, the flow behavior of a water-blown urethane foam prior to appreciable chemical gelation taking place. The objectives are:

- to generate a quantifiable flow field associated with appreciable (macroscopic) shear stresses,
- to investigate the nature of momentum transfer involved,
- to make a quantitative assessment of the time-dependent shear stress field leading to an evaluation of the apparent viscosity as a function of time,
- to examine briefly the effect of the flow field on the terminal foam morphology.

0097-6156/81/0172-0167\$05.00/0

© 1981 American Chemical Society

GROWING FOAM AS A FLUID MEDIUM

From a phenomenological standpoint, gas-liquid mixtures can be divided into dispersions, macro-mixed and stratified systems. Fine dispersions are considered pseudo-homogeneous, their flow mechanics being essentially those established for true homogeneous fluids.

Fine dispersions contain fluid particles that are small by both geometrical and dynamic criteria. Thus, the growing foam may be regarded as a pseudo-homogeneous mixture as long as:

- the bubbles are small when compared to the characteristic dimension of the apparatus, and
- the bubble Reynolds number is vanishingly small ($Re_B \ll 1$).

In growing polyurethane foams these two criteria are usually satisfied.

In the following treatment the foaming medium is considered a pseudo-homogeneous fluid. In contrast to conventional fluids, however, this fluid gradually expands as the foaming progresses, generating a macroscopic flow field of measurable intensity. The velocity is a function of both the position and time.

Analogously to the well-behaved systems, the flow of the foaming mass should be described by a pressure drop-flow rate relationship (the foam flow characteristic). (In view of the fact that the flow is generated by volume expansion only, the foam flow characteristic, for a given formulation and a given set of geometrical and operational conditions, can be characterized by a (unique) pressure drop-nominal density function.)

APPROACH PROBLEM DEFINITION

Using a continuum rather than cellular model implies that the growing foam is regarded as a fluid with a continuously distributed source of flow. Hence, the flow rate is also a function of position; the (hydrodynamic) pressure gradient is resulted from inertia, gravity and stress mechanisms operating in the fluid.

Although the proper understanding of the overall momentum transfer pattern is the ultimate goal, at this stage, a choice has been made to concentrate on a study of the shear component of the stress field. At the same time, it is convenient to suppress the accelerating nature of the flow. (In addition to the methodological aspect stressing a separation of the major participating transport mechanisms, this choice has been supported by the belief that viscous stresses concentrated in the neighborhood

of the mold walls are responsible for a variety of defects in the foam structure observed in large scale processing.)

The relative importance of the viscous stresses can be increased by letting the foam flow through a narrow channel or a capillary: e.g., when connecting a capillary of inner diameter d to a cylindrical reservoir of diameter D serving as a foam source, a flow governed by viscous forces establishes in the capillary as long as $d \ll D$, and the capillary Reynolds number being sufficiently small. (Additionally, the above criteria for pseudo-homogeneous mixture must be satisfied.)

Accepting this concept, the present problem is conveniently formulated as one of laminar flow through a circular tube. The axial pressure profile and flow rate are identified as the key macroscopic variables.

The availability of the pressure gradient-flowrate relationship forms a basis for the determination of apparent viscosity.

A post-mortem evaluation of the terminal cell structure in the capillary is to serve the purpose of a qualitative examination of the processing-morphology correlation.

EXPERIMENTAL

The apparatus built to measure the intensity of viscous forces is shown in Fig. 1. A cylindrical steel vessel of an inner diameter of 122 mm and height of 150 mm is used as a source of foam. It is fitted with a carefully sealed aluminum lid 12.7 mm thick. A perspex thick-walled "capillary" of 12.7 mm inner diameter has been installed at the center of the lid; its length has been varied from 600 to 1500 mm by 300 mm increments. In all cases, strain gauge pressure transducers (Entran EPS-1032) have been installed at 1/4, 1/2 and 3/4 of the total tube lengths. Temperatures at the inlet and outlet of the tube were measured using thermocouples. After the passage through the instrumented test section the foaming mass was collected in a cylindrical overhead vessel of an inner diameter 92 mm. The foam rise has been monitored using a modified ultrasonic depth measuring device (CRANE PRO-TECH, MODEL UDX). To facilitate the measurements of the foam rise a styrofoam float was installed in the overhead vessel.

Output signals from the pressure and ultrasonic transducers and from the thermocouples were registered using multichannel recorders (HOUSTON INSTRUMENT, OMNISCRIBE B-5000).

As a model system, a conventional flexible urethane foam formulation developed by Union Carbide for automotive seat applications has been used. It consists of:

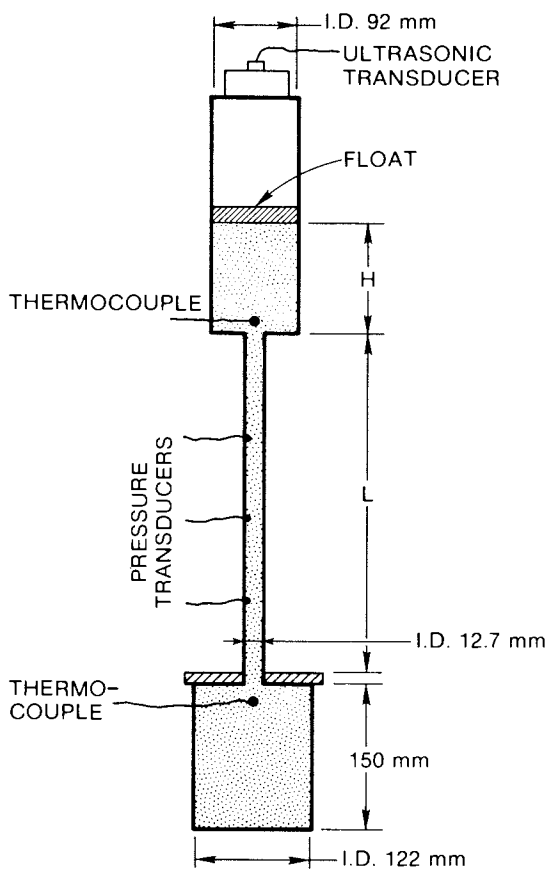


Figure 1. Scheme of the apparatus ($L_1 = 600$ mm; $L_2 = 900$ mm; $L_3 = 1200$ mm; $L_4 = 1500$ mm).

60/40 blend of NIAx polyols 11-34/34-28	300 pbw
catalysts (A-1, DABCO, A-4) water	11.85 pbw
surfactant (L-5308) and catalyst (T-12)	2.31 pbw
80/20 blend of TDI/PAPI (SF-58)	96.00 pbw

This mixture (410.16 g) was thoroughly mixed in the lower vessel at about 14°C. After the mixing step the vessel was promptly attached to the instrumented test section (Fig. 1).

After each experiment the foam was removed from the apparatus and analyzed.

The mixing equipment, the lower and upper vessels were thoroughly cleaned and recoated with a teflon spray.

RESULTS DISCUSSION

Preceding an evaluation of the flow characteristics, visual examinations were made of the terminal foam morphology in the tube. In the absence of explicit information on the cell size distribution during the foaming stage, results on morphology of the cured foam have been used to support an earlier assumption of fine dispersion. Plate 1 shows an enlarged view (15X) of the cross-section of a cured foam sample taken from the downstream end of a 6.35 mm I.D. tube. (For a conservative estimate a small diameter tube has been chosen.) As can be seen, even the largest "cells" in the cured foam are more than an order of magnitude smaller than the tube diameter.

It is also interesting to note that inside the tube a significant orientation exists. Long cylindrical cells (tunnels) parallel to the flow axis can be observed rather than the usual dodecahedra commonly found in free-rise foams. Moreover, the pattern of Plate 1 indicates appreciable shear sensitivity of the cell structure to exist; at the wall where most shearing has occurred the largest cell defects are found.

Data on the time-dependent flow of foam through the test section (c.f. Fig. 1) consists of continuous records* of the axial pressure profile, and of foam rise in the overhead reservoir. (An example is given in Fig. 2.)

Generally, the measurements indicated the existence of the following distinct regimes:

- developing flow

The instrumented section is getting filled with a highly

*The time was measured from the instant when the isocyanates were added to the mixture.

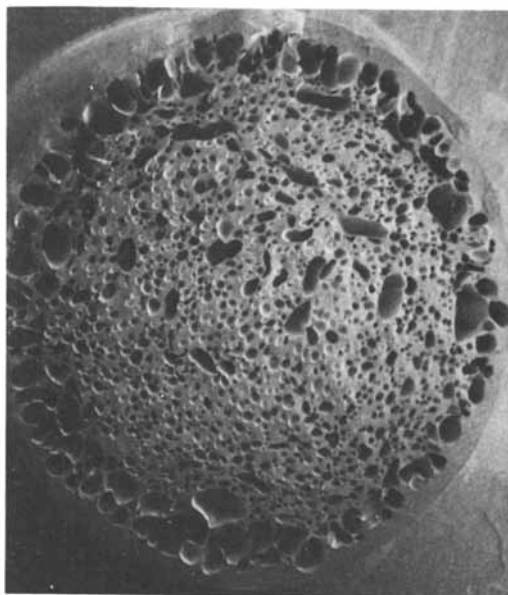


Plate 1. Scanning electron micrograph of a foam sample from the flow measurement apparatus (enlargement 12 \times).

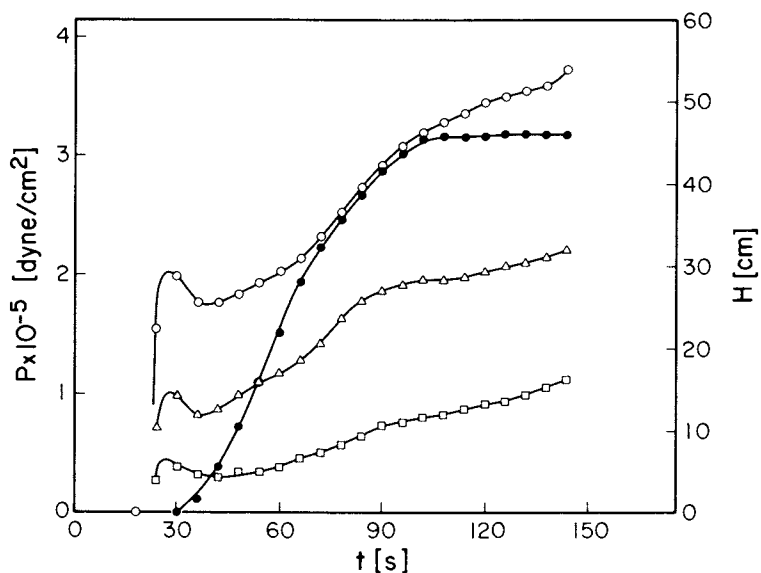


Figure 2. Experimental results ($L = 120$ cm). Key: \circ , pressure at $z = 30$ cm; \triangle , pressure at $z = 60$ cm; \square , pressure at $z = 90$ cm; \bullet , foam height in overhead reservoir.

mobile, relatively high density, foaming mass. The flow is governed by unsteady-state effects.

- viscous flow
Viscous stresses dominate the flow (in Fig. 2, after cca. 30s).
- static pressurization
The foam appears to be chemically gelled, flow stops (after cca. 100s have elapsed).

The subsequent analysis is limited to the viscous flow regime. As shown below, the foam apparent viscosity is high enough to give $Re < 1$. Also, changes in momentum due to the unsteady nature of the flow are small compared to the viscous forces beyond the initial developing flow stage.

When replotting the pressure data of Fig. 2 against axial position a linear function (within an experimental error) has been found; see Fig. 3. The same finding applies to the pressure measurements on the tubes 600, 900 and 1500 mm long.

The fact that the axial pressure profile is linear over a relatively broad time interval is extremely important. Most probably, it indicates that under the present experimental conditions:

- the properties of the foaming mass are virtually independent of the axial position within the instrumented portion of the tube,
- the flow rate along the tube is nearly constant (as it should for $d \ll D$).

These conclusions are valid within the present limits of accuracy. They also exclude a possibility of the linear pressure profile being resulted from a compensation effect balancing axial dependences of the phenomenological quantities involved. (It should also be noted that the entrance and end effects have been eliminated experimentally by placing the pressure transducers no closer than $11.8 L/d$ from either end.)

Results of the pressure measurements are collected in Fig. 4. The pressure gradients show a scatter particularly visible at the lower end of the time interval. As there is no clear indication of the tube length effect on the pressure gradient, the spread can most likely be attributed to mixing problems. (The progressive mixing due to the elongational flow associated with the bubble growth may lead to a reduced scatter with the increasing time.) In view of the data scatter, a linear approximation of the pressure gradient-time dependence has been used.

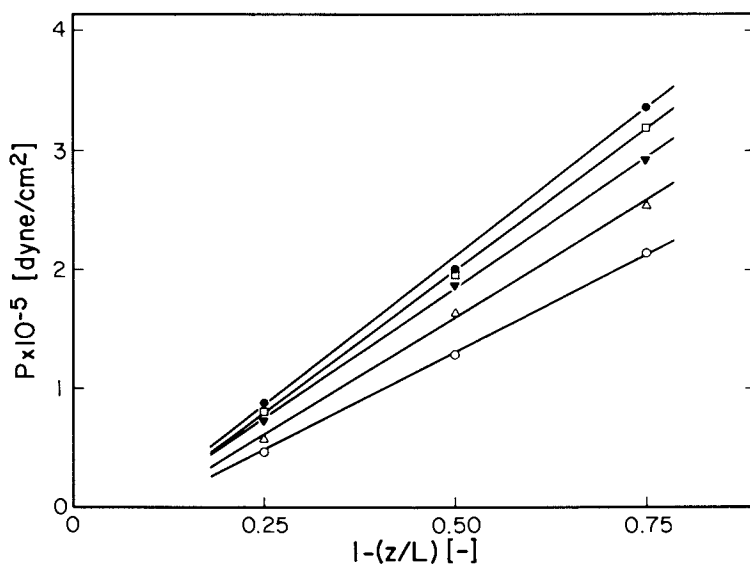


Figure 3. Pressure profile as a function of time ($L = 120$ cm). Key: \circ , 66 s; \triangle , 78 s; \blacktriangledown , 90 s; \square , 102 s; \bullet , 114 s.

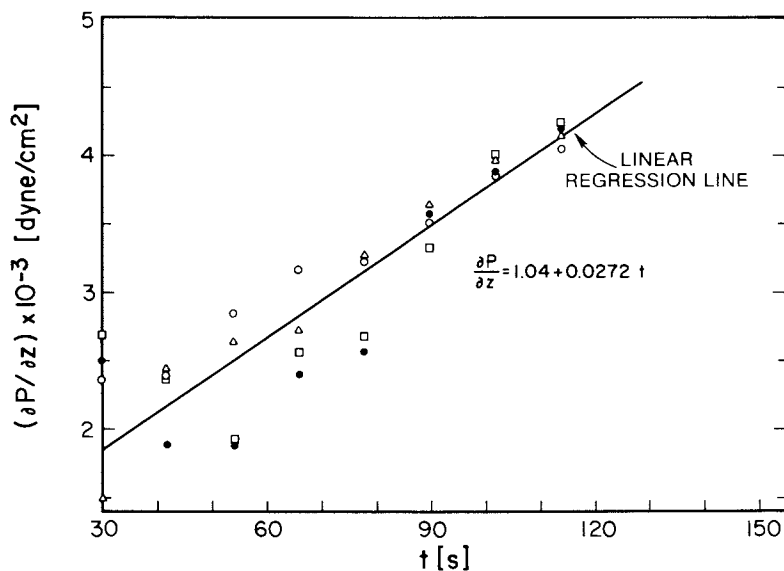


Figure 4. Pressure gradient as a function of time. Key: \square , $L = 60$ cm; \bullet , $L = 90$ cm; \triangle , $L = 120$ cm; \circ , $L = 150$ cm.

The average density of the foaming mass contained in the apparatus as a function of time has been determined from the readings of the foam rise in the upper vessel (c.f. Fig. 1). Assuming no loss of mass, the mean density can be evaluated from the ultrasonic transducer readings by:

$$\bar{\rho} = \frac{M}{V_1 + V_T + \pi R_2^2 H} \quad (1)$$

where M is the total (initial) mass, V_1 and V_T volumes of lower vessel and tube, respectively. R_2 is the radius of the upper vessel, and H is the changing foam height in it.

The present data on the mean density are given in Fig. 5. The scatter is relatively small.

The density data of Fig. 5 can be converted into flow rate through the tube. Assuming constant density throughout the apparatus* at a given instant, the flow rate as a function of time can be determined from:

$$Q = - \frac{V_1}{\bar{\rho}} \frac{d\bar{\rho}}{dt} \quad (2)$$

Based on data points of Fig. 5, the volumetric flow rate in the tube as a function of time has been calculated and plotted in Fig. 6. (The relatively large spread in Q has been introduced by numerical differentiation.)

Finally, the information on the pressure gradient and flow rate is used for an assessment of the viscosity buildup during the foaming stage. The apparent viscosity η_A is determined by:

$$\eta_A = \tau_A / \dot{\gamma}_A \quad (3)$$

where the apparent shear stress τ_A and shear rate $\dot{\gamma}_A$ are given by, resp., :

$$\tau_A = \frac{\partial p}{\partial z} R/2 \quad \text{and} \quad \dot{\gamma}_A = 4Q/\pi R^3 \quad (4)$$

In view of the crude concept of apparent viscosity, the viscosity function given in Fig. 7 has been evaluated using the statistical representations of the consistency variables (solid lines in Figs. 4 and 6) rather than the actual data points.

*The average densities in the lower and upper vessels have been found not to differ by more than 10 percent.

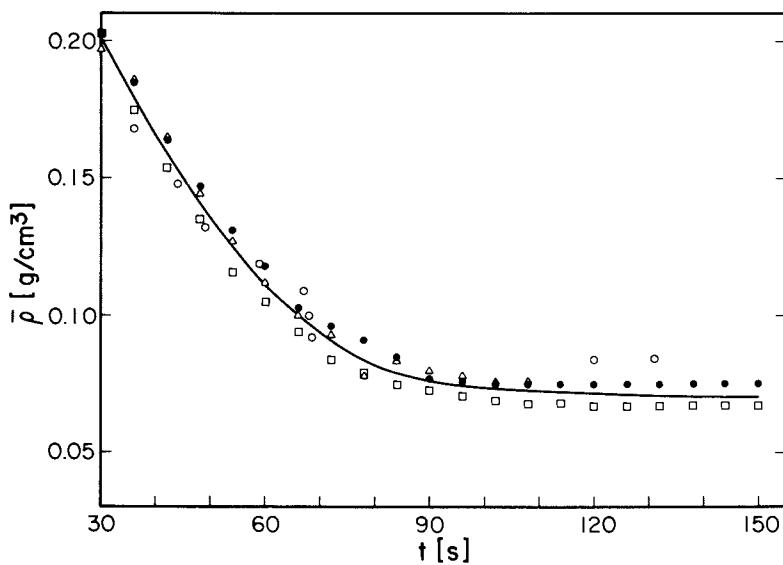


Figure 5. Mean density as a function of time. Key: \square , $L = 60$ cm; \bullet , $L = 90$ cm; \triangle , $L = 120$ cm; \circ , $L = 150$ cm.

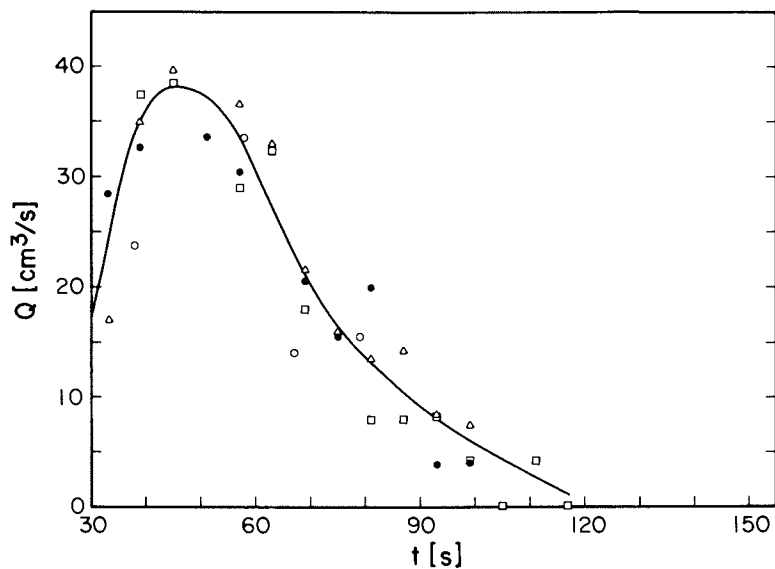


Figure 6. Volumetric flowrate in capillary as a function of time. Key: \square , $L = 60$ cm; \bullet , $L = 90$ cm; \triangle , $L = 120$ cm; \circ , $L = 150$ cm.

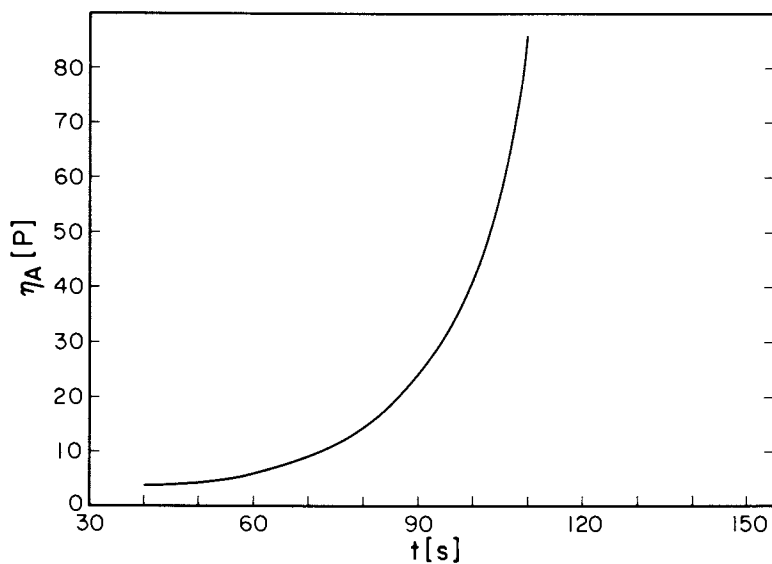


Figure 7. Apparent viscosity as a function of time.

CONCLUSIONS

The above results indicate that:

1. The foam formation process can be analyzed as a macroscopic flow problem.
2. For a given set of physico-chemical, geometrical and operational parameters, the flow characteristics can be specified fully by measurements of the foam rise and of the pressure profile in the mold.
3. From the characterization standpoint, data on the foam rise and pressure profile can be converted into the time-dependent density and viscosity functions.

In addition to the determinations of the density and viscosity functions, the present technique can be used for examinations of the shear sensitivity of the foam cell structure.

ACKNOWLEDGEMENT

Financial assistance and technical help made available by Union Carbide Corporation is gratefully acknowledged.

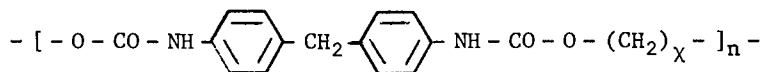
RECEIVED May 19, 1981.

The Structure of the Hard Segments in MDI/diol/PTMA Polyurethane Elastomers

J. BLACKWELL, M. R. NAGARAJAN, and T. B. HOITINK

Department of Macromolecular Science, Case Western Reserve University, Cleveland, OH 44106

Polyurethane elastomers derive their elastomeric properties from phase separation of the hard and soft copolymer segments, such that the hard (urethane) segment domains serve as cross-links between the amorphous soft segment domains, which are usually polyesters or polyethers. We are interested in the systems in which the hard segments are prepared from diphenylmethane 4,4'-diisocyanate (MDI) with a linear diol as the chain extender:



The soft segments are poly(tetramethylene adipate) (PTMA; $\bar{M}_n \approx 2089$). In these preparations the hard domains are crystalline and there has been considerable interest in the way the hydrogen bonding and chain packing contribute to the structural stability. The mechanical properties are dependent on the choice of chain extender, which affects the extent of phase separation. Development of crystallinity is thought to be an important factor controlling phase separation, and we are investigating the effect on the molecular conformation, packing, and the crystallite perfection, due to variation of the chain extender.

In our initial studies we concentrated on the structure of poly(MDI-butandiol). Initial proposals for the structure of these hard segments were made by Bonart and co-workers (1-3) and by Wilkes and Yusek. (4) The x-ray pattern of the oriented annealed elastomer film showed a single reflection which could be assigned to the hard segments, at $d \approx 7.9\text{\AA}$, azimuthally inclined at $\sim 30^\circ$ to the meridian. This reflection must originate from Bragg planes inclined at $\sim 60^\circ$ to the chain axis, and Bonart *et al* proposed that these planes arise from a staggering of adjacent chains so that intermolecular hydrogen bonds can be formed between the urethane groups. Formation of $C=O \cdots H-N$ hydrogen bonds which are approximately perpendicular to the chain necessitates staggering of the chains, as occurs for example in the structure of the α -form of Nylon 66. (5)

0097-6156/81/0172-0179\$05.00/0
© 1981 American Chemical Society

The above studies provided insight into the structure of the hard segments, but more detailed proposals could not be developed without a knowledge of the stereochemistry of the MDI unit. In addition to the standard bond lengths and angles for the phenyl, urethane, and butandiol groups, we need to determine

- (i) the bond angle at the central C-CH₂-C bridge;
- (ii) the orientation of the phenyl rings with respect to each other and to the central C-CH₂-C plane;
- (iii) the degree of planarity of the urethane groups and their orientations with respect to their adjacent phenyls; and
- (iv) the conformation of the -(CH₂)₄- chain and its orientation with respect to the diphenylmethane diurethane.

In order to determine the above parameters we are investigating the structures of model compounds prepared by capping MDI with alcohols. The first of these structures was methanol-capped MDI (6) [MeMMe, CH₂(C₆H₄NHCOOCH₃)₂]. This compound crystallizes in two polymorphic structures, which will be designated MeMMeI and II. The structure of MeMMeI has been determined in this laboratory, (6) and reveals many features which can be expected to occur in the polymer structure. The conformation of the molecule is shown in fig. 1a and the bc projection of the crystal structure is shown in fig. 1b. The central C-CH₂-C bridge angle is 114.5° and the phenyl planes are mutually inclined at 90.0°. Despite the chemical symmetry, the molecule is not physically symmetrical, and the two ends of the molecule are differentiated by A and B labels in fig. 1 (a and b); this asymmetry probably occurs in order to optimize the hydrogen bonding and packing.* The phenyl groups are inclined at 74.5°(A) and 34.7°(B) to the bridge C-CH₂-C plane. The urethane groups are planar and inclined at 39.4°(A) and 10.2°(B) to their adjacent phenyls; the terminal methyl carbons lie approximately in the planes of the urethane groups. The B-urethane groups form C=O...H-N hydrogen bonds approximately in the bc plane, as seen in fig. 1b. The molecules are stacked on top of each other along the a axis (perpendicular to the bc plane), and the A-urethane groups are hydrogen bonded to each other along this stack.

In considering the type of packing possible in the polymer structure, it is clear that the hydrogen bonding seen for the A-urethanes is likely to occur for the polymer, but not that for the B-urethanes. Another feature of the MeMMe structure is that the molecules have crystallized end-to-end: see the shaded molecules in fig. 1b. A model for the polymer chain was derived (9)

* It is interesting that in the structure of MeMMeII, as determined by Born *et al.*, (7) the molecules are symmetrical, with the two ends of the molecule related by a twofold axis through the CH₂ group. This twofold molecular symmetry also occurs for HO-BMB-OH (butandiol-capped MDI; CH₂[C₆H₄NHCOO(CH₂)₄OH], as determined in this laboratory. (8) However, neither of these two structures has intermolecular hydrogen bonding networks that could be analogous to situation in the polymers.

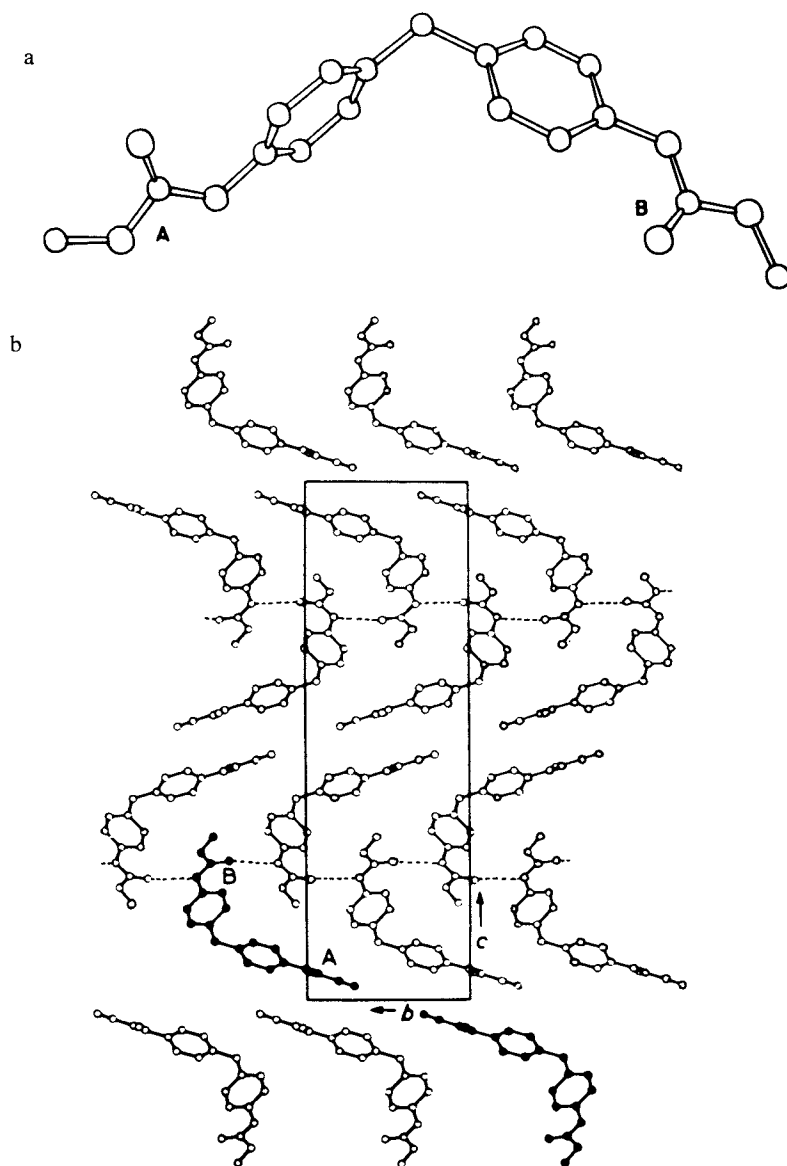


Figure 1. Structure of MeMME (methanol-capped MDI) (6): (a) conformation of molecule; (b) bc projection of the structure showing the packing and intermolecular hydrogen bonding.

by addition of a $-\text{CH}_2-\text{CH}_2-$ chain to form the butandiol unit, which was assumed to have a planar zigzag conformation (as in polyethylene). The stacking of the molecules along the a axis of the MeMMe structure was retained for the polymer, such that the ac projection of the polymer structure is as shown in fig. 2, where the hydrogen bonding of the A-urethane groups can be seen. The B-urethane groups are hydrogen bonded to the next sheet of chains, and thus the structure is stabilized by hydrogen bonding in two (approximately perpendicular) directions. This proposed structure has a triclinic unit cell with dimensions $a = 5.2\text{\AA}$, $b = 4.8\text{\AA}$, $c = 35.0\text{\AA}$, $\alpha = 121^\circ$, $\beta = 116^\circ$, and $\gamma = 85^\circ$. The space group is $P\bar{1}$ since the center of symmetry between molecules in the MeMMe structure relates the two monomer units forming the polymer fiber repeat.

Confirmation for this structure was obtained in later x-ray work, (10) in which a more highly resolved x-ray fiber diagram was obtained for the poly(MDI-butandiol) hard segments. Twelve unique reflections were observed and these were indexed by a triclinic unit cell with dimensions $a = 5.05\text{\AA}$, $b = 4.67\text{\AA}$, $c = 37.9\text{\AA}$, $\alpha = 116^\circ$, $\beta = 116^\circ$, and $\gamma = 83.5^\circ$. Given the experimental uncertainty in the measured d-spacings, and the assumptions in the model building, the agreement between the observed and predicted unit cells is striking. The most significant difference is probably in the fiber repeat (c), which indicates a more elongated conformation than that predicted from the "monomer" structure.

This paper describes a continuation of the above work, firstly to apply conformational analysis to predict the conformation of the poly(MDI-butandiol) chain, and secondly to extend these x-ray diffraction and model building techniques to investigate the structures formed with other chain extenders, notably propandiol and ethylene glycol. More detailed accounts of this work have been published elsewhere. (11,12)

EXPERIMENTAL

Specimens

The polyurethane specimens used in this research were generously provided by Dr. C.S. Schollenberger of B.F. Goodrich Co., Brecksville, Ohio. The specimens were prepared from reactant mixtures containing the ratio 6 moles MDI:5 moles diol: 1 mole PTMA ($\bar{M}_n \approx 2089$), corresponding to approximately 50% hard segment content; the diol chain extenders were ethylene glycol (EDO), propandiol (PDO), and butandiol (BDO).

Oriented films of the BDO and PDO polymers were prepared by slowly stretching 1mm thick unoriented films to 700% extension on a stainless steel rack at 130°C over a period of 7 days. As will be seen, these specimens showed no evidence for soft segment crystallinity. This procedure was unsuccessful for the EDO

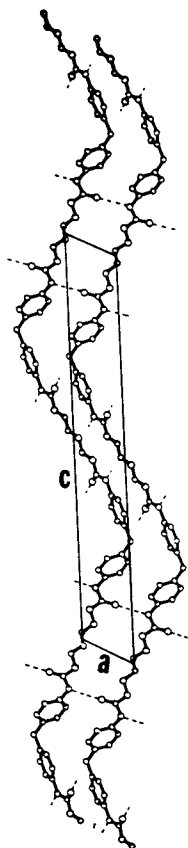


Figure 2. The ac projection of the structure of poly(MDI-butandiol) hard segments proposed by Blackwell and Gardner (9).

polymer, in that the films always broke during stretching above 60°C. The latter specimens were oriented by stretching 400% at room temperature. The x-ray patterns obtained showed both hard and soft segment crystallinity.

X-ray Diffraction

X-ray diffraction patterns were recorded using a Searle toroidal focusing camera with nickel filtered $\text{CuK}\alpha$ radiation generated by a Rigaku-Denki rotating anode source.

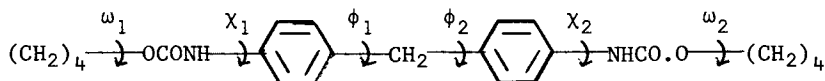
Conformational Analysis

The chain conformations of poly(MDI-BDO), poly(MDI-PDO), and poly(MDI-EDO) were investigated (11) using both semiempirical potential energy functions and CNDO/2 quantum mechanical methods. (13) Standard interatomic distances and angles were used for the diphenylmethane and $-(\text{CH}_2)_x-$ units. Similar parameters for the urethane group were obtained from a survey of 24 crystal structures of low molecular weight urethane compounds. The semiempirical calculations determined the total conformational energy by summing non-bonded (van der Waals), torsional, angular deformations, and electrostatic energies. Point charges for the calculation of the electrostatic contributions were calculated using the CNDO/2 method. The coefficients used for the potential functions were due to Sheraga and co-workers. (14) CNDO/2 calculations were also used to estimate the effects of interaction of the π -orbitals of the phenyl and urethane groups.

RESULTS AND DISCUSSION

Conformational Analysis of Poly(MDI-BDO)

The conformation of the poly(MDI-BDO) chain is defined by six torsion angles as shown below.



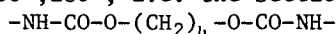
The phenyl and urethane groups are planar and are assumed to be rigid; the conformation of the $-(\text{CH}_2)_4-$ chain must also be defined. The definitions of the origins for the six torsion angles are given in reference 11.

This polymer has a long chemical repeat and conformational analysis would be a formidable task were it not that the x-ray data indicate a highly extended conformation: two monomer units repeat in 37.9Å, i.e. a rise of 18.95Å per repeat. Consequently, the conformation will be determined by interactions between contiguous groups. Conformational energy calculations have been used to investigate the phenyl-phenyl, the phenyl-urethane, and, after consideration of the possible $-(\text{CH}_2)_4-$ conformations, the

urethane $-(\text{CH}_2)_4$ interactions. These results have then been combined to predict the conformation of the polymer chain.

For the phenyl-phenyl interactions, the energy of the diphenylmethane unit was minimized as a function of ϕ_1 and ϕ_2 for different values of the C-CH₂-C bridge angle, τ . Minimum energy occurs for $\tau = 110^\circ$, the tetrahedral angle. However there is a subsidiary minimum at $\tau = 118.3^\circ$, with energy 1.9 kcal/mole higher than the $\tau = 110^\circ$ minimum. The subsidiary minimum is at $\phi_1, \phi_2 = (-60^\circ, -60^\circ)$ for which the phenyl rings are mutually perpendicular and exactly *gauche* to the central CH₂ group (c.f. $\tau = 114.5^\circ$ in the structure of MeMMeI. (6) This subsidiary minimum also leads to a more extended conformation and for these reasons was selected for the diphenylmethane section of the polymer chain. For the phenyl-urethane interactions, minimum energy occurs at $\chi = \pm 90^\circ$, for which the phenyl and urethane planes are perpendicular. The most extended conformation is $\chi_1, \chi_2 = -90^\circ, +90^\circ$; a monomer repeat of $\underline{c} = 18.95\text{\AA}$ cannot be achieved for the other combinations of χ_1, χ_2 for any conformation of the rest of the chain.

The above conformation: $\chi_1 = -90^\circ, \phi_1 = -60^\circ, \phi_2 = -60^\circ, \chi_2 = +90^\circ$ has a length of 14.0\AA measured from the terminal oxygens of the urethane groups. Minimum energy for the O-(CH₂)₄-O section is for an all-*trans* conformation which is coplanar with the urethanes, $\omega_1, \omega_2 = 180^\circ, 180^\circ$, i.e. the section



is a planar zigzag. Examination of subsidiary minima containing *gauche* bonds show that the monomer repeat of $\underline{c} = 18.95\text{\AA}$ cannot be attained with any but the all-*trans* conformation.

Thus the predicted polymer conformation is defined by the following torsion angles $\omega_1 = 180^\circ, \chi_1 = -90^\circ, \phi_1 = -60^\circ, \phi_2 = -60^\circ, \chi_2 = +90^\circ, \omega_2 = 180^\circ$, with an all-*trans* $-(\text{CH}_2)_4$ - unit. The monomer repeat for our model was 18.95\AA which matches the observed value. (Variation of the bond lengths and angles is possible within the standard ranges, resulting in a variation of approximately $\pm 0.5\text{\AA}$ in the monomer repeat; the exact agreement is contrived for convenience in later packing analyses.) A projection of the predicted conformation is shown in fig. 3.

We can be reasonably confident that the actual torsion angles in the solid state structure will be close to the predicted values, except for χ_1 and χ_2 , which define the phenyl-urethane orientations. The model diphenyl-diurethane structures (6-8) have χ angles in the range $10-37^\circ$. The deviations from $\chi = 90^\circ$ could be due to electron delocalization between the phenyl and urethane groups, which would favor the sterically disallowed $\chi = 0^\circ$ conformation. Such electron delocalization has been considered elsewhere for aromatic polyamides and polyesters. However, a simpler explanation may be that significant space occurs between the molecules if they are hydrogen bonded in the $\chi = \pm 90^\circ$ conformations, and that this is eliminated when χ is varied i.e. the urethanes are twisted away from a position

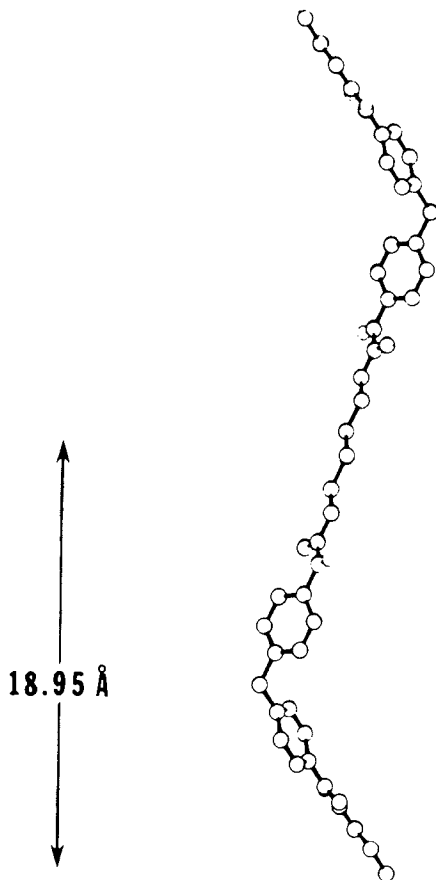


Figure 3. Projection of the minimum energy conformation of poly(MDI-BDO) (11). The fiber repeat is 37.9 Å and contains two monomers, that is, the monomer repeat along the fiber axis is 18.95 Å.

perpendicular to the phenyl rings. The energy increase for the molecular conformation would be more than compensated by that due to the packing effects.

Variation of χ has little effect on the length of the monomer repeat, owing to the fact that the terminal oxygen of the urethane group is almost colinear with the N-C (phenyl) bond. Table 1 shows the monomer repeats for centrosymmetric chains with a range of values of χ_1 and χ_2 , where it is seen that $c/2$ does not vary by more than 0.2\AA . We are now considering the packing of the poly(MDI-BDO) chains in the proposed triclinic unit cell, and will report on this in due course.

Poly(MDI-PDO) and Poly(MDI-EDO)

X-ray diffraction patterns of oriented films of the BDO, PDO, and EDO preparations (12) are shown in fig. 4. The poly(MDI-BDO) pattern has been analyzed previously and indicates a triclinic unit cell in which the base plane is tilted, i.e. it is not perpendicular to the fiber axis, such that the chains are in a staggered hydrogen bonded array. The conformational analysis above shows that the polymer chain is fully extended, with the all-trans $-(\text{CH}_2)_4-$ unit coplanar with the urethane groups.

The x-ray pattern of poly(MDI-PDO) and the EDO preparation can be seen to be quite different from that of poly(MDI-BDO). Poly(MDI-PDO) shows meridional reflections at $d=16.2\text{\AA}$, 8.1\AA , and $\sim 4.0\text{\AA}$, and an equatorial at $d \approx 4.7\text{\AA}$, with a row line at that position. This pattern is characteristic of a monoclinic unit cell with the base plane perpendicular to the fiber axis, i.e. the chains are not staggered but are arranged in register. The poly(MDI-BDO) and poly(MDI-PDO) specimens had been prepared in the same manner, and the lower quality of the x-ray pattern for the latter indicates a lower degree of crystalline order in the poly(MDI-PDO) hard segments. In the pattern of the EDO preparation, meridional reflections are seen at 15.0\AA and 7.5\AA , and there is a strong equatorial at $d=4.05\text{\AA}$. This specimen had been prepared at room temperature, and consequently crystalline reflections for the soft segments are to be expected. The equatorial reflection matches that at $d=4.05\text{\AA}$ for the α -form of PTMA, (15) the more probable polymorph given the method of preparation. However the meridional reflections are not observed for either α - or β -PTMA and these can be assigned to the poly(MDI-EDO) hard segments. Analogy with the poly(MDI-PDO) pattern suggests that the PDO and EDO hard segments have similar chain conformations, with monomer repeats of 16.2 and 15.0\AA respectively, and are packed in an unstaggered array.

The 1.2\AA difference in the monomer repeats for poly(MDI-PDO) and poly(MDI-EDO) is probably due to deletion of a trans-CH₂-group: in polyethylene the repeat is 1.27\AA per CH_2 group. However, the difference between the poly(MDI-BDO) repeat of 18.95\AA and that for poly(MDI-PDO) of 16.2\AA cannot be explained so simply.

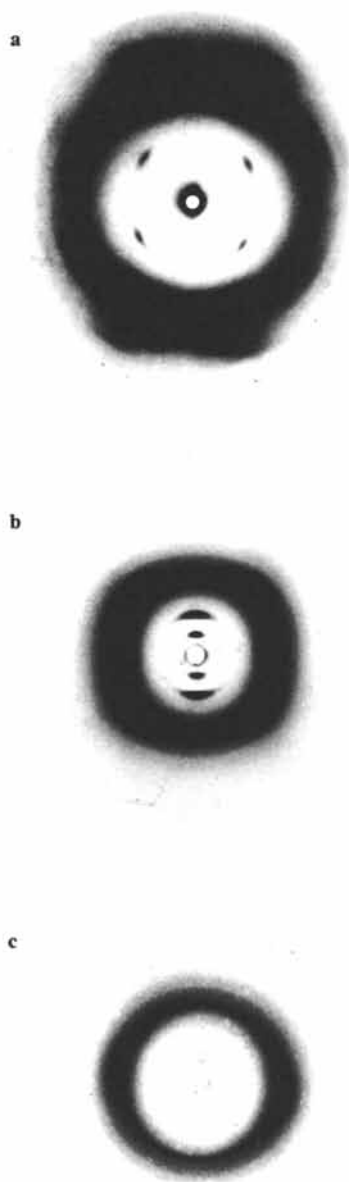
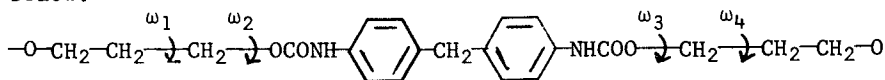


Figure 4. X-ray diffraction patterns of oriented polyurethane films: (a) MDI/BDO/PTMA stretched 700% at 130°C (10); (b) MDI/PDO/PTMA stretched 700% at 130°C (12); (c) MDI/EDO/PTMA stretched 400% at room temperature (12).

From the conformational analysis poly(MDI-BDO) is seen to be fully extended, with an all-trans butandiol unit. Thus it must be concluded that the poly(MDI-PDO) and poly(MDI-EDO) conformations are contracted and that there are some gauche conformations in the $O-(CH_2)_x-O$ sections of the chains.

Our procedure in predicting poly(MDI-PDO and poly(MDI-EDO) conformations has been to take the extended minimum energy conformation for the diphenylmethane diurethane section ($\chi_1 = -90^\circ$, $\phi_1 = -60^\circ$, $\phi_2 = -60^\circ$, $\chi_2 = +90^\circ$) and to look at possible conformations of the diol sections, comparing their relative energies and fiber repeats. (12) These conformations are defined by the torsion angles $\omega_1, \omega_2, \omega_3$ and [for poly(MDI-PDO) only] ω_4 , as shown below.



The chemical repeats are symmetrical and it is likely that this will lead to symmetry in the conformations on either side of the center of the diol unit i.e. $\omega_1 = \omega_4$ and $\omega_2 = \omega_3$ for poly(MDI-PDO) and $\omega_1 = -\omega_3$ for poly(MDI-EDO). These symmetries lead to monomer repeats. The x-ray data appear to be compatible with multiple repeats e.g. where successive monomer units are related by a screw axis, and we are in the process of considering these options. However, there is no positive x-ray evidence for anything more complex than a monomer repeat, and the multiple repeat possibilities will not be discussed further.

An energy map was obtained for the ω_1, ω_2 conformations for poly(MDI-PDO) and the positions and relative energies of the minima are listed in table 2. Not surprisingly, the lowest energy is for $\omega_1, \omega_2 = 180^\circ, 180^\circ$, corresponding to the fully extended all-trans conformation. This has a monomer repeat of 17.6Å which is significantly longer than the observed value of 16.2Å. In addition it can be seen that such a chain cannot form straight intermolecular hydrogen bonds since the N-H groups of urethanes adjacent to the central $-(CH_2)_3-$ are pointing in the same direction.

The next lowest minimum, 0.9 kcal/mole above the all-trans conformation is for $\omega_1, \omega_2 = 180^\circ, \pm 60^\circ$ ($+60^\circ$ and -60° correspond to the gauche⁺ and gauche⁻ conformations for the CH_2 groups). This trans-gauche⁺-gauche⁺-trans (and trans-gauche⁻-gauche⁻-trans) option has a fiber repeat of 16.20Å. Following this, the third minimum is 1.4 kcal/mole higher than all-trans at $\omega_1, \omega_2 = \pm 80^\circ, 180^\circ$ (deviation from $\pm 60^\circ$ is due to the CH_2- carbonyl interaction). This corresponds to the gauche⁺-trans-trans-gauche⁺ (and gauche⁻-trans-trans-gauche⁻) conformation, and has a fiber repeat of 16.24Å. The second and third conformations are both compatible with the observed monomer repeat. The remaining minima are for all-gauche options, of which the most extended conformation has a repeat of 15.31Å, significantly shorter than the observed value.

The two possible conformations of poly(MDI-PDO) are shown in fig. 5. We are currently considering packing models for these conformations, which may allow for selection of one or the other as the more likely. However, evidence in favor of the lower energy form (trans-gauche⁺-gauche⁺-trans) comes from the structure of another model compound determined in this laboratory: butandiol-capped MDI[CH₂{C₆H₄NHCOO(CH₂)₄OH}₂; HO-BMB-OH], which is shown in fig. 6. The terminal -C₄-O chains are approximately planar, but are gauche⁺ to the urethane: $\omega_1, \omega_2 = 170.5, 69.5^\circ$. As indicated in fig. 6, the C...C distance corresponding to the poly(MDI-PDO) repeat is 16.34Å. It should be noted that in the HO-BMB-OH structure $\chi = 10.4^\circ$, i.e. the phenyl and urethane groups are almost coplanar. However, symmetrical variation of χ_1 and χ_2 changes the fiber repeat by no more than $\pm 0.2\text{\AA}$, i.e. c is relatively insensitive to the phenyl-urethane orientations, as was the case for poly(MDI-BDO).

The same energy calculations can be used to investigate the possible poly(MDI-EDO) conformations. The energy minima and monomer repeats are listed in table 3. The all-trans and trans-gauche⁺-trans conformations have monomer repeats that are significantly longer than the observed value of 15.0Å, which coincides with that for the third minimum: gauche⁺-trans-gauche⁻. This conformation is proposed for the poly(MDI-EDO) structure, and is shown in fig. 7. As was the case for the other polymers, symmetrical variation of χ_1 and χ_2 have little effect on the fiber repeat. We are currently studying packing models for all three polymers, which should throw light on the more likely χ angles.

At this point the following conclusions can be drawn from these investigations. The BDO hard segments have better crystalline order than the PDO hard segments, suggesting more effective phase separation in the BDO preparation. This may have the simple explanation that the poly(MDI-BDO) chains can crystallize more easily, since in the crystal structure they have the lowest energy fully extended conformation, which forms straight intermolecular hydrogen bonds in both dimensions perpendicular to the chain axis. Poly(MDI-PDO) however cannot form an equivalent hydrogen bonding network if it adopts the lowest energy fully extended conformation, and thus will need to rearrange to a higher energy contracted conformation. This structure will then be stabilized by intermolecular hydrogen bonds, but will be of higher energy than the poly(MDI-BDO) structure, and thus there will be less of a driving force for phase separation due to crystallization of the hard segments. The results for poly(MDI-EDO) are more surprising in that one might expect that this polymer would adopt a structure similar to poly(MDI-BDO), since EDO has an even number of CH₂ groups. It may be however that the ethylene glycol chain is too short to allow adequate packing of the diphenylmethane diurethane units in the extended conformation, resulting in adoption of a contracted conformation more analogous to poly(MDI-PDO).

Table 1

Minimum Energy Conformations of the MDI-butandiol Fragment

No.	Initial Conformation (degrees)						Relative Energy (kcal/mole)	Length of the MDI-butandiol Fragment $\underline{c}/2$ (Å)
	ω_1	χ_1	ϕ_1	ϕ_2	χ_2	ω_2		
1	-180	-90	-60	-60	90	180	0.00	18.95
2	-180	-100	-60	-60	80	180	0.32	19.02
3	-180	-110	-60	-60	70	180	0.88	19.06
4	-180	-120	-60	-60	60	180	1.62	19.09
5	-180	-130	-60	-60	50	180	2.58	19.06
6	-180	-140	-60	-60	40	180	3.92	19.02
7	-180	-150	-60	-60	30	180	5.35	18.95
8	-180	-160	-60	-60	20	180	7.03	18.86
9	-180	-170	-60	-60	10	180	9.12	18.77

Table 2

Minimum Energy Conformations of MDI-PDO Fragment

Conformational Angles (degrees)								Relative Energy (kcal/mole)	Fiber Repeat \underline{c} (Å)
ω_1	ω_2	χ_1	ϕ_1	ϕ_2	χ_2	ω_3	ω_4		
180	180	-90	-60	-60	90	180	180	0.00	17.60
180	60	-90	-60	-60	90	60	180	0.90	16.20
80	180	-90	-60	-60	90	180	80	1.39	16.24
60	80	-90	-60	-60	90	80	60	1.64	15.31

Table 3

Minimum Energy Conformations of MDI-EDO Fragment

Conformational Angles (degrees)							Relative Energy (kcal/mole)	Fiber Repeat \underline{c} (Å)
χ_1	ϕ_1	ϕ_2	χ_2	ω_1	ω_2	ω_3		
-90	-60	-60	90	180	180	180	0.00	16.45
-90	-60	-60	90	180	60	180	0.94	15.80
-90	-60	-60	90	60	180	-60	1.28	15.00
-90	-60	-60	90	60	60	-60	1.98	14.16

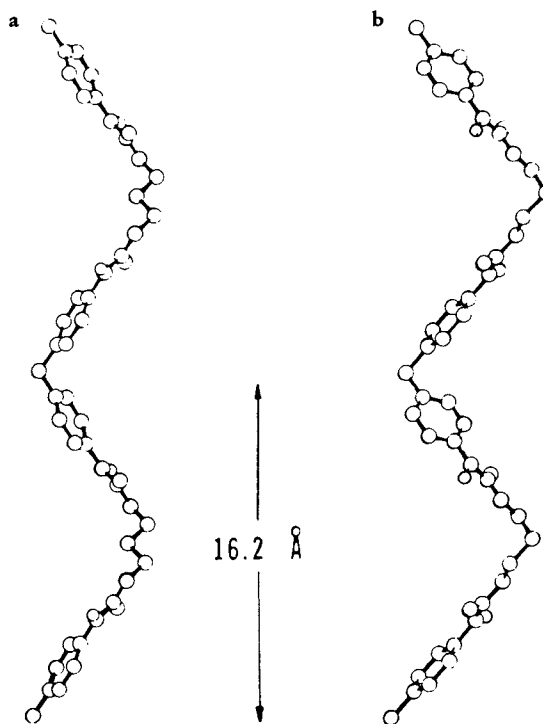


Figure 5. Projection of predicted conformations of poly(MDI-PDO) (12): (a) trans-gauche'-gauche'-trans; fiber repeat 16.20 Å; (b) gauche'-trans-trans-gauche'; fiber repeat 16.24 Å.

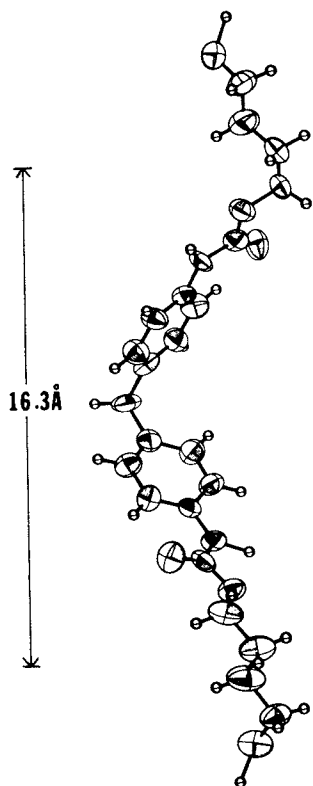


Figure 6. Molecular conformation of HO-BMB-OH (butandiol-capped MDI) (8).

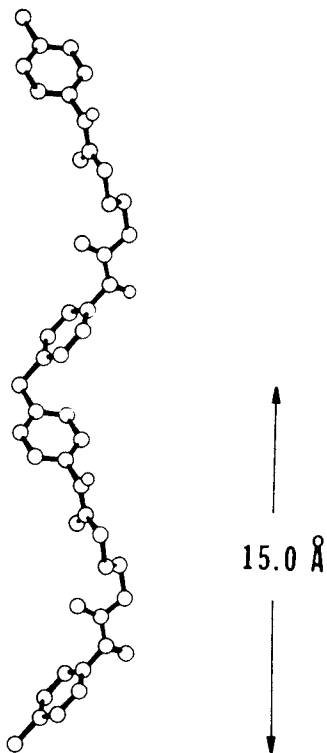


Figure 7. Predicted conformation for poly(MDI-EDO) (12). The ethylene glycol unit has the gauche-trans-gauche* conformation; the fiber repeat is 15.0 Å.*

We have recently obtained x-ray diffraction diagrams of equivalent preparations using pentandiol and hexandiol and are extending the above considerations to these and systems prepared with other chain extenders. Our research is supported by A.R.O. grant number DAAG29-79G-0070.

Abstract

We are using x-ray methods to determine the structure of the poly(MDI-diol) hard domains in polyurethane elastomers, in order to understand the effect of chemical structure on the crystalline order and extent of phase separation. Oriented films containing approximately 50% hard segments have been obtained for preparations using butandiol (BDO), propandiol (PDO), and ethylene glycol (EDO) as the chain extender; the soft segment is polytetramethylene adipate ($\bar{M}_n \approx 2089$). Poly(MDI-BDO) is the most crystalline, and has a triclinic unit cell with a tilted base plane such that there is a staggering of adjacent chains in the crystal structure. In contrast, poly(MDI-PDO) and poly(MDI-EDO) have monoclinic unit cells with adjacent chains in register. In order to develop molecular models for these polymers we have used single crystal x-ray methods to determine the structures of methanol- and butandiol-capped MDI. Based on the data from these structures, conformational analysis has been used to predict the likely chain conformations for the polymers. A model has been developed for poly(MDI-BDO) in which fully extended chains are staggered to give a hydrogen bonding network in two dimensions perpendicular to the chain axis. In contrast poly(MDI-PDO) and poly(MDI-EDO) crystallize in higher energy contracted conformations, which are necessary for the non-staggered packing of the chains. This difference may explain the higher crystalline perfection of the hard segments in the butandiol preparation.

Literature Cited

1. Bonart, R.J. *J. Macromol. Sci. (B)*, 1968, 2, 115.
2. Bonart, R.J.; Morbitzer, L.; Hentze, G. *J. Macromol. Sci. (B)*, 1969, 3, 337.
3. Bonart, R.J.; Morbitzer, L.; Muhler, E.H. *J. Macromol. Sci. (B)*, 1974, 9, 447.
4. Wilkes, C.W.; Yusek, C. *J. Macromol. Sci. (B)*, 1973, 7, 157.
5. Bunn, C.W. and Garner, E.V. *Proc. Roy. Soc. (London)*, 1947, A189, 39.
6. Gardner, K.H. and Blackwell, J. *Acta Crystallogr.*, 1980, B36, 1972.
7. Born, L.; Hocker, J.; Paulus, H.; Wölfel, E. *Krist. Struct. Commun.*, (in press); Hocker, J. and Born, L. *J. Polymer Sci.-Polymer Letters Edns.*, 1979, 17, 723.
8. Forcier, P.G. and Blackwell, J. *Acta Crystallogr.*, 1980, B37, 286.

9. Blackwell, J. and Gardner, K.H. Polymer, 1979, 20, 13.
10. Blackwell, J. and Ross, M. J. Polymer Sci.-Polymer Letters Edns., 1979, 17, 447.
11. Blackwell, J. and Nagarajan, M.R. Polymer, 1981, 22, 202.
12. Blackwell, J.; Nagarajan, M.R.; Hoitink, T., submitted to Polymer.
13. Pople, J.A. and Beveridge, D.L. "Approximate Molecular Orbital Theory"; McGraw-Hill, New York, 1970.
14. Ooi, T.; Scott, R.A.; Vanderkooi, G.; Scheraga, H.A. J. Phys. Chem., 1967, 46, 4410.
15. Minke, R. and Blackwell, J. J. Macromol. Sci.-Phys. (B), 1979, 16(3), 407.

RECEIVED May 11, 1981.

Polyether Glycols from Tetrahydrofuran and Ethylene Oxide

I. M. ROBINSON, E. PECHHOLD, and G. PRUCKMAYR

Chemicals and Pigments Department, E. I. du Pont De Nemours & Co., Inc.,
Wilmington, DE 19898

Polyether glycols have found wide acceptance as soft segment components for polyurethanes. Representative examples of useful polyether glycols are obtained by ring-opening polymerization of propylene oxide to polypropylene ether glycol and tetrahydrofuran (THF) to polytetramethylene ether glycol (PTMEG). However, the copolymerization of ethylene oxide (EO) and THF produced copolyether glycols which were reported to give polyurethanes with inferior properties (1). It is now known that these early EO/THF copolymers contained macrocyclic oligomers. The formation of macrocyclics in the cationic polymerization of certain cyclic ethers has been known for some time (2). McKenna *et al.* (3) have reported on the macrocyclics from THF. Dale (4) has studied the formation of cyclic oligomers from EO, and Hammond (5) has identified some of the macrocyclics produced in the copolymerization of propylene oxide and THF. We have recently reported (6) on the formation of crown ethers from EO and THF using $\text{CF}_3\text{SO}_3\text{H}$ as a catalyst.

The present paper deals broadly with the copolymerization of ethylene oxide and tetrahydrofuran using cationic ring-opening polymerization catalysts. A comparison is made of EO/THF polyether glycol with PTMEG and their respective polyurethanes.

Polymerization

In typical experiments, THF and EO were mixed in the presence of H_2O and polymerized at temperatures from 0-60°C using $\text{BF}_3 \cdot \text{OEt}_2$ as a catalyst. Gas chromatograms of samples showed both linear and macrocyclic oligomers at the early stages of the copolymerization. As the copolymerization proceeded, the initially formed linear low molecular weight glycols were consumed. Macrocyclics were generated steadily during the polymerization. Polymerization ceased when essentially all the EO was used. Conversion and degrees of polymerization were calculated from 100 MHz NMR spectra using tetramethylsilane as an internal reference.

The composition of the copolymer was varied by adjusting the EO/THF ratio, and the molecular weight was controlled by the amount of H_2O present. Glycols, such as ethylene, tetramethylene

0097-6156/81/0172-0197\$05.00/0

© 1981 American Chemical Society

and hexamethylene, were also used for molecular weight control and to influence end group structure. A range of other cationic initiations were effective, such as acid forms of Nafion[®] perfluorosulfonic acid resin and certain clays.

Results and Discussion

Gas chromatograms taken at the end of EO:THF polymerization, producing polyether glycols with number average molecular weights above 1000, show only the presence of macrocyclics, as discussed earlier (6). Identification of each of the macrocyclics was made by chemical ionization mass spectroscopy. Figure 1 shows a typical gas chromatogram for the EO/THF macrocyclic ethers. The cyclic cotetramers are the dominant species--an event in keeping with other cyclization phenomena where tetramers are found in highest concentration. Some of these cyclics present the possibility for isomer forms, but none have been found to date. The 28-membered ring, EO:THF crown 1:5, is shown as the largest ring, although larger rings are present, as apparent by GC peaks at longer retention times. It is interesting that no homologs of EO or THF crowns are detected - with the exception of very small amounts of dioxane.

The relative concentration of EO:THF crowns formed is usually in the range of 8-20% of the linear polyether glycol. Variables influencing macrocyclic concentration and composition are polymerization conditions, monomer ratio, and catalyst.

Figure 2 shows the EO:THF crown ethers identified by chemical ionization mass spectroscopy from a polymerization using Nafion[®] perfluorosulfonic acid resin as the catalyst. All of the cyclic ethers shown in Figure 1 were obtained but in significantly different concentrations. Again, no homologous EO or THF rings were detected. However, the dominance of species high in the THF component, such as 1:3, 1:4 and 1:5, may be a result of the efficacy of this catalyst for THF propagation.

The chemical ionization mass spectra for two of these EO:THF crowns are shown in Figures 3 and 4. The fragmentation patterns indicate down-sizing by extrusion of THF and EO moieties. In the example of the EO:THF 3:2 crown, the relative abundance of 1:1 and 2:1 species may point to direct formation from the 3:2 ring rather than stepwise fragmentation via $3:2 \rightarrow 2:2 \rightarrow 2:1 \rightarrow 1:1$ and $3:2 \rightarrow 3:1 \rightarrow 2:1$. Interestingly, the 1:1 ion is seen as a dominant component in the decay process although this represents a normally strained 8-membered ring and one which is not formed to any significant extent during the polymerization process.

Formation of EO/THF macrocyclics probably occurs via tail-biting and back-biting mechanisms as outlined in Figure 5. The back-biting reaction route appears most likely for this system. Since no THF homocyclic oligomers have been found in this copolymerization and are extremely limited in THF

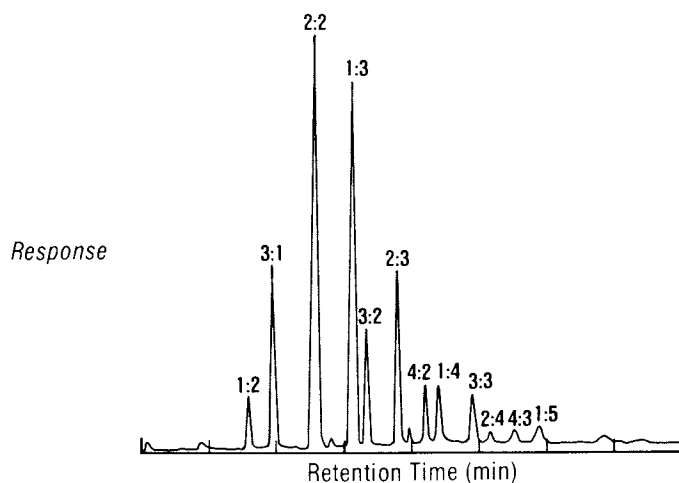


Figure 1. Gas chromatograph for EO:THF crowns. The nomenclature, for example, EO:THF crown 2:3, has been found convenient with the smaller monomer designated as the leading number.

Crown Ether (EO:THF)	Molecular Weight (m/e-1)	GC area %
1:2	188	3
3:1	204	1
2:2	232	16
1:3	260	51
3:2	276	3
2:3	304	5
4:2	320	1
1:4	332	10
3:3	348	2
2:4	376	1
4:3	392	t
1:5	404	4

+small amounts of higher mol. wt. crown ethers

Figure 2. Crown ethers identified by chemical ionization mass spectroscopy for EO/THF polymerization using Nafion perfluorosulfonic acid resin as catalyst.

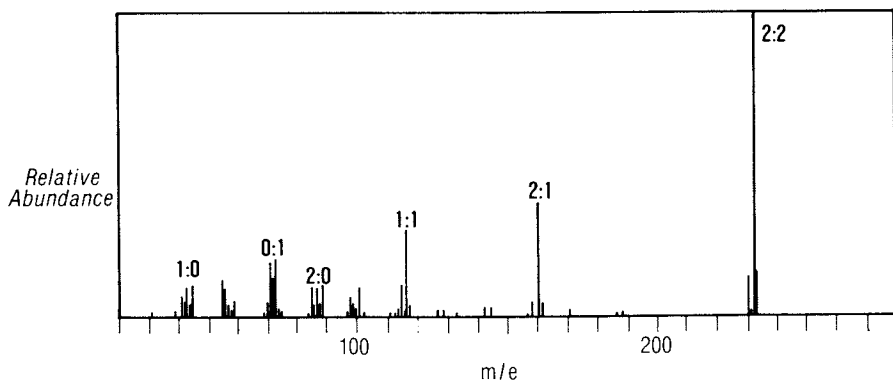


Figure 3. Chemical ionization mass spectrum for EO:THF crown 2:3 with fragmentation pattern to down-sized rings.

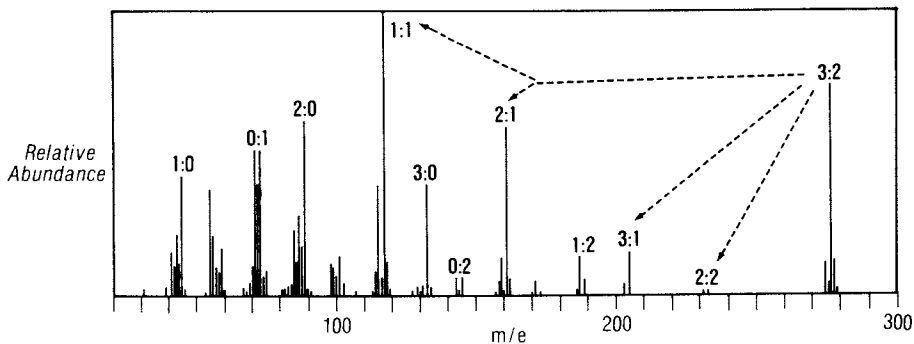


Figure 4. Chemical ionization mass spectrum for EO:THF 3:2 crown with speculative pathways for ion decay.

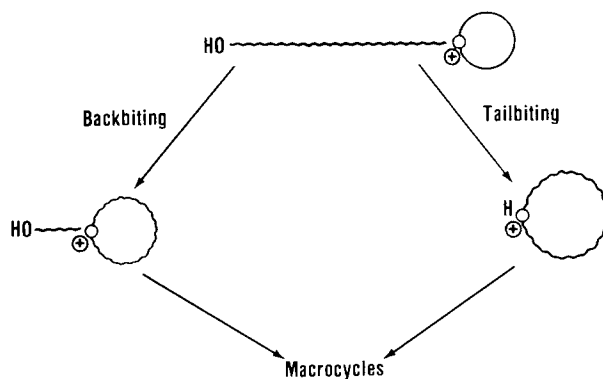


Figure 5. Mechanism for formation of EO/THF macrocycles involving both back-biting and tail-biting routes.

Composition	PTMEG	EO:THF Copolymer
Viscosity 40°C PA.S	.26-.36	.15
Melting Range °C	14-23	<-11
% Crystallinity (-20°C)	55-60	30-35
H ₂ O Solubility	Negligible	~50%
Chain End Groups	HO(CH ₂) ₄ O~	HOCH ₂ CH ₂ O~ 80-85%

Figure 6. Comparison of PTMEG and EO/THF copolyether glycols stressing significant property differences.

homopolymerization, the THF propagating oxonium ion does not seem a likely source for involvement in macrocycles to the high degree we see in EO/THF systems. The highly strained EO oxonium ion on the other hand is a favored candidate for reaction site. We know that chain initiation in aqueous or hydroxylic environments will not occur with THF but will take place with EO to generate initiating chain ends with resultant hydroxy ethyl ether structures. From such systems with hydroxy ethyl ether chain ends and EO oxonium ions, if tail biting was the dominant route to macrocyclics, the species having two adjacent EO's in the ring would be most favored. Such is not the case, and back biting appears most likely. If the random composition of the macrocyclics found is indicative of the polymer backbone, the copolyether glycols produced are also of random EO/THF structures.

The macrocyclic EO/THF crowns have been removed from the linear polyether glycol by several methods, including distillation under high vacuum.

EO/THF Copolyether Glycol

A comparison of the physical properties of an EO/THF copolyether glycol with PTMEG is shown in Figure 6. The number average molecular weight range for each was 950-1050. The mole % EO content in the copolymer was 46-52. Major differences are seen in viscosity, melting point, % crystallinity, water solubility and chain-end group structure.

A comparison of polyurethanes prepared from this EO/THF polyether glycol with PTMEG, polyester glycols, and polycaprolactone glycol was given at the ACS meeting in May, 1980. The EO/THF polyether glycol provides soft segment for polyurethanes with good low-temperature properties, oil resistance and favorable compression set.

LITERATURE CITED

- 1a. Murbach, W. J.; Adicoff, A. Ind. Eng. Chem., 1960, 52, 772.
- b. Dickinson, L. A. J. Polymer Sci., 1962, 58, 857.
2. Goethals, E. J. Adv. Polym. Sci., 1977, 23, 103 - a review on the formation of cyclic oligomers.
3. McKenna, M.; Wu, T. K.; Pruckmayr, G. Macromolecules, 1977, 10, 877.
4. Dale, J.; Borgen, G.; and Daasvatn, K. Acta Chem. Scand., 1974, 28, Series B, 378.

Dale, J.; Borgen, G.; and Daasvatn, K. British Patent 1,434,672, 1976.

Dale, J.; Daasvatn, K. Chem. Soc., Chem. Commun., 1976, 295.

Dale, J.; K. Daasvatn, K.; and Gronneberg, T. Makromol. Chem., 1977, 178, 873.

5. Hammond, J. M.; Hooper, J. F.; and Robertson, W. G. P. J. Polym. Sci., 1971, 9, 281, Part A-1.
6. Robinson, I. M.; Pruckmayr, G. Macromolecules, 1979, 12, 1043.
7. Pechhold, E.; Pruckmayr, G.; Robinson, I. M., ACS Meeting, Rubber Division, Las Vegas, May, 1980, Paper No. 40.

RECEIVED May 14, 1981.

Catalysis of Isocyanate Reactions with Protonic Substrates

A New Concept for the Catalysis of Polyurethane Formation via Tertiary Amines and Organometallic Compounds

GIA HUYNH-BA

Experimental Station, Polymer Products Department,
E. I. Du Pont De Nemours & Co. Inc., Wilmington, DE 19898

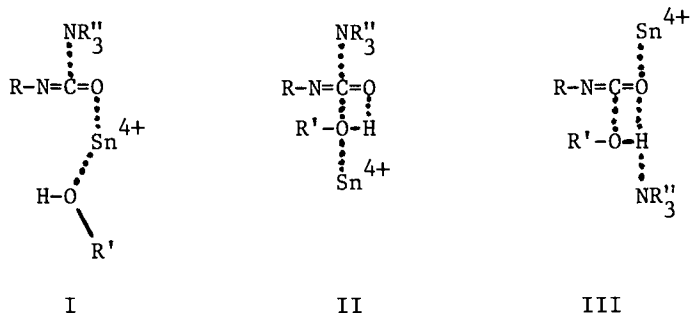
R. JERÔME

Laboratory of Macromolecular Chemistry and Organic Catalysis,
University of Liege, Sart-Tilman, 4000 Liege, Belgium

A survey of the literature indicates that the catalysis of isocyanate-alcohol reactions has produced a variety of mechanistic explanations. The proposed reaction pathways in the literature are often based on limited information and are unable to explain many of the experimental observations well known to scientists and technologists active in the field (1, 2, 3, 4).

The catalysis of the polyurethane formation by organometallic compounds has especially lead to a number of very different interpretations.

Entelis assumes the formation of an activated alcohol-isocyanate binary complex during the catalysis of the methanol-phenyl isocyanate reaction by dibutyltin dilaurate (DBTDL) (3, 5). Activated alcohol-isocyanate-catalyst ternary complexes have also been proposed by others. However, significant differences can be noted in the structures of either the postulated one (2, 4, 6, 7) or two (8) coordination positions of the isocyanate to the metal. To explain the synergistic effects observed when tertiary amine and organometallic compounds are combined, several authors suggest the formation of an activated quaternary complex: I, II or III (2, 6, 9, 10, 11, 27).



0097-6156/81/0172-0205\$05.00/0
© 1981 American Chemical Society

In these schemes, amine and metal are coordinated on separate atoms. In spite of contradictory views of the electronic distribution of isocyanates (3, 12, 13) the metal is always shown as interacting with the oxygen and never with the nitrogen atom. Furthermore, the organometallic compound is noted by M^{n+} so that the fate of the ligands is disregarded (6) and clearly oversimplified structures are accordingly proposed.

Thus, several mechanistic pathways based on polarization effects have been proposed to explain the catalysis of the alcohol-isocyanate reaction. These propositions appear to be often unsatisfactory and cannot explain even the majority of the experimental results reported in the literature. For an example, why is the polyurethane formation catalyzed by potassium acetate (1) and not at all by $MgCO_3$ nor $CsCl$ (14)? The role played by the nature of the metal remains also unexplained. Robins reports the incremental temperature rise noted 1 minute after the mixing of reagents and catalyst (7, 16). This parameter is related to the catalytic activity and is an effective way to show the role played by the organometallic compound in its interaction with the alcohol. A similar conclusion can be drawn from Table I (15) where the Sn^{+4} derivative is much more active than the Sn^{+2} oxidation state or Pb^{+2} .

This paper is an attempt to further evaluate and to suggest a new mechanistic view for these important reactions. Knowledge of the complexation between reagents and catalysts will be the basic premise.

Discussion

Literature data confirm the possibilities of complexation between reagents (isocyanate, alcohol) and catalyst (tertiary amine, organometallic compound) considered two by two.

The alcohol-tertiary amine complexation is well established by NMR (2, 17), cryoscopy (10), UV spectroscopy (2) and other techniques (18-20). According to Frisch, 10 to 20% of the amine is complexed by the alcohol (2).

The evidence for the alcohol-metal complexation is from UV and NMR spectroscopy (2, 5, 17, 21). By cryoscopy, Frisch concluded that the metal is complexed at about 10-20% by the alcohol (10). NMR measurements agree with the formation of a metal-alcohol-tertiary amine complex (17). The proton of the alcohol is indeed shifted by the addition of a tertiary amine (0.22 ppm), an organometallic compound (0.25 ppm) and the combination of these two catalysts (0.72 ppm) respectively. Structure IV could account for the alcohol activation.

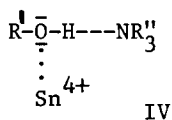


Table I
Rate Constant of Phenyl Isocyanate-Alcohol Reactions Catalyzed by Organometallic Compounds (15)

Catalyst	K X 10 ⁴ l/equiv.-sec									
	BuOH-1	BuOH-2	$\frac{K_{\text{BuOH-1}}}{K_{\text{BuOH-2}}}$	A	B	C	$\frac{K_A}{K_B}$	$\frac{K_A}{K_C}$	$\frac{K_B}{K_C}$	
non-catalyzed	0,9	0,3	3,0	0,5	0,4	0,2	1,2	2,5	2,0	
DBTDL	290,0	24,2	12,0	262,0	75,7	15,2	3,5	17,2	4,9	
Sn ²⁺ Octoate	12,0	3,4	3,5	60,3	-	48,5	-	1,2	-	
Sn ²⁺ Oleate	6,9	2,0	3,5	40,4	-	41,4	-	1,0	-	
Pb ²⁺ (naphtenate)	6,3	0,9	7,0	32,0	106,5	68,0	0,3	0,5	1,6	

BuOH-1 = butanol-1, BuOH-2 = butanol-2; A = methoxy-3-propanol-1

B - methoxy-2-propanol-1; C = methoxy-1-propanol-2

K - rate constant

Conditions = Solvent = toluene
temperature = 30°C
[catalyst] = 10⁻⁴ mole/l

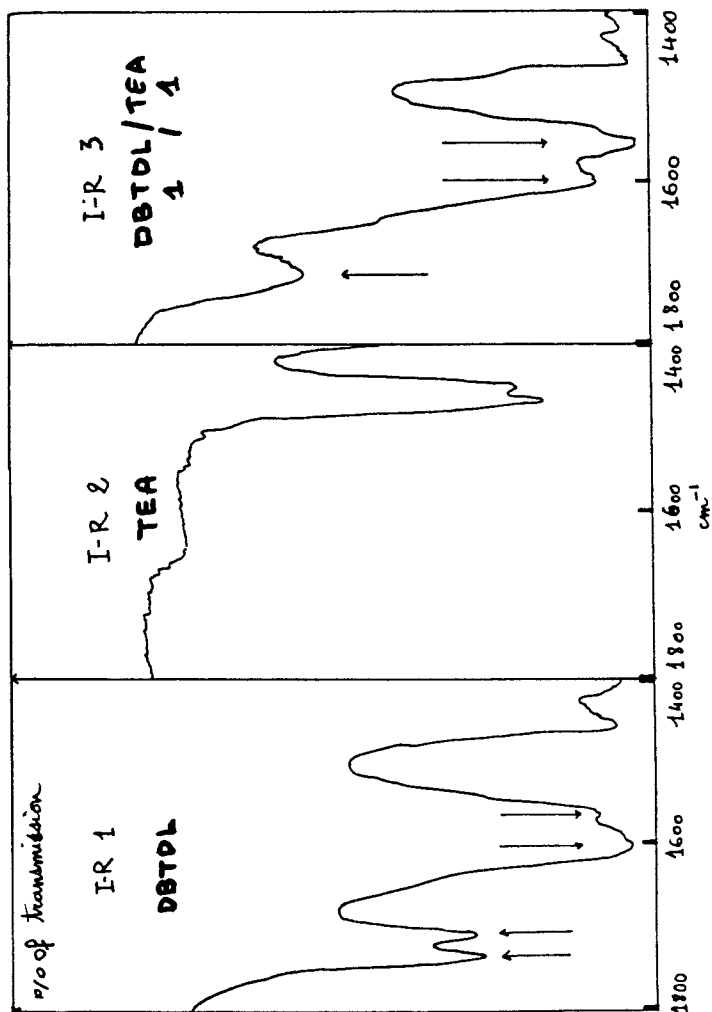


Figure 1. Infrared spectrum of dibutylindilaurate (DBTDL, IR 1), triethylamine (TEA, IR 2), and 1:1 mixture of DBTDL and TEA (IR 3) in the region 1800-1400 cm⁻¹.

considered by Davies, who reports that Sn becomes linked to the nitrogen atom of PhNCO (29). The interaction between PhNCO and Sn^{4+} could accordingly take place on the C=N double bond. Under these conditions, Fig. 2 describes the isocyanate-metal interaction by assuming:

- a σ donor-type bond between the vacant 5 p_y orbital of Sn^{4+} and the occupied π orbital of the isocyanate.
- a π type back bonding between the occupied 4 d_{yz} orbital of the metal M and the π^* antibonding orbital of the isocyanate. This interaction decreases the double bonding character between the C and N atoms of the isocyanate (30).

If the metal, noted M_x , has not an occupied d orbital with an energy similar to that of the vacant p_y or s type orbital, the σ coordination (a, Fig. 2) takes place whereas the back bonding π type (b, Fig. 2) is now impossible; that is the case for Mg^{2+} and Cs^{1+} derivatives.

From the above interactions schemes, Fig. 3 is proposed as a model for the structure of the activated alcohol-isocyanate-metal ternary complex; M and M_x metals are considered separately.

The potential energy curves derived from the angular vibration of both metal-O (alcohol) and metal- $\overset{\text{O}}{\underset{\text{N}}{\text{C}}}$ (isocyanate) bonds are qualitatively shown. The curves (1) and (1') relative to M-O bond are similar (see Fig. 3). On the contrary, the curves (2) and (2') are not. Due to the π type backbonding, M- $\overset{\text{O}}{\underset{\text{N}}{\text{C}}}$ bond is indeed shorter than M_x - $\overset{\text{O}}{\underset{\text{N}}{\text{C}}}$ and the potential energy curve (2') is broader than (2). The overlap of the curves (1') and (2') is accordingly more important than this one of (1) and (2) and the activation energy for the reaction ($\Delta E_{R'}$) is more favorable for metal M than for M_x (ΔE_R).

A non-concerted rearrangement can be anticipated (Fig. 4): after complexation there is formation of an oxygen (RO:alcohol)-carbon(isocyanate) bond together with a donor-type bond between nitrogen and metal (via p_y); the latter bond would then hydrolyzed by the proton (from alcohol) already present around the coordination sphere of the metal.

Consequences of the Proposed Reaction Mechanism

The mechanism has only qualitative significance but it enables one to explain the experimental results more satisfactorily than the more often accepted models. Let us now use this new concept to interpret some of the until now unexplained observations.

-To be valid, the mechanism (Figs. 3 and 4) implies the participation of orbitals characterized by a similar energy: vacant p and occupied d_{yz} orbitals of the metal, lone pair n_2

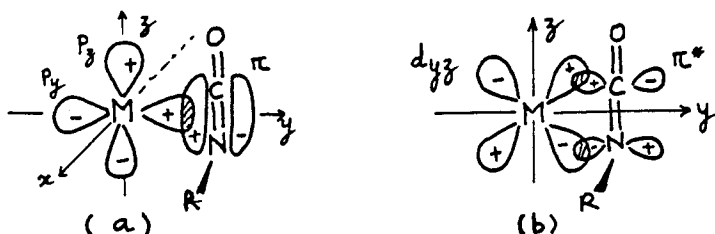


Figure 2. (a) The σ bonding between π isocyanate and unoccupied p_y of the metal (M). (b) The π back bondings between π^* of isocyanate and occupied (or partially) d_{yz} of the metal (M).

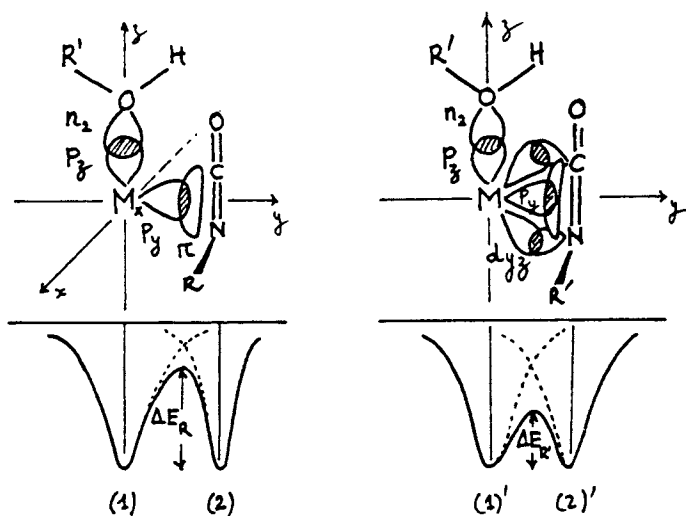


Figure 3. Potential energy curve of the angular vibration of alcohol-metal (M_x) (1) and isocyanate-metal (M_x) (2). The rearrangement energy for that system is the collapse region of curves 1 and 2 (ΔE_R). Similarly, in the case of M we have alcohol-metal (M) (1'), isocyanate-metal (M) (2'), and $\Delta E_{R'} < \Delta E_R$.

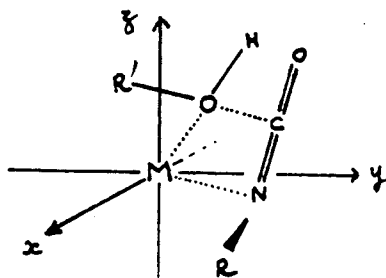


Figure 4. Transition structure during the rearrangement of the alcohol and isocyanate.

of the alcohol, π and π^* orbitals of the isocyanate. For a given alcohol-isocyanate pair, the nature of the metal must play an important role. The inactivity of CsCl and $MgCO_3$ salt (M_x type metals) can be easily explained by the absence of any activation process.

-The mechanism assumes a nucleophilic attack of $R'O^-$ on the carbon atom of the isocyanate. The rearrangement is accordingly favored by a decrease of the electronic density of the carbon atom. The polyurethane formation rate is indeed higher for an aromatic than for an aliphatic isocyanate (1); the substituent R of the isocyanate has a favorable inductive effect in the former but an unfavorable effect in the latter.

-The nature of the alcohol has also an influence on the polyurethane formation; the activity increases from tertiary, to secondary and finally to primary in the case of non-activated alcohols (1, 15). The energy of the lone pair n_2 of these alcohols is weakly affected by their molecular structure, the alcohol-metal interaction should accordingly be sensitive to steric groups near the hydroxyl group (Fig. 3).

-The kinetic results summarized in Table I can be explained on the basis of the activated ternary complex (Fig. 3). In the presence of DBTDL (R_2L_2Sn), the rate constants relative to different alcohol are to be classified as follows:

$$K_{BuOH1} > K_A > K_B \quad \text{and} \quad K_{BuOH2} > K_C$$

where BuOH1 = 1-butanol and BuOH2 = 2-butanol are non-activated alcohol, A = $CH_3-O-CH_2-CH_2-CH_2-OH$, B = $CH_3-CH(OCH_3)-CH_2OH$ and C = $CH_3-O-CH_2-CHOH-CH_3$ are activated alcohols.

DBTDL is described as an octahedral complex (31, 32); four of its coordination vacancies are occupied by the ligands whereas the alcohol and the isocyanate can occupy the two last positions. The methoxy group of the activated alcohols is unable to participate to the crystalline field and has only a steric and therefore, negative effect on the rate.

With Sn^{2+} and Pb^{2+} based catalysts, two ligands are coordinated and the methoxy group of the activated alcohol can be involved in the crystalline field (ether-metal bond) and be responsible for a donor-type effect on the metal. The reactivity sequence is now reversed (Table I):

$$\begin{array}{l} Sn^{2+} \quad K_A > K_{BuOH1} \\ \\ K_C > K_{BuOH2} \\ Pb^{2+} \quad K_B > K_A > K_{BuOH1} \\ \\ K_C > K_{BuOH2} \end{array}$$

Similarly, Robins reports an increasing activity (17x) when 1-butanol is replaced by β -dimethylaminoethanol in the presence of Pb^{2+} (7, 16). It is well known that the lone pair of nitrogen is more donor than that of oxygen (ether); it could therefore be concluded that the amino group exerts its donor effect through coordination with the metal. This view is non-consistent with the structure of the activated quaternary complexes reported elsewhere (I, II, III).

With DBTDL as a catalyst, the replacement of a non-activated alcohol (1 or 2-butanol) by an activated one (A, B, or C) has a depressive kinetic effect. Surprisingly, the same behavior is not observed when 1-butanol is substituted by β -dimethylaminoethanol. This apparent contradiction can be explained by the coordination of the amine instead of the isocyanate. Two arguments can be forwarded that are in favor of this hypothesis.

-The donor character of the tertiary amine is higher than that of an isocyanate. Tertiary amines are indeed recognized as powerful donor ligands for metals such as Cu^{2+} , Sn^{4+} , Sn^{2+} (24, 31, 32).

-Outside the coordination sphere of the metal, the isocyanate can be activated by the carboxylate group of laurate or acetate ligands. It is to be recalled that carboxylate salts are efficient catalysts in the trimerization of isocyanate (1) as well as in polyurethane formation (4). The interaction probably takes place through the lone pair of carboxylate and π^* orbitals of the isocyanate.

Figure 5 is proposed to explain the activation effect observed in the systems: isocyanate-organometallic compound- β amino alcohol. This phenomenon is conclusively related to the donor effect of the amine onto the metal and not to the activation of the isocyanate by the metal [structures I and II (2, 6, 27)].

Conclusions

The main experimental results relative to the catalysis of the polyurethane formation by organometallic compounds can be explained by taking into account the structure of the catalysts and of coordination vacancies. Several cases are to be considered.

Case 1. The alcohol is non-activated (no donor group in β or γ position of the alcohol) and the metal has at least two vacancies. The latter are occupied by the alcohol and the isocyanate respectively and the process takes place in accordance to Fig. 6. This mechanism implies metals characterized by at least partially or completely occupied d orbitals with an energy similar to the one of the first unoccupied s, p levels (Sn^{2+} , Cu^{2+} -----).

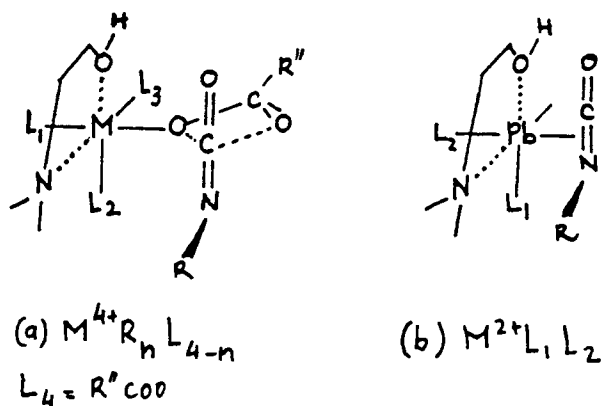


Figure 5. (a) Structure of an octahedral complex of the metal carrying four ligands. The two remaining vacancies will be occupied by an alcohol and amine (isocyanate, alcohol, amine, and metal present simultaneously); (b) Same situation as in (a) but the metal carries only two ligands.

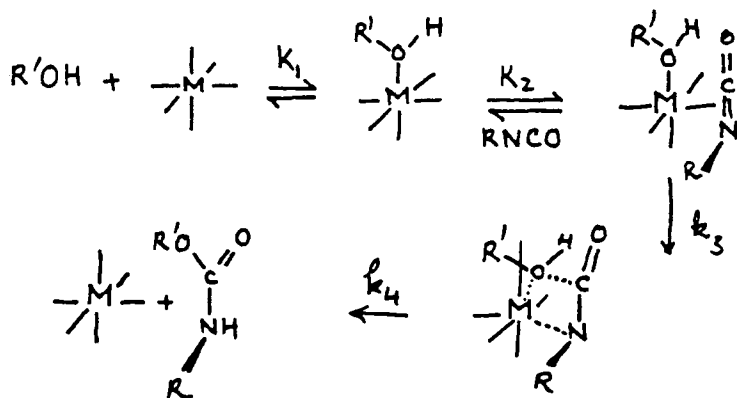


Figure 6. Proposed mechanism for the urethane formation catalyzed by organometallic compounds.

Case 2. The same system as in Case 1 is now added with a tertiary amine. The amine occupies a vacancy on the metal instead of the isocyanate. If the isocyanate is activated outside the coordination sphere of the metal, i.e. by a carboxylic ligand, the process takes place (Fig. 5a).

Case 3. Case 2 but the metal has more than two vacancies. All these components (alcohol, isocyanate and amine) are coordinated onto the metal (Fig. 5b). The results of Frisch (15) (Pb^{2+} and Sn^{2+} in Table I), Smith (6), and Robins (7) are now accordingly explained.

Case 4. When a β -amine or ethero-alcohol is used, Cases 2 or 3 are encountered. In the Case 2, the isocyanate can however be coordinated onto the metal in preference to the ether group. Under these conditions, a steric hindrance due to the ether group can exert a depressive effect on the kinetics of the process.

Further research, of course, is needed to support the new concepts developed in this paper. Recently we found in the literature that the results obtained by Bechara (33) supported our concepts.

Acknowledgements

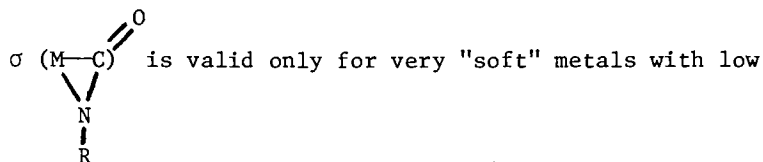
The authors want to express their gratitude to Professors: K. C. Frisch (University of Detroit, Michigan - 48221), J. E. McGrath (Virginia Polytechnic Institute and State University, Blacksburg, VA 24061), P. Teyssie (University of Liege, Sart-Tilman, 4000 Liege, Belgium) for very fruitful discussions and comments.

Literature Cited

- 1) Saunders, J. H., Frisch, K. C., "Polyurethanes, Chemistry, and Technology" Part I Chemistry Interscience, New York (1962)
- 2) Frisch, K. C., Rumao, L. P., Jour. Macromol. Sci. Revs. Macromol. Chem. (1970) (1), C5, 103
- 3) Entelis, S. G., IUPAC International Symposium on Macromolecular Chemistry, Budapest (1969), 89
- 4) Farkas, A., Mills, G.A., Adv. Catalysis, (1962), 13, 393
- 5) a) Nesterov, O.V., Zabrodin, V.B., Chirkov, Yu. N., Entelis, S. G., Kinetic Cat. (1974), 15, 1183
 b) *ibid*; Kinetic Cat. (1972), 13, 200
 c) Zabrodin, V. B., Nesterov, O. V., Entelis, S. G., Kinetic Cat. (1970), 11, 877
 d) *ibid*; Kinetic Cat., (1970), 11, 91
 e) *ibid*; Kinetic Cat., (1969), 10, 544

- 6) Smith, H. A., Jour. Appl. Polym. Sci. (1963) 7, 85
- 7) Robins, J., Jour. Appl. Polym. Sci. (1965) 9, 821
- 8) Williams, F., Ulrich, H., Jour. Appl. Polym. Sci. (1969) 13, 1929
- 9) Willeboorse, F. C., Critchfield, F. E., Meeker, R. L., Jour. Cellular Plast. (1965), 1, 76
- 10) Reegan, S. L., Frisch, K. C., Jour. Polym. Sci. (1970) A1, 8, 2883
- 11) Smith, H. A., Jour. Poly. Sci. (1968) A1, 6, 1299
- 12) Entelis, S. G., Nesterov, O. V. Russ. Chem. Revs., (1966) 35, (12) 917
- 13) Zabrodin, V. B., Zhur. Phys. Khim. (1971) N3, 45
- 14) Anzuino, G. Pirro, A., Rossi, G., Polofriz, L., Jour. Polym. Sci. Polym. Chem. Ed. (1975) 13, 1667
- 15) Rand, L. Thir, B. Reegan, S. L., Frisch, K. C., Jour. Appl. Polym. Sci. (1965) 9, 1787
- 16) Huynh-ba, G. Teyssie, Ph. Jerome, R., Polym. Preprint, (1980) 21 (2) 307
- 17) Frisch, K. C., Reegan, S. L., Floutz, W. V., Silver, J. P., Jour. Polym. Sci. (1967) A1, 5, 35
- 18) Farkas, A., Strohm, P. F., Industr. and Eng. Chem. Fundamental (1965) 4, 32
- 19) Oberth, A. E., Brunner, R. S., Jour. Phys. Chem. (1968) 72, 845
- 20) Zharkov, U. V., Zhitinlainer, A. V., Zhokhova, F. A., Zh. Fiz. Khimie. (1970) 44, 223
- 21) a) Entelis, S. G., Nesterov, O.V., Kinet. Kataliz. (1966) 7, 464
b) ibid., Kinet. Kataliz.(1966), 7, 627
c) ibid., Kinet. Kataliz. (1966) 7, 805
- 22) Pestemer, H., Lauerer, D., Angew Chem. (1960) 72, 612
- 23) Frisch, K. C., "Polyurethane Technology", Bruins, P. F., ed. Wiley Inters., New York (1969)
- 24) Dyer, E., Pinterton, R. B., Jour. Appl. Polym. Sci. (1965) 9, 1713
- 25) Bloodworth, A. J., Davies, A. G., Proc. Chem. Soc. (1963) 264
- 26) Lipatova, T. E., Bakalo, L. A., Niselsky, Yu. N., Sirotinskaya, A. L., Jour. Macromol. Sci. Chem. (1970) A4, (8) 1743
- 27) Chirkov, Y.N., Nesterov, O. V., Entelis, S. G., Kinetic Cat. (1973), 14, 798
- 28) Thiele, L., Becker, R. Frommelt, H., Faserforsch Textiltech. (1977) 28 (7), 343
- 29) Bloodworth, A. J., Davies, A. G., Jour. Chem. Soc., (1965) 5328

30) Teyssie, Ph. Private Communication: structure type double



oxidation stage. Our example on Sn⁴⁺ is "hard" type and high oxidation stage.

31) Okawara, R., Wada, M., Adv. Organomet. Chemistry, (1967) 5, 137

32) Zubieta, J. A., Zuckerman, J. J., Progress in Inorganic Chemistry, Lippard, S. J. Ed., Interscience, New York (1978) 24, 251

33) Bechera, S., Org. Coat. and Plast. Chem., (1980) 43, 914

RECEIVED May 14, 1981.

Structure and Segmental Mobility of Polyester Urethanes Using Photochromic Azobenzene Probes

CLAUS D. EISENBACH

Institut für Makromolekulare Chemie, Universität Freiburg,
Hermann-Staudinger-Haus, Stefan-Meier-Strasse 31, D-7800 Freiburg, West Germany

Photochromic processes in a solid matrix such as polymers generally proceed with considerable deviations from solution. This phenomenon is ascribed to particular interactions between the photoreactive molecule and the surrounding matrix (1,2) on a molecular scale (3) as will be shortly illustrated below. It can be inferred from these findings that photochromic molecules, on the other hand, should be suitable probes to detect, e. g., particular motions in solid polymers and changes of the overall chain segmental mobility. This is a challenging technique to be applied in the field of polyurethane elastomers, since quite a few questions are still unsolved in this area.

For segmented polyurethane elastomers of the $\{AB\}_n$ type it is established that the elastomeric properties are due to physical crosslinks of the urethane hard segments B via hydrogen bonding (4,5,6), whereas the soft segments A form the continuous soft phase. However, the question of 1) how complete the phase separation between the soft phase and the hard domains is, 2) of the extent to which single hard segments are dissolved in the soft phase and how much they influence the elastomeric properties via hydrogen bonding to soft segments and 3) of size and shape of the domains and the structure and dimension of the interlayer between soft and hard phase are still not yet solved (7,8,9).

For completeness and better understanding of the method described in this paper and the conclusion drawn, the main results obtained with azaromatic chromophores incorporated in linear poly(acrylates) and poly(methacrylates) (3,10) are first presented and shortly discussed; then the investigation of the photochromic polyurethanes will be described and evaluated.

Experimental

The two-phase polyurethanes were synthesized in the usual way starting from a polyester diol which is reacted with a diisocyanate and finally the chain extension reaction is achieved by

0097-6156/81/0172-0219\$05.00/0
© 1981 American Chemical Society

addition of a diamine. In case of the polyurethanes with chromophoric soft segments (11), the starting polyester was obtained by a copolycondensation reaction of a 4,4'-diaminoazobenzene derivative, 1,4-butandiol and adipic acid; 2,4-tolylene diisocyanate (TDI) was used for the formation of the prepolymer and the final polyurethane was obtained by addition of carbohydrazid. The polyurethanes with partly chromophoric hard segments (12) were obtained by using 4,4'-diaminoazobenzene (DAAB) together with ethylene diamine (EDA) as chain extenders in the final reaction step, starting with poly(tetramethylene adipate) as macrodiol and TDI or 4,4'-methylenebis(1,4-phenylene) diisocyanate (MDI) as diisocyanates. The experimental details for these two types of photochromic poly(ester urethane)s are given elsewhere (11,12).

The single phase polyurethanes were obtained by first reacting a small amount of DAAB with MDI or TDI in DMF solution and subsequent addition of poly(tetramethylene adipate) diol, i. e., no EDA chain extender was used (13).

The polymers were purified by reprecipitation from DMF/methanol and dried for 48 hrs. at 60°C under vacuo.

Clear, thin films of all polymers could be obtained by melting the polymer at 140°C under compression between teflon coated steel plates.

The samples were characterized by DSC-measurements and by torsional pendulum experiments.

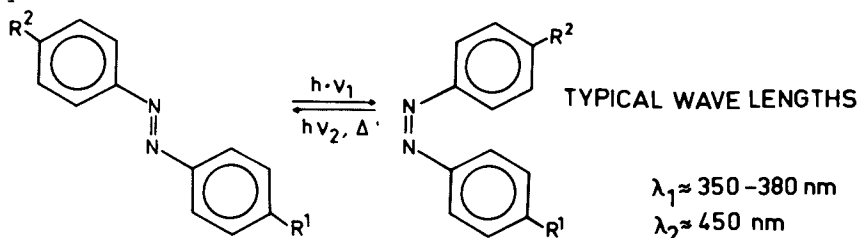
For the photochemical isomerization, a 150 W Xe-lamp or a 200 W Super Pressure Mercury Lamp were used. The light was filtered either by using a monochromator or an interference filter with transmission in the wavelength range of the maximum absorption band of the trans isomer. The other conditions were the same as previously described (3). The proceeding of the photochemical and the thermal cis-trans isomerization was followed by measuring the change in the absorption of the trans-isomer in the area of 370-400 nm.

Results and Discussion

1) General discussion of photochromism in polymer matrices

Photochromism means the reversible change of a single chemical species between two different states having distinguishable different absorption spectra; the change is induced in at least one direction by the interaction with electromagnetic radiation (14).

Typical photochromic molecules which best fulfil these requirements are the aromatic azo benzenes:



A reversible cis-trans isomerization around the azo-linkage occurs upon irradiation with UV-light of the appropriate wavelength; the typical UV-absorption spectra of these chromophores incorporated in a poly(methyl methacrylate) matrix after different periods of irradiation are shown in Fig. 1.

In the following the thermal back reaction of the cis-isomers to the thermodynamically more stable trans-isomer will be discussed; in the experiment, the polymer film is irradiated until the photostationary state is reached, then the light source is cut off and the reformation of the trans-isomer with time is followed by measuring the increase of the UV-absorption at the maximum absorption band of the trans-form.

Whereas the thermal cis-trans isomerization follows single first order kinetics in rubbery specimen, this is not the case in glassy polymers (Fig. 2). The experimental curve can be resolved by two simultaneous first order processes, one of these reactions (line 3) being much faster than the thermal back reaction in solution at the same temperature (3).

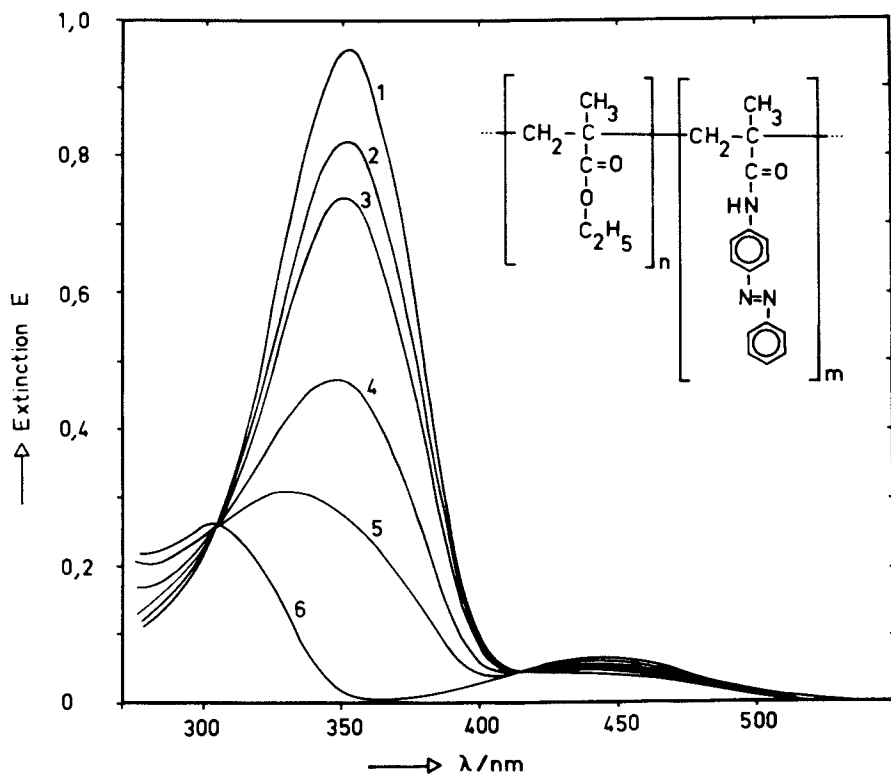
Since the cis-isomers can only be present as a single species, this phenomenon has to be attributed to two different relaxation mechanisms. This is evident from the reduced Arrhenius plot of the rate constant k of the thermal cis-trans back reaction in terms of a_T (Fig. 3); a_T is the ratio of the thermal cis-trans relaxation time τ ($1/k$) at temperature T to its value at T_g .

For all glassy polymers investigated, a_T of the normal and the so-called anomalously fast reaction is given by two linear branches. The apparent energies of activation as determined from the slopes are 68.7 kJ/mol and 26.8 kJ/mol. These values coincide with the characteristic activation energies for rotational (crankshaft (15)) and translational chain segmental motions in glassy polymers (3,10). It was therefore concluded that only chain segmental relaxation processes, which depend on the local environment of the chromophore, are the controlling factors for the isomerization.

The temperature dependency of the apparent energy of activation of the bleaching process as exhibited by the curvature in the Arrhenius plot (Fig. 3) is typically found for, e. g., dynamic mechanical relaxation processes (17), which leads to the connection with the free volume theory. The latter processes are best described by the WLF-equation (18), $\log a_T = C_1(T-T_g)/(C_2+T-T_g)$, i. e., a master plot is obtained when plotting the logarithm of a_T vs. $T-T_g$.

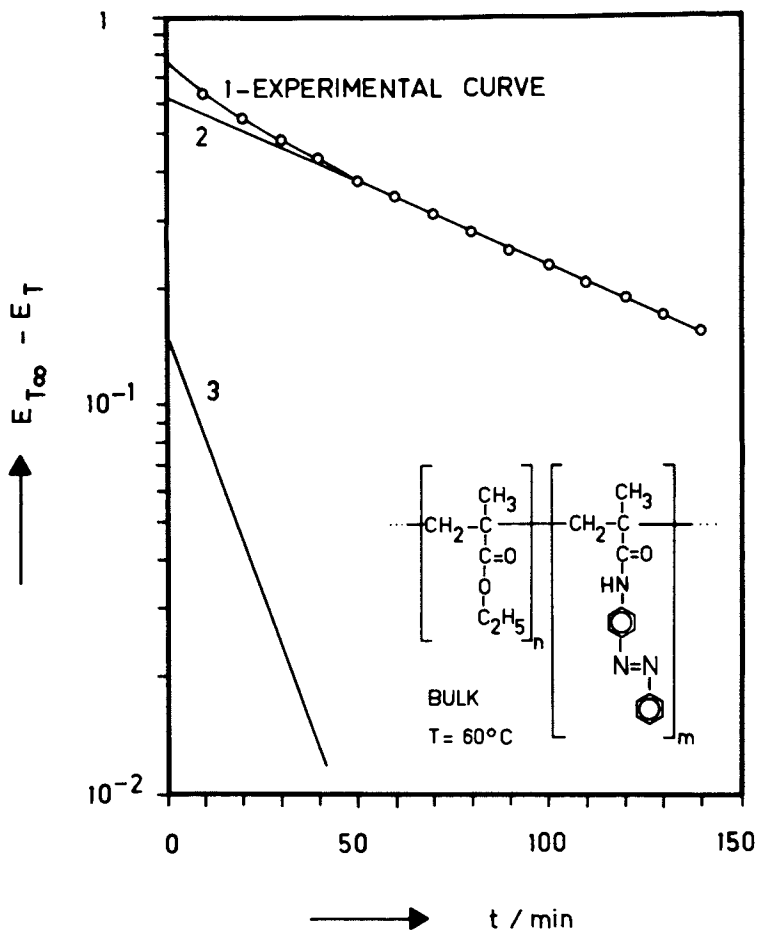
The form of the WLF-equation, indeed, is also valid for photochromic relaxation processes (3,10); this is shown by the corresponding WLF-plot of the relaxation time of the azochromophore (Fig. 4).

In conclusion it can be stated from these general studies that photochromic processes in polymer matrices can be described by the free volume theory; moreover, these processes are controlled by the kind of local environment around the photochromes,



Die Makromolekulare Chemie

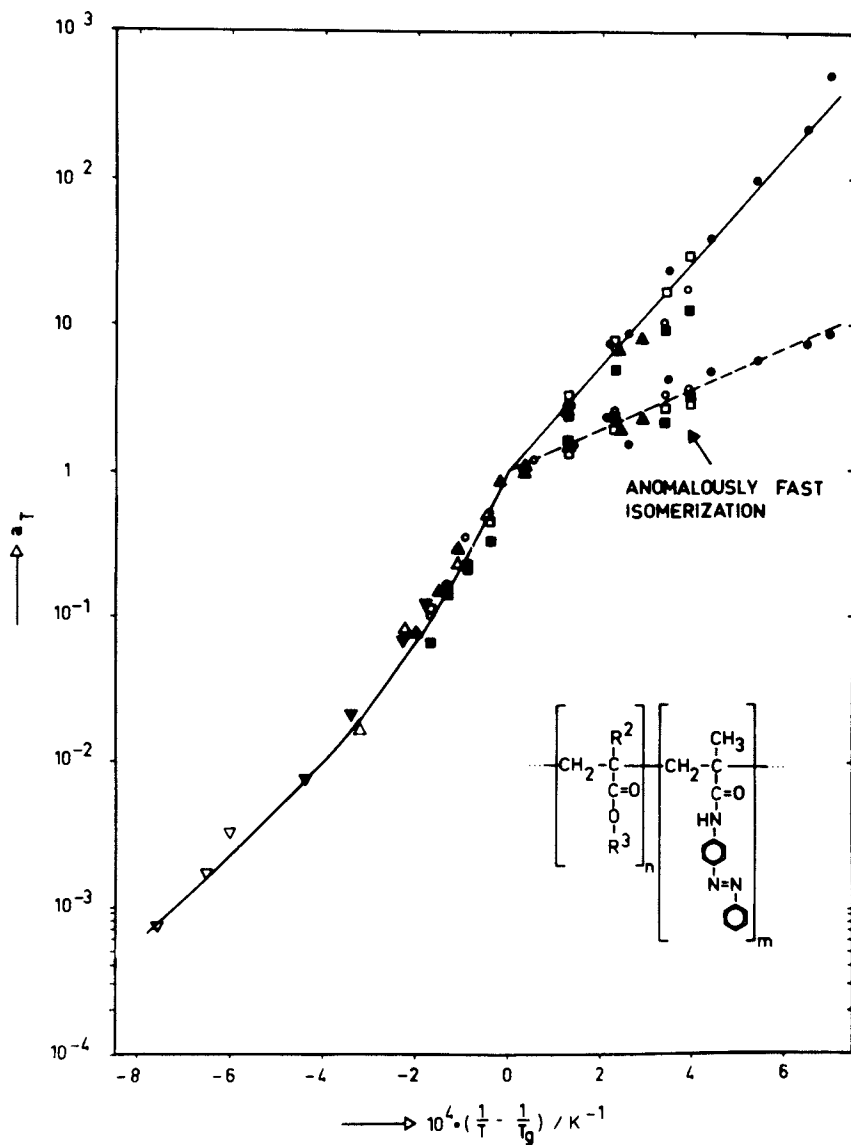
Figure 1. The UV absorption of a film of methylmethacrylate/4-methacrylaminoazobenzene-copolymer after different periods of irradiation ($\lambda = 355 \text{ nm}$) (3).



$$[T_{\infty}] - [T] = \underbrace{[c_N]_0 \cdot e^{-k_1 t}}_{\text{CURVE 2}} + \underbrace{[c_A]_0 \cdot e^{-k_2 t}}_{\text{CURVE 3}}$$

Die Makromolekulare Chemie

Figure 2. Resolution of the experimentally obtained time-conversion curve by two simultaneous first-order reactions (3).



Die Makromolekulare Chemie

Figure 3. Reduced Arrhenius plot of a_T (ratio of the relaxation time at temperature T and T_g) for the thermal *cis*-*trans* isomerization of azoaromatic chromophores in bulk polymers (3).

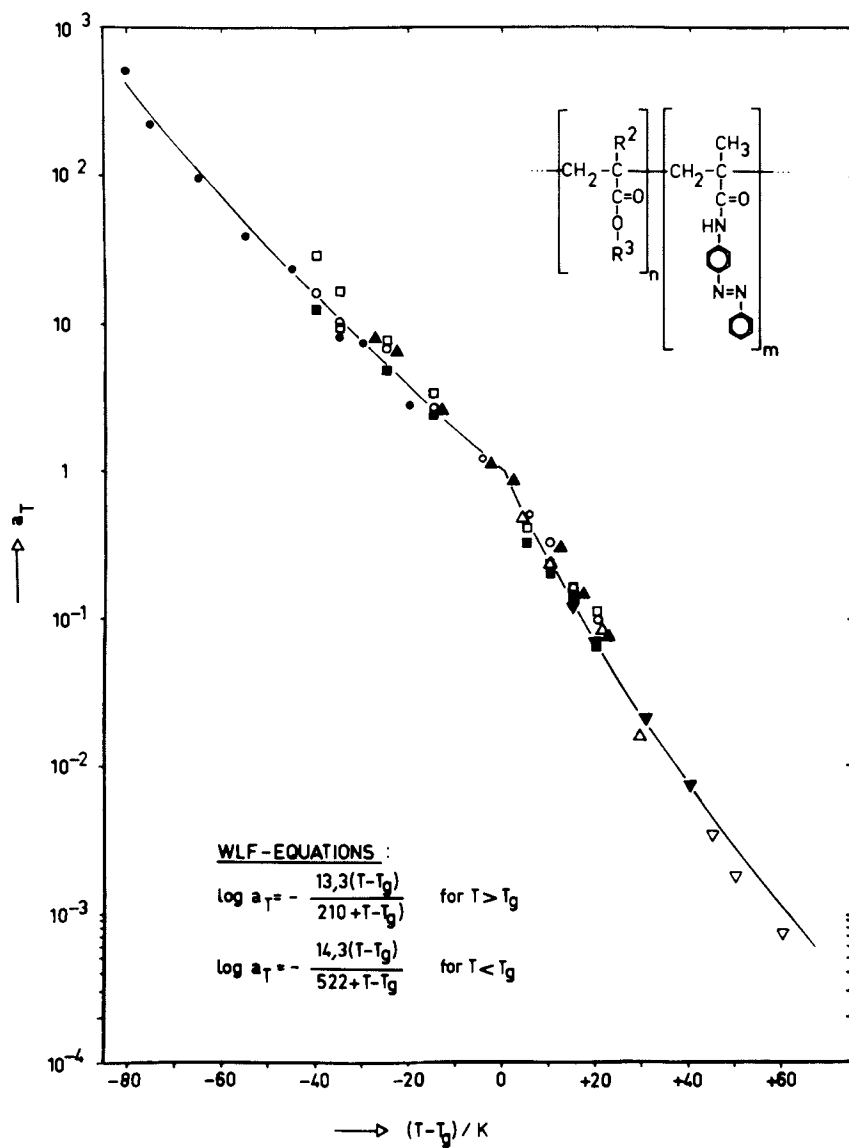


Figure 4. The WLF plot of a_T for the thermal *cis-trans* isomerization of azo-aromatic chromophores in bulk polymers (3, 10).

particularly the mobility of chain segments. As a consequence, a photochromic molecule can be expected to probe polymer properties on a molecular scale what will be shown in the following with the example of polyurethanes.

2) Photochromism in polyurethanes

As outlined before, the question of interest now is first, how the photochrome would react when incorporated in the backbone of amorphous and semicrystalline polymers such as segmented polyurethanes and if the isomerization behaviour of the photochrome would allow conclusions on the structure, morphology, and segmental mobility of this matrix.

The segmented structure of polyurethane elastomers and the chain organization in the solid polymer is schematically shown in Fig. 5a and b. These polymers are usually made by subsequent addition polymerization reactions: a high molecular weight macrodiol (e.g., poly(tetramethylene adipate) or poly(tetramethylene oxide), molecular weight between 1000 and 2000) is reacted with a diisocyanate (TDI or MDI) to form a so-called macrodiisocyanate and by the addition of a low molecular weight diol or diamine the chain extension reaction to the final segmented elastomer (Fig.5a) takes place. Due to the incompatibility of the hard and soft segments in the temperature range of application, phase separation occurs resulting in a domain structure (Fig. 5b);

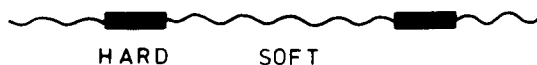
The hard segment aggregates act as physical crosslinks and this thermoreversible three-dimensional network formation accounts for the properties of these thermoplastic elastomers.

This basic view of the structure and morphology of segmented polyurethane elastomers is well established (19), but as mentioned before, on a microscopic level these polymer systems are far from being fully understood; the key questions are linked to the phase separation (e. g., sharpness of interlayer between hard and soft phase, fraction and effect of isolated hard segments in the soft phase) and to the resulting chain segmental mobility of hard and soft segments in the regions of different morphology.

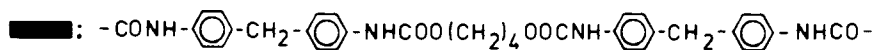
The approach of using a photochromic probe for the study of these problems was undertaken with three types of photochromic segmented polyurethanes (one-phase and two-phase systems) with an aromatic azochromophore incorporated in different sections of the polymer chain; this is schematically represented in Fig. 6. In the two-phase systems the chromophore is statistically incorporated either in the soft segment or in the hard segment; in the single phase system, which is obtained by a polyaddition reaction of macrodiol and diisocyanate without using a particular chain extender except for a small amount of DAAB, the azochromophore is part of an isolated hard segment unit. Thus, the azochromophore is located in a variety of representative regions and segments in these polymers, allowing a general study of the influence of structural and morphological changes of the matrix on the photochromism as well as of the use of a photochromic probe in multi-phase polymer systems.

SEGMENTED POLYURETHANE ELASTOMERS

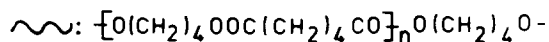
SCHEME OF THE CHAIN STRUCTURE:



HARD SEGMENT:



SOFT SEGMENT:



SCHEMATIC REPRESENTATION OF DOMAIN STRUCTURE:

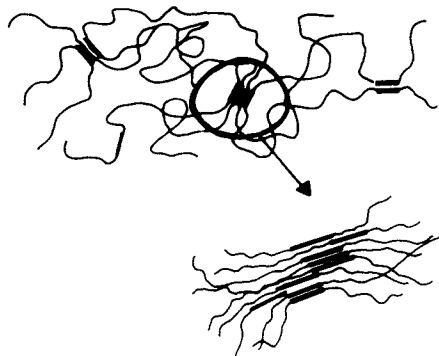


Figure 5. Scheme of primary chain structure of segmented polyurethane elastomers and chain segment organization.

2a) Two-phase polyurethanes with chromophoric soft segments (11)

The basic structure of these poly(ester urethane)s with a DAAB derivative randomly incorporated in the polyester soft segment in various concentrations is shown in Fig. 7.

The photochemical cis-trans isomerization of the azochromophore can be achieved by irradiation at the maximum absorption band of the trans isomer at $\lambda=378$ nm; the change in the absorption spectra of a polymer film before and after irradiation is given in Fig. 8. Similar fractions of cis-isomers can be obtained in samples quenched from the melt (i.e., from above the melting temperature T_m of the soft phase; $T_m=45^\circ\text{C}$) and in samples annealed at temperature some degrees below T_m of the soft phase, by which some soft segment crystallization was caused.

In contrast to this, distinct differences were observed for the thermal cis-trans isomerization depending on the samples thermal history; the increase in the trans-isomer content was followed by measuring the change in the absorption at $\lambda=378$ nm (Fig. 8).

At temperatures above T_m , single first order kinetics were found for the thermal back reaction as one would expect for this reaction in an amorphous matrix, in agreement with the results obtained for, e. g., the polyacrylate systems (3) (s. above). The same behaviour is also found at temperatures below T_m in samples quenched from the melt with still completely amorphous soft phase (Fig. 9, line 4), and the rate constants k_3 of the thermal back reaction in these samples were similar to those found in solution over the whole temperature range. In contrast to this, the kinetics do not follow single first order kinetics in the annealed samples (Fig. 9, line 1), but the experimental curve is given by two exponentials (line 2 and 3, Fig. 9), similar to what was already found in glassy polymers. As could be shown by DSC-measurements of annealed samples, partial crystallization of soft segments occurs due to the annealing procedure at about 5 K below T_m of the soft phase; therefore the phenomenon of two simultaneous first order processes in these samples with semicrystalline soft phase as compared to only one single first order process in samples with completely amorphous soft phase clearly shows the sensitivity of the photochrome to changes in the morphology of the surrounding matrix.

The rate constants k obtained for thermally differently treated polyurethanes are represented in the Arrhenius plot, Fig. 10. The apparent energy of activation E_A for the thermal cis-trans isomerization, as determined from the slopes in Fig. 10, is about 80 kJ/mol (k_3) in polymers with completely amorphous soft phase, a similar figure as found in solution; in samples with partially crystallized soft segments, values of about 60 kJ/mol (k_1) and 19 kJ/mol (k_2) are found for the two simultaneous first order processes (line 2 and 3, Fig. 10). The occurring of these two apparent energies of activation, which are similar to the energies required for rotational (crankshaft (15)) and translational (3)

PHOTOCHROMIC SEGMENTED POLYURETHANES

TWO-PHASE SYSTEM:

(MACRODIOL+DIISOCYANATE+CHAIN EXTENDER)

1)PHOTOCHROME (●)IN THE SOFT SEGMENT(~~~):



2)PHOTOCHROME (●)IN THE HARD SEGMENT(■):



SINGLE-PHASE SYSTEM:

(MACRODIOL+DIISOCYANATE, NO CHAIN EXTENDER)

PHOTOCHROME (●) IN THE "HARD SEGMENT" (—):

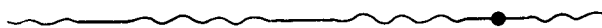
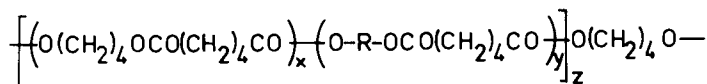


Figure 6. Scheme of the primary chain structure of photochromic segmented polyurethanes with aromatic azochromophores built in the polymer chain.

PHOTOCHROMIC POLY(ESTER URETHANES)Soft Segment A

$$30 < x/y < 500 ; z \sim 12$$

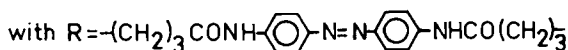
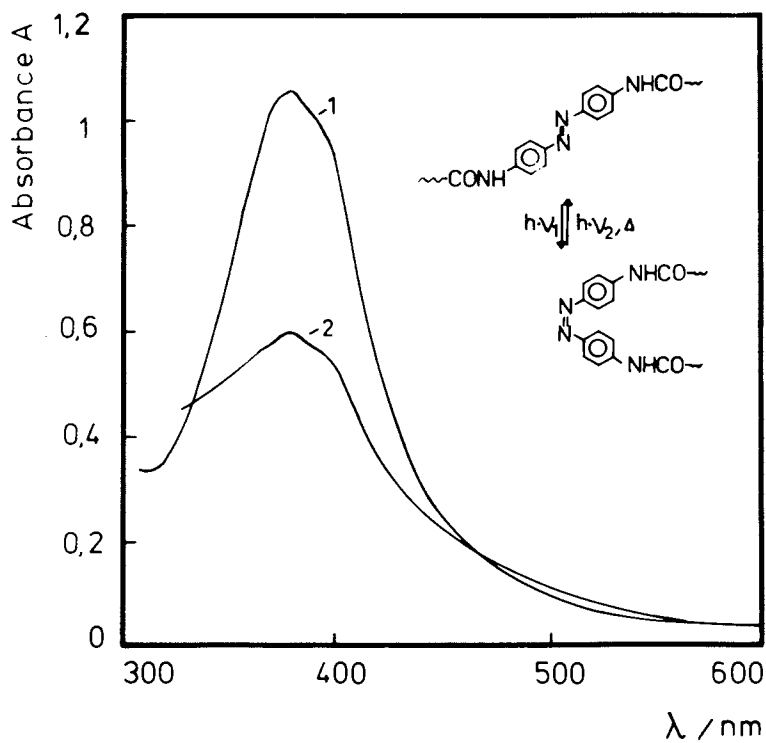
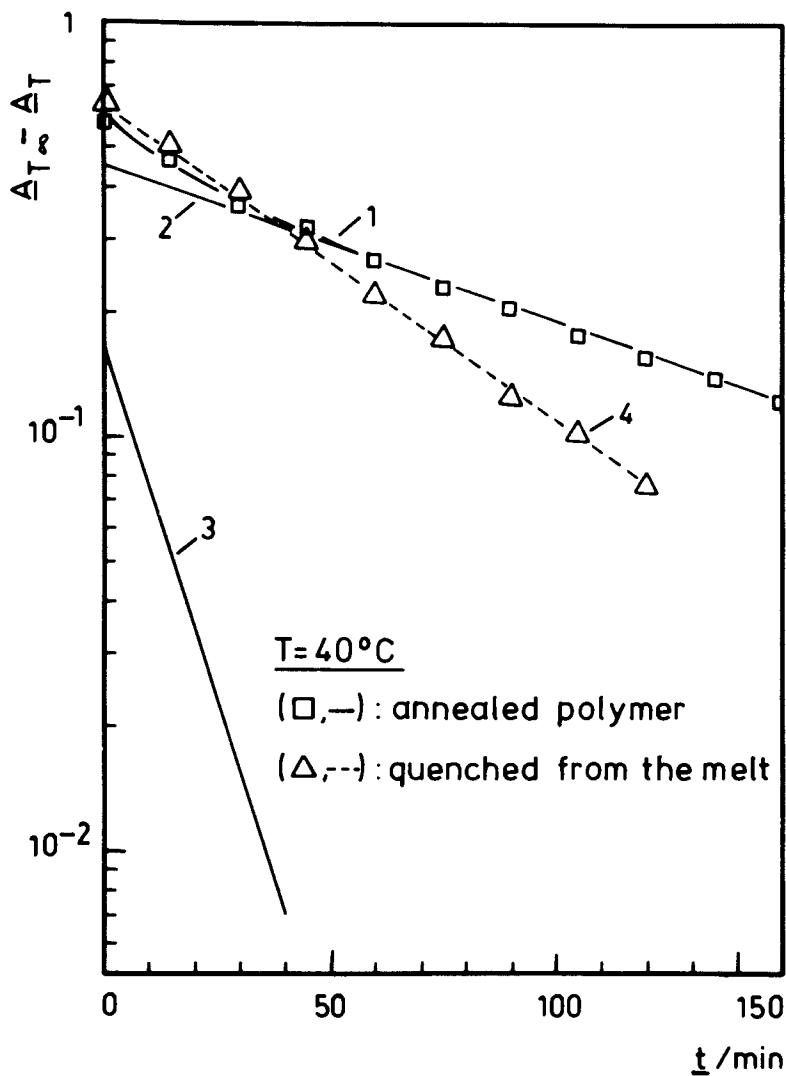
Hard Segment B

Figure 7. Molecular structure of soft and hard segment of photochromic polyester urethane with partly photochromic soft segments.



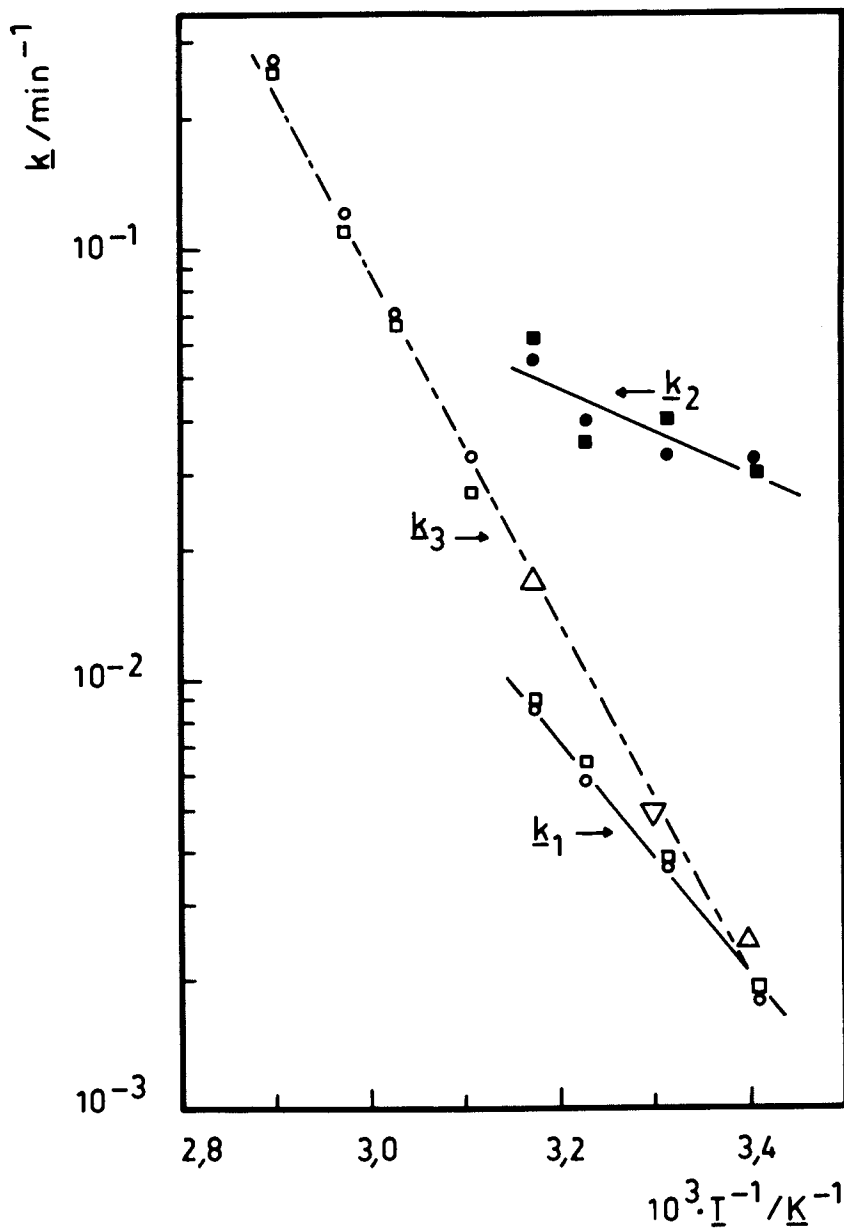
Polymer Bulletin

Figure 8. The UV absorption spectra of polyurethane film with photochromic soft segment before (1) and after (2) irradiation at $\lambda = 378$ nm (11).



Polymer Bulletin

Figure 9. First-order plot of the thermal *cis-trans* isomerization of the azochromophore incorporated in the soft segment (solid film) (11).



Polymer Bulletin

Figure 10. Arrhenius plot of the rate constants k of the thermal *cis-trans* isomerization of the azochromophore incorporated in the soft segment (solid film): k_1 and k_2 , annealed polymer; k_3 , quenched polymer (11).

chain segmental motions, were also found for the two first order processes in glassy polymethacrylates (3,10,11). Since the activation parameters of photochromic processes in polymers reflect the chain segmental mobility of the polymer matrix, it can be inferred, that the local segmental mobility in the soft phase with additional physical crosslinks (due to crystallization of polyester segments by annealing) is reduced to an extent comparable to the glassy state not too far below T_g (10,16). The photochromic probe is not only able to detect changes in the morphology of the surrounding matrix, but also allows some conclusion on the restrictions in the overall segmental mobility and on the kind of chain segmental motions in the matrix upon changes of the morphology.

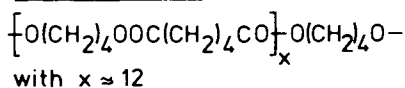
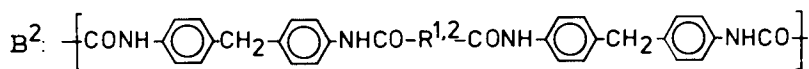
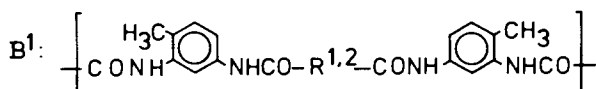
2b) Two-phase polyurethanes with chromophoric hard segments (12)

The polymers investigated had a small amount of chromophoric hard segments incorporated and randomly distributed within the poly (ester urethane) chain; the basic structure of these systems is illustrated in Fig. 11.

In contrast to the polyurethane systems with chromophoric soft segments discussed above, in these polymers no photoisomerization of the incorporated azoaromatic group could be achieved in the solid state for both types of polyurethanes with MDI or TDI based hard segments. In solution, however, photoisomerization of the azochromophore occurs by exposure to light in the region of the maximum trans absorption and the same fraction of cis-isomers in the photostationary state could be reached for the chromophoric polyurethane as for a model compound of the azoaromatic hard segment unit, 4,4'-di(phenylurea)azobenzene.

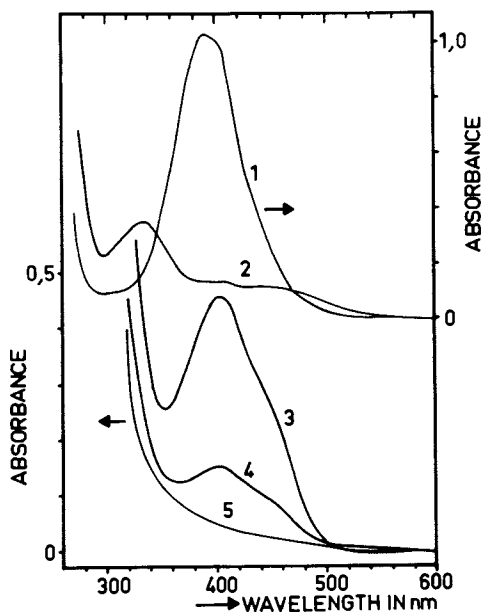
In Fig. 12 the absorption spectra of the low molecular model compound (curve 1,2) and the polyurethane (curve 3,4) before and after irradiation are depicted. The coinciding spectra of the model compound and the polymer in solution and their coinciding photoresponse are clear evidence for the fact that the chromophore is built into the polymer backbone as part of the hard segments as shown in Fig. 11. The UV-spectra obtained from polyurethane films were similar to the one in solution shown in curve 3, Fig. 12, but did not change upon irradiation of the films.

The fact that in these bulk polymer samples no photoisomerization could be detected has to be attributed only to the severe restrictions of the local chain segmental mobility around the chromophore, i. e., it is due to the predominant incorporation of the azochromophoric units in the hard phase; the mobility of chain segments within the hard domain is widely suppressed in this system, causing a nearly complete immobilization of the chromophore in the hard phase. This behaviour is comparable to systems where the photochrome was incorporated in highly crystalline polyamide or polyimide (2,20,21).

Soft Segment AHard Segment B

with $\text{R}^1 = \text{HN}-(\text{CH}_2)_2\text{NH}$ and $\text{R}^2 = \text{HN}-\text{C}_6\text{H}_4\text{N}=\text{N}-\text{C}_6\text{H}_4\text{NH}$
 mol ratio $\text{R}^1/\text{R}^2 = 100$

Figure 11. Molecular structure of soft and hard segment of photochromic polyester urethane with partly photochromic hard segments.



Die Makromolekulare Chemie, Rapid Communications

Figure 12. The UV absorption spectra of 4,4'-di(phenylurea)azobenzene (Curves 1 and 2) and polyurethane with photochromic hard segment (Curves 3 and 4) in DMF solution before (1,3) and after (2,4) irradiation at $\lambda = 405 \text{ nm}$; Curve 5: pure poly(tetramethylene adipate urethane) (12).

2c) Single-phase polyurethanes with chromophoric hard segments (13)

Polyurethanes with a few chromophoric hard segment units which do not show phase separation can be obtained by a polyaddition reaction of only a macrodiol and a diisocyanate in nearly stoichiometric amount (slight excess of diisocyanate) together with a small amount of a difunctional chromophore (DAAB), counterbalancing the diisocyanate excess. The structure of such polyurethanes investigated here are given in Fig. 13.

As compared to the systems discussed in the previous section, due to the absence of a chain extender (EDA) in the synthesis of these polyurethanes, the length of the carbamate units is not sufficient to enable phase separation; consequently, the small amount of photochromic hard segments here exist in a medium similar to isolated hard segments in the soft-phase of two-phase polyurethanes.

For these polyurethanes, photoisomerization of the azochromophore in solid films again is possible, as it was the case for the two-phase polyurethanes with chromophoric soft segments. These results confirm similar observations of relatively facile photoisomerization of azochromophores in the hard segment of corresponding poly(propyleneoxid urethanes) (22).

These findings reveal that photoisomerization of aromatic azo compounds is only possible if the chromophore is incorporated in a sufficiently flexible matrix. This is a basic requirement not only because of the fact that sufficient free volume has to be provided for the trans-cis photoisomerization, but also because a chain segment pendent to the azochromophore has to be slipped through the matrix since the distance between the para carbons in the azobenzene derivative is decreased by about 50 % when going from the trans- to the cis-isomer (23).

For the case of the polyurethanes it can be assumed that, independent of the nature of the matrix, the cis-trans isomerization of azobenzene containing hard segments is possible as long as no phase separation occurs, which would cause an incorporation of these chromophoric segments into the hard domain. It means that the mobility of the chromophoric hard segments in the single phase system, which are representative for isolated hard segments in two-phase systems not contributing to the hard domains, is, by far, not as restricted as the mobility of the segments in the hard domains; furthermore, it can be assumed from the photochromic behaviour that these isolated hard segments rarely influence the properties of polyurethane elastomers to an appreciable extent since their mobility is similar to the soft segments themselves.

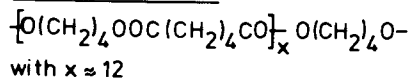
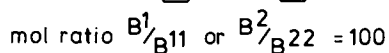
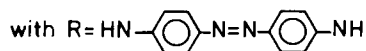
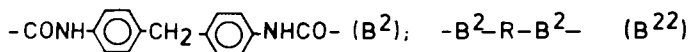
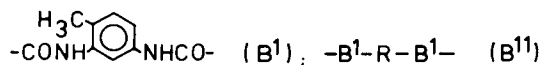
SOFT SEGMENT AHARD SEGMENT B

Figure 13. Molecular structure of a single-phase polyurethane containing a few chromophoric hard segments.

Conclusion

It is clearly evident from the data discussed above that the isomerization of the aromatic azochromophore incorporated in the backbone of polyurethanes is markedly affected by its position in the backbone of the polyurethanes and also by the morphology of the polymer matrix. The kinetics of the photoisomerization and the thermal cis-trans isomerization both reflect the structure, morphology and segmental mobility of the surrounding polymer. In particular it was shown that the soft segment mobility is highly restricted in ordinary two-phase polyurethanes with additional soft phase crystallization, that the segmental mobility of hard segments in the hard domains is neglectably small compared to the segmental mobility of soft segments in the soft phase and finally that the mobility of isolated hard segments in the soft phase is comparable to that of soft segments.

In conclusion it can be stated that, based on the already positive results and new findings discussed above, photochromic molecules can be used as probes for the study of some of the open questions in the area of polyurethanes mentioned at the beginning; this technique will further be employed in future work with photochromic polyurethane elastomers of known segment length distributions.

Literature Cited

- 1) G. Smets, *Pure Appl. Chem.* 30, 1 (1972)
- 2) C. S. Paik, H. Morawetz, *Macromolecules* 5, 171 (1972)
- 3) C. D. Eisenbach, *Makromol. Chem.* 179, 2489 (1978)
- 4) R. Bonart, *Angew. Makromol. Chem.* 58/59, 259 (1977)
- 5) R. Bonart, *Polymer* 20, 1389 (1979)
- 6) R. W. Seymour, G. M. Estes, S. L. Cooper, *Macromolecules* 3, 579 (1970)
- 7) R. Bonart, E. H. Müller, *J. Macromol. Sci., Phys. B* 10, 345 (1974)
- 8) G. M. Estes, R. W. Seymour, S. L. Cooper, *Macromolecules* 4, 452 (1971)
- 9) J. W.C. van Bogart, J. C. West, S. L. Cooper, *Am. Chem. Soc., Div. Org. Coat. Plast. Chem., Prepr. Vol.* 37 (2), 503 (1977)
- 10) C. D. Eisenbach, *Ber. Bunseng. Physikal. Chem.* 84, 680 (1980)
- 11) C. D. Eisenbach, *Polym. Bull.* 1, 517 (1979)
- 12) C. D. Eisenbach, *Makromol. Chem. Rapid. Commun.* 1, 287 (1980)
- 13) C. D. Eisenbach, *Polym. Bull.*, in preparation
- 14) G. H. Brown, *Techniques of Chemistry, Vol. III, "Photochromism"*, Wiley Interscience, New York 1971
- 15) T. Schatzki, *J. Polym. Sci.* 57, 496 (1963); *Polym. Prepr., Am Chem. Soc., Div. Polym. Chem.* 6, 646 (1965)
- 16) C. D. Eisenbach, *Europhys. Conf. Abstr., Europ. Phys. Soc., Vol. 4A*, 212 (1980)
- 17) N. G. McCrum, B. E. Read, G. Williams, *Anelastic and Dielectric Effects in Polymeric Solids*, John Wiley and Sons, London 1967

- 18) M. L. Williams, R. F. Landel, J. D. Ferry, *J. Am. Chem. Soc.* 77, 3701 (1955)
- 19) S. L. Cooper, G. M. Estes, *Multiphase Polymers*, *Advanc. in Chem. Ser.* 176, Am Chem. Soc., Washington, D. C. 1979
- 20) F. Agolini, F. P. Gay, *Macromolecules* 3, 349 (1970)
- 21) D. Ta-Li Chen, H. Morawetz, *Macromolecules* 9, 463 (1976)
- 22) C. S. Paik Sung, L. Lamarre, M. K. Tse, *Macromolecules* 12, 666 (1979)
- 23) J. J. de Lange, J. M. Robertson, I. Woodward, *Proc. Roy Soc., Ser. A* 171, 398 (1939); G. V. Hampson, J. M. Robertson, *J. Chem. Soc.* 1941, 409

RECEIVED June 23, 1981.

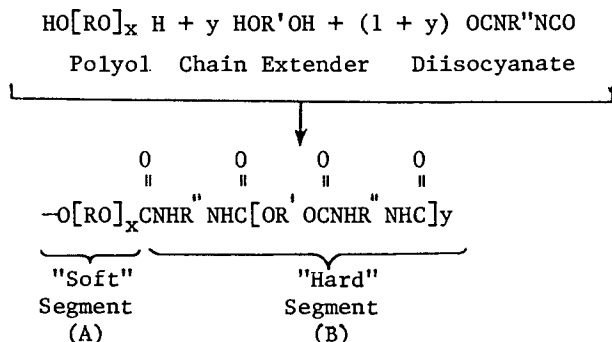
Thermoplastic Polyurethanes Based on Poly(oxyethylene–oxypropylene) Glycols

The Dependence of Properties and Injection Moldability on Molecular Structure

F. X. O'SHEA

Uniroyal, Inc., World Headquarters, Middlebury, CT 06749

Thermoplastic polyurethanes (TPU) are a versatile family of elastoplastic materials characterized by outstanding toughness and abrasion resistance. These materials are prepared from three principal reactants, a difunctional polyol, a difunctional chain extender and a diisocyanate in accordance with the following reaction:



They are linear block copolymers of the (AB)_x type in which A is the "soft" segment derived from the polyol and B is the "hard" segment derived from the diisocyanate and chain extender. Theoretically, infinite molecular weight would be achieved at an isocyanate to total hydroxyl ratio of 1.0. Thus the number of moles of diisocyanate is equal to the sum of the number of moles of polyol and chain extender as shown. Hardness of the materials can be varied by altering the molar ratio of chain extender to polyol which in turn affects the weight ratio of hard segment to soft segment in the polymer.

A principal obstacle to growth in TPU usage has been the high cost of these polymers because of the expensive raw materials required. Among commercially available diisocyanates only methylenebis(phenylisocyanate), pure MDI, produces

0097-6156/81/0172-0243\$05.00/0
 © 1981 American Chemical Society

acceptable injection moldable polymers and then only with a limited number of chain extenders such as 1,4-butanediol and the bis(hydroxyethylether) of hydroquinone. The structures of these compounds are shown in Figure 1.

Until recently, the polyol component was restricted to poly(oxytetramethylene)glycol (PTMG), polycaprolactone diol and to adipate ester diols such as poly(ethyleneadipate)diol. The structures of these polyols are shown in Figure 2.

This paper describes work which we have carried out on TPU elastomers derived from poly(oxypropylene)glycols (PPG polyols) and from poly(oxyethylene-oxypropylene)glycols as the polyol components of the elastomers. Our interest in these materials is based on the lower cost of these polyols, especially since the polyol comprises about 45 to 65 percent by weight of the raw materials used in preparing most TPU elastomers.

Figure 3 shows the structure of these polyols. The poly-(oxyethylene-oxypropylene)glycols are often referred to as "tipped" PPG polyols since they are commonly prepared by post-reacting a PPG polyol with ethylene oxide. The reaction increases the polyol reactivity by converting secondary hydroxyl groups to primary hydroxyl groups although the kinetics of the reaction precludes 100% conversion to primary hydroxyl terminated polyol. Therefore, in the structure shown in Figure 3, z equals zero on some polyol molecules.

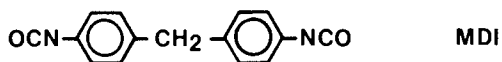
The principal focus of this paper will be on the effects of polyol molecular weight, polyol oxyethylene group content, NCO/OH ratio and chain extender structure on low temperature and elevated temperature properties, thermal stability during processing, and processability, in particular injection molding behavior.

Experimental

Materials. 1,4-Butanediol was vacuum dried (60°C., 2mm Hg) for six hours and then stored over molecular sieves. The PPG polyols used were PPG 1025 and PPG 2025 from Union Carbide Corporation. Tipped PPG polyols were supplied through the courtesy of F. J. Preston of the Olin Corporation Research Center, New Haven, Connecticut. Polyols were vacuum dried (100°C., 2 mm. Hg) for one hour immediately prior to use. The MDI, Isonate 125 MF from Upjohn Company, was stored at 50°C. and decanted prior to use so that only water white, clear material was used. The BHEHQ was from Eastman Chemical Products.

Preparation of Elastomers. Two methods for preparing TPU elastomers are commonly used. In the prepolymer method, the polyol is prereacted with all of the MDI and the resultant prepolymer, often containing free MDI, is subsequently reacted with the chain extender. In the masterbatch method, the polyol and chain extender are premixed and then combined with the MDI,

DIISOCYANATE



CHAIN EXTENDERS

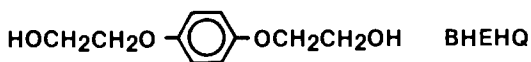


Figure 1. Hard segment chemical components.

POLYOLS

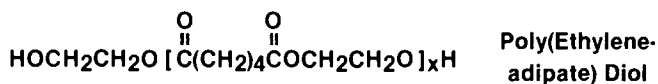
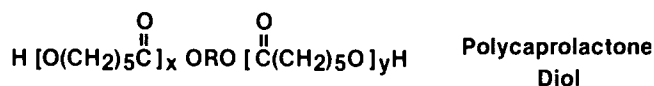


Figure 2. Typical polyols.

PPG



"TIPPED" PPG



Figure 3. PPG-type polyols.

random polymerization being allowed to take place. We used both methods in our studies. Slabs cast from the reactions were granulated, extruded, pelletized, and then injection molded into test plaques. The prepolymer method was used primarily with the untipped or lightly tipped PPG polyols to avoid polymerization difficulties arising from the difference in reactivity between the secondary hydroxyl group of the polyol and the primary hydroxyl group of the chain extender. Structure-property relationship comparisons were always made between polymers prepared by the same method.

Test Methods. The standard physical-mechanical properties of the elastomers were measured at ambient temperature with an INSTRON Tensile Tester.

Cold impact was measured by the falling dart test in which a 3" x 6" x 0.125" sample is positioned in an inverted U shape, conditioned four hours at -30°C., and impacted at the highest point of the specimen by a weighted two-inch diameter rod-shaped plunger rounded on the end to a one-inch radius. The plunger is dropped from a predetermined height to give 5 mph impact velocity.

Heat sag was determined in a test in which a four-inch extension of a 2" x 6" x 0.125" plaque is heated for 30 minutes at 121°C. and its deflection from horizontal is measured.

The DTA measurements were made on a DuPont Model 900 Thermal Analyzer using a heat-up rate of 20°C./min.

The DSC cooling curves were obtained using a Perkin-Elmer DSC-1B at a cooling rate of 20°C./min.

Molecular weight determinations were made in THF at room temperature using a Waters Model 200 gel permeation chromatograph.

The hardness build-up test was carried out on a one-half ounce laboratory injection molding machine. Using a 2.5" x 2.5" x 0.125" plaque mold held at a constant temperature, polymer melt was injected into the mold. The mold was opened at various times after injection, the piece removed, and its Shore A hardness measured exactly five seconds after opening the mold. The development of hardness could be followed as a function of quench time starting with quench times as short as 10 seconds.

Results and Discussion

When this work began, an important application for TPU elastomers was in automobile exterior body components associated with impact absorbing bumper systems. Cold impact strength, resilience, resistance to heat distortion at paint oven temperatures and rapid injection molding cycles were all required.

Polymers prepared from untipped PPG polyols have some inherent deficiencies. Table 1 shows data on injection molded TPU elastomers based on PTMG and PPG polyols.

Table 1. TPU Elastomers From PPG & PTMG Polyols, MDI and 1,4-Butanediol.
1.04 NCO/OH, 52% by Weight Polyol.

	A	B	C
Polyol	PTMG	PPG	PPG
Polyol Molecular Weight	1000	1000	2000
-30°C. Drop Impact	Pass	Fail	Pass
Tg, DTA	-54°C.	-30°C.	-53°C.
Heat Sag, 4" Extension, 121°C.	2.5"	3.5"	1.5"
Bashore Rebound	38	21	34

Comparisons were made between polymers containing an equal weight percent of soft segment so that the effects of segment length could be evaluated independent of segment content. Thus the polymer based on 2000 molecular weight PPG polyol in Table 1 has both a soft segment length and an average hard segment length twice that of the other polymers even though the weight percent of soft and hard segments is the same for all three polymers.

The data show that the TPU based on 1000 molecular weight PPG has poorer low temperature properties than the PTMG based polymer as indicated by its lack of cold impact resistance and its higher soft segment glass transition temperature. It also displays poorer heat sag resistance and is less resilient than the PTMG based polymer. In addition, the polymer from PPG 1000 does not injection mold well because of slow "freeze-off" and high shrinkage.

The comparison to PTMG is much more favorable when 2000 molecular weight PPG is used instead of 1000 molecular weight. In addition to improved cold impact resistance, heat sag and resilience, this polymer freezes off rapidly on injection molding and does not shrink excessively.

The differences between the two PPG based polymers can be attributed to differences in polymer morphology. It has been well established through work by Cooper (1), by Seefried (2), by Wilkes (3) and others that the properties of TPU elastomers result from thermodynamic incompatibility of the soft and hard segments which leads to microphase separation, domain formation and the development of long-range order in the hard segment domains. The data in Table 1 suggest that the PPG soft segment is more compatible with the MDI/butanediol hard segment than is PTMG, resulting in less complete phase separation. The glass transition of the PPG soft segment, theoretically -78°C. at infinite length, is shifted to a higher temperature because of restraints imposed by segment mixing. In the same way, the softening temperature of the hard segment is shifted downward leading to poorer resistance to heat distortion. Increasing the segment lengths through the use of 2000 molecular weight polyol gives more

American Chemical
Society Library

1155 16th St. N. W.

complete phase separation and less segmental mixing resulting in improved cold impact resistance and better resistance to heat sag. The effectiveness of increased soft segment molecular weight in promoting phase segregation has been demonstrated by Schneider and Paik Sung (4) for polyester-TDI polyurethanes.

Processing Stability. Despite its improved properties, the polymer based on PPG 2000 was found to be impractical because of instability at processing temperatures. Retention of the polymer melt at 204°C. in the barrel of an injection molding machine for times as short as 10 minutes gave molded parts with reduced tensile strength and loss of impact resistance. Ineffectiveness of antioxidants and nitrogen blankets in preventing this breakdown indicates that it is thermal and not oxidative.

Work by Beachell (5) and by Dyer (6) has established that the polyurethane bond can dissociate at these temperatures to give polymer fragments terminated by isocyanate and hydroxyl functionality as shown in Figure 4.

Although this reaction is reversible it could be driven to the right if the dissociated fragments undergo subsequent side reactions or in some way become less available to one another for recombination. Morphology could play a role since the polymer prepared from PPG 1000 is stable at 204°C. even though it has twice the number of polyol to isocyanate urethane bonds available for dissociation.

Effect of Oxyethylene Content on Stability. The processing instability of TPU elastomers based on PPG 2000 can be overcome by the use of ethylene oxide "tipped" PPG polyols, especially those containing high levels of oxyethylene groups, e.g., 30% to 45% by weight. The improved stability of the polymers based on such polyols is demonstrated in Table 2.

Table 2. Effect of Oxyethylene Group Content of 2000 M.W. Polyol on Stability of TPU Elastomer.

<u>Wt. % EO</u>	<u>Min. @ 204°C.*</u>	<u>Tensile, MPa</u>	<u>\bar{M}_w</u>
10	2	22.1	1.78×10^5
	20	5.5	0.88×10^5
30	2	24.8	1.86×10^5
	20	15.9	1.16×10^5
45	2	24.8	2.05×10^5
	20	23.4	1.47×10^5

*Retention time in barrel of injection molding machine before injection into mold.

Increased oxyethylene group content in the polyol results in improved stability as reflected in better retention of tensile strength with thermal exposure. In turn, this coincides with better retention of the weight average molecular weight of the polymers as determined by GPC measurements.

There is strong evidence that thermal stability is dependent primarily on oxyethylene group content rather than primary hydroxyl content. Table 3 shows that polymer prepared from a 2000 molecular weight polyol with 45% by weight oxyethylene group content but only 46% primary hydroxyl content is more stable than one prepared from a polyol with 30% by weight oxyethylene groups but with 82% primary hydroxyl.

Table 3. Dependence of Stability on Oxyethylene Group Content of Polyol.

	A	B	C
Polyol Molecular Weight	2000	2000	2000
Weight % EO	45	45	30
1° -OH Content	93	46	82
% Tensile Retention*	94	85	64

*Melt retained 20 minutes in the barrel at 204°C. before injection into mold compared with melt held for two minutes.

These data suggest that the thermal instability of the polymer based on PPG 2000 arises from dissociation of the urethane bonds in the melt but with slow recombination because of segmental incompatibility which gives rise to fragment separation making the reactive ends unavailable for recombination. High oxyethylene group content appears to improve compatibility of the soft and hard segments sufficiently to allow recombination, thus resulting in a more stable polymer. By this reasoning, the polymer based on untipped PPG 1000 is thermally stable because of greater compatibility between the soft and hard segments in the melt as a result of the shorter segment lengths.

The effects of polyol molecular weight and oxyethylene group content on the thermal stability of these polymers have been reported independently by Bonk and Shah (7).

Injection Moldability. The injection molding behavior of these materials is another response which can be influenced significantly by structural variations. For example, commercial scale molding trials on a 45 Shore D automotive polymer based on a 2000 molecular weight poly(oxyethylene-oxypropylene)glycol which contained 45% by weight oxyethylene groups showed that achievable cycle times were strongly influenced by the NCO/OH

ratio of the formulation used to produce the polymer. Although an NCO/OH ratio of 1.0 theoretically would produce infinite molecular weight polymer, in practice a small excess of diisocyanate is often used in order to account for impurities and minor side reactions which would reduce molecular weight. The excess isocyanate ensures high molecular weight through the branching mechanisms shown in Figure 5.

With the automotive grade polymer an NCO/OH ratio of 1.05 or higher gave polymers which were difficult to demold in reasonable cycle times and tended to stick in the mold. When made at an NCO/OH ratio of 1.01, the polymer demolded very readily but tended to show stress marks after painting and drying of the demolded parts and, in some tools, did not fill out the part adequately. These differences could not be reconciled on the basis of melt viscosity but appeared instead to reflect differences in the "freezing off" of the polymer during molding. It was possible to measure these differences by the hardness build-up test described in the experimental section.

Effect of NCO/OH Ratio on Hardness Build-up. Figure 6 shows the dramatic effect of NCO/OH ratio on the development of hardness with quench time for the 45 Shore D automotive polymer. A ratio of 1.01 gives a polymer which develops hardness very rapidly while increasing the NCO/OH ratio leads to slower and slower hardness development, particularly in the critical early seconds after injection. This slow hardness build-up can account for the long demolding time and tendency for mold sticking observed with materials made at an NCO/OH ratio of 1.05 or higher. On the other hand, the very rapid freeze-off of the polymer made at the 1.01 ratio could account for molded-in stresses because of premature hardening of the polymer over the long distances traveled by the cooling melt in a commercial tool.

Polymer made at an NCO/OH ratio of 1.03 was found to have an optimum rate of hardness build-up. Its hardness build-up curve, shown in Figure 6, was essentially superimposable with that of a commercially acceptable PTMG-based polymer and in field trials it molded at the same cycle time without difficulty. Thus molding behavior in large automotive molds could be related to a simple test which can be carried out on a relatively small sample. Control of NCO/OH ratio was demonstrated to be critical in these materials to obtain polymer which can be molded acceptably and reproducibly.

Another way to represent hardness development is to select two quench times representing critical points in a hardness build-up curve for the polymer type of interest and adding together the two readings to obtain a hardness build-up index. Table 4 shows index values obtained from the addition of the 10 second and 15 second readings for the polymers described in Figure 6.

These differences in hardness build-up (HBU) are believed to result from differences in the kinetics of domain formation taking

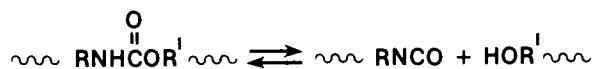
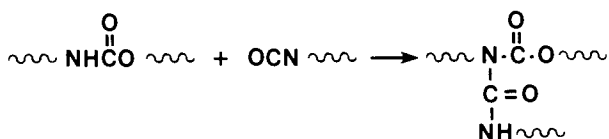


Figure 4. Thermal dissociation of polyurethane.

ALLOPHANATE FORMATION



BIURET FORMATION

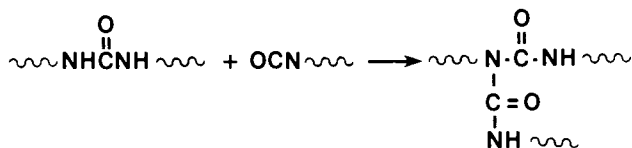


Figure 5. Branching reactions.

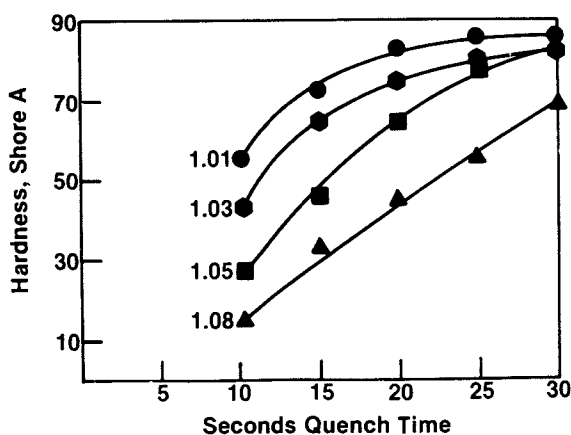


Figure 6. Effect of NCO/OH ratio on hardness build-up for polymer made from tipped PPG polyol (45% EO) at NCO/OH ratios of 1.01 (●), 1.03 (●), 1.05 (■), and 1.08 (▲).

Table 4. Hardness Build-up Index Values Obtained By Addition of 10 Second and 15 Second Readings of Polymers Described in Figure 6.

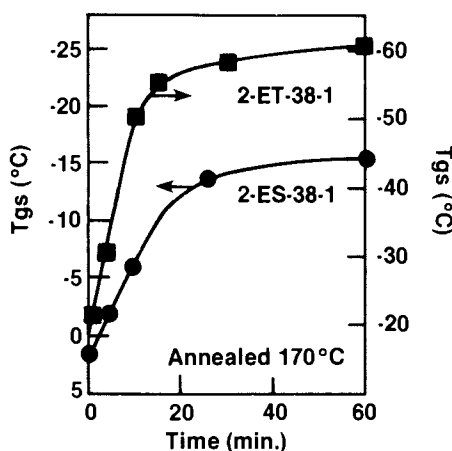
<u>NCO/OH Ratio</u>	<u>10 Sec. + 15 Sec. Shore A</u>
1.01	128
1.03	107
1.05	72
1.08	47

place when the polymer melts are quenched. Wilkes (8, 9, 10) and coworkers have published several studies on the properties of TPU elastomers which change with time after quenching from the melt. Figure 7, taken from one of their publications (9), shows that the soft segment glass transition shifts to progressively lower temperature with time after quenching. This result is consistent with continuing microphase separation of soft and hard segments and increasing domain formation with time. Wilkes proposed that in the melt, the soft and hard segments of the polymer are mixed but on quenching, thermodynamic incompatibility and hydrogen bonding act as restoring forces of the domain morphology. The kinetics of this "demixing" process can be affected by structural features of the polymer chain. He proposed that the rate of "demixing" can be influenced by temperature, solubility parameter differences, hydrogen bonding, crystallizability and rate of crystallization.

In the polymers described in Figure 6, branching introduced by excess isocyanate can slow down the demixing process and the re-establishment of the domain morphology. Branching can exert this effect by disrupting chain alignment and the re-establishment of hydrogen bonding thus slowing the rate of development of long-range order and crystallinity which lead to developing hardness in the cooling polymer.

The effect of NCO/OH ratio on slowing the rate of crystallization also can be seen through the use of DSC cooling curves. Figure 8 shows DSC cooling curves obtained for a series of TPU samples varying only in NCO/OH ratio. They show a shift in the position and broadness of the hard segment crystallization exotherm. The peak becomes broader and appears at progressively lower temperatures as the NCO/OH ratio is increased, an observation consistent with slower hardness development.

Effect of Segment Length. Among other structural variations which can affect the rate of domain formation on quenching from the melt are segment length and hard segment structure as influenced by the chain extender. The poor injection molding characteristics of a polymer derived from 1000 molecular weight



Journal of Applied Physics

Figure 7. Plot of glass transition temperature of the soft segment vs. time after quenching for polyester and polyether polyurethanes (9).

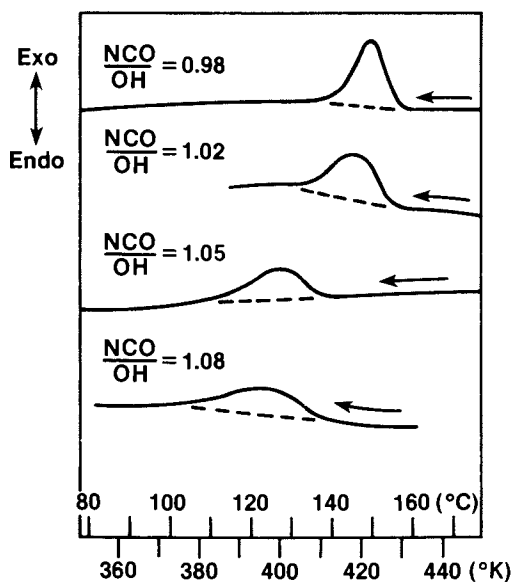


Figure 8. DSC cooling curves of TPU elastomers (based on 2000 M.W. tipped PPG polyol (45% EO) varying in NCO/OH ratio).

PPG compared with one from 2000 molecular weight PPG was mentioned previously. Polymers made with an equal weight percent of polyol but based on polyols of increasing molecular weight have increasing lengths of both the soft and the hard segments. This increase in segment length should give increasing rates of domain formation on quenching from the melt, not only because of the driving force of decreased compatibility of the segments but also because of the increased capability for the rapid development of long-range order resulting from the longer hard segment.

That this does take place is shown in Figure 9 which shows hardness development curves for three polymers varying only in segment length. The dramatic effect of segment length on hardness build-up is apparent.

Effect of Chain Extender Structure. From hardness build-up studies it is also easy to understand why 1,4-butanediol and the bis(hydroxyethylether) of hydroquinone are preferred chain extenders for TPU elastomers for injection molding applications. Table 5 gives hardness build-up index values for two polymers which illustrate that changing the chain extender from 1,4-butanediol to 1,6-hexanediol results in poorer injection molding behavior. The longer polymethylene sequence of the 1,6-hexanediol apparently results in a poorer hard segment fit, slowing down re-alignment and subsequent crystallization enough to make it a poor choice as chain extender.

Table 5. Effect of Chain Extender on Hardness Build-up.

	A	B
% by Weight Polyol	50	50
Polyol Molecular Weight	3000	3000
Weight % EO	30	30
NCO/OH Ratio	1.03	1.03
Chain Extender	1,4-Butanediol	1,6-Hexanediol
HBU Index (10 + 15 Sec.)	140	20

A similar effect on hardness development can be obtained by mixing two polymers made with different chain extenders. Table 6 shows that a polymer made with 1,4-butanediol as chain extender and another with the bis(hydroxyethylether) of hydroquinone as chain extender each have hardness build-up index values higher than does a 50/50 blend of the two. It is suggested that the poor spatial fit of the mixed hard segments results in slow domain formation on cooling. There is an important practical consequence of this observation as it relates to the mixing of TPU elastomers from different suppliers in an industrial molding operation.

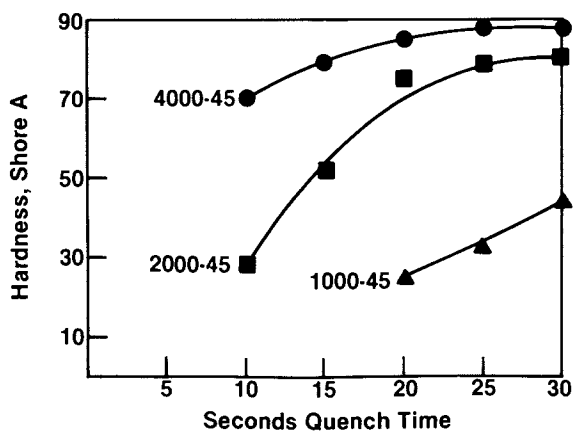


Figure 9. Hardness build-up curves of polymers containing 50 wt % polyol made at 1.04 NCO/OH ratio and based on 1000 M.W. (▲), 2000 M.W. (■), and 4000 M.W. (●) polyols.

Table 6. Effect of Dissimilar Chain Extenders
in TPU Blends.

Polymer	A	B	50/50 A/B
Chain Extender	1,4-BD	BHEHQ	1,4-BD/BHEHQ
HBU Index (10 + 15 Sec.)	71	90	19

Conclusions

Certain aspects of thermoplastic polyurethanes derived from poly(oxyethylene-oxypropylene)glycols have been described. Low temperature impact resistance and heat sag properties are dependent on segment length with 2000 molecular weight polyols being required for acceptable performance in automobile parts. The beneficial effect of oxyethylene group content on processing stability is ascribed to improved segmental compatibility. Several variables show a dramatic influence on injection moldability. Most notable examples are NCO/OH ratio, segment length as determined by polyol molecular weight, and hard segment structure as determined by the chain extender. These influences are attributed to the effects of these variables on the kinetics of domain formation on quenching from the melt.

Acknowledgments

The assistance of W. Tullo and J. Super in much of the experimental work is gratefully acknowledged. Thanks are due also to C. C. Ho of UNIROYAL Chemical Company for the DSC cooling curves and for many helpful discussions. The author is indebted to G. P. Roberts for his encouragement and to UNIROYAL, Inc. for permission to publish this work.

Literature Cited

1. Cooper, S. L. and Tobolsky, A. V., J. Appl. Polym. Sci., 1966, 10, 1837.
2. Seefried, C. G., Jr., Koleske, J. V. and Critchfield, F. E., J. Appl. Polym. Sci., 1975, 19, 3185.
3. Ophir, Z. H. and Wilkes, G. L., Adv. Chem. Ser., 1979, 176, 53.
4. Schneider, N. S. and Paik Sung, C. S., Poly. Eng. Sci., 1977, 17, 73.
5. Beachell, H. C. and Ngoc Son, C. P., J. Appl. Polym. Sci., 1963, 7, 2217.
6. Dyer, E. and Wright, G. C., J. Am. Chem. Soc., 1959, 81, 2138.
7. Bonk, H. W. and Shah, T. M., U. S. Patent 4,202,957, 1980 to Upjohn Company.

8. Wilkes, G. L., Bagrodia, S., Humphries, W., and Wildnauer, R., Polymer Letters Ed., 1975, 13, 321.
9. Wilkes, G. L. and Wildnauer, R., J. Appl. Phys., 1975, 46, 4148.
10. Wilkes, G. L. and Emerson, J. A., J. Appl. Phys., 1976, 47, 4261.

RECEIVED May 11, 1981.

Bonding of Isocyanates to Wood

ROGER M. ROWELL and W. DALE ELLIS

Forest Products Laboratory, U.S. Department of Agriculture,
Forest Service, Madison, WI 53705

Bonding of chemicals to wood cell wall components--cellulose, hemicellulose and lignin--can change the physical and chemical properties of the wood. For example, reaction of southern pine with simple epoxides results in a modified wood which is resistant to attack by subterranean termites in laboratory tests (1). Wood modified with acetic anhydride, dimethyl sulfate, β -propiolactone and epoxides are highly resistant to attack by microorganisms in standard soil block laboratory tests (2,3). Southern pine modified by reaction with acetic anhydride and propylene and butylene oxides has a reduced tendency to swell in the presence of water (4).

It is speculated that the biological resistance of chemically modified wood is due to chemical alteration of cellulosic substrate so that the very specific hydrolytic enzymatic reactions cannot take place. Resistance may also be due, in part, to reducing the available cell wall moisture to below a level required for biological attack. The decrease in swelling of wood in contact with moisture--that is, dimensional stability--which results from chemical modification of wood is due to the bulking action of the added chemical to the cell wall. The bulked wood cell walls are kept in a swollen state as long as the bonded chemical is retained. In this swollen condition, wood cannot expand or contract further in response to contact with water.

Cellulose, the hemicelluloses, and lignin are distributed throughout the wood cell wall (Figure 1), and the hydroxyl groups they contain are the most abundant reactive chemical sites. These three hydroxyl-containing polymers make up a three-dimensional polymer composite with a solid phase (cell wall) and voids (lumens) (Figure 2). The lumens can be viewed as bulk storage reservoirs for chemicals. For example, the void volume of southern pine springwood or earlywood with a density of 0.33 g/cm^3 is $0.77 \text{ cm}^3 \text{ voids/cm}^3 \text{ wood}$ or $2.3 \text{ cm}^3/\text{g}$. For summerwood or latewood with a density of 0.70 g/cm^3 , the void volume is

This chapter not subject to U.S. copyright.
Published 1981 American Chemical Society

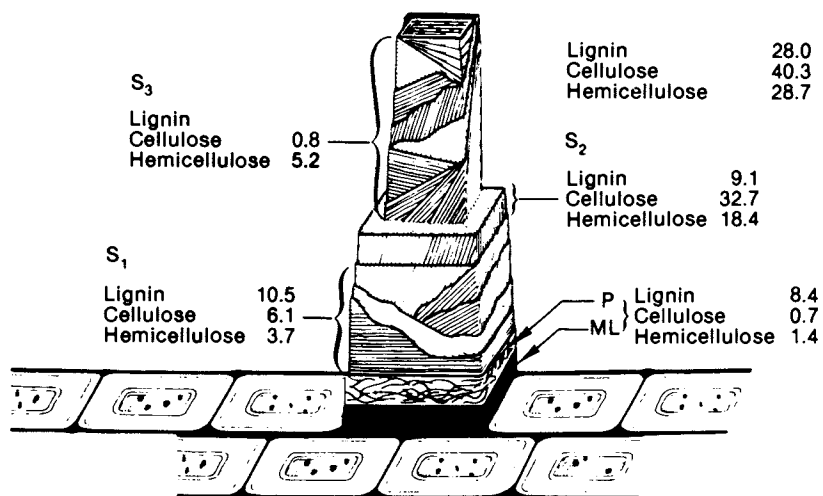


Figure 1. Chemical composition of a softwood cell wall.

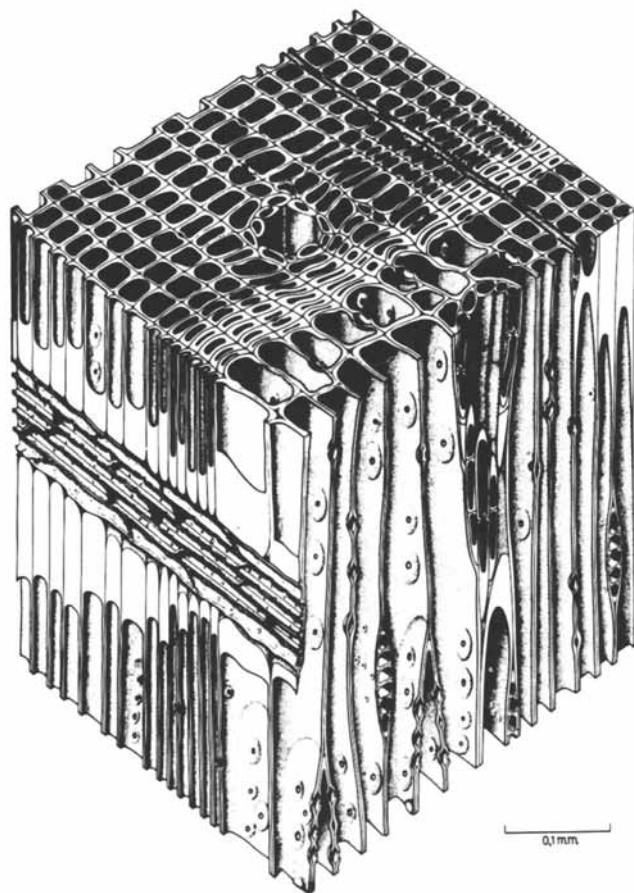
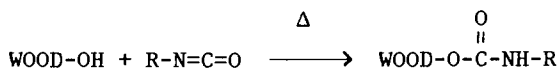


Figure 2. Three-dimensional view of a softwood.

0.52 cm³/cm³ or 0.74 cm³/g. The cell wall can also swell and act as a chemical storage reservoir. For southern pine the cell wall storage volume from oven dry to water swollen is 0.077 cm³/cm³.

Several requirements must be met for successful wood modification with a chemical bonding system. In whole wood, accessibility of the treating reagent to the reactive chemical sites (hydroxyls in the cell wall) is a major consideration. It is necessary, therefore, that the reagents used for chemical modification swell the wood structure to facilitate penetration of the cell wall by the reagent. The reagent should be volatile for ease of removal of unreactive chemical. The reagent must react quickly with the wood component hydroxyl groups under mild conditions (generally, under neutral or slightly alkaline conditions at temperatures below 120° C). There should be 100% carbon skeleton add-on of reagent so that no by-products are formed that need to be removed. The chemical bonds formed must be stable to ensure permanence and the treated wood must still possess the desirable properties of untreated wood.

One class of chemicals that meet these criteria for chemical reagents is the isocyanates (5):



Isocyanates swell wood and react at 100° to 120° C without a catalyst or with a mild alkaline catalyst. The resulting urethane bond is very stable to acid and base hydrolysis. There are no by-products generated from the chemical reaction of isocyanate with dry wood.

Evidence of Bonding

Evidence that chemical reaction has taken place with wood cell wall hydroxyl groups is evident from the infrared (IR) spectra of methyl isocyanate-modified southern pine (Figure 3). All samples run in the IR were first milled to pass a 40-mesh screen and extracted first with benzene/ethanol (2/1, v/v) followed by water in a Soxhlet extractor. Any unreacted reagent and isocyanate homopolymer formed during the reaction with wood would be removed by this extraction procedure. The spectrum for unreacted wood in the region of 1,730 cm⁻¹ shows some carbonyl stretching vibrations (Figure 3A). After modification to 17.7 weight percent gain (WPG), the carbonyl band is stronger (Figure 3B) and at 47.2 WPG (Figure 3C) this band becomes one of the major bands in the IR spectra. The increase in carbonyl is due to the formation of R-O-C-N-R in the urethane bond. There is also an increase in

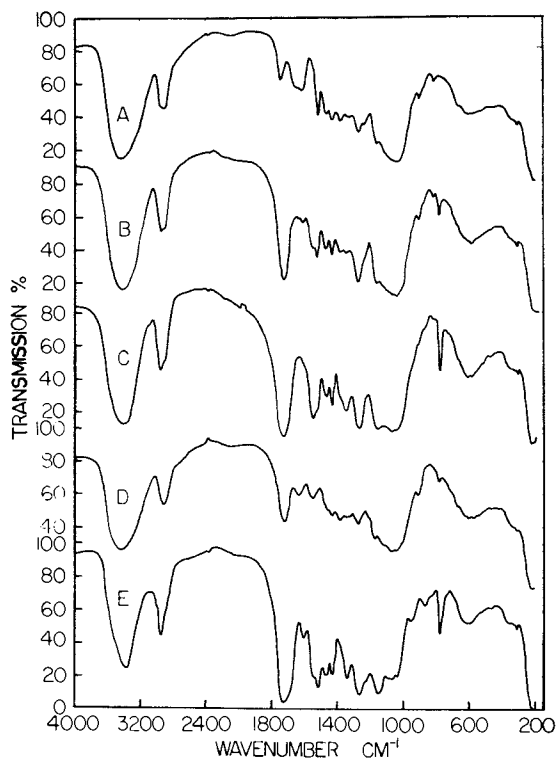


Figure 3. Infrared spectra of methyl isocyanate-modified southern pine. Key: A, unreacted wood (control); B, 17.7 WPG; C, 47.2 WPG; D, holocellulose from sample treated to 17.7 WPG; E, lignin from sample treated to 47.2 WPG.

the absorption bands as the WPG increases: at 1550 cm^{-1} , due to the NH deformation frequencies of secondary amines; at $1,270\text{ cm}^{-1}$, which is C-N vibration of disubstituted amines; and at $770\text{ to }780\text{ cm}^{-1}$, which may be due to NH deformation of bonded secondary amines (6). No unreacted reagent remains in the samples as the isocyanate absorption at $2,275\text{ to }2,240\text{ cm}^{-1}$ is absent (Figure 3B, C).

The strong absorption at $3,400\text{ cm}^{-1}$ and $2,950\text{ cm}^{-1}$ in all the IR spectra is due to hydroxyl absorption. Because substitution is not high enough to eliminate all hydroxyl groups, these bands are always present.

The holocellulose (cellulose and hemicellulose) from a methyl isocyanate-modified sample at 17.7 WPG was isolated by the sodium chlorite procedure (7). The IR spectra of the holocellulose (Figure 3D) shows that urethane bonding has taken place in the carbohydrate component of wood. Isolating the lignin from a methyl isocyanate-modified sample at 47.2 WPG by the sulfuric acid procedure (8) and running the IR spectrum (Figure 3E) also shows that urethane bonding has occurred in the lignin component of wood. The lignin spectrum shows the characteristic aromatic skeletal vibration at $1,515\text{ cm}^{-1}$ (9). This band is missing from the modified holocellulose curve (Figure 3D) which shows that the chlorite procedure does remove substituted lignins.

Volume of Chemical Added to Wood

Additional evidence that bonding has occurred in the cell wall of methyl isocyanate-modified southern pine can be seen by considering the volume increase in the treated wood and comparing that to the theoretical volume of chemical added after thorough leaching of the treated wood. If the chemical has entered the wood cell wall, the increase in wood volume as a result of modification should be proportional to the volume of chemical added.

Southern pine specimens ($2.5 \times 2.5 \times 0.75\text{ cm}$, radial by tangential by longitudinal) were treated with methyl isocyanate at 120° C without catalyst for varying lengths of time. After reaction, the specimens were extracted for 2 hours. Table I shows the increase in wood volume and the calculated volume of chemical added. Assuming a density of 0.967 g/ml for methyl isocyanate monomer and polymer, the calculated volume of chemical added to the wood is approximately equal to the volume expansion of the wood. Even at very high weight gains, this relationship held, showing that most of the chemical ended up as cell-wall bulking chemical and not as lumen-filling material.

This is not the case with higher molecular weight isocyanates such as ethyl, *n*-propyl, *n*-butyl, phenyl and *p*-tolyl isocyanates, 1,6-diisocyanate hexane and tolylene-2,4-diisocyanate.

At lower weight add-ons for ethyl, *n*-propyl and *n*-butyl isocyanates the increase in wood volume is approximately equal to the volume of isocyanate added (Table II). At higher weight add-ons for these and for phenyl and *p*-tolyl isocyanates, 1,6-diisocyanate hexane and tolylene-2,4-diisocyanate, there is far more volume of chemical added to the wood than there is in expansion of wood volume. This means that polymerization of the isocyanate is taking place in the lumen (homopolymer formation) and little of the chemical ends up in the cell wall.

Table I. Volume changes in southern pine reacted with methyl isocyanate

<u>1/</u> WPG	Increase in wood volume with treatment (cm ³)	<u>2/</u> Calculated volume of chemical added (cm ³)
12.4	0.16	0.14
25.7	0.21	0.27
47.7	0.46	0.54
51.9	0.54	0.58

1/ Weight percent gain.

2/ Density used in volume calculations for methyl isocyanate, 0.967 g/ml.

Dimensional Stability

The decrease in tendency of wood to swell in contact with moisture or dimensional stability is calculated as (10):

$$S = \frac{V_2 - V_1}{V_1} \times 100$$

where

S = volumetric swelling coefficient

V₂ = wood volume after wetting with liquid water

V₁ = wood volume of oven-dried sample before wetting

and

$$ASE = \frac{S_2 - S_1}{S_1} \times 100$$

where

ASE = antishrink efficiency (reduction in swelling resulting from treatment)

S_2 = treated volumetric swelling coefficient

S_1 = untreated volumetric swelling coefficient

Table II. Volume changes in southern pine reacted with isocyanates

Isocyanate	WPG	Increase in wood volume with treatment	Calculated volume of chemical added
		cm^3	cm^3
Ethyl	11	0.21	0.26
	34	0.55	0.90
<u>n</u> -Propyl	13	0.25	0.34
	24	0.34	0.61
<u>n</u> -Butyl	8	0.17	0.22
	24	0.35	0.64
Phenyl	25	0.13	0.52
<u>p</u> -Tolyl	22	0.08	0.48
1,6-Diisocyanate hexane	22	0.05	0.49
Tolylene-2,4-diisocyanate	27	0.02	0.53

In those reactions where the isocyanate enters the cell wall and bulking takes place, the ASE values will be high. If, on the other hand, the isocyanate polymerizes in the lumen and no cell wall bulking takes place, there will be little, if any, ASE as a result of the treatment. Table III shows varying degrees of dimensional stability by reacting southern pine with ethyl, n-propyl and n-butyl isocyanate. Less dimensional stability is achieved with phenyl and p-tolyl isocyanates, and 1,6-diisocyanate hexane and none with tolylene-2,4-diisocyanate.

In a more detailed study with southern pine reacted with methyl isocyanate (5) repeated ASE values were obtained during two water-soaking cycles. A maximum ASE of 76% is achieved at

Table III. Reaction and dimensional stability resulting from isocyanate reactions with southern pine

Isocyanate	Time	Catalyst	WPG	$\frac{1}{ASE}_1$	$\frac{2}{ASE}_3$
	<u>Min</u>				
Ethyl	30	None	11	28	23
	120	None	34	54	49
<u>n</u> -Propyl	60	None	3	8	6
	300	None	21	36	31
	300	5% TEA	24	42	39
	120	5% DMF	35	43	36
<u>n</u> -Butyl	120	None	5	17	11
	360	5% TEA	8	17	12
	1080	None	19	35	36
	180	5% DMF	24	44	34
	15	35% DMF	32	70	68
Phenyl	120	None	3	7	1
	120	5% DMF	19	12	12
	1080	None	25	29	18
	360	5% TEA	28	10	3
<u>p</u> -Tolyl	180	None	4	16	8
	60	5% DMF	16	15	11
	420	5% TEA	22	10	6
1,6-Diisocyanate hexane	360	None	13	16	7
	120	5% DMF	22	6	4
	240	5% TEA	52	8	0
Tolylene-2,4- diisocyanate	180	None	5	4	0
	420	None	27	0	0
	30	35% DMF	44	19	0
	240	5% TEA	48	4	0

$\frac{1}{ASE}_1$ determined from first oven-dry volume to water-swollen volume.

$\frac{2}{ASE}_3$ determined from second oven-dry volume to second water-swollen volume.

40 WPG after the first water wetting (Table IV). A more realistic value, however, is obtained from the second water-swelling test. Specimens treated to 16 to 28 WPG have ASE values of 60.

Table IV. Dimensional stability (ASE) of methyl isocyanate modified southern pine as a function of weight percent gain (WPG)

WPG	$\frac{1}{ASE_1}$	$\frac{2}{ASE_2}$	$\frac{3}{ASE_3}$	$\frac{4}{ASE_4}$
11.3	48	39	42	40
16.3	68	62	62	59
25.0	72	61	64	61
28.6	75	60	60	59
40.4	76	47	46	36
47.7	71	43	46	34
52.7	57	30	41	38

$\frac{1}{ASE_1}$ determined from first oven-dry volume to water-swollen volume.

$\frac{2}{ASE_2}$ determined from water-swollen volume to second oven-dry volume.

$\frac{3}{ASE_3}$ determined from second oven-dry volume to second water-swollen volume.

$\frac{4}{ASE_4}$ determined from second water-swollen volume to third oven-dry volume.

At high weight add-ons the ASE values start to decrease (Figure 4). Scanning electron micrographs clearly show the effects of high cell wall added chemical. The untreated southern pine specimen shows no swelling (Figure 5A). At 16 WPG and 32.2 WPG (Figure 5B and C) swelling occurs up to the green volume. At 36.9 WPG (Figure 5D) a few checks become visible, which are more pronounced (Figure 5E) at 47.4 WPG and cell wall rupture is very pronounced at 72.3 WPG (Figure 5F). The splitting occurs in the tracheid wall--not in the intercellular spaces--and in some cases the splits go through the bordered pits. Once this splitting occurs, ASE starts to drop and continues to drop as WPG increases. Splitting exposes new fiber surfaces where water can cause swelling. Swelling beyond the green volume takes place because the cell wall is ruptured and no longer acts as a restraint to swelling.

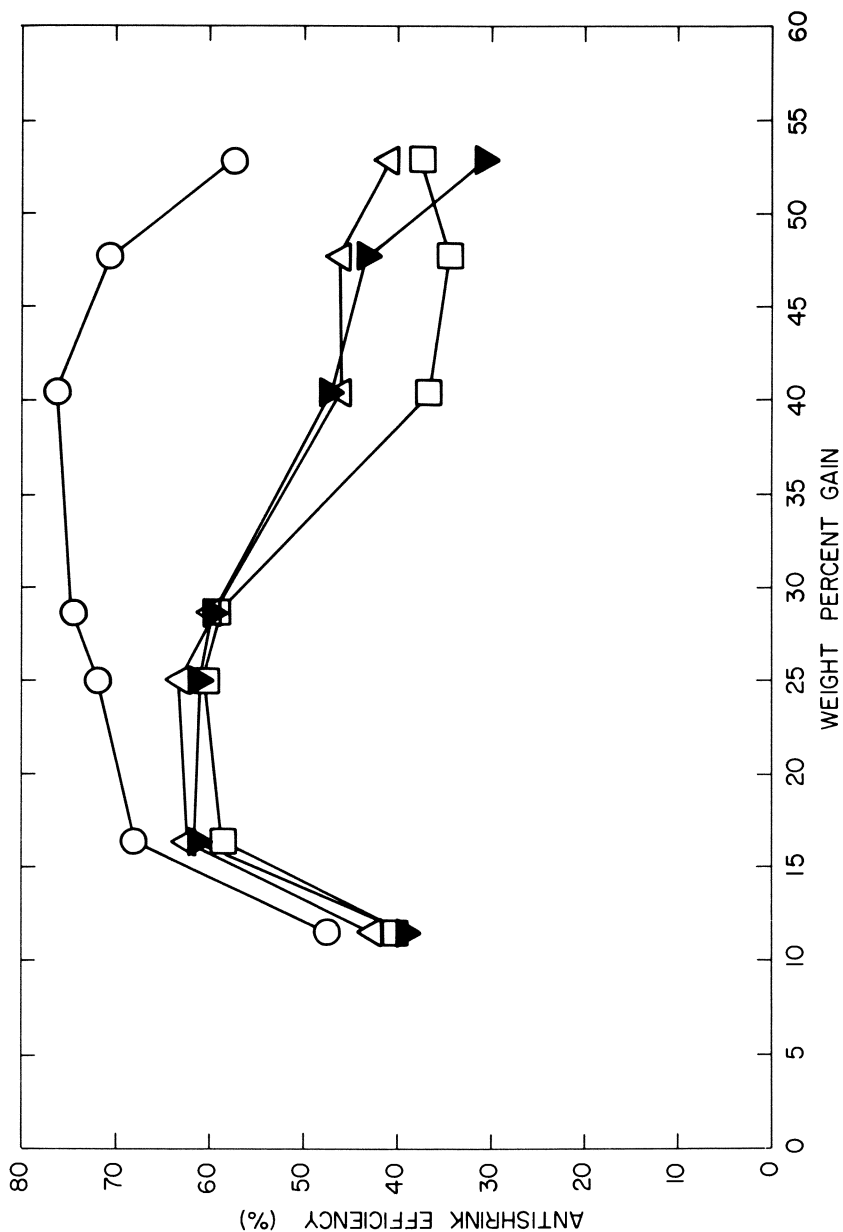


Figure 4. Antishrink efficiency of methyl isocyanate-modified southern pine as a function of WPG.
Key: ○, ASE₁; ▼, ASE₂; △, ASE₃; □, ASE₄.

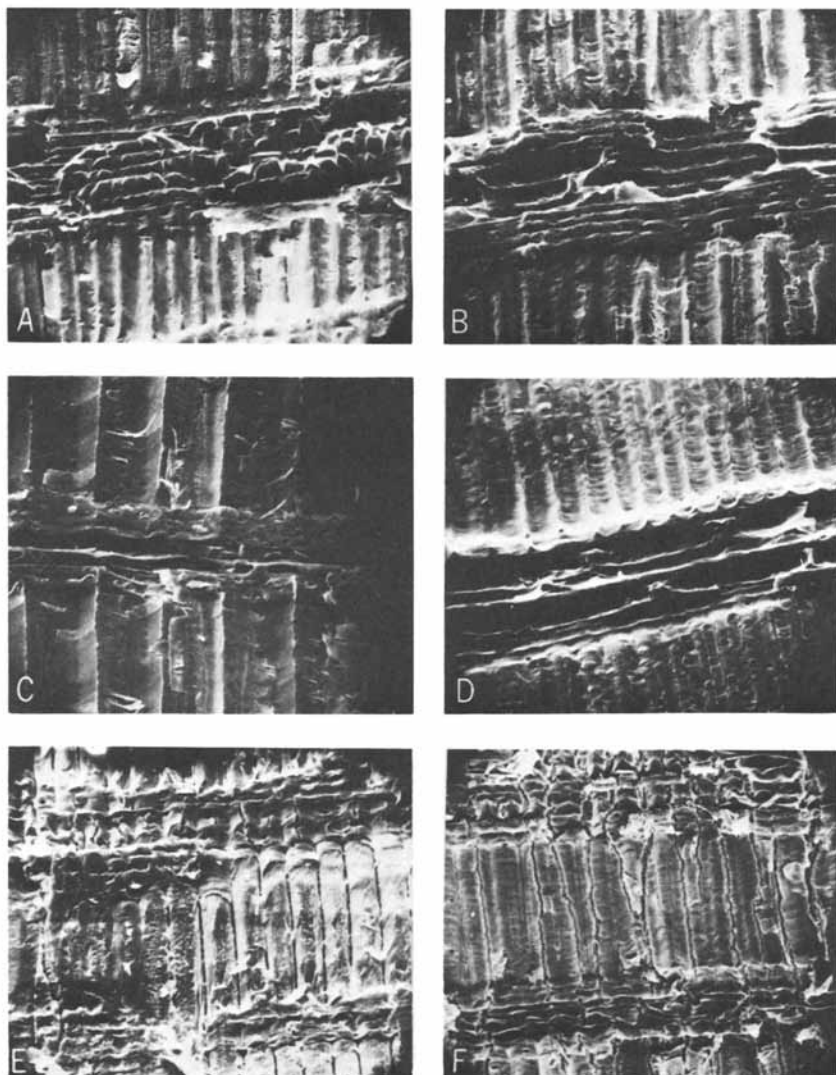


Figure 5. Scanning electron micrographs of radially-split southern pine showing swelling of wood treated with methyl isocyanate. Key: A, untreated control (245 \times); B, 16.0 WPG (224 \times); C, 32.2 WPG (224 \times); D, 36.9 WPG (224 \times); E, 47.4 WPG (224 \times); F, 72.3 WPG (196 \times).

Resistance to Attack by Microorganisms

Standard laboratory soil-block tests were run on chemically modified woods according to specifications outlined in ASTM D 1413 (11). The brown-rot fungus Gloeophyllum trabeum was chosen as a test organism because it causes extensive damage to untreated southern pine. Southern pine blocks, 2 x 2 x 2 cm, both untreated (control) and chemically modified to various WPG's with different isocyanates were evaluated. All samples were extracted 2 hours in a Soxhlet extractor with benzene/ethanol (2/1, v/v) prior to soil-block testing to ensure removal of any unreacted monomer. Samples were removed after 12 weeks of exposure to the fungus and extent of decay determined by oven-dry weight loss.

Southern pine modified with ethyl isocyanate at WPG 15-26, n-propyl isocyanate at 10-26 WPG and n-butyl isocyanate at 18-36 WPG give good resistance to decay (Table V). A detailed study of southern pine chemically modified with methyl isocyanate gives a clear picture of the WPG required to achieve decay resistance. A large variability in decay resistance below about 13 WPG is evidenced by the wide range in weight loss obtained (Table VI). The largest variability is in those samples with WPG's up to 13. Some of these samples must have an adequate distribution of chemicals to prevent specific hydrolytic enzyme reactions from taking place while others at nearly equal WPG do not. The data show that above 19 WPG methyl isocyanate-modified wood is very resistant to attack by Gloeophyllum trabeum.

Table V. Soil block test of isocyanate-treated southern pine inoculated with Gloeophyllum trabeum

Isocyanate	Catalyst	WPG	Weight loss
			in 12 weeks
		%	%
Control	None	0	39
Ethyl isocyanate	None	7	23
		15	6
		26	3
<u>n</u> -Propyl isocyanate	5% TEA	10	4
	5% DMF	11	7
		19	4
		26	4
<u>n</u> -Butyl isocyanate	35% DMF	18	2
		36	2

Table VI. Soil block test of methy isocyanate-treated southern pine inoculated with *Gloeophyllum trabeum*

WPG	Weight loss in 12 weeks		Number of samples	Standard deviation
	Range	Average		
%	%	%		
None (control)	39.5 - 61.8	48.8	8	7.6
6-8	7.0 - 25.5	15.8	10	6.4
8-13	1.1 - 24.9	9.2	10	8.1
13-18	2.0 - 5.8	3.4	8	1.3
19-22	1.6 - 3.1	2.4	7	0.53
23-28	2.0 - 3.0	2.3	7	0.34
29-33	2.0 - 3.2	2.7	7	0.39

Distribution of Bonded Isocyanates
in Cell Wall Components

It is thought that decay resistance of chemically modified wood is due to the blocking of hydroxyl groups required for very selective enzymatic reactions to take place. Because of this, it is of great interest to determine the distribution of bonded isocyanates in the holocellulose and lignin fractions of the wood cell wall. Protection from biodegradation is mainly required in the holocellulose components because it is the main food source for microorganisms. It has been shown that biological attack results in large weight and strength losses in wood due to hydrolysis and depolymerization (12).

The distribution of isocyanate bonded to wood was determined by reacting southern pine with methyl isocyanate to various WPG's, isolating the holocellulose component by the chlorite method (7), and the lignin component by the sulfuric acid method (8), and determining the amount of nitrogen present by the Kjeldahl method (8). Five samples were prepared at WPG's of 5.5, 10.0, 17.7, 23.5 and 47.2. Nitrogen content was determined on each delignified sample from the chlorite procedure, as well as on the isolated lignin samples from the sulfuric acid procedure. As WPG increases so does the nitrogen content of both the lignin and holocellulose components.

If nitrogen content is plotted against lignin remaining in the holocellulose samples (Figure 6), a straight-line plot results. The lines are nearly parallel for each WPG and displaced from one another by higher nitrogen content at higher WPG's. If each line is extrapolated to 0% lignin remaining, this point is the nitrogen content of the holocellulose at that WPG. This value correlates closely with the holocellulose nitrogen content calculated by subtracting the product of the percent lignin remaining times the nitrogen content for the sulfuric acid isolated lignin divided by the weight fraction of the holocellulose from the total nitrogen in the sample (Table VII).

Table VII. Distribution of nitrogen in methyl isocyanate-modified southern pine

WPG	$\frac{1}{N}$ in lignin	$\frac{2}{N}$ in holocellulose, calculated	N in holocellulose from Figure 6
	%	%	%
5.5	1.42	0.78	0.65
10.0	2.36	1.50	1.20
17.7	3.44	2.70	2.25
23.5	4.90	3.64	3.05
47.2	7.46	6.41	6.32

1/ Analytical Kjeldahl method.

2/ $\frac{\% N \text{ in total sample} - (\% N \text{ in isolated lignin}) (\% \text{ lignin remaining})}{0.70}$

If the chemical composition of southern pine (lignin, 27.9%; holocellulose, 67.0%; cellulose, 48.1%; hemicellulose pentosans, 9%; hemicellulose hexosans, 9.9%) is used in these calculations, the nitrogen content of each component can be determined on a whole-wood basis (Table VIII): At low WPG's the amount of nitrogen in the holocellulose and lignin are about equal. As the WPG increases, the ratio of nitrogen in holocellulose/lignin increases. This ratio should continue to increase as the WPG increases because there are many more hydroxyl groups available for substitution in the holocellulose than in the lignin. Theoretically, this ratio can be as high as 3 (Table IX) if all available hydroxyl groups on both holocellulose and lignin are substituted.

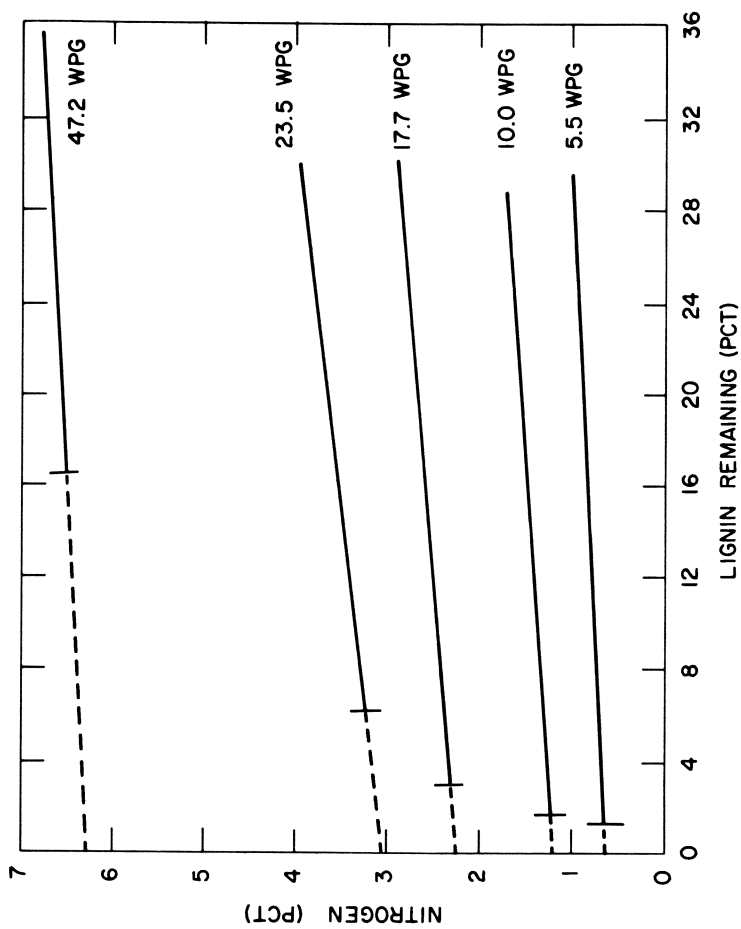


Figure 6. Nitrogen in partially delignified holocellulose samples from methyl isocyanate-modified southern pine.

Table VIII. Distribution of nitrogen in methyl isocyanate-modified southern pine on a whole wood basis^{1/}

WPG	N in holocellulose	N in lignin	Ratio
	%	%	
5.5	0.546	0.426	1.3
10.0	1.05	0.708	1.5
17.7	1.89	1.03	1.8
23.5	2.55	1.47	1.7
47.2	4.49	2.24	2.0

^{1/} Based on 70% holocellulose and 30% lignin.

Table IX. Theoretical nitrogen content of all available hydroxyl groups in southern pine

Component	Hydroxyl group	Nitrogen content
		%
Holocellulose ^{1/}	30H 20H	25.11
Hexosans	30H/C ₆	25.92
Pentosans	20H/C ₅	21.20
Lignin	1.16 OH/C ₉	8.37
Ratio		
holocellulose:lignin = 3.0		

^{1/} Holocellulose = 87% hexosans + 13% pentosans = 71.8% cellulose + 14.8% hemicellulose hexosans + 13.4% hemicellulose pentosans.

Table X. Degree of substitution of hydroxyl groups in lignin in methyl isocyanate-modified southern pine

Lignin (theoretical maximum 8.37% N)		
WPG	N in lignin	Degree of substitution
	%	
5.5	1.42	0.17
10.0	2.36	0.28
17.7	3.44	0.41
23.5	4.90	0.59
47.2	7.46	0.89

Table XI. Degree of substitution of hydroxyl groups in holocellulose in methyl isocyanate-modified southern pine

Holocellulose (theoretical maximum 25.11% N)			
WPG	N in holocellulose	Degree of substitution	Ratio lignin DS/holocellulose DS
	%		
5.5	0.59	0.025	7.4
10.0	1.19	0.047	6.0
17.7	2.11	0.084	4.9
23.5	2.94	0.117	5.1
47.2	5.24	0.209	4.3

Correlating the substitution data with the soil-block decay test data (Table VI) the 23.5 WPG sample represents a WPG where very little weight loss occurs due to decay. Assuming that the holocellulose fraction is the most important fraction that must be substituted to prevent decay, the data show that protection is achieved when only about 12% of the hydroxyl groups are substituted. It is important to note that the hydroxyl substitution calculations are based on the assumption that all hydroxyl groups are accessible and that the methyl isocyanate is a single-site substitution reaction, i.e., only one methyl isocyanate reacting with one hydroxyl and no polymerization. It has been shown that only 60% of the total hydroxyl groups in spruce wood are accessible to tritiated water (14). It has been further estimated that 65% of the cellulose in wood is crystalline and therefore probably not accessible for reactions involving these hydroxyl groups (10).

Assuming that only 35% of the cellulose hydroxyls are accessible for substitution, recalculating 2A gives a maximum WPG value of 53.72 and a maximum theoretical nitrogen value (Eq. 2B) of 13.19. Using these values to calculate the DS of holocellulose at the 23.5 WPG, the DS is 0.22. The 17.7 WPG sample has a DS 0.16, assuming 35% accessibility.

Southern pine modified with methyl isocyanate was resistant to attack by *Gloeophyllum trabeum* at weight gains (WPG) above 19. A sample analyzed at 23.5 WPG showed a DS in the lignin fraction of 0.59 and in the holocellulose fraction of 0.12. These findings indicate that at the point where resistance to biological degradation is attained, 59% of the lignin hydroxyls were substituted but only 12% of the holocellulose hydroxyls, assuming that all hydroxyls in both fractions were accessible for reaction and that no polymerization of the methyl isocyanate took place.

These data suggest that high lignin substitution did not contribute significantly to the overall protection of wood from decay. The degree of substitution in lignin was high in samples at lower WPG where little or no protection was observed. If the DS in lignin does have an effect in the protection mechanism it is only observed at very high levels.

Degree of substitution in the holocellulose fraction seemed to be the most important factor in the protection mechanism. A minimum DS of 0.12 was required for decay resistance, assuming 100% accessibility of both cellulose and hemicellulose hydroxyls, or approximately 0.22, assuming 100% accessibility in the hemicellulose fraction but only 35% in the cellulose fraction.

Conclusions

Methyl, ethyl, propyl, and butyl isocyanates react quickly with dry wood to give good substitution of cell wall component hydroxyl groups. Phenyl and *p*-tolyl isocyanates and difunctional isocyanates tend to polymerize in the lumen with much lower

levels of cell wall component reaction. Reacted methyl, ethyl, propyl, and butyl isocyanates give good dimensional stability to wood except at very high levels of chemical add-ons. At these high levels, the chemical added to the cell wall components causes the cell wall to rupture and swelling in water can go beyond the green volume.

Bonding methyl, ethyl, propyl, and butyl isocyanates to wood gives good decay resistance at weight gains above about 20%. Determination of the distribution of bonded chemical with methyl isocyanate in southern pine shows that 60% of the lignin hydroxyls are substituted and 12% of the holocellulose hydroxyls are substituted at the point where resistance to biological attack occurs.

Literature Cited

1. Rowell, R. M., Hart, S. V., and Esenther, G. R. Resistance of alkylene-oxide modified southern pine to attack by subterranean termites. Wood Sci. (1979) 11(4):271-274.
2. Rowell, R. M. Chemical modification of wood: Advantages and disadvantages. Proc. Am. Wood Pres. Assoc. (1975) 71:41-51.
3. Rowell, R. M. and Gutzmer, D. I. Chemical modification of wood. Reactions of alkylene oxides with southern yellow pine. Wood Sci. (1975) 7(3):240-246.
4. Rowell, R. M. and Ellis, W. D. Determination of dimensional stabilization of wood using the water-soak method. Wood Fiber (1979) 10(2):104-111.
5. Rowell, R. M. and Ellis, W. D. Chemical modification of wood: Reaction of methyl isocyanate with southern pine. Wood Sci. (1979) 12(1):52-58.
6. Bellamy, L. J. "The Infra-Red Spectra of Complex Molecules," John Wiley and Sons, New York (1962).
7. Green, J. W. "Wood Cellulose. Methods in Carbohydrate Chemistry, Vol. II." R. L. Whistler and M. L. Wolfrom, eds. Academic Press, New York (1963) p. 239-241.
8. Moore, W. E., and Johnson, D. B. Procedures for the chemical analysis of wood and wood products. USDA For. Serv. unnumbered report, For. Prod. Lab., Madison, Wis. (1967).
9. Sarkanen, K. V., Chang, H.-m., and Ericsson, B. Species variation in lignin. I. Infrared spectra of guaiacyl and syringyl models. Tappi (1967) 50(11):572-575.

10. Stamm, A. J. "Wood and Cellulose Science," Ronald Press Co., New York (1964).
11. American Society for Testing and Materials. Standard method of testing wood preservatives by laboratory soil-block cultures. ASTM Stand. Desig. D 1413, ASTM, Philadelphia, Pa. (1973).
12. Cowling, E. B. Comparative biochemistry of the decay of sweetgum sapwood by white-rot and brown-rot fungi. USDA For. Serv. Tech. Bull. No. 1258, Washington, D.C. (1961) p. 50.
13. Kirk, T. K. Effects of a brown-rot fungus, Lenzites trabea, on lignin in spruce wood. Holzforschung (1975) 29:99-107.
14. Sumi, Y., Yale, R. D., Meyer, J. A., Leopold, B., and Ranby, B. G. Accessibility of wood and wood carbohydrates measured with tritiated water. Tappi (1964) 47(10):621-624.

RECEIVED April 30, 1981.

Isocyanate Binders for Wood Composite Boards

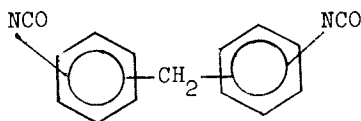
J. W. FRINK

Mobay Chemical Corporation, Pittsburgh, PA 15205

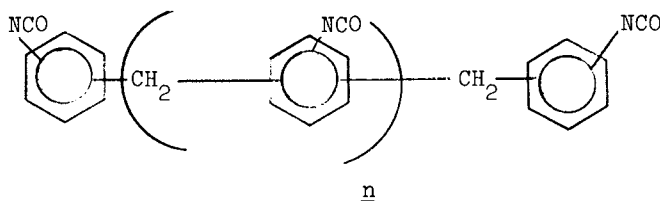
H. I. SACHS

Bayer AG, Leverkusen, West Germany

This paper is intended to present the history and current development status of a relatively new application for commercially produced polymeric MDI and to demonstrate its potential. The monomer upon which polymeric MDI is based is diphenylmethane diisocyanate:

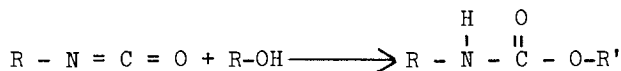


In polymeric MDI's the 4-4' isomer usually predominates but varying amounts of 2-4' and some 2-2' are also present. The polymeric are represented by the generalized structure:



Commercial polymeric MDI's consist of a mixture of molecules of varying n values with small amounts of high molecular weight species present with n as large as 8.

Isocyanates are very reactive toward compounds containing labile hydrogen atoms, forming addition compounds with the hydrogen donors. One such reaction, with hydroxyl-bearing compounds to form carbamates, or urethanes,



0097-6156/81/0172-0285\$05.25/0
© 1981 American Chemical Society

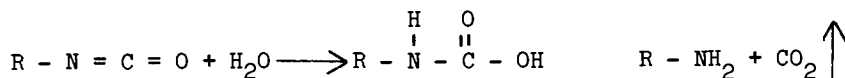
is the basis for the commercial use of isocyanates. Polyisocyanates, such as polymeric MDI, are reacted with polyfunctional alcohols, or polyols, to produce polyurethanes.

Wood contains a multiplicity of hydroxyl-bearing constituents such as cellulose, hemi-cellulose and lignin. Rowell and Ellis (1) have published evidence that isocyanates can react chemically with wood to produce urethane linkages. Hartman (2) has prepared rigid polyurethane foams by mixing polymeric MDI with catalysts, surfactant, blowing agent and ground Douglas Fir or Ponderosa Pine bark. The bark served as the sole polyol in the system.

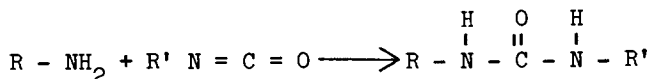
The initial development of polymeric MDI as a particleboard binder predates the above work but it is, we believe, based upon the same chemistry. Exterior or structural particleboard has been manufactured in North America and in Europe for years with predominantly phenol-formaldehyde binders and, in a few cases, with melamine-modified urea-formaldehyde binders. The familiar urea-formaldehyde resins are subject to hydrolysis and are thus suitable for interior board only.

Proposed Chemistry of Isocyanate Bonding

Most investigators agree that the strength and durability of isocyanate-bound wood panels are due to the chemical reaction of the isocyanate group with wood hydroxyls as illustrated by the above equation. Thus, the multifunctional isocyanate molecule forms a chemically bonded bridge between two or more adjacent wood particles. This reaction is only one of several involving isocyanates that can and probably do occur in a hot press during formation of particleboards when isocyanate binder is used. A very important reaction is that of isocyanate with water to produce a very unstable carbamic acid which immediately decomposes to form a primary amine and CO₂:



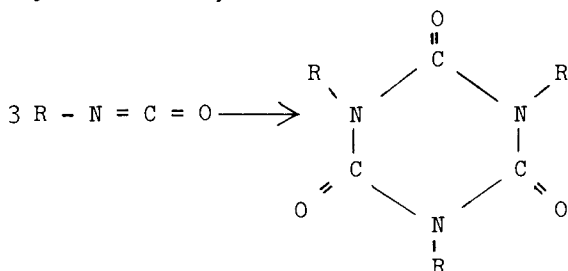
The resultant amine rapidly consumes another equivalent or isocyanate to form a symmetrical disubstituted urea:



By collecting and measuring the CO₂ evolved from a laboratory particleboard press, Wittman (3) has calculated that 1/4 to 1/3 of the isocyanate groups present, depending upon wood moisture content and binder level, are consumed in the water reaction. This means that a like amount of isocyanate must react with the resultant amine to form substituted ureas. Since at least 50%, and likely more, of the isocyanate is apparently consumed by the water reaction, chemical bonding through urethane linkages appears to be

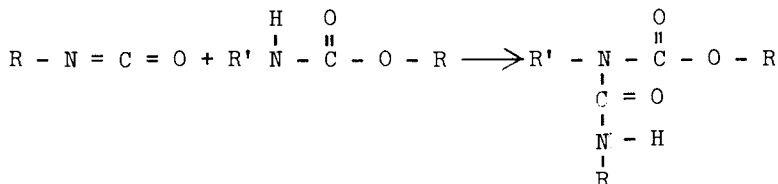
effective at rather low levels. Loss of some isocyanate moieties through urea formation is not necessarily harmful to board properties. Urea formation is probably the principle cross-linking mechanism in the polymer matrix that is formed between wood particles.

Another possible cross-linking reaction is isocyanurate, or isocyanate trimer, formation:

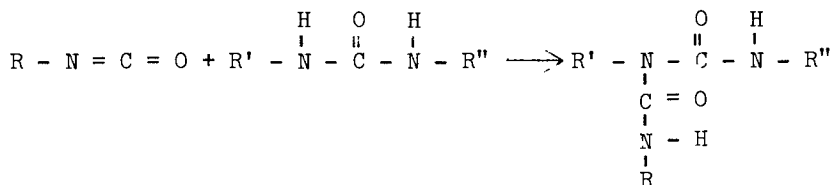


The reaction is known to occur at elevated temperatures and could occur during hot pressing depending on the stoichiometry and steric environment of the system.

The isocyanate-urethane reaction to form allophanates,



and the isocyanate-substituted urea reaction to form biurets,



are other possible cross-linking mechanisms. It is not known whether these reactions take place during particleboard formation.

In summary, it can be postulated that chemical bonding of the isocyanate to wood occurs through urethane linkages while other isocyanate groups on the same molecule can cross-link with other isocyanate-wood ligands through urea or possible isocyanurate linkages. Figure 1 shows this concept schematically. One three-functional isocyanate molecule is shown binding to a wood hydroxyl and cross-linking with three other isocyanate-wood ligands through a urea and an isocyanurate structure. It must be emphasized that this is only a simplified representation of some of the cross-linking mechanisms that could take place.

History

Development of isocyanate binders for particleboard began in Europe in the late 1960's. The development gained momentum in the early '70's. Deppe and Ernst (4) were among the first to report the achievement of V₁₀₀ (West German exterior structural grade) boards suitable for building construction using polymeric MDI as the binder. They demonstrated strength values at least equivalent to phenolic-bound boards and, in particular, found the isocyanate-bound boards to be more hydrophobic as determined by the West German test method.

The first commercial production of an isocyanate-containing particleboard was achieved by Deutsche Novopan of West Germany. They commercialized a product called Phenapan-V-100-Iso-Spanplatte which consists of a polymeric MDI-bound core with phenolic-bound face layers. This configuration accommodated one of the major problem areas characteristic of isocyanate binders - namely adhesion to metal surfaces during pressing (4, 5). Ernst (6) describes Phenapan-V-100-Iso-Spanplatte as a technological advance vs. the previous phenolic V-100 boards and cites moisture resistance and better performance under permanent load in outdoor conditions among its advantages.

Pioneering work in the development of an isocyanate-bound particleboard in the U.S. has been conducted by the Ellingson Lumber Company. This work has resulted in a proprietary process for bonding cellulosic materials with polymeric MDI to produce a multiple-ply structure panel (7, 8, 9). Advantages cited for this process include a tolerance for up to 22% moisture in the wood raw material without predrying and the ability to also include significant quantities of bark and needles.

As a result of this work, Ellingson has become the first, and at present, the only commercial producer of a wood panel product utilizing isocyanate binder in North America. This product, called Elcoboard (10, 11) consists of an isocyanate-bound saw mill waste core and two surface veneers of varying grades. Elcoboard differs from similar composite panels not only in the use of isocyanate, but also in that the entire composite is pressed in one step. Elcoboard has gained International Conference of Building Officials' (ICBO) approval as an exterior grade plywood substitute in building applications.

The West German parent of Mobay Chemical Corporation was very active, along with Deutsche Novopan, in the development of isocyanate as a particleboard binder in Europe. The work of Sachs (12, 13, 14) and of Deppe (4, 5), along with the aforementioned commercial developments, has provided a background for interest in isocyanate binders in North America. This interest is beginning to be reflected in the literature. For example, Hse (15) has published papers on the development of both plywood and flakeboard adhesives which combine isocyanate and phenolic resins. In the former case, he claims adequate bonding with wetter veneers than can be used with conventional phenolic adhesive. In the case of

southern hardwood flakeboard, Hse has found a superior performance vs. phenolic resin at high flake moisture content, low binder content and low panel density. He has recently been awarded a U.S. patent on this development (16).

During the past two years, papers have been given at the annual Washington State University Symposium on Particleboard by Udvardy (17), Wilson (18) and Johns (19). Their laboratory studies along with some of the others cited in this paper have shown that a number of advantages are possible when using polymeric MDI, as compared to conventional phenolic resins, for binding wood composite panels including particleboards, flakeboards and waferboards. Mobay has also developed data which contributes to the current state of the technology, partially in joint research programs at recognized wood research laboratories.

There are two major disadvantages often cited in the use of isocyanate wood binders. The first is a higher raw material cost as compared to conventional binders and the second is a tendency to adhere to metal transfer plates or press platens. The latter problem has been solved on a commercial scale by producing a multi-layer product with solid veneers or phenolic-bound particles as face layers. All isocyanate-bound non-veneered board can be made by treating the metal surfaces with a release material or, more recently, using a self-releasable isocyanate.

The increased costs represented by the above can be offset only if processing advantages are possible with isocyanates that are not possible with competing binders. It is the purpose of this paper to illustrate some of these advantages for the production of exterior grade wood composite panels.

Red Oak Flakeboard

A joint program involving Mobay, Purdue University and the U.S. Forest Products Laboratory (USFPL) has been documented as part of a Purdue University Research Bulletin authored by Hunt, et.al. (20).

The wood raw material used was red oak flakes. Red oak, an abundant species in the North Central United States, is a relatively dense hardwood, known to be rather difficult to bind. The ultimate goal was the development of a roof decking panel which required a 1-1/8 inch (29mm) board, considerably thicker than typical flakeboard products. An exterior grade binder had to be used but conventional aqueous phenolics are relatively slow curing resins. Polymeric MDI was evaluated in an attempt to achieve the necessary exterior durability without the excessively long press times otherwise needed for curing such thick boards.

Procedure. A description of the type of panels made is given in Table I. Both the core and face flakes as received from USFPL were milled in a Condux hammer mill so that flake geometry was constant throughout the study. Table II gives the processing

Table I

Panel Characteristics - Red Oak Flakeboard

Type: 3-layer lab flakeboard, hand formed
Dimensions: 460x460x299mm (18-1/8"x18-1/8"x1-1/8")
Target Density: 750 Kg/m³ (46.9 PCF)
Raw Material: Red oak flakes - 65% by wt. in core
17.5% by wt. in ea. face

Table II

Constants For All Panels - Red Oak Flakeboard

Flake Moisture Content¹: Face layers - 13%
Core layer - 11%

Paraffin Wax: 1% solids based on oven-dry wood
wt. added as 47% aqueous emulsion

Binder Content: Face layers - 5% solids on OD wood wt.
Core layer - 6% solids on OD wood wt.

Press Temp.: 176°C (349°F)

Press Closing Time: 40 sec. to stops

Open Time: 15-35 min. blender to press

¹Water added to flakes to equal
these levels when isocyanate used

parameters that were constant for all panels. Binder and paraffin wax were introduced to the flakes through an atomizing nozzle in a Drais FSP 80 discontinuous laboratory blender. The two binders evaluated were:

- 1) Aqueous phenol-formaldehyde resin solution (43.5% solids)
- 2) Desmodur PU-1520A 20 polymeric MDI (Bayer AG, West Germany)

Figure 2 is a photograph of a section of one of the panels bound with Desmodur PU-1520A 20.

Testing. Two panels were made for each experimental point and physical properties measured for each according to the appropriate West German "Deutschen Normvorschriften" (DIN) standards. The principle difference between these and the ASTM D-1037-72 ("Standard Methods of Evaluating the Properties of Wood-Base Fiber and Particle Panel Materials") procedures is in the durability test. In the German procedure this is determined by measuring the internal bond (tensile stress applied in the thickness direction to failure) on wet specimens after boiling two hours in water. This is called the V100 test. Other properties measured were dry internal bond (V20), bending modulus of rupture (MOR) and elasticity (MOE), density and thickness swell, the latter after 2 and 24 hour water soaks.

The pattern used for cutting test specimens is shown in Figure 3. The property values given in this report are mean values of the number of specimens indicated times two since each board was duplicated. Densities were measured on all thickness swell, internal bond (IB) and bending modulus specimens before those respective tests were run.

In addition, four panels (representing two experimental points) were submitted to Purdue University for linear expansion testing. Two specimens were cut from each board at right angles to each other. After conditioning at 80°F (27°C) and 50% relative humidity, the samples were brought to constant weight in an 80°F (27°C) and 90% relative humidity environment and linear expansion measured over a 10 inch (254mm) gauge length.

Variable Levels. The variable studied in the work reported here was press time, since we were seeking to produce a faster curing panel. Each binder was evaluated at three press time levels - 0.2, 0.3 and 0.5 seconds per mm panel thickness. For the nominal 29mm thickness, this resulted in design press times of 5.8, 8.7 and 14.5 minutes.

Results. Physical property values for the panels produced are given in Table III. A more rapid curing rate with the Desmodur PU-1520A 20 is strongly indicated by the modulus of rupture and internal bond relationships as illustrated by Figures 4 and 5, respectively. In both instances it appears that the phenolic resin has not totally cured at 8.7 minutes press time and perhaps not at 14.5. The isocyanate, on the other hand, has developed essentially full MOR and IB values at 5.8 minutes. The IB in

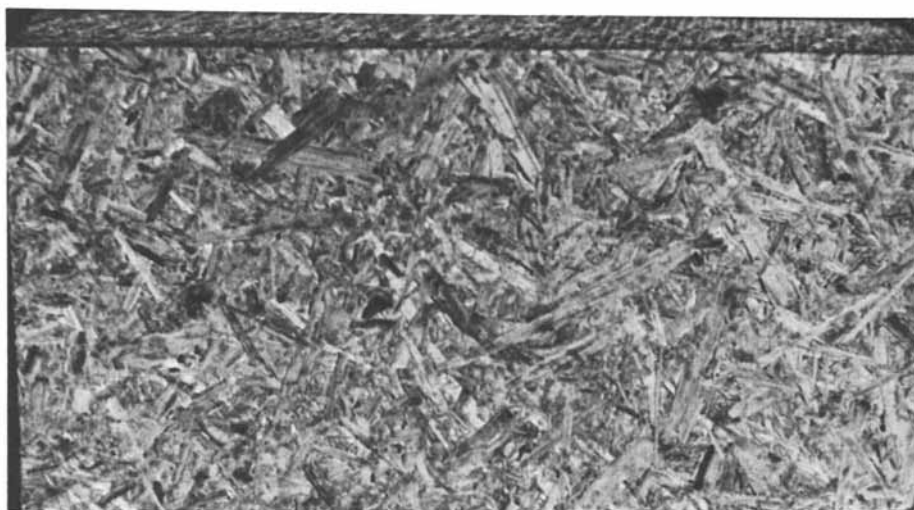
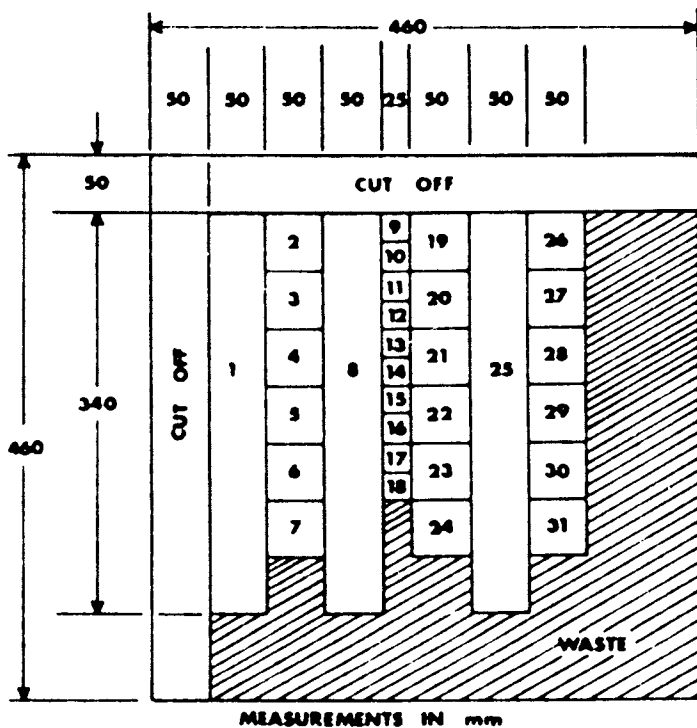


Figure 2. Red oak flakeboard with Desmodur PU-1520A 20 binder.



IB, DRY (V20): 2, 4, 6, 20, 24, 26, 28, 30

IB, WET (V100): 3, 5, 7, 19, 21, 23, 27, 29, 31

BENDING (MOR, MOE) - TEST PIECE 340 × 50 mm,
SPAN LENGTH 290 mm: 1, 8, 25

MOISTURE ANALYSIS: 9, 13, 16, 18

THICKNESS SWELL: 2 hrs. 24 hrs.: 10, 11, 12, 14, 15, 17

Figure 3. Cutting pattern for test specimens.

Table III
Physical Properties of Red Oak Flakeboards

<u>Binder</u>	<u>Press Time</u> <u>Min.</u>	<u>Density</u> <u>PCF</u>	<u>Modulus of Rupture</u> <u>psi</u>	<u>Modulus of Elasticity</u> <u>psi x 10³</u>	<u>Thickness Swell, %</u> <u>2 Hrs.</u>	<u>Thickness Swell, %</u> <u>24 Hrs.</u>	<u>Internal Bond, psi</u> <u>Dry</u>	<u>Internal Bond, psi</u> <u>Wet</u>
PF	5.8	45.2	4946	703	7.4	16.8	84	14
PF	8.7	46.8	6613	658	5.1	14.4	129	14
PF	14.5	46.7	7049	569	5.3	14.5	162	18
Desmodur PUI520A 20	5.8	47.0	7136	743	1.3	5.4	260	95
Desmodur PUI520A 20	8.7	46.9	7208	756	1.5	5.7	268	93
Desmodur PUI520A 20	14.5	46.6	7107	725	1.3	5.7	264	89

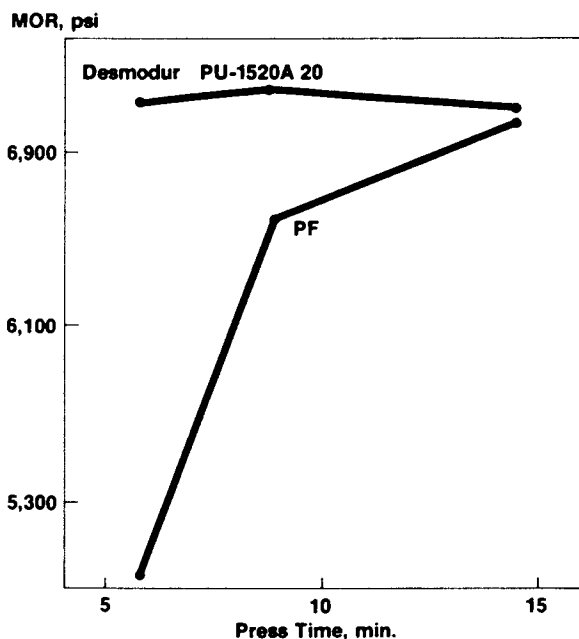


Figure 4. Modulus of rupture vs. press time for red oak flakeboard.

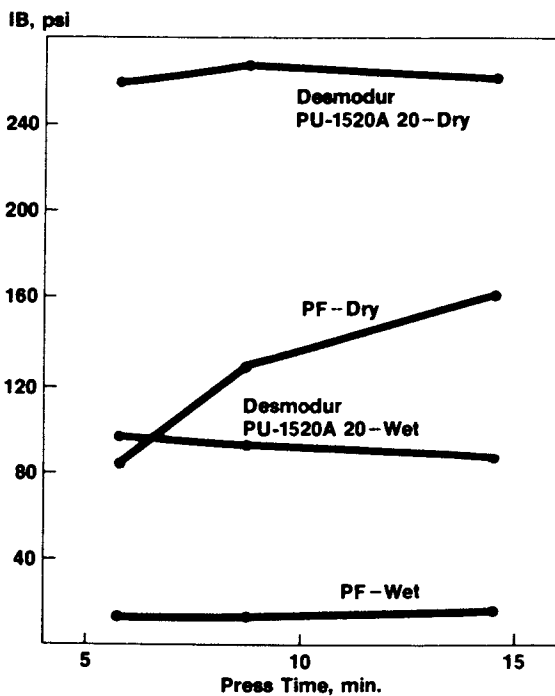


Figure 5. Internal bond vs. press time for red oak flakeboard.

particular is a good indicator of degree of cure since it is a core property, whereas MOR, which measures bending strength, is highly related to surface characteristics.

A comparison of the durability of the adhesive bonds formed by the two binders is provided by the wet internal bond and by the thickness swell values shown graphically in Figures 5 and 6, respectively. The former, measured after a 2 hour water boil, are strikingly superior for the Desmodur PU-1520A 20 vs. the phenolic binder at all press times. The same can be said for thickness swell after 2 and 24 hour water soaks.

It seems safe to say that a 50% reduction in press time is possible with the isocyanates vs. the phenolic resin while maintaining equivalent bending strength and vastly improved wet and dry internal bond. This is further shown, although perhaps not quite so dramatically, by the dimensional stability data given in Table IV.

Mixed Hardwood Flakeboard

Among other hardwoods indigenous to the North Central United States are maple, birch and aspen. These species have little commercial value but are found in areas close to major markets. Mobay sponsored a study, conducted by the Institute of Wood Research at Michigan Technological University, to determine the effects of processing variables on isocyanate-bound flakeboard prepared from a mixture of these species and to compare resultant panel properties with those of a standard panel prepared with a commercial aqueous phenolic resin under typical processing conditions for that type of resin.

Procedure. Panel characteristics are given in Table V. Table VI gives the processing parameters for the standard panels. Binders and paraffin wax were introduced into the blender by spraying. The binders employed in this study were an aqueous phenol-formaldehyde resin and Mobay's Mondur MR polymeric MDI.

Testing. Three replicate panels were made for each experimental point and properties were measured, in general, according to ASTM D-1037-72. One slight deviation was in the durability, or accelerated aging test. The ASTM method calls for the following:

- Immerse in water @ 120°F (49°C) for 1 hour
- Spray with steam and water vapor at 200°F (93°C) for 3 hours
- Store at 10°F (-12°C) for 20 hours
- Heat in dry air at 210°F (100°C) for 3 hours
- Spray with steam and water vapor at 200°F (93°C) for 3 hours
- Heat in dry air at 210°F (100°C) for 18 hours

The cycle is run six times. Since IWR's unit required some time for steam generation, the freezing phase and long dry phase were each reduced by one hour so that the total cycle could be completed in 48 hours.

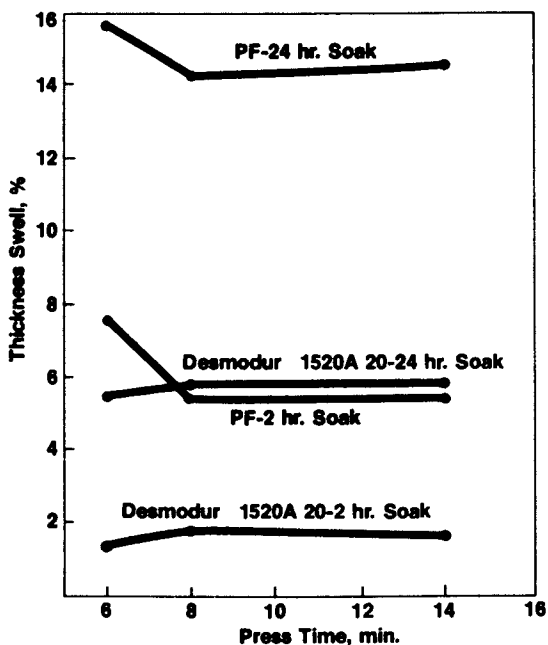


Figure 6. Thickness swell of red oak flakeboards.

Table IV

Dimensional Stability: 50 to 90% R.H.

<u>Binder</u>	<u>Press Time</u> <u>Min.</u>	<u>Water</u> <u>Absorption %</u>	<u>Thickness</u> <u>Swell %</u>	<u>Linear</u> <u>Expansion %</u>
PF	14.5	8.8	6.8	0.20
Desmodur PU-1520A 20	5.8	6.4	4.4	0.14

Table V

Panel Characteristics - Mixed Hardwood Flakeboard

Type: Single layer

Dimensions: 460x460x11mm (18-1/8"x18-1/8"x7/16")

Target Density: 720 Kg/m³

Raw Material: 52.5% maple, 17.5% birch, 30.0% aspen flakes
(2.0" x 0.4" to 1.2" x 0.025")

Table VI

Processing Parameters For Standard Panels
Mixed Hardwood Flakeboard

Flake Moisture Content	- 10%
Paraffin Wax	- 1% solids based on O.D. wood wt.
Binder Content	- 5% solids on O.D. wood wt.
Press Temperature	- 190°C (375°F) for phenolic 163°C (325°F) for isocyanate
Press Closing Time	- 1 min. to stops
Total Press Time	- 7 min. for phenolic 5 min. for isocyanate

Thickness swell measurements were made on 2 x 12 x 7/16" (51 x 305 x 11mm) specimens after conditioning at 21°C (70°F) and 90% relative humidity for two months.

Since bending strength values were affected by specimen density, and as the densities varied somewhat (from 43-46 PCF [688-736 Kg/m³]), these values were adjusted to correspond to the target density. Normalization factors used were based on earlier work with these wood species. The adjusted MOR after accelerated aging (AA/MOR) was calculated by applying the percent retention of the original MOR to the original adjusted MOR. Considering the number of test specimens cut from each of the three replicate panels for each experimental point, the thickness swell data are averages of three specimens; all other properties are averages of nine.

Variable Levels. In addition to the standard panels as described above, panels were made with the Mondur MR with variations from standard conditions as shown in Table VII.

Results. Physical properties for the standard, or control, panels are given in Table VIII. Although the Mondur MR panels were cured two minutes less and at 50°F (28°C) lower press temperature, original strength properties and thickness swell values are clearly superior to those of the phenolic-bound panels. There did appear to be a slight lag in modulus of rupture retention after accelerated aging.

Binder Level. Mondur MR-bound panels were made at 3 and 4% binder levels while maintaining all other parameters at the control levels. The resulting property values are given in Table IX. The 5% binder column represents the control board values for each of the binders and is included for comparative purposes. Modulus of rupture values, both original and after accelerated aging, are shown graphically in Figure 7. It is surprising to note that bending strength values are higher at 4% than at 5% Mondur MR level. Durability of the MR boards also seems best at the intermediate binder level as indicated not only by the MOR's after accelerated aging, but also by the thickness swell values illustrated in Figure 8. Durability of the isocyanate boards at 4% binder exceeds that of the phenolic control boards. Values for the latter are shown as single points in Figures 7 and 8.

At the 3% level the Mondur MR boards retain too little MOR after accelerated aging, although this may not be the case at a higher press temperature.

Flake Moisture Content. Panels were made with Mondur MR in which the moisture content of the flakes was adjusted to 20% into the press. It is well known that panels cannot be made with phenolic resins at such a high moisture content, since steam pressure blows them apart upon opening of the press. Even to attain 10% moisture content into the press, raw material must be dried to

Table VII
Variable Levels Studied With Mondur MR
Mixed Hardwood Flakeboard

Binder Level	-	3% 4% 5%
Flake Moisture Content	-	10% 20%
Total Press Time	-	3 minutes 5 minutes

Table VIII
Average Property Values For Control
Mixed Hardwood Panels

Property	PF ¹	Mondur MR ²
Modulus of Rupture* (psi)	5245	5340
Modulus of Elasticity* (psi x 10 ³)	675	721
Internal Bond (psi)	138	286
Aged MOR* (psi)	3472	3028
Thickness Swell (%)	20.33	17.08

*Adjusted to 45 pcf

¹Press time of 7 min. with 375^oF press temperature

²Press time of 5 min. with 325^oF press temperature

Table IX

Effect Of Binder Level On Mixed
Hardwood Flakeboard Properties

Property	Binder	Binder Level		
		3%	4%	5%
Modulus of Rupture* (psi)	MR ¹	5223	6673	5340
	PF ²	--	--	5245
Modulus of Elasticity* (psi x 10 ³)	MR	696	867	721
	PF	--	--	675
Internal Bond	MR	226	233	286
	PF	--	--	138
Aged MOR* (psi)	MR	1917	4691	3028
	PF	--	--	3472
Thickness Swell (%)	MR	18.95	16.58	17.08
	PF	--	--	20.33

*Adjusted to 45 PCF

¹Press time of 5 min. with 325^oF press temperature

²Press time of 7 min. with 375^oF press temperature

1 and 2 at 10% MC level

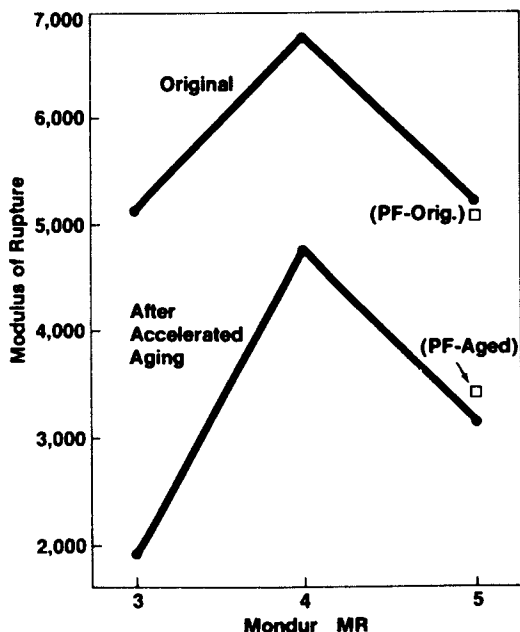


Figure 7. Modulus of rupture vs. Mondur MR level for mixed hardwood flakeboards.

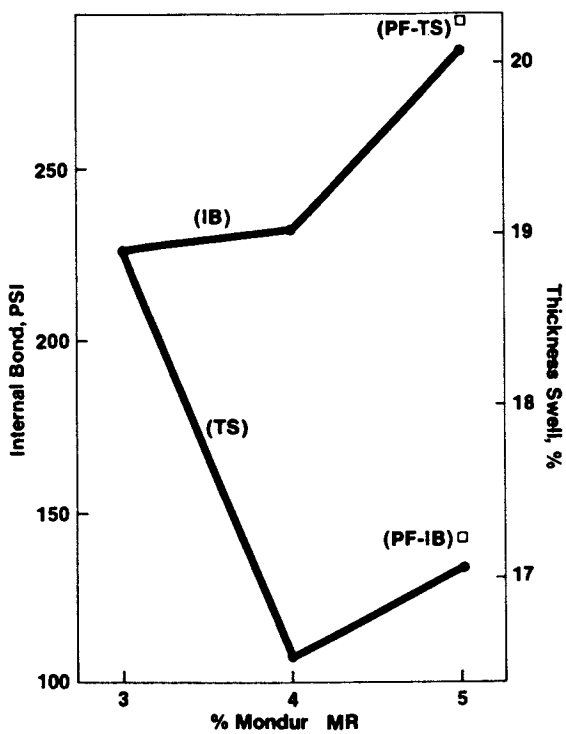


Figure 8. Internal bond and thickness swell vs. % Mondur MR for mixed hardwood flakeboards.

a level well below that if aqueous phenolic resins are used. If panels can be made with isocyanates at 20% moisture content into the press, the material need not be dried below 19% (assuming 1% water added with the paraffin wax), since no additional water is added with the binder.

Properties of the panels made with the high moisture raw material are compared with those of the control boards in Table X. Bending strengths are somewhat higher and internal bonds are lower at 20% MC. This is to be expected since the plasticizing effect of the excess water on the wood flakes tends to increase the density gradient between the core and surface of the board, weakening core properties and increasing surface-related properties. This can be corrected by lengthening the press closing time. That wasn't done here since internal bonds are still considerably higher than those of the phenolic control panels.

MOR after accelerated aging increases slightly in going from 10 to 20% flake moisture content. The dramatic improvement in thickness swell at the higher moisture content is unexplained.

The data show the feasibility of making good quality flake-board with Mondur MR at flake moisture content levels as high as 20%.

Press Time. Properties of the Mondur MR-bound boards pressed only 3 minutes vs. those of the control boards are given in Table XI. The internal bond strength of the Mondur MR boards did drop, as expected, although even at 3 minutes press time at 325°F (163°C), it is higher than that of the phenolic-bound board cured 7 minutes at 375°F (191°C). The surprise comes in the bending strength and durability properties where the performance actually appears better at the shorter press time.

To summarize the mixed hardwood flakeboard study, it can be said that good quality panels were made with Mondur MR at reduced press time, temperature and binder levels and increased flake moisture content vs. the commercial phenolic resin.

Aspen Waferboard

Another parameter in which savings can be made with the use of polymeric MDI binder is panel density. Although density variations were not studied in either of the two above programs, they were in a program Mobay sponsored at the former Eastern Canadian Forest Products Laboratory, now Forintek Canada Corp. - Eastern Forest Products Laboratory. The work was done with 3 layer aspen waferboard with cores bound with Mondur E-441, another Mobay polymeric MDI, and the faces with a spray-dried powdered phenolic novolac resin. Controls were homogeneous boards bound entirely with the novolac. Although homogeneous boards bound entirely with Mondur E-441 were not included in this study, one such board is shown in Figure 9 to illustrate the appearance of aspen waferboard. Note the much wider wafers as compared to the red oak flakes shown earlier.

Table X

Effect Of Flake Moisture Content On
Mixed Hardwood Flakeboard Properties

Property	Binder	Moisture Content	
		10%	20%
Modulus of Rupture* (psi)	MR ¹	5340	5785
	PF ²	5245	--
Modulus of Elasticity* (psi x 10 ³)	MR	721	749
	PF	675	--
Internal Bond (psi)	MR	286	215
	PF	138	--
Aged MOR* (psi)	MR	3028	3483
	PF	3472	--
Thickness Swell (%)	MR	17.08	8.91
	PF	20.33	--

*Adjusted to 45 PCF

¹Press time of 5 min. with 325°F press temperature

²Press time of 7 min. with 375°F press temperature

1 and 2 at 5% binder level

Table XI

Effect of Press Time on Mixed
Hardwood Flakeboard Properties

Property	Binder	Press Time		
		7 Min.	5 Min.	3 Min.
Modulus of Rupture* (psi)	MR ¹	--	5340	5950
	PF ²	5245	--	--
Modulus of Elasticity* (psi x 10 ³)	MR	--	721	733
	PF	675	--	--
Internal Bond (psi)	MR	--	286	167
	PF	138	--	--
Aged MOR* (psi)	MR	--	3028	4230
	PF	3472	--	--
Thickness Swell (%)	MR	--	17.08	15.74
	PF	20.33	--	--

*Adjusted to 45 PCF

¹at 325°F press temperature

²at 375°F press temperature

1 and 2 at 10% M.C and 5% binder levels

Subsequent to publication of the original work done by Udvardy (17), a multiple correlation analysis of all replicates of the data points was conducted at Mobay. A set of regression equations was generated for each binder studied. Each equation predicted one of the board properties in terms of a number of processing variables including panel density. Correlation coefficients were 0.8 for internal bonds for the Mondur E-441 panels with all others being 0.9 or greater.

Some of the predictive property equations were plotted vs. panel density for each binder with binder level and press time held constant at 2% and 5 minutes, respectively. Figure 10 shows that comparable MOR's are attainable with the Mondur E-441 at about a 10% lower density than with the phenolic. Aged MOR (Figure 11) determined in this study by MOR measurement after a two hour water boil (Canadian Standard CSA 0188-OM78) indicates the possibility of a savings of about 7.5-10% in density. Finally, Figure 12 shows that comparable internal bonds can be achieved by the isocyanate at up to 25% lower density vs. the phenolic resin.

Summary

The purpose of this presentation has been to illustrate some advantages that are possible in the use of polymeric MDI as a binder for exterior grade wood composite panels. The data given have indicated the potential for savings in press time, press temperature, flake moisture content, resin level and panel density (as compared to conventional phenol-formaldehyde binders) in several types of such panels.

The panel producer must optimize his processing parameters to take full advantage of the savings isocyanates can offer. The answer as to what the optimum conditions are must be determined on a case-by-case basis. To date these optimized conditions for polymeric MDI have been found favorable versus those of alternate binders by several European and at least one U.S. panel producer.

Acknowledgement

We wish to thank Dr. Darrell D. Nicholas, Mr. Roy D. Adams and Ms. Susan Mateer of the Institute of Wood Research at Michigan Technological University for their work in conducting the mixed hardwood flakeboard experimental program. We also wish to thank Dr. Michael O. Hunt of Purdue University and Dr. William F. Lehmann of Weyerhaeuser Corporation for their help in the red oak flakeboard work and Mr. Otto G. Udvardy of Borden Chemical for the aspen waferboard study. Finally, we would like to thank Dr. Ronald Taylor of Mobay Chemical Corporation for his considerable advice and help with the multiple correlation analysis.

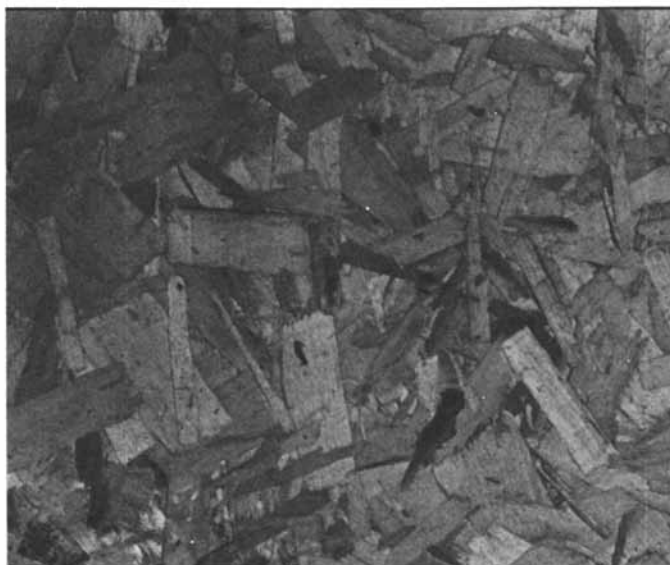


Figure 9. Homogeneous aspen waferboard with Mondur E-441 binder.

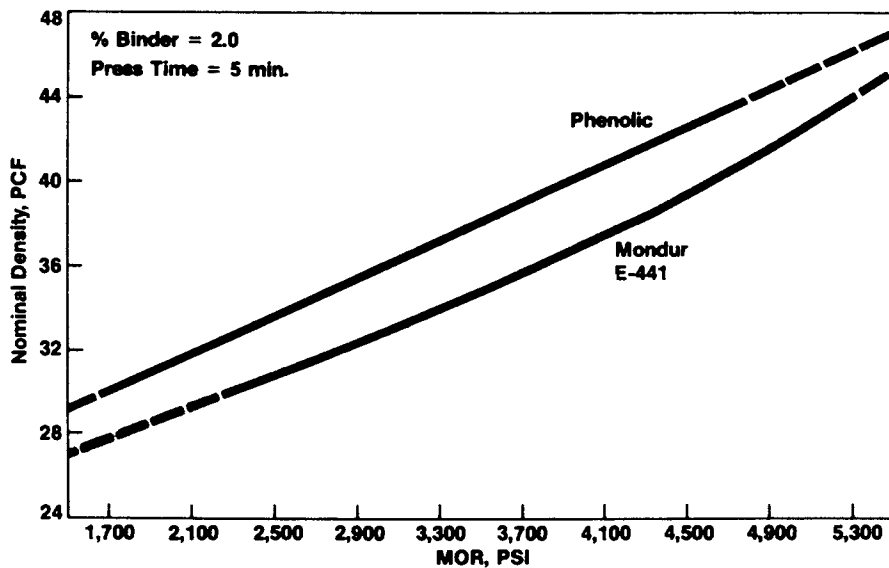


Figure 10. Predicted modulus of rupture vs. nominal density-aspen waferboard.

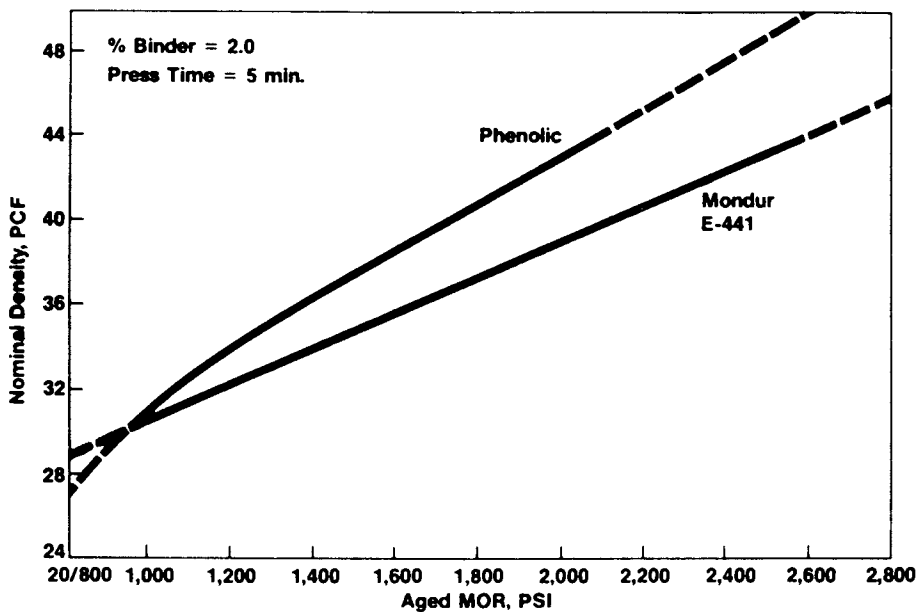


Figure 11. Predicted aged modulus of rupture vs. nominal density-aspens waferboard.

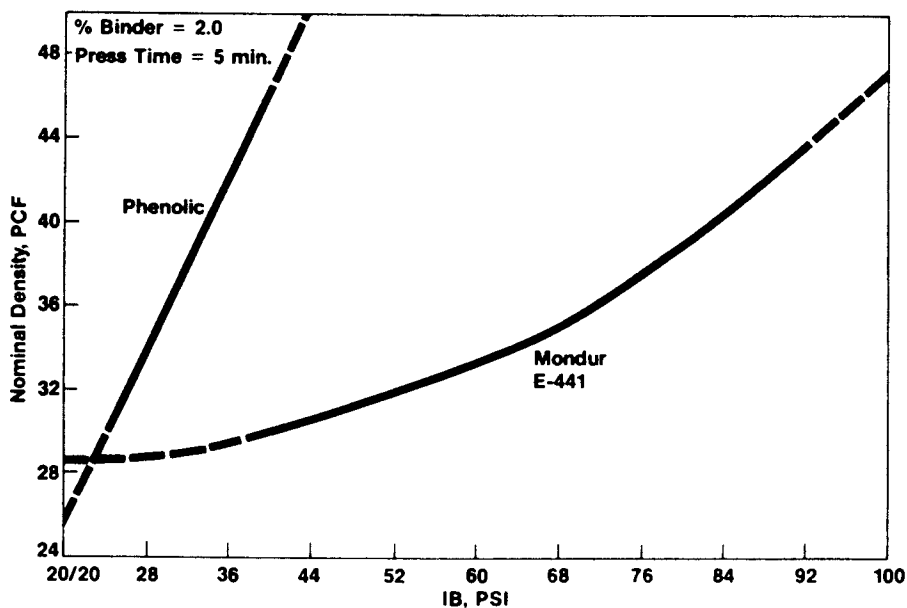


Figure 12. Predicted internal bond vs. nominal density-aspens waferboard.

Literature Cited

1. Rowell, R.M. and Ellis, W.D., Wood Science, (1979) 12 (1)
2. Hartman, S., Wood Technol.: Chem. Aspects Symp., 1976 (1977), 43
3. Wittman, O., Holz als Roh-und Werkstoff, (1976) 34 (11)
4. Deppe, H.-J. and Ernst, K., Holz als Roh-und Werkstoff (1971), 29 (2)
5. Deppe, H.-J., Proc. of Washington State University Symposium on Particleboard, (1977), 11
6. Ernst, K., Holz-Zentralblatt, (1975) 122
7. Shoemaker, P.D. and McQueary, H.O., U.S. Patent No. 3,919,017 (1975)
8. Shoemaker, P.D. and McQueary, H.O., U.S. Patent No. 3,930,110 (1975)
9. Shoemaker, P.D. and McQueary, H.O., U.S. Patent No. 4,946,952 (1977)
10. Ellingson, G.P., Proc. of Washington State University Symposium on Particleboard (1977), 11
11. Braun, F.W. and Ellingson, G.P., ibid, (1979) 13
12. Loew, G. and Sachs, H.I., ibid, (1977) 11
13. Sachs, H.I., Holz-Zentralblatt, (1977), 103 (20)
14. Sachs, H.I., ibid (1977), 103 (25)
15. Hse, C.-Y., Proc. of Complete Tree Utilization of Southern Pine Symposium, (1978)
16. Hse, C.-Y., U.S. Patent No. 4,209,433, (1980)
17. Udvardy, O.G., Proc. of Washington State University Symposium on Particleboard, (1979), 13
18. Wilson, J.B., ibid, (1980), 14
19. Johns, W.E., ibid, (1980), 14
20. Hunt, M.O., Hoover, W.L., Fergus, D.A., Lehmann, W.F., and McNatt, J.D., Purdue University Agricultural Experiment Station Research Bulletin 954, (1978)

RECEIVED April 30, 1981.

Lignin-Derived Polyols, Polyisocyanates, and Polyurethanes

W. G. GLASSER, O. H.-H. HSU¹, D. L. REED², R. C. FORTE³, and L. C.-F. WU

Department of Forest Products and Department of Chemical Engineering,
Virginia Polytechnic Institute and State University, Blacksburg, VA 24061

Lignin. Lignin is a natural polymer of plants which is exceeded in abundance only by cellulose. Plants gain the ability of lignifying when they acquire the need for developing "woody tissues." This need may be triggered by the requirement for mechanical support (reinforcing fibers by binding them together with a glue-like substance, lignin); the requirement for a sealed water-conducting system; or the requirement for an improved natural decay resistance. In response to such requirements, lignin is deposited as a polyphenolic, three-dimensionally crosslinked network polymer by maturing plants. Lignin contents range from 20 to 30% by weight of plant materials, or between 30 and 45% by enthalpy (1,2).

In the common process of making paper by chemical means, lignin is separated from mostly cellulosic fibers by dissolution processes which often involve structural modification and macromolecular breakdown (1). Pulp and paper mills generate approximately 24 million tons of dissolved lignin annually in the United States (2,3,4), and this compares to a combined total production of all synthetic organic materials of approximately 18.5 million tons per year in the U.S. in 1975 (5). Only about 3%, or 1.5 billion pounds per year, of solubilized lignin from spent pulping liquors are marketed, mostly (ca. 95%) as lignin sulfonic acids for roughly 6-8¢ per pound, and the remaining 5% as kraft lignin for approximately 20¢ per pound (6). Total market value for lignin products is estimated at roughly \$100 million per year in the United States (6).

The supply of kraft lignin is limited by the need of pulp mills to incinerate their lignin and chemicals containing spent

¹ Current address: Masonite Corp., St. Charles, IL.

² Current address: Hammermill Paper Co., Erie, PA.

³ Current address: Kimberly-Clark of Canada, Ltd., St. Catherines, Ontario.

pulping liquors for the purpose of recovering inorganic pulping chemicals. Thus, the practical available supply of kraft lignin in the United States is probably less than 2 million tons per year. However, additional sources of lignin are likely to become available in the future if any of the novel biomass-to-ethanol conversion processes designed for agricultural residues, waste paper, newsprint, or various types of wood sources, ever materialize. Such lignin sources will probably be similar in nature to kraft lignin (6).

Polyurethanes. Polyurethanes are a versatile group of polymers which span a wide range of physical properties and applications. Polyurethane markets are predicted to grow at an annual rate of 7-10% in the next 10 years (7). Many polyurethane applications are for network polymers, and these have been reviewed elsewhere in this treatise (7).

There have been several accounts in the literature for the involvement of wood or wood components in polyurethane systems. Thus, Senzyu and Ishikawa oxyalkylated wood with ethylene oxide in the presence of alkali in 1948 (8). Using appropriate lignin-like model compounds, Ishikawa, Oki and Fugita (9) observed that phenolic hydroxyl groups react quantitatively with ethylene oxide if the side chains do not contain carbonyl groups or other unsaturated moieties. Phenolic hydroxyl groups of model compounds with unsaturated side chains exhibited great resistance to hydroxyl-ethylation, probably reflecting the reduced nucleophilicity of the resulting phenoxide anions. In another series of experiments with model compounds, Kratzl et al. (10) studied the reactivity of the various functional groups which are present in lignin and which may react with isocyanate and diisocyanates. Since the alcoholic and phenolic hydroxyl groups differ in reactivity towards isocyanates, Kratzl et al. (10) were able to prepare both a mono- and diurethane from guaiacyl propanol-2 using a phenyl isocyanate. With hexamethylene diisocyanate, slower reactions were observed and selectivity between alcoholic and phenolic hydroxyl model compounds yielded only polymeric oily or tarry products. However, naphthalene diisocyanate yielded diurethanes in every case. When these studies were applied to technical hydrolysis lignins, reactions with isocyanates were described as very poor. This reaction behavior was in contrast to the behavior of kraft and sulfite lignins in combinations with commercial polyols (11,12).

Moorer, Dougherty and Ball (13) have employed lignin in the formation of polyurethane foams by dissolving it in glycols which are rich in active hydroxyl groups, and then reacting it with diisocyanates. The reaction was described as the isocyanate acting as a bridge substance linking the two kinds of polyol together. The phenolic hydroxyl groups in lignin were assumed to play a key role in this reaction. However, results showed that most lignin by-products yielded urethanes of inferior quality when compared with products made with polyethylene glycol.

The conversion of the phenolic hydroxyl groups to aliphatic hydroxyl functions was recognized as an important step toward the activation of functional hydroxyl groups by Allan (14) and by Christian et al. (15). Reactions with ethylene oxide, propylene oxide, and an alkyl sulfide were shown to produce oils with viscosities and hydroxyl numbers suitable for mixing and reacting with diisocyanates in the formation of rigid polyurethane foams. Brittleness, high water absorption and low strength appeared to constitute the main drawbacks of the resulting oxyalkylated lignin-urethane foams. These difficulties could largely be overcome by a carboxylation pretreatment with maleic anhydride (16). Carboxyl-rich lignins were converted into ester-rich polyols by oxyalkylation, and these were employed for the preparation of polyurethane foams (17), adhesives, and coatings (18) with acceptable properties. The enrichment of lignin with carboxylic functionality has also been accomplished by carboxymethylation with bromoacetic acid (19).

Approach and Objectives. In general, inherent disadvantages of lignin in regard to its utilization for materials concern (a) its resistance to degradative depolymerization to low molecular weight chemical feedstocks, and (b) its structural complexity which presents difficulties in altering, controlling, and manipulating the chemical and physical properties of polymeric lignin-derived materials via structural features. In addition, polymeric uses of lignin are burdened by an inherent resource variability, which, when it finds entrance to end product characteristics, gives rise to intolerable performance variations (2).

Therefore, a lignin utilization approach was explored which promised to satisfy the following prerequisites: (a) that lignin be used in its polymeric form for products which depend in their performance on *typical lignin characteristics* (structural reinforcement, antioxidant behavior, etc.); (b) that the chemical treatment or treatments involved in the utilization scheme amount to a *homogenation* capable of alleviating some of the natural variabilities; (c) that the chemical modification(s) introduces a measure of flexibility with regard to end product characteristics, such that it becomes possible to *tailor-make* lignin-derived materials for specific end uses; and (d) that the end product type belongs to a *growth market* in which lignin can conquer a sizable market share without displacing other raw materials.

Various types of lignin-derived polyurethane products and their precursors appeared to satisfy these constraints. This paper summarizes experimental efforts aimed at developing lignin-derived polyol, polyisocyanate, and polyurethane products.

Results and Discussion

Lignin-Derived Polyols. Polyhydroxy (polyol) components may be prepared from lignin using a one-, two-, or three-step modi-

fication procedure involving copolymerization with maleic anhydride (optional), saponification or solvent extraction (optional), and oxyalkylation with propylene oxide. The general reaction sequence is illustrated in Figure 1. The result of this lignin modification is a liquid polyol with unique functionality in regard to reactivity with isocyanates. This transformation of lignin via several chemical modification steps offers flexibility in terms of degree of carboxylation; concentration of ester groups; concentration of aliphatic ethers; ratio of aromatic vs. aliphatic polymer components; and extent of network vs. chain polymer constituents. Polyol characteristics may be influenced by variations in the reaction of lignin with maleic anhydride; by the method of copolymer purification; and by the conditions of the oxyalkylation reaction. Copolymer purification may involve solvent extraction, saponification (NaOH), or reprecipitation; and oxyalkylation may be varied via reaction time and/or temperature, type of catalyst (acidic or basic), and presence of initiator (ethylene glycol).

The effect of the maleic anhydride content in the copolymerization reaction mixture on the degree of carboxylation is illustrated by the data in Table I. Carboxylation of kraft lignin and ligninsulfonates may easily reach levels of 0.7 to 0.8 maleic anhydride units per lignin-building C₉-unit, if the lignin to maleic anhydride ratio in the reactor increases to 2:1.

The degree of copolymerization of the carboxylated lignin with propylene oxide, and the degree of homopolymerization of propylene oxide, can be expected to vary with the reactor pressure at the end of the oxyalkylation reaction. A typical pressure-temperature diagram of this reaction is presented in Figure 2. Polymerization usually commences between 165 and 185°C as is indicated by a retardation of the temperature rise and a distinct peaking of the reactor pressure. The entire reaction is completed after three to four hours, when the final pressure declines to around 180 psi.

Parameters which influence the functionality of the resulting polyols include the ratio of copolymer to propylene oxide, and the presence and concentration of catalyst and initiator. The influence of those parameters on hydroxyl number, carboxyl number, and polyol yield are summarized in Tables II and III. Low copolymer to propylene oxide ratios make it obviously difficult to totally liquefy lignin, Table II. Such conditions, however, seem to favor polyols with low total hydroxyl numbers. The oxyalkylation reaction appears to require catalyzation by zinc chloride or base catalysts in concentrations of about 10% or less for successful completion. The presence of an initiator (ethylene glycol) helps completion of the reaction in particular when the unhydrolyzed copolymer is used as substrate (Table III).

The degree to which physical properties of polyols depend on the nature and prior treatment of the lignin employed in the oxyalkylation reaction is indicated in Table IV. Polyols pre-

Table I
Semi-Empirical Formulas and Maleic Acid Contents of Lignins
and Lignin-Maleic Anhydride Copolymers

	Ratio of Lignin to Maleic Anhydride	Semi-Empirical Formula	Content of Maleic Acid/C ₉
Kraft Lignin	10:0	C _{9.0} H _{8.0} O _{2.7} S _{0.16} (OCH ₃) _{0.82}	--
"	10:1	C _{9.9} H _{8.4} O _{2.9} S _{0.13} (OCH ₃) _{0.82}	0.23
"	7.5:1	C _{10.1} H _{8.4} O _{3.1} S _{0.13} (OCH ₃) _{0.82}	0.28
"	5:1	C _{10.5} H _{9.0} O _{3.4} S _{0.14} (OCH ₃) _{0.82}	0.38
"	2:1	C _{11.7} H _{9.9} O _{4.3} S _{0.13} (OCH ₃) _{0.82}	0.67
Lignin Sulfonates	10:0	C _{9.0} H _{10.7} O _{6.5} S _{0.48} (OCH ₃) _{0.70}	--
"	10:1	C _{10.1} H _{10.2} O _{6.8} S _{0.22} (OCH ₃) _{0.70}	0.27
"	7.5:1	C _{10.1} H _{9.9} O _{7.0} S _{0.25} (OCH ₃) _{0.70}	0.29
"	5:1	C _{10.9} H _{10.5} O _{7.7} S _{0.16} (OCH ₃) _{0.70}	0.48
"	2:1	C _{12.1} H _{11.4} O _{7.6} S _{0.23} (OCH ₃) _{0.70}	0.79

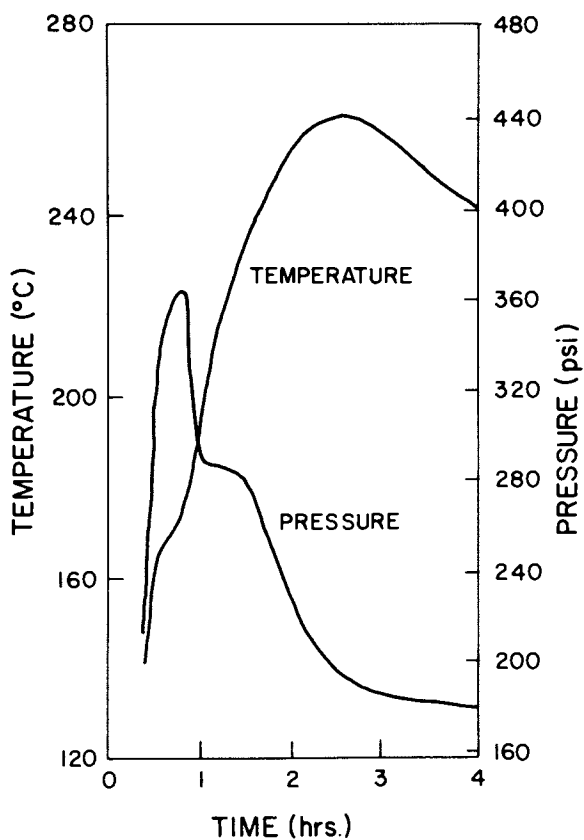


Figure 2. Pressure-temperature diagram for an oxyalkylation reaction of a carboxylated kraft lignin.

Table II

Polyol Functionality in Relation to Method of Preparation--
 Ratio of Lignin Copolymer to Propylene Oxide
 (All Reactions: 4 hrs. reaction time;
 temperature: 200-250°C)

Lignin Preparation	Ratio of Propylene Oxide to Lignin Copolymer	Catalyst System		OH Number	COOH Number
		A ¹	B ²		
Unhydrolyzed Kraft L.-M.A. (2:1) Copolymer	12:1	X		333	9
"	10:1	X		309±2%	11±2%
"	8:1	X		430±2%	13±12%
"	8:1		X	362	12
"	6:1 ³	X		289	26
"	6:1		X	307	18
"	4:1 ³	X		167	36
"	4:1 ³		X	260	32
Unhydrolyzed L. Sulfonates-M.A. (2:1) Copolymer	10:1	X		509	9

¹Catalyst System A: 10% catalyst (ZnCl₂) and 10% initiator (ethylene glycol).

²Catalyst System B: 10% catalyst and 30% initiator.

³Resulted in incomplete solubilization of the lignin-M.A. copolymer.

Table III

Polyol Functionality in Relation to Method of Preparation--
Initiator and Catalyst Concentrations
(All Reactions: 4hrs. reaction time; Ratio of Propylene Oxide:
Lignin 10:1; Temperature: 220-250°C)

Lignin Preparation	Initiator (%)	Catalyst (%)	OH Number	COOH Number	Polyol Yield ⁴
Unhydrolyzed Kraft L.-M.A. (2:1) Copolymer ¹	0	0	318	0.8	12
" ²	3.3	3.3	295	10	67
"	10	0	354	2	11
"	0	10	419	10	79
"	10	10	315	11	72
" ³	10	10	289	26	54
" ³	10	30	56	36	19
" ³	30	10	307	18	74

¹Reaction time of 2 hrs.

²Reaction time of 6 hrs.

³Propylene oxide:lignin ratio 6:1.

⁴Liquid polyol obtained after dissolving/suspending reactor content in methanol, filtration of methanol solution/suspension, and evaporation of filtrate at 80°C and 25 mm Hg; in % of total reactor content.

Table IV
Physical Properties of Three Types of Polyols

Property	Kraft Lignin Polyol	Hydrolyzed Copolymer Polyol	Unhydrolyzed Copolymer Polyol
<u>Solubility</u> ¹ :			
Methanol	V (clear)	V (clear)	V (cloudy)
DMF	S	V	V
Diethyl ether	I	S (cloudy)	I
Acetone	S (cloudy)	S (clear)	S (cloudy)
Benzene	S (cloudy)	S (clear)	σ
Carbon tetrachloride	σ	S	I
Chloroform	V	V	V
Toluene	σ	V	I
Ethylacetate	I	S (cloudy)	S (cloudy)
Propyleneglycol	V	V	V
Dioxane	V	V (cloudy)	V
Water	S	I	I
Acetic acid	I	S	V
<u>Functionality</u> :			
OH Number	560	420	0.8 meq/g
COOH Number	0	0.16 meq/g	1230
<u>Viscosity</u> :	220	430	
<u>Color</u>	Brown	Yellow	Brown

¹Abbreviated with V, very soluble; S, soluble; σ, slightly soluble; and I, insoluble.

pared with the hydrolyzed copolymer have apparently a less polar solubility character than those polyols prepared with the unhydrolyzed copolymer or the uncarboxylated lignin. Similar differences are detected for chemical functionality, viscosity, and color (Table IV).

Suitable liquefaction during oxyalkylation seems to require a ratio of propylene oxide to copolymer (or lignin) of 4:1 or greater. This epoxide excess presently constitutes the greatest constraint for optimizing the incorporation of lignin into a polyurethane product. A polyol prepared with such an excess of propylene oxide will not contain more than 25% lignin assuming that all propylene oxide polymerizes.

Lignin-Derived Polyisocyanates: Efforts to increase the incorporation of lignin into polyurethane products have concentrated on transforming polymeric lignins into polyisocyanates useful for reacting with polyols. Two alternative reaction pathways have been explored with the three lignin-like model compounds shown in Figure 3. These models were vanillic acid or a derivative thereof (Model Type A); a derivative of tetralin dicarboxylic anhydride (Model Type B); and a derivative of a styrene-maleic anhydride copolymer (Model Type C).

The two reaction pathways studied involve a route from the carboxylic acid to the isocyanate via the acyl chloride and azide (Sodium Azide Pathway, Pathway A), Figure 4; and a route from the carboxylic acid to the isocyanate via the hydrazide (Hydrazide Pathway, Pathway B), Figure 5. The reactions were monitored by isolating the intermediate reaction products and characterizing them by melting points, elemental composition, or IR spectroscopy.

The sodium azide pathway (Pathway A), Figure 4, begins with a thionylchloride treatment of the free acid to form the acyl chloride. Subsequent treatment with sodium azide may involve a non-aqueous environment (1,2-dimethoxy ethane, "dry method"), or an aqueous medium ("wet method"). The organic azide is recovered from the reaction mixture and converted into the isocyanate by the Curtius rearrangement. This may be accomplished in solid form ("dry method"), or in a non-aqueous solvent like dioxane or DMF ("solution method").

The hydrazide pathway (Pathway B), Figure 5, was first attempted by treating the acyl chloride with hydrazine. Since this reaction, however, produced the secondary hydrazide in almost quantitative yields, this approach was abandoned in favor of one employing the methyl ester derivative. Hydrazinolysis of the ester, formed by refluxing the free acid in anhydrous methanol/ H_2SO_4 , proceeded in dry methanol to the hydrazide in good yield. Subsequent reaction of the hydrazide with nitrous acid, which was generated in the presence of the hydrazide in aqueous acetone/HCl solution at 0-5°C, yielded the organic azide. This, again, was rearranged either dry or in solution to the isocyanate.

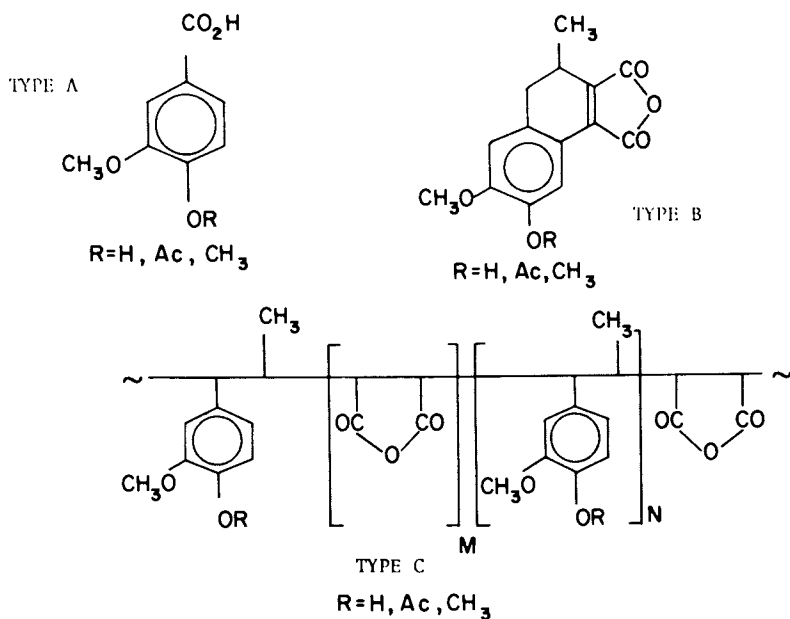


Figure 3. Lignin-like model compounds.

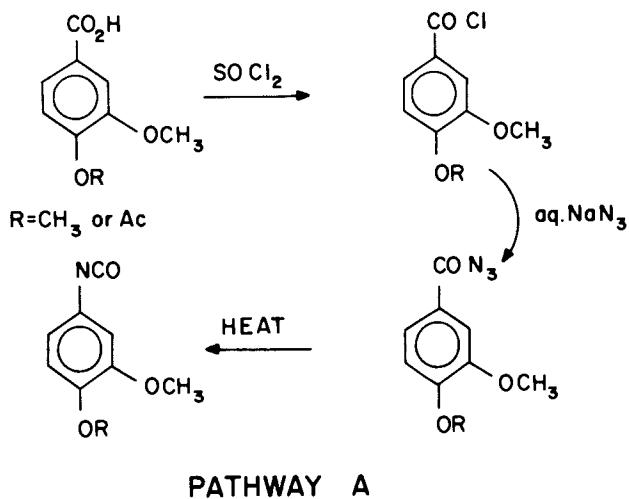


Figure 4. Reaction scheme of the sodium azide pathway.

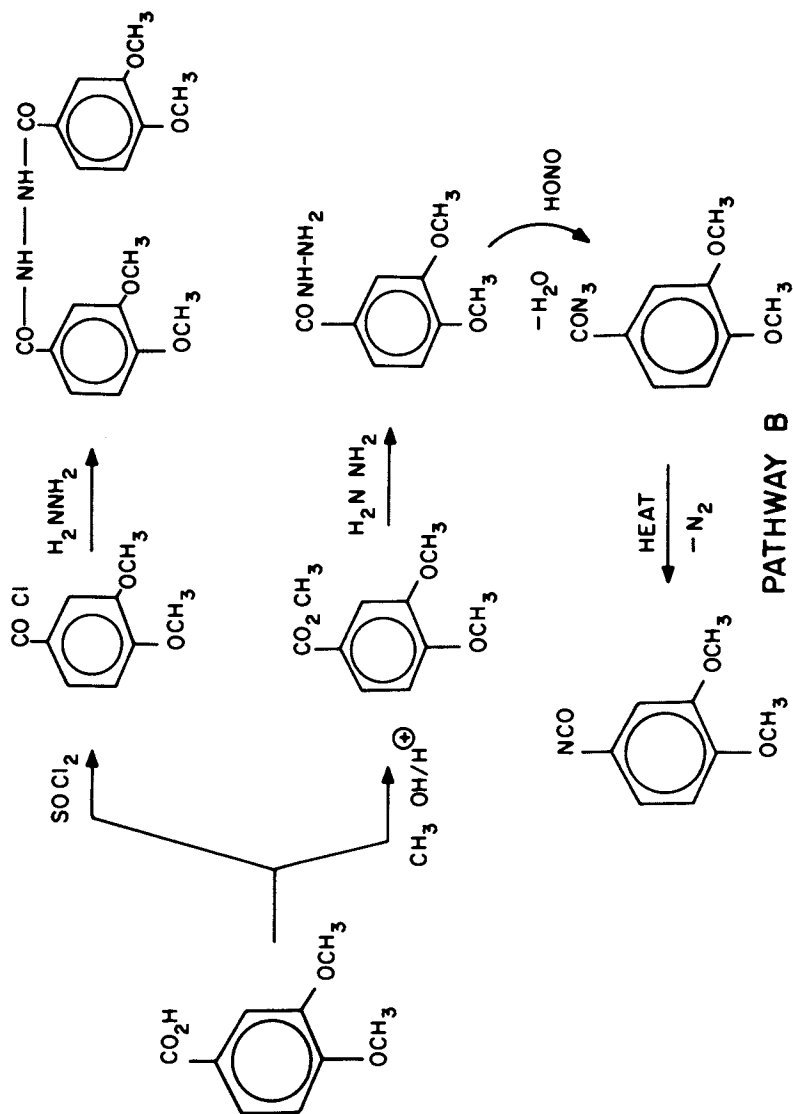


Figure 5. Reaction scheme of the hydrazide pathway.

Model Type A, vanillic acid and its acetylated or methylated derivative, generated the expected isocyanate without major problems either via the sodium azide or the hydrazide pathway. Yields and analysis results are summarized in Table V. IR spectra of the various intermediary reaction products are given in Figure 6. Formation of the organic azide by the wet method from the acyl chloride was superior to "dry" formation; but hydrazinolysis of the methyl ester followed by HNO_2 -treatment worked satisfactorily as well.

Model Type B (Figure 3), tetralin dicarboxylic acid and its derivatives, failed to form a stable free acid. Its anhydride regenerated consistently from its sodium salt, which was temporarily formed in aqueous alkaline solution, upon acidification. Therefore, conversion attempts with this model were abandoned.

Model Type C, a copolymer formed by the reaction of isoeugenol or its methyl ether with maleic anhydride at 170°C in an autoclave and purified by precipitating its ethyl acetate solution from ether, was reacted following both pathways. The results in Table VI indicate that, although eventual formation of azide groups can be documented at least for the sodium azide and probably also for the hydrazide pathway, the accumulation of impurities along the multi-step conversion pathways present mounting problems. Incomplete transformation of functionalities of intermediary steps is indicated in the sodium azide pathway by the retention of chlorine after treatment with sodium azide and in the hydrazide pathway by incomplete methylation and incomplete hydrazide transformation to azide by HNO_2 , resulting in a product with low N-content.

Model Type C, the isoeugenol-maleic anhydride copolymer, forms an organic azide and isocyanate by the sodium azide pathway as is indicated by the IR spectra (A and B) of Figure 7. However, overall isocyanate yields remain low.

Another approach at introducing isocyanate functionality into polymeric lignin derivatives concentrated on "capping" hydroxyl groups of lignin-derived polyols with diisocyanates. Results of these experiments, which employed anhydrous benzene solutions of polyols and excess HDI, are given in Table VII. That this method of introducing N-containing functionality into polyols is highly successful is indicated by the high nitrogen contents of capped polyols A and B. A strong NCO band in the IR spectrum of the derivatized polyol, Figure 7C, suggests that this polyol has been successfully transformed into a polyisocyanate. This simple polyol conversion may eliminate the difficulties associated with the formation of a polyisocyanate from lignin by multi-step transformation procedures applied to carboxylated lignin derivatives, which are caused by the accumulation of multiple functionalities.

Lignin-Derived Polyurethanes. The manufacture of polyurethane foams, adhesives and coatings from lignin-derived polyester-ether-polyols and various commercial diisocyanates has been accomplished and reported earlier (16,17,18). Foam properties

Table V
Melting Points, Elemental Analysis, Yield, and IR-Data of Model Type A Intermediates

Compound (cf. Fig. 3)	Theory/ Found	Melting Point (°C)	Elemental Analysis (%)			Yield ¹ (% of Theory)	Characteristic IR-Band(s) (cm ⁻¹)
			C	H	N		
Vanillin	Th	81-82	63.15	5.26	---	---	CHO: 1700-1725
	F	80-81	62.99	5.31	---	---	
Veratraldehyde	Th	44-45	65.06	6.02	---	87	CHO: 1700-1725
	F	44-45	64.77	6.06	---		
Veratric Acid	Th	179-180	59.34	5.49	---	81	COOH: 1680-1700
	F	179	59.24	5.31	---		
Veratric Acid Chloride	Th	69-70	53.86	4.48	---	95 ²	COCl: 1760-70
	F	71-73	52.03	5.12	17.70		
Veratric Acid Methyl Ester	Th	60-61	61.22	6.12	19.86	71	COCH ₃ : 1720
	F	60-61	60.12	5.81	---		
Veratric Acid Hydrazide	Th	144	55.10	6.12	14.28	89	CONHNH: 1640-1700; 3180-3320; 1602-1633
	F	205	55.01	6.17	14.21		
Diveratric Hydrazide (2°)	Th	205	60.00	5.56	7.77	69	CON ₃ : 1660-1700; 2150-2175
	F	51-52	59.79	5.81	7.81		
Veratric Acid Azide	Th	51-52	60.33	5.02	7.82	88	NCO: 2230-2300
	F	N160	61.99	6.01	8.43		NHR: 2850-3000
Veratric Acid Isocyanate	Th	205-206					
	F						

¹Based on previous step.

²Unpurified.

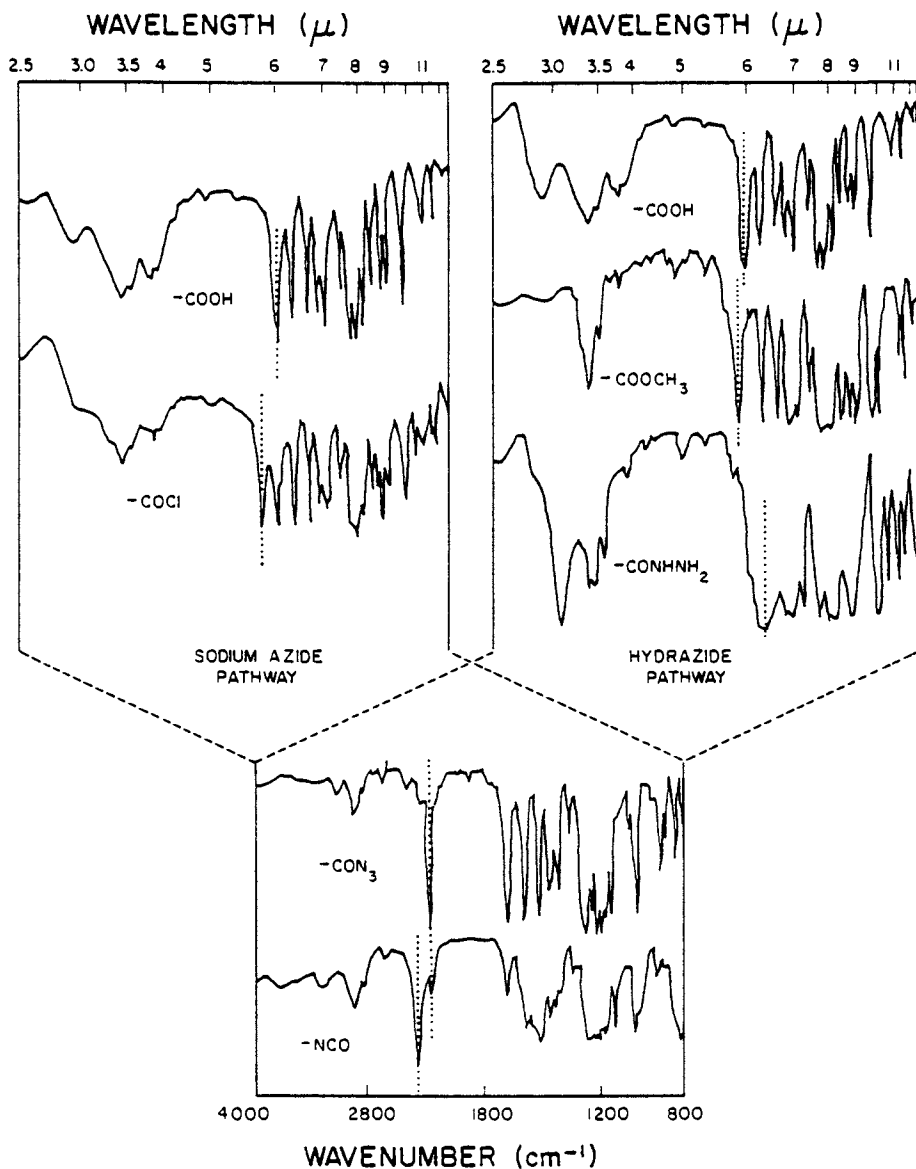


Figure 6. Infrared spectra of isocyanate formation of model Type A ($R = CH_3$) via the sodium azide and the hydrazide pathways.

Table VI
Elemental Analysis and Functionality Data of Model Type C Intermediates

Compound	Elemental Analysis (%)						Functionality					
	SODIUM AZIDE PATHWAY - MODEL TYPE C (R = CH ₃)			HYDRAZIDE PATHWAY - MODEL TYPE C (R = CH ₃)			Mal. Acid/ C ₉	COOH/ C ₉	Cl/ COOH	Ester- OCH ₃ / COOH	Hydra- zide/ COOH	N ₃ / COOH
	C	H	N	Cl	OCH ₃	9.74						
Acid - A(1.trial) B(2.trial)	55.87	5.97	--	---	9.74	1.32	2.64					
	57.28	5.39	--	---	7.31	2.24	4.48					
Acid Chloride - A B	48.00	3.91	1.27	13.70					0.53			
	50.43	4.31	1.38	12.86					0.38			
Azide-Wet Method-A -B	54.04	3.93	4.25	4.13							0.10	
	54.73	4.12	3.23	7.51							0.05	
Azide-Dry Method-B	33.68	2.49	16.44	8.13							0.21	
HYDRAZIDE PATHWAY - MODEL TYPE C (R = CH ₃) - ANHYDRIDE												
Anhydride Methylester Hydrazide Azide	61.70	5.42	--	---	17.90	1.71	3.42		0.49		0.44	
	60.72	6.00	--	---	29.73							
	55.60	5.31	9.76	---	15.54							
	56.3	5.92	3.63 (max)	---	16.91							0.01

¹Determined by IR-spectroscopy.

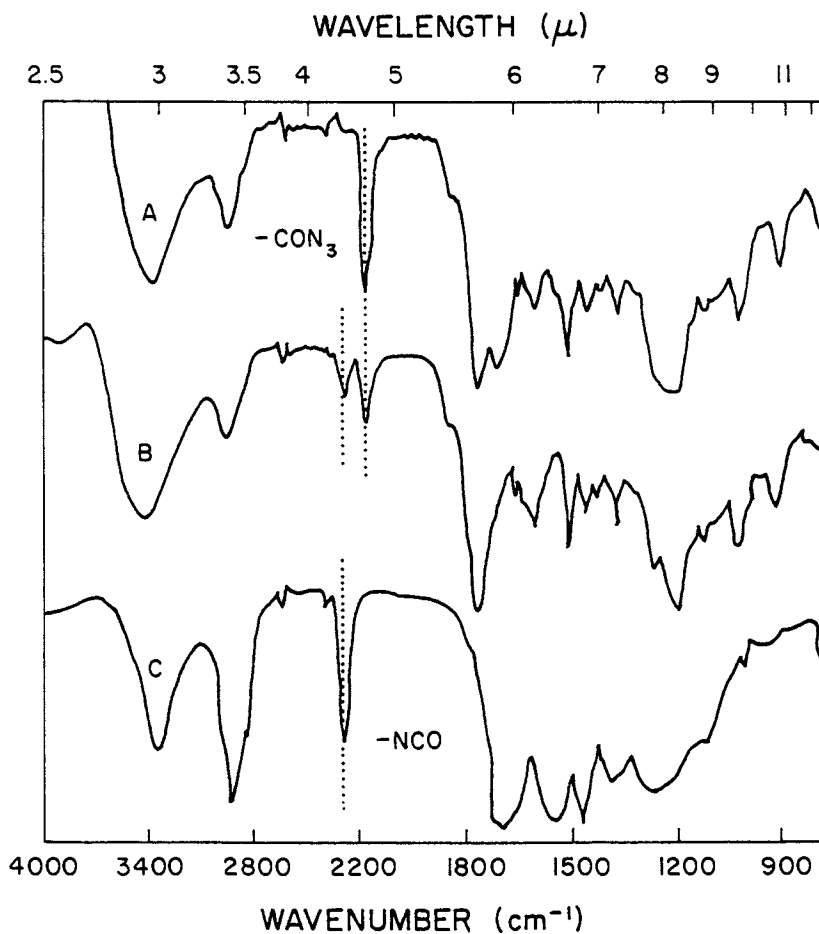


Figure 7. Infrared spectra of isocyanate formation of model Type C ($R = CH_3$) (Spectrum A, azide and Spectrum B, isocyanate) and of capped lignin-derived polyol.

Table VII

Analysis Data of Two HDI-Capped Polyols

Preparation	Elemental Analysis (%)					Functionality NCO/OH ¹
	C	H	N	S	Total OH	
Kraft Lignin					10.39	
Polyol-A					6.23	
-B					9.3	
HDI-Capped Polyol ² -A	52.01	7.51	13.52	0.69		2.1
-B	52.55	7.48	12.08	0.74		1.5

¹Assuming that one of the two NCO-groups of HDI survives the reaction as NCO.

²Analyses were performed on ether-insoluble fractions recovered from the total reaction mixtures in low (unrepresentative) yields.

are summarized in Table VIII, where they are compared to a commercial low-density foam and to a foam prepared from an uncarboxylated lignin-derived polyether-polyol. The results demonstrate superior performance characteristics of lignin-polyester-ether-polyol-based urethane foams in terms of compressive strength, recovery, and density, as compared to the two other foams. Water sorption ranges generally below 10% for lignin polyester-polyols, and between 10 and 20% for the non-carboxylated kraft lignin-polyol foams and the commercial product.

Adhesive properties are listed in Table IX. Shear strength, wood failure, and swelling data for two wood species, southern pine and hard maple, illustrate excellent performance properties of lignin-based urethane products.

Urethane coatings for wood surfaces, prepared with lignin-based polyester-ether-polyol, have demonstrated exceptional properties in terms of solvent and chemical resistance (18), and they provide the coated wood surface with an attractive appearance.

Capped polyols, prepared by reacting polyols in non-polar solvents (benzene or ethyl acetate) with excess diisocyanate (HDI), reacted with cellulose fibers at ambient temperature. Simple immersion of preformed fiber mats (blotting paper) followed by air-drying resulted in drastic increases in sheet strength properties. This is indicated in Table X.

Economic Considerations. The economic feasibility of producing lignin-derived polyols from carboxylated and oxyalkylated kraft lignin has been assessed in a publication series entitled "How to Design Chemical Plants on the Back of an Envelope," by J. P. Clark (20). The results of this economic evaluation, which was completed in 1975 and published in 1976, are highlighted in Table XI. The "back-of-the-envelope" evaluation concluded that commercial production of lignin-derived polyester-ether-polyols was commercially feasible at that time. Where similar polyester-polyols were selling for 40-60¢/lb., lignin-derived polyols could be manufactured at a profit for 34¢/lb. This would require a capital investment of below \$2 million for a plant with a 30,000-tons per year capacity. It is likely that this economic situation has changed in the past five years to the benefit of the concept on the basis of renewable resources.

Experimental

Materials. Kraft lignin samples were obtained from WESTVACO Corp., Charleston, South Carolina; they were commercial preparations traded under the name INDULIN-AT. Lignin sulfonate preparations were procured from GEORGIA PACIFIC Corp., Bellingham, Washington; their commercial name is LIGNOSITE (spray-dried from fermented calcium spent sulfite liquor).

Methods. Carboxylation of Lignin: Mixtures of lignin and maleic anhydride were sealed in a 3.5 x 20 cm thick-walled glass tube and placed inside a steel autoclave. The vessel was heated

Table VIII

Comparison of Foam Properties--
Strength, Appearance, Water Sorption of Three Types of Foam

Property	Kraft Lignin Polyol ¹	Carboxy-lated Kraft Lignin Polyol ¹	Commercial Foam ²			
I. Strength Properties:						
At Density (lbs/ft ³)	6.10±0.27	2.54±0.15	2.54			
Compressive Strength (psi) ³	11±1.0	23±2.2	17			
Modulus of Elasticity (psi)	531±65.4	381±34.5	80			
Recovery (%) ⁴	0	90	80			
II. Appearance:						
Cell Structure	Collapsed	Uniform				
Color	Brown	Yellow				
III. Water Sorption⁵ at						
	lbs/ft ³	%	lbs/ft ³	%	lbs/ft ³	lbs/ft ³
1.5 lbs/ft ³ Density			0.15	9		
2.0 lbs/ft ³ Density			0.21	10		
3.0 lbs/ft ³ Density			0.26	8	0.38 ⁶	19 ⁶
4.0 lbs/ft ³ Density			0.34	8		
5.0 lbs/ft ³ Density	0.72	18	0.44	9	0.39 ⁶	10 ⁶
6.0 lbs/ft ³ Density	0.93	19	0	7		
	0.97	16	0.40	7		

¹Foams prepared with a mixture of 2.4- to 2.6-toluene diisocyanate of 4:1.

²Data from "Polyurethanes," 2nd ed., B. M. Dombrow, Reinhold Publ. Co. (1965), pp. 82-84.

³Based on 20% deflection at 23°C.

⁴Following 50% compressive deflection.

⁵After subjection to saturated humidity at 23°C for 2 months.

⁶After subjection to 98% relative humidity for 120 hrs; from same source as given in footnote #2, p. 89.

Table IX
Comparison of Adhesive Properties--Strength, Wood Failure, Swelling of Several Types of Adhesives¹

Property	TDI ^{2,4}			HDI ^{2,4}			MDI ^{3,4}		
	BNZ	EtOAc	DMF	BNZ	EtOAc	DMF	BNZ	EtOAc	DMF
I. Shear Strength (psi) ⁵									
--Southern Pine	2031±13	1708±5	1470±9	1651±8	1366±18	798±13	482±18	884±27	1693±17
--Hard Maple	1885±5	2320±4	1205±48	2010±7	2200±5	1210±0	300±23	498±6	2437±6
II. Wood Failure (%) ⁶									
--Southern Pine	95±5	94±4	54±54	81±32	72±40	5±100	10±100	10±70	90±16
--Hard Maple	10±1	60±35	1±100	26±27	32±25	0	0	0	40±18
III. Swelling (%) ⁷									
--12 hours	1.1±18	1.1±10	---	2.2±18	---	---	2.3±18	---	1.0±20
--48 hours	2.0±7	2.0±10	---	3.1±6	---	---	4.4±14	---	1.9±16
--1 week	3.1±5	2.8±5	---	4.3±9	---	---	6.0±10	---	2.5±8

¹Values given are averages of 5 determinations with maximum deviation indicated in percent.

²Assembly time of 5 minutes.

³Assembly time of 20 seconds.

⁴BNZene (BNZ) and ethylacetate (EtOAc)-formulated adhesives were used at room temperature; DMF-formulated adhesives were cured at 150°C.

⁵Comparable shear strength values (hard maple) for resorcinol-formaldehyde and epoxy resins are 2308±2 and 2320 psi, respectively (from F. L. Williamson and W. T. Nearn, For. Prod. J., 1958, 8(6), 181; and from J. T. Clark and W. T. Nearn, For. Prod. J., 1957, 7(1), 20).

⁶Comparable wood failure data (hard maple) for resorcinol-formaldehyde and epoxy resins are 92±2 and 30%, respectively (from same sources as given under footnote #5).

⁷Determined on sheets prepared by curing the adhesive at 100°C on silicone-coated glass plates; values given refer to weight gained (in %) during water immersion. The sheets were aged for 3 weeks prior to testing.

Table X

Strength Properties of Untreated
and Polyisocyanate-Coated Paper Strips
(Each figure represents an average of 10 measurements)

	Untreated	Polyisocyanate-Coated	% Increase through Treatment
Tensile Strength (kg/m)	802.4	1659.2	106
Breaking Length (m)	3379.6	6942.8	106
Elongation at Rupture (%)	10	24	135
Energy Absorbed at Rupture (kg/m)	0.023	0.115	404
O.D. Wt. of Strip (g)	1.18	1.44	22
Basis Wt. (g/m ²)	228	279	22
Thickness (μm)	501	502	<1
Density	0.46	0.56	22

Table XI

Economic Analysis (1975) of the Production
of Lignin-Derived Polyols (After Clark (20))

Price of Competitive Polyols:	40-60¢/lb.
Plant Capacity (polyol):	30,000 mt/yr
Mode of Operation:	batchwise
Capital Investment	\$ 1,540,000
<u>Fixed Costs</u> (annual basis):	
Depreciation (7 years, straight line)	220,000
Taxes and Insurance (5% of T.C.I.)	77,000
Plant Overhead (70% of labor)	<u>37,800</u>
Total Fixed Costs	\$ 334,000
<u>Direct Costs:</u>	
Raw Materials	\$16,770,139
Energy	148,643
Labor	540,000
Maintenance (10% of T.C.I.)	154,000
Other Expenses (20% of Direct Costs)	<u>4,403,195</u>
Total Direct Costs	<u>\$22,015,978</u>
Total Product Costs	\$22,350,778
Cost of Polyol	34¢/lb.
Cost of Polyol at 20% return after taxes on investment, at 48% tax rate, before tax profit	35¢/lb.

at 170°C (oven or oil bath) for two hours. After cooling and opening, the copolymer was removed, ground to a fine powder using a mortar and pestle, and either Soxhlet extracted with diethyl-ether ("unhydrolyzed") or saponified by refluxing with 2N NaOH (1 hr) followed by acidification (1N H₂SO₄) and recovery of the resulting precipitate by centrifugation ("hydrolyzed").

Oxyalkylation: Lignin or lignin-copolymer was mixed with varying parts of propylene oxide, initiator (ethylene glycol) and catalyst (1% by wt. KOH or ZnCl₂), and sealed in a 1.5-liter stainless steel pressure reactor equipped with heating mantle and mounted on a shaking platform (8-20 cycles/sec with 0.05 in. oscillation). The reaction vessel was heated by a Glass-Coil heating mantle. After cooling, the reactor content was centrifuged, and the viscous liquid portion freed from unreacted propylene oxide by vacuum evaporation.

Polyurethane Products: Polyurethane foams were prepared by reacting a 10% excess of diisocyanate component over the amount required by stoichiometric calculation, based on hydroxyl and carboxyl number determination with the polyol, and either water or freon for blowing agent, silicone surfactant (Union Carbide L-520), and two catalysts, Union Carbide's NIA X A-1 (70% by weight solution of bis-dimethyl-amino-ethyl ether), and a stabilized stannous complex (Union Carbide's Metals and Thermit T-9). Blowing agent, surfactant, and catalysts were added in concentrations of 1.5, 1.5, 0.2 and 0.3%, respectively, on basis of polyol weight. The mixture was agitated vigorously for about 10-15 seconds and then allowed to rise. The foams were conditioned for three days before they were cut into the dimensions recommended by ASTM standards.

Polyurethane adhesives were prepared by mixing polyol, diisocyanate (MDI, TDI or HDI), solvent (DMF, benzene or ethylacetate), and catalyst (T-9) in the following fashion: The diisocyanate dissolved in half of the total solvent volume was mixed with two-thirds of the polyol in one-fourth of the solvent in the presence of a trace of the catalyst. The mixture was heated to 50°C until an exothermic reaction starts; then, heat was temporarily removed and reapplied for 10 min to maintain a temperature of 80°C. The rest of the polyol, catalyst, and solvent were then added and mixed completely. The resin was ready for application when the consistency of the mixture had reached a suitable level. The adhesive was spread on 11 3/4" x 4 1/2" x 3/4" wood (hard maple or southern pine) strips. The moist adhesive-coated surfaces were exposed to ambient air (vented hood) for 20-30 seconds if DMF was used as solvent, or for 3-5 minutes if either benzene or ethylacetate was used. After pressing (100 psi), the strips were cut into small shear blocks and tested according to ASTM Standard D905-49. Polyurethane coatings were prepared by mixing the polyol (80 parts) in ethylacetate (60 parts) and toluene (40 parts), with a solution of TDI (53 parts) in 80 parts ethylacetate and 30 parts toluene, and T-9 catalyst

(0.5 parts). The resin is ready for application when the temperature of the mixture has returned to ambient.

Sodium Azide Pathway: The free carboxyl group-containing compound was dissolved in thionyl-chloride and refluxed for 10 hours, followed by vacuum evaporation. To a solution of acyl chloride in 1,2-dimethoxyethane was added, under stirring, an excess of freshly activated sodium azide in solid form ("dry method"), or in aqueous solution ("wet method"). In the dry method, the mixture was refluxed overnight, filtered, and evaporated to dryness. In the wet method, the mixture was stirred for 20 minutes and precipitated by the addition of water (10 times its original volume). The precipitate was filtered, washed, and freeze-dried. The organic azide was either heated for 1 hour to 100-120°C (oil bath) as a dry powder ("dry method"), or refluxed for 1 hour in dioxane- or DMF-solution ("solution method"), which was followed by vacuum evaporation.

Hydrazide Pathway: The unhydrolyzed copolymer (anhydride form) was methylated for 20 hrs by pressure-heating to 110°C its absolute methanol solution containing a small amount (ca. 0.5% of methanol) of N-N-4 dimethylaminopyridine followed by vacuum evaporation. The concentrated solution was precipitated from ether-pet ether 2:1 by dropwise addition, filtered and washed (ether-pet ether).

A dimethylester solution in dry methanol (ca. 1%) was mixed with excess anhydrous hydrazine and refluxed for 6 hours. The residue from vacuum evaporation was the hydrazide, which was freeze-dried from its aqueous solution. A solution of the hydrazide in 10% aqueous HCl was cooled to 0 to 5°C, and to this solution was added dropwise an aqueous solution of NaNO₂. A precipitate formed overnight, which was collected and dried. This product, the acid azide, was subjected to the same kinds of Curtius rearrangement conditions as described above.

Polyol Capping: A polyol (hydroxyl no. 315, carboxyl no. 11) solution in benzene was added dropwise to a stirred benzene solution of HDI, which was kept in a 50°C water bath. After heating the mixture for 1 hour, the solution was cooled and used for impregnating strips of bleached board (blotting paper) by immersion for 30 seconds. After removing the coated strips from the solution, excess solution was wiped off from the paper surface, and the strip was air-dried. After conditioning, the tensile strength of the samples was determined following TAPPI Standard T4940S-70. Elongation, tensile energy absorption (TEA), basis weight, and density were calculated.

Conclusions

Lignin by-products from kraft and sulfite pulping were found to constitute useful raw materials for polyols for polyurethane products. Their employment in the manufacture of semi-rigid polyurethane foams as well as polyurethane adhesives and coatings

has been reported previously. The manufacture of lignin-based polyols by carboxylation with maleic anhydride and oxyalkylation with propylene oxide has been studied with regard to economic feasibility, and was found to be competitive with commercial polyols of similar characteristics, and profitable if sold for about 40¢/lb. (1975) (20).

The limitations of the use of lignin in polyols for urethanes are determined by the difficulties encountered during the liquefaction step of its preparation. This step generally reduces the lignin content of the polyol to between 10 and 30%.

Attempts to increase the lignin content in polyurethane products via either increased lignin contents of the polyols, or via the formulation of lignin-derived polyisocyanates, have so far largely failed. This is primarily attributed to lignin's limited solubility characteristics.

Acknowledgement

Financial support for this study was provided by the National Science Foundation, Washington, D.C., under grant No. PFR79-13135; the Research Division of VPI & SU; and the Crown Zellerbach Corporation of Camas, Washington. This support by all sponsors is gratefully acknowledged. The authors wish to thank Dr. P. L. Hall and Dr. J. McGrath, both Department of Chemistry, VPI & SU, for helpful counsel.

Literature References

1. Glasser, W. G.; "Lignin," Chapter 2 in "Pulp and Paper--Chemistry and Technology," 3rd ed., Vol. I, J. P. Casey, ed.; John Wiley and Sons, Inc.: New York, 1980; pp. 39-111.
2. Falkehag, S. I.; Appl. Polym. Symp., 1975, No. 23, 247.
3. Kringstad, K.; "The Challenge of Lignin," in "Future Sources of Organic Raw Materials--CHEMRAWN I," L. E. St.-Pierre and G. R. Brown, eds.; Pergamon Press, 1980; pp. 627-636.
4. Allen, B. R., M. J. Cousin, G. E. Pierce; "Pretreatment Methods for the Degradation of Lignin," Final Report to NSF; Battelle Columbus Laboratories: Columbus, OH, 1980; pp. 1-176.
5. Goldstein, I.; "Potential for Converting Wood into Plastics," in "Materials: Renewable and Nonrenewable Resources," P. L. Abelson and A. L. Hammond, eds.; American Association for the Advancement of Science, 1976; pp. 179-184.
6. Glasser, W. G.; For. Prod. J., 1981, 31, in press.

7. Manno, P. J.; "Outlook for Worldwide Polyurethane Markets," ACS Symposium on Urethane Chemistry and Applications, Las Vegas, NE, Aug. 24-29, 1980.
8. Senzyn, R.; H. Ishikawa; J. Agr. Chem. Soc. Japan, 1948, 22, 72.
9. Ishikawa, H.; T. Oki; F. Fugita; Nippon Mokuzai Gakkaishi, 1961, 7, 85.
10. Kratzl, K.; K. Buchtela; J. Gratzl; J. Zauner; O. Ettingshausen; Tappi, 1962, 45(2), 113.
11. Allan, G. G.; "Modification Reactions," in "Lignins--Occurrence, Formation, Structure and Reactions," K. V. Sarkanen and C. H. Ludwig, eds.; Wiley-Interscience, 1971; pp. 511-573.
12. Saunders, J. H.; K. C. Frisch; "Polyurethanes--Chemistry and Technology," Part 1, Interscience Publishers: New York, 1962; 368pp.
13. Moorer, H. H.; W. K. Dougherty; F. F. Ball; U.S. Patent 3,519,581 (1970).
14. Allan, G. G.; U.S. Patent 3,476,795 (1969).
15. Christian, D. T.; M. Look; A. Nobell; T. S. Armstrong; U.S. Patent 3,546,199 (1970).
16. Glasser, W. G.; O. H.-H. Hsu; U.S. Patent 4,017,474 (1977).
17. Hsu, O. H.-H.; W. G. Glasser; Appl. Polym. Symp., 1975, No. 28, 297.
18. Hsu, O. H.-H.; W. G. Glasser; Wood Science, 1976, 9(2), 97.
19. Lange, W.; W. Schweers; Wood Sci. Technol., 1980, 14(1), 1.
20. Clark, J. P.; Chem. Tech., 1976, 6, 235.

RECEIVED April 30, 1981.

Dynamic Mechanical and Thermal Properties of Seven Polyurethane Adhesives

D. MARK HOFFMAN

Lawrence Livermore National Laboratory, University of California,
Livermore, CA 94550

The dynamic mechanical behavior of block copolymers depends on the mechanical and morphological nature of each block. If polymer block A is thermodynamically incompatible with polymer block B, microphase domains form (1-5). The concentration and chemical structure of these domains can be controlled to produce desired mechanical and thermal properties.

Seven polyurethane adhesives have been developed at Lawrence Livermore National Laboratory (LLNL). These adhesives, designated Halthanes were synthesized because of OSHA restrictions on the use of the curing agent methylene bis(2-chloroaniline). Four of the Halthanes were made from LLNL-developed 4,4'-methylene bis(phenylisocyanate) terminated prepolymers cured with a blend of polyols; three were made from an LLNL-developed prepolymer terminated with Hylene W and cured with aromatic diamines. In this paper we report the dynamic mechanical and thermal behavior of these seven segmented polyurethanes.

Segmented polyurethanes have domains called hard and soft segments (3) because of their modulus differences. Relaxations in the dynamic mechanical spectrum can be associated with transitions in the hard and soft segments. In the Halthane adhesives, the soft segment is always the reaction product of a hydroxy-terminated poly(tetramethylene glycol) and an isocyanate. Since domain insolubility depends on molecular weight, the degree of polymerization of the polyether can be changed to produce different degrees of microphase separation.

0097-6156/81/0172-0343\$05.00/0

© 1981 American Chemical Society

Lower molecular weight polyether in the soft segment increases the glass transition temperature and therefore decreases the low temperature limit of elastomeric character of the adhesive.

Diisocyanates and low molecular weight diols or amines used to form the polyurethane or polyurea hard segments act as physical crosslinks and particulate filler in the soft rubbery domains increasing the modulus and improving toughness and creep resistance. The transition behavior of the hard segments depends on their chemical structure. We found that hard segments made from aromatic or cyclic monomers produced stiff, high modulus adhesives while aliphatic monomers produced more rubbery adhesives.

Experimental

Compositions of Halthane adhesives are given in Tables I and II. Information on polymerization procedures is described elsewhere (6).

The dynamic shear storage modulus (G') and loss modulus (G'') were measured from -150° to 50°C using the forced torsion fixture on a Rheometric Mechanical Spectrometer (RMS)*. When the storage modulus dropped below 10^6 Pa, this fixture became insensitive. For moduli less than 10^7 Pa, the parallel plate fixture with serrated disks was used. The parallel plate fixture was used to extend the dynamic mechanical measurements to high temperatures. Degradation above about 250°C dictated this temperature as an upper limit for RMS measurements. Further discussion of equations and use of these fixtures are given elsewhere (7,8).

Results

This section is subdivided into two parts based on the two types of LLNL Halthane adhesives. The basic distinction between these adhesives is the modulus of the rubbery plateau. Halthane 73-series adhesives are tough, rubbery polyurethanes with a modulus of about 10^6 Pa at room temperature. On the other hand, Halthanes 87-1, 87-2, and 88-2 are stiff, almost glassy adhesives with a modulus of about 10^8 Pa at room temperature.

Halthane 73-Series Adhesive

Soft Segment Behavior. The soft segments of all the 73-series Halthanes consist mainly of a low molecular weight

*Reference to a company or product name does not imply approval or recommendation of the product by the University of California or the U.S. Department of Energy to the exclusion of others that may be suitable.

Table I. 73-series prepolymer and curing agent formulations.

Component	Curing Agents			
	14	15	18	19
Polymeg 1000	90	90	85	85
1,4-butanediol	10	10	10	10
Quadrol	-	-	5	5
FAA	-	0.0156	-	0.0107
	Prepolymer			
Polymeg 1000	47.6	47.6	47.6	47.6
Polymeg 2000	7.4	7.4	7.4	7.4
MDI	45.0	45.0	45.0	45.0
Prepolymer: Curing Agent	62/38	62/38	65/35	65/35

Table II. Prepolymer and curing agent formulations for polyurea hard segment adhesives.

Component	Curing Agents		
	87-1	87-2	88-2
Tonox 60/40	100	-	-
XU-205	-	100	100
	Prepolymer		
Polymeg 2000	77.6	77.6	74.0
HMDI	22.4	22.4	26.0
Prepolymer: Curing agent	93/7	92/8	88/12

polyether Polymeg 1000 extended by a difunctional isocyanate, MDI. Three low temperature transition maxima are found in the loss modulus (G'') of the 73-series Halthanes (see Fig. 1). Two low temperature secondary relaxations below the glass transition of the soft segment are arbitrarily labeled T_β (-100°C) and T_γ (-155°C). These relaxations are probably associated with molecular motions in the urethane (9) and polyether (10) components of the soft segment, respectively. The glass transition of the soft segment occurs at about -50°C and is responsible for the drop in the storage modulus G' by two orders of magnitude.

The soft segment transitions of 73-15, 73-18, and 73-19 are very similar to those shown for 73-14 in Fig. 1. Table III lists these transitions for each adhesive. The presence of tetrafunctional alcohols in the 73-18 and 73-19 polymers raises the soft segment glass transition temperature of these adhesives slightly as compared to 73-14 and 73-15.

The apparent activation energies (E_{ACT}) of the dynamic mechanical transitions can be calculated from the temperature at the maximum in the loss modulus ($T(G''_{\text{max}})$) as a function of frequency. A typical Arrhenius plot (see Fig. 2) of the apparent activation energy of the soft segment glass transition for 73 series polymers yields E_{ACT} values of approximately 75 ± 5 kcal/mole (314 kJ/mole) over a frequency range of 2 decades.

Hard Segment Behavior. The hard segment transitions of the 73-series Halthane adhesive are very complex. Hard segments containing the tetrafunctional chain extender, quadrol (73-18 and 73-19), show strikingly different dynamic mechanical behavior compared to hard segments of difunctional butanediol (73-14 and 73-15). Because of the low concentration of hard segments, their transitions are difficult to identify. The transition behavior is also complicated by a small amount of crystallinity shown as a melting endotherm in the DSC traces in Fig. 3. Poorly crystallized paracrystalline (11) urethane segments exhibit broad, weak melting endotherms, which occur at different temperatures depending on the thermal history of the sample (12).

The glass transition of the hard segments is presumed to be between 50° and 80°C based on the DSC data. It is followed by a melting endotherm beginning at about 80°C and ending at about 120°C . The exotherm is smaller in the crosslinked hard segments (73-18 and 73-19) than in the linear hard segments.

The dynamic mechanical relaxations in the high temperature region are very weak and the glass transition was indistinguishable from the melting point (Fig. 4). However, the mechanical properties of polyurethanes with chemically crosslinked hard segments were quite different from uncrosslinked polyurethanes. In the linear adhesives (73-14 and 73-15), the rubbery plateau ends at the melting point of the

**American Chemical
Society Library**

1155 16th St. N. W.

Washington, D. C. 20036

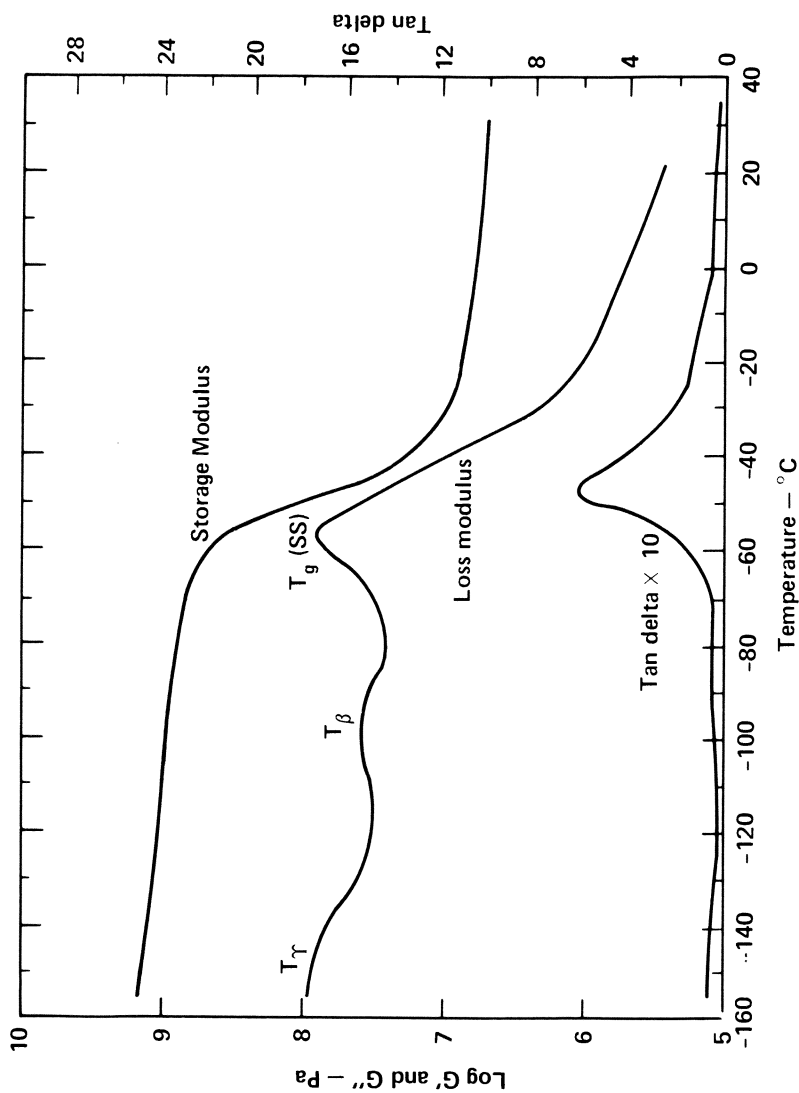


Figure 1. The low-temperature dynamic mechanical spectrum of Halthane 73-14 is typical of the 73-series polyurethane adhesives. Two secondary relaxations, T_{β} and T_{γ} , are shown as peaks in the loss modulus at -100°C and -150°C . The soft segment glass transition, $T_g(\text{SS})$, occurs at about -50°C . The frequency of oscillation was held constant during the measurement at 0.1 Hz.

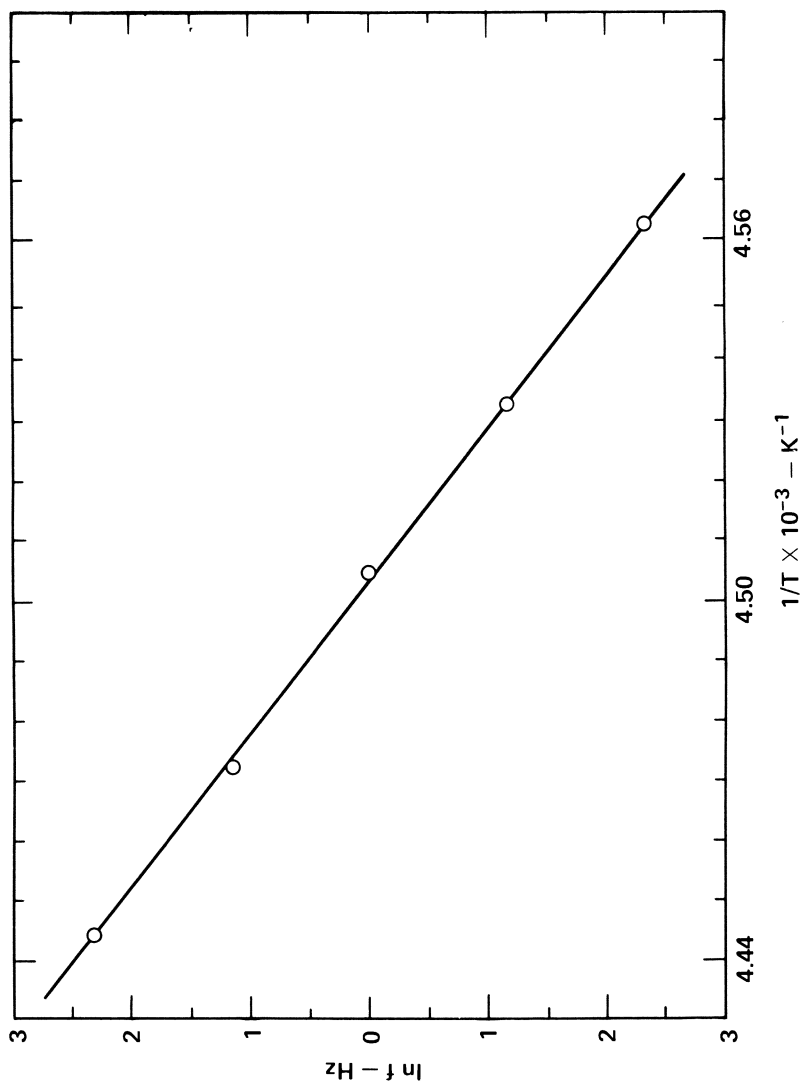


Figure 2. The apparent activation energy of the soft segment glass transition for Halthane 73-15 is determined from the slope of a plot of $\ln f$ vs. $1/T(G''_{max})$.

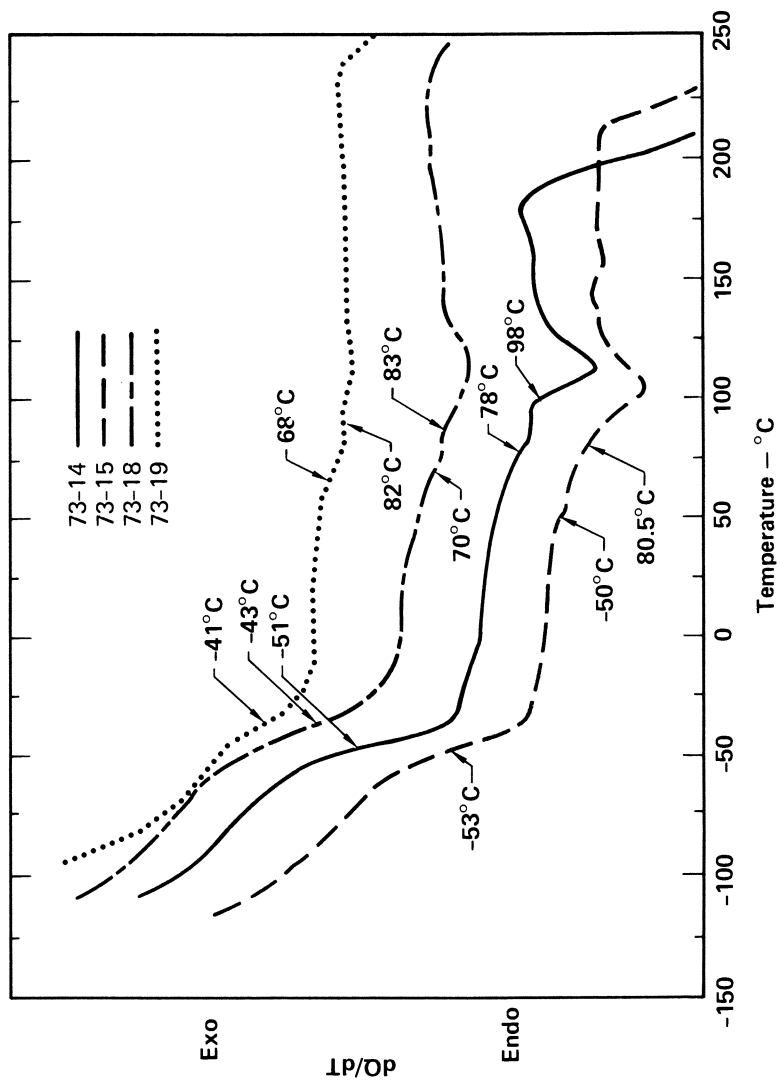


Figure 3. Differential scanning calorimeter traces of 73-series Halthanes show the soft and hard segment glass transitions and a melting endotherm. The temperatures of these transitions are consistent with the dynamic mechanical measurements.

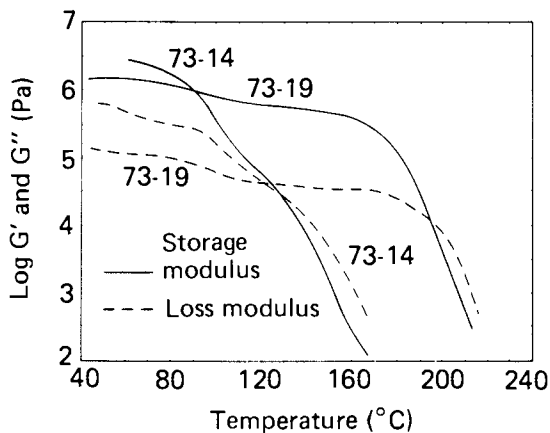


Figure 4. The high-temperature shear storage and loss moduli of Halthane 73-14 and 73-19 adhesives are controlled by the presence or absence of the cross-linking agent quadrol in the hard segments. In the linear urethane (73-14), viscous flow follows the melting of the hard segments, whereas in the cross-linked urethane (73-19), the modulus drops only when the polymer begins to degrade.

hard segment and the polymer begins to flow (about 90°C). This is shown by the drop in the storage modulus (G') above this temperature (Fig. 4). The shoulder on the loss and storage modulus of 73-14 at about 120°C is probably the final melting out of the hard segment crystals. In contrast, the 73-19 adhesive remains rubbery and will not flow below 200°C. Above this temperature, these polymers begin to degrade. Clearly, the chemically crosslinked adhesive is superior to the uncrosslinked adhesive, because it retains its integrity above the melting point of the hard segment. The melting of the hard segments causes only a slight change in storage modulus and the adhesive does not flow.

Table III. Transition temperatures of 73-series Halthanes.^a

Transition ^b	73-14	73-15	73-18	73-19
T_{γ}	-155	-160	-160	-160
T_{β}	-100	-100	- 99	-100
E_{ACT} (kJ/mole)			57.3	62.3
$T_g(SS)$	- 56.7	- 53.8	- 49.2	- 49.4
E_{ACT} (kJ/mole)	339	323	298	195
$T_g(SS)^c$	- 51	- 53	- 43	- 41
$T_m(HS)^d$	92	81	85	85
$T_g(HS)^c$	78	50	70	68
$T_m(HS)^c$	98	80	83	82

^a Dynamic mechanical transition temperatures were measured at the maximum in the loss modulus at 0.1 Hz.

^b Temperatures in °C.

^c Differential scanning calorimeter measurements from Fig. 3.

^d This transition shifts from sample to sample characteristic of urethane hard segment multiple melting behavior.

The addition of tetrafunctional quadrol has two effects on the mechanical properties. (1) It chemically crosslinks the polymer, extending the rubbery plateau beyond the melting point of the hard segments. (2) It weakens the load bearing capability of the hard segments causing the rubbery modulus of crosslinked systems to be lower than the linear materials at temperatures below the melting transition of the hard segments. That is to say, the crosslinked adhesives (73-18 and 73-19) have a lower modulus (10^6 Pa as compared to 10^7 Pa) over a wider temperature range (-50° to 200°C as compared to -50° to 100°C) than the uncrosslinked 73-14 and 73-15 adhesives.

Polymer degradation, as measured by TGA, begins at about 250°C in air for all the 73-series adhesives (see Fig. 5). This is somewhat higher than the degradation indicated by the decrease in storage modulus; this is because the initial stages of degradation involve chain scission, which reduces the modulus, whereas at higher temperatures, reversion and pyrolysis produce gaseous degradation products and therefore, weight loss.

Halthane 87- and 88-Series Adhesives

Soft Segment Behavior. The soft segment storage and loss moduli of 87-1, 87-2, and 88-2 Halthane polyurethanes (Fig. 6) are very similar to the dynamic mechanical moduli of poly(tetramethylene glycol) (10). From the loss modulus peaks a low temperature secondary relaxation is found at about -150°C and the soft segment glass transition is -70°C . From the storage modulus, the relaxation strength of the soft segment (the difference between the storage modulus of the glass and the rubber) is much less than the 73-series polymers. This means that 87 and 88 series adhesives are stiffer or harder than the 73-series adhesives. DSC soft segment glass transition temperatures for 87- and 88-series adhesives (Fig. 7) are slightly higher than dynamic mechanical transition temperatures probably because of the higher heating rates used in the DSC measurements.

Hard Segment Behavior. The high temperature dynamic mechanical behavior of Halthane 88-2 shows some apparent post curing above 90°C (Fig. 8). The aromatic polyurea hard segments have glass transitions at about 180°C (14). If these polymers are cured at room temperature, the hard segments do not polymerize completely. As the temperature increases, further curing occurs causing the storage and loss moduli to rise. This behavior is also shown in the DSC curves (Fig. 7). Since these polyurea hard segments are less flexible, they are more effective in bearing the stress than the MDI-butanediol hard segments. Therefore, the modulus of these adhesives is about two orders of magnitude larger than the 73-series Halthanes

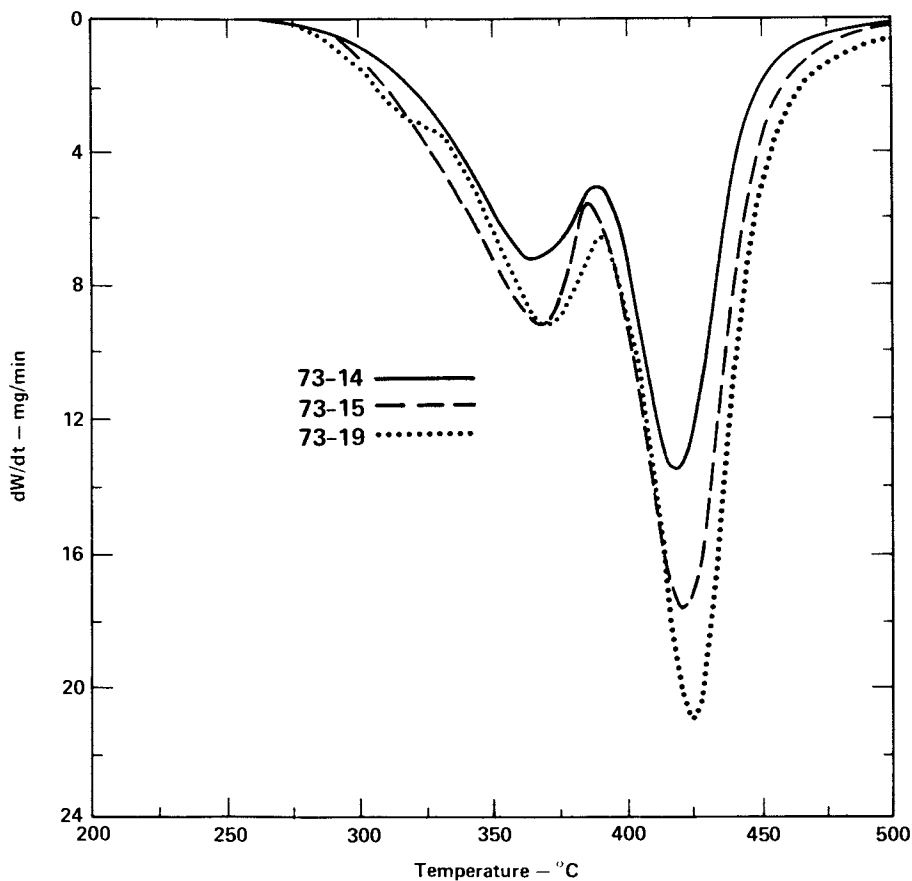


Figure 5. Thermogravimetric analysis curves of 73-series Halthanes show bimodal pyrolysis behavior starting at about 250°C. The rate of change in weight of the adhesive with time, dW/dt is plotted against temperature for a programmed heating rate of 12°C/min.

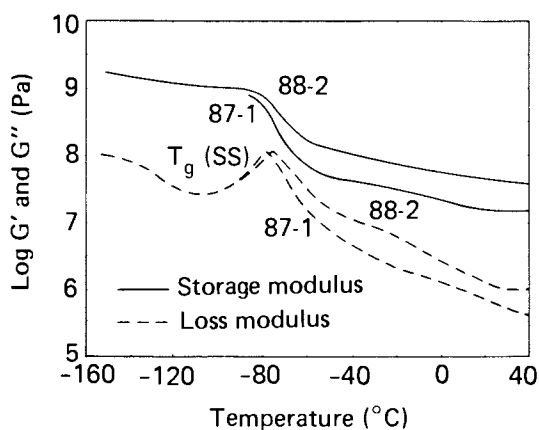


Figure 6. The low-temperature storage moduli of 87- and 88-series Halthanes show a smaller relaxation strength than 73-series Halthanes because of the aromatic hard segments' stiffness.

Higher concentrations of hard segments are responsible for the higher modulus of Halthane 88-2 above the soft segment glass transition, $T_g(SS)$, at -80°C . The low-temperature loss moduli of 87- and 88-series Halthanes show the glass transition of the soft segments and a secondary relaxation at about -150°C . The frequency of oscillation was held constant during the measurements at 0.1 Hz.

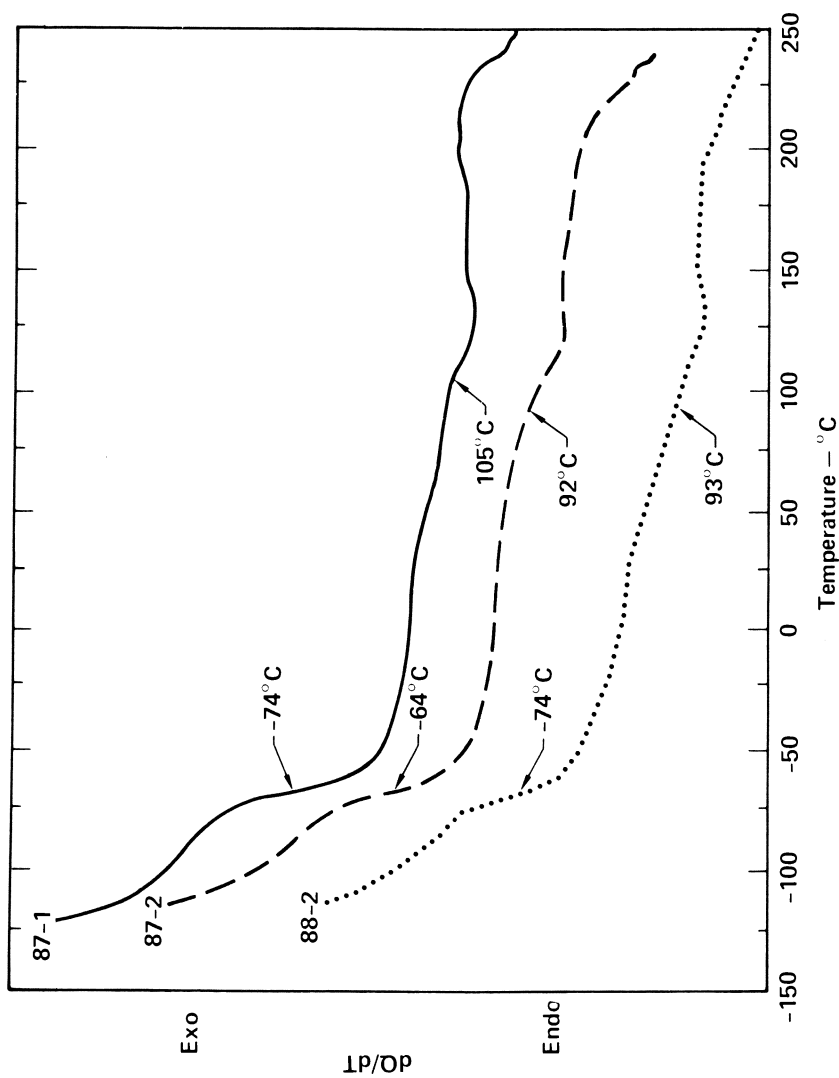


Figure 7. Differential scanning calorimeter traces of 87- and 88-series Halthanes show the soft segment glass transition and a curing endotherm at about -70°C and 100°C , respectively.

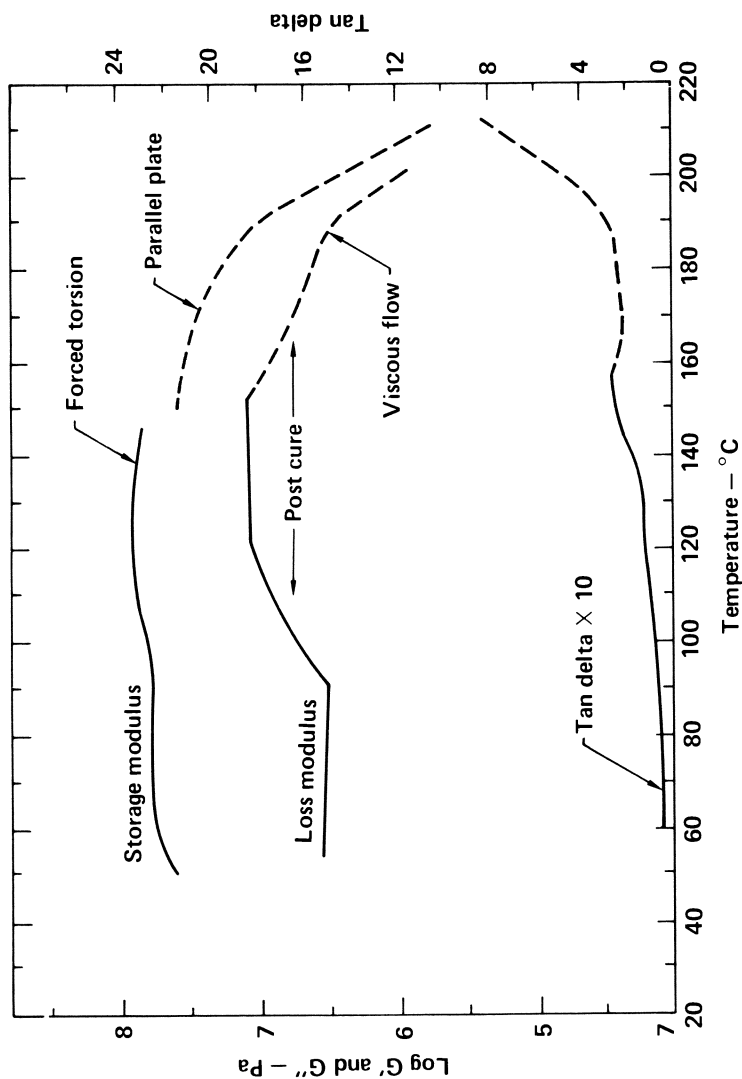


Figure 8. The high-temperature dynamic mechanical spectrum of Halthane 88-2 shows that some further curing is occurring above 100°C because both storage and loss modulus increase over a broad range of temperatures.

The onset of viscous flow above 200°C indicates that the hard segment glass transition temperature has been exceeded. Solid line data were obtained using the RMS forced-torsion fixture and dashed line data using the parallel-plate fixture.

(10^8 Pa as compared to 10^6 Pa) over the temperature range between hard and soft segment glass transitions. Table IV lists the transition temperatures for 87- and 88-series adhesives.

As in the case of 73-series adhesives, degradation of 87 and 88-series polyurethanes was bimodal (Fig. 9). These adhesives were somewhat more stable than the 73-series (compare Fig. 6 with Fig. 9). Volatilization began at about 250°C. Assuming that the hard segments degrade first, this implies that the polyurea hard segments of 87- and 88-series polymers have better thermal stability than the polyurethane hard segments of the 73-series adhesives.

Table IV. Transition temperatures of 87 & 88-series Halthanes.^a

Transition ^b	87-1	87-2	88-2
T_γ	-150	-150	-150
T_g (SS)	- 79	- 77	- 76
E_{ACT} (kJ/mole)	189	162	256
T^C (post cure)	105	92	93
T_g (HS)	185	196	188

^a Dynamic mechanical transitions were measured at the maximum in the loss modulus at 0.1 Hz.

^b Temperatures in °C.

^c Differential scanning calorimeter measurements from Fig. 7.

Discussion

Comparison of Hard and Soft Segments in the Different Adhesives. Each chemically distinct block in these segmented polyurethanes exhibits mechanical and thermal transitions characteristic of the homopolymer from which that block was made, unless the transitions are inhibited by the proximity of the second block. Five types of transitions are found in most homopolymers: secondary relaxations, a glass transition, melting transitions, viscous flow, and polymer degradation. Secondary relaxations are usually unaffected by other blocks because they involve small, localized molecular motions. Degradation is usually unaffected by other blocks. The other transitions (the glass transition, melting transition, and viscous flow) often depend on the structure of the second block in the copolymer.

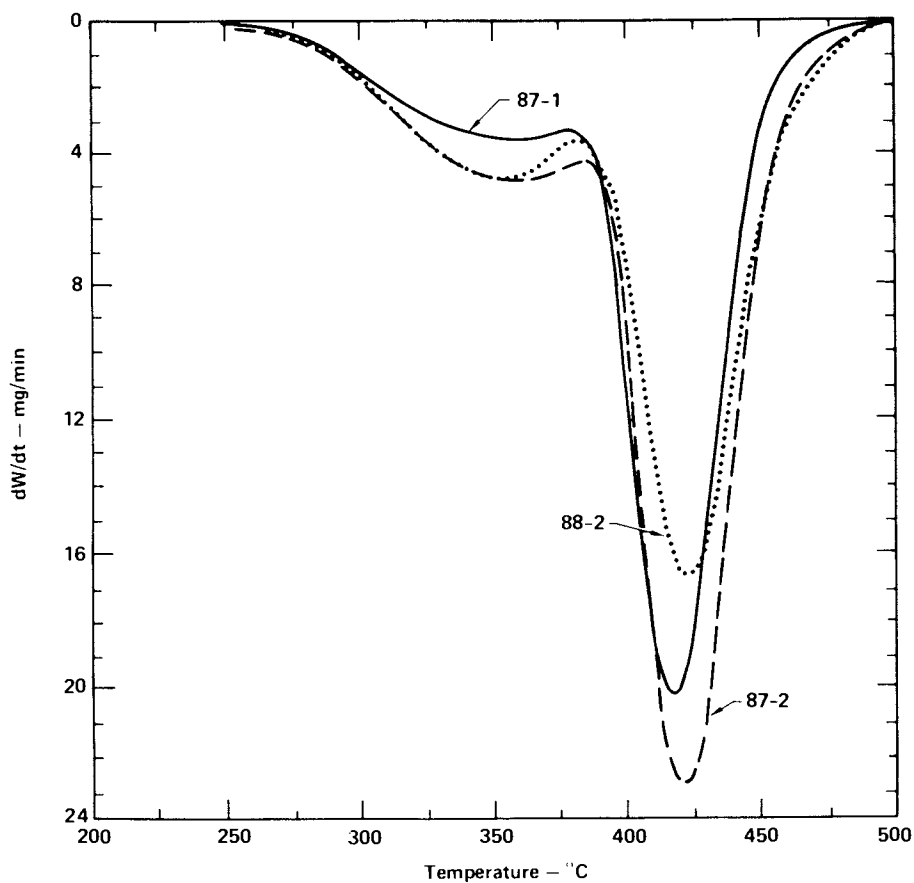


Figure 9. Thermogravimetric analysis curves of 87- and 88-series Halthanes show degradation behavior similar to 73-series Halthanes (Figure 6).

The glass transition of the low molecular weight soft segments in the Halthane 73-series adhesives is 20°C higher than the glass transition of the higher molecular weight soft segments in the 87 and 88 adhesives because of the constraints on the shorter poly(tetramethylene glycol) chain motion by the more frequent placement of urethane hard segments (15,16). The addition of tetrafunctional monomer to the hard segments of the 73-series Halthanes also increases the glass transition slightly, probably by disrupting the hard segment packing and increasing the interfacial zone between the two blocks.

There are several ways of changing the properties of segmented polyurethane copolymers. In this study, the chemical structure of the hard segments was changed to adjust the modulus of the adhesive. Further fine tuning is possible by varying the concentration of the different blocks. For example, the 87-series adhesives have a lower modulus than the 88-series adhesives because their hard segment concentration is lower. Studies of concentration effects (16) have shown that much wider variation of modulus is possible than was achieved here.

Conclusions

The chemical structure of the hard and soft segments, the concentrations of each block, and the presence of tetrafunctional crosslinker determined the dynamic mechanical and thermal properties of the three types of polyurethane adhesives, 73-, 87-, and 88-series Halthanes studied. Aromatic-aliphatic MDI- butanediol urethane hard segments produce lower modulus (10^6 Pa) materials in the rubbery region than cyclic unsaturated-aromatic urea hard segments. Incorporation of chemical crosslinks in the hard segments extended the rubbery plateau beyond the hard segment transitions up to temperatures where the polymer begins to degrade. Concentration of hard and soft segments can also be used to control the modulus between the glass transition temperatures of the two blocks.

Acknowledgments

We would like to thank Barbara McKinley and Patricia Crawford for the thermal measurements and LeRoy Althouse for supplying the polymers. Discussions with George Hammon and John Kolb are also gratefully acknowledged.

Work performed under the auspices of the U.S. Department of Energy by Lawrence Livermore National Laboratory under contract No. W-7405-Eng-48.

This document was prepared as an account of work sponsored by an agency of the United States Government. Neither the United States Government nor the University of California nor any of their employees, makes any warranty, express or implied, or assumes any legal liability or responsibility for the accuracy, completeness, or usefulness of any information, apparatus, product, or process disclosed, or represents that its use would not infringe privately owned rights. Reference herein to any specific commercial products, process, or service by trade name, trademark, manufacturer, or otherwise, does not necessarily constitute or imply its endorsement, recommendation, or favoring by the United States Government or the University of California. The views and opinions of authors expressed herein do not necessarily state or reflect those of the United States Government thereof, and shall not be used for advertising or product endorsement purposes.

Literature Cited

1. Morton, M., J. Polym. Sci., Polym., Symposium, 1977, 60, 1. Encyclopedia of Polymer Science and Technol., 1971, 15, 508.
2. Dickie, R. A., in "Polymer Blends" (D. R. Paul and S. Newman, eds.), Academic Press: New York (1978) pp. 353-392.
3. Estes, G. M., Cooper S. L., and Tobolsky, A. V., J. Macromol. Sci., Rev. Macromol. Chem., 1970, C4, 167.
4. Meier, D. J., J. Polym. Sci., Pt. C., 1969, 26, 81.
5. Krause, S., Macromol., 1970, 3, 84.
6. Hammon H. G., and Althouse, L. P., Lawrence Livermore Laboratory, Rept. UCID-17348, 1977.
7. Rheometrics Mechanical Spectrometer Operations Manual, Rheometrics, Inc., 1974.
8. McCrum, N. G., Read, B. E., and Williams, G., "Anelastic and Dielectric Effects in Polymeric Solids," Wiley: New York, 1967.
9. Huk D. S., and Cooper, S. L., Polym. Eng. Sci., 1971, 11, 369.
10. Wetton, R. E., and Allen, G., Polym., 1966, 7, 331.
11. Bonart, R., J. Macromol. Sci. Phys., 1968, B2, 115. Bonart, R., Morbitzer, L., and Hantze, G., J. Macromol. Sci. Phys., 1969, B3, 337.

12. Seymour, R. W., and Cooper, S. L., Macromol., 1973, 6, 48.
13. Lipatov, Yu. S., Privalko, V. P., Kercha, Yu. Yu., Krafchik, S. S., and Kuz'mina, V. A., Kolloid Z. Z. Polym., 1976, 254, 41.
14. Work, J. L., Macromol., 1976, 9, 759.
15. Illinger, J. L., Schneider, N. S., and Karasz, F. E., Polym. Eng. Sci., 1972, 12, 25.
16. Minoura, Y., Yamashita, S., Okamoto, H., Matsuo, T., Izawa, M., Kohmoto, S., J. Appl. Polym. Sci., 1978, 22, 1817.

RECEIVED April 30, 1981.

Phase Mixing in Urethane Polymers

ROBERT J. LOCKWOOD and LOUIS M. ALBERINO

Donald S. Gilmore Research Laboratories, The Upjohn Company,
North Haven, CT 06473

It has become well established⁽¹⁻⁸⁾ that urethane polymers are two-phase segmented block copolymers. The blocks consist of hard segments formed from the isocyanate and the short chain diol and soft segments formed from the isocyanate and long chain polyol. The interconnection between these two phases and the degree of phase separation are of major importance in determining the final polymer properties.^(9-14,16,17) If a polymer system consisted of compatible segments which were not phase separated then properties such as glass transition are considerably different from the case where the segments are incompatible and, hence, phase separated.

In this research, the concept of compatible and incompatible hard and soft segments was investigated by first looking at physical mixtures of model amorphous hard segments and model soft segments. The physical blends then were analyzed by DSC and the glass transitions were measured. DSC has been demonstrated to be a very useful tool for studying polymer morphology.⁽¹⁵⁾ If the mixture of the amorphous hard and soft segments was compatible then one glass transition should result. However, if the mixture was incompatible, then the individual distinct T_g's would be observed. These ideas were further extended to actual polymers which were produced from prepolymers and various extender/polyol combinations.

Experimental

The extenders used were urethane grade dipropylene glycol (DPG) obtained from Dow Chemical, and urethane grade 1,4 butanediol (1,4-BDO) obtained from GAF Corporation. The polyols used were Poly Gtm 53-56 (Olin Chemical) a 2000 molecular weight polyoxyethylene-oxypropylene diol containing 11% EO (ethylene oxide), Poly Gtm 55-56 (Olin Chemical) a 2000 M.W. polyoxyethylene-oxypropylene diol containing 45% EO, and Niox PPG-2025tm

0097-6156/81/0172-0363\$05.00/0
© 1981 American Chemical Society

(Union Carbide) a 2000 M.W. polyoxypropylene glycol containing no EO. The isocyanate used was Upjohn 125M, 4,4' diisocyanato diphenyl methane (MDI). Polyols and extenders were dried by degassing under vacuum.

Model Preparation

In order to provide solubility, the MDI-DPG model oligomeric hard segment was prepared at a hydroxyl to isocyanate equivalent ratio of 1.0 to 0.9. The model soft segments were prepared at 1 to 1 equivalent ratios. Both hard and soft segments were prepared by mixing the two components together at 50°C with (0.01%) dibutyl tin dilaurate catalyst in plastic cups. The model hard and soft segment mixtures were then dissolved in reagent grade N,N-dimethyl formamide (stored over sieves - Fisher) and cast into glass crystallizing dish covers. The solvent was removed by oven drying at 80°C followed by vacuum drying at 110°C for two hours. TGA showed the resulting material to be solvent free. DSC scans on these materials were then run on a DuPont 990 at 10°C/min. under nitrogen from -100°C to +250°C.

Polymer Preparation

Preparation of the polymers was carried out by a two step method. First, MDI prepolymers were prepared in a 5 liter round bottom flask equipped with a stirrer, thermometer, addition funnel, and nitrogen inlet. The dried polyols were added dropwise to MDI at 75°C and the reaction temperature was maintained at 85°C. The mole ratios of MDI to polyol listed in Table II gave prepolymers containing 18.67% free NCO groups by weight or an isocyanate equivalent weight of 225. In the case of prepolymers 2 and 4, the DPG was added first and then the 2000 molecular weight polyol was added.

In the second step, the urethane polymers were prepared from each of the four prepolymers by mixing with a stoichiometric amount of 1,4-butanediol (1,4-BDO). To a plastic cup was added 125 grams of prepolymer, 25 grams of 1,4-BDO, and 0.1 cc of UL-1, a dibutyl tin mercaptide from Witco Chemical Co. These room temperature components were mixed for 10 seconds using a high shear mixing blade at 2400 rpm. The prepared polymers were allowed to cure at room temperature for at least one week and then DSC's and TMA's were run.

DSC's were run on a DuPont 990 at 10°C/min. with a nitrogen purge. One sample series was run over the range -120°C to 0°C and another sample series was run from 20°C to 250°C.

TMA's were run over a temperature range of -20°C to 210°C on a Perkin Elmer Thermomechanical Analyzer TMS-1. They were run with a 40 mil diameter penetration probe loaded with 200 grams to give a pressure of 394 psi. The program rate was 10°C/min. under a helium atmosphere and the Y-axis sensitivity was 10⁻³ inches/inch of chart paper.

Results and Discussion

Model hard segments of MDI-DPG at a 0.9/1.0 mole ratio gave a T_g of 85°C which was used in the physical blending study, while at a 1.0/1.0 mole ratio gave a T_g of 110°C. No melting endotherms were observed so these hard segments are described as glassy-amorphous.

Model soft segments of MDI/PPG-2025tm, MDI/Poly G-53-56tm, and MDI/Poly G-55-56tm gave T_g's of -50°C, -52°C, and -56°C, respectively (see Table I).

As such, these amorphous (glassy) hard segments and amorphous (rubbery) soft segments follow classical rules of mixing. For example, the Fox equation ⁽¹⁸⁾ for the T_g of a compatible blend is given by (1),

$$(1) \frac{1}{Tg_M} = \frac{W_A}{Tg_A} + \frac{W_B}{Tg_B}$$

where T_{gM} = glass transition of compatible mixtures (°K)

T_{gA} = glass transition of Polymer A (°K)

W_A = weight fraction of Polymer A.

Thus, if two polymers are compatible - SINGLE PHASE - there will be one T_g given by equation (1). If two polymers are incompatible - TWO PHASES - there will be two T_g's - those of the individual polymers. These concepts are demonstrated in Figure 1 which shows blends of the hard segment (MDI-DPG) in soft segments (MDI/Poly G 53-56tm and MDI/Poly G 55-56tm). Figure 1 shows that the hard segment MDI-DPG is essentially completely compatible in the soft segment MDI/Poly G-55-56tm, a 45% EO polyol and essentially completely incompatible in the soft segment MDI/Poly G-53-56tm, an 11% EO polyol. The theoretical line derived from Equation 1 is in good agreement with the compatible blend.

An example of a crystalline hard segment is MDI/1,4-BDO which has a T_m or melt point by DSC. Table 1 shows that MDI/1,4-BDO has a small T_g at 110°C, a T_c or crystallization temperature at 182°C and a series of three successive crystallite melting points at 202°C, 220°C, and 236°C; the upper temperature being the mp of the pure equilibrium crystal.

The same compatibility/incompatibility rules as discussed for amorphous hard segments and soft segments do not apply with crystalline hard segments. Extenders which form crystalline hard segments with MDI aggregate into bundles or form a hard segment domain within the amorphous soft segment phase (3). Thus, crystalline hard segment based polymer systems will generally have separate hard and soft segment glass transitions.

TABLE I
DSC ANALYSIS OF HARD & SOFT
URETHANE SEGMENTS

Hard Segments	Mole Ratio	T _g °C	T _c °C	T _m °C
MDI - DPG	0.9/1.0	85	-	-
MDI - DPG	1.0/1.0	110	-	-
MDI - 1,4 BDO	1.0/1.0	110	182	202
				220
				236

Soft Segments	Mole Ratio	T _g °C
MDI - PPG-2025®	1/1	-50
MDI - Poly G-53-56®	1/1	-52
MDI - Poly G-55-56®	1/1	-56

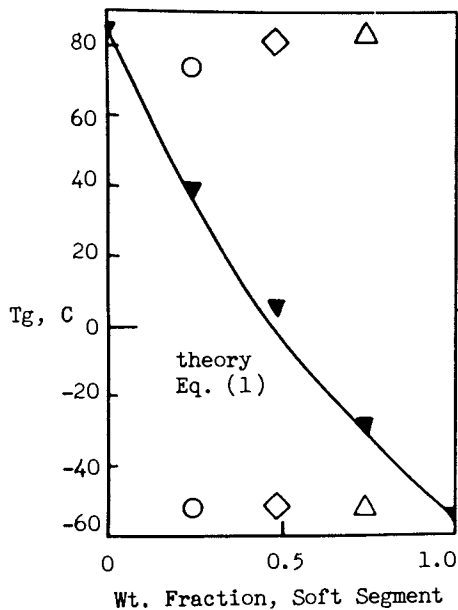


Figure 1. DSC results of physical blending of hard and soft segments. Key: ▼, MDI-DPG/MDI-Poly G (55-56 [®]); ○, ◇, and △, MDI-DPG/MDI-Poly G (53-56 [®]).

Table II lists the thermal transitions by DSC and TMA of four different urethane polymer systems based on the preceding hard and soft segment combinations. While PPG-2025tm was used in place of Poly G-53-56tm, it should behave the same since it has no compatibilizing EO. Figures 2 and 4 exhibit the respective DSC and TMA curves of these polymers:

Polymer 1 based on MDI/PPG-2025tm/1,4-BDO shows an incompatible two phase polymer with a well defined soft segment Tg at -40°C and sharp melting endotherms at 203°C, 222°C, and 238°C characteristic of a pure MDI/1,4-BDO hard segment. The TMA curve has an initial softening at 41°C, a second softening at 130°C and a major softening at 165°C. This two step softening might be due to the influence of the well defined soft segment domains in the hard segment domain.

Polymer 2 based on MDI/DPG/PPG-2025tm/1,4-BDO is also two phase; however, the crystalline hard segment phase has been transformed to a glassy-amorphous phase as shown by the Tg at 105°C and the soft segment glass transition is not as well defined as in Polymer 1. The major softening observed at 99°C by TMA very closely corresponds to the 105°C Tg measured by DSC.

Polymer 3 based on MDI/Poly G 55-56tm/1,4-BDO exhibits an incompatible two phase polymer consisting of an amorphous soft segment Tg at -38°C and crystalline hard segment Tm's at 222°C and 241°C. TMA shows a high 160°C onset softening temperature and a major softening at 205°C, which is very close to the melt temperature of the hard segment.

Polymer 4 based on MDI/DPG/Poly G-55-56tm/1,4-BDO can be described as a basically one-phase compatible polymer system. The soft segment Tg is almost non-existent and there is no definable Tm. Extreme intermixing between the hard and soft segments has taken place, resulting in an intermediate glassy amorphous Tg by DSC of about 81°C. The TMA curve shows a major softening at about 74°C, which once again is in close agreement with the Tg by DSC.

Conclusions

Physical blending of model homopolymers can be used to predict the compatibilities of urethane hard and soft segments and agrees well with actual reaction blending. As shown by physical blending studies MDI-DPG is compatible with a 2000 M.W.-45% EO containing polypropylene glycol based polyol, and incompatible with a 2000 M.W. - 11% EO containing polypropylene glycol based polyol. When urethane polymers based on the above or similar polyols had 25% of the hard segment based on MDI-DPG

TABLE II
DSC'S & TMA'S OF URETHANE POLYMERS

225I.E. PREPOLYMERS	Extender	Weight Fraction Hard Segment	DSC Results, °C		TMA Results, °C			
			Tg1	Tg2	Tm	S1	S2	S3*
1)	MDI/PPG-2025® (11.5/1/.....10.5)Δ	0.63	-40	-	203 222 238	41	130	165
2)	MDI/DPG/PPG-2025® (35/7.7/1/.....26.3)Δ	0.84	-40	105	-	80	-	99
3)	MDI/Poly G-55-56® (12.3/1/.....11.3)Δ	0.63	-38	-	222 241	160	-	205
4)	MDI/DPG/Poly G-55-56® (34.8/7.7/1/.....26.1)Δ	0.84	-	81	-	52	-	74

Δ Mole Ratio

* S₁ Onset Softening S₂ Intermediate Softening S₃ Major Softening

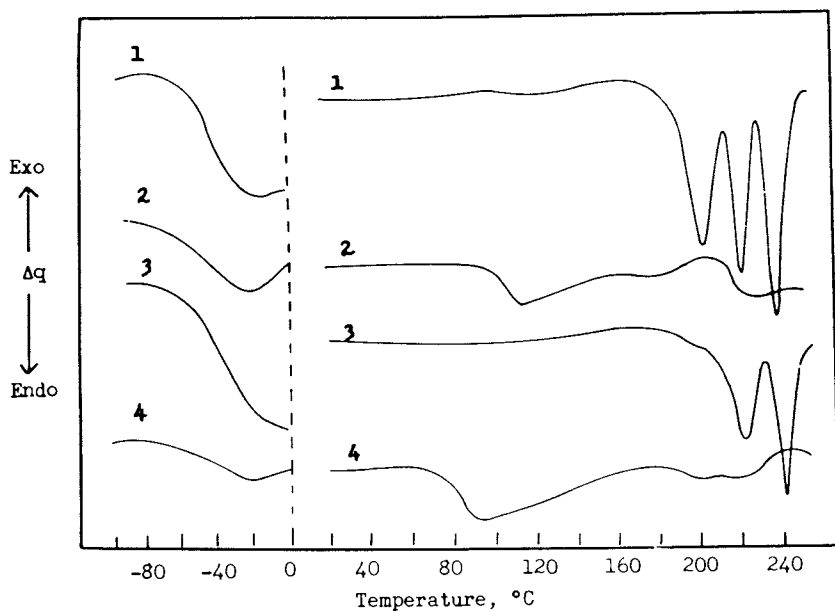


Figure 2. DSC's of model polymers.

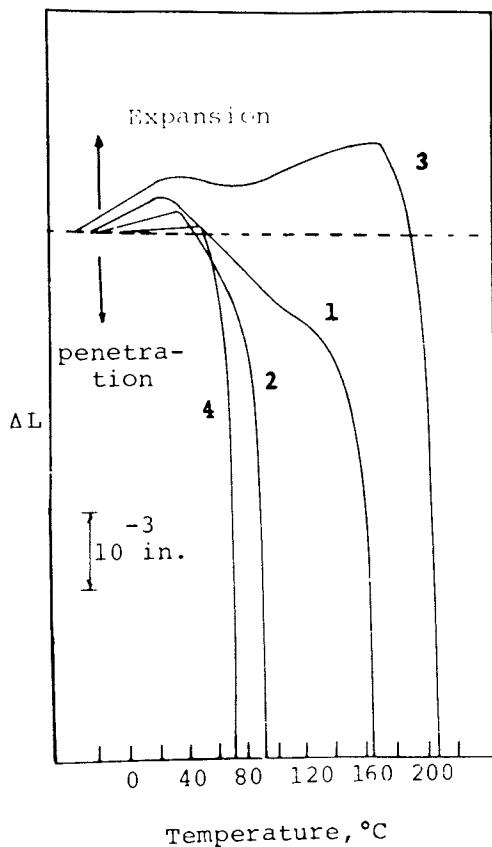


Figure 3. TMA's of model polymers.

and 75% of the hard segment based on MDI/1,4-BDO, the compatibilizing influence of the MDI-DPG predominated. This level of MDI-DPG was found to destroy the crystallinity of a normally crystalline 1,4-butanediol hard segment, making the total hard segment glassy-amorphous and produced a basically one-phase compatible polymer when a high EO (45%) containing polyol is used. Thus, the level of MDI-DPG in a urethane polymer can be critical to the polymer's performance and final properties.

Urethane polymer morphology can be quickly characterized by means of DSC and TMA analyses. These thermal analyses are valuable tools in determining the interrelationship of the many formulation variables of urethane polymer systems: polyol type and molecular weight, hard segment type and concentration, and various prepolymer compositions.

Literature Cited

1. Clough, S. B., and Schneider, N. S., J. Macromol. Sci., 1968, B2, 553.
2. Clough, S. B., Schneider, N. S. and King, A. O., J. Macromol. Sci.-Phys., 1968, B2(4), 641.
3. Estes, G. M., Cooper, S. L. and Tobolsky, A. V., J. Macromol. Sci.-Rev. Macromol. Chem., 1970, C4(2), 313.
4. Samuels, S. L. and Wilkes, G. L., J. Polym. Sci., 1973, 43, 149.
5. Seymour, R. W., Allegrezza, A. E., Jr., and Cooper, S. L., Macromolecules, 1973, 6(6), 896.
6. Chang, Y. P., and Wilkes, G. L., J. Polym. Sci., 1975, 13, 455.
7. Blackwell, J. and Gardner, K. H., Polymer, 1979, 20, 13.
8. Bonart, R., Morbitzer, L., and Hentze, G., J. Macromol. Sci., Phys., 1969, 3(2), 337.
9. Harrell, L. L., Jr., Macromolecules, 1969, 2(6), 607.
10. Huh, D. S., and Cooper, S. L., Polym. Eng. and Sci., 1971, 11(5), 369.
11. Ng, H. N., Allegrezza, A. E., Seymour, R. W., and Cooper, S. L., Polymer, 1973, 14, 255.
12. Smith, T. L., J. Polym. Sci. - Phys., 1974, 12, 1825.
13. Zdrahala, R. J., Gerkin, R. M., Hager, S. L., and Critchfield, F. E., J. Appl. Polym. Sci., 1979, 24, 2041.
14. Seefried, C. G., Jr., Koleske, J. V., Critchfield, F. E., J. Appl. Polym. Sci., 1975, 19, 2493, 2503, 3185.
15. Seymour, R. W., and Cooper, S. L., Polymer Letters, 1971, 9, 689.
16. Samuels, S. L. and Wilkes, G. L., J. Polym. Sci., 1973, 11, 807.
17. Seymour, R. W., and Cooper, S. L., Macromolecules, 1973, 6, 48.
18. Fox, T. G., Bull. Amer. Phys. Soc., 1956, 2, 123.

RECEIVED April 30, 1981.

Characterization of Polyurethane Networks

B. ERSHAGHI, A. J. CHOMPF, and R. SALOVEY

Department of Chemical Engineering, University of Southern California,
Los Angeles, CA 90007

Linear polymers are usually characterized in solution. However, if enough crosslinking has occurred, such as in the vulcanization of elastomers, the polymer will swell but cannot dissolve in typical solvents. Then, it is impossible to derive molar mass (molecular weight) information from solution behavior. However, the average molar mass of the chains in the polymer network can be determined from swelling (1,2).

If a polymer network attains an equilibrium degree of swelling, one can relate the number of "effective" chains per unit volume (v^*) or the average molar mass between crosslinks (M_c) to the degree of swelling (q_1), if certain assumptions are made; namely, a constant polymer/solvent interaction parameter (χ) and a reference degree of swelling in the unperturbed state (q_0) equal to unity for polymerization in bulk. However, we have calculated that M_c derived from swelling measurements did not agree with values determined analytically by labelling crosslinks with C^{14} (3). Indeed, M_c derived from swelling was about ten times that derived analytically. The origin of this discrepancy is examined in this paper. Selected polyurethane networks are swelled over polymer solutions with varied solute concentration in order to determine the equilibrium degree of swelling as a function of solvent activity. From these data, M_c , χ and q_0 can be independently determined. In addition, swollen networks are subjected to stress relaxation in tension. The initial and equilibrium stress are related to M_c and q_0 .

Experimental Details

Materials Two commercial polypropylene glycols (polyols) of different functionality were used. The trifunctional polyol is Union Carbide NIAX 16-56, and the difunctional polyol is Union Carbide NIAX 2025. Each has an equivalent weight approximating 1.00 kg. The polyols were dried with bubbling dry nitrogen while

0097-6156/81/0172-0373\$05.00/0
© 1981 American Chemical Society

heating to 110°C. Solid MDI (4-4'-diphenylmethane diisocyanate) was supplied by the Upjohn Company. MDI was purified by vacuum distillation. Since MDI dimerizes on storage, samples were always freshly distilled before use. The catalyst was dibutyltin dilaurate from Witco Chemical. Dioxane solvent was obtained from Union Carbide, and polystyrene "standards" from Pressure Chemicals.

Network Synthesis (4) Solid MDI was weighed into a flask and an equivalent amount of polyol added. The mixture was heated to about 40°C to dissolve the MDI. The mixture was then cooled to room temperature and degassed for several minutes under vacuum in order to remove dissolved air. Catalyst was then added and the contents of the flask mixed under vacuum to ensure uniformity and then poured into a mold. All operations were carried out in a dry glove bag to minimize reaction with atmospheric water. The cross-linking process was also carried out in dioxane solution at 70% volume fraction of solids. Polyurethane networks with different crosslink densities were prepared by varying the ratio of difunctional and trifunctional polyols. All samples were extracted with dioxane to remove unreacted and uncrosslinked material before swelling.

Swelling A temperature controlled air bath, a balance and small modified weighing bottles were used to study swelling. Polymer network samples were suspended over polystyrene solutions. Vapor absorption was measured by gravimetry and by monitoring the weight of the bottles, correction could be made for changes in solute concentration.

Stress Relaxation Polyurethane networks were also polymerized in a mold with a cylindrical cavity. Uniform rings were cut from the cylinders and weighed. The cross sectional area was then derived from the sample diameter and polymer density and approximated 0.05 cm². Stress relaxation was measured at several strains between 10 and 43% with an Instron tensile tester. During stress relaxation, the samples were immersed in dioxane and swelled to equilibrium.

Theory The swelling behavior of polymer networks is described by several network parameters: χ_g , a polymer network-solvent interaction parameter; ν^* , the concentration of elastically effective network chains; and q_0 , a reference degree of swelling which is related to the unperturbed end-to-end distance of the polymer chains during network formation.

At an equilibrium degree of swelling, the chemical potentials of mixing and of elastic deformation of the network balance, so that:

$$(1) \quad \left(\frac{\partial \Delta G}{\partial N} \text{ mixing} \right) + \left(\frac{\partial \Delta G}{\partial N} \text{ elastic} \right) = 0$$

where, ΔG_{mixing} and $\Delta G_{\text{elastic}}$ are the Gibbs free energies due to mixing and elasticity, respectively, and N is the number of moles of solvent. Ordinarily, a single swelling test is combined with assumed values for χ_2 and q_0 to determine v^* or M_c , the molecular weight between crosslinks (2). Additional information can be derived by studying variations in the equilibrium degree of swelling as a function of solvent activity, a_1 . If μ_1 is the chemical potential of solvent, then

$$(2) \quad \mu_1 = \mu_1^0 + k T \ln a_1$$

and the swelling of a crosslinked network may be expressed as follows (5):

$$(3) \quad (\ln a_1 - \ln (1 - q_i^{-1})) q_i^2 = \chi_g - \bar{V}_1 B v^* q_i + \bar{V}_1 A v^* q_0^{-2/3} q_i^{5/3}$$

q_i is the degree of swelling, expressed as the swollen volume/dry volume, \bar{V}_1 is the molar volume of the solvent, A and B are arbitrary constants from the theory of rubber elasticity. Values for A and B have been suggested (6,7,8).

Another method of varying the equilibrium degree of swelling is to stretch the polymer during swelling. Then, the chemical potential of the solvent inside the gel will decrease so that the degree of swelling in the stretched state increases. For a swollen network, one can calculate the degree of swelling in the stretched state (q) from the initial (f_0) and equilibrium (f_∞) forces and the stretch ratio in the swollen state (Λ_x). If σ_d is the force per unit dry unstrained cross-sectional area, then

$$(4) \quad \sigma_d = A k T v^* q_0^{-2/3} q_i^{1/3} \left(\Lambda_x - \frac{q}{q_i \Lambda_x^2} \right)$$

since for a swollen network, the retractive force in stress relaxation is almost purely entropic. Then, $A v^* q_0^{-2/3}$ can be calculated and compared to values from swelling.

Since the interaction parameter (χ) in most polymer solutions is concentration dependent (10), we can write:

$$(5) \quad \chi_g = \chi_1 + \chi_2 q^{-2}$$

In order to evaluate χ , we can combine data from stress relaxation and swelling. From stress relaxation, the value of $A v^* q_0^{-2/3}$ can be calculated (equation 4) and substituted into equation 3. If we represent all of the quantities in equation 3 which are determined experimentally by D , then we can write:

$$(6) \quad D = \chi_1 + \chi_2 q^{-2} + \bar{V}_1 B v^* q_i$$

The values of χ_1 , χ_2 , and $\bar{V}_1 \text{BU}^*$ may then be obtained by linear programming.

Results and Discussion

A polyurethane gel network prepared with 80% diol and 20% triol showed the highest degree of swelling in dioxane among polyurethanes prepared from the bulk polymerization of different polyol mixtures. Compositions higher than 80% diol yielded soluble polymers. When an 80/20 polymerization was run in dioxane solution, the degree of swelling of the resultant network was increased. Dioxane solvent produced maximum swelling of the polyurethane networks when compared to various solvents. From swelling studies in a series of solvents, the solubility parameter (δ) of a polyurethane network prepared with 100% trifunctional polyol was estimated to equal 11.

The swelling of polyurethane networks was also conducted in dioxane vapor. Such experiments generally take a long time to reach equilibrium. The diffusion time was reduced by using thin (50 μ) samples. The variation of the degree of swelling with the volume fraction of polystyrene solute in dioxane is shown in Figure 1. The stress relaxation of swollen polyurethane networks is illustrated in Figure 2.

The Flory-Rehner equation (2,13) was used to interpret the swelling of the polyurethane networks in pure dioxane in order to calculate M_c , the molecular weight between crosslinks. Here, we set $q_0 = 1$ and χ , the network-solvent interaction parameter, constant and assumed equal to 0.35 (3). Networks with degrees of swelling (q_1) of 6.41, 11 and 21.1 yielded M_c values of 7,700, 23,000, and 76,500, respectively.

Values of M_c approximating 10^5 were derived from measurements of the sol fractions of these networks (11). Such results did not correlate with the degree of swelling and are believed to be inaccurate.

The swelling data in Figure 1 were analyzed by linear programming in order to determine values of M_c , q_0 , and χ , assuming that χ is constant for each network. Results for the three networks are shown in Table I. Values of q_0 are much larger and M_c much smaller than expected.

Stress relaxation calculations on the swollen networks (Figure 2) are summarized in Table II. The values of $AU^* q_0^{-2/3}$ are in fairly good agreement with those derived from swelling over polymer solutions (Table I). It is possible to determine M_c by setting $q_0 = 1$. Then, from stress relaxation, the networks with degrees of swelling 6.41, 11, and 21.1 gave M_c values of 14,000, 21,000, and 31,500, respectively.

An alternative and, perhaps, preferable treatment of these data involves the method described in the section on theory. In this case, the interaction parameter, χ , is assumed to be a simple function of concentration and stress relaxation and swell-

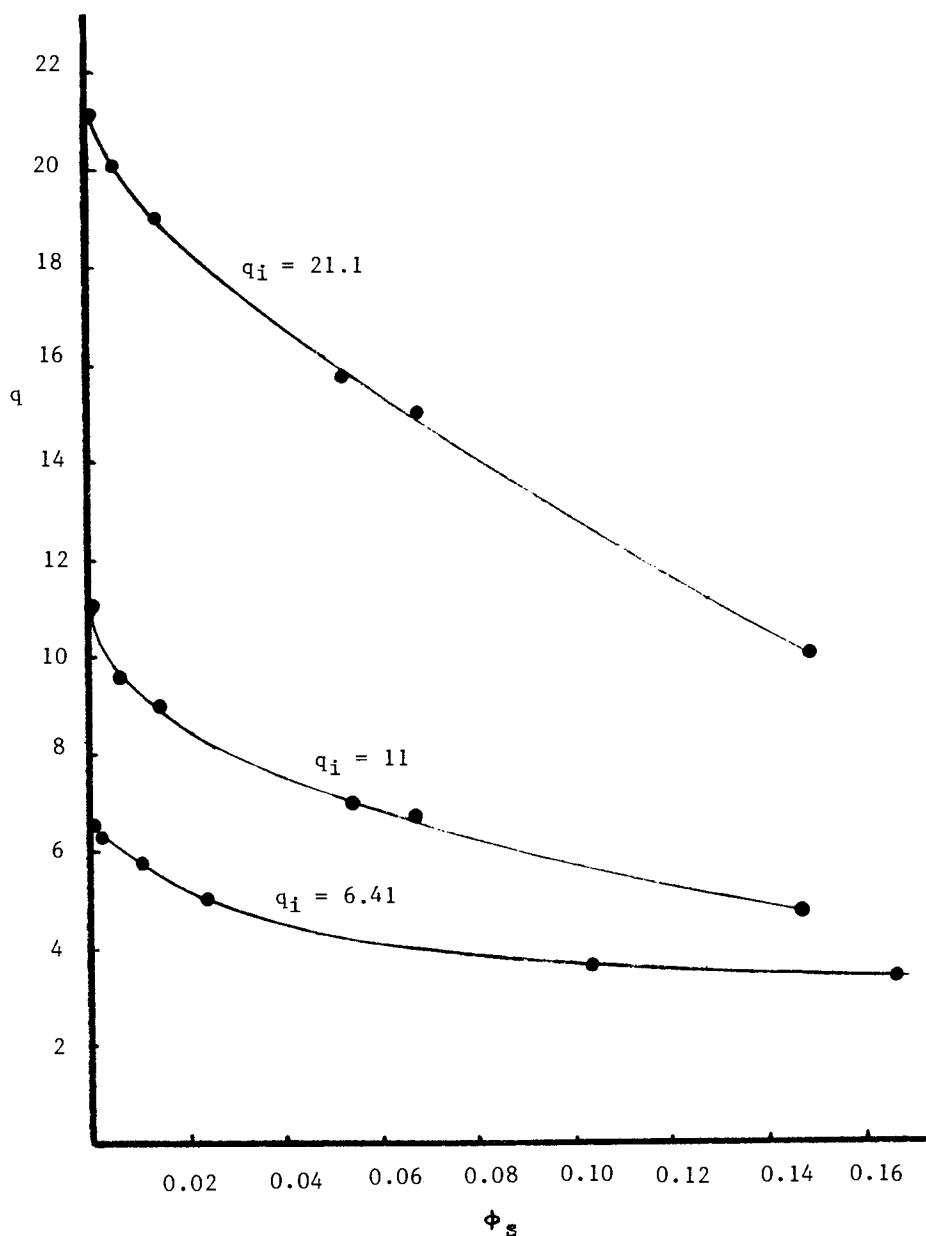


Figure 1. The degree of swelling (q) of polyurethane networks in dioxane vapor over polystyrene solutions of various volume fractions (Φ_s).

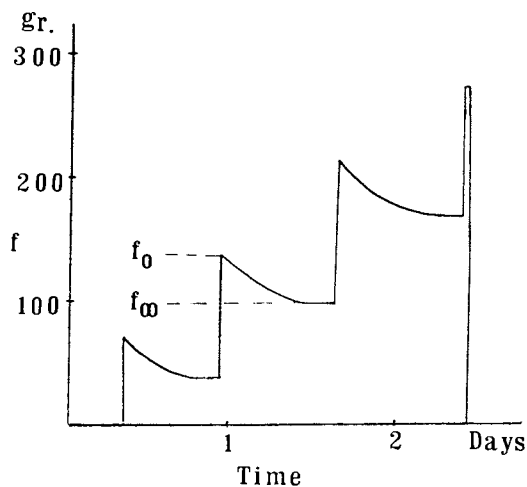


Figure 2. Stress relaxation of a swollen polyurethane network.

Table I

Swelling of Polyurethane Networks
over Polystyrene Solutions in Dioxane

q_i	χ	$AU^*q_0^{-2/3}$	q_0	M_c
6.41	0.720	7.92×10^{-5}	19.4	1800
11.1	0.642	5.717×10^{-5}	17.8	2600
21.1	0.436	4.810×10^{-5}	16.8	3260

A=B=1

Table II

Stress Relaxation of Swollen Polyurethane Networks

	Λ_x	f_o (gm)	f_∞ (gm)	q	σ_d (gm/cm ²)	$AU^* q_o^{-2/3}$
$q_i=6.41$	1.10	61	56	6.58	960	8.16×10^{-5}
	1.25	114	110	6.62	1886	6.85×10^{-5}
	1.32	154	147	6.79	2520	7.5×10^{-5}
$q_i=11.00$	1.065	50	41.5	11.38	415	4.85×10^{-5}
	1.24	150	144	11.41	1440	4.74×10^{-5}
	1.324	201	194	11.51	1940	4.78×10^{-5}
	1.432	272	263.6	11.65	2636	5.15×10^{-5}
$q_i=21.10$	1.10	31	26	22.22	542	3.35×10^{-5}
	1.14	40	35.5	22.24	739	3.19×10^{-5}
	1.21	62	57	22.41	1187	3.46×10^{-5}
	1.32	78	73	22.86	1570	3.08×10^{-5}

ling data are combined to yield values of M_c . Results of this treatment are tabulated in Table III. Apparently, by allowing q_0 to vary, very low values of M_c are derived.

Inordinately low M_c may result from an anomaly associated with polyurethane networks (12). The persistence of hydrogen bonding in the swollen state may lead to high apparent crosslink density and low values of M_c . In addition, it is possible that the Gaussian approximation implicit in all our treatments is inadequate for an extensively swollen network.

Conclusions

In the characterization of polymer networks by swelling, the average molar mass between crosslinks (M_c) is usually derived from the degree of swelling (q_i) (13). However, such values often do not agree with independent measurements (3). The swelling of polyurethane networks has been examined at varied solvent activity and during stress relaxation in tension in order to determine M_c . As expected, the degree of swelling decreased with solvent activity and small increases in the degree of swelling could be effected by the application of stress.

Alternative treatments of swelling and stress relaxation data gave varied results for M_c . For the least densely crosslinked network ($q_i = 21.1$), a simple application of the Flory-Rehner equation (13) to swelling in pure dioxane gave M_c equal to 76,500. Allowing the interaction parameter (χ), the reference degree of swelling in the unperturbed state (q_0) and M_c to vary, analyses of the swelling data at various dioxane activity using linear programming gave unreasonably low values of M_c . For example, $M_c = 3,260$ for the least densely crosslinked network. From stress relaxation of this swollen network, the corresponding value of M_c was calculated to be 31,500. Assuming χ to be concentration dependent, stress relaxation and swelling data were combined to calculate M_c . In this case, M_c was found to be equal to 10,400.

It is concluded that by allowing q_0 and M_c to vary independently, swelling studies at varied solvent activity do not yield reasonable values of M_c . Higher and more likely values of M_c result from either swelling studies or stress relaxation of swollen networks by constraining q_0 to unity.

Values of $AU^*q_0^{-2/3}$ calculated from stress relaxation of the swollen networks agreed fairly well with those derived from swelling of polyurethane networks. The anomalous behavior of polyurethanes has been reported (12). Swelling at different solvent activity and stress relaxation of swollen networks are valuable techniques for network characterization. Other networks such as crosslinked polystyrene will be examined by these methods. The role of the Gaussian approximation in rubber elasticity will be evaluated in calculating M_c for highly swollen networks.

Table III

Characteristics of Polyurethane Networks

q_i	$AU^*q_o^{-2/3}$	χ_g	q_o	M_c
6.41	7.5×10^{-5}	$0.669 + 0.364q^{-2}$	16.5	2,100
11.00	4.88×10^{-5}	$0.611 + 0.265q^{-2}$	17.25	3,100
21.10	3.27×10^{-5}	$0.250 + 6.84q^{-2}$	5.2	10,400

A=B=1

Acknowledgement

We gratefully acknowledge the financial support and encouragement of the Urethane Group at the University of Southern California.

Literature Cited

1. P. J. Flory, "Principles of Polymer Chemistry", Cornell University Press, Ithaca, New York (1953).
2. E. A. Collins, J. Bares and F. W. Billmeyer, Jr., "Experiments in Polymer Science", Wiley, New York (1973).
3. B. Mukherji and W. Prins, *J. Poly. Sci.*, A2, 4367 (1964).
4. G. Allen, *Rubber Chem. and Tech.*, 49, 1206 (1976).
5. A. J. Chompff, *ACS Organic Coatings and Plastics Preprints*, 38, 456 (1978).
6. J. J. Hermans, *Trans. Faraday Soc.*, 43, 591 (1947).
7. F. T. Wall, *J. Chem. Phys.*, 11, 527 (1953).
8. H. M. James and E. Guth, *J. Chem. Phys.*, 21, 1039 (1953).
9. S. Yamada and W. Prins, *J. Poly. Sci.*, A1, 2335 (1963).
10. R. A. Orwoll, *Rubber Chem. and Tech.*, 50, 451 (1977).
11. H. E. Marsh, *Jet Propulsion Labs. Publication* 79-10 (1979).
12. W. Nierzwicki and Z. Majewska, *J. Appl. Poly. Sci.*, 24, 1089 (1979).
13. M. Ruthowska and A. Kwiatkowski, *J. Poly. Sci.*, Symposium No. 53, 141 (1975).

RECEIVED April 30, 1981.

Polyisobutylene-Based Diols and Polyurethanes

J. P. KENNEDY, B. IVAN¹, and V. S. C. CHANG

Institute of Polymer Science, The University of Akron, Akron, OH 44325

Fundamental studies directed toward the elucidation of the mechanism of olefin i.e., isobutylene, polymerizations yielded a new method for the synthesis of novel linear and tri-arm star telechelic polymers and oligomers [1,2]. The synthesis involves the use of bi- or tri-functional initiator/transfer agents, so called inifers (binifers and trinifers), in conjunction with BCl_3 coinitiator and isobutylene, and gives rise to polyisobutylenes carrying exactly two or three terminal $-\text{CH}_2-\text{C}(\text{CH}_3)_2\text{Cl}$ groups. These liquid telechelic polyisobutylene chlorides can be readily and quantitatively converted to telechelic polyisobutylene di- or tri-olefins [2,3] which in turn can quantitatively yield by hydroboration/oxidation telechelic polyisobutylene di- and triols [4,5].

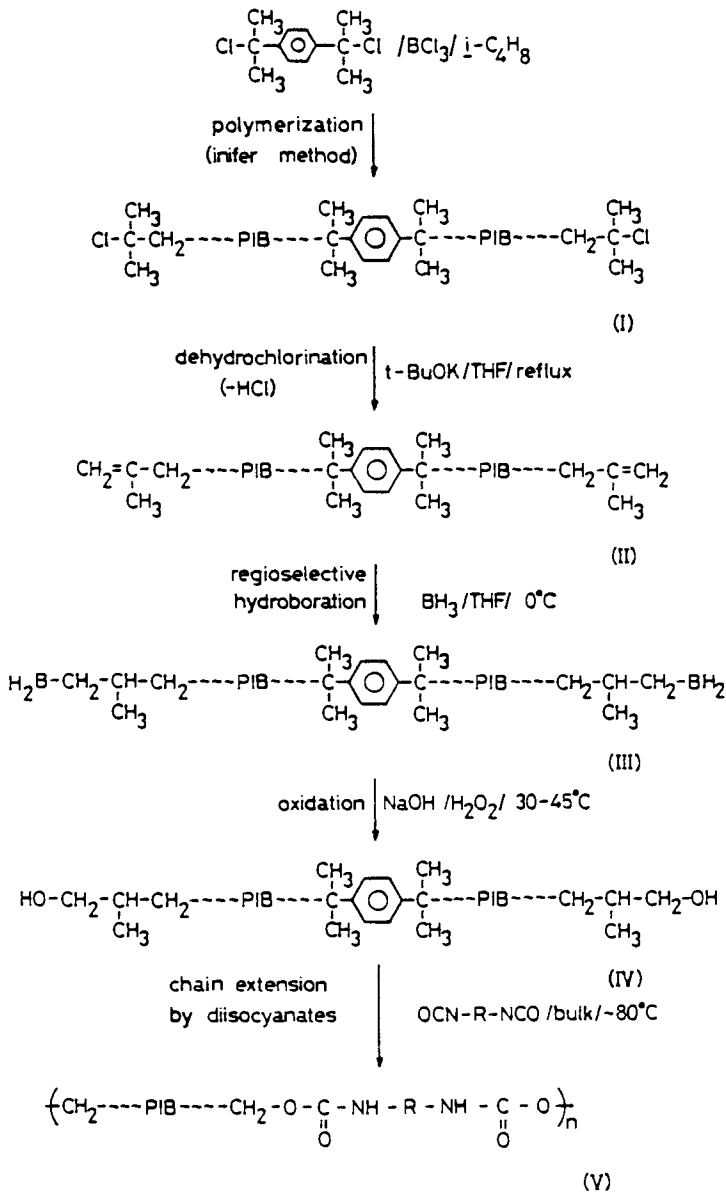
This paper concerns the synthesis of a new telechelic polyisobutylene diol, α,ω -di(hydroxy)polyisobutylene (formula IV in Scheme I), and the preparation of new linear polyurethanes containing polyisobutylene (PIB) soft segments by the use of this diol and conventional extension techniques with TDI.

Experimental

A. Materials. Solvents were purified by conventional techniques and freshly distilled before use. Potassium tert.butoxyde (t-BuOK) (Aldrich), 9-borabicyclo[3.3.1]nonane (9-BBN), 0.5 M solution in THF (Aldrich), 1 M solution of $\text{BH}_3 \cdot \text{THF}$ complex in THF

¹ Current address: Central Research Institute for Chemistry of the Hungarian Academy of Sciences, Budapest II Pusztaszeri ut 57-69 Hungary.

Scheme 1. Synthesis of polyisobutylene-based diols and polyurethanes.



(Aldrich), and dibutyltindilaurate (DBTDL) (Poly-sciences) were used as received. Phenyl isocyanate (PhNCO) (Aldrich), tolylene diisocyanate (TDI) (Aldrich), and 1,4-butanediol (BD) (Aldrich) were distilled under reduced pressure before use.

B. Techniques. The synthesis and purification of α, ω -di(tert.-chloro)polyisobutylene Cl-PIB-Cl (formula I in Scheme I) and the preparation of α, ω -di(isobutenyl)polyisobutylene (formula II in Scheme I) by quantitative regioselective dehydrochlorination of Cl-PIB-Cl have been described [1,3]. Details of the synthesis of α, ω -di(hydroxy)polyisobutylenes HO-CH₂-PIB-CH₂-OH (formula IV in Scheme I) by hydroborations of α, ω -di(isobutenyl)polyisobutylene with 9-BBN or BH₃·THF, have been given elsewhere [4].

Chain extension of polyisobutylene diols have been carried out with TDI under a dry N₂ atmosphere in a stainless steel enclosure at ~80°C on a heating plate. The diol containing a trace amount of DBTDL catalyst and TDI (NCO/OH \approx 1.0) were rapidly mixed with a glass rod and the charge was maintained at 78-80° for two days. Molecular weights were determined by GPC; the equipment and procedure used have been described [1].

Comparative extension experiments in the absence, PU-1, and presence, PU-2, of 1,4-butanediol, BD, have been carried out to obtain Tg information. The M_n (by VPO) of the PIB-diol used was 1,850. The stoichiometries were PU-1: NCO/OH = 1.05; PU-2: NCO/OH/BD = 1.0/0.5/0.5. DSC measurements were carried out on a 990 Thermal Analyzer (DuPont Instruments) under N₂ at 20°C/min. heating rate.

Results and Discussion

A. Synthesis of Linear Telechelic Polyisobutylene Diols. According to model calculations [5-7] efficient chain extension of telechelics can be carried out only with prepolymers having \bar{F}_n (number average functionality) = 2.00. The preparation of such telechelic prepolymers has been demonstrated to be possible by the inifer synthesis method [1,3,8-10]. The synthesis of a telechelic polyisobutylene diol as outlined in Scheme I includes three major steps: 1) the synthesis of Cl-PIB-Cl(I) by the inifer method [1] 2) the conversion of I into the diolefin II by dehydrochlorination using a hindered base [3] and 3) conversion of II into the desired telechelic polyisobutylene diol(IV) by hydroboration/oxidation [4].

In regard to Step 1, the principle of the inifer synthesis is that certain bifunctional initiator/transfer agents (inifers) induce polymerizations and subsequently control the termini of the polymers that are formed by chain transfer to inifer steps. Scheme II shows a simplified inifer mechanism (XRX = inifer, M = monomer) [1].

The p-dicumyl chloride/ BCl_3 /isobutylene inifer system has been thoroughly investigated. Detailed characterization research including various chemical techniques [3,8,10], ^1H NMR spectroscopy [1,3,8], GPC equipped by dual RI and UV detectors [1], end-group determination by dehydrochlorination [9], and kinetic studies [8] proved that the structure of the product is as shown by formula I in Scheme I and that the molecule is perfectly bifunctional ($\bar{F}_n = 2.0$).

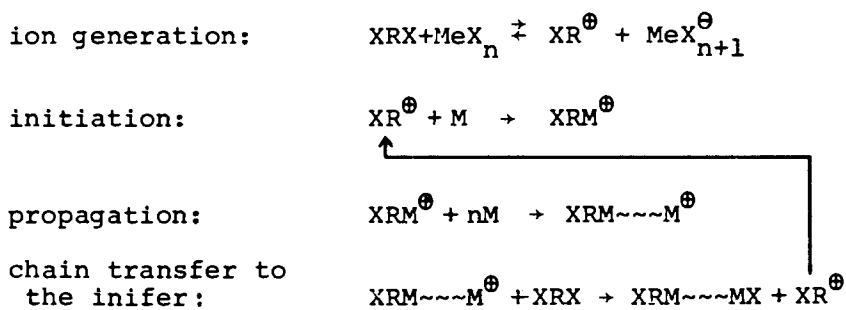
In regard to Step 2, it has been shown that I can be quantitatively converted to the telechelic diolefin II by regioselective dehydrochlorination with a strong hindered base e.g., *t*-BuOK, in refluxing THF [3]. This diolefin is a valuable starting material for the synthesis of a large variety of other products e.g., telechelic diols [4], diepoxides [11], dialdehydes [12], diacids [13], etc., whose exploration is actively pursued in our laboratories.

In regard to Step 3, the telechelic diolefin II can be quantitatively converted to the diol V by hydroboration/alkaline oxidation. Specifically, hydroboration of II by $\text{BH}_3 \cdot \text{THF}$ (or 9-BBN) yields an intermediate III which without isolation can be converted *in situ* by alkaline oxidation ($\text{NaOH}/\text{H}_2\text{O}_2$) to the diol IV, the starting material for polyurethane synthesis. The number average functionality of IV was found to be 2.0 within experimental error. The analytical methods used were ^1H NMR and UV spectroscopy [4]. The latter method involved the reacting of the diol with phenyl isocyanate, PhNCO, removing the excess PhNCO, filtration, \bar{M}_n determination and differential UV spectroscopy. Table I shows representative data.

Table I. \bar{F}_n of HO-CH₂-PIB-CH₂-OH's prepared by 9-BBN and $\text{BH}_3 \cdot \text{THF}$

Hydroborating agent	Number average functionality \bar{F}_n	
	^1H NMR	PhNCO method
9-BBN	2.05±0.08	1.99±0.05
$\text{BH}_3 \cdot \text{THF}$	2.02±0.08	1.98±0.07

B. Polyurethane Synthesis. We proceeded to prepare polyurethanes by reacting a series of well

Scheme II. Simplified inifer mechanism.

characterized liquid telechelic polyisobutylene diols having molecular weights in the range 1,7000-3,000, with TDI in the conventional manner. Table II shows the results obtained with three diols at $\text{NCO/OH} \sim 1.0$.

Table II. Chain Extension of α, ω -Di(hydroxy)polyisobutylene with Tolylene Diisocyanate^a

Sample #	Starting Material		Product		Extension	
	$\bar{M}_n \cdot 10^{-3}$	$\bar{M}_w \cdot 10^{-3}$	$\bar{M}_n' \cdot 10^{-3}$	$\bar{M}_w' \cdot 10^{-4}$	$\frac{\bar{M}_n'}{\bar{M}_n}$	$\frac{\bar{M}_w'}{\bar{M}_w}$
1	1.70	2.86	9.8	2.48	5.8	8.7
2	2.05	3.66	9.51	2.69	4.64	7.4
3	2.95	5.46	18.4	3.0	6.24	5.5

^aReaction conditions: bulk, $\text{NCO/OH} \sim 1.0$, 75-80°C, trace of DBTDL catalyst in PIB-diol, under dry N_2 ; data obtained after 2 days; obtained by GPC.

The viscosity of the clear and colorless charge increased rapidly during the first three-four minutes and stirring became difficult after about 24 hours. After two days the products exhibited rubbery behavior (very rapid recovery upon releasing the strain of stretched samples). The rubbery masses were completely soluble in THF at room temperature.

It is not too surprising that the molecular weight extension rose only 5.5-8.7 fold considering the difficulties one may encounter during the linking reaction, e.g., relatively high molecular weights reached after 6-9 fold extension, H-bonding between urethane linkages, diminished endgroup concentration, and minute deviations from perfect 1:1 functionality. Extended heating to somewhat higher temperatures and/or varying the NCO/OH ratios may result in higher extensions. Further investigations along these lines are in progress.

Another series of experiments have been carried out to study the T_g of these new polyurethane rubbers. In these experiments a diol of $\bar{M}_n = 1,850$ was chain extended with TDI ($\text{NCO/OH} \sim 1.05$) in the absence and presence of 1,4-butanediol extender. The product obtained in the absence of BD was colorless (PU-1) whereas that in the presence of this extender was yellowish (PU-2). Both films were tough elastomers. Extraction with n-pentane (Soxhlet, 48 hrs) did not change the appearance of the films. These products were largely THF soluble (5-10% gel) and insoluble in DMF. The

elongation of PU-1 was 500-600% and exhibited rapid relaxation. The elongation of PU-2 was only ~100%.

Figure 1 shows DSC traces of HO-CH₂-PIB-CH₂-OH, PU-1 and PU-2. The appearance of Tg's characteristic of soft PIB segments at low temperatures and hard TDI segments at high temperature indicates a high degree of phase segregation. High amplification was needed to detect the high temperature Tg's: i.e., at 81°C and 93°C for PU-1 and PU-2, respectively. The slight increase in PIB Tg's from -72°C in HO-CH₂-PIB-CH₂OH to -64°C and -61°C in PU-1 and PU-2, respectively, may indicate a slight degree of intermingling between the low molecular weight PIB and urethane segments. Similar phenomena have been observed recently for polybutadiene-based polyurethanes [14].

In conclusion, these experiments indicate the possibility of synthesizing polyurethanes with polyisobutylene soft segments. The polyisobutylene diols have been synthesized by the inifer method and careful characterization techniques indicate $\bar{F}_n = 2.0$. It is anticipated that polyurethanes with polyisobutylene soft segments will exhibit superior thermal, UV, oxidative and chemical resistance to conventional polyurethanes having polyester, polyether, or polybutadiene soft segments.

Abstract

A novel polyisobutylene-based diol has been synthesized and subsequently used in conjunction with tolylene diisocyanate (TDI) to yield polyurethanes. The diol was obtained by quantitative hydroboration/oxidation from the corresponding telechelic diolefin which in turn was prepared by quantitative dehydrochlorination of the corresponding dichloride (Scheme I). The number average functionality of the diol is exactly two and its molecular weight polydispersity is 1.5. Extension of telechelic polyisobutylene diols ($\bar{M}_n = 1,700-3,000$) with TDI (NCO/OH = 1.0, bulk, 80°, two days) yielded a 5.5-8.7 fold increase in molecular weight. The products are strong rubbers exhibiting rapid recovery upon releasing the strain of stretching. The Tg's of polyurethanes prepared in the absence (PU-1) and presence of 1,4-butanediol (PU-2) extender have been determined. DSC showed two transitions, at -64° and 81°C for PU-1 and -61° and 93° for PU-2. The first transition is due to rubbery polyisobutylene domains while the second to hard TDI domains.

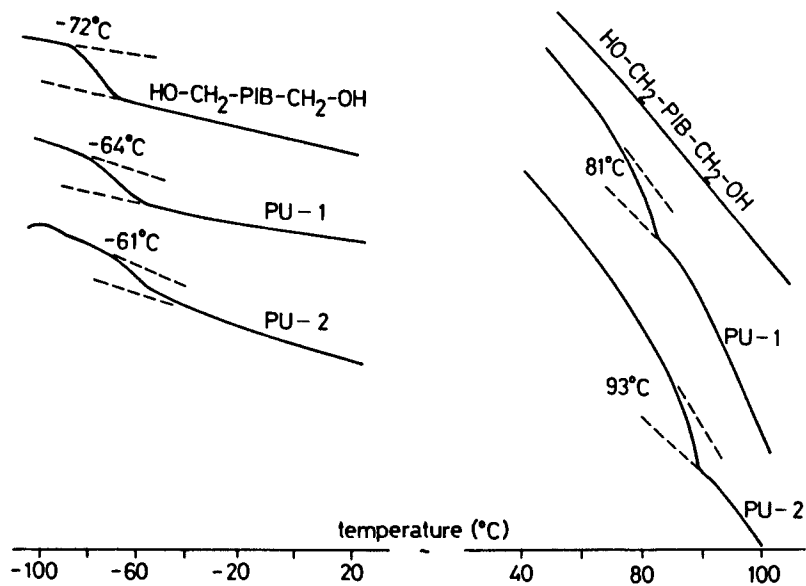


Figure 1. DSC traces of HO-CH₂-PIB-CH₂-OH, PU-1, and PU-2.

Acknowledgement

Financial assistances by the Institute for Cultural relations, Hungary and the National Science Foundation, U.S.A. (INT-78-27245) are gratefully acknowledged.

Literature Cited

1. Kennedy, J.P.; Smith, R. A. J. Polym. Sci., Polym. Chem. Ed., 1980, 18, 1523.
2. Kennedy, J. P.; Ross, L.; Lackey, J. E.; Nuyken, O. Polymer Bulletin, in press.
3. Kennedy, J. P.; Chang, V.S.C.; Smith, R. A.; Iván, B. Polymer Bulletin, 1979, 1, 575.
4. Iván, B.; Kennedy, J. P.; Chang, V.S.C. J. Polym. Sci., Polym. Chem. Ed., 1980, 18, 3177.
5. Baldwin, F. P.; Burton, G. W.; Griesbaum, K.; Hanington, G. Adv. Chem. Ser., 1969, 91, 448.
6. Athey, R. D., Jr.; 1974, Ph.D. Dissertation, University of Delaware.
7. Iván, B.; Kennedy, J. P. Polymer Bulletin, 1980, 2, 351.
8. Fehérvári, A.; Kennedy, J. P.; Tüdös, F. J. Macromol. Sci.-Chem., 1980, A15, 215.
9. Iván, B.; Kennedy, J. P.; Kelen, T.; Tüdös, F. J. Macromol. Sci.-Chem., in press.
10. Chang, V. S. C.; Kennedy, J. P.; Iván, B.; Polymer Bulletin, in press.
11. Chang, V. S. C.; Kennedy, J. P.; Iván, B. to be published.
12. Kennedy, J. P.; Francik, W. P. to be published.
13. Kennedy, J. P.; Hongu, Y. to be published.
14. Schneider, N. S.; Sung, C. S. Paik Polym. Eng. Sci., 1977, 17, 73.

RECEIVED April 30, 1981.

The Mechanism of Tin–Amine Synergism in the Catalysis of Isocyanate Reaction with Alcohols

IBRAHIM S. BECHARA

Air Products and Chemicals, Inc., Linwood, PA 19061

Tertiary amines and tin carboxylates are important catalysts in the production of polyurethane foams from polyisocyanates and polyhydroxy compounds. Many articles have been written on the mechanism of the catalysis of the isocyanate-alcohol reactions by such compounds. Farkas and Mills (1), Entelis and Nesterov (2), Frisch and Rumao (3) and Petrus (4) have written excellent reviews on this subject. Wolf (5) has shown that these catalysts are synergistic to each other.

Various explanations for this synergism have already been proposed. Willeboordse and co-workers (6) explained the synergism by the coordination of the amine to the isocyanate in a tin-isocyanate-alcohol complex, thereby increasing the complex's stability as shown in Figure 1.

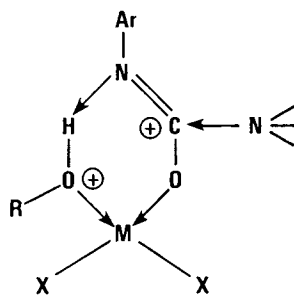
Reegen and co-workers (7) studied the effect of tin and amine on the chemical shift of the alcohol's proton. Their NMR studies showed that the greatest downfield shift of the OH proton occurred when tin and amine were added to the solution of alcohol; thus, they reported that both hydrogen bonds and oxygen-metal bonds are formed and that the observed increase in the shift appears to correlate with the synergistic effect noted when preparing urethanes with a mixture of these catalysts. Frisch (3) later explained the synergism as due to complex formation between the alcohol-isocyanate and tin where the OH proton is hydrogen bonded to the nitrogen of the isocyanate as shown in Figure 2. The amine was presumed to coordinate to the already complexed isocyanate in a manner similar to that proposed by Willeboordse (6).

These explanations, however, are unlikely in view of the fact that the amine is certainly a much better ligand than the isocyanate or alcohol and therefore its coordination to the metal ion should be favored over that of the isocyanate. It was shown by Graddon and Ranna (8) that dialkyltin dicarboxylates form a 1:1 complex with tertiary amines quite readily. Using calorimetric techniques, these workers calculated the formation constants in benzene solution for numerous complexes of alkyltin carboxylates with tertiary amines.

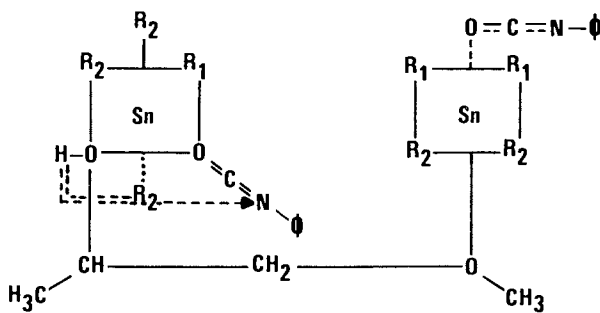
0097-6156/81/0172-0393\$05.00/0

© 1981 American Chemical Society

Figure 1. Tertiary amine-activated ternary complex of tin-alcohol-isocyanate (6).



Journal of Macromolecular Sciences



Reviews of Macromolecular Chemistry

Figure 2. Alcohol-bridged isocyanate-tin complex (3).

Experimental

Materials. Phenyl isocyanate (Eastman Kodak) and 2-butanol were fractionally distilled under reduced pressure prior to use. Dioxane was purified by first refluxing with sodium metal, then distilling under reduced pressure. Triphenyl phosphine, dibutyltin dilaurate (DBTDL) and cobalt acetylacetonates were used as received from Eastman Kodak and M&T companies, respectively. DABCO catalyst (triethylenediamine, Air Products and Chemicals, Inc.) was purified by sublimation and stored in a desiccator.

Kinetic Experiments. Stock solutions were prepared by weighing out the correct amount of material and diluting to the proper level, using volumetric flasks. Reaction mixtures were prepared by adding the desired amount of catalyst and active hydrogen compound to a volumetric flask, diluting with solvent short of the calibration mark, and adding the proper amount of phenyl isocyanate solution and then solvent to the mark.

The reaction flasks were stoppered with rubber caps, so that samples could be withdrawn at the proper time interval with a hypodermic syringe. The flasks were immediately placed in a water bath controlled at 25°C. Samples withdrawn from the reaction flasks were placed in a 0.1 mm cell (Connecticut Instrument Corporation, Type FT) using Irtran-2 crystals. The infrared spectrum was scanned in the 4.5 micron region using a Perkin-Elmer Infracord, Model 257 Spectrometer. When the isocyanate peak was reached, the time was noted. NMR studies were carried out on a Varian A-60 high resolution spectrometer.

Discussion

We have measured the synergism of dibutyltin dilaurate (DBTDL)-triethylenediamine catalyzed reactions of phenyl isocyanate with butanol and water at various concentrations of the tin and amine. As Tables I and II show, there is a lack of proportionality between the acceleration of the reaction and the concentration of the additives. If one assumes the tin catalyzed reaction is of second order and calculates the increase in rate constant due to the addition of amine co-catalyst, one finds that the addition of 0.02% amine based on isocyanate increases the rate of DBTDL catalyzed ϕ NCO-2-butanol by a factor of 4.2. If one increases this amount of amine ten times, the resulting increase in the rate is only 5.30 times, while increasing the concentration of the amine by a factor of 100 results in an increase of the rate constant only by a factor of 7.1.

It is also noteworthy that the acceleration of the reaction provided by each of the catalyst components when added to the other is about the same. This symmetrical effect of the catalyst components on the activity of the system suggests a 1:1 complex between the catalyst components as the active species. The lack

TABLE I . SYNERGISTIC EFFECT OF DABCO CATALYST AND DIBUTYLTIN DILAURATE FOR THE CATALYSIS OF PHENYL ISOCYANATE (0.07M) REACTION WITH BUTANOL-2 (0.07M) IN DIOXANE AT 25°C

RATE CONSTANT, LITER/MOLE/HOUR					
DABCO, MOLE/LITER	DBTDL MOLE/LITER	0.0	0.000014	0.00014	0.0014
		0.0	0.000014	0.00014	0.0014
0.0	0.0	—	0.8	9.0	
0.000014	0.0	—	14.7	38.0	
0.00014	1.0	9.7	28.0	48.0	
0.0014	1.8	12.5	38.5	64.6	

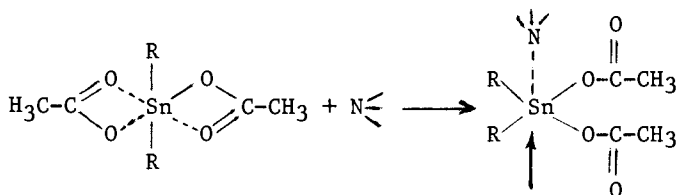
TABLE II. SYNERGISTIC EFFECT OF DABCO CATALYST AND DIBUTYLTIN DILAURATE FOR THE CATALYSIS OF PHENYL ISOCYANATE (0.07M) REACTION WITH WATER (0.035M) IN DIOXANE AT 25°C

RATE CONSTANT, LITER/MOLE/HOUR					
DABCO, MOLE/LITER	DBTDL MOLE/LITER	0.0	0.000014	0.00014	0.0014
		0.0	0.0	0.000014	0.00014
0.0	0.0	—	0.5	4.9	
0.000014	0.0	0.8	1.2	5.6	
0.00014	0.2	6.3	12.2		
0.0014	0.7	6.0	12.0	19.0	

of proportionality between the acceleration and catalyst concentration must be due to the transformation of the 1:1 complex to a lesser active species (perhaps a dimer) in accordance with the following equations:



On the basis of these observations, the following configuration is proposed as the highly active catalytic species:



Evidence for this complex formation between DBTDL and DABCO catalyst was obtained from nuclear magnetic resonance studies. The dimethyl tin diacetate was selected for investigation because of its simple spectrum and its known structure. In dioxane solution we observed two small CH_3 doublets that appear because of the $\text{CH}_3\text{-Sn}119$ and $\text{CH}_3\text{-Sn}117$ coupling. Each of these two tin isotopes are present in about 8% concentration. The coupling constant for $\text{CH}_3\text{-Sn}119$ was 82 cps in the absence of amine (TEDA) and changed to 98 cps in the presence of added excess TEDA (Figure 3). In accordance with work by Okawara (9) and Drago (10) on complexes of related tin compounds, the change in coupling constant indicates a complexing between tin compound and the amine.

Another supporting evidence for complex formation as a prerequisite to synergism was obtained from the study of the catalysis of phenyl isocyanate-butanol reaction by soluble organic cobalt compounds in presence and absence of DABCO catalyst. The results obtained are presented in Figures 4 and 5. It is evident that the combination of DABCO catalyst with divalent cobalt compounds shows synergistic effects while the trivalent cobalt acetylacetonate shows relatively low activity. The explanation of these observations is the structure of these compounds.

Cobalt^{III} acetylacetonate is an octahedral complex with the central metal ion fully coordinated to its maximum coordination number. As there is no free coordination position or easily displaceable ligand in this complex, neither the amine nor the hydroxyl compound can coordinate with it. Therefore, neither high catalytic activity nor synergism are observed.

On the other hand, the cobalt^{II} compounds are tetrahedral complexes which can be converted to octahedral complexes by coordination with amines and the alcohol yielding catalytically active species.

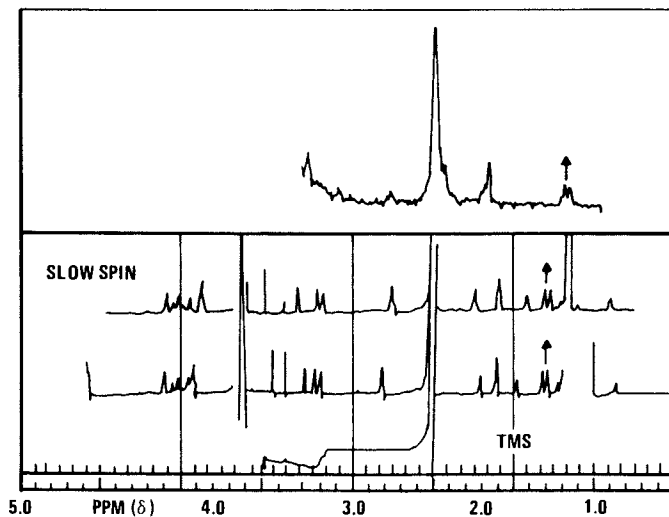


Figure 3. Effect of added TEDA on the $^{119}\text{Sn}-\text{CH}_3$ coupling constant solvent dioxane at 25°C .

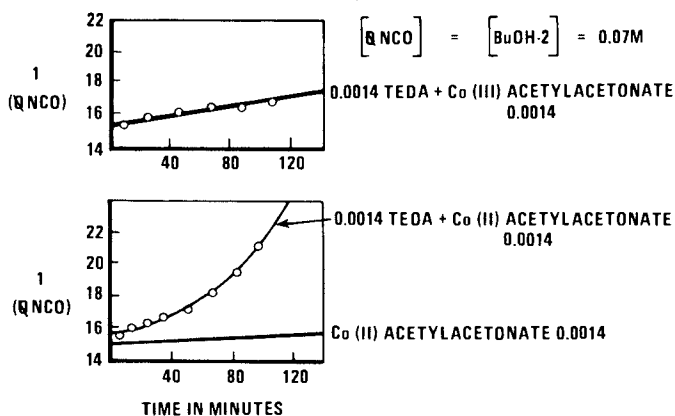


Figure 4. Effect of TEDA in the catalysis of $\text{PhNCO}-\text{BuOH}-2$ reaction in dioxane at 25°C by cobalt compounds.

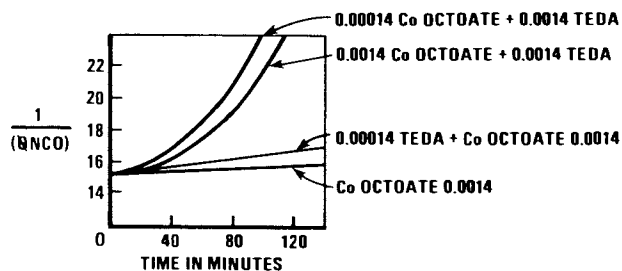
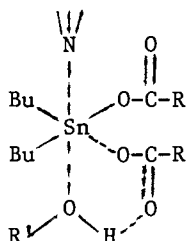
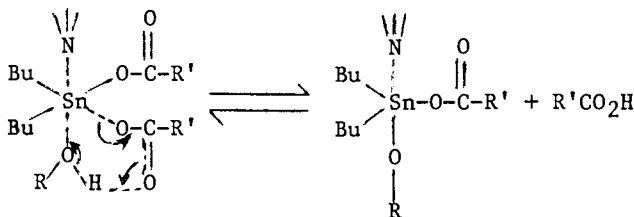


Figure 5.

The aforementioned 1:1 complex of DBTDL-amine can activate the alcohol by coordinating at the position indicated by the arrow and form the following structure:



The occurrence of such a complex is in agreement with the NMR chemical shift of the OH proton of the alcohol observed by Reagen and co-workers (7). The addition of tin to alcohol will result in an alcohol-tin complex and deshielding of the alcoholic proton due to the filling of vacant d orbitals of the tin by the nonbonding electrons of the alcohol's oxygen. The added amine will also coordinate with the tin via its unshared electron pair and further weaken the tin carboxylate bond which will tend to form a stronger bond with alcoholic protons as depicted in the following equilibrium:



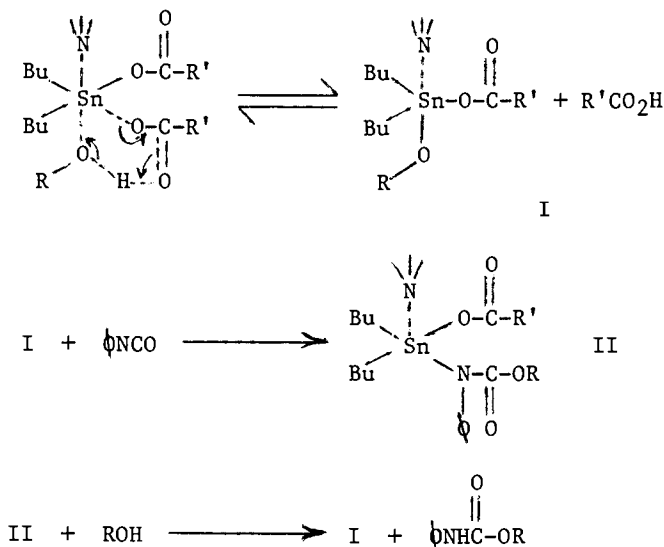
If the mechanism of the catalysis of isocyanate-alcohol reaction by tin carboxylates does indeed proceed via the alkoxide as proposed by Bloodworth and Davies (11), then the synergism of the amine to tin can readily be explained from the above equilibrium. The amine will assist in the alcoholysis step and speed up the decomposition of the tin-carbamate complex by the alcohol to the urethane and tin alkoxide.

The presently proposed mechanism of synergism implies that ligands other than amine which can coordinate with the tin ion should also synergize its catalytic activity toward alcohol-isocyanate reactions. This apparently is the case for triphenyl phosphine-DBTDL combination. When triphenyl phosphine was added to DBTDL, it accelerated the rate of reaction of isocyanate with alcohol and water (Figure 6). Although triphenyl phosphine is known to dimerize isocyanates, (12), the dimerization

rate is negligible under the conditions employed for the above described reactions because the addition of triphenyl phosphine to DBTDL-DMEA produced no change in the rate of reaction (Figure 7), indicating that triphenyl phosphine has no catalytic activity of its own, under the conditions used for converting isocyanates. Triphenyl phosphine is, however, a good ligand and can readily complex with alkyltin carboxylates in the absence of amine ligands. The observed increase in the catalytic activity of DBTDL in the presence of triphenyl phosphine must be due to the complex formed between them which is in agreement with the above proposed mechanism of tin-amine synergism.

Conclusion

The mechanism of the amine-tin carboxylate synergism in the catalysis of isocyanate reactions with alcohol involves the formation of a highly active complex between the tin and the amine. In the presence of alcohol this complex probably facilitates the alcoholysis step of the tin carboxylates to the highly active tin alkoxides, which then rapidly adds isocyanate across the tin-oxygen bond to form the carbamate adduct of tin. The adduct breaks up by another molecule of alcohol to form the urethane and regenerate the tin alkoxide. This mechanism is in full agreement with the mechanism postulated by Bloodworth and Davies (11) for the tin carboxylate catalyzed reaction of isocyanate with alcohols. It is also in agreement with Reegen's and Frisch's observation of the effect of tin-amine on the NMR's chemical shift of the OH proton of the alcohol. Kinetic studies to verify the Bloodworth-Davies postulated mechanism is the needed next step.



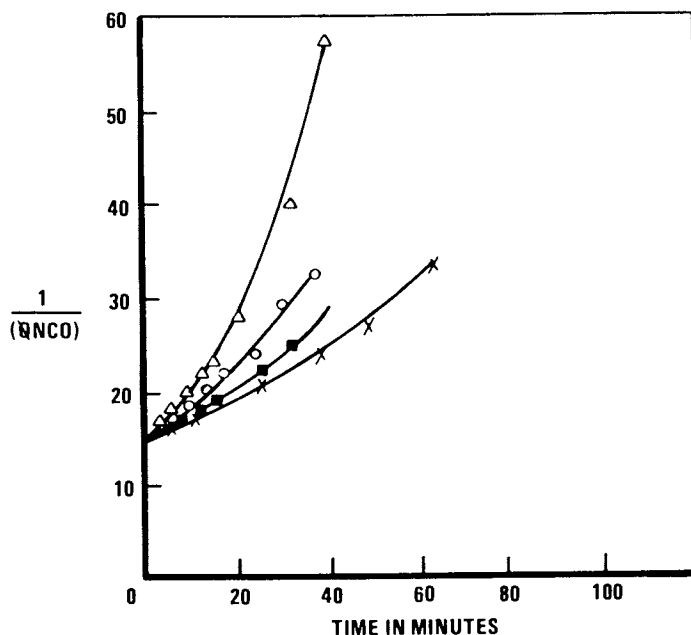


Figure 6. Effect of Ph_3P on the catalysis of isocyanate reactions by DBTDL. Key: solvent = dioxane; 30°C ; catalyst concentration = 0.0014M ; $[\text{PhNCO}] = [\text{OH}] = 0.07\text{M}$. $\text{PhNCO} + \text{H}_2\text{O}$: X, DBTDL; \blacksquare , DBTDL + Ph_3P . $\text{PhNCO} + 2\text{-BuOH}$: \circ , DBTDL; \triangle , DBTDL + Ph_3P .

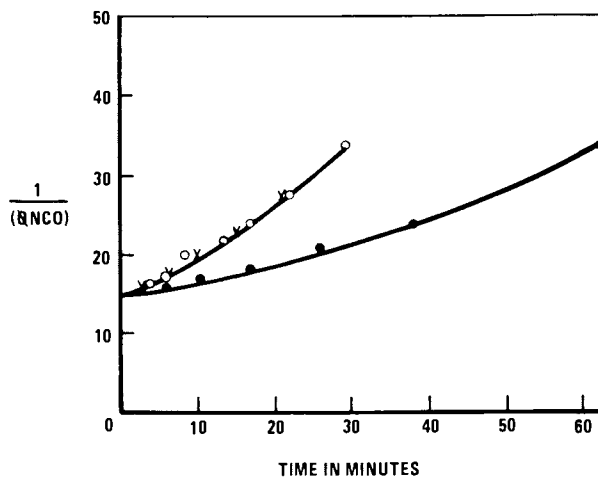


Figure 7. The effect of triphenyl phosphine on the rate of tin-amine catalyzed reaction of PhNCO with water. Key: \circ , DBTDL + DMEA; X, DBTDL + DMEA + Ph_3P ; \bullet , DBTDL. $\text{PhNCO} = 0.07\text{M}$; $\text{H}_2\text{O} = 0.035\text{M}$; solvent dioxane, 30°C .

Acknowledgment

The author wishes to express his gratitude to Air Products and Chemicals, Inc. for allowing the publication of this work. I am also indebted to Dr. A. Farkas and Dr. R. L. Mascioli under whose supervision this work was done.

Literature Cited

1. Farkas, A; Mills, G. A., Advances in Catalysis, 1962, 15, 393-446
2. Entelis, S. E.; Nesterov, O. V., Russian Chem. Rev., 1966, 35 (12), 917-930
3. Frisch, K. C.; Rurnao, L. P., J. of Macromolecular Science, Rev. of Macromolecular Chem., 1970, 5 (1), 103-149
4. Petrus, A., International Chemical Engineering, 1971, 11 (2), 314-323
5. Wolf, H. W., Urethane Foam Bulletin, E. I. duPont de Nemours & Company, 1960
6. Willeboordse, F. G.; Critchfield, F. E.; Meeker, R. L., J. of Cellular Plastic, 1965, 1, 76-84
7. Reegen, S. L.; Frisch, K. C.; Floutz, W. V., J. of Polymer Science, 1967, 5, 35-42
8. Graddon, D. P.; Ranna, B. A., J. of Organometallic Chem., 1977, 136, 19-24
9. Maeda, Y.; Dillard, C. R.; Okawara, R., J. of Inorganic and Nuclear Chem. Letters, 1966, 2, 197-199
10. Bolles, T. F.; Drago, R. S., J. of American Chemical Society, 1966, 88, 5730-5734
11. Bloodworth, A.; Davies, A. G., Chemical Society Proceeding, 1963, 264
12. Zharkov, V. V.; Bakhitov, M. I.; Apanasenko, G. A.; Gerasimova, S. S., Chem. Abstracts, 1974, 81, 104242u

RECEIVED May 28, 1981.

Model Studies of Phenolic-Urethane Polymers

J. E. KRESTA, A. GARCIA, and K. C. FRISCH
Polymer Institute, University of Detroit, Detroit, MI 48221

G. LINDEN
Ashland Chemical Co., Columbus, OH 43216

Phenolic-based urethane foams have been described by various investigators [1-19]. The phenolic resins used were either resoles or novolacs, as well as derivatives of phenol-formaldehyde, or phenol-aniline-formaldehyde condensation products [1-17], in particular poly(oxyalkylene) derivatives [7,9-14] and also Mannich reaction products of phenol with formaldehyde and alkanolamines [15-17]. More recently, new types of phenolic-urethane foams were reported using phenolic resins containing both benzylic ether linkages and methylol groups with polymeric isocyanate (polymeric MDI) [18]. These foams were characterized by low combustibility even without the addition of flame retardants, good compressive strength, and a low K factor (0.113).

Very recently Papa and Critchfield [19] described the preparation of foams based on a resole resin containing a high ortho-methylol content and a blend of quasi prepolymer of tolylene diisocyanate, a phosphorus-containing polyol and polymeric isocyanate containing a minor portion of tris-(2-chloro-ethyl) phosphate. The resulting foams had relatively low friability, low combustibility and smoke evolution. However, the foams were open-celled and the K factor was more characteristic of that of phenolic foams (0.254).

Relatively little basic information has been published regarding the kinetics of phenol-formaldehyde intermediates, especially of phenols, methylol phenols, benzyl alcohol and benzylic ethers with isocyanates. Due to the fact that a typical resole contains both phenolic and benzylic hydroxyl groups, it was of interest to determine their reactivity toward isocyanates in the presence of various catalysts, as well as the effect of substitution on their reactivity. This investigation describes the kinetics of model phenols and model benzyl alcohols with phenyl isocyanate catalyzed with either a tertiary amine (dimethylcyclohexylamine, DMCHA) or an organotin catalyst, dibutyltin dilaurate (DBTDL) in either dioxane or dimethylformamide solution.

0097-6156/81/0172-0403\$05.00/0
© 1981 American Chemical Society

Experimental

Materials. All model compounds and dimethylcyclohexylamine (DMCHA) used in this study were reagent grade and were purified by distillation under nitrogen. Dibutyltin dilaurate (DBTDL) was used as received from the supplier. Reagent grade 1,4-dioxane was dried by refluxing first with NaOH, then with metallic sodium for 24 hours each and then distilled under nitrogen. Toluene was purified by refluxing with sodium for 24 hours, followed by distillation. Dimethylformamide (DMF) was dried using Linde 4A molecular sieves. Phenyl isocyanate was purified by vacuum distillation.

Measurement of Kinetics. The reactions were carried out in a dried 300 ml three-necked flask, equipped with a nitrogen inlet, magnetic stirrer, reflux condenser, and dropping funnel. The reaction flask was immersed in a thermostatically controlled oil bath. Fifty ml of 1.0 mole/kg isocyanate solution in 1,4-dioxane was pipetted into the flask and was stirred magnetically while the model compound solution in dioxane (1 mole/kg) and containing variable amounts of catalyst was placed in a temperature-controlled dropping funnel. When constant temperature was reached (25°C) in the flask, as well as in the dropping funnel, the solution was poured into the flask and the whole mixture was thoroughly mixed. Samples of approximately 2.5 g were withdrawn at regular intervals and the isocyanate content determined by means of the di-n-butylamine method. Corrections due to the consumption of the hydrochloric acid by the amine catalyst were made in the determination of the isocyanate content.

Results and Discussion

The reactivity of the model phenols and benzyl alcohols with phenyl isocyanate was determined in the presence of a tertiary amine (DMCHA) and a tin catalyst (DBTDL) by measurement of the reaction kinetics. The experimental results based on initial equal concentrations of phenyl isocyanate and protic reactants showed that the catalyzed reactions followed second order reaction with respect to the disappearance of isocyanate groups (see Figure 1). It was also found that a linear relationship exists between the experimental rate constant k_{exp} , and the initial concentration of the amine catalyst (see Figure 2). In the case of the tin catalyst, the reaction with respect to catalyst concentration was found to be one-half order (see Figures 3-4). A similar relationship for the tin catalyzed urethane reaction was found by Borkent [20].

In Table I are summarized the kinetic results for the model phenols with phenyl isocyanate in the presence of DMCHA catalyst in dioxane solution. It is apparent that substitution in the 2 and 6 positions decrease significantly the reaction constant k_{cat} . In the case of model benzyl alcohols using DMCHA catalyst, the

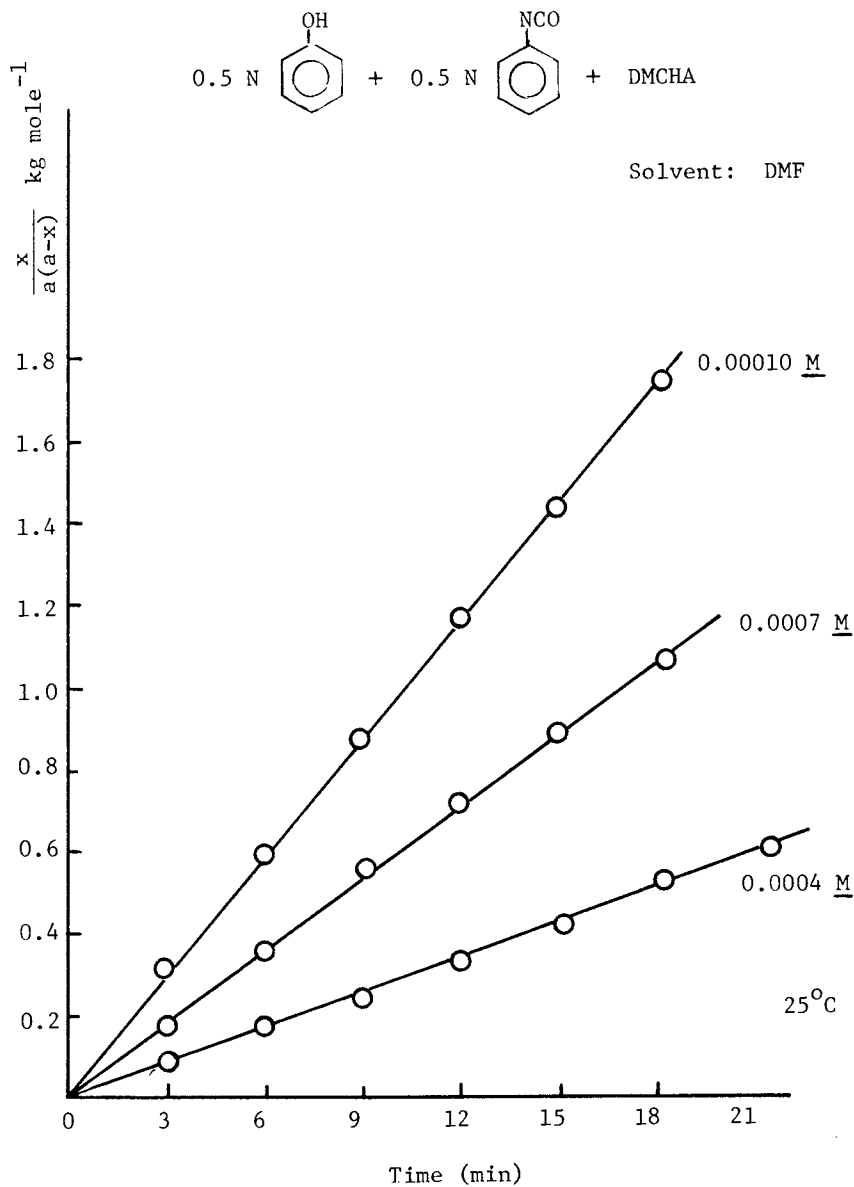
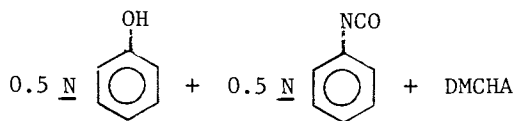


Figure 1.



Solvent: DMF

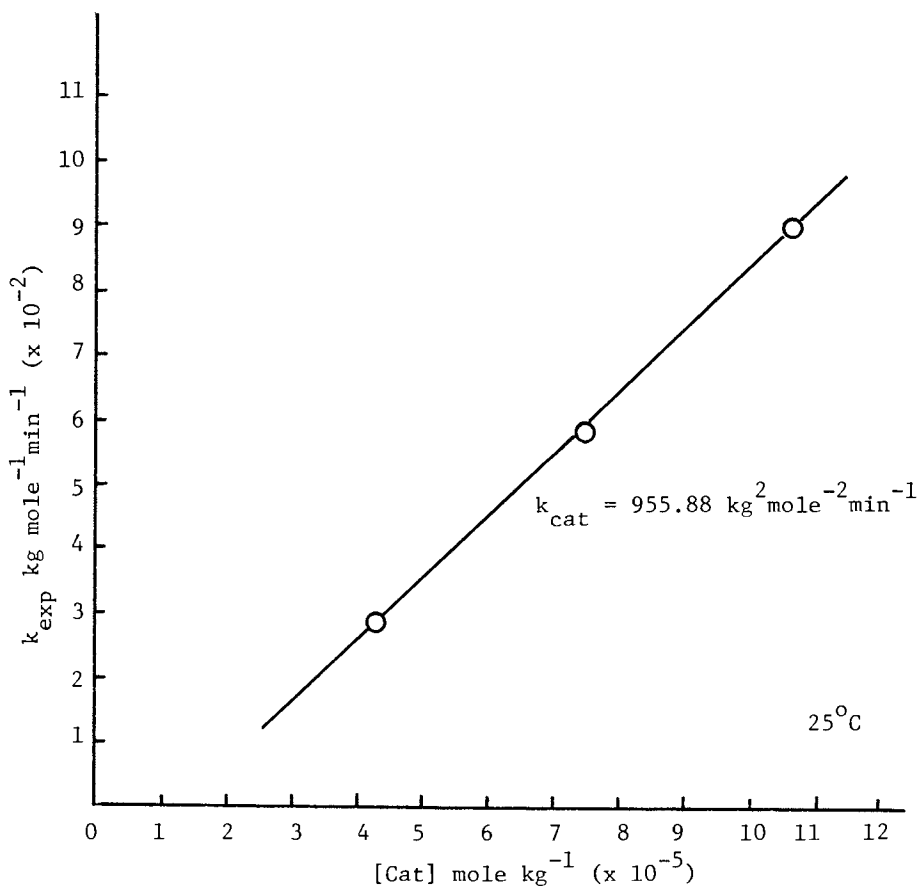
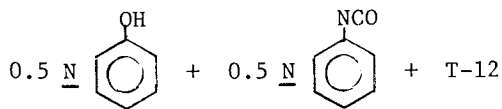


Figure 2.



Solvent: Dioxane

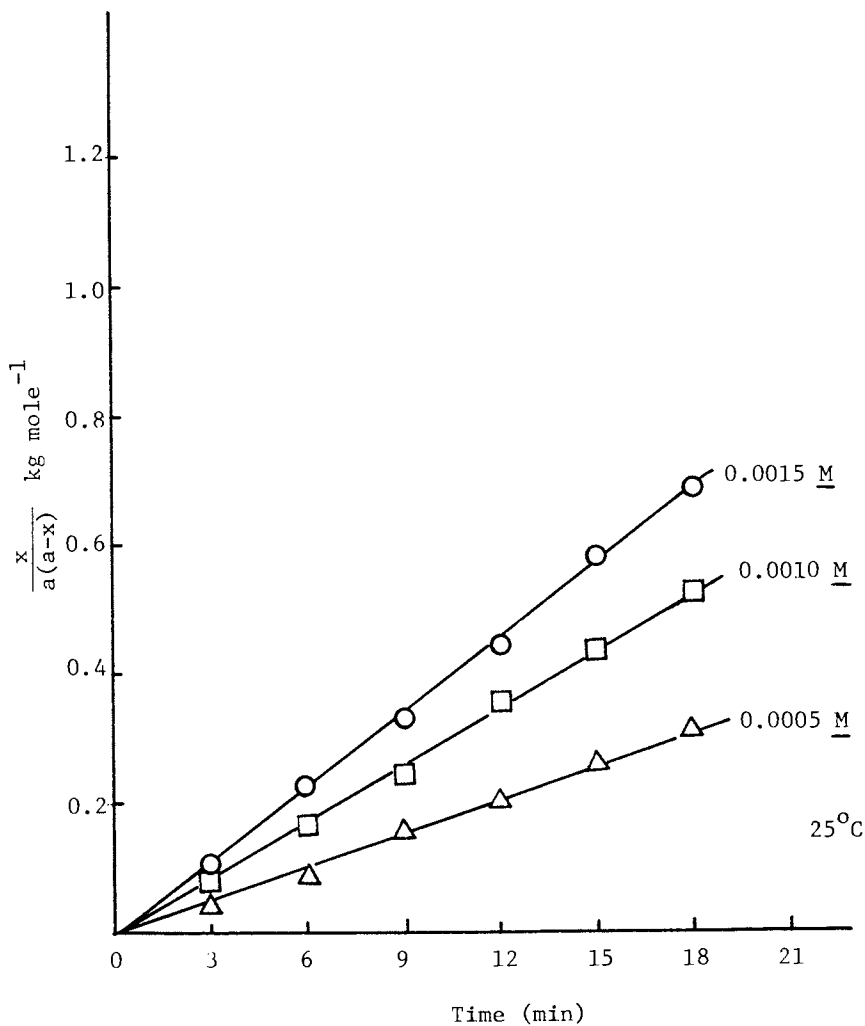


Figure 3.

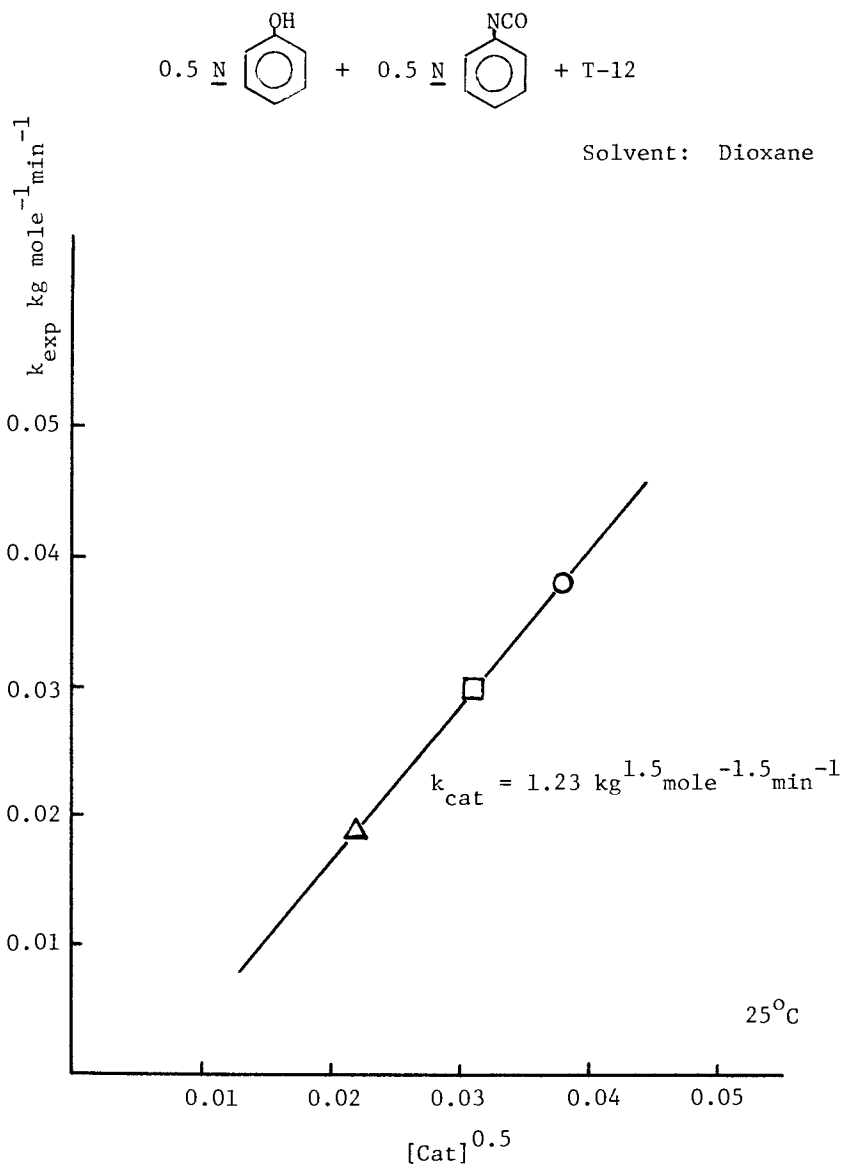
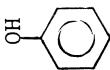
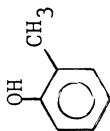
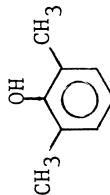
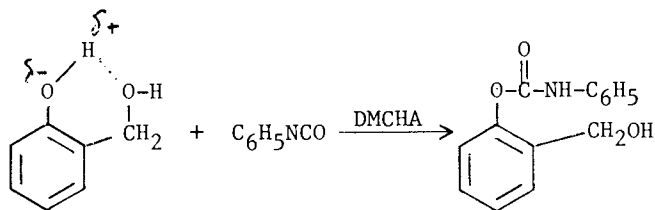


Figure 4.

TABLE I
EFFECT OF SUBSTITUTION ON REACTIVITY OF MODEL PHENOLS
WITH PHENYL ISOCYANATE IN DIOXANE AT 25°C

Model Phenol	pK	Catalyst DMCHA mole/l	k_{exp} $\frac{1}{\text{kg mole}^{-1} \text{min}^{-1}}$	k_{cat} $\frac{1}{\text{kg}^2 \text{mole}^{-2} \text{min}^{-1}}$
	9.89	0.005 0.010 0.015	0.0414 0.0892 0.1415	10.35
	10.20	0.010 0.015 0.020	0.0479 0.0786 0.0990	5.28
	10.60	0.005 0.0075 0.010	0.0309 0.0464 0.0567	5.34

decrease in the reactivity due to the substitution in the 2 position was relatively small as can be seen in Table II. A substantial increase in k_{cat} for *o*-hydroxy benzyl alcohol was observed. This increase in the reactivity can be attributed to the formation of internal hydrogen bonding which activated the phenol group resulting in the preferential formation of the corresponding *o*-(hydroxymethyl) phenyl *N*-phenylcarbamate:



Similar results were obtained by Papa and Critchfield [19].

The effect of type of catalyst on the reactivity of phenol and benzyl alcohol with phenyl isocyanate can be seen in Table III. In the case of tertiary amine (DMCHA), there is a relatively small difference in the reactivity of both the phenol and benzyl alcohol with phenyl isocyanate. Using DBTDL as catalyst, benzyl alcohol was found to be 26 times more reactive than phenol in the reaction with phenyl isocyanate.

It is also of interest to point out that DBTDL is about three times more effective a catalyst than DMCHA in the reaction of phenol with phenyl isocyanate. Baker and Gaunt [21] found that ethyl alcohol was 30 times more reactive than phenol in the uncatalyzed reaction with phenyl isocyanate. However, in the presence of a tertiary amine (triethylamine), the reactivity of phenol increased significantly and was found to be similar to that of ethyl alcohol (see Table IV).

The effect of solvents on the kinetics of the phenol-phenyl isocyanate reaction is seen in Table V. The reactivity increased in the following order: dioxane < toluene < DMF (1:3.3:92). The difference in reactivity is due to the combined effects of the relative permittivity and the specific solvation.

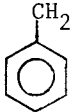
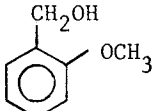
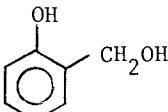

Conclusions

It was found that the reactivity of typical functional groups present in resole type of polyols with isocyanates is affected to a great extent by the structural configuration of the polyols and the type of catalyst used.

Model studies based on substituted phenols and benzyl alcohols showed that the presence of substituents in the *ortho* position in benzyl alcohol had a relatively small effect on the reactivity of the hydroxyl group with isocyanate in the presence of tertiary amine catalyst (DMCHA). In contrast, similar substitution in phenols significantly affected the reactivity of the

TABLE II

EFFECT OF SUBSTITUTION ON REACTIVITY OF MODEL BENZYL
ALCOHOLS WITH PHENYL ISOCYANATE IN DIOXANE AT 25°C

Model Phenol	Catalyst DMCHA mole/l	k_{exp} kg mole ⁻¹ min ⁻¹	k_{cat} kg ² mole ⁻² min ⁻¹
	0.010	0.0709	9.88
	0.015	0.1278	
	0.020	0.1664	
	0.010	0.0657	8.29
	0.015	0.1071	
	0.020	0.1459	
	0.001*	0.0125**	18.94***
	0.002*	0.0297**	
	0.003*	0.0491**	
	0.005	0.0414	10.35
	0.010	0.0892	
	0.015	0.1415	

*equiv l⁻¹**kg equiv⁻¹ min⁻¹***kg² equiv⁻² min⁻¹

TABLE III

COMPARISON OF TERTIARY AMINE (DMCHA) WITH ORGANOTIN (DBTDL) CATALYSTS IN THE REACTION OF PHENOL AND BENZYL ALCOHOL WITH PHENYL ISOCYANATE IN DIOXANE AT 25°C

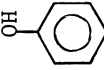
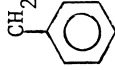
	DMCHA		DBTDL	
	k_{cat}	$(\text{kg mole}^{-2} \text{min}^{-1})$	mole/l	$\text{kg mole}^{-1} \text{min}^{-1}$
				$\text{kg}^{1.5} \text{mole}^{-1.5} \text{min}^{-1}$
	10.35		0.0005	0.0186
			0.0010	0.0299
			0.0015	0.0382
	9.88		0.0001	0.0918
			0.0002	0.1979
			0.0003	0.3268
Relative reactivity:				
$\frac{(k_{cat})_{\text{PhCH}_2\text{OH}}}{(k_{cat})_{\text{PhOH}}}$	0.95		-	26.27

TABLE IV

EFFECT OF TERTIARY AMINE CATALYST ON REACTIVITY OF PHENOL AND ETHYL ALCOHOL WITH PHENYL ISOCYANATE²¹

[PhNCO] = [ROH] = 0.24 mole/l

Solvent: Bu₂O

Temp.: 25°C

Catalyst	$k_o \times 10^{-4}$ 1 mole ⁻¹ sec ⁻¹	$k_c \times 10^4$ 1 mole ⁻¹ sec ⁻¹	k_c/k_o
	None	[Et ₃ N] = 0.03 mole l ⁻¹	
PhOH	0.01	12.0	1200
C ₂ H ₅ OH	0.3	12.7	42.3
Relative reactivity:			
$\frac{k_{\text{EtOH}}}{k_{\text{PhOH}}}$	30	1.06	-

TABLE V
EFFECT OF SOLVENTS ON REACTIVITY OF PHENOL WITH PHENYL ISOCYANATE AT 25°C

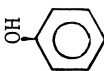
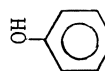
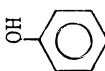
Model Phenol	Solvent	Catalyst DMCHA mole/l	k_{exp} $\frac{\text{kg mole}^{-1} \text{min}^{-1}}{\text{kg mole}^{-1} \text{min}^{-1}}$	k_{cat} $\frac{\text{kg mole}^{-2} \text{min}^{-1}}{\text{kg mole}^{-1} \text{min}^{-1}}$
	Dioxane	0.005	0.0414	10.35
		0.010	0.0892	
		0.015	0.1415	
	Toluene	0.001	0.0276	34.89
		0.002	0.0664	
		0.003	0.1082	
	DMF	0.00004	0.0283	955.88
		0.00007	0.0572	
		0.00010	0.089	

TABLE VI
EFFECT OF CATALYSTS ON THE REACTIVITY OF PHENOL BENZYL
ALCOHOL AND ETHYL ALCOHOL WITH PHENYL ISOCYANATE

	Non-Catalyzed	DBTDL Catalyzed	Amine Catalyzed	
$\frac{(k)_{EtOH}}{(k)_{PhOH}}$	30*	-	1.06*	$\frac{(k_{cat})_{EtOH}}{(k_{cat})_{PhOH}}$
$\frac{(k)_{PhCH_2OH}}{(k)_{PhOH}}$	-	26.27**	0.95**	$\frac{(k_{cat})_{PhCH_2OH}}{(k_{cat})_{PhOH}}$

* (21) T = 20°C; Bu₂O

** T = 25°C; Dioxane

hydroxyl groups, which is presumably due to electronic effects of the substituents on the polarizability of phenols. The electron donating substituent ($-\text{CH}_3$) increased the electron density on the hydroxyl group of the phenol and consequently decreased the overall polarizability resulting in lower reactivity. In this case the electronic effect of the substituent had a significantly more pronounced influence on the reactivity than the steric hindrance due to the substituent.

The presence of the electron donor ($-\text{O}-$) in the vicinity of the phenolic hydroxyl activated the $-\text{OH}$ group through induced polarization due to hydrogen bonding and therefore, increased reactivity was observed. Similarly, the polarizability of the phenolic hydroxyl groups by the tertiary amine catalyst is responsible for the multi order (1200 x) increase in the reactivity compared to the non-catalyzed reaction with isocyanate (see Table IV).

The action of the tin catalyst was found to be quite different from the action of the tertiary amine catalyst. In the presence of the amine catalyst the reactivity of the phenol and benzyl alcohol was approximately equal (see Table IV). In the case of DBTDL, the reactivity ratio was similar to that of the non-catalyzed reaction, which indicates that the polarization of the isocyanate by the tin catalyst due to complex formation presumably played an important role in the reaction catalysis (see Table VI).

The reaction of the phenol with isocyanate, catalyzed by the tertiary amine, was very sensitive to the type of solvent used. The observed increase in the reactivity is due to the combined effects of the relative permittivity and the specific solvation of the reactants by the solvents.

Acknowledgments

The authors wish to express their appreciation for the financial support of this investigation to the Ashland Chemical Company.

Literature Cited

1. A. Khawam, U. S. Pat. 3,063,964 (to Allied Chemical Corp.), Nov. 13, 1962.
2. R. F. Sterling, U. S. Pat. 2,608,536 (to Westinghouse Electric Corp.), Aug. 26, 1952.
3. H. H. Ender, U. S. Pat. 3,271,313 (to Union Carbide Corp.), Sept. 6, 1966.
4. R. W. Quarles and J. A. Baumann, U. S. Pat. 3,298,973 (to Union Carbide Corp.), Jan. 17, 1967.
5. M. Cenker and P. T. Kan, U. S. Pat. 3,732,187 (to BASF Wyandotte Corp.), May 8, 1973.

6. E. A. Dickert, U. S. Pat. 3,872,034 (to Cook Paint and Varnish Co.), March 18, 1975.
7. D. B. Davis, E. E. Jones and R. E. Morgan, Jr., U. S. Pat. 3,598,771 (to Dow Chemical Co.), Aug. 10, 1971.
8. A. Heslinga and P. J. Napjus, Ger. Pat. 1,197,614 (to Chemische Fabrik Kalk G.m.b.H.), July 29, 1965.
9. J. S. McFarling, U. S. Pat. 3,770,671 (to Owens-Corning Fiberglass Corp.), Nov. 6, 1973.
10. W. C. Forster, U. S. Pat. 3,470,118 (to Reichhold Chemicals, Inc.), Sept. 30, 1969.
11. K. D. Longley, F. Park and C. Bernstein, U. S. Pat. 3,682,845 (to Witco Chemical Corp.), Aug. 8, 1972.
12. E. F. Cox, W. H. Cook and F. Hostettler, U. S. Pat. 3,186,969 (to Union Carbide Corp.), June 1, 1965.
13. F. M. Kujawa and J. A. Stone, U. S. Pat. 3,499,961 (to Hooker Chemical Corp.), March 10, 1971.
14. E. F. Cox, W. H. Cook and F. Hostettler, U. S. Pat. 3,245,924 (to Union Carbide Corp.), April 12, 1966.
15. G. D. Edwards, D. M. Rice and R. L. Soulen, U. S. Pat. 3,297,597 (to Jefferson Chemical Co.), Jan. 10, 1967.
16. D. H. Chadwick, Can. Pat. 856,311 (to Mobay Chemical Co.), Nov. 11, 1970.
17. E. F. Cox and R. J. Knopf, U. S. Pat. 3,436,373 (to Union Carbide Corp.), April 1, 1969.
18. R. J. Schafer, L. A. Baker, G. L. Linden, K. C. Frisch and V. Tripathi, *J. Cell. Plastics* 14, No. 3, 146 (1978).
19. A. J. Papa and F. E. Critchfield, *J. Cell. Plastics* 15, No. 5, 258 (1979).
20. G. Borkent, *Advances in Urethane Science and Technology*, edited by K. C. Frisch and S. L. Reegen, Vol. 3, p. 1 (1973), Technomic Publishing Co., Westport, Conn.
21. J. W. Baker and J. Gaunt, *J. Chem. Soc.* (1949), 9, 19, 27.

RECEIVED April 30, 1981.

Reactivity Studies and Cast Elastomers Based on *trans*-Cyclohexane-1,4-Diisocyanate and 1,4-Phenylene Diisocyanates

S. W. WONG, W. J. JUANG, V. OLGAC, and K. C. FRISCH
Polymer Institute, University of Detroit, Detroit, MI 48221

G. HEINRICHS, and P. HENTSCHEL

Research Department, Akzo Corporation, Oburnberg, West Germany

p-Phenylene diisocyanate (PPDI) and *trans*-cyclohexane-1,4-diisocyanate (CHDI), produced by the Hofmann degradation of the corresponding acid amides (1) have become available in developmental quantities for polyurethane production (2). Due to the symmetrical structure of both these molecules and their rigid, rod-like molecular shape, a very orderly structure in the build-up of the hard segments will be promoted in the polyurethane system. These structural features could enable the resulting elastomers to perform better under high and low temperature conditions and to achieve high modulus. Previous kinetic studies (3-7) showed that PPDI had a high reactivity, but no kinetic data were available for the reactivity of CHDI. Three model isocyanate reactions catalyzed with both tertiary amine and organotin catalysts were carried out with PPDI or CHDI and *n*-butanol (urethane formation) and water (urea formation) as well as cyclotrimerization (isocyanurate formation) in suitable solvents (toluene, cellosolve acetate and butyl acetate). Four widely used commercial diisocyanates, 4,4'-diphenylmethane diisocyanate (MDI), 1,5-naphthalene diisocyanate (NDI), isophorone diisocyanate (IPDI) and 4,4'-methylene bis(cyclohexyl) diisocyanate (HMDI) were included for comparison.

Sample formulations of cast urethane elastomers applicable to conventional industry processing techniques were developed, and the physical properties of the resulting products determined.

Experimental

Materials and Purification. The diisocyanates employed for kinetic studies were distilled prior to use. Reagent grade *n*-butanol was treated with sodium

(10% by weight) and distilled. Distilled water was used for the study of the urea formation. Solvents used were toluene, cellosolve acetate and butyl acetate. Reagent grade toluene was purified by boiling under reflux over sodium and distilled. Cellosolve acetate was refluxed over phosphorus pentoxide and distilled. Catalysts employed in these reactions were dibutyltin dilaurate (T-12), diazabicyclo(2,2,2)octane (Dabco) and N,N',N''-tris(dimethylaminopropyl) hexahydrotriazine (Polycat 41) were used directly without any further purification.

Kinetic Studies. Kinetic studies of the three types of reactions of PPDI and CHDI, together with those of the four commercially available diisocyanates, MDI, NDI, IPDI and HMDI, with catalysts were carried out in solvents. The reaction conditions for the kinetic runs are described in Table I.

The reactions were carried out in a 300 ml round-bottom flask, equipped with a magnetically stirring device, a reflux condenser, and a nitrogen inlet tube. 25 ml of the diisocyanate solution was introduced into the reactor and placed in a thermo-regulated oil bath. The solution of the hydroxyl component containing the catalyst in a 25 ml volumetric flask was also kept in the same oil bath. After the reactants had reached the desired temperature, the hydroxyl component-catalyst solution was poured into the reactor. The time when half of the solution had been added was recorded as the starting point of the reaction. Constant stirring and flow of nitrogen was maintained during the reaction. Samples of the reaction mixture were pipetted at measured time intervals and the isocyanate content determined by means of the di-*n*-butylamine method.

Preparation of Cast Elastomers. The cast elastomers were prepared in a two-step procedure. First prepolymers were made from one polyether polyol (poly(oxytetramethylene) glycol of 1000 M.W., (POTMG)) and two polyester polyols (adipate polyester of 2000 M.W. (PAG) and polycaprolactone of 1250 M.W. (PCL)) by reaction with the corresponding diisocyanates (MDI, PPDI, CHDI or NDI) at an NCO/OH ratio of 2/1. The temperature was maintained at 80°C and periodic samples were withdrawn to determine the isocyanate content. When the isocyanate content of the mixture reached within 0.3% of the calculated value, the reaction was stopped by cooling. The prepolymer could be kept for a period of six months in the absence of moisture. The isocyanate-terminated prepolymers were then chain-extended with

TABLE I. REACTION RATES OF CATALYZED DIISOCYANATE REACTIONS.

OH Components	Reaction Conditions					
	Urethane			Urea		
Diisocyanate	n-BuOH	0.12 mole l ⁻¹	H ₂ O	0.12 mole l ⁻¹		
Catalyst	R(NCO) ₂	0.06 mole kg ⁻¹	R(NCO) ₂	0.12 mole kg ⁻¹		
Solvent	T-12	0.0002 mole l ⁻¹	Dabco	0.004 mole l ⁻¹		
Temp., °C	Toluene		Cellosolve acetate			
	50		50			40
	Reaction Rate and Activation Energies					
	k _{exp} (A)	t _{1/2} min	ΔE _a kcal	k _{exp} (A)	t _{1/2} min	ΔE _a kcal
Diisocyanates	l mole ⁻¹ min ⁻¹	min	kcal	l mole ⁻¹ min ⁻¹	min	kcal
PPDI	9.17 (8.56 x 10 ⁸)	1.18	11.76	0.43 (5.95 x 10 ³)	19	6.19
NDI	1.81	9.2		0.29	29	
MDI	4.93	3.4		0.20	42	
CHDI	1.40 (1.57 x 10 ¹²)	11.9	17.78	0.002 (1.41 x 10 ⁶)	3623	13.12
IPDI	0.73	22.8		0.001	8089	
HMDI	0.64	26.0		0.001	8226	
				k _{exp} (A)	t _{1/2} min	ΔE _a kcal
				l mole ⁻¹ min ⁻¹	min	kcal
				0.0675 (6.34 x 10 ⁷)	53	12.87
				0.045	79	
				0.0011 (2.05 x 10 ⁴)	3247	10.37
				0.0006	6374	
				0.0006	6374	

T-12 : dibutyltin dilaurate
 Dabco : diazabicyclo(2,2,2)octane
 Polycat 41 : N,N',N"-tris(dimethylaminopropyl)hexahydrotriazine.

1,4-butanediol (1,4-BD), 2,2'-p-phenylenedioxydiethanol (HQEE) or a blend of trimethylolpropane (TMP) with 1,4-BD. The final NCO/OH ratio was kept at 1.05/1. The prepolymers were heated to 80-100°C to give a workable viscosity and the liquid or molten chain extender was then added to the prepolymer. The respective catalysts were used in CHDI-prepolymers in order to accelerate the cure. The mixture was then press-molded in a Carver press at 100°C for from 1/2 to 1 hour and post-cured for 16 hours at the same temperature.

Results and Discussion

Kinetic Studies. Plots of the experimental data are shown in Figures 1-3, which indicate that both the urethane and urea formations followed second order reaction up to 50% conversion. Although PPDI has two isocyanate groups on the same benzene nucleus, the two isocyanate groups did not exhibit a large activating influence on the reactivity of each other in the reaction with n-butanol catalyzed by T-12. Unlike the study by Burkus and Eckert (4) on the reaction of diisocyanates and l-butanol catalyzed with triethylendiamine having a k_1/k_2 of 8.40, the k_1/k_2 of this reaction was 2. This means that catalyst T-12 activates the second isocyanate group nearly to the same reactivity level as the first isocyanate group. In the case of MDI, the methylene bridge effectively isolates the two isocyanate functions. In the case of the aliphatic isocyanates, this effect was even less apparent. The isocyanate-water reactions (formation of urea) showed the same results. The reaction of the cyclotrimerization of the diisocyanates catalyzed with Polycat 41 in butyl acetate followed second order up to 30% conversion as shown in Fig. 3; then the trimer started to precipitate. It was also found that the least square fitted straight line did not pass through the origin. This may be due to the mechanism of a complex formed between the diisocyanates with the catalyst at the beginning of the reaction; then the cyclotrimerization proceeds at a much slower rate. This has to be proven with more studies.

The rates of these three catalyzed reactions of diisocyanates are listed in Table I under identical conditions of reactants and catalyst concentrations and temperature. The half time, $t_{1/2}$, of the reactions was calculated from the reaction constants. The reactions of PPDI and CHDI were carried out at three different temperatures and the calculated activation energies and frequency factors are listed in Table I.

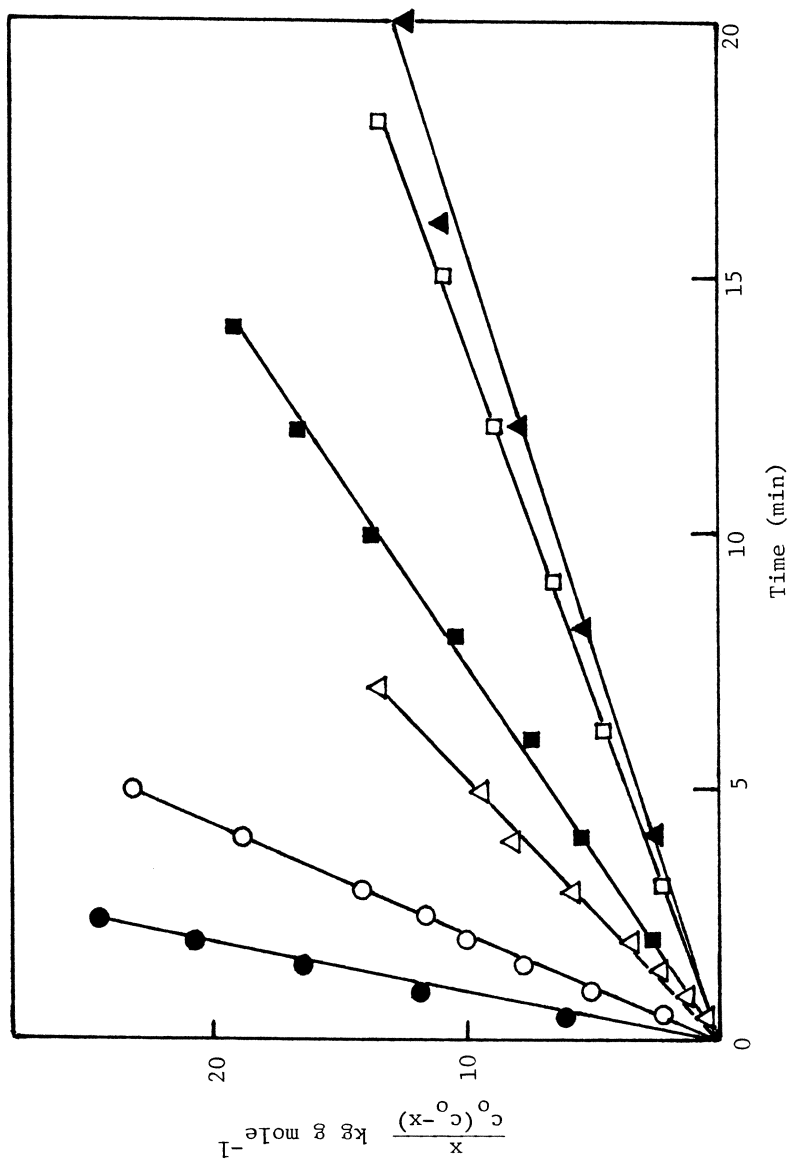


Figure 1. Second-order plot for reaction between diisocyanates and n-butanol in toluene catalyzed by T-12 at 50°C: $[R(NCO)_2] = 0.06$ g mol/kg; $[n\text{-BuOH}] = 0.12$ g mol/L; $[T-12] = 0.0002$ g mol/L. Key: ●, PPDI; ○, MDI; △, CHDI; ■, HMDI; ▲, IPDI; □, NDI.

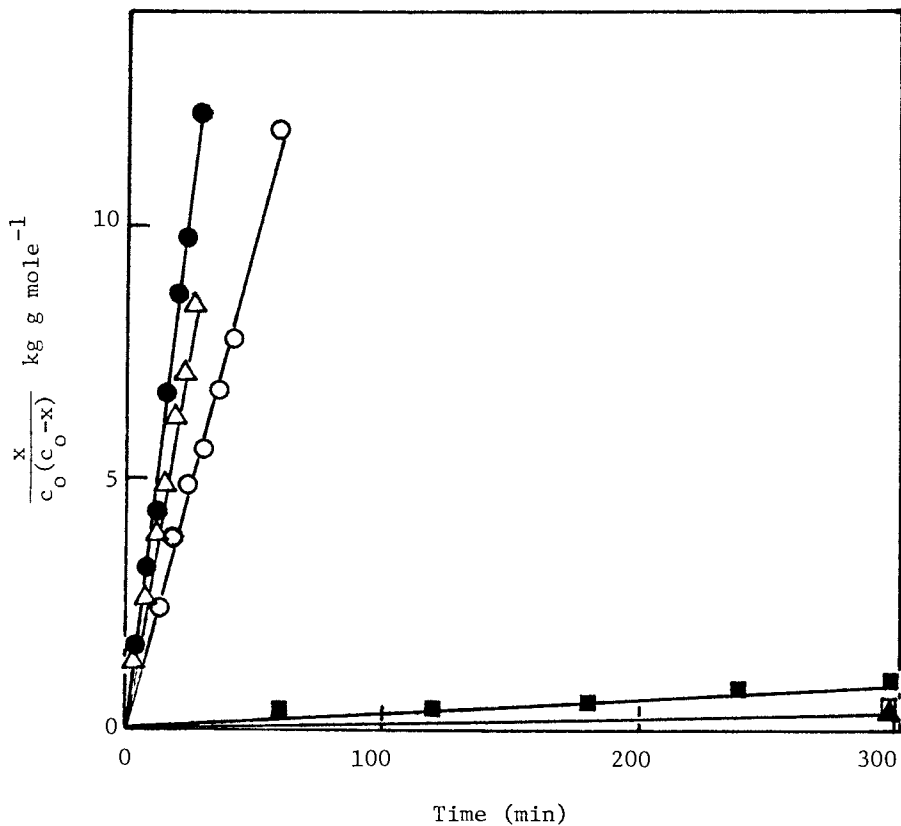


Figure 2. Second-order plot of reaction of diisocyanates and water in cellosolve acetate catalyzed by triethylene diamine at 50°C: $[R(NCO)_2] = 0.12 \text{ g mol/kg}$; $[H_2O] = 0.12 \text{ g mol/L}$; $[Dabco] = 0.004 \text{ g mol/L}$. Key: ●, PPD1; ○, MDI; ■, CHDI; □, IPDI; ▲, HMDI; △, NDI.

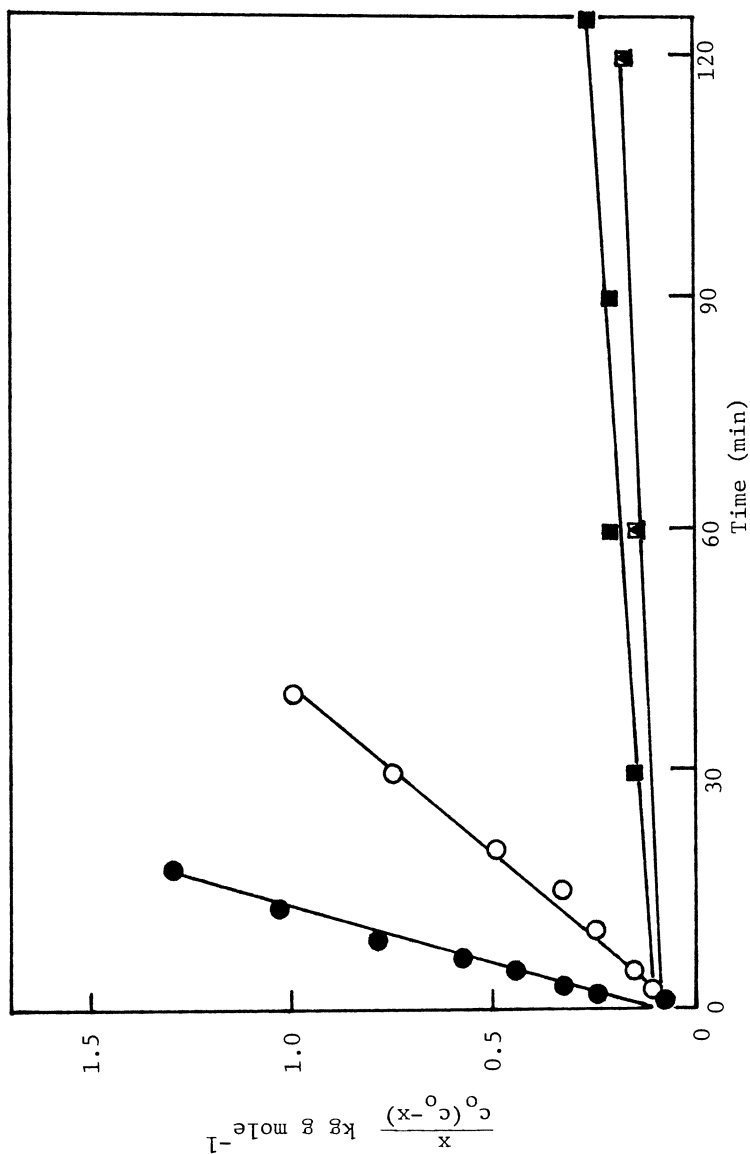


Figure 3. Second-order plot of trimerization reaction of diisocyanate in butyl acetate catalyzed by polycat 41 at 40°C: $[R(NCO)_2] : 0.28 \text{ mol kg}^{-1}$, $[Polycat 41] : 0.0025 \text{ mol}^{-1}$. Key: ●, PFDI; ○, MDI; ■, CHDI; □, IPDI; ▲, HMDI.

Based on the reactivity of MDI as 1, the relative reactivities of the diisocyanates in the three catalyzed reactions were as follows:

1. Urethane formation (with *n*-butanol in toluene at 50°C using dibutyltin dilaurate as catalyst) -
 PPDI : MDI : NDI : CHDI : IPDI : HMDI = 1.85 : 0.37 : 1 : 0.28 : 0.15 : 0.13.

2. Urea formation (with water in cellosolve acetate at 50°C using diazabicyclo(2,2,2)octane as catalyst -
 PPDI : NDI : MDI : CHDI : IPDI : HMDI = 2.15 : 1.45 : 1 : 0.01 : 0.0005 : 0.005.

3. Isocyanurate formation (cyclotrimerization catalyzed with *N,N',N''*-tris(dimethylaminopropyl) hexahydrotriazine) -
 PPDI : MDI : CHDI : IPDI : HMDI = 1.5 : 1 : 0.024 : 0.013 : 0.013.

These conclusions were in general agreement with the study carried out by Akzo Research Laboratories, Oburnberg, Germany (8), on the reaction between diisocyanates and excess ethanol or *n*-octanol at 80°C. The order of reactivities of the diisocyanates were as follows: MDI > TDI > XDI >> HDI > trans-CHDI > IPDI ≈ cis-CHDI > HMDI.

Cast Elastomers. Table II shows the elastomers prepared from MDI, PPDI, CHDI and NDI with POTMG, M.W. 1000, chain-extended with 1,4-BD. Catalyst T-12 was used in the CHDI-based prepolymer to accelerate the reaction and to reduce the molding time. As expected, the PPDI elastomers had a very short pot life but were still manageable in processing. The resulting elastomers exhibited substantially better properties compared to the corresponding MDI-based elastomers, especially the high temperature resistance and the tensile strength at 300% elongation at temperatures ranging from -20° to 150°C, as shown in Fig. 4. The CHDI-based elastomers exhibited lower physical properties at room temperature, but exhibited a surprisingly high retention of properties at higher temperatures. CHDI also had the advantage of light stability over the two aromatic diisocyanates. Table III shows the elastomers prepared from MDI, PPDI and CHDI with PAG, M.W. 2000, chain-extended with 1,4-BD, 1,4-HQEE or blends of TMP and 1,4-BD at a 25/75 ratio. Catalyst Dabco 33 LV was used in all the cases. Again, the PPDI-based elastomers showed excellent properties both at room and elevated temperatures (Fig. 5). The high value of compression set could be overcome by introducing the aromatic chain-extender HQEE or crosslinkers such as TMP.

TABLE II
COMPOSITION AND PROPERTIES OF POLYURETHANE CAST
ELASTOMERS

COMPOSITION:

Prepolymer - POTMG 1000: diisocyanate at 1:2

Extender - 1,4-BD (95% theoretical)

Diisocyanates	MDI	PPDI	CHDI	NDI
Diisocyanate, %	31.94	23.10	23.76	28.27
NCO Content, %	5.70	6.36	6.34	5.79
T-12, %	-	-	0.0037	-

PROPERTIES:

Density, g/ml	1.12	1.14	1.21	1.14
Shore Hardness:				
A	78	94	97	95
D	33	48	50	47
Stress, MPa:				
At 100% Elongation	5.65	13.12	12.16	8.96
At 300% Elongation	10.04	17.31	14.53	13.69
Tensile Strength	26.41	33.19	22.26	22.87
Elongation, %	563	512	565	800
Tear Resistance, KN/m				
Graves	64.09	98.76	83.35	55.16
Split	21.36	20.14	37.47	11.38
Bashore Rebound, %	54	58	60	46
Compression Set, % (70°C, 22 Hrs.)	25	31	37	32

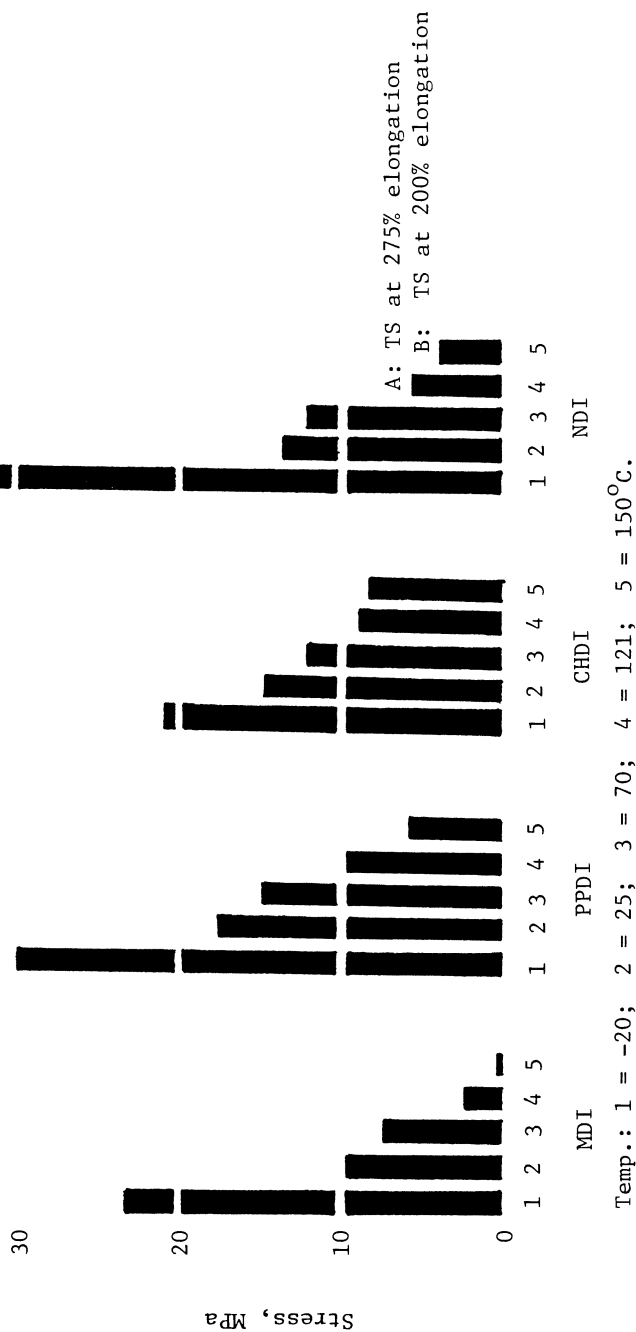


Figure 4. Stress properties at 300% elongation of polyether polyol elastomers at various temperatures (NCO/POI/MG/1,4-BD = 2/1/0.95).

TABLE III. COMPOSITION AND PROPERTIES OF POLYURETHANE CAST ELASTOMERS

	1,4-BD			HQEE			TMP/1,4-BD		
	MDI	PPDI	CHDI	MDI	PPDI	CHDI	MDI	PPDI	CHDI
<u>COMPOSITION:</u>									
Prepolymer - PAG : Diisocyanate at 1 : 2									
Extender - 95% Theoretical									
Diisocyanates									
Diisocyanate, %	19.01	13.06	13.48	18.26	12.51	12.92	19.01	13.06	13.48
NCO Content, %	3.31	3.56	3.54	3.31	3.56	3.54	3.31	3.56	3.54
Dabco 33LV, %	0.025	0.013	0.025	0.024	0.012	0.024	0.025	0.025	0.025
<u>PROPERTIES:</u>									
Density, g/ml	1.21	1.16	1.13	1.25	1.16	1.14	1.19	1.13	1.11
Shore Hardness:									
A	55	80	80	82	84	86	55	67	78
D	15	30	30	33	36	35	15	20	28
Stress, MPa:									
At 100% Elongation	2.08	4.10	5.83	4.73	5.59	7.61	1.72	2.63	4.40
At 300% Elongation	3.64	7.57	11.15	9.20	11.33	15.13	3.18	4.24	9.27
Tensile Strength	32.70	37.21	29.87	34.65	43.29	28.70	27.94	39.68	38.56
Elongation, %	591	822	713	590	730	635	577	698	720
Tear Resistance, KN/m:									
Graves	47.8	82.5	94.6	74.0	93.5	68.6	38.2	49.0	78.6
Split	18.7	60.8	71.6	36.4	58.7	47.1	11.6	30.5	45.4
Bashore Rebound, %	39	46	48	42	48	51	26	38	48
Compression Set, % (70°C, 22 Hrs.)	57	65	56	36	21	33	12	12	33

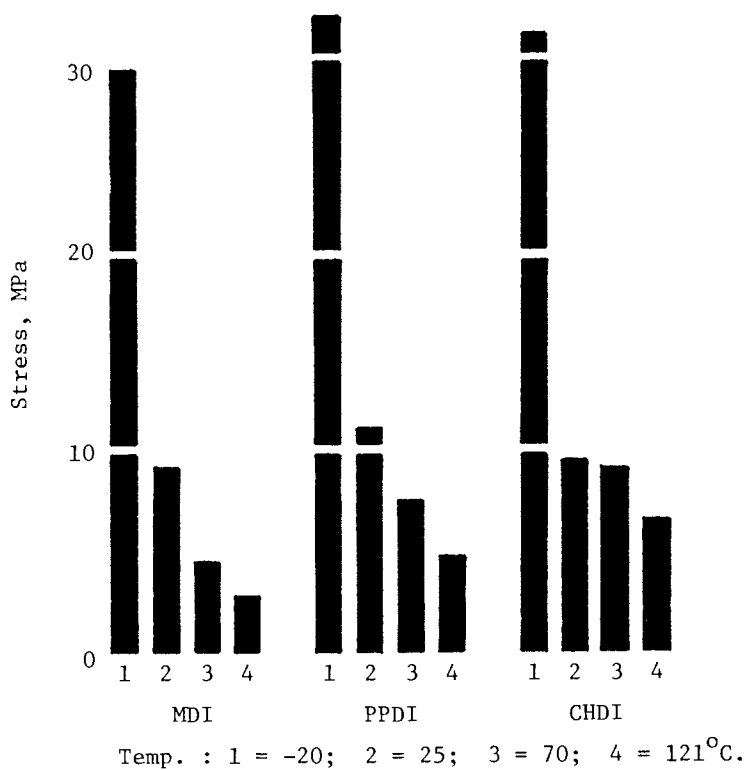


Figure 5. Stress properties at 300% elongation of polyester polyol elastomers at various temperatures (NCO/PAG/HQEE = 2/1/0.95).

Both PPDI- and CHDI-based elastomers had high modulus and hardness which resemble those of diamine-cured elastomers. The diol-cured case elastomers of PPDI (CHDI) can be seriously considered as a replacement for diamine-cured TDI-based cast elastomers.

Acknowledgments

The financial support of this work was granted by the Armak Company and Akzo Chemie and is gratefully acknowledged.

Literature Cited

1. H. G. Zengel, International Conference on Cellular and Non-cellular Urethanes, S.P.I. and S.F.K. Strasbourg, France, June, 1980. Preprint Book, Carl Hauser Verlag, pp. 315-325.
2. Technical Data Sheet on PPDI and CHDI, Armak Co.
3. M. E. Bailey, V. Kirss and R. G. Spaunburgh, Ind. Eng. Chem. **48**, 794 (1956).
4. J. Burkus and C. F. Eckert, J. Am. Chem. Soc. **80**, 5948 (1958).
5. W. Cooper, R. W. Pearson and S. Darke, The Industrial Chemist, **36**, 121 (1960).
6. T. Yokoyama and T. Iwasa, Kogyo, Kagaku Zasshi, **63**, 1835-9 (1960).
7. T. Tanaka, T. Yokoyama and T. Iwasa, Kogyo, Kagaku Zasshi, **66**, 158-60 (1963).
8. Akzo Corp., Research Dept., Oburnberg, Germany, private communication.

RECEIVED April 30, 1981.

Thermoplastic Polyurethane Elastomer Melt Polymerization Study

C. S. SCHOLLENBERGER, K. DINBERGS, and F. D. STEWART

BF Goodrich Research & Development Center, Brecksville, OH 44141

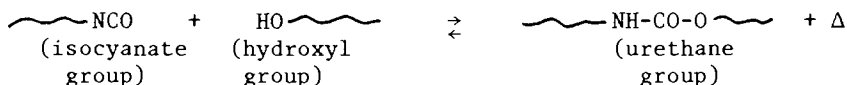
Due to the relatively low volatility, compatibility, high reactivity, and liquid or low melting nature of their reactant components - the diisocyanate, the macroglycol, and the small chain-extender glycol - polyurethanes can be produced readily in the melt by the polyaddition process, even at moderate temperatures and atmospheric pressure. Such polymerizability is attractive in that it enables the polymers to be formed quickly, efficiently, and in a relatively small space. There are no large solvent storage tanks to accommodate, no solvents nor reactants to recover and repurify for recycle, no contaminated water to clean before discharge, and no atmospheric pollution by gases or particulates to deal with. In an era of high capital costs, keen commercial competition, and worldwide concern for a clean environment a manufacturing process such as polyurethane elastomer melt polymerization obviously has much to recommend it.

Polymer Formation. In the formation of thermoplastic polyurethane elastomers the reactants - diisocyanate, macroglycol, and small chain extender glycol - interact and join together end-to-end to produce essentially linear polymer chains. The chemical bond produced in the chain-building linkages is the urethane group which is covalent in nature and reasonably strong, although the strength varies with structure. Urethane formation is shown in Equation 1.

0097-6156/81/0172-0433\$09.25/0

© 1981 American Chemical Society

Equation 1. Urethane Formation



Heat of reaction is reported to be -52 kcal/mole in the case of the hexamethylene diisocyanate and 1,4-butanediol reaction.¹ The same diisocyanate, reacting with poly(ethylene adipate) glycol at 100°C was found to show a reaction velocity constant, k , of $0.00083 \text{ l mol}^{-1} \text{ sec}^{-1}$, with an activation energy, E , of 11.0 kcal/mole.^{2,4} At the same temperature diphenylmethane-4,4'-diisocyanate (MDI) reportedly reacted with poly (diethylene adipate) glycol in mono-chlorobenzene with $k = 0.00091 \text{ l mole}^{-1} \text{ sec}^{-1}$, and $E = 10.5 \text{ kcal/mole}$.^{3,4}

As Equation 1 indicates, urethane formation is an equilibrium reaction. The degree of dissociation of urethane product into reactant isocyanate and hydroxyl groups is dependent upon the ambient temperature and is a constant at given temperature (Equation 2).

Equation 2. Urethane Equilibrium Constant

$$\frac{[\text{NHCOO}]}{[\text{NCO}][\text{OH}]} = K$$

We will later note manifestations of the chemical equilibrium in urethane polymerizations.

Polymer Structure. In thermoplastic polyurethane elastomer formation the polymerization produces polymer primary chains which consist of alternating urethane-sparse soft segments (diisocyanate-macroglycol linear reaction product) and urethane-rich hard segments (diisocyanate-chain extender linear reaction products). These primary chains tend to "virtually crosslink" and "virtually chain extend" with one another, principally through the association of their hard segments, due to the hydrogen bonding of their urethane groups, the association of aromatic π electrons, etc., producing a giant "virtual network" of polymer chains, and thus elasticity in the product. These virtual linkages are relatively labile and are reversible with heat and solvation, permitting thermoplastic and solution processing of the polymers. The foregoing is depicted schematically in Figure 1.

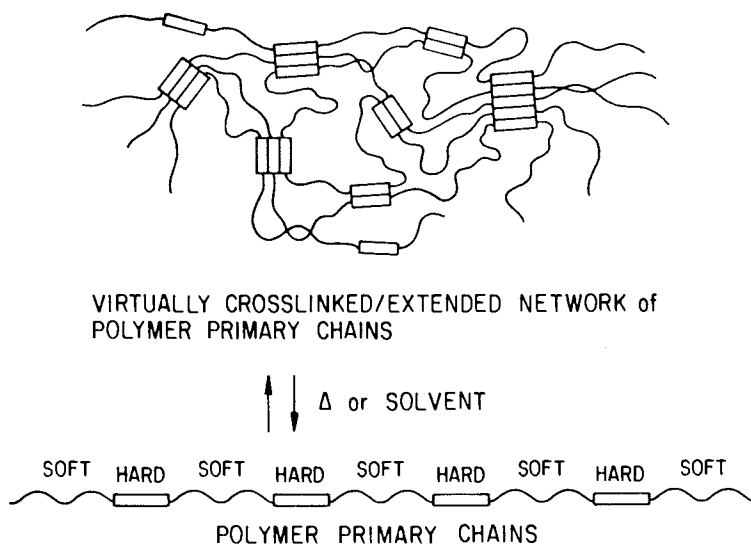


Figure 1. Thermoplastic urethane elastomer chain organization.

It is thus seen that thermoplastic polyurethane elastomers have two types of thermal lability. That depicted in Figure 1 is benign and the basis of the versatile processability of this polymer class. That depicted in Equation 1 becomes important at high temperatures and cannot be considered to be totally benign in that it involves the reversible dissociation of polymer primary chain bonds, which separations can be irreversible depending upon the polymer environment. It would seem that such dissociation must predominate in the areas of highest urethane group concentration, namely the polymer hard segments and this suggests the possibility of some "scrambling" of polymer segmented structure, e.g., during polymer melt processing, rheology studies, etc. and other problems which we do not address in this paper. It is the polymer changes related to Equation 1 that are the primary concern of the present paper.

Although there is considerable published literature on the relation of polyurethane properties to their chemical and physical structures, considerably less has appeared concerning the detailed nature of urethane polymerization. The thermoset nature of the classical polyurethane systems, which has provided fewer opportunities and thus less scientific interest for the study of the intermediate stages and course of urethane polymerization, likely helps account for this.

Published information on urethane polymerization detail largely concerns thermoset urethane elastomers systems.⁴⁻¹³ In particular, the work of Macosko et. al. is called to attention. The present paper supplements this literature with information on the full course of linear thermoplastic urethane elastomer formation conducted under random melt polymerization conditions in a slightly modified Brabender PlastiCorder reactor. Viscosity and temperature variations with time were continuously recorded and the effects of several relevant polymerization variables - temperature, composition, catalyst, stabilizer, macroglycol acid number, shortstop - are reported. The paper will also be seen to provide additional insight into the nature and behavior of thermoplastic polyurethane elastomers.

Experimental Part

Materials. The reactants used in this study and their designations are listed in Table I.

Table I
Reactants Used in the Present Study

Name	Designation	\bar{M}_n	Acid Number	Purity (%)	Hydrolyzable Chloride (ppm)	Boiling Point (°C)
PTAd ^a	I	1073	2.40	-	-	-
PTAd ^a	XVI	1105	2.00	-	-	-
PTAd ^a	III	1014	0.10	-	-	-
PTAd ^a	V	999	0.10	-	-	-
PTAd ^a	VI	963	0.30	-	-	-
PTAd ^a	VII	1068	0.15	-	-	-
MDI ^b	II	-	-	99.5	9	-
MDI ^b	IV	-	-	99.0	5	-
MDI ^b	VIII	-	-	99.6	1	-
1,4-BDO ^c	IX	-	-	100	-	-
1,4-BDO ^c	X	-	-	100	-	-
EDO ^d	XI	-	-	100	-	-
Stannous Octate ^e	XII	-	-	-	-	-
1-Propanol ^f	XIII	-	-	-	-	98
1-Decanol ^g	XIV	-	-	-	-	231
TPU ^h	20	-	-	-	-	-
Irganox 1010 ⁱ	XV	-	-	-	-	-

^a poly(tetramethylene adipate) glycol (our laboratory)

^b diphenylmethane-4,4'-diisocyanate (Multrathane M, Mobay Chemical Corp.)

^c 1,4-butanediol (Antara, General Aniline & Film Corp., distilled from calcium hydride, b.p. 118-120°C/8 mm)

^d ethylene glycol (Union Carbide & Carbon Co., Urethane Grade, distilled from calcium hydride, b.p. 110°C/23 mm)

^e M&T Chemicals, Inc., T9 Catalyst

^f Fisher Scientific Co., No. A-414

^g Eastman Organic Chemicals, No. 370

^h (2.00) MDI/PTAd (MW 1000)/1,4-BDO (thermoplastic polyurethane elastomer, our laboratory)

ⁱ Ciba-Geigy Corp.

Table II provides information on the combinations of Table I reactants that were polymerized in this study, and other additives charged. Urethane polymerization rates prove to be so sensitive to the influence of many adventitious trace contami-

nants that polymerization variables are best studied in sets of runs made from the same reactant batches or lots. Such sets will be apparent in Table II.

The Plasticorder, described as a "torque rheometer" by the supplier, is one version of a practical tool well known and used in the plastics and rubber industries. We believe that our use of the Plasticorder as a polymerization reactor may be unique, and that the instrument is probably not well known in polymer science laboratories, so we felt it appropriate to picture it. Additional detail of the mixing chamber/measuring head and the removable sigma blade rotors is also pictured (see Photographs A, B, and C).

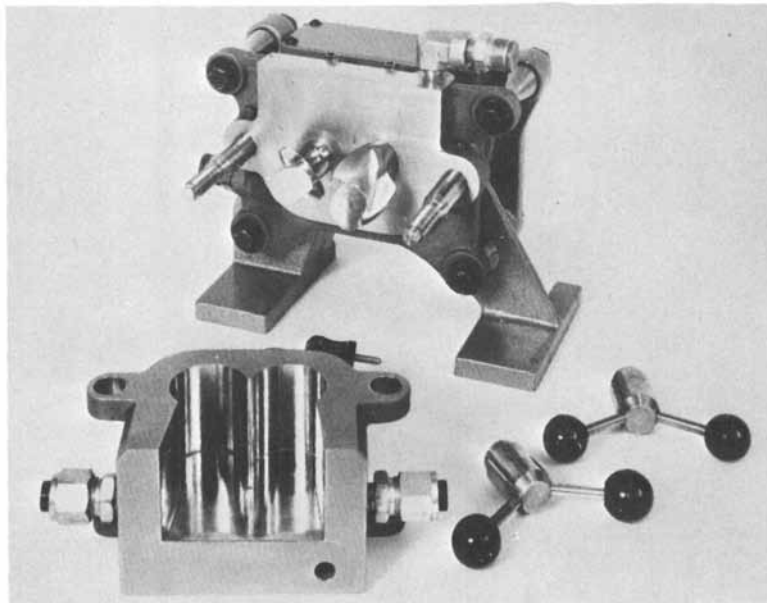
Table II
Reactant Combinations, Additives, and Polymers Used in Present Study

Polymer	Fig.	Ratio (Molar)	Reactants			Other	Polymer Properties Table
			MDI	PTAd	1,4-BDO		
1	2	2.00	II	I	IX	-	III
2	2	2.00	II	I	IX	-	III
3	2	2.00	IV	XVI	X	-	III
4	3	2.00	IV	III	X	-	IV
5	3,9	2.00	IV	III	X	-	IV,X
6	4	2.00	IV	VII	X	0.25% Irganox 1010	XV VI
7	4,11	2.00	VIII	VII	X	0.25% Irganox 1010	XV VI
8	4	2.00	IV	VII	X	0.25% Irganox 1010	XV VI
9	5,7	3.00	IV	VI	X	-	VII,IX
10	6	2.00	IV	VII	EDO XI	0.25% Irganox 1010	XV VIII
11	7	3.00	IV	VI	X	47 ppm stannous octoate XII	IX
12	8	2.00	VIII	V	X	-	-
13	8	2.00	VIII	V	X	71 ppm stannous octoate XII	-
14	9	2.00	IV	III	X	1.0% n-propanol	XIII X
15	9	2.00	IV	III	X	3.0% n-propanol	XIII X
16	10	2.00	IV	VII	X	-	XI
17	10	2.00	IV	VII	X	0.24% 1-decanol	XIV XI
18	10	2.00	IV	VII	X	0.51% 1-decanol	XIV XI
19	11	1.95	VIII	VII	X	0.25% Irganox 1010	XV XIII
20	12	2.00	-	-	-	-	-



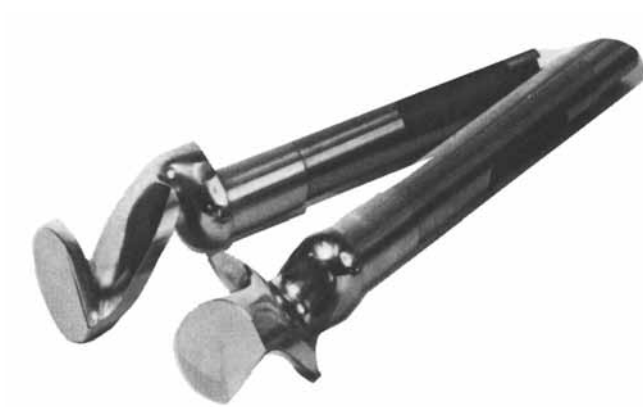
C. W. Brabender Instruments, Inc.

Photograph A. Polymerization reactor and ancillary equipment.



C. W. Brabender Instruments, Inc.

Photograph B. Plasticorder mixing chamber (electrically heated) and measuring head.



C. W. Brabender Instruments, Inc.

Photograph C. Plasticorder removable sigma blade rotors.

Apparatus

Polymerization Reactor. Below is a photograph (A) of the C. W. Brabender Instruments, Inc. (South Hackensack, New Jersey) "Plasti-Corder", and ancillary equipment as was assembled for use as polymerization reactor in the present study.

For the purposes of our study we modified our Plasticorder measuring head slightly by having a ring machined into the steel backplate around each rotor shaft bearing - to accommodate replaceable Teflon O-rings. And we cut a removable U-shaped gasket, conforming to the mixing chamber cross section form, from 10 mil thick Teflon sheet. This gasket was then placed between the removable mixing chamber and the fixed measuring head. The O-ring and the gasket sealed the mixing chamber effectively, preventing the loss of liquid reactants during charging and early polymerization stages.

The Plasticorder mixing chamber unit we used (see photograph (B)) was Catalog No. 28-B (nominal 120 ml capacity, 1450 watts, 230 volts, 60 cycle, with air cooling channel, stock temperature thermocouple, and nitrogen injection ram). We equipped the mixing chamber with removable, stainless steel, sigma blade rotors (catalog No. 2-17AR, see photograph (C)). The drive assembly for the rotors, the measuring head, etc., which we used was part of the C. W. Brabender Instruments, Inc., Plasticorder No. 2G-12, Model PL-V340 (0-200 rpm, etc.).

In the present study we utilized Plasticorder torque values (polymer viscosity) on a relative basis, principally to follow the course of thermoplastic polyurethane elastomer polymerization, and the effect of several relevant variables on this polymerization. These torque data, expressed in meter-grams, served our purposes well, and we have not attempted to translate them to absolute rheological units. Such translation, which is a rather complex problem, has been addressed by others using a different rotor type and other polymers in the Plasticorder.¹⁴ That study concluded that the shear rate, $\dot{\gamma}$, of the Brabender Plasticorder with a somewhat different rotor configuration (roller blade) is in the range of 23 - 228 sec⁻¹ over the rotor speed range of 30 - 200 rpm.

The supplier of the Plasticorder has provided the following approximate relationship, which is relevant to the present study in that it applies to a Plasticorder with a 120 ml mixing chamber with sigma blade rotors:¹⁵

$$\eta \text{ (poises)} = \frac{5 \times T(162)}{\text{rpm}}$$

where T = Plasticorder torque reading in meter-grams
rpm = rotor speed (60 in the present study)

The above relationship could presumably be applied to translate the meter-gram torque values appearing in this study to the approximate level in the standard rheological unit, poises.

Procedure. The procedure we followed in conducting melt polymerizations in the Brabender Plasticorder reactor was as follows. The clean mixing chamber was heated to temperature and ~50g of molten (140°C), previously dried (~0.02% water) PTAd was added. The ~4g of dry 1,4-butanediol at room temperature was added to the PTAd via a hypodermic syringe. The mixing chamber was closed with a Teflon plug cut to fit the mixing chamber throat snugly. Then the rotors were started and the macroglycol and chain extender were mixed together for a half minute. Next, after removing the Teflon plug, ~24g of melted (120°C) MDI (corrected for purity) was added from a wet-tared beaker to the mixing blend in the reaction chamber. The exact amounts of all reactants added were known, of course, and varied slightly depending on the exact amount of PTAd charged and its molecular weight. The addition of the 120°C molten MDI cooled the system momentarily, and this registered on the temperature gauge and chart. The chamber was then closed with the Teflon plug again (the Plasticorder ram was not needed since one starts with a liquid system which neither then nor later needs force to compact it in the chamber). Data-taking (torque, temperature, time) commenced with complete MDI addition. The polymerizing mixture was heated and mixed at 60 rpm for 8 to 20 minutes noting torque and temperature values every minute.

Catalyst and antioxidant when used were thoroughly mixed through the hot macroglycol-chain extender glycol blend before MDI addition. Shortstop when used was added quickly and cleanly to the polymerizing reaction mixture through the mixing chamber throat.

When sampling for isocyanate analysis the mixer rotors were stopped and a sample was quickly withdrawn from the sticky polymerizing mixture by dipping two or three clean spatulas in quick succession through the reactor throat, then resuming mixing and data taking.

At the end of the polymerization stirring and heating were stopped and the mixing chamber was promptly removed from the measuring head. Then, within no more than 2.5 minutes, enough polymer (50 - 60g) for subsequent polymer characterization and mechanical tests was dug from the mixing chamber and pulled from the more rapidly cooling rotor blades. Full polymer recovery for test purposes was not attempted since that takes too long and autoxidation of the hot polymer in air during even moderately long recovery periods is apparent by polymer coloration.

Complete and prompt reactor cleanup is a chore but quite necessary. While still hot the mixing chamber and rotors are

scraped reasonably clean of polymer. Then the mixing chamber is reassembled and PVC or ABS granules are masticated in it as a cleaning compound for 20 minutes. The mixing chamber is again removed and scraped clean. The mixing blades are removed and cleaned. Solvent polishing is required in some areas.

Mastication studies of fully polymerized thermoplastic polyurethane elastomer were performed in the Plasticorder by adding polymer granules at room temperature to the preheated mixing chamber with the rotors in motion.

Following the polymerization method described above, the reactants of Table I were polymerized in the combinations shown in Table II, for the most part in the molar reactant ratio, 2.00 moles MDI/1.00 mole PTAd/1.00 mole chain extender glycol (e.g., 1,4-BDO or EDO). Such a recipe is seen to be in stoichiometric balance with respect to hydroxyl and isocyanate content, and our convention is to refer to it as a (2.0) ratio polymer, the index being the MDI level, with the macroglycol level always set at unity. Thus, a (3.0) ratio polymer is 3.00 MDI/1.00 PTAd/2.00 1,4-BDO with the chain extender glycol level increased to maintain stoichiometric balance of isocyanate and hydroxyl groups.

In one example cited in this paper we polymerized with a deficiency of isocyanate. In such unbalanced recipes it is our convention to write the full recipe so as to make the imbalance clear, e.g., 1.95 MDI/1.00 PTAd/1.00 1,4-BDO.

It will be appreciated that conducting melt polymerizations in the Brabender Plasticorder as described requires adeptness as well as careful attention and the utmost care to avoid burns from the very hot mixing chamber. Heavy gloves must be worn in removing the hot mixing chamber from the measuring head, in sampling from it, in cleaning it, etc. And Photograph (A) shows that we installed the entire Plasticorder unit in a vented hood to avoid contact with reactant vapors.

Test Methods. Prior to testing, the polyurethane preparations were sheeted out on a 4 inch plastics mill at 120° - 140°C and samples for tests or molding were taken from this sheet.

Dilute Solution Viscosity: Polymer dilute solution viscosity was measured at a concentration of 0.400g/dl of N,N-dimethylformamide [DMF, contained 0.05% n-propyliodide stabilizer¹⁶] at 25°C ±0.1°C using an Ostwald-type viscometer.

Solubility: Polymer solubility was checked in tetrahydrofuran and in DMF on polymer samples both 1 and 14 days after polymer preparation. In the test one gram of small pieces of the polymer was rolled in 19 grams of solvent at ~25°C for 24 hours.

Dynamic Extrusion Rheometer T_2 Value: The dynamic extrusion rheometer T_2 values (~processing temperature) were determined in the proprietary BFGoodrich Research dynamic extrusion rheometer¹⁷ according to the established procedure.

Isocyanate Content: Isocyanate levels in polyurethane preparations were measured on ~2g samples taken from the polymerizate and immediately cut into small pieces which were then promptly immersed in excess 0.05 N di(n-butyl)amine solution in dry tetrahydrofuran which was contained in an iodine flask. The gross weight of reagent plus flask was very accurately determined ahead of time to enable the exact weight of the added polyurethane sample to be subsequently determined by difference. Excess di(n-butyl)amine was titrated with 0.05N hydrochloric acid to the bromocresol green endpoint to enable calculation of the sample isocyanate concentration.

Stress-Strain Values: Polyurethane stress-strain properties were measured with the Scott Tensile Tester operated at a jaw separation rate of 20 inches per minute. Test pieces were microdumbbells died out of 25 mil thick compression-molded sheets. The test pieces were pre-conditioned for 24 hours at 50% relative humidity and 25°C, and then tested in this environment.

Results and Discussion

I. Natural Polymerizations

A. (2.0) Ratio Polymers. 1. High Acid Number Polyester Glycol Effects: Figure 2 shows the polymerization viscosity-time-temperature relations for three (2.0) ratio thermoplastic poly(ester-urethane) elastomers. Numbers 1 and 2 were both made from the same reactant lots (I, II, and IX - Table I) at about the same reaction temperatures. High acid number (2.4) polyester was used in these runs. Number 3 was made from reactant lots IV, XVI and X. The polyester used also had high acid number (2.00) and the polymerization temperature was ~200°C. None of these polymerizations was deliberately shortstopped.

Polymers 1 and 2 showed almost identical polymerization rates, but 1 slowed at 5 minutes, and 2 at 5.7 minutes. The longer life of 2 produced a higher torque (viscosity) polymer. This indicated a higher degree of polymerization (DP) in 2 which is attributed to better balanced charging stoichiometry (i.e., OH = NCO). But the DSV and T_2 values of Table 3 indicate a lower final DP for Polymer 2.

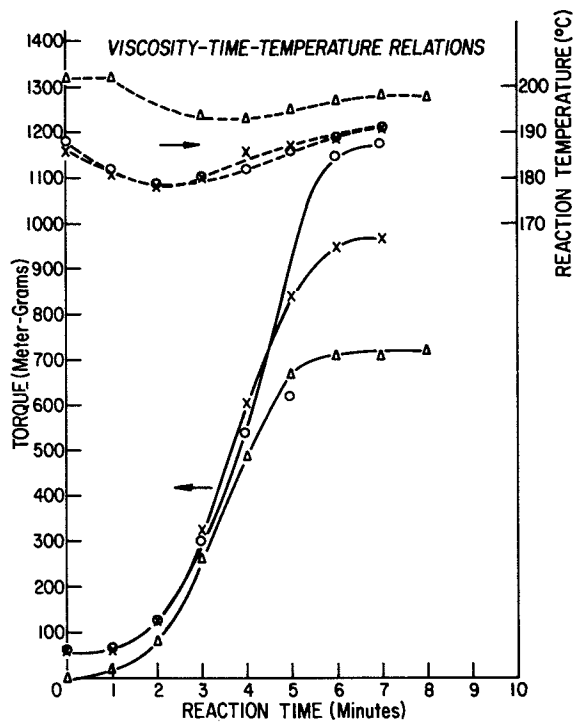


Figure 2. Thermoplastic urethane melt polymerization. Key: X, Polymer 1; O, Polymer 2; Δ, Polymer 3.

Since the foregoing polymers were not deliberately shortstopped, it is likely that the polymerization of 1 subsided earlier than 2 due to a slight isocyanate excess in the initial charge, then subsequently grew during storage due to the spontaneous, unregulated reaction of its unreacted terminal isocyanate groups with atmospheric moisture. This excess NCO might be the amount charged which is equivalent to the (relatively high) carboxyl content of the polyester glycol (PTAd) since such carboxyl does not react with NCO to any degree in such thermoplastic polyurethane elastomer polymerizations.¹⁸

Moderate atmospheric humidity would favor the Polymer 1 post reactor change, whereas high humidity would tend to shortstop the polymer, and low humidity would result in slow but sure molecular weight growth. Polymer 3 formed at about the same rate but leveled off in 6 minutes at lower torque (~700 meter-grams) due in part to its higher polymerization temperature and an inherently lower melt viscosity that the higher MW macroglycol component should confer.

Further data for polymers 1, 2 and 3 appear in Table III.

Table III
Data for Natural Polymers 1, 2, & 3 from
High Acid Number Polyester Glycol

Polymer	1	2	3
Polymerization			
Torque (meter-grams)	970	1175	710
Time (min.)	7	7	7
DSV ^a	1.04	0.927	1.820
Gel (%) ^a	trace	trace	nil
Solubility ^b (THF, DMF)	+,+	-,+	+,+
D.E.R.T ₂ (°C) ^c	136	133	145
Tensile Strength [psi(MPa)]	9500 (65.5)	8900 (61.4)	9700 (66.9)
300% Modulus [psi(MPa)]	1100 (7.58)	1200 (8.27)	1200 (8.27)
Elongation (%)	560	580	505

^aDilute solution viscosity, aged polymer;

^b+ soluble, - insoluble;

^cDynamic extrusion rheometer.

2. Low Acid Number Polyester Glycol Effects: Figure 3 shows the polymerization viscosity-time-temperature relations for two additional (2.0) ratio polymers, Numbers 4 and 5. Both were made from reactant lots III, IV and X

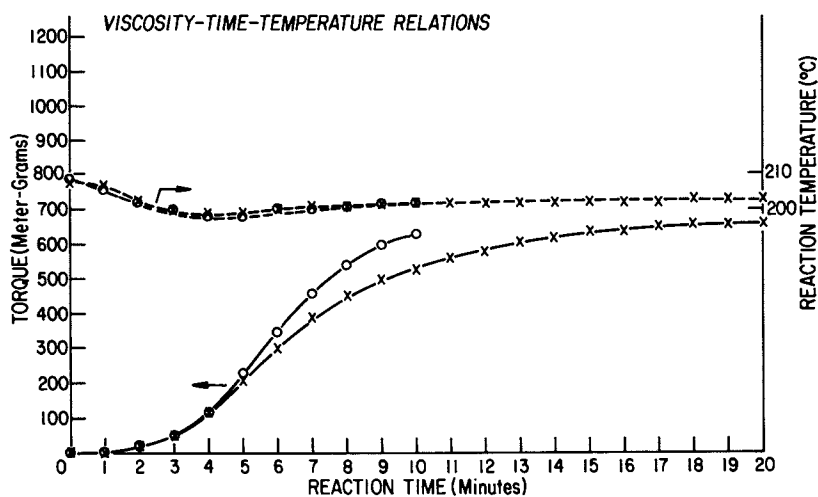


Figure 3. Thermoplastic urethane melt polymerization. Key: \circ , Polymer 4; \times , Polymer 5.

American Chemical
Society Library
1155 16th St. N. W.

(Table I). A major difference from the preceding polymer set was the use of low acid number (0.1) PTAd. Comparison shows that both polymerizations with 0.1 AN PTAd were considerably slower than those with high AN (2.4, 2.0) PTAd. We believe that this comparison illustrates the known weak catalysis of the isocyanate-hydroxyl reaction by acids (2,19, etc.).

Notice that Polymer 4 was still growing at the end of its measurements, as was Polymer 5 at the same reaction time. This indicates that the potential for continued polymerization via the NCO-OH reaction still remained. The torque level achieved in polymerizations 4 and 5 was less than that of 1 and 2, reflecting the higher polymerization temperature of 4 and 5.

Polymerization 5 was followed for 20 minutes. Figure 3 shows a steady torque (DP) increase for 18 minutes, then a leveling tendency. This result is taken to indicate that for eighteen minutes the concentration of unreacted isocyanate and hydroxyl groups remaining in the polymerizing mixture exceeded their equilibrium concentration at ~203°C, so polymerization via urethane formation continued up to this point, exceeding chain cleavage by thermally induced urethane dissociation (Equation 1).

Further data for Polymers 4 and 5 appear in Table IV.

Table IV
Data for Natural Polymers 4 & 5 from
Low Acid Number Polyester Glycol

Polymer	4	5
Polymerization		
Torque (meter-grams)	460	390,640
Time (min.)	7	7, 16
DSV ^a	1.639	2.441
Gel (%) ^a	4	2
Solubility (THF, DMF)	+ ^a , +	+ ^a , +
D.E.R.T ₂ (°C)	167	161
Tensile Strength [psi(MPa)]	8500 (58.6)	9600 (66.2)
300% Modulus [psi(MPa)]	1700 (11.72)	1500 (10.34)
Elongation (%)	420	450

^a Mostly

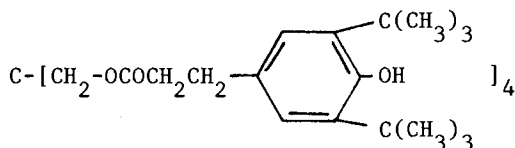
Table IV data show that the 0.1 AN PTAd ultimately produced higher molecular weight (MW) aged polyurethanes

than the 2.4 AN PTAd did (Table III). This tendency was expected since we know that polyester terminal carboxyl groups do not readily participate in uncatalyzed thermoplastic polyurethane polymerizations but act as limiting, very reluctant, or "dead" chain ends which can catalyze subsequent hydrolytic degradation of the poly(ester-urethane).^{18,20} This higher MW is apparent in the significantly higher DSV, T_2 , and gel values of the low acid number PTAd-based polymers, 4 and 5.

The very high DSV value for Polymer 5 (2.441) is not consistent with its moderate T_2 value and its THF solubility.

The higher MW of Polymers 4 and 5 (vs. 1, 2, and 3) is also reflected in the higher 300% modulus values of the former polymers. The 300% modulus value has been shown to increase with thermoplastic polyurethane elastomer number average molecular weight, M_n .¹⁷

Figure 4 shows the viscosity-time-temperature relations for three additional (2.0) ratio poly(ester-urethane) elastomers. These polymers, #6, #7, and #8 were all prepared from the same low acid number (0.15) PTAd (VII). And the antioxidant, Irganox 1010 (Ciba-Geigy), was added at 0.25 phr to the polymerization charges of these polymers.



(Irganox 1010)

The somewhat acidic phenolic hydroxyl groups of Irganox 1010 are believed to be too sterically hindered to react with isocyanate groups in urethane polymerizations.

In Figure 4 the temperature and viscosity curves for Polymers #6 and #7 are seen to be much alike and similar to that of Polymer 5 (Figure 3) which was prepared from another low acid number (0.1) PTAd. But notice the difference in the torque curve for Polymer 8 of Figure 4 which levels off at a value of only 150 meter-grams after eight minutes of reaction time. We attribute the lower torque in the Polymer 8 polymerization to the 20°C higher reaction temperature imposed which we believe reduced polymer viscosity in two ways: 1) by increasing the normal "thermal thinning" process which overcomes intact polymer chain interchain attractive forces (hydrogen bonding, van der Waals forces, etc.) and 2) by driving the urethane dissociation equilibrium of Equation 1 farther to the left, thus

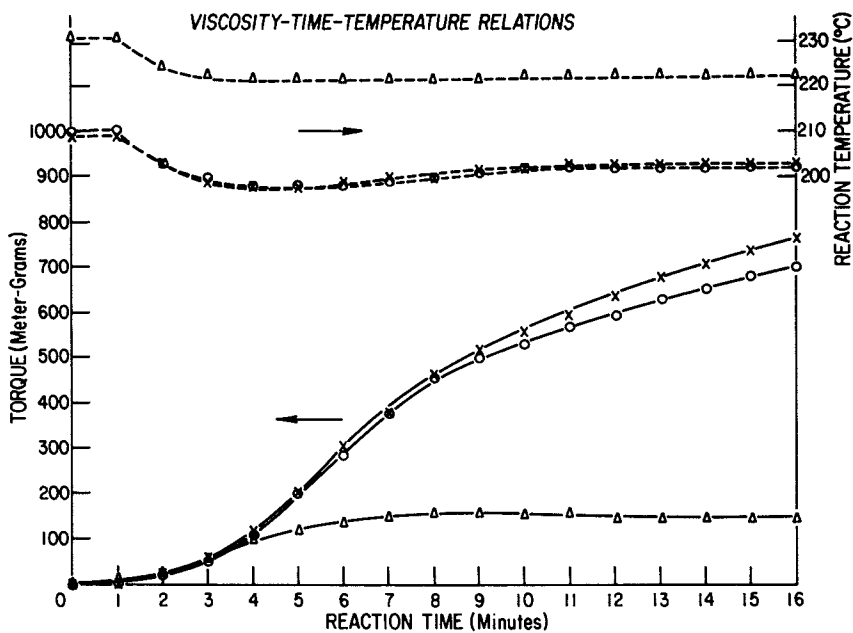


Figure 4. Thermoplastic urethane melt polymerization. Key: \circ , Polymer 6; \times , Polymer 7; \triangle , Polymer 8.

increasing the degree of (reversible) thermal dissociation/cleavage of polyurethane chains.

In spite of its sustained high polymerization temperature (~222°C), after eight minutes Polymer 8 torque remained quite steady during the last 8 minutes of the polymerization reaction with only a slight drop indicative of minor polymer reversion.

Isocyanate analysis performed during the polymerization of Polymers 6, 7, and 8 after 7 and 16 minutes of reaction time afforded the interesting results of Table V.

The data of Table V indicate a gradual decrease of [NCO] in the later stages of each of these natural polymerizations. But a significant amount of isocyanate remained in the reaction mixtures at the full term of the reactions. One might argue that this is due to a slight initial excess of isocyanate charged. But we feel that it is more likely manifestation of the urethane dissociation equilibrium (Equation 1).

Table V
Isocyanate Level During (2.0) Ratio Polymer Melt Polymerizations

Polymerization [NCO] (%) ^a	<u>6</u>	<u>7</u>	<u>8</u>
Initial ^a	10.1	10.05	10.1
7 Minute	0.190	0.193	0.191
Consumed	98.12	98.08	98.11
16 Minute	0.137	0.153	0.128
Consumed	98.64	98.48	98.73
Comment	Active polymer- ization at 16 minutes	Active polymer- ization at 16 minutes	Slight rever- sion then steady after 13 minutes

^aCharged

Further data for Polymers 6, 7, and 8 appear in Table VI.

The high 300% moduli of Polymers 7 and 8 seems to be a tendency in polymers made from low acid number PTAd.

Table VI
Data for Irganox 1010-Stabilized Polymers 6, 7, and 8
from Low Acid Number Polyester Glycol

Polymer	6 ^a	7 ^a	8 ^a
Polymerization			
Torque (meter-grams)	380,700	380,760	150,150
Time (min.)	7,16	7,16	7,16
DSV	1.485	1.812	1.31
Gel (%)	nil	nil	nil
Solubility (THF, DMF)	+,+	+,+	+,+
D.E.R.T ₂ (°C)	149	139	154
Tensile Strength [psi(MPa)]	9700 (66.9)	8800 (57.2)	7400 (51.0)
300% Modulus [psi(MPa)]	1400 (9.65)	2000 (13.79)	1700 (11.72)
Elongation (%)	470	415	435

^aPolymerization charge contains 0.25% Irganox 1010.

B. (3.0) Ratio Polymers: Effect of Urethane Group Concentration. Figure 5 shows the polymerization viscosity-time-temperature relations for a (3.0 ratio) thermoplastic poly(ester-urethane) elastomer, Polymer 9. This polymer was made from reactants VI, IV, and X (Table I) the polyester glycol component being intermediate acid number PTAd (0.30).

It can be seen from Figure 5 that this (3.0) ratio melt polymerization was very rapid and faster than those of Polymers 1 and 2. It achieved high melt viscosity quickly but immediately began to lose this viscosity, presumably due to shear-induced polymer chain cleavage, which is usually most pronounced at high melt viscosity levels.

The rapid polymerization rate was likely related to the polymer composition wherein the high urethane concentration not only increased polymer melt viscosity but also autocatalyzed further urethane formation.¹⁹ However, the intermediate acidity of the polyester glycol is also believed to contribute to the increased polymerization rate due to what may be the particularly favorable balance of its catalytic but reluctant terminal carboxyl groups (at intermediate level) and its reactive terminal hydroxyl groups (in preponderance).

Further data for Polymer 9 appear in Table VII.

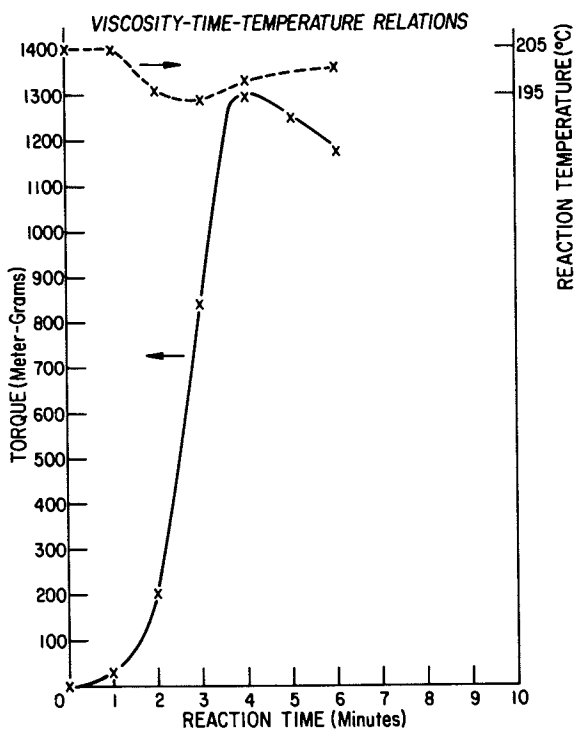


Figure 5. Thermoplastic urethane melt polymerization. Key: X, Polymer 9.

Table VII
Data for (3.0) Ratio Polymer 9

Polymer	9
Polymerization	
Torque (meter-grams)	1300 ^a , 1180
Time (min.)	4, 6
DSV	-
Gel (%)	-
Solubility (THF, DMF)	-, -
D.E.R.T ₂ (°C)	200
Tensile Strength [psi(MPa)]	4800 (33.1)
300% Modulus [psi(MPa)]	>4800 (>33.1)
Elongation (%)	220

^aMaximum

Table VII data show that Polymer 9 was an unusual polymer. This is seen in its very high modulus, low extensibility at break, high T₂ value, and insolubility even in DMF. Apparently Polymer 9 is an unusually high molecular weight polymer which we feel resulted from the use of (intermediate) acid number PTAd.

C. Ethylene Glycol Chain Extender Effects. Figure 6 shows the polymerization viscosity-time-temperature relations for a thermoplastic poly(ester-urethane) elastomer, Polymer 10, made from monomers VII, IV, and XI (Table I). VII is low acid number PTAd (0.15) and XI is ethylene glycol chain extender. The polymerization charge also contained 0.25% (on charge) of Irganox 1010 antioxidant.

The polymerization of Polymer 10 reached its maximum torque in 7 minutes (390 meter-grams) then died and began to degrade with loss of melt viscosity, even at this low polymer melt viscosity level and familiar polymerization temperature. Ethylene glycol chain extended polymers have been anomalous polymerizations and polymers in our experience due, we believe, to abnormal chemistry that can occur during their preparation.

The data of Table VIII show that Polymer 10 is a high quality thermoplastic polyurethane elastomer.

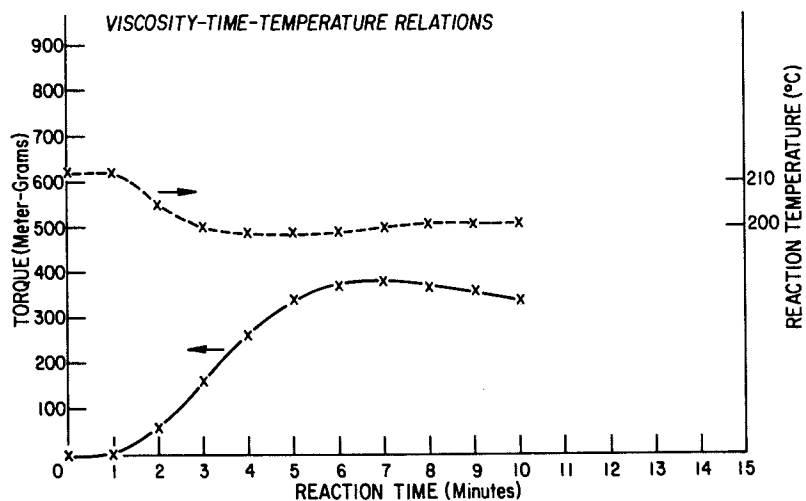


Figure 6. Thermoplastic urethane melt polymerization. Key: X, Polymer 10.

Table VIII
Data for (2.0) Ratio Polymer 10

Polymer	10^a
Polymerization	
Torque (meter-grams)	380,340
Time (min.)	7,10
DSV	1.15
Gel (%)	nil
Solubility (THF, DMF)	+,+
D.E.R.T ₂ (°C)	137
Tensile Strength [psi(MPa)]	8400 (57.9)
300% Modulus [psi(MPa)]	1200 (8.27)
Elongation (%)	495

^aPolymerization charge contains 0.25% Irganox 1010.

II. Catalyzed Polymerizations

A. Stannous Octoate. 1. (3.0) Ratio Polymers: Figure 7 shows the polymerization viscosity-time-temperature relations for two thermoplastic poly (ester-urethane) (3.0) ratio elastomers, Polymers 9 and 11, made from the same monomer lots, VI, IV, X (Table I). Stannous octoate catalyst (47 ppm) (XII - Table I) was mixed into the macroglycol-chain extender glycol blend prior to MDI addition in polymerization Number 11.

Examination of Figure 7 shows that stannous octoate strongly catalyzed the already rapid (3.0) ratio polymerization. The highest torque was realized in uncatalyzed Polymer 9 but prompt, substantial melt viscosity reduction, indicative of polymer degradation via shear-induced chain cleavage followed. Catalyzed Polymer 11 showed polymerization die-out at about 4 minutes of reaction time but no polymer degradation tendency is apparent even at these high torque and temperature levels.

Further data on Polymers 9 and 11 appear in Table IX.

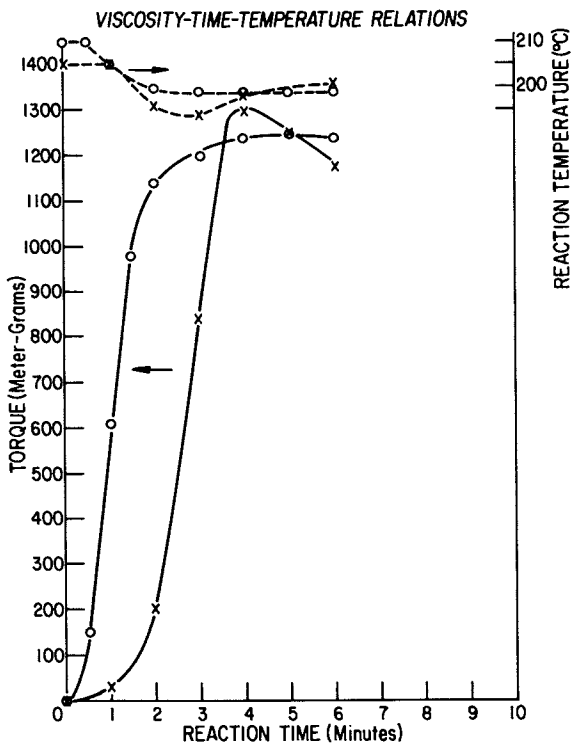


Figure 7. Thermoplastic urethane melt polymerization. Key: X, Polymer 9 (natural); O, Polymer 11 (47 ppm stannous octoate).

Table IX
Data Showing Stannous Octoate Catalyst Effect:
Polymers 9 & 11

Polymer	9	11
Polymerization		
Torque (meter-grams)	200,1300 ^a	1140,1240
Time (min.)	2,4	2,4
DSV	-	-
Gel (%)	-	-
Solubility (THF, DMF)	-, -	-, -
D.E.R.T ₂ (°C)	200	189
Tensile Strength [psi(MPa)]	4800 (33.1)	9600 (66.2)
300% Modulus [psi(MPa)]	>4800 (>33.1)	5900 (40.7)
Elongation (%)	220	380

^aMaximum

Table IX data show that neither Polymer 9 nor Polymer 11 was soluble, apparently due to their high molecular weights, which are also apparent in their high T₂ and 300% modulus values.

2. (2.0) Ratio Polymers: Figure 8 shows the polymerization of (2.0) ratio polymers made from reactants V (PTAd, AN 0.1), VIII, and X without added catalyst (Polymer 12) and with 58 ppm of stannous octoate (Polymer 13). Again strong catalysis by the tin compound is apparent. The catalyzed run, Polymer 13, required only 4 minutes to reach maximum torque whereas the uncatalyzed run, Polymer 12, needed about 16 minutes to reach this same torque level.

Again there is no evidence for polymer viscosity loss by reversion in the catalyzed polymerization even on extended reaction at ~200°C. Note that the uncatalyzed polymer was still growing at the end of its term in the reactor in keeping with the behavior of Polymers 6 and 7 (Figure 4) which were also made from low acid number polyester glycol, PTAd.

III. Shortstopped Polymerizations

A. 1-Propanol. Figure 9 shows the polymerization viscosity-time-temperature relations for three (2.0) ratio thermoplastic poly(ester-urethane) elastomers, Polymers 5,

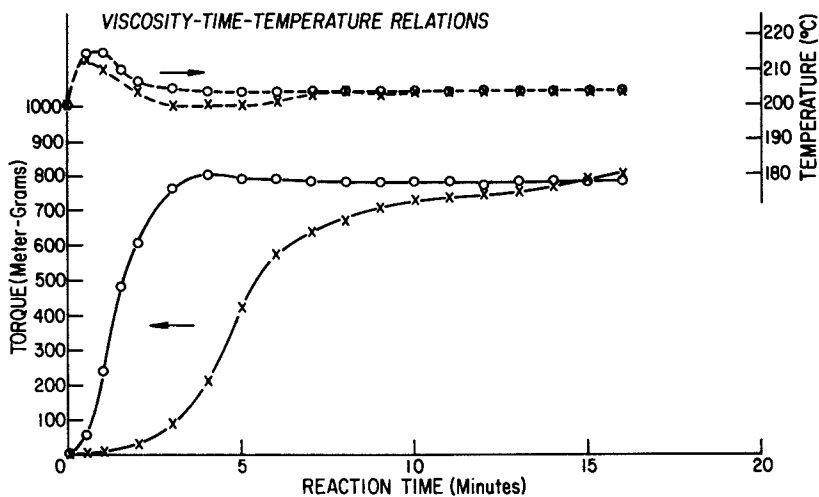


Figure 8. Thermoplastic urethane melt polymerization. Key: X, Polymer 12 (natural); O, Polymer 13 (58 ppm stannous octoate).

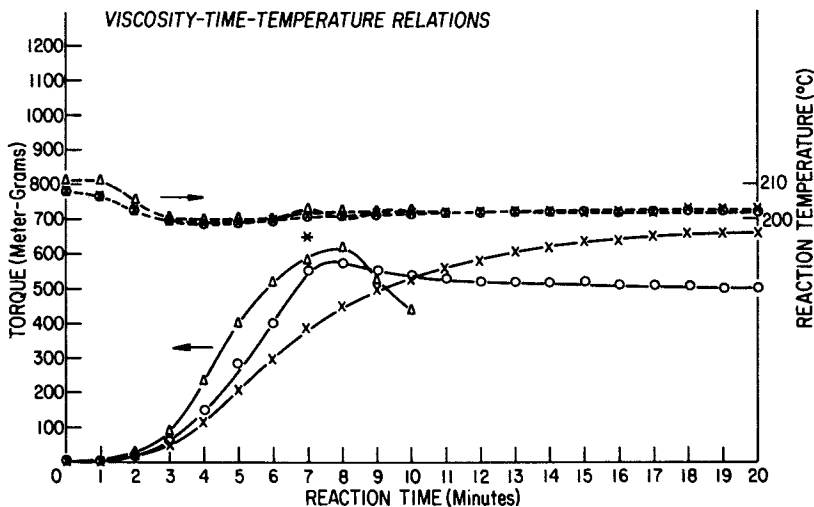


Figure 9. Thermoplastic urethane melt polymerization. Key: X, Polymer 5; O, Polymer 14 (1% n-propanol); Δ, Polymer 15 (3% n-propanol).

14, and 15. The two latter were shortstopped with 1-propanol (XIII, Table I). These polymers were all made from the same monomer lots, III, IV and X (Table I). The polyester glycol, III, has low acid number (0.1).

In Polymers 14 and 15 the shortstop, 1-propanol, was added to the polymerizing reaction mixture in the Brabender Plasticorder reactor 7 minutes after the polymerization had been started (see asterisk in Figure 9).

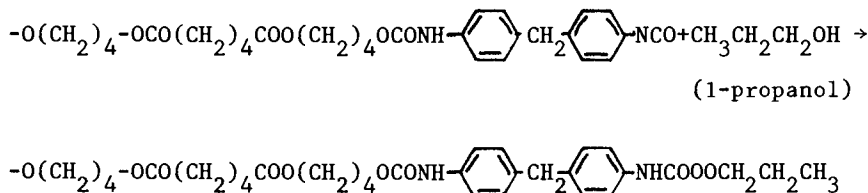
Comparison of Polymers 14 and 15 in Figure 9 shows fairly similar polymerizations up to the point of shortstop addition. The control, Polymer 5, was slower but alive and growing at 18 minutes of polymerization time, reaching a final torque value of 660 meter-grams. Its steady intermediate polymerization rate is seen to be characteristic of uncatalyzed thermoplastic polyurethane elastomer polymerizations based on low acid number PTAd while Polymers 14 and 15 formed faster than usual from such a low acid number polyester glycol component.

In Polymer 14 (1.0% SS) the polymerization showed a torque increase of 30 meter-grams peaking at 580 meter-grams one half minute after shortstop addition (+ ΔT 30/0.5, 580 maximum) with 80 units reversion in the subsequent 12.5 minutes of polymerization (- ΔT 80/12.5).

In Polymer 15 (3.0% SS) behavior was (+ ΔT 40-60/1, 580-620 maximum) with strong reversion (- ΔT 130-180/2). The polymerization of 15 was notably faster than the polymerization of 14 and the rate differences in this set are more than are normally encountered or desired.

The apparent partial reversion of the polymerizing mixture after torque peaking, its dependence on shortstop concentration, and its ultimate decline with polymerization time are interesting phenomena. The desired shortstopping chemistry is pictured in Equation 3. It involves the reaction of the hydroxyl group of the added 1-propanol shortstop molecules with the unreacted terminal isocyanate groups on the poly(ester-urethane) chains. This permanently stops chain growth as desired.

Equation 3. Shortstopping a Polyester Urethane Chain by Terminal Urethane Formation



But we believe some unwelcome chemistry may also occur, and the course of the reversion, particularly the fact that it eventually subsides (e.g., Polymer 14), suggests that the following occurs.

Shortstop molecules, added in substantial excess of the isocyanate groups in the polymerizing mixture (to shortstop quickly and completely) upset the urethane equilibrium shown in Equation 1, driving the reaction to the right by the Law of Mass Action in order to produce more urethane groups and thus re-establish the equilibrium constant (Equation 2) for that temperature.

Since 1-propanol is monofunctional and reacts with "matched dissociation isocyanate" (at internal urethane chain positions) as well as "unmatched isocyanate" (at polymer chain terminal positions) its effects include cleavage of some polyurethane chains in the process of generating more urethane groups. As a result, polymer DP, melt viscosity, and torque drop until the shortstop is consumed, or escapes the mixture by volatilization. Figure 9 shows that the more 1-propanol used to shortstop the polymerizations, the more pronounced the polymer reversion was.

Further data on Polymers 5, 14, and 15 appear in Table X.

Table X
Data Showing 1-Propanol Shortstop Effect: Polymers 5, 14 and 15

Polymer	5	14	15
[Shortstop] (%) ^a	0	1.0	3.0
Polymerization			
Torque (meter-grams)	390,500,660	550,580 ^b ,500	580,620 ^b ,440
Time (min.)	7,9,20	7,7.5,20	7,8,10
DSV	2.441	1.257	0.910
Gel (%)	2	nil	nil
Solubility (THF, DMF)	+,+	+,+	+,+
D.E.R.T ₂ (°C)	161	141	136
Tensile Strength [psi(MPa)]	9600 (66.2)	9600 (66.2)	8600 (59.3)
300% Modulus [psi(MPa)]	1500 (10.34)	1600 (11.03)	1300 (8.96)
Elongation (%)	450	470	530

^a % wt. (on reactants) of 1-propanol;

^b Maximum

The data of Table X indicate the pronounced effectiveness of 1-propanol as a urethane polymerization shortstop. It does its job in about 1 to 2 minutes under the conditions investigated and DSV and T_2 values decrease with increasing shortstop concentration.

B. 1-Decanol. Figure 10 shows the polymerization viscosity-time-temperature relations for a set of (2.0) ratio thermoplastic poly(ester-urethane) elastomers, Polymers 16, 17 and 18, where 17 and 18 were shortstopped with a higher molecular weight primary alcohol, 1-decanol (XIV - Table I). The polymers of this set were all made from the same reactant lots (VII, IV, and X - Table I). The polyester glycol had a low acid number, 0.15.

Comparison of Polymer 16 polymerization (control) with 17 shows essentially identical polymerization rates up to the point of shortstop addition after 8 minutes of polymerization time. In Polymer 16 we see the polymerization begin to slow down after about 8 minutes of reaction at 420 meter-grams but to achieve 490 meter-grams in 10 minutes without die-out.

The behavior of Polymer 17 polymerization (0.24% SS at 8 minutes) showed less than complete shortstop action (+ ΔT 30/2) and a final torque of 470 meter-grams. Note the total absence of shortstop-induced polymer reversion even after 16 minutes of reaction time.

Polymerization of Polymer 18 (0.51% SS at 8 minutes) was a bit faster than 17. Subsequent to shortstop addition, behavior was + ΔT 10/0.5 with 500 meter-grams maximum torque realized 0.5 minute after shortstop addition. But this 0.51% of shortstop resulted in pronounced polymer reversion in the next 7.5 minutes of reaction time and showed no leveling tendency even then. This behavior contrasts with that of Polymer 14 polymerization which was shortstopped with n-propanol (Figure 9). It probably indicates a deleterious excess concentration of shortstop hydroxyl over polymer chain terminal isocyanate, the situation resulting in polyurethane chain cleavage as discussed earlier. And the fact that the reversion continued steadily with reaction time is believed to reflect the nonfugitive nature of the high boiling 1-decanol shortstop relative to that of 1-propanol (Table I).

Further data on Polymers 16, 17, and 18 appear in Table XI.

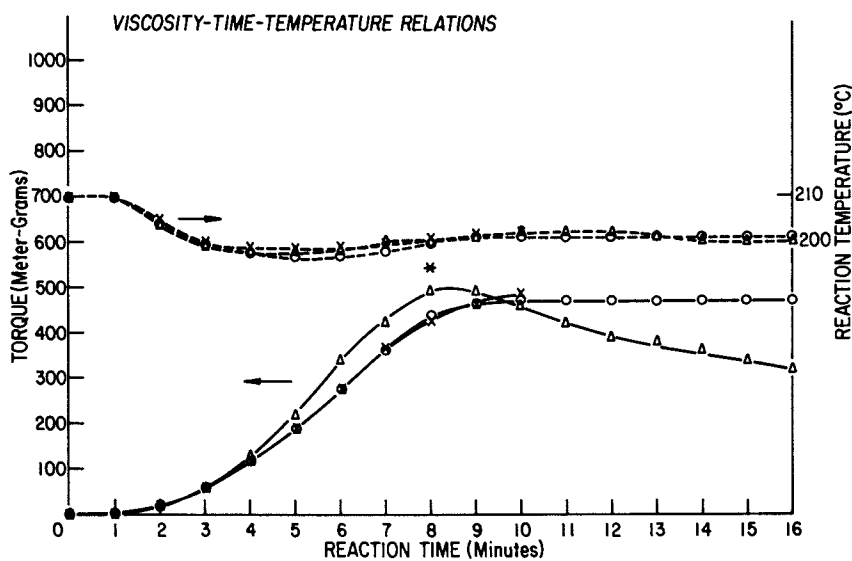


Figure 10. Thermoplastic urethane melt polymerization. Key: X, Polymer 16 (control); O, Polymer 17 (0.24% 1-decanol); Δ, Polymer 18 (0.51% 1-decanol).

Table XI
Data Showing 1-Decanol Shortstop Effect: Polymers 16, 17, and 18

Polymer	16	17	18
[Shortstop] (%) ^a	0	0.24	0.51
Polymerization Torque (meter-grams)	370,490	360,440,470	420,490,500 ^b ,320
Time (min.)	7,10	7,8,10 ^a	7,8 ^a ,8.5,16
DSV	1.450	0.862	0.705
Gel (%)	nil	nil	nil
Solubility (THF, DMF)	+,+	+,+	+,+
D.E.R.T ₂ (°C)	145	138	126
Tensile Strength[psi(MPa)]	9800 (67.6)	8900 (61.4)	6400 (44.1)
300% Modulus [psi(MPa)]	1800 (12.41)	1200 (8.27)	1000 (6.90)
Elongation (%)	450	500	565

^a Shortstop added

^b Maximum

Isocyanate analyses of the shortstopped polymers, performed during the polymerization before and after short-stop addition, afforded the results of Table XII.

Table XII
Isocyanate Levels During 1-Decanol Shortstopped Polymerization of Polymers 17 & 18

Polymer	17	18
[NCO] (%) ^a		
Initial ^a	10.05	10.05
7 Minute	0.198	0.176
Consumed	98.03	98.25
16 Minute	0.107	0.066
Consumed	98.93	99.34
Comment	Steady final state	Reversion

^a Charged

Table XII data show that all of the 1-decanol short-stopped polymerizations, measured after 16 minutes of polymerization, contained less isocyanate than the natural polymerizations, e.g., 6, 7, and 8 (Table V). But even so,

a significant concentration of unreacted isocyanate groups remained in the shortstopped polymers, providing more evidence of the urethane thermal equilibrium (Equation 1).

D. Diisocyanate Deficiency. Another way of modifying polyurethane molecular weight during polymerization is to deliberately avoid stoichiometric reactant balance in the polymerization charge, favoring a hydroxyl excess. This has been done in the case of Polymer 19 where a deficiency of diisocyanate was charged in a (2.0) ratio polymer recipe so that the molar reactant ratio was 1.95/1.00/1.00 (MDI/PTAd/1,4-butanediol). The control polymer for this set was 7. Both Polymers 7 and 19 were prepared from the same lots of low (0.15) acid number PTAd (VII), 1,4-butanediol (X), and MDI (VIII). Both contained 0.25% wt. Irganox 1010 in the polymerization charge. The polymerizations of 7 and 19 are seen in Figure 11.

Comparison of the polymerizations of Polymers 7 (balanced control) and 19 (MDI-deficient) shows 7 to be high viscosity, live, and vigorous after 16 minutes of reaction whereas 19 was much slower and apparently dying out at only about one-third the viscosity of the control polymer. Isocyanate analyses after 7 minutes of reaction showed 0.191% wt. in Polymer 7 and only 0.094% wt. in Polymer 19. After 16 minutes of reaction the values were 0.128% for 7 and 0.042% for 19.

Thus, substantial polymer molecular weight modification (reduction) is seen to be a consequence of deliberate stoichiometric reactant imbalance via MDI deficiency. This not only represents a method of thermoplastic polyurethane elastomer molecular weight control but also demonstrates what inadvertent reactant imbalance can do to the polymerization and the polymer product.

Further data on polymers 7 and 19 appear in Table XIII.

Table XIII
Data for Polymers 7 & 19 Prepared from Balanced
and Diisocyanate-Deficient Recipes

Polymer	7	19
Modifier		
Type	none	MDI deficiency
Polymerization		
Torque (meter-grams)	380,760	165,270
Time (min.)	7 ^a , 16 ^b	7 ^c , 16 ^d
DSV	1.812	0.787
Gel (%)	nil	nil
Solubility (THF, DMF)	+,+	+,+
D.E.R.T ₂ (°C)	139	122
Tensile Strength [psi(MPa)]	8300 (57.2)	7400 (51.0)
300% Modulus [psi(MPa)]	2000 (13.79)	1200 (8.27)
Elongation (%)	415	590

% Wt. NCO: ^a0.191, ^b0.128, ^c0.093, ^d0.042

It can be seen from Table XIII data that control Polymer 7 is a high molecular weight and high quality polyurethane whereas the modified polymerization yielded lower molecular weight Polymer 19 with good but lesser properties. The lowest final (16 minute) [NCO] was obtained in the polyurethane prepared with a diisocyanate deficiency in the charging recipe.

IV. Polymer Mastication

The Brabender Plasticorder is also a useful device for studying the effect of shear and heat on fully formed polymeric materials. And this is another way that we used it in the present study. The technique employed was to bring the Plasticorder mixing chamber to temperature, then add granules of thermoplastic polyurethane elastomer (at 25°C) to the chamber and record the viscosity-time-temperature pattern that developed.

Figure 12 shows an example of the characteristic pattern we encountered in this type of experiment in the mastication of a high quality (2.00) MDI/PTAd (MW 1000)/1.4-BDO composition, Polymer 20, taken from the shelf. Granules of Polymer 20 were pre-dried (75°C/1 mm Hg/6 hours, then 25°C/1 mm Hg/over Drierite/20 hours) before mastication.

As can be seen in Figure 12 the Plasticorder mixing chamber was heated to 200°C, a temperature frequently applied in the

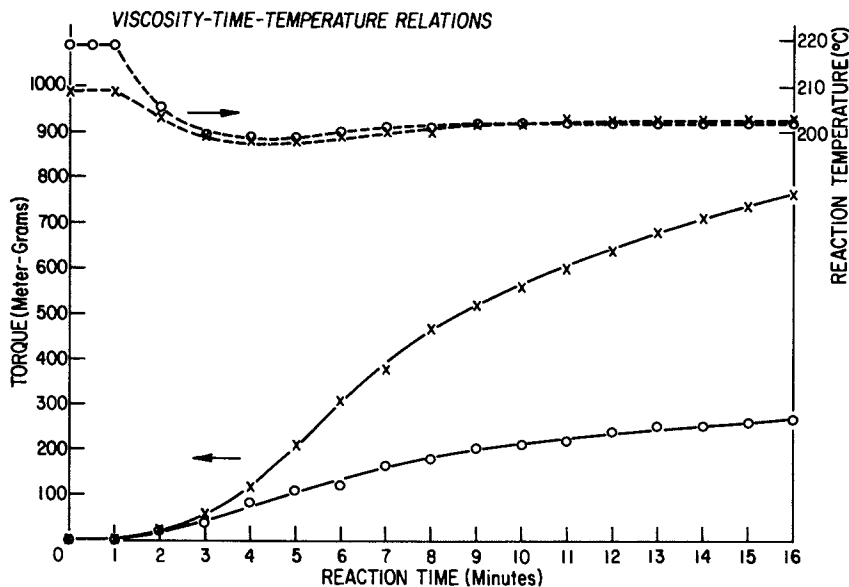


Figure 11. Thermoplastic urethane melt polymerization. Key: X, Polymer 7; O, Polymer 19.

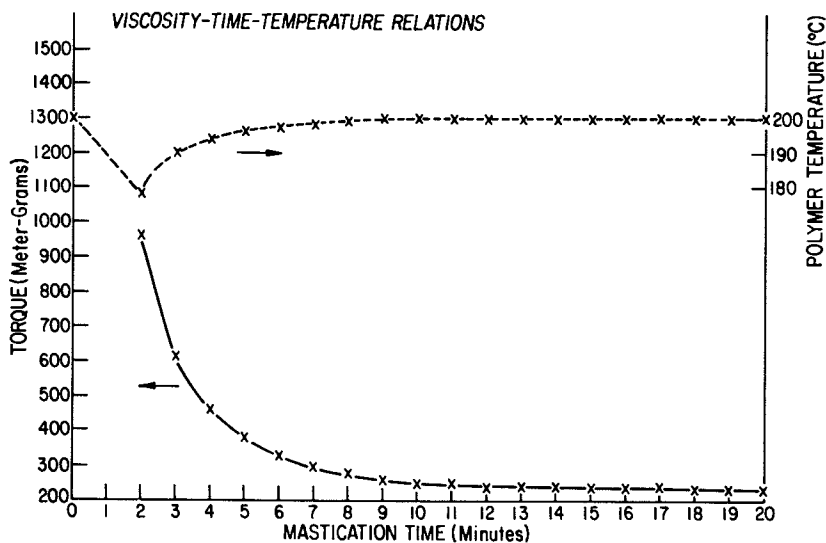


Figure 12. Thermoplastic urethane mastication. Key: X, Polymer 20 (predried).

polymerizations of this study. Two minutes after addition of the granules (79.4g) the fluxed polymer registered $\sim 180^{\circ}\text{C}$ and ~ 960 meter-grams torque. This torque level will be recognized as being fairly high for a polymer of this composition forming at 200°C , but of course very high initial levels would be expected at the formed polymer solid-to-melt transition point.

At six minutes the polymer flux had essentially regained the selected mastication temperature, 200°C , but notice that during this interval mastication reduced torque precipitously to the low level of 320 meter-grams. After a total mastication time of 10 minutes the polymer melt torque level fell a bit further to 250 meter-grams and declined little more during the full 20 minute term of the experiment.

The foregoing mastication pattern is characteristic of the several fully formed thermoplastic polyurethane elastomer compositions we have examined. An obvious question the pattern raises is why mastication reduces already formed polymer to such essentially constant low viscosity level under a given set of shear/temperature/time conditions while the same conditions raise the viscosity of the same composition of forming polymer to a much higher and growing or constant viscosity level, (e.g., Polymer 5, Figure 3).

Some possible answers to the foregoing question occur. Perhaps, in spite of our efforts to dry Polymer 20 granules some tightly absorbed water remained in the polymer. This moisture would then be on site to react with the isocyanate-terminated polymer chain ends as they are generated by the thermal/shear-induced cleavage of polymer urethane bonds. Such a process would reduce polymer average molecular weight, and thus melt viscosity, until the water is used up or has escaped.

In contrast, trace moisture in the polymerization charge quickly reacts with isocyanate in a chain-extending process, and is thereafter not available to react with and seal off isocyanate-terminated polymer chains.

Again, it is likely that the virtual crosslinks (hard segment aggregation into domains, urethane hydrogen-carbonyl group bonding, aromatic π electron associations, van der Waals interchain forces, etc.) in formed segmented thermoplastic polyurethane elastomers, such as the polymers of this study, have become well developed by phase segregation relative to their potential, in stored polymer samples. Under the shear of mastication such virtual crosslinks may hold well enough before disruption to restrict polymer chain slippage, with the consequence that many chains are broken irreversibly and polymer viscosity is permanently reduced.

But, such an extensive virtual network has not yet developed in the forming polymer and chain growth dominates shear-induced chain cleavage, eventually producing a much higher viscosity polymer melt.

We feel it likely that both of the above factors, trace moisture and virtual networks, are involved as suggested in the foregoing incongruous polymer melt viscosity phenomena.

Literature Cited

1. Bayer, O., Angewandte Chemie, A59, 257, (1947).
2. Cooper, W., Pearson, R. W., Darke, S., Ind. Chem., 1960, 36, (421), 121.
3. McGinn, C. E., Spaunburgh, R. G., Dyestuffs, 1958, 42, (7), 224.
4. Wright, P., Cumming, A.P.C., "Solid Polyurethane Elastomers", Gordon and Breach, N.Y., N.Y., 1969.
5. Lipshitz, S. D., Mussatti, F. G., Macosko, C. W., SPE Antech Tech. Papers, 1975, 21, 239-241.
6. Lipshitz, S. D., Macosko, C. W., Poly. Eng. Sci., 1976, 16, (12), 803-810.
7. Broyer, E., Macosko, C. W., Critchfield, F. E., Lawler, L. F., Poly. Eng. Sci., 1978, 18, (5), 382-387.
8. Miller, D. R., Valles, E. M., Macosko, C. W., Poly. Eng. Sci., 1979, 19, (4), 272-283.
9. Martin, R. A., Hoy, K. L., Peterson, R. H., I and EC Prod. Res. & Devel., 1947, 6, (4), 218-222.
10. Iobst, S. A., Cox, H. W., J. Appl. Poly. Sci., 1979, 23, (8), 2513-2527.
11. Peebles, L. H., Jr., Macromolecules, 1974, 7, (6), 872-881.
12. Peebles, L. H., Jr., Macromolecules, 1976, 9, (1), 58-61.
13. Rausch, K. W., Jr., McClellan, T. R., U.S. Patent 3,642,964, Feb. 15, 1972, The Upjohn Company.
14. Goodrich, J. E., Porter, R. S., Polymer Preprints, 1966, 7, (1), 292-305.
15. Private communication, P. R. VanBuskirk (C. W. Brabender Instruments, Inc.) to C. S. Schollenberger.
16. Dinbergs, K., U.S. Patent 3,660,341, May 2, 1972, The BFGoodrich Company.
17. Schollenberger, C. S., Dinbergs, K., J. Elastoplastics, 1973, 5, 222-251.

18. Schollenberger, C. S., Stewart, F. D., J. Elastoplastics, 1971, 3, 28-56.
19. Saunders, J. H., Frisch, K. C., "Polyurethanes - Chemistry and Technology, Part I, Chemistry", High Polymers Vol. XVI, Interscience - John Wiley, 1962.
20. Stewart, F. D., U.S. Patent 3,463,758, Aug. 26, 1969, The BFGoodrich Company.

RECEIVED April 30, 1981.

Biodegradation of Polyurethanes Derived from Polycaprolactonedioles

SAMUEL J. HUANG, CHRISTOPHER MACRI, MARK ROBY,
CHRISTINE BENEDICT, and J. A. CAMERON

Department of Chemistry, Biological Science Group, and Institute of Materials Science,
University of Connecticut, Storrs, CT 06268

Earlier studies on the biodegradation of synthetic polymers were initiated by the desire to avoid biodegradation, thereby obtaining long lasting materials. Disposing of nondegradable synthetic polymers after use is a problem that grows more serious every day. Designing the polymer to be biodegradable avoids the problem of accumulation of expended polymers. The disposal of biodegradable polymers, on the other hand, is less difficult. Moreover, the increasing uses of biodegradable polymers in medicine and agriculture as sutures, surgical implants, and components of controlled release formulations of drugs and agricultural chemicals require knowledge concerning the biodegradabilities of synthetic polymers. Since natural macromolecules are generally degraded in biological systems by hydrolysis followed by oxidation, we have been studying biodegradable polymers containing hydrolyzable linkages (1). In addition to the semi quantitative method of following biodegradation recommended by ASTM (2) we have developed quantitative methods to study enzymic and microbial degradation (3). We report here some of our recent results on the biodegradation of polyurethanes.

Experimental

Materials. Polyurethanes were prepared in the usual manner using suitable diols, polyols and diisocyanates. Catalysts were not used to avoid the possibility that metal ions might act as fungicides. Polyurethanes were purified by reprecipitation before subjection to biodegradation testing.

The reaction of 0.01 mole of a polyesterdiol (Aldrich Chemical Co., Milwaukee, WI.) with 0.01 mole (plus a 1-3% excess) of a diisocyanate (Aldrich Chemical Co., Milwaukee, WI.) was

0097-6156/81/0172-0471\$05.00/0

© 1981 American Chemical Society

performed under an argon atmosphere by premelting the PCL-diol to which the specified amount of diisocyanate was added. The reaction vessel, consisting of a three neck round bottom flask equipped with a condenser, gasbubbler, and stirrer was heated to 110°C for a period of 12 hrs. resulting in a highly viscous, slightly colored polymer. This polymer was then THF extracted overnight with refluxing and subsequently precipitated out in distilled H₂O. This reprecipitation was carried out twice more to insure the removal of impurities. The product was dried while under vacuum at room temperature for at least one week. The result was an off-white, tough material which was redissolved overnight in preparation for the biodegradation studies. The commercial polyurethane was obtained from Upjohn Company.

The following organisms were used: Cryptococcus laurentii, a yeast; Aspergillus fumigatus sp. (Aspergillus fischeri), an enrichment culture isolate; and a Fusarium sp. isolated in the laboratory. The fungi were stored as spore suspensions washed from Sabouraud's Dextrose Agar (Difco; Detroit, MI) with 0.1% (v/v) Triton X-100 in distilled water and standard volumes of each were used as the inocula for growth studies. The yeast was stored on glucose (0.4% w/v) basal salts solution containing a suspension of polyester(polycaprolactonediol 1250). The medium used consisted of a basal salts solution (BMS) containing, per liter of glass distilled water: K₂HPO₄, 0.7 g and KH₂PO₄, 0.7 g sterilized separately from MgSO₄·7H₂O, 0.7 g; NH₄Cl, 1.0 g; NaNO₃, 1.0 g; and 1.0 ml of trace salts solution. This consisted of, per milliliter: NaCl, 0.005 g; FeSO₄·7H₂O, 0.002 g; ZnSO₄·7H₂O, 0.002 g; and MnSO₄·H₂O, 0.0007 g. The pH was adjusted to 6.5 with 10% (w/v) NaOH. For solid media, BMS was supplemented with 10.0 g of Noble Agar (Difco, Detroit, MI) per liter. For experiments with nitrogen-free medium, both NH₄Cl and NaNO₃ were omitted, NaCl, 1.0 g/l. was substituted.

Biodegradation. The ASTM recommended procedure was used for the fungal degradation experiments (2). The enzymatic degradation procedure developed in our laboratory has been described recently (3).

The protocol outlined by the American Society for Testing Materials (ASTM) was followed for the solid surface growth studies. A film of the polymer was cast on the surface of a BMS-agar plate by spreading 2.0 ml of 10 mg/ml poly(ester-urethane) in THF over the surface of the plate and evaporating the THF. The centers of the plates were inoculated with 0.1 ml of the spore suspensions or 0.1 ml of a turbid culture of yeast grown on 0.2% (w/v) Casamino Acids (Difco, Detroit, MI), after which the plates were incubated at 25°C for one month.

For the quantitative assays of degradation, films were cast in the bottom of 25 x 125 mm glass tubes and rotated overnight for solvent evaporation. BMS (5 ml.) and a 0.1 ml inoculum were added aseptically and the tubes incubated at 25°C for one month. Controls for stability of the polymer to nonbiological hydrolysis with incubation and viability of the inoculum were included. These experiments were terminated by lyophilization of the culture in the growth tube.

Both the qualitative and the quantitative studies were done in duplicate.

High pressure liquid chromatography (HPLC) was performed using a series of three 60 x 0.75 cm columns: two 3 x 10⁴ Å Styragel followed by one 500 Å Styragel (Waters Assoc., Milford, MA.). The exclusion limit of this column system is 1.7 x 10⁶ determined with polystyrene standards (Waters Assoc., Milford, MA). The HPLC system consists of a piston pump (mini-pump, Milton Roy Co., Hollywood, Fla.), the columns, a Rheodyne injector 7125 an R-4 Differential Refractometer, and a Speedomax H recorder (Leeds and Northrop, Phila., PA), with THF as the eluant.

The described column system is capable of separating polystyrene standards (Waters Assoc.) of 950,000 to 3,600 MW. Because of differing molecular configurations, however, a polystyrene standard curve cannot be used to accurately describe apparent molecular weights of the poly(ester-urethanes).

Lyophilized samples were extracted with 2.5 ml of THF overnight with rotation at 37°C. Sterile 4.0 mm glass beads were added to increase dissolution. The samples were filtered through 0.45 µm Millipore HF filters and 100 µl sample volumes were chromatographed. The molecular weight distribution post degradation was recorded and compared to control samples treated in an identical manner.

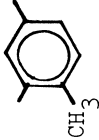
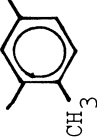
Results and Discussion

Darby and Kaplan reported in 1968 that polyester based polyurethanes were better nutrients for fungi than polyether based polyurethanes (4). A similar finding was reported by Potts et. al. later (5). Both of these reports were based upon experiments using polyurethane samples as the only available carbon nutrient for the growth of fungi and the extents of fungal growth after the testing period were taken as an indication of the extents of polymer degradation. Our studies on fungal degradation of polymers have shown that the growth of fungi is a good indication of polymer biodegradation. However, the absence of fungal growth cannot be viewed as definite proof of lack of biodegradation. Occasionally we found that some microorganisms degraded polymer samples without being able to utilize the degraded end products.

In these cases, the absence of extensive fungal growth does not mean lack of biodegradation. Studies on the changes of the polymer samples (molecular weight, molecular weight distribution, morphology, etc.) together with changes of the microorganisms provide a better understanding of the biodegradation processes. Enzymatic degradation, being experimentally less complicated than fungal degradation, has been also carried out in our laboratory together with fungal degradation.

Most of the commercial polyurethanes are derived from the polymerization of polyesterdiols or polyetherdiols with diisocyanates giving poly(ester-urethanes) and poly(ether-urethanes). The question can thus be raised whether the observed biodegradation of polyurethanes is due to the degradation of ester (or ether) linkages but not the degradation of the urethane linkages. We have studied the fungal and enzymatic degradation of polyurethanes derived from ethylene glycol and phenylethylene glycol. These simple polyurethanes contain only urethane linkages that are hydrolyzable. The observed degradation listed in Table 1 can thus be attributed to the degradation of the urethane linkages. Although no growth of *Aspergillus niger* on the polyurethane samples could be detected the polyurethanes were found to be readily degraded by the enzyme containing detergent Axion. It is interesting to note that the phenylated polymers 1 and 3 are less degradable than the nonsubstituted polymers 2 and 4. Since racemic monomer was used to prepare 1 and 3 it is quite possible that only one of the two enantiomeric forms can be attacked by the enzyme. Earlier we found that the poly(amide-urethane) derived from natural mandelic acid was degraded more readily by both enzymes and fungi than the corresponding non-substituted poly(amide-urethane) derived from glycolic acid (6). As is true in most enzyme catalyzed reactions, biodegradation of synthetic polymers has been found by us to proceed in a stereospecific manner. Kim, Gilbert, and Stannett reported in 1973 that the polyurethanes derived from cellulose hydrolysates were degraded by the enzyme cellulysin (7). Compared to polyamides having similar structural features the simple polyurethanes were found to be more susceptible to biodegradation. Earlier reports (4,5) on biodegradable polyurethanes included mostly polyurethanes derived from low molecular weight polyesterdiols prepared from diols and diacids. Recently polycaprolactonediolols have gained increasing importance as commercial prepolymers for polyurethanes. In view of the well known biodegradability of polycaprolactone (5) we decided to study the biodegradation of polyurethanes derived from polycaprolactonediolols.

Table 1. Biodegradation of Polyurethanes

Polymer	R	R'	$[\eta]^a$	T _m ^{o,b}	% Degrad. ^c Axion	A. niger Growth
1	Ph	-(CH ₂) ₆ -	0.12	43-59	1.1(18.6)	0
2	H	-(CH ₂) ₆ -	0.20	136-168	4.9(10.2)	0
3	Ph		0.13	146-173	3.0(17.3)	0
4	H		0.21	152-185	9.6(14.4)	0

a In *m*-cresol at 40°C.

b By DSC.

c % Degradation due to enzyme, total degradation minus degradation due to buffer, (% degradation due to buffer), 10 days, at 30°C, pH 7.0, measured by weight loss.

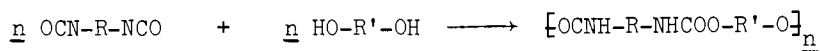
Polyurethanes were prepared from polymerizations of polycaprolactonediol (MW 3000, 1250, and 530) with 1,6-hexamethylene diisocyanate, Scheme 1. To avoid the possibility that some of the traditional metallic catalysts for polyurethane polymerization might be biocides the polymerizations were carried out without catalyst. Purified polyurethanes were cast into films from THF solutions. Dry films were then subjected to semi quantitative (ASTM and zone clearing) and quantitative (GPC) studies of biodegradation by two fungi (Aspergillus fumigatus and a Fusarium solanii) and a yeast (Cryptococcus laurentii). All these microorganisms were found by our previous studies to be effective in the degradation of polycaprolactone.

ASTM Analysis and Zone Clearing Analysis. All the polymers can be considered very biodegradable by these methods except the commercial sample, which degraded slowly. In general, there is no discrimination between polymers. All received the highest growth rating except for polyurethane derived from PCL (MW 1250), exposed to Fusarium sp. (Table 2). The presence of added nitrogen in the growth medium did not apparently inhibit the degradation by repressing the synthesis of enzymes for nitrogen metabolism. It was anticipated that the utilization of nitrogen containing subunits might be inhibited in the presence of excess nitrogen. In fact, the lack of added nitrogen was seen to result in less extensive hyphal development for the sample, as mentioned above.

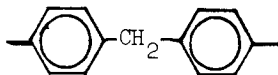
An example of this is seen in Figure 1. These results were difficult to quantitate by ASTM ratings because the surface of the nitrogen deficient plates was covered, but aerial hyphae were sparse, as compared to the parallel plates containing nitrogen. In these cases the organisms were growth limited due to a lack of sufficient nitrogen.

Cr. laurentii could not be evaluated on the same basis because as a yeast it does not produce hyphae, and only colony development (or the lack thereof) or zone production could be used as criteria. An example of a zone can be seen in Figure 2, presumably caused by the action of an extracellular enzyme on the polymer film which altered the light scattering characteristics. These zones were also detected in areas of high hyphal concentration.

GPC Analysis. The organisms chosen were ones found to be effective degraders of polyesters; specifically polycaprolactones. It was thought that they would prove to be effective degraders of these poly(ester-urethanes). All the investigated polymers were found to have molecular weights in the area of 90,000 as estimated by GPC. An enrichment of the culture media, set up as a parallel experiment, was done in hopes of discovering the effects of nitrogen incorporation into the polymer backbone. Some of the

Scheme 1

R: $-(\text{CH}_2)_6-$,



R': Polycaprolactonediois

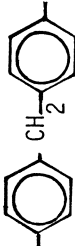
PCL(MW 3000)

PCL(MW 1250)

PCL(MW 530)

\overline{Mn} 40,000

Table 2. Biodegradation of Polyurethanes by *Fusarium solani* Evaluated by ASTM method

R	R'	Extent of Growth ^a	
		+ Nitrogen ^b	-Nitrogen ^c
$-(\text{CH}_2)_6-$	PCL(MW 3000)	4	4
	PCL(MW 3000)	4	3
	PCL(MW 1250)	3	3
	PCL(MW 530)	4	4
	PCL-Commercial	4	1

a ASTM rating: 4--60 to 100% surface covered with fungal growth

3--30 to 60% surface covered

2--10 to 30% surface covered

1-- 1 to 10% surface covered

0-- no visible growth

b With added nitrogen nutrient.

c Without added nitrogen nutrient.

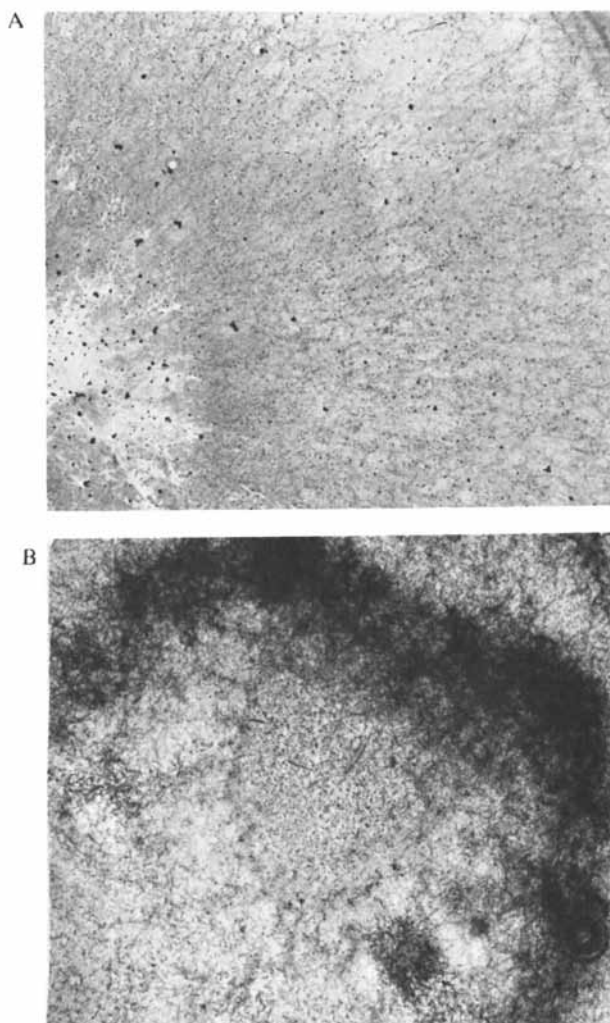


Figure 1. An example of the effects of added nitrogen on hyphal development. (A) Polyurethane from PCL(MW 1250) inoculated with Fusarium sp. lacking added nitrogen nutrient and without extensive hyphal development. (B) The same polymer and organism but with added nitrogen nutrient and, as a result, much more highly developed hyphal structures seen as the dark areas. Both micrographs are at 3 \times .

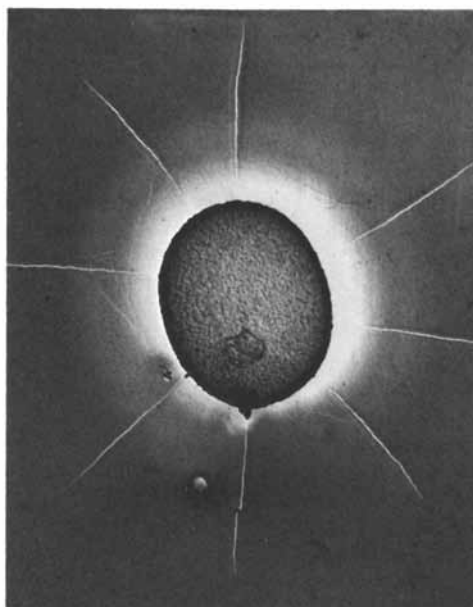


Figure 2. An example of zone clearing found in the yeast inoculated sample—polyurethane from PCL(MW 1250) inoculated with Cr. laurentii on a nitrogen-enriched plate.

observed effects are reported in this study. The lack of added nitrogen was thought to force the organism to disassemble the urethane linkages to satisfy its nitrogen nutrient requirements. The tetrahydrofuran (THF) extracts of the degraded films were subjected to gel permeation chromatography (GPC). By measuring the percent decrease in area of the high molecular weight peak component as compared to the peak areas of uninoculated chromatographed controls, the amount of microbial degradation was determined. The areas of all peaks were determined using a planimeter. This change in peak area is regarded as an indication of microbial action (or polymer susceptibility to attack) in which the organisms are utilizing the polymer as a substrate.

With the exception of the commercial sample, all the polymers were degraded with significant differences discernible by this analysis (Tables 3-7). In the presence of added nitrogen, all three organisms have higher activity towards the two polymers which contain the longest chain of polyester subunits. This is not unexpected - the organisms were selected for their ability to hydrolyze polyester substrates. For the two fungi, the relationship holds that the longer the polyester chain the more degradable the polymer. This did not hold for the yeast.

In the absence of added nitrogen, degradation is more markedly delineated on the basis of polymer composition. In all cases, except for degradation by *Cr. laurentii*, hydrolysis was reduced. *A. fumigatus* and *Cr. laurentii* displayed enhanced activity towards the long polyester chain containing poly(ester-urethanes).

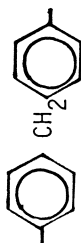
From the chromatograms, two non-quantitative observations were made. Degradation was non-selective in that the molecular weight distribution was not affected by the action of the organisms. All molecular weight species were reduced in concentration. Secondly, accumulation of low molecular weight material was detected in most of the samples. In five cases, the amount of this material is reduced or absent in the tubes lacking added nitrogen as compared to the parallel tubes containing nitrogen. This could be the result of an increased dependence of the organism on the nitrogen in the polymer for growth, which yields a more complete utilization of substrate.

It is interesting to note that both polyurethanes derived from aliphatic diisocyanate and aromatic diisocyanate were degraded. With a few exceptions, the more rigid aromatic polymers degraded at slower rates than the aliphatic polymers.

Conclusions

Polyurethanes were found to be biodegradable by the enzyme, fungi, and yeast studied. In the case of poly(ester-urethanes) a relation between the polyester chain length of the copolymer

Table 3. Biodegradation of Polyurethanes by *Aspergillus fumigatus* Evaluated by ASTM Method


		Extent of Growth ^a	
		+ Nitrogen ^b	-Nitrogen ^c
R	R'		
$-(CH_2)_6-$	PCL(MW 3000)	4	4
	PCL(MW 3000)	4	4
	PCL(MW 1250)	4	4
	PCL Commercial	2	2

a ASTM rating

b With added nitrogen nutrient

c Without added nitrogen nutrient

Table 4. Biodegradation of Polyurethanes by *Cryptococcus laurentii* Evaluated by Zone Clearing

R	R'	Zone Size, mm ^a	
		+ Nitrogen ^b	-Nitrogen ^c
$-(\text{CH}_2)_6-$	PCL(MW 3000)	40-45	41-42
	PCL(MW 3000)	12-22	13
	PCL(MW 1250)	11-15	12
	PCL(MW 530)	d	d
	PCL-Commercial	0	0

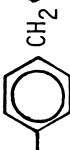
a. The area of polymer affected by degradation

b With added nitrogen nutrient

c Without added nitrogen nutrient

d Film too transparent to evaluate but degradation visible

Table 5. Biodegradation of Polyurethanes by Fusarium solanii Evaluated by GPC

R	R'	% Degradation ^a	
		+ Nitrogen ^b	-Nitrogen ^c
$-(\text{CH}_2)_6-$	PCL(MW 3000)	68 ^d	14 ^d
	PCL(MW 3000)	49 ^d	43
	PCL(MW 1250)	38 ^d	23 ^d
	PCL(MW 530)	31 ^d	29
	PCL-Commercial	8	4


^a Obtained from the area decrease of GPC peak as compared with that of uninoculated control

^b With added nitrogen nutrient

^c Without added nitrogen nutrient

^d Accumulation of low MW products was observed

Table 6. Biodegradation of Polyurethanes by *Aspergillus fumigatus* Evaluated by GPC

$\left[\text{OCNH-R-NHC(OO-R')-O} \right]_n$		% Degradation ^a	
R	R'	+ Nitrogen ^b	-Nitrogen ^c
$-(\text{CH}_2)_6-$	PCL(MW 3000)	98 ^d	22 ^d
	PCL(MW 3000)	45 ^d	38 ^d
	PCL(MW 1250)	42 ^d	19 ^d
	PCL(MW 530)	36 ^d	6 ^d
	PCL-Commercial	7	5


a Obtained from the area decrease of GPC peak as compared with that of uninoculated control

b With added nitrogen nutrient

c Without added nitrogen nutrient

d Accumulation of low MW products was observed

Table 7. Biodegradation of Polyurethanes by *Cryptococcus laurentii* Evaluated by GPC

$\left[\text{OCNH-R-NHCOO-R}'-O \right]_n$		% Degradation ^a	
R	R'	+ Nitrogen ^b	-Nitrogen ^c
$-(\text{CH}_2)_6-$	PCL(MW 3000)	42 ^d	48 ^d
	PCL(MW 3000)	33	31
	PCL(MW 1250)	5 ^d	15 ^d
	PCL(MW 530)	31 ^d	6
	PCL-Commercial	14	9

a Obtained from the area decrease of GPC peak as compared with that of uninoculated control

b With added nitrogen nutrient

c Without added nitrogen nutrient

d Accumulation of low MW products was observed

and susceptibility to these organisms was noted, with biodegradability increasing with increasing ester chain length. This held true for nitrogen enriched or deficient culture conditions, although in the absence of added nitrogen general degradation was reduced. Low molecular weight material produced in most cases indicates an incomplete utilization of hydrolysis products, which, with time, are expected to be metabolized.

Acknowledgements

We thank the National Science Foundation (through Grant DMR7813402) for support of our research.

Literature Cited

1. S. J. Huang, M. Bitritto, K. W. Leong, J. Pavlisko, M. Roby, and J. R. Knox, "Advances in Chemistry Series, No. 169, Stabilization and Degradation of Polymers", D. L. Allara and W. L. Hawkins, Eds., Am. Chem. Soc., 1978, pp. 205-214.
2. ASTM Annual of ASTM Standard, Part 27, ASTM-D-1929, p. 593.
3. S. J. Huang, D. A. Bansleben, and J. R. Knox, *J. Appl. Polym. Sci.*, 23, 429 (1979).
4. R. T. Darby and A. M. Kaplan, *Appl. Microbiol.*, 16, 900 (1968).
5. J. E. Potts, R. A. Clenning, W. B. Ackart, and W. D. Niegisch, "Polymer and Ecological Problems", J. Guillet, Ed., Plenum Press, New York, 1973, pp. 61-79.
6. M. M. Bitritto, J. P. Bell, G. M. Brinkle, S. J. Huang, and J. R. Knox, *J. Appl. Polym. Sci.: Appl. Polym. Symposium* 35, 405 (1979).
7. S. Kim, V. T. Stannett, and R. D. Gilbert, *J. Polym. Sci. Polym. Letter Ed.*, 11, 731 (1973).

RECEIVED April 30, 1981.

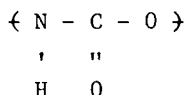
Development of a Biomedical Polyurethane

Orthopedic Implant Applications

EDWARD W. C. WONG¹

Biomaterials Group, Ontario Research Foundation,
Sheridan Park, Mississauga, Ontario, Canada L5K 1B3

Polyurethanes are block copolymers containing blocks of low molecular weight polyesters or polyethers linked together by a urethane group:



These have the versatility of being either rigid, semi-rigid or flexible. These materials, in general, have excellent flex-life, strength and other mechanical properties. They have been described as resistant to gamma radiation, oils, acids and bases.

The first generation of polyurethanes used for implant studies were industrial grade and are commercially available. Mirkovitch and Associates, (1) however, found the Estane^R (B.F. Goodrich, Company) polyester urethanes to degrade rapidly when implanted in the muscle of dogs or when used as monocusp valvular prosthesis. Sharp (2) and co-workers observed thromboresistance of a polyester-polyether polyurethane (Goodyear Tire and Rubber Company) in intravascular replacement.

The first biomedical grade polyether polyurethane was synthesized by two groups. Boretos and Pierce (3) introduced the biomedical application of segmented polyether polyurethanes containing hard segments of urea and soft segments of polyether linked by the urethane group. These materials sustained high modulus of elasticity, biocompatibility, resistance to flex-fatigue and excellent stability over long implant periods. (4)

From their previous experience in the synthesis of polyurethanes for dialysis membranes, Lyman and Associates (5) also introduced a segmented polyether polyurethane which has shown excellent thromboresistance. (6)

¹ Current address: Avco Everett Research Laboratory, Inc., 2385 Revere Beach Parkway, Everett, Massachusetts 02149

Nyilas, the developer of Avcothane^R, synthesized a copolymer of polyurethane and polydimethyl siloxane(7) which is blood compatible and used in the making of heart assist balloon pumps.

Another biomedical grade segmented polyether urethane Biomer^R which is now available commercially from Ethnor, Division of Ethicon, Incorporated, is based on polyether from polybutanediol-1,4.

In 1968, Ontario Research Foundation developed a series of segmented polyether polyurethanes as polymer membrane materials for reverse osmosis, ultrafiltration and hemodialysis. The elastomers of recent implant studies are polyurea-urethanes(8) with modification of the synthesis limited to only one variable-- the chain length of the polyether component.

Synthesis and Modification. A series of polyurethanes and polyurethane-ureas of varying degrees of hydrophilicity and hydrophobicity and mechanical property were synthesized. The polymers were prepared by a solution polymerization method and consisted of three components: a polyether, a diisocyanate, and a chain extender. In our studies, polyurethanes (Table I) were based on a carbowax (polyoxyethylene glycol), MDI (methylene bis-4-phenyl isocyanate) and 1,5-pentanediol. Polyurethane-ureas (Table II) were obtained by substituting the chain extender from a diol to a diamine. The polyurethane-ureas (Table II) were obtained by changing the chain extender from a diol to a more reactive diamine. The polyurea-urethanes (Table III) were obtained by using a diamine terminated polyether instead of the carbowax.

The hydrophilicity and hydrophobicity of the polymer could be modified chemically by changing the following variables:

- Increasing hydrophilicity by selecting polyethers longer carbon chain: polyoxyethylene (2 C) < polyoxypropylene (3 C) < polytetrahydrofuran (4 C).
- Increasing hydrophilicity by raising the molar ratio of polyether/chain extender.
- Increasing hydrophilicity by lengthening the chain length of polyether.

In most of our studies, modification of the synthetic route was limited to only one variable, the chain length of the polyether component. The same molar ratio of polyether/chain extender diisocyanate (MDI) and chain extender (diethylene glycol) were used. The molecular weight of the polyether component of J-20, J-9 and J-6 was 2,000, 1,000 and 600 respectively. A wide range of properties was obtained from this series of polyurethanes. Properties intermediate between J-20 and J-9 were also obtained by

TABLE I

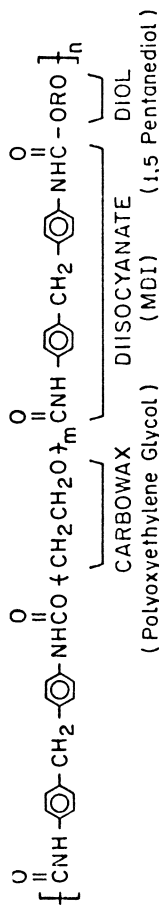


TABLE II

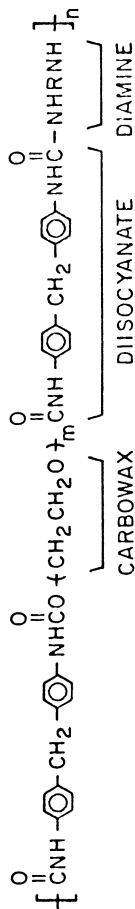
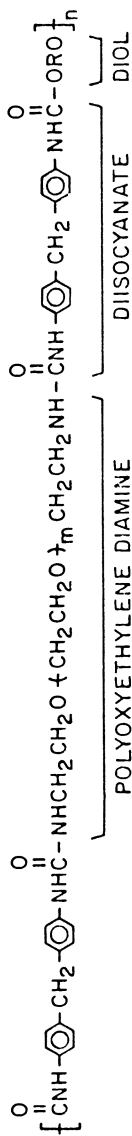


TABLE III



using a 1:1 molar ratio of J-20 and J-9 polyether without changing other variables.

Even though the polymer is linear and has no chemical cross-linking, it behaves like a rubber. There are physical cross-linking from crystalline packing of urethane hard segments. These crystalline domain structures also explain why the longer the polyether chain, the more flexible the system, lower elastic modulus and more hydrophilicity. The hydrophilic property of these polymers was measured by the % moisture absorption of dry polymer film.⁽⁹⁾ Films of a uniform size and thickness (2" diameter disc, 1 mil thickness) were dried under high vacuum and then exposed to 98% RH in a desiccator containing a saturated solution of $Pb(NO_3)_2$ until no more water was absorbed. The percent of water absorbed increased from J-20 > J-9 > J-6. Results are shown in Table IV.

TABLE IV

% MOISTURE ABSORPTION OF DRY POLYMER
FILMS (THICKNESS = 1 mil, DIAMETER OF DISC = 2")

Film	Dry Wt. (gms)	Water Pickup	% Water Absorbed
J-6-1	0.1567	0.0155	9.9
J-9-1	0.1526	0.0409	26.8
J-20-1	0.0636	0.0397	62.4
JD-4-1	0.1591	0.0111	7.0
JD-6-1	0.2767	0.0115	4.2

Biocompatibility and Mechanical Properties. Currently, their are no suitable artificial materials for the prosthetic replacement of articular cartilage. The biocompatibility is considered the primary criterion in the selection of such a material. In a recent study, Furst and co-workers⁽¹⁰⁾ compared the biocompatibility of the polyurethane to the well known medical grade silicone polymer. The tissue reactions to small polymer discs, inserted in an articulating space--the suprapatellar bursa of rabbits, was examined. The foreign body reaction of the tissue at the implantation site was evaluated at intervals of 7 days, 21 days and 6 months. The tissue reaction was characterized by the thickness of the patellar articular cartilage and the presence or absence of morphonuclear leukocytes, macrophages, and foreign body giant cells in synovium and menisci tissue samples.

Histological results indicated that the J-9 polyurethane produced less foreign body tissue reaction than did the medical grade silicone rubber control. The polyurethane articulating patellas showed normal articular cartilage and little cartilage appeared on the patellas of the silicone control knees. All menisci samples from both the experimental and control knees. All menisci samples from both the experimental and control knees appeared normal regardless of the time interval. The synovium samples from the polyurethane knees appeared normal but the samples from the silicone control knees contained many uniform holes that appeared to be lipid deposits.

Mechanical testing of the polyurethanes was performed by a modified indentation/shear method described by Parsons and Black.⁽¹¹⁾ Relaxed and unrelaxed shear moduli of these polymers were measured in a simulated body fluid environment and compared to moduli of rabbit and human articular cartilage. This is shown in Table V. These tests, in addition to viscoelastic measurements of those polymers, indicate that this new polyurethane formulation is an excellent candidate for synthetic cartilage fabrication.

TABLE V

VISCOELASTIC AND HYDROPHILIC PROPERTIES OF CARTILAGE
AND SYNTHETIC MATERIALS
(at 37°C in Saline Solution)

<u>Materials</u>	<u>Unrelaxed Shear Modulus (MPa)</u>	<u>Relaxed Shear Modulus (MPa)</u>	<u>Amount of Water (Weight %)</u>
Human Cartilage	1.04	0.24	60-80
Rabbit Cartilage (Alive)	0.53	0.11	-
Polyurethane			
J-20	0.57	0.33	62
J-9	1.72	0.66	27
J-6	2.58	0.92	10

Wear and Lubrication In-Vitro Study. Polyurethane surface layers with viscoelastic properties similar to natural articular cartilage has been proposed for use with hemiarthroplasty, a single component joint replacement in which the implant is intended to bear against a natural cartilage surface. Medley and

co-workers(12) have carried out in vitro experiments to study the effects of fluid film lubrication on the wear of polyurethane.

The test apparatus is shown in Figure 1. The experimental model consists of a flat polyurethane block sliding over a stationary loading pin with a linear reciprocating motion. A variable speed motor was connected via a scotch yorke arrangement to produce a range of sinusoidal velocities and a constant stroke length. A load was set by placing the appropriate amount of lead shot in the cup. The pin tip could be detached thus allowing either a glass or a metal sphere to be used against the polyurethane.

In the wear tests, the polyurethane under the tip of the sphere was subjected to a maximum stress of 2.4 MPa whereas articular cartilage(13) typically is subject to average contact stresses of 2.75 MPa. A typical "average" velocity, if only one surface moves, for human hip and knee(14) is 0.05 m/s. The polyurethane was subject to velocity from zero to 0.126 m/s. Thus, except for higher deformation rates, specific regions of the polyurethane were subject to approximately physiological conditions. Fluid film protection is shown to greatly reduce, if not eliminate, wear. The results of this study suggest the possibility of designing a prosthesis with a polyurethane surface layer for hemiarthroplasty or a prosthetic replacement for articular cartilage such that a fluid film will be formed to protect both surfaces during implant functioning.

Total Elbow Joint Replacement. A common problem encountered with the hinge-type total elbow joint replacement is the loosening of the humeral component as a result of loading across the joint.(15,16) A new concept for a total elbow replacement with the capability to absorb loading and reduce peak force levels at the humeral component/bone interface has been investigated. The design, Figure 2, is based on two elastomeric spheres serving as a pivot in the replacement with their elastomeric properties allowing for the absorption of loading through deformation.(17) In this study, the modification of synthetic route in relation to the damping coefficient has been examined. The method of measuring the damping coefficient of the polymer spheres and the impact testing using the model elbow has been described previously by Wong and White.(17) The damping coefficient (quality factor) of the system can be readily calculated from the following impression:(18)

$$\text{Quality Factor, } Q = \frac{f_R}{f_2 - f_1}$$

where f_R = frequency at resonance (peak power) and f_2 and f_1 are frequencies respectively above and below f_R at the point of one-half peak power. The damping coefficient of the system is equal to the reciprocal of Q . Figure 3 and 4 showed the measurement

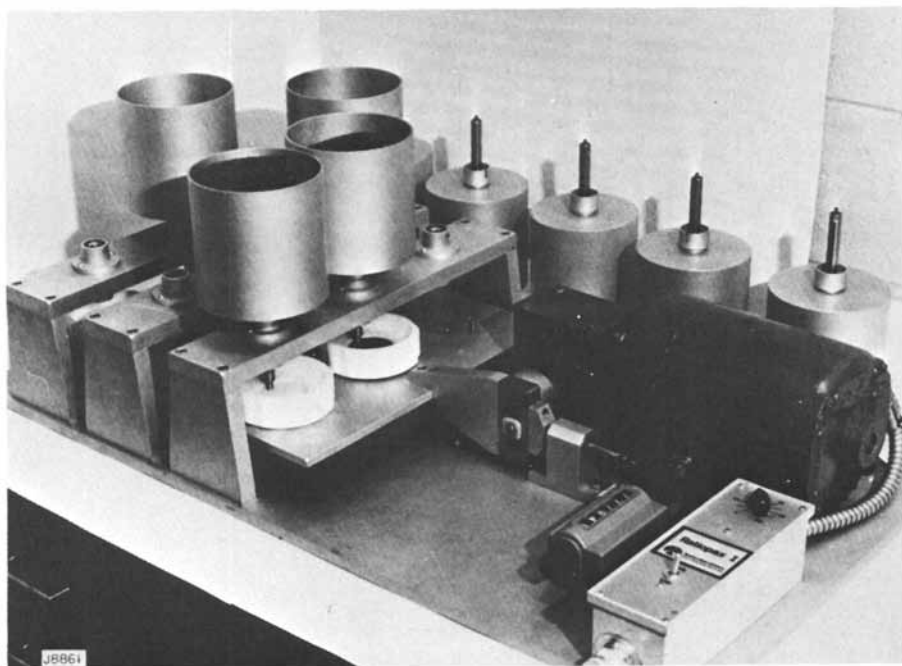


Figure 1. Wear test apparatus.

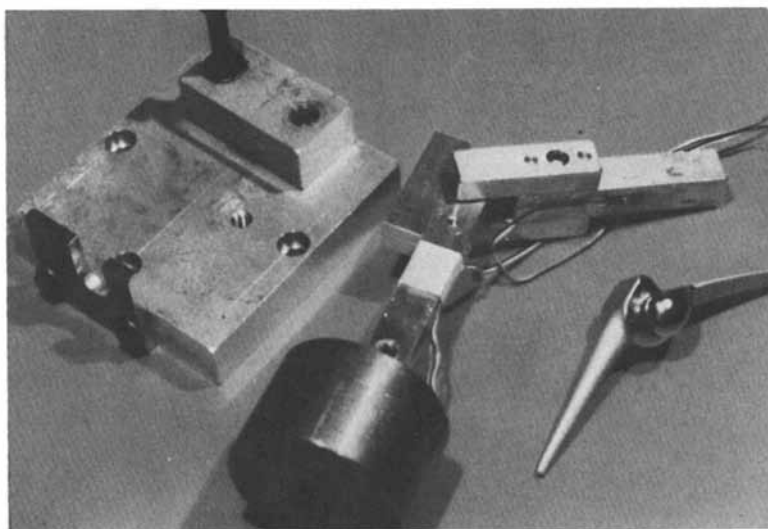


Figure 2. Model elbow and new total elbow joint replacement design.

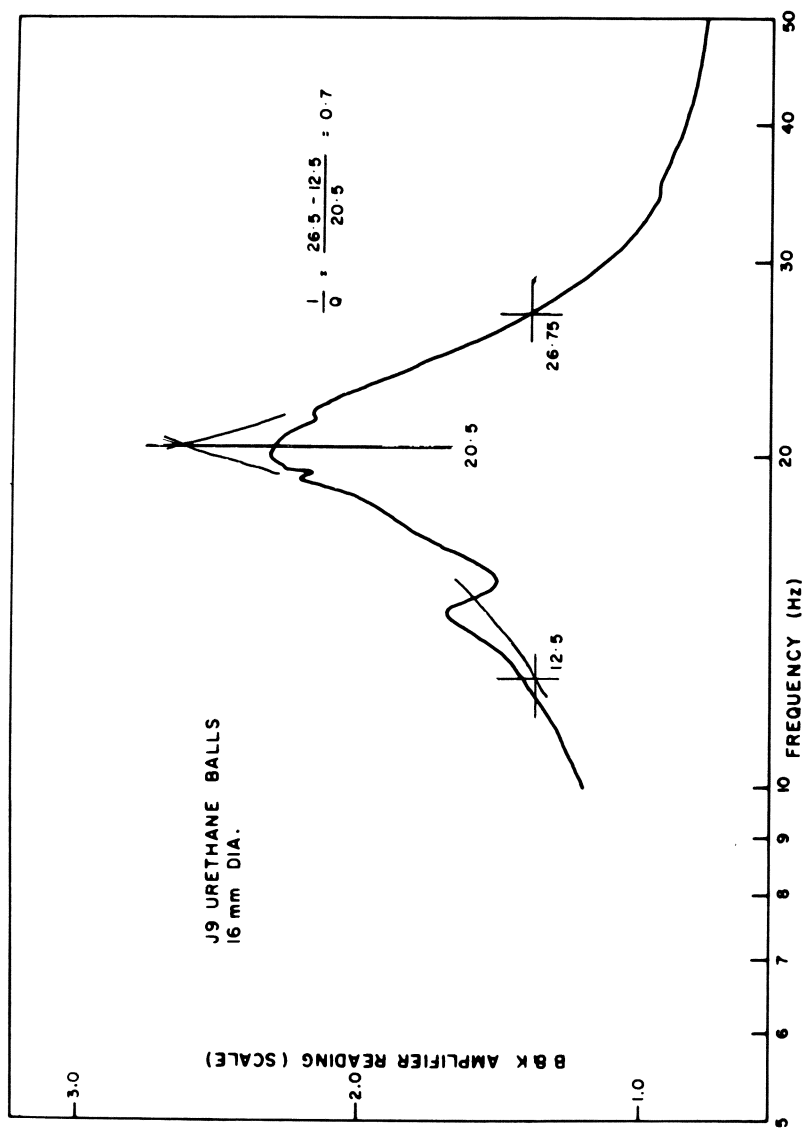


Figure 3. Measurement of damping coefficient of J-9 urethane spheres.

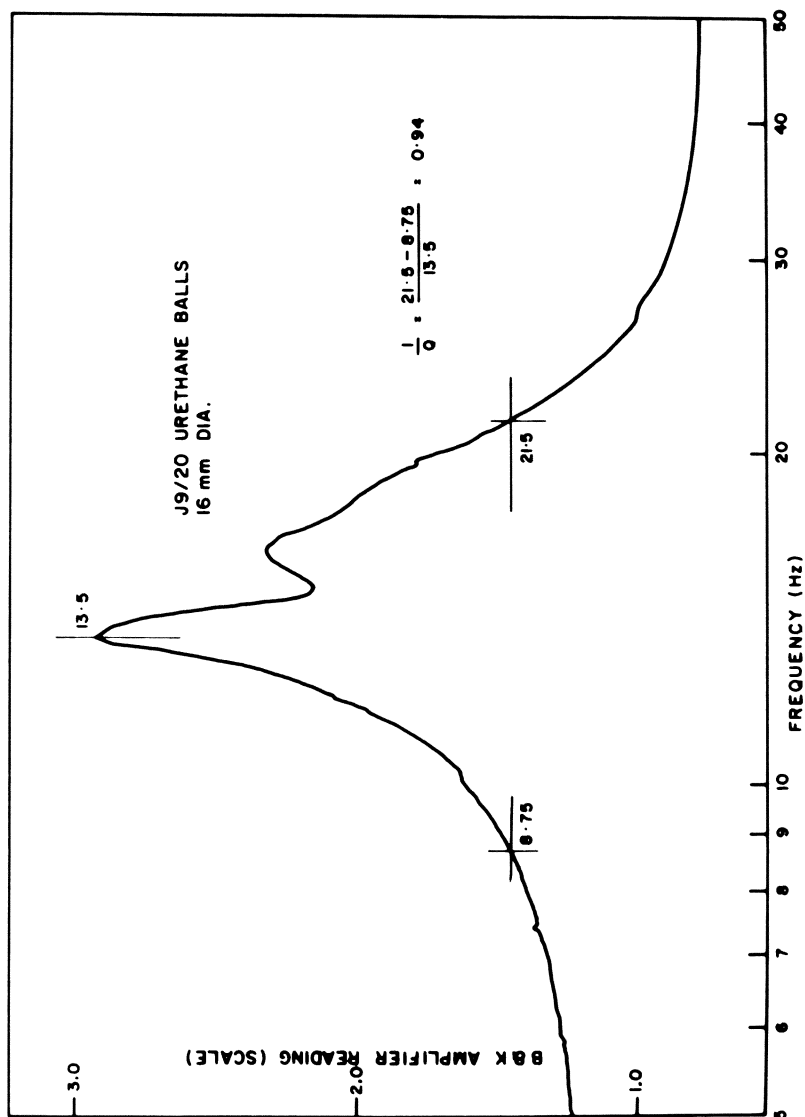


Figure 4. Measurement of damping coefficient of J-9/J-20 urethane sphere.

of 1/Q. The damping coefficient of J-9 polymer sphere was 0.7 which is the optimum in many vibration damping applications.

Figure 5 of the impact test showed that J-9 polyurethane was able to reduce the peak force value down to 36% that of steel balls without sacrificing mechanical strength. The result from the impact test and the measurement damping coefficient indicate that polyurethane J-9 is the optimum sphere material in the new total elbow joint replacement design.

In-Vivo Percutaneous Implant Experiment. The principle of percutaneous attachment has extensive application in many biomedical areas, including the attachment of dental and orthopedic prostheses directly to skeletal structures, external attachment for cardiac pacer leads, neuromuscular electrodes, energy transmission to artificial heart and for hemodialysis. Several attempts to solve the problem of fixation and stabilization of percutaneous implants(19) have been made. Failures were also attributed to the inability of the soft tissue interface to form an anatomic seal and a barrier to bacteria. In the current studies, the effect of pore size on soft tissue ingrowth and attachment to porous polyurethane (PU) surface and the effect of the flange to stem ratio and biomechanical compliance on the fixation and stabilization of the percutaneous devices have been investigated.(20)

Solid discs (2.5 cm diameter) were molded from J-9 polyurethane. A series of porous J-9 PU surfaces with two different thicknesses (1 mm and 10 mm) and two porosities (fine, 47-75 μm ; coarse, 150-250 μm) was prepared and bonded on the solid discs. A series of percutaneous implant devices with three stem/flange ratios (1:1, 1:2 and 1:4) was fabricated from three materials (Dacron velour - silicone, porous PU and porous metal). The implants were totally porous (coarse, 150-250 μm) with 1.5 mm diameter holes drilled throughout the device. Figure 6 shows the mold and the polyurethane percutaneous devices with three stem/flange ratios and 1.5 mm diameter drilled holes.

Discs were implanted subcutaneously in the abdomen and in the thigh against abraded muscle. Vigorous tissue ingrowth into the coarse porous PU was observed, as shown in Figure 7. The muscle tissue could be seen to be separated only by a thin fibrous tissue sheath ($\sim 30 \mu\text{m}$), demonstrating its biocompatibility. The cross section of one of the drilled discs showed how the fibrous tissue through-growth helped anchor the soft tissue even to the non-porous side of the implant, as shown in Figure 8.

Percutaneous devices were implanted dorsally along the spine in three pigs (Figure 9). Gross examination of six-month implants showed that the porous metal device with the 1:2 flange had excellent stabilization and formed the best anatomic seal and barrier to bacteria. Due to their weight, metal devices with a large flange or no flange sank beneath the skin pulling the skin down. However, one-year implants showed signs of tissue necrosis after 9 months which led to infection and eventual rejection. The

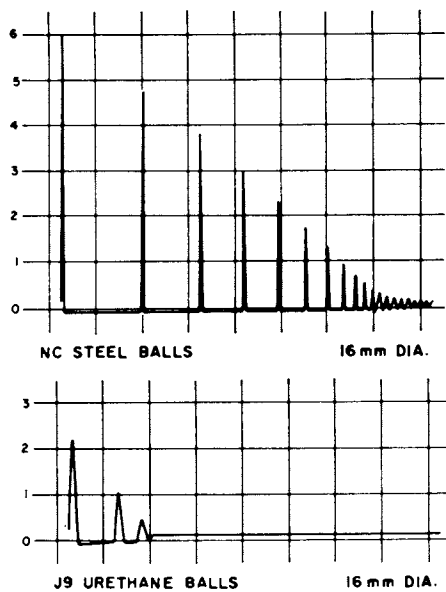


Figure 5. Impact test: measurement of peak force and vibration.

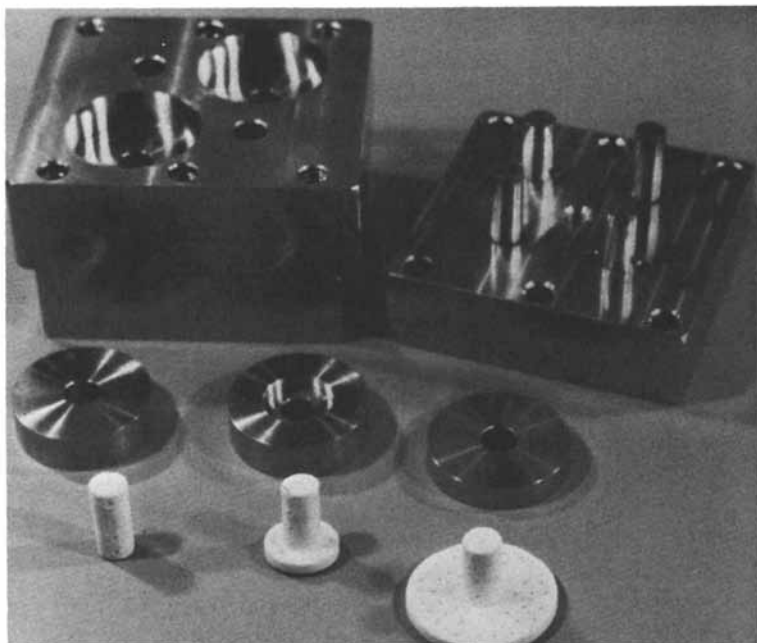


Figure 6. Porous polyurethane percutaneous implantable devices and molds.



Figure 7. Histological section showing vigorous tissue ingrowth into coarsest porous polyurethane (150–250 μm pores).

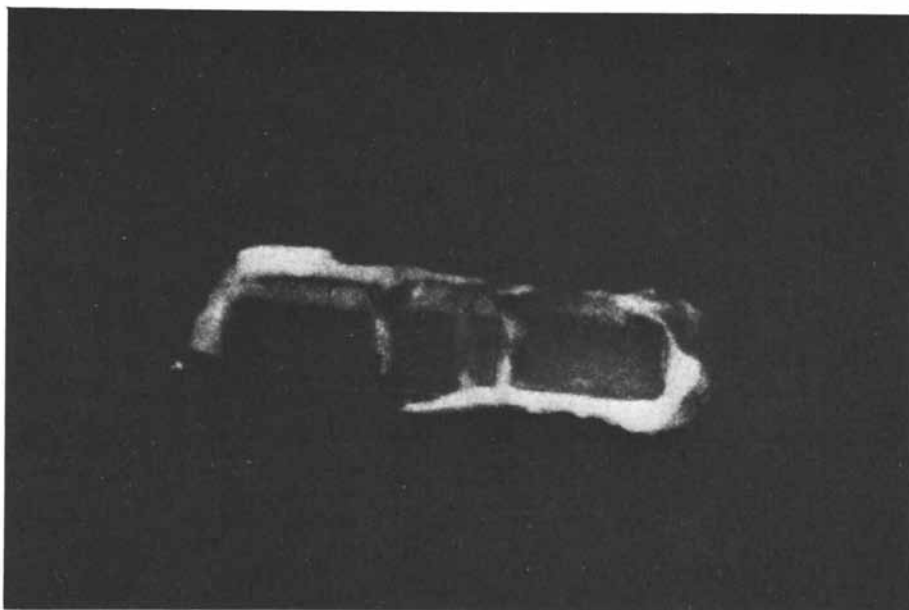


Figure 8. A cross section of drilled disc showing fibrous tissue through growth for fixation of device.

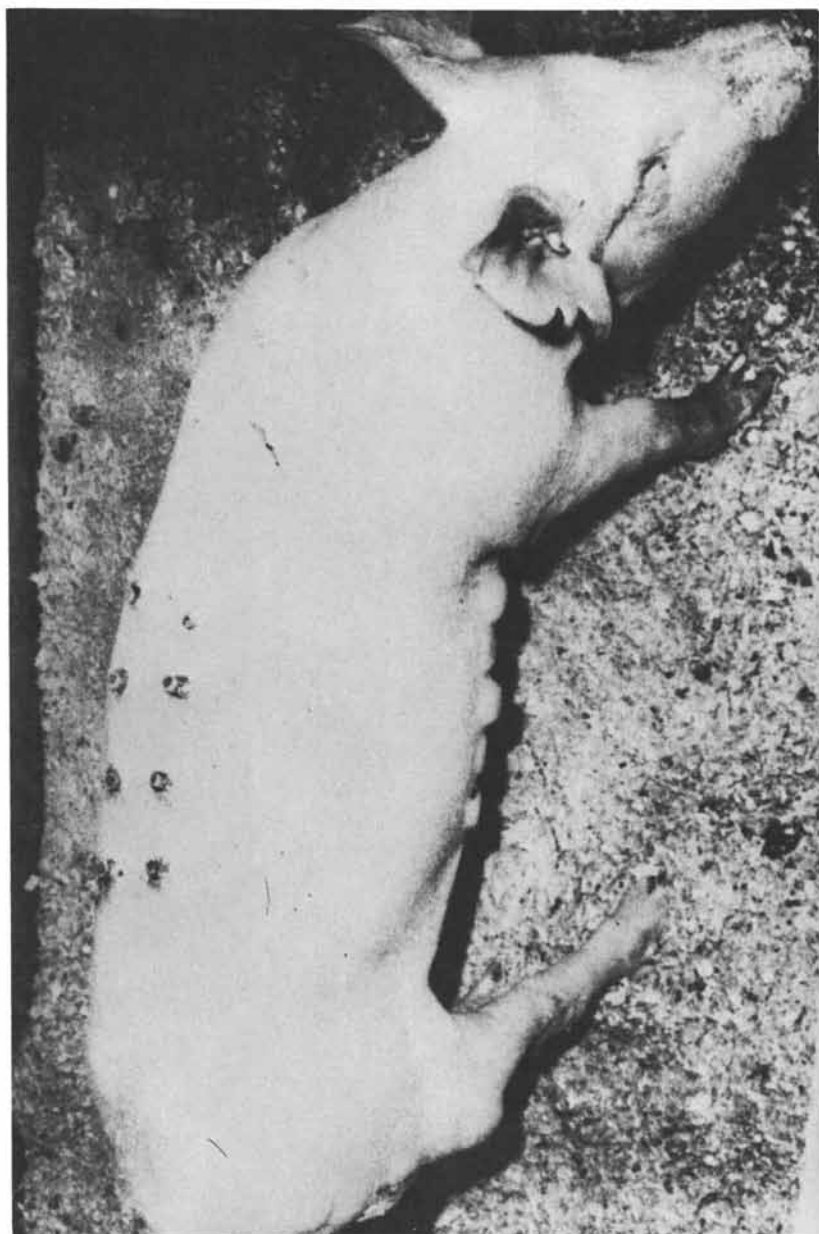


Figure 9. Sites for the percutaneous implantation of the porous devices in the dorsum and subcutaneous implantation of discs in thigh and belly.

failure has been attributed to the incompatibility of interface compliance leading to cyclic fatigue of the tissue at tissue/metal interface as load transfer is taking place.

Percutaneous PU devices showed excellent results in three-month implantations. However, evidence of mechanical breakdown of the polymer due to vigorous tissue ingrowth and load transfer appeared in the six-month implants. The polymer percutaneous devices were totally porous. The pores were interconnecting voids and the devices were drilled with 1.5 mm holes throughout. Therefore, structurally this porous material was not strong although its compliance matched well with the soft tissue. As the load transfer taking place due to vigorous tissue ingrowth, the fatigue failure was at the polymer interface rather than tissue in the metal implants. Early rejection of Dacron velour/silicone rubber implants in less than 2 to 4 weeks was caused by infections and delamination of Dacron velour/silicone rubber interface.

From these in-vivo implant studies, we learn that the following factors may contribute to the success of a percutaneous device:

- Porous interface with large porosity to provide vigorous ingrowth of soft tissue to form an anatomic seal and a barrier to bacteria.
- Holes drilled throughout the device to promote soft tissue through growth for fixation and to prevent marsupialization of the epidermal cells.
- Importance of flange/stem ratio and the weight of the device in stabilizing and anchoring the percutaneous device.
- Biomechanical compliance or impedance matching of the tissue/material interface is not important for short-term implant experiments. However, for long implanting periods, cyclic fatigue failure of the tissue/material interface is caused by compliance mismatching.

Conclusions. Results from the biocompatibility studies in rabbit supratellar bursa, measurement of hydrophilic properties, lubrication and wear in-vitro studies, determination of viscoelastic properties, measurement of damping coefficient and impact test, total elbow joint replacement design and in-vivo percutaneous implant experiment, all indicate that this series of polyurethanes is an excellent candidate biomaterial for the prosthetic replacement of articular cartilage, artificial joint prostheses and percutaneous implantable devices.

Further testing, in vivo fatigue and wear tests and clinical evaluation, are recommended.

Literature Cited

1. Mirkovitch; V., Akutsu, T. and Kolff, W.J.; Polyurethane Aortas in Dogs - Three-Year Results, Trans. Am. Soc. Artif. Intern. Organs, 1962, 8, 79 .
2. Sharp, W.V.; Gardner, D.L.; Andresen, G.J. A Bioelectric Polyurethane Elastomer for Intravascular Replacement, Trans. Am. Soc. Artif. Intern. Organs, 1966, 12, 1979 .
3. Boretos, J.W.; Pierce, W.S. A Polyether Polymer, J. Biomed. Mat. Res., 1968, 2, 121 .
4. Boretos, J.W., "Concise Guide to Biomedical Polymers, Their Design, Fabrication and Molding"; Charles C. Thomas - Publisher, Springfield, IL, 1973; p. 10 .
5. Lyman, D.J.; Loo, B.H. New Synthetic Membranes for Dialysis IV--A Copolyether Urethane Membrane System, J. Biomed. Mat. Res., 1967, 1, p. 17-26 .
6. Lyman, D.J.; Brash, J.L.; Klein, K.G. The Effect of Chemical Structure and Surface Properties of Synthetic Polymers on Coagulation of Blood, Proceeding Artificial Heart Program USGPO, Washington, D.C., 1969, p. 113 .
7. Nyilas, E. Development of Blood Compatible Elastomers, Theory, Practice and In-Vivo Performance, 23rd Conference on Engineering in Medicine and Biology, 1970, 12, 147 .
8. Wong, E.W. Urethane-Polyether Block Copolymer Membranes for Reverse Osmosis, Ultrafiltration and Other Membrane Processes, ORF Record of Invention No. 335, 1969.
9. Pilliar, R.M.; Wong, W.E.; Black, J. Development of More Compatible Synthetic Articular Surfaces, Digest of 11th International Conference on Med. and Biol. Engineering, 1976, 492 .
10. Furst, L.; Black, J.; Pilliar, R.M.; Wong, E.W. The Bio-Compatibility and Mechanical Properties of a Candidate for Articular Cartilage Replacement, Trans. of the 4th Annual Meeting Society of Biomaterials, 1978, 2, 159 .
11. Parsons, J.R.; Black, J. The Viscoelastic Shear Behavior of Normal Rabbit Cartilage, J. Biomechanics, 1977, 10, 21 .
12. Medley, J.B.; Strong, A.B.; Pilliar, R.M.; Wong, E.W. The Breakdown of Fluid Film Lubrication in Elastic Isoviscous Point Contacts, Wear, 1980, 63, 1, 25 .

13. Keinpson, G.E. Mechanical Properties of Articular Cartilage, "Adult Articular Cartilage" Edited by M.A.R. Freeman, Pitman, London, 1973.
14. Dowson, D. Modes of Lubrication in Human Joints, Proc. Inst. Mech. Engrs., 1966, 181, 3J, 45.
15. Joyce, G.C.; Rack, P.M. The Effects of Load and Force on Tremor at the Normal Human Elbow Joint, J. Physiol. London, 1974, 240, 2, 375 .
16. Ewald, F.C. Total Elbow Replacement Orthop. Clinics, North Am., 1975, 6, 3, 685 .
17. Wong, E.W.; White, R.C. Development of a Stock Absorbing Biomedical Elastomer for a New Total Elbow Replacement Design, Biomat. Med. Dev., Art. Org., 1979, 1, 2, 283 .
18. Kinsler, L.E. Fundamentals of Accoustics, 2nd Ed., Wiley & Sons, New York, 1962 (p. 43).
19. Fernie, G.R.; Kostwik, J.P.; Lobb, R.J.; Pilliar, R.M.; Wong, E.W.; Bennington, A.G. A Percutaneous Implant Using a Porous Metal Surface Coating for Adhesions to Bone and a Velour Covering for Soft Tissue Attachment, Results of Trials in Pigs, J. Biomed. Mat. Res., 1977, 11, 883 .
20. Wong, E.W.; Fernie, G.R.; Pilliar, R.M.; Bennington, A.G. A Percutaneous Implant Experiment Using Porous Coatings for Soft Tissue Attachment: A Preliminary Report, accepted for presentation at International Congress of Implantology and Biomaterials in Stomatology, June 9-12, 1980, in Kyoto, Japan.

RECEIVED April 30, 1981.

Specialty Urethanes for Solventless Coatings and Adhesives

CLAIRE BLUESTEIN

Captan Associates, Inc., Rutherford, NJ 07070

This paper is a commercial survey covering recent developments in urethane coatings and adhesives with reduced solvent contents. There are many aspects of urethane chemistry which make polyurethanes an ideal base for nonsolvent coatings developments. However, in order to achieve practical handling behavior for coatings & adhesives, modifications of classical urethane chemistry are needed.

The major commercial market in polyurethanes, foam, has always been predominantly non-solvent. Solvents had only entered the commercial picture in urethanes in the 1960's when early efforts to make specialized coatings out of state of the art urethanes required a free flowing form. The sizes and distribution of these and other polyurethane commercial markets have been discussed in papers presented earlier in this symposium. In the United States alone, total urethane consumption is presently over 2 billion pounds.

The polyurethane derivatives used in solventless coatings and adhesives systems form a relatively small part of the market. There were about 50 million pounds sales in 1979, however, the solventless segment can be expected to grow at more than the 10% rate expected for all polyurethane coatings & adhesives.

Our problem is that these numerous varieties of commercial polyurethane materials are very slippery to define, particularly in a chemical sense. The name polyurethane attached to a coating or adhesive has a good public relations image, one that generates the impression that it has superior properties. Are all urethane coatings equal, either chemically or property-

0097-6156/81/0172-0505\$05.00/0

© 1981 American Chemical Society

wise? Certainly not. Does the purchaser or user of the coating or adhesive know this? Yes he does, but he does not always know how to select from what is available. Further, how much polyurethane must a coating contain to exhibit so-called "polyurethane properties?"

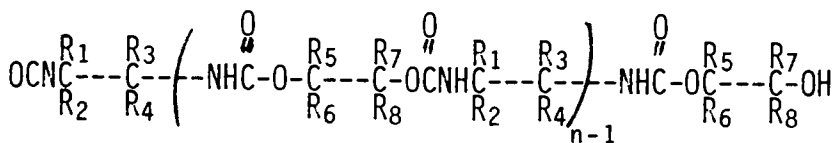
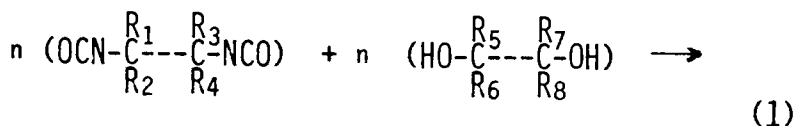
There is no industry guide to answer these questions. This has led many users of both solvent containing and solventless technology to hire their own polyurethane chemical experts and to produce their own multitude of proprietary variants.

Classification

We believe it is a good time to initiate a comprehensive classification system. The system would be oriented to the commercial user and not intended to be limited by chemical considerations, because in the practical world frequently more than one composition will perform an equivalent job. We also believe that such a system would encourage a healthier industrial growth situation. The present ASTM urethane coatings classification (1) covers chiefly the solvent types and is thus an extremely limited one from the viewpoint of the new developments in the past ten years.

Thus, we are proposing such a classification system here. The system presented appears broad enough to encompass all specialized industrial urethanes, including elastomers & moldings and also the solvent containing urethanes. But first, we must define the base polyurethane.

1. Definition. A polyurethane is a polymeric product which has been formed by the reaction of a di- or polyisocyanate and a di- or polyhydroxyl bearing molecule (Equation 1). Equation 1 shows in theory what might happen if precise equimolar amounts of hydroxyl and isocyanate terminated intermediates were reacted. In the practical manufacturing situation it is more complex. Many of the interesting properties and varying behavior of polyurethanes are feasible because a wide range of mole ratios can be used. We believe that the lowest molecular weight range of polymers is about 600. Commercially available materials below that range should be classified as intermediates.



Polyurethane intermediate chemicals have been thoroughly studied and described with regard to the commercial markets (2). They should be incorporated in this classification system, but we do not plan to devote much space to their description in this paper. However, the growing markets for polyurethanes have helped encourage the chemical manufacture of a wide variety of intermediates. The isocyanates most readily available are TDI, MDI and polymeric MDI, but hydrogenated MDI, IPDI, HDI, and their derivatives are frequently chosen for use in coatings. The most economical hydroxyl bearing intermediates are the polyether polyols based on polyethylene and polypropylene oxide, but there are also the polyadi-pate polyglycols (polyesterpolyols). These commodity materials are widely available because they form the basis of the major portion of polyurethane foams. Yet, for the reasons stated above, there are presently many sources of specialty polyol materials for synthesizing polyurethanes.

2. Coreactive and prereacted. All polyurethanes can be subdivided into two broad categories, using the reactive isocyanate functional group to distinguish them. Those that have available NCO (for further reaction) can be called coreactive and those that have essentially no pendant NCO are prereacted. Table I contains an outline and description of some of the available materials that fit each type. It should be noted that some of the prereacted urethanes do contain other chemical functional groups that may be available for non-urethane forming reactions.

3. System design. All commercial coatings and adhesives are prepared with some particular application system in mind. The system design is a highly

TABLE I

POLYURETHANE CLASSIFICATION BASED ON RNCO

<u>A. COREACTIVE</u>	<u>B. PREREACTIONED</u>
1. NCO TERMINATED PREPOLYMERS	1. THERMOPLASTIC URETHANES SOLIDS IN SOLVENTS IN OTHER DILUENTS
2. BLOCKED PREPOLYMERS BLOCKING AGENTS: PHENOLS OXIMES	2. URETHANE ALKYD (ASTM I)
3. NCO TERMINATED ISOCYANURATES	3. URETHANE ACRYLATE
	4. HYDROXYL TERMINATED URETHANE
	5. URETHANE EPOXY

TABLE II

SYSTEM DESIGN

A, ONE COMPONENT

1. CONTAINS COREACTIVE URETHANE
 - A. TO BE MOISTURE CURED (INCLUDES ASTM II)
 - B. TO BE HEAT CURED (INCLUDES ASTM III)
2. CONTAINS PREREACTIONED URETHANE
 - A. TOGETHER WITH SOLVENT OR INERT DILUENT (INCLUDES ASTM VI)
 - B. TOGETHER WITH REACTIVE DILUENTS AND PHOTOINITIATOR FOR UV CURE
 - C. TOGETHER WITH REACTIVE DILUENTS AND/OR OTHER INTERMEDIATE AND CATALYST FOR HEAT CURE

B, TWO COMPONENT

COMPONENT A	COMPONENT B
1. COREACTIVE URETHANE	CATALYST (ASTM IV)
2. COREACTIVE URETHANE	REACTIVE INTERMEDIATE
3. COREACTIVE URETHANE	PREREACTIONED URETHANE (ASTM V)
4. PREREACTIONED URETHANE	CROSSLINKING AGENT
5. PREREACTIONED URETHANE	REACTIVE INTERMEDIATE (FOR GROUPS IN TABLE IV)

important factor, and when a user ignores this, he will not obtain satisfying results from the polyurethane coating. This is not molecular behavior, but processing behavior. Initially we must distinguish between one and two-component systems. In each of these categories we can further subdivide systems performance. A number of examples are shown in Table II.

4. Backbone elements R-N $\overset{\text{O}}$ C-O-R'. In order to assess the general properties a polyurethane film exhibits one must identify the backbone elements: the R and the R' in the title formula. This harkens back to the original intermediate chemicals. But, it has been found in the real world of applications that some reasonably similar combinations are virtually identical. In Table III, therefore, we are able to establish some generalized categories.

<u>R ATTACHED TO N</u>	<u>R' ATTACHED TO O</u>
aromatic	polyether
aliphatic	polyester
non carbon	polycaprolactone
	hydrocarbon
	non carbon

However, identifying the general category of backbone element is not the only thing that should be classified. We should be able to estimate the average molecular weight, or, really better, the NCO to OH ratio used in the urethane synthesis, the overall %

-N- $\overset{\text{O}}$ C-O- in an average molecule, and whether it is a linear, branched, or crosslinked polyurethane. These are more easily said than done. In pure chemical and model compound studies, these quantities can be controlled quite closely, but in the manufacturing kettle, control, though not that precise, will make a real difference in use properties.

A realistic system for assessing classification of these factors may take further time to develop. In current practice, a competent analytical chemist derives most of this information via spectrometry, usually infrared and NMR.

Additional details of backbone elements are shown in Tables IV and V.

TABLE IV

EXAMPLES OF $\begin{array}{c} R_1 \quad R_3 \\ -C---C- \\ R_2 \quad R_4 \end{array}$

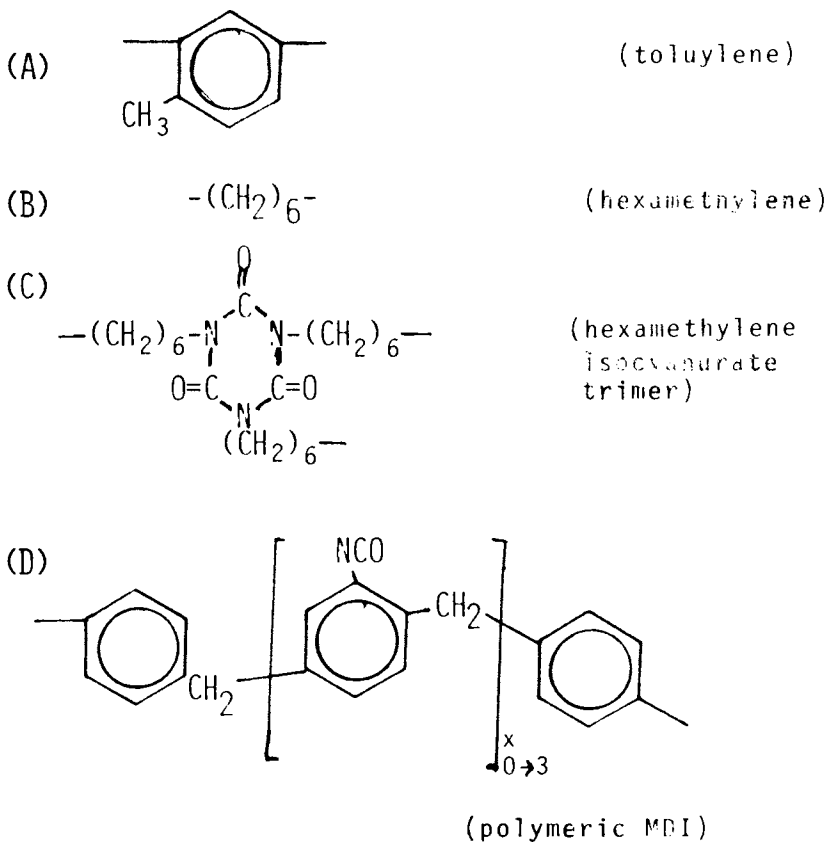


Table IV shows some examples of what might be in the molecule in place of the generalized grouping $\begin{matrix} R_1 & R_3 \\ -C- & -C- \\ R_2 & R_4 \end{matrix}$ in Equation 1. Table V shows some examples of what might be in the molecule in place of the generalized grouping $\begin{matrix} R_5 & R_7 \\ -C- & -C- \\ R_6 & R_8 \end{matrix}$ in Equation 1.

5. Other functional moieties. Other functional moieties that are in the polyurethane coating or adhesive will have a large effect on its properties. These exert both a qualitative and a quantitative effect. This means that as the relative ratio of urethane moiety diminishes, the coating will behave more nearly like the class of coating as defined by the major functional moiety content. Table VI provides a listing together with each formula.

6. Multiphase description. The nature of polyurethane requirements for a coating or adhesive makes it highly unlikely that we are talking about simple homopolymers. Thus we are more likely to have copolymers, segmented copolymers, grafts, block copolymers, polyblends, networks, and even other complexes. Whatever is in the coating solution is less important than what happens when it dries or cures to its final film. What will the morphology of the film be? Will it become crystalline, have domains, form networks, or be amorphous? These would be good and helpful to know, but it is unlikely that anything beyond hypothesis can be determined for the commercial systems. Nevertheless, the numerous excellent studies on model systems in recent years (3) have helped to shape the path of development for industrial chemists to improve film formation in polyurethane coatings and adhesives.

7. Catalyst content. The catalyst content does make a significant difference in applications properties of coatings and adhesives. This is especially true where the user is seeking a long wearing film. Where multistage preparations have been made, the cumulative effects of catalysts used in each stage have been known to cause startling results in usage, because each stage was done independently of the others without being aware of prior catalyst content.

For urethane reactions, the catalysts are either metallic or tertiary amine or a combination of both.

TABLE V

EXAMPLES OF $\begin{array}{c} R_5 \\ -C- \\ R_6 \end{array} - \begin{array}{c} R_7 \\ -C- \\ R_8 \end{array}$

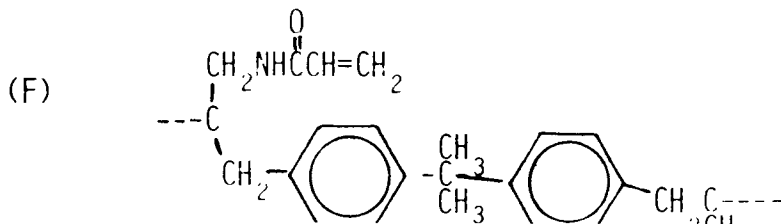
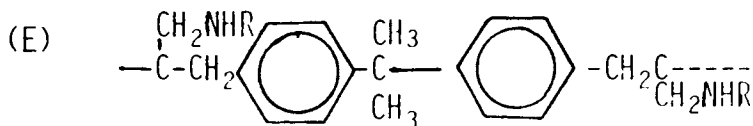
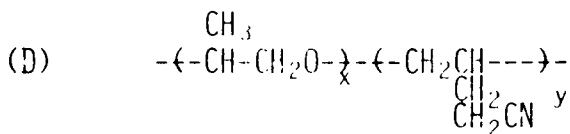
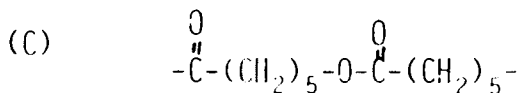
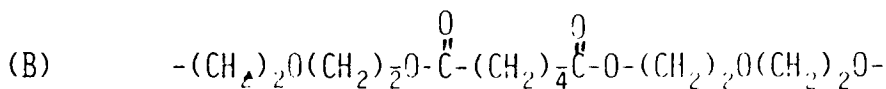
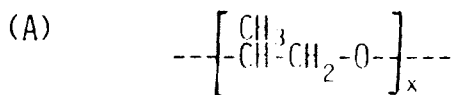


TABLE VI

OTHER FUNCTIONAL MOIETIES

$\begin{array}{c} \text{O} \\ \parallel \\ \text{-NH-C-NH-} \end{array}$	UREA
$\begin{array}{c} \text{O} \\ \parallel \\ \text{-}\overset{\text{,}}{\underset{\text{,}}{\text{C}}}\text{-}\overset{\text{,}}{\underset{\text{,}}{\text{C}}}\text{-O}\overset{\text{,}}{\underset{\text{,}}{\text{C}}}\text{-} \end{array}$	ESTER
$\begin{array}{c} \text{O} \\ \parallel \\ \text{-}\overset{\text{,}}{\underset{\text{,}}{\text{C}}}\text{-O-}\overset{\text{,}}{\underset{\text{,}}{\text{C}}}\text{-O-}\overset{\text{,}}{\underset{\text{,}}{\text{C}}}\text{-} \end{array}$	CARBONATE
$\begin{array}{c} \text{O} \\ \parallel \\ \text{-}\overset{\text{,}}{\underset{\text{,}}{\text{C}}}\text{-}\overset{\text{,}}{\underset{\text{,}}{\text{C}}}\text{-}\overset{\text{,}}{\underset{\text{,}}{\text{C}}}\text{-} \end{array}$	EPOXY
$\overset{\text{'}}{\text{C}}\equiv\text{C-} \text{ OR } \overset{\text{'}}{\text{C}}=\overset{\text{'}}{\text{C-}}$	UNSATURATION
$\text{CH}_2=\overset{\text{'}}{\underset{\text{'}}{\text{C}}}\text{-}$	ALLYL
$\text{CH}_2=\overset{\text{'}}{\underset{\text{'}}{\text{C}}}\text{-}$	VINYL
$\begin{array}{c} \text{O} \\ \parallel \\ \text{CH}_2=\overset{\text{'}}{\underset{\text{'}}{\text{C}}}\text{-O}\overset{\text{,}}{\underset{\text{,}}{\text{C}}}\text{-} \end{array}$	ACRYLIC
$\text{ROSO}_2\text{-}\overset{\text{'}}{\underset{\text{'}}{\text{C}}}\text{-}$	SULFONATE
$\begin{array}{c} \text{O} \\ \parallel \\ \text{-}\overset{\text{,}}{\underset{\text{,}}{\text{C}}}\text{-}\overset{\text{,}}{\underset{\text{,}}{\text{C}}}\text{-NH}\overset{\text{,}}{\underset{\text{,}}{\text{C}}}\text{-} \\ \text{-}\overset{\text{,}}{\underset{\text{,}}{\text{C}}}\text{-} \end{array}$	AMIDE
$\begin{array}{c} \text{-}\overset{\text{,}}{\underset{\text{,}}{\text{C}}}\text{-O-}\overset{\text{,}}{\underset{\text{,}}{\text{Si}}}\text{-O} \\ \text{-}\overset{\text{,}}{\underset{\text{,}}{\text{C}}}\text{-} \end{array}$	SILICONE

The metallic catalyst most widely employed is some form of tin. However, some specialized uses of titanium, mercury, and even lead exist in industry. Based on my industrial experience I do not recommend the use of tin in a coating or adhesive that is designed for long ageing or wearing.

If crosslinking or other functional moieties are designed into the coating, most frequently the same classes of catalysts are employed. However, it is feasible to expect that a manufacturer might use another catalytic material. With respect to catalysts, identification and classification should be easy.

8. Nonresinous compounding ingredients. Though the polyurethane resin or blend with other resins determines the key properties of a coating or adhesive, its application utility is not evident until the proper compounding ingredients are added. The supplier may or may not add all of the necessary compounding ingredients and thus, one might argue that these may not be necessary to include in a classification system. Nevertheless, it should be pointed out that in current applied polyurethane coatings and adhesives, the polyurethane resin content can range anywhere from 15 to 95%. Further, it requires much probing on the part of the user to determine what level he is buying. Even a guess based on price may be misleading. We feel that this percentage should be an important part of an industry designation.

The classes of compounding ingredients that may be present as follows:

- A. Diluents - solvents, water, monomer, cross-linking agents
- B. Fillers, reinforcing agents, flame retardants
- C. Pigmentation and gloss modifiers
- D. Surfactants and coupling agents
- E. Stabilizers and antioxidants

Commercial materials used are selected from those that are available for compounding use with all of the major plastics materials (4). The resin manufacturer normally takes responsibility for designating to formulators which materials are more compatible with his products. But the formulator of a coating is frequently less informative on which of these classes of additives are present. A yes or no answer to each class, A through E, should thus be included in the comprehensive description.

Review

We have shown eight factors which could be used to characterize polyurethane coatings and adhesives: Intermediate chemicals, coreactive and prereacted, system design, backbone elements, other functional moieties, multiphase description, catalyst content, and compounding ingredients. Descriptive terms for subcategories have been given as examples under each factor. The tabulation and organization of a more complete set of terms can now be set up and appropriate code letters and numbers assigned so that industry could be encouraged to clarify to its customers the products that are available. Much of the terminology is presently in use informally. We hope that a good system will develop communication which encourages users to feel they have a sensible way to select an appropriate product.

Conclusions

We have described the current state of the industry market in solventless polyurethane coatings and adhesives. There is a wide variety of specialty materials available, all selling for widely different prices and consisting of a wide variety of chemical compositions.

We are proposing a classification system which could form a guide to the purchaser and user of these products. We hope that such a system could help eliminate confusion that presently exists among many purchasers of these products.

Literature Cited

1. ASTM D-3726-9, "Annual Book of ASTM Standards," American Association for Testing and Materials, Philadelphia, PA., 1980, Vol. 29.
2. a. Pigott, K.A., Polyurethanes, "Encyclopedia of Polymer Science and Technology," Interscience Division, J. Wiley, New York, 1969, Vol. 11, pp. 506-563.
b. Buist, J.M., Crowley, G.P., & Lowe, A., Polyurethane Technology, "Encyclopedia of Polymer Science and Technology," Interscience Division, J. Wiley, New York, 1971, Vol. 15, pp. 445-479.

- c. Cooper, S.L., Seymour, R.W., and West, J.C., Polyurethane Block Polymers, "Encyclopedia of Polymer Science and Technology," Interscience Division, J. Wiley, New York, 1976, Suppl. I, pp. 521-543.
- d. Patton, J.T., Chemtech, 1976, 6, pp. 780-4.
3. Cooper, S.L. & Estes, G.M., Eds., "Multiphase Polymers," American Chemical Society, Washington, D.C., 1979.
4. Agranoff, J., Ed., "Modern Plastics Encyclopedia," McGraw-Hill Publication, New York, 1979, pp. 152-229.

RECEIVED April 30, 1981.

Novel Masked Aliphatic Diisocyanates

HENRI ULRICH

Donald S. Gilmore Research Laboratories, The Upjohn Company, North Haven, CT 06473

Blocked aliphatic diisocyanates are used in light stable one-component polyurethane systems. Typical examples include baking enamels, wire coatings and powder coatings. A variety of active hydrogen containing compounds have been used as **blocking agents**, notably oximes and phenol.⁽¹⁾ Heating of the blocked isocyanates generates the free isocyanates with release of the blocking agent. Attempts have been made over the years to develop blocking agents which are incorporated into the polymer backbone upon thermal release, thereby eliminating the need for well-ventilated working areas. All these efforts have met with failure.

We selected a novel approach to design a masked or blocked aliphatic diisocyanate based on the fact that 1,3-disubstituted ureas undergo facile thermal dissociation to produce an isocyanate and an amine derivative.⁽²⁾ In the dissociation of mono acyl and aroyl ureas an isocyanate and a carboxylic acid amide is simultaneously produced. If the urea group is part of a cyclic system both fragments are parts of the same molecule.

The required novel bifunctional monomers are synthesized by reacting cyclic ureas with aliphatic or aromatic dicarboxylic acid chlorides in the presence of triethylamine as hydrogen chloride scavenger. This reaction is best conducted in an inert organic solvent using an excess of the cyclic urea to prevent polymer formation (Scheme I).

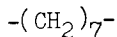
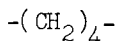
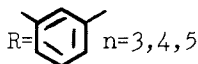
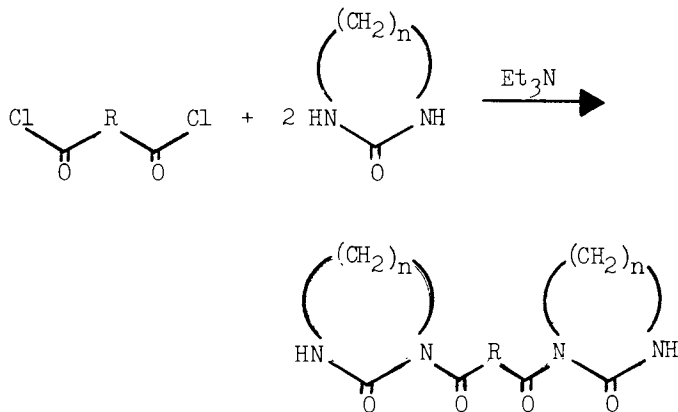
The cyclic ureas are synthesized from the corresponding diamines and carbon dioxide or carbonyl sulfide.⁽³⁾ The eight-membered ring cyclic urea can be obtained from caprolactam.⁽³⁾

The stability of the difunctional monomers in alcohols or polyols was demonstrated by the fact that no ring opening was observed upon refluxing in lower boiling alcohols. Heating of the difunctional monomers in *o*-dichlorobenzene produces the corresponding aliphatic diisocyanates as evidenced by infrared spectroscopy and trapping with methanol to give biscarbamates.⁽³⁾

Recyclization does not occur because the reaction of aliphatic isocyanates with carboxylic acid amide groups occurs only under very severe conditions.

SCHEME I

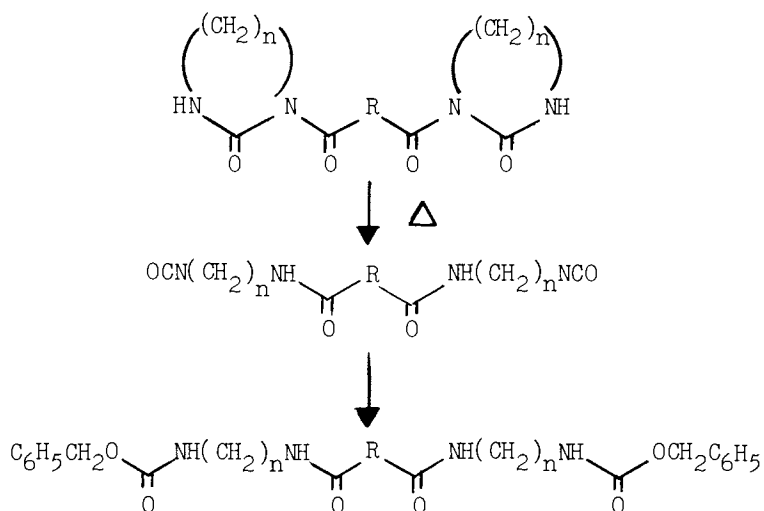
Synthesis of Difunctional Macrocylic Ureas



The rate of ring opening of the bis cyclic ureas was studied in a model system using nitrobenzene as solvent to simulate a polar environment and to achieve the necessary high dissociation temperatures. Benzyl alcohol was used as the trapping reagent. Heating the macrocylic bis urea based on isophthaloyl chloride and 1,3-diazepin-2-one without a catalyst at 170°C effected a 48% conversion to the carbamate within ten minutes. Complete reaction was achieved within five minutes in the presence of triethylenediamine (DABCO) and the temperature could be lowered to 155° if 0.5 mole % (based on the bis cyclic urea) of dibutyltin dilaurate (T-12) were used as catalyst. The extent of reaction was monitored by measurement of the signal due to benzylic protons, in the formed carbamate, in the ¹H-NMR-spectrum.

SCHEME II

Ring Opening Of Difunctional Macrocylic Ureas



The utility of the bis cyclic ureas for curing of coatings was demonstrated by dispersing them in a functional acrylic polymer formulated for powder coating application, or by using them as additive in solvent based coatings or in aqueous polymer emulsions for electrocoating.

To achieve good compatibility with functionalized acrylic and epoxy resins a bis cyclic urea with $n=3$, and $R=-(CH_2)_7-$ (see Scheme I) was synthesized. Acrylic- and epoxy polymer solutions were prepared using 15% by weight of the bis cyclic urea (based on the dry polymer) and methyl ethyl ketone as solvent. Films cast from these solutions on steel sheets were clear, and had a thickness of ~ 0.4 mil.

Indicated below are the baking temperatures for the films to become insoluble in methyl ethyl ketone using a 30 minute baking cycle. The required temperatures were lower by adding a catalyst (15% by weight based on the bis cyclic urea of dibutyltin dilaurate).

	<u>with catalyst</u>	<u>without catalyst</u>
acrylic polymer	175°C	195°C
epoxy polymer	160°C	175°C

The given temperatures serve as a guideline since they may vary with film thickness, crosslinker and catalyst concentrations and solvent.

In this process the aliphatic diisocyanates are formed and reaction with hydroxyl groups attached to the polymer backbone occurs. The resulting carbamate linkages lead to crosslinking of the polymer matrix, thus creating tough and solvent resistant films. The polymer derived from the reaction of bis acylamido-alkyl isocyanates with macroglycols contain urethane and amide groups as well.

Further work is in progress to optimize solvent free one component systems based on macroglycols and the novel difunctional cyclic urea monomers.

Literature Cited

1. Wicks, Z. W., Jr., "Blocked Isocyanates", Progress in Organic Coatings, 3, 73 (1975), Elsevier (Neth.).
2. Ulrich, H., and Sayigh, A.A.R., Angew. Chem., Int. Ed. Engl., 5, 704, 724 (1966).
3. Ulrich, H., Tucker, B. and Richter, R., J. Org. Chem. 43, 1544 (1978).

RECEIVED April 30, 1981.

Comparison of Diol Cross-Linkers in Castable Urethane Elastomers

I. SIOUN LIN, JEROME BIRANOWSKI, and DONALD H. LORENZ

Polymer Department, GAF Corporation, 1361 Alps Road, Wayne, NJ 07470

There are regulatory and handling problems in using methylene bis(2-chloroaniline) as a chain extender (curative or cross-linker) for toluene diisocyanate (TDI)-terminated prepolymers, to produce urethane elastomers (1,2). There is, therefore, a strong interest in achieving similar elastomer properties with other curatives and methylene diphenyl diisocyanate (MDI)-terminated prepolymers(3,4).

EXPERIMENTAL

A. Materials

The materials used are listed in Table I. All curatives were dried overnight at 80°C in vacuum. MDI prepolymer were used as received.

B. Polyurethane Elastomer Preparation

Amine stoichiometry was kept at 95% based on prepolymer content. Except where noted, prepolymers were preheated at 93°C and mixed with curatives at desired temperature. The prepolymer, curative and prepolymer-curative mixture were each vacuum degassed prior to pouring the mixture into a preheated mold. Degassing before and after mixing is especially important to achieve optimum cures. The mold was closed when gelation started. Demolding time was one hour or less. The sample was then post-cured for 16 hours at 120°C. The elastomer was conditioned for one week at 50% relative humidity at room temperature prior to physical properties measurement.

B. Physical Testing

After the samples had been aged and conditioned, the following tests were run according to the following specifications:

1. Shore Hardness
Durometer A ASTM D-2240
2. Stress-Strain Properties ASTM D-412
3. Tear Resistance
Grave, die C, pli ASTM D-624

0097-6156/81/0172-0523\$05.00/0

© 1981 American Chemical Society

4. Resilience (Rebound, Bashore) ASTM D-2632
5. Compression set
Method B (22 hrs. at 70°C) ASTM D-395

RESULTS AND DISCUSSION

Urethane elastomers based on MDI type prepolymer extended with 1,4-butanediol and other curatives have been formulated. The results of this work are summarized in Tables II-IV. In general, polyether and polyester-based urethane elastomers both have excellent physical properties. There are several differences between them. Among them are: (1) Polyesters usually are more viscous at processing temperatures, making processing difficult. (2) Polyester generally have shorter pot life than polyethers. (3) Polyether-based urethanes exhibit higher resilience and lower compression set. It appears that diamine curative (Polacure) is more reactive than glycols. 1,4-Butanediol/MDI systems show not nearly as much sensitivity to stoichiometry as ethylene glycol or polyol 50-1180. HQEE and Polacure have relatively low tensile strength and high compression set. However, both gave improved elastomer hardness and tear strength. Vibracure cured elastomers have approximately the same physical properties as HQEE cured urethanes. This may be due to their chemical composition. Similar results also found in ethylene glycol/MDI and polyol 50-1180/MDI systems. The conclusions which can be drawn from this work are summarized as follows:

1. 1,4-Butanediol vs. Ethylene Glycol
 - a) Stoichiometry less sensitive
 - b) Inferior on compression set characteristics
2. 1,4-Butanediol vs. Polyol 50-1180
 - a) Stoichiometry less sensitive
 - b) Superior tensile modulus, tear strength and rebound
 - c) Inferior on compression set
3. 1,4-Butanediol vs. HQEE
 - a) Superior tensile and rebound
 - b) Somewhat inferior tear and elongation
4. 1,4-Butanediol vs. Vibracure
same as HQEE
5. 1,4-Butanediol vs. Polacure
 - a) Superior tensile and compression set
 - b) Inferior in modulus and tear
6. 1,4-Butanediol vs. 4,4'-Methylene bis (2-chloroaniline)
(published properties)
 - a) Superior tensile modulus, tensile and tear
 - b) Inferior in elongation

TABLE I - MATERIALS

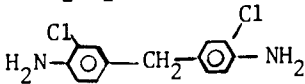

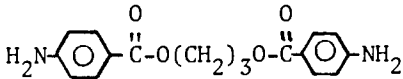

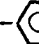
	Eq. Wt.	Chemical Composition
1,4-Butanediol (B ₁ D)	45.06	HOCH ₂ CH ₂ CH ₂ CH ₂ OH
Ethylene glycol (EG)	31.03	HOCH ₂ CH ₂ OH
4,4'-Methylene bis (2-chloroaniline) (MOCA)	133.5	
Hydroquinone bis (2-hydroxyethyl) ether (HQEE)	99	HOCH ₂ CH ₂ O-  -OCH ₂ CH ₂ OH
Trimethylene glycol di-p-aminobenzoate (Polacure #740M)	157	
Polyol 50-1180	47.26	Mixture of ethylene glycol plus short chain diol
Vibracure 3095	97.86	HQEE plus other curative
Toluene diiso- cyanate (TDI)	87	80/20, 2,4/2, 6-tolylene diisocyanate, a mixture of isomers
Methylene diphenyl diisocyanate (MDI)	125	OCN-  -CH ₂ -  -NCO
Vibrathane B-635	530 \pm 15	Polytetramethylene ether glycol-based MDI prepolymer
Vibrathane 6020	665 \pm 25	Polyester-based MDI pre- polymer
Adiprene L-100	1050	Polytetramethylene ether glycol-based TDI prepolymer
Adiprene APX 381	1072	Polyester based TDI prepolymer

TABLE II - Properties of Elastomers Prepared from Polyester-MDI Prepolymer (Vibrathane 6020) Cured with B₁D, EG, HQEE Polacure No. 740M, Polyol 50-1180 and Vibracure 3095.

<u>Formulation</u>	<u>1</u>	<u>2</u>	<u>3</u>
VIBRATHANE 6020 (AE=640 ± 25), g	100	100	100
1,4-Butanediol, g	6.64	--	--
Ethylene glycol, g	--	4.70	--
HQEE, g	--	--	14.97
Polacure No. 740M, g	--	--	--
Polyol 50-1180, g	--	--	--
Vibracure 3095, g	--	--	--
Curative Mole Ratio,	0.95	0.95	0.95
<u>Conditions</u>			
Curative, Temp., °C	60	60	120
VIBRACURE 6020, Temp. °C	93	93	93
Mix. Temp. °C (curative/prepolymer	60/93	60/93	120/93
Pot Life at Mix. Temp., min.	8	7	3
Cured in Mold, min/°C	60/120	60/120	60/120
Post Cure, hrs/°C	24/120	16/120	16/120
<u>Physical Properties</u>			
Hardness, Shore A	85	84	97
Shore D	35	35	44
100% Modulus, psi (MPa)	866 (6.0)	892 (6.2)	1578 (10.8)
300% Modulus, psi (MPa)	1498 (10.4)	1624 (11.2)	2001 (13.8)
Tensile Strength, psi (MPa)	6427 (44.4)	5385 (37.2)	4265 (29.4)
Elongation, %	555	581	650
Tear Strength, Die C, pli (kN/m)	543 (95)	596 (104.3)	754 (131.9)
Bashore Rebound, %	37	32	27
Compression Set, 22 Hrs/70°C Method B, %	40	30	25

TABLE II - Properties of Elastomers Prepared from Polyester-MDI
(cont'd.) Prepolymer (Vibrathane 6020) Cured with B₁D, EG, HQEE
Polacure No. 740M, Polyol 50-1180 and Vibfacure 3095.

<u>Formulation</u>	<u>1</u>	<u>2</u>	<u>3</u>
VIBRATHANE 6020 (AE=640 + 25), g	100	100	100
1, 4-Butanediol, g	--	--	--
Ethylene glycol, g	--	--	--
HQEE, g	--	--	--
Polacure No. 740M, g	23.07	--	--
Polyol 50-1180, g	--	6.69	--
Vibfacure 3095, g	--	--	15.02
Curative Mole Ratio,	0.95	0.95	0.95
<u>Conditions</u>			
Curative, Temp., °C	125	60	120
VIBRATHANE 6020, Temp °C	93	93	93
Mix. Temp. °C			
(curative/prepolymer	125/93	60/93	120/93
Pot Life at Mix. Temp., min.	1	10 15	7
Cured in Mold. min/°C	30/120	60/120	60/120
Post Cure, hrs/°C	16/80	16/120	16/120
<u>Physical Properties</u>			
Hardness, Shore A	--	75	96
Shore D	55	30	43
100% Modulus, psi (MPa)	1782 (12.3)	490 (3.4)	1372 (9.5)
300% Modulus, psi (MPa)	2324 (16.0)	1125 (7.8)	2040 (14.1)
Tensile Strength, psi (MPa)	4070 (28.1)	6164 (42.5)	4680 (32.3)
Elongation, %	550	544	526
Tear Strength, Die C, pli (kN/m)	800 (140.0)	478 (83.6)	725 (126.8)
Bashore Rebound, %	42	24	34
Compression Set, 22 Hrs/70°C Method B, %	39	20	29

TABLE III - Properties of Elastomers Prepared from Polyether-MDI Prepolymer (VIBRATHANE B-635) Cured with B₁D, EG, HQEE, Polacure No. 740M, Polyol 50-1180 and Vibracure 3095.

<u>Formulation</u>	<u>1</u>	<u>2</u>	<u>3</u>
VIBRATHANE B-635 (AE-530 + 15), g	100	100	100
1,4-Butanediol, g	8.31	--	--
Ethylene glycol, g	--	6.24	--
HQEE, g	--	--	17.93
Polacure No. 740M, g	--	--	--
Polyol 50-1180, g	--	--	--
Vibracure 3095, g	--	--	--
Curative Mole Ratio	0.95	1.05	0.95
<u>Conditions</u>			
Curative, Temp. °C	60	60	120
VIBRATHANE B-635, Temp. °C	93	93	93
Mix. Temp., °C (Curative/Prepolymer)	60/93	60/93	120/93
Pot Life at Mix. Temp., min.	7	20	10
Cured in Mold, min/°C	60/120	60/120	60/120
Post Cure, hrs/°C	16/120	16/120	16/120
<u>Physical Properties</u>			
Hardness, Shore A	93	84	--
Shore D	37	31	55
100% Modulus, psi (MPa)	1386 (9.6)	1089 (7.5)	2433 (16.8)
300% Modulus, psi (MPa)	3778 (26.1)	-- --	2783 (19.2)
Tensile Strength, psi (MPa)	6115 (42.2)	5788 (39.9)	3450 (23.8)
Elongation, %	338	268	432
Tear Strength, Die C, pli (kN/m)	590 (103.2)	423 (74.0)	680 (119.0)
Bashore Rebound, %	39	19*	42
Compression Set, 22 hrs/70°C Method B, %	24	18	31

*sample was soft and sticky after demolding.

TABLE III - Properties of Elastomers Prepared from Polyether-MDI (cont'd.) Prepolymer (Vibrathane B-635) Cured with B₁D, EG, HQEE, Polacure No. 740M, Polyol 50-1180 and Vibracure 3095.

<u>Formulation</u>	<u>1</u>	<u>2</u>	<u>3</u>
VIBRATHANE B-635 (AE-530 + 15),	g 100	100	100
1,4-Butanediol,	g --	--	--
Ethylene glycol,	g --	--	--
HQEE,	g --	--	--
Polacure No. 740M,	g 28.44	--	--
Polyol 50-1180,	g --	8.56	--
Vibracure 3095,	g --	--	17.39
Curative Mole Ratio	0.95	0.95	0.95
<u>Conditions</u>			
Curative, Temp. °C	125	60	120
VIBRATHANE B-635, Temp. °C	80	93	93
Mix. Temp., °C			
(Curative/Prepolymer	125/80	60/93	60/93
Pot Life at Mix. Temp., min. (40 sec)		10	10
Cured in Mold, min/°C	30/120	60/120	60/120
Post Cure, hrs/°C	16/80	16/120	16/120
<u>Physical Properties</u>			
Hardness, Shore A	--	82	--
Shore D	60	31	52
100% Modulus, psi	3160	919	2224
(MPa)	(21.8)	(6.4)	(15.4)
300% Modulus, psi	4868	3610	2641
(MPa)	(33.6)	(24.9)	(18.2)
Tensile Strength, psi	5335	4681	4000
(MPa)	(36.8)	(32.3)	(27.6)
Elongation, %	342	305	466
Tear Strength, Die C, pli	871	415	657
(kN/m)	(152.4)	(72.6)	(115)
Bashore Rebound, %	40	15*	35
Compression Set, 22 hrs/70°C	50	19	29
Method B, %			

*Sample was soft and sticky after demolding.

TABLE IV - GENERAL SUMMARY OF PHYSICAL PROPERTIES

<u>Compound</u>	<u>B₁D[†]/MDI</u>	<u>Polacure*/TDI</u>	<u>MOCA*/TDI</u>
Polyether-MDI prepolymer	100	--	--
ADIPRENE APX-381	--	100	--
ADIPRENE L-100	--	--	100
Polacure No. 740M	--	14.2	--
MOCA	--	--	12.5
1,4-Butanediol	8.31	--	--
Curative Mole Ratio	0.95	0.95	0.95
<u>Mixing and Curing</u>			
Polymer Mix Temp. °C	93	100	100
Cured: hours/°C	16/120	16/120	3/100
Pot Life	7	4	10-12
<u>Physical Properties</u>			
Hardness, Shore D	93	93	90
100% Modulus, psi (MPa)	1386 (9.6)	1100 (7.6)	1100 (7.6)
300% Modulus, psi (MPa)	3778 (26.1)	2200 (15.2)	2100 (14.5)
Tensile Strength, psi (MPa)	6115 (42.2)	6425 (44.3)	4500 (31.0)
Elongation, %	338	460	450
Tear Strength, Die C, pli (kN/m)	590 (103.3)	350 (61.3)	240 (42.0)
Bashore Rebound, %	39	40	40
Compression Set, 22 hrs/70°C Method B, %	24	42	27

*Data from 1978 Fall Meeting PMA, Point Clear, Alabama, October, 1978.

†1,4-Butanediol

These data show that urethane elastomers based on MDI type prepolymer cured with 1,4-butanediol exhibit equivalent or even better physical properties, such as tensile strength, compression set, resilience, tear strength and elongation when compared to elastomers extended with methylene bis (2-chloroaniline), trimethylene glycol di-p-aminobenzoate or hydroquinone bis(2-hydroxyethyl) ether in MDI or TDI system (at equal hardness). Other advantages for 1,4-butanediol curative are low toxicity, liquid state at room temperature, ease of handling and lower cost than other well-known curatives.

REFERENCES

1. Polaroid Corporation, Recent Developments in the Use of Polacure® No. 740M Diamine Curative, October, 1978.
2. Polaroid Corporation, Trimethylene Glycol Di-p-Aminobenzoate - A Development Diamine Curative for Cast Elastomers, October, 1977.
3. The Quaker Oats Company, Polyurethane Elastomers Based on MDI-QO® Polymeg® Prepolymer Extended with 1,4-Butanediol, 1976.
4. Uniroyal Chemical, MDI-Prepolymer Systems - Viable Alternatives to MOCA Cured Urethanes. April 18, 1978.

RECEIVED April 30, 1981.

A New Aromatic Diol Chain Extender for Urethane Elastomers

D. KLEMPNER and K. C. FRISCH

Polymer Institute, University of Detroit, Detroit, MI 48221

A significant effort has been carried out in recent years on chain extenders for urethane elastomers. This has been prompted primarily by the search for a suitable replacement for 4,4'-methylene bis(o-chloroaniline) (MOCA), a widely used chain extender and curing agent which gives a positive Ames test (screening test for mutagenicity).

A number of different hindered diamines have been investigated as a substitute for MOCA (1). In addition to diamine curing agents, which are used most frequently with elastomers based on polyether polyols and toluene diisocyanate (TDI), prepolymers based on polyether or polyester polyols and 4,4'-diphenylmethane diisocyanate (MDI), can be cured with diols to yield elastomers with similar properties to those of diamine-cured polyester-TDI elastomers. The most common chain extender is butanediol. However, to achieve improved mechanical properties, especially at elevated temperatures, aromatic diols are often used. The most common one is hydroquinone di-(beta-hydroxyethyl) ether (HEQ).

One basic problem with HEQ is its high melting point (102°C). As a result, the chain extension process must take place above 102°C, normally around 120°C. If lower temperatures are used, "starring" (crystallization or precipitation of this curative out of the system) occurs, since HEQ is not soluble in the rest of the components at temperatures below its melting point.

In order to alleviate these processing problems, the meta-substituted analog of HEQ was studied. This material, resorcinol di-(beta-hydroxyethyl) ether (HER) has a lower melting point (89°C), due to the lack of symmetry in the molecule.

In this study, the properties and processing of elastomers cured with HER were compared with those cured with HEQ. Studies were made using a variety of prepolymers and catalysts.

0097-6156/81/0172-0533\$05.00/0

© 1981 American Chemical Society

Experimental

Materials. The materials used are described in Tables I and II. All materials were used as received, with no further purification.

The tentative specifications of HER are as follows:

Appearance	White to tan flake
Hydroxyl number	547-545
Equivalent wt.	99.1
Molecular wt., empirical	198.2
Melting point, °C	89 min.
Boiling point, °C/5	206-212
Water content	0.1 wt. %, max.
Solubility 25°C, approximate wt. %:	
Water	2
Acetone	11
Ethanol	13
Ethyl acetate	3
Benzene	< 1
Hexane	< 1
Specific heat	0.25 cal/°C/gm
Melt density	1.16 gm/cc at 100°C
Melt viscosity	13.50 cc at 100°C

Elastomer Preparation

Phase I. In this phase of the study, the feasibility of chain extending polyurethane elastomers with HER was determined. A variety of elastomers were prepared by chain extending the following prepolymers with HER (see Table I for their chemical descriptions):

<u>Polyether</u>	<u>% NCO</u>	<u>Viscosity cps</u>	<u>Eq. Wt.</u>	<u>Appearance at 75° F</u>
B-625	6.6	750	636.36	liquid
B-605	3.15	2900	1333.33	solid
B-635	7.7	430	545.46	liquid
B-665	9.55	540	439.79	liquid
<u>Polyester</u>				
V-6001	3.23	3000	1300.31	solid
V-6012	6.68	1000	628.74	solid

The catalyst used was Dabco 33LV (triethylene diamine). Preliminary studies indicate that Dabco 33LV is an efficient catalyst for HER. Although there is indication of good stability of 33LV in HER, the true stability and retention of activity are unknown.

Elastomers were prepared using 0.06% by weight (based on HER) Dabco 33LV as a catalyst. A 105 isocyanate index was used (95% stoichiometry). The prepolymer and the chain extender were heated to 120°C. When the chain extender was completely melted, they were mixed together with the required amount of catalyst. The mixing temperature was 105-110°C. Castings were made using metal plates and a spacer on a heated platen press. Two cure temperatures were employed, 115°C and 130°C. The mold residence time was 1 hour. This was followed by a post cure at 100°C overnight. Green strength measurements were also carried out on each prepolymer.

Phase II. In this phase, polyurethane elastomers were prepared using only one prepolymer, B-625, and several catalysts and concentrations in order to determine the optimum properties possible with HER

Phase III. In this phase a direct comparison of HER with HEQ was made. Elastomers were prepared as above using both polyether and polyester prepolymers and both HER and HEQ as chain extenders. No catalyst was used. The mixing temperature was 120°C. The elastomers were cured for one hour in the mold at 130°C and post-cured overnight at 100°C.

Phase IV. In this final phase, the lowest possible processing temperatures for HER and HEQ extended elastomers were determined as well as the pot lives. Combinations of

TABLE I
PREPOLYMERS AND CHAIN EXTENDERS

<u>Designation</u>	<u>Description</u>	<u>%Isocyanate</u>	<u>Eq. Wt.</u>	<u>Supplier</u>
Vibrathane B605	A prepolymer based on di-phenyl-methane diisocyanate (MDI) and poly-tetramethylene glycol	3.02	1333	Uniroyal
Vibrathane B625	Above	6.42	636	Uniroyal
Vibrathane B635	Above	7.97	545	Uniroyal
Vibrathane B665	Above	9.39	440	Uniroyal
PCA 6-3	Above	6.-6.6	635-690	Polyurethane Corp. of America
Vibrathane V6001	An MDI-terminated polyester prepolymer	3.23	1300	Uniroyal
Vibrathane V6012	Above	6.33	629	Uniroyal
HEQ	Hydroquinone di (beta-hydroxyethyl) ether			Tennessee Eastman
HER	Resorcinol di (beta-hydroxyethyl) ether			Koppers

TABLE II
CATALYSTS

<u>Designation</u>	<u>Description</u>	<u>Supplier</u>
Dabco 33LV	33% Solution of triethylene diamine in dipropylene glycol	Air Products
Dabco	Triethylene diamine	Air Products
Dabco WT	Salt of diethylene triamine and formic acid	Air Products
Armeen DMOD	Proprietary amine	Armak
T-9	Stannous octoate	M & T Chemicals
T-1	Dibutyltin diacetate	M & T Chemicals
T-12	Dibutyltin dilaurate	M & T Chemicals
T-31	Dibutyltin isoocetyl-mercaptoacetate	M & T Chemicals
T-20	Dibutyltin dilauryl-mercaptide	M & T Chemicals
Cotin 222	Proprietary organotin	Cosan Chemical

HEQ and HER were also studied in order to see if a minimum azeotrope might result to allow even lower processing temperatures.

Elastomers were made from B-625 at various initial mixing temperatures, using an isocyanate index of 1.05.

The prepolymers and the chain extenders were both heated to temperatures ranging from 130°C to as low as 70°C in some cases, and mixed with no catalyst.

Temperature intervals of 10°C were used and the crystallization and starring tendencies of HER and HEQ elastomers were determined as well as the pot lives.

Only one cure temperature was used, 130°C. The mold residence time was one hour. This was followed by a post cure of 100°C overnight. No testing was performed on the samples.

Test Methods

The elastomers made after being aged and conditioned for one week were subjected to the following tests to determine their physical properties:

1. Stress-strain properties (ASTM D 412)
Tensile strength, psi
Elongation at break, %
Elongation set, %
2. Tear resistance (ASTM D 1938)
Split tear
Die C
3. Shore hardness (ASTM D 2240)
Durometer A
Durometer D
4. Bashore rebound (ASTM D 2632)
5. Compression set%, (ASTM D 395), Method B

The green strengths of the Phase I elastomers were determined by measuring the mechanical properties immediately after demolding.

Results and Discussion

Phase I: The properties of the phase I elastomers are shown in Tables I and II. The mechanical properties of all the elastomers, both polyether based (Table III) and polyester based (Table IV) were, in general, comparable with conventionally chain extended MDI-based polyurethane elastomers (3). In general, the higher processing temperature (130°C) resulted in elastomers with superior properties.

The green strength studies (Tables V and VI) showed that even shorter mold residence times could be used to obtain

TABLE III
 PROPERTIES OF PHASE I ELASTOMERS - POLYETHERS

Prepolymer:	B 605	B 605	B 625	B 625	B 635	B 635	B 665	B 665
Pot life, min/°C	35/110	23/110	16/130	9/115	17/130	16/115	11/110	9/110
Cured in mold, min/°C	109/130	64/115	54/130	60/115	75/130	68/115	81/130	79/115
Physical Properties:								
Shore A Hardness	77	76	88	88	91	92	96	95
Shore D Hardness	24	24	39	39	44	44	65	66
Stress-strain:								
100% M, psi	510	485	965	1057	1282	1323	3406	3424
300% M, psi	820	841	1572	1745	2804	2248	4503	4169
TS, psi	3363	3231	3303	3387	4372	3451	5081	4393
Elongation, %	742	646	604	589	463	471	274	245
Elongation set, %	21.2	15.1	20.4	20.3	22	29	11.3	9.5
Tear resistance:								
Graves, pi (die C)	316	309	390	340	414	415	834	868
Split -								
Initial, pi	141	107	114	104	180	111	191	156
Max., pi	206	148	191	176	358	379	505	544
Bashore rebound	61	64	51	51	38	42	34	34
Compression set, %	46	46	18	34	32	25	32	42

TABLE IV
 PROPERTIES OF PHASE I ELASTOMERS - POLYESTERS

Prepolymer:	V 6012	V 6012	V 6001	V 6001
Pot life, min/ ^o C	12/100	12/100	7/115	20/105
Cured in mold, min/ ^o C	47/130	42/115	60/115	93/130
Physical Properties:				
Shore A Hardness	93	90	76	76
Shore D Hardness	48	46		31
Stress-strain:				
100% M, psi	1204	1411	425	432
300% M, psi	2629	3499	667	879
TS, psi	4440	5360	3546	3612
Elongation, %	451	418	721	697
Elongation set, %	10.3	8.7	15	8.9
Tear resistance:				
Graves, pi (die C)	446	443	254	257
Split -				
Initial, pi	84	83		96
Max., pi	275	183	245	214
Bashore rebound	32	27	42	32
Compression set, %	35	28	4	52

TABLE V
GREEN STRENGTH RESULTS - PHASE I ELASTOMERS - POLYETHERS

Prepolymer:	B 605	B 605	B 625	B 625	B 635	B 635	B 665	B 665
Pot life, min/°C	13/110	16/110	10/115	12/130	10/115	12/130	12/110	11/110
Cured in mold, min/°C	48/115	64/130	45/115	45/130	45/115	45/130	70/115	31/130
Physical Properties:								
Shore hardness A	47	39	62	48	82	72	94	95
Stress-strain:								
100% M, psi	99	105	845	882	992	804	3008	2409
300% M, psi	168	191	1465	1462	1471	1383	-	-
TS, psi	866	901	3380	3043	1471	2521	3200	2645
Elongation, %	820	945	700	700	300	575	220	200
Elongation set, %	114.2	126.7	149	40	17	35	12	13.3
Tear resistance:								
Graves, pi (die C)	103	80	373	422	229	254	485	358

TABLE VI
GREEN STRENGTH RESULTS - PHASE I ELASTOMERS - POLYESTERS

<u>Prepolymer:</u>	V 6001	V 6001	V 6012	V 6012
Pot life, min/°C	6/115	20/105	14/110	15/110
Cured in mold, min/°C	30/115	85/130	51/115	41/130
Physical Properties:				
Shore hardness A	34	44	72	50
Stress-strain:				
100% M, psi	121	138	687	309
300% M, psi	176	161	1285	614
TS, psi	1309	2332	1392	2873
Elongation, %	1067	1055	315	530
Elongation set, %	42	110	10	49.3
Tear resistance:				
Graves, pi (die C)	68	101	249	292

good elastomers. Even in the green or "cheesy" state, the freshly demolded elastomers had good mechanical properties. In general, the polyesters showed better green strengths with a mold temperature of 130°C, while the polyethers yielded mixed results.

Phase II: The phase I studies showed the potential of HER as a polyurethane chain extender. Excellent elastomers resulted with no processing problems. In phase II, the optimum catalyst and catalyst concentration was determined by curing one prepolymer, B-625, using a variety of tertiary amine and organo-tin catalysts. The results are shown in Tables VII and VIII.

In general, increasing catalyst concentration results in decreased pot life, as expected. However, the elastomers made with the higher catalyst concentration do not necessarily exhibit higher mechanical properties. The Bashore rebounds and hardness for all the catalysts are about the same (within the experimental error). The compression sets for the elastomers catalyzed with the metal catalysts (Table VIII) are generally lower (superior) to those for the amine catalyzed elastomers (Table VII). The mechanical properties are generally slightly higher for most of these elastomers than for the elastomers catalyzed with Dabco 33LV.

Of all the catalysts, Armeen DMOD resulted in the highest strength properties, particularly at the lower concentration. The compression set, however, appeared unusually high.

Phase III: In this phase, elastomers were prepared using HEQ as well as HER in order to obtain a direct comparison. No catalyst was used since at the necessarily high processing temperature (120°C), the pot life of HEQ elastomers was too low with catalyst to allow molding. The results are shown in Tables IX and X.

In general, HEQ elastomers were slightly harder than HER elastomers.

B 605 - HER was found to yield the best elastomers with B 605 showing good tensile, elongation and tear properties.

B 625 - HEQ showed mechanical properties superior to those of HER

B 635 - HEQ and HER both yielded elastomers with similar properties.

B 665 - HER was the best extender with B 665, showing excellent tensile and elongation. But HEQ yielded somewhat better tear strengths.

V 6001 - HEQ yielded better tensile properties while HER resulted in superior tear properties.

V 6012 - HEQ yielded elastomers with slightly superior properties to the HER extended elastomers.

Phase IV: The major problem with HEQ as a urethane curative is its high melting point, which results in crystallization, or "starring" of the elastomers if processed at too low a temperature. Since HER has a lower melting point than HEQ, due to the lack of symmetry in the molecule, it is expected that HER cured elastomers will have less of a tendency to star.

HER exhibited remarkable processing characteristics with this prepolymer, as shown in Table XI. When just HER (100%) alone was used there was no crystallization or starring until a temperature of 70°C was reached.

But as HER's concentration was lowered (in combination with HEQ) crystallization was observed at higher temperatures as shown in Table XI. Pure HEQ could only be formulated at 130°C without crystallization.

No benefits were realized by mixing HEQ and HER. HEQ was found to be the faster reacting material, as evidenced by the pot lives. Decreasing HEQ concentration resulted in increased pot lives.

Conclusions

1. HER is an effective chain extender for MDI-based polyurethane elastomers, with both polyether and polyester-based prepolymers. Good overall properties and green strengths resulted.
2. Catalyst type and concentration has a strong influence on the properties of HER cured elastomers. A tertiary amine, Armeen DMOD, resulted in the best overall mechanical properties.
3. HER cured elastomers are comparable in properties to HEQ cured elastomers, although they are slightly softer.
4. HER exhibits significant benefits in processing over HEQ, due to its lower melting point and difficulty in crystallizing.

TABLE VII
 PROPERTIES OF AMINE CATALYZED PHASE II ELASTOMERS

<u>Sample</u>	<u>DABCO</u>	<u>DABCO-WT</u>	<u>ARMEEN DMOD</u>	<u>DABCO 33LV</u>
	0.005	0.06	0.03	0.16
Prepolymer	B625	B625	B625	B625
Pot life, min/°C	16/110	2/110	5/110	2/110
Shore hardness A	91	93	92	90
Stress-strain:				
100% M, psi	1167	1137	1272	1339
300% M, psi	1941	1900	2390	2475
TS, psi	3536	2725	4844	4403
Elongation, %	550	484	368	460
Tear resistance:				
Graves, fi (die C)	426	394	442	392
Split, initial, pi	59	104	34	48
Bashore rebound	56	57	58	57
Compression set, %	34	34	27	36

TABLE VIII
 PROPERTIES OF ORGANOMETAL CATALYZED PHASE II ELASTOMERS

Sample	T-31		T-9		COTIN 222	
	0.01	0.0125	0.001	0.005	0.003	0.0005
Prepolymer	B625	B625	B625	B625	B625	B625
Pot life, min/°C	19 120	19 120	9 120	1 120	14 120	16 120
Shore hardness A	91	92	93	91	90	91
Stress-strain:						
100% M, psi	1434	1544	1735	1439	1575	1457
300% M, psi	2333	2597	2892	2456	2828	2494
TS, psi	3186	3430	3520	3061	3525	3497
Elongation, %	440	430	368	369	373	408
Tear resistance:						
Graves, pi (die C)	495	357	474	434	432	447
Split, initial, pi	122	75	80	50	61	60
Bashore rebound	58	57	58	52	56	56
Compression set, %	20	22	34	19	15	17

TABLE VIII (CONTINUED)
 PROPERTIES OF ORGANOMETAL CATALYZED PHASE II ELASTOMERS

Sample	T-20		T-12		T-1	
	0.012	0.015	0.009	0.0116	0.004	0.005
Prepolymer	B625	B625	B625	B625	B625	B625
Pot life, min/ ^o C	$\frac{16}{120}$	$\frac{11}{120}$	$\frac{10}{120}$	$\frac{2}{120}$	$\frac{11}{120}$	$\frac{3}{120}$
Shore hardness A	91	91	90	91	89	90
Stress-strain:						
100% M, psi	1462	1420	1233	1432	1320	1158
300% M, psi	2388	2344	2123	2179	2201	1992
TS, psi	3562	3631	3761	4211	3629	3893
Elongation, %	444	434	517	635	445	490
Tear resistance:						
Graves, pi (die C)	454	412	413	550	371	412
Split, initial, pi	38	40	61	59	55	44
Bashore rebound	56	57	55	54	57	57
Compression set, %	38	40	19	20	27	25

American Chemical
 Society Library
 1155 16th St. N. W.
 Washington, D. C. 20036

TABLE IX
 PROPERTIES OF PHASE III ELASTOMERS - POLYETHERS

PREPOLYMER	B 605	B 605	B 625	B 625	B 635	B 635
NCO %	3.02	3.02	6.42	6.42	7.97	7.97
g	100	100	100	100	100	100
Mixing Temp., °C	120	120	120	120	120	120
Curing Agent	HEQ	HEQ ^R	HEQ	HEQ ^R	HEQ	HEQ ^R
NCO/OH	1.051	1.04	1.06	1.06	1.05	1.043
Pot life, min/°C	13/130	20/130	8/130	13/130	5/130	11/130
Physical Properties:						
Shore hardness A	81	75	93	88	94	94
Shore hardness D	32	30	45	39	54	50
Stress strain:						
100% M, psi	644	557	1478	1182	1961	2048
300% M, psi	1138	959	2103	1901	3315	3194
TS, psi	4237	4427	4809	3786	4648	4488
Elongation, %	661	700	529	622	403	400
Elongation set, %	17	17	36	26	14	18
Tear resistance						
Graves, pi (die C)	367	323	485	419	473	498
Split: Max., pi	120	155	240	236	162	179
Bashore rebound	62	64	53	55	44	41
Compression set	7	22	23	32	24	26

TABLE X
 PROPERTIES OF PHASE III ELASTOMERS - POLYESTERS

PREPOLYMER	V 6001	V 6012	V 6012
NCO %	3.33	6.33	6.33
g	100	100	100
Mixing Temp., °C	120	120	120 R
Curing Agent	HEQ	HEQ	HEQ
g	7.4	14.16	14.2
NCO/OH	1.048	1.046	1.048
Pot Life, min/°C	3/130	6/130	6/130
Mold Residence, min/°C	60/130	60/130	60/130
Post cure, hrs/°C	16/100	16/100	16/100
Physical Properties:			
Shore Hardness A	77	91	90
Shore Hardness D	31	45	41
Stress Strain:			
100% M, psi	685	1731	1471
300% M, psi	1086	3225	3021
TS, psi	3546	4074	3617
Elongation, %	681	404	425
Elongation set, %	14	12	9
Tear Resistance			
Graves, pi (die C)	400	480	479
Split: Max., pi	200	332	280
Bashore Rebound	55	38	42
Compression Set	11	3	7

TABLE XI
PHASE IV PROCESSING STUDIES

Temp.	130°C	120°C	110°C	100°C	90°C	80°C	70°C	60°C
HER 100%	1.05 13'30"	1.07 18'	1.04 16'	1.10 21'	1.04 28'	1.31 29'		
	Crystalline No	No	No	No	No*	No*	Yes	
HER 75%	1.10	1.01	1.00	1.03	1.04			
HEQ 25%	13'	14'30"	15'	17'	22'	Yes		
	Crystalline No	No	No	No	No*			
HER 50%	1.08	1.06	1.07	1.04	1.05			
HEQ 50%	11'	14'	13'30"	15'	17'			
	Crystalline No	No	No	No	Yes			
HER 25%	1.09	1.02	1.01	1.04	1.22			
HEQ 75%	9'	9'30"	8'	14'	12'			
	Crystalline No	No	No	No	Yes			
HEQ 100%	1.04	1.05	1.05	1.15				
	5'	6'	6'	10'				
	Crystalline No	Yes	Yes	Yes				

* crystallization of chain extender occurred separately from prepolymer, but starrng did not occur in elastomer

Acknowledgement

The authors would like to acknowledge Koppers Co., Inc., for their support of this research.

Literature Cited

1. Frisch, K.C., Paper presented at the First IMPAC Symposium, San Juan del Rio, Mexico, 1978; Rubber Chem. & Techn., 1980, 53, (1), 126.
2. Fujiwara, E., unpublished work.
3. Uniroyal Product Bulletins.

RECEIVED April 30, 1981.

Fluid Film Processing Applied to Manufacturing of Foam Core Insulating Panels

VIJAY VIMAWALA

Kornylak Corporation, 400 Heaton Street, Hamilton, OH 45011

Kornylak Corporation's recent development of the Process Tunnel is expected to have a significant impact on a variety of operations in the plastic field. A number of lines incorporating this process have already been built and are in operation in the United States and abroad. Their spectacular performance indicates that this development is indeed a breakthrough. This chapter will cover some of the technical aspects of this new process.

To avoid repetition of our company's trade name we will, in this chapter, use a generic name to describe the equipment and its process. We will call it the "Fluid Film Process". The fluid film process permits a high speed continuous treatment of sheet, strip, panel and billet material requiring cooling, heating, pressure confinement or shape and surface control. Many products presently manufactured in molds or platen presses can now be much more rapidly produced continuously on machinery incorporating fluid film processing.

The first major application of this process has been in the production of foam core panels used by the construction industry for the manufacture of roofing and sheathing panels. The use of urethane foam insulation for roofing in the United States dates back to the 1950's.

The earliest machine was a four-sided Armorbelt pressure tunnel built in 1958. This machine produced a continuous rectangular block of urethane foam which was cut to length and multiple sawed to desired thicknesses and roofing felt was laminated to the cut slabs. This line of machinery was soon followed by machines capable of pressures up to 5 psi (0.35 Kg/sq. cm) and panel widths to 9 ft. (2.74 meters) (See Figure 5).

These machines are well known as double belt units which produce the major share of today's urethane foam panels for building roofing and sheathing in the USA. We also know that through the years both designers and users have been concerned with undesirable features of double belt units. Double belt lines are large and massive. The size is necessary to

0097-6156/81/0172-0553\$05.00/0

© 1981 American Chemical Society

accommodate the large drive sprockets to reduce the chordal action of the belt chain to achieve a reasonably uniform belt speed.

Belts must be of heavy duty construction to prevent deflection under the pressure of the expanding foam. A deflection of .030 inch (0.76 mm.) in each belt results in a .060 inch (1.52 mm) difference in panel thickness across the width of the panel.

The high pressure loads of up to 3000 lbs. (1364 Kg) per lineal foot for a 4 foot (1.22 meter) wide conveyor requires a heavy duty frame to avoid frame deflections which, added to the belt deflections, further increase the inaccuracy of the panel.

These high pressures require the use of antifriction rollers to avoid excessive drive horsepowers. Even with such efficient rollers, the drive for a panel line running at 50 ft./min. (15 meters/min.) is 30 H.P. Tracks for the belt rollers must be machined and ground for panel thickness accuracy and power reduction. However, unless they are hardened or of special wear and brinnelling resistant steel, the continuous heavy rolling action of the rolls soon wears a deep groove in the track.

Even with frequent or continuous lubrication, the rollers subjected to heat and high loads, soon reach the end of their life span, requiring replacement and expensive down time.

Minute differences in alignment of adjacent conveyor slats results in belt marks which mar the appearance of the finished panel. This is in spite of all the care possible to build a precision conveyor. Even though the difference is only several thousandths of an inch, reflected light shows up the slat marks very distinctly. This condition worsens as rolls and tracks wear.

Another important concern, in view of the oil crisis, is the extravagant use of energy needed to support this chemical process and to move the panel through the process area. The heavy machinery and the belt pressure load result in high motor power requirements. More serious, however, is the inefficiency of heat transfer to the belt and to the product and the great loss of heat from the belt to the atmosphere. These and other needs for improvement were representative of the state of the urethane foam panel manufacturing art at the time of introduction of fluid film processing.

All of these problems had been a concern to my company during its years of pioneering work with foam panel production. A number of piecemeal improvements were made through the years, but the grand solution, one which solved them all, came with the development of the fluid film process.

The fluid film process not only eliminates all of these problems but goes on to add new advantages, most of them of very significant magnitude.

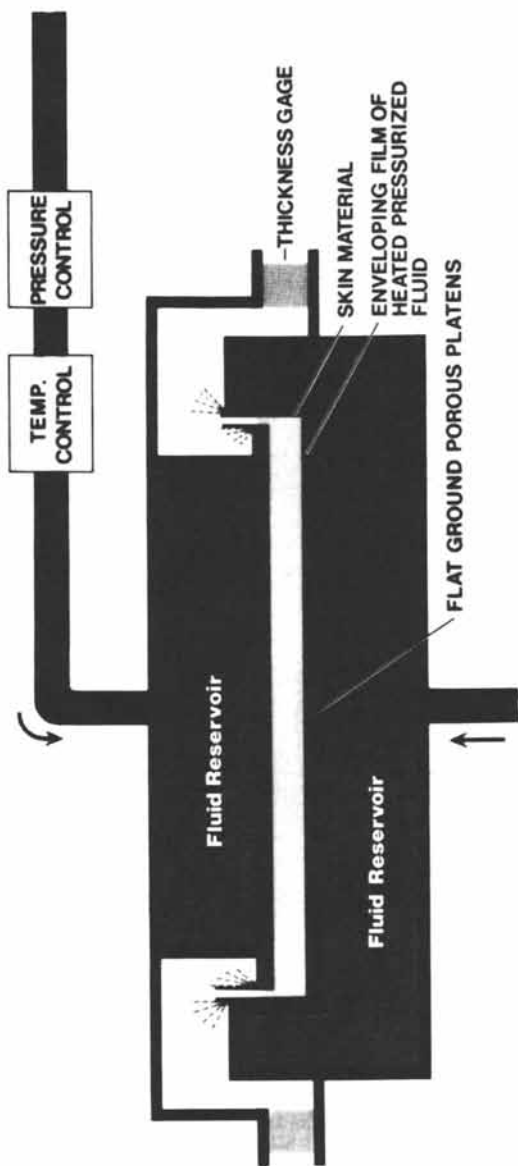


Figure 1. Cross section of process tunnel.

Figure 1 shows a cross section through a fluid film process panel production line. Air is introduced through the porous platen surfaces. The air forms a .005" (0.127 mm) thick film of rapidly moving air, enveloping the panel for maximum heat transfer and preventing physical contact of the panel with the platens. The platens are separated by precise gage blocks to achieve accurate thickness and to permit the production of a broad range of panel thicknesses.

A fluid film process line is shown in Figure 2. It is a series of modules, each consisting of the pair of platens illustrated in the previous slide. Each module is 5 feet (1.524 meters) long and each can have controls to adjust the temperature and pressure of the entering air. Thus, knowing the profile of temperature and pressure needs of a specific foam chemical formulation, the line can be adjusted for optimum operation and minimum energy waste.

The following are some of the other revolutionary features of the process:

- FASTER
- MORE ACCURATE
- SMOOTH SURFACE
- MODULAR CONTROL
- HIGHER PRESSURE
- LOWER ENERGY USE
- HIGHER TEMPERATURE
- LOWER MAINTENANCE
- QUIETER
- SAFER
- COMPACT
- INTERCHANGEABLE WITH DOUBLE BELTS

Each of these is discussed in detail below:

Faster

Foam panels have moved thru the tunnel in a smooth effortless manner at any speed we have tried. Meanwhile, existing "wet-end" and cutoff equipment have been strained to capacity. Because of these wet end and cutoff limitations, the top speed tested at the writing of this paper, has been 170 ft./min. (52 meters/min.) However, there appears to be no apparent limit to the speed capability of the process, and for this reason, we are in the process of developing the auxiliary equipment for higher speeds. Naturally, as the line speed increases there develops a need for increasing the length of the line to permit complete cure of the foam. This new speed capability, now presents a challenge to the chemical manufacturers and formulators to develop formulations which will match the machine. This challenge has been passed on to the industry, but meanwhile we are looking into other technologies to speed the curing process of existing formulations.



Figure 2. Fluid film process line.

More Accurate

Where $+1/32$ inch ($+0.8$ mm) has been the standard thickness tolerance for 4 foot (1.22 meter) wide panels produced in double belt lines, the standard for the fluid film process is $+0.010$ inch ($+0.25$ mm). At times, an accuracy within $+0.005$ inch ($+0.127$ mm) has been achieved. Such accuracy is possible because of the precision and rigidity of the tunnel construction. The platens are reinforced weldments, stress relieved after welding and then ground and chrome plated. They are separated by precise gage blocks to form the two faces of the tunnel. Deflection is practically non-existent since the foam pressure on the platen is balanced by the fluid pressure within the platen reservoir. The fluid film is accurately controlled to maintain it at a normal working thickness of 0.005 inch (0.127 mm).

This new accuracy, in addition to easing the job of meeting customer specifications is also an opportunity for savings in costly chemicals, particularly significant for thin panels. In the case of a 0.125 inch (3 mm) thick panel, a 0.040 inch (1 mm) saving is equal to $1/3$ of the thickness.

Smoothness

Belt marks and the usual random plane slat impressions are non-existent on fluid film process panels. The absence of conveyor belts and the extremely accurate tunnel, produce a smooth continuous surface on both sides of the panel.

This feature combined with the improved thickness accuracy opens the door to many new markets which were previously denied for the lack of acceptable appearance and accuracy.

Lower Energy Use

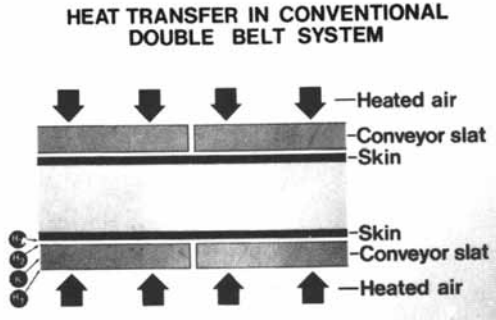
Energy conservation stems from the following features of the fluid film process:

- 1) More efficient heat transfer
- 2) Absence of heat losses
- 3) Friction-free movement of panel

Each of these energy conserving features is reviewed in detail below:

More Efficient Heat Transfer. In the conventional double belt system, hot air is normally introduced into each conveyor body. This air heats the belts which in turn transfer the heat to the product. The equation for heat transfer coefficient for this process is shown in Figure 3.

In the fluid film process, the heat is supplied via the hot air film which is in direct contact with the product. In addition, the rapid movement of the air film further increases



$$U = \frac{1}{\frac{1}{h_1} + \frac{L}{K} + \frac{1}{h_2} + \frac{1}{h_3}}$$

$$= \frac{1}{\frac{1}{1.34} + \frac{3}{5.2} + \frac{1}{1.34} + \frac{1}{1.34}}$$

U = heat transfer coefficient

h_1, h_2 & h_3

are transfer coefficient of the film on both sides of the conveyor slat and the panel skin surface.

L is the plate thickness (inches)

K is the conductivity coefficient of the plate

= .435 BTU / degF / hour / square foot

Reference – MARKS HANDBOOK

Figure 3.

the transfer rate. The formula for the fluid film transfer is shown in Figure 4.

At a temperature of 180°F (82°C) and a conveyor slat thickness of 0.375 inch (9.5 mm), the fluid film heat transfer rate is approximately 4 times that of the double belt unit.

Absence of Heat Losses. There are two major heat losses in a double belt system. One is the leakage of hot air through the gap between the conveyor belt and the conveyor body. The combination of inefficient heat transfer previously explained and the size of the gap around the entire periphery of the conveyor on both sides, wastes most of heat fed into the conveyor to the atmosphere.

The second loss is by radiation from the belt. The belt, which is of heavy construction for rigidity and flatness is a very significant heat sink. Some of this heat transfers to the panel where it is needed and some where it is not needed. The remainder is lost to the atmosphere by radiation during its idle return to the input end. This loss can be reduced by insulation but the problem of removing and restoring this insulation for inspection and maintenance access makes it impractical. A measurement on a double belt revealed a 20°F (11°C) loss in belt temperature during the return run.

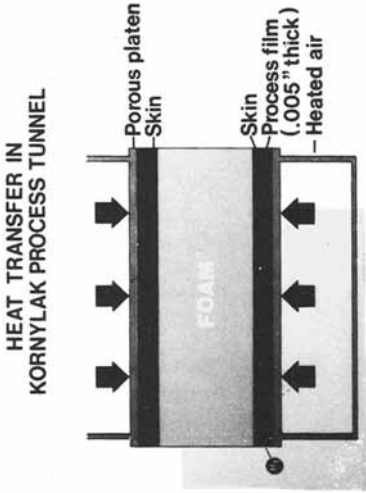
The fluid film system completely eliminates the heat sink/radiation loss since the platens remain stationary. The heat in the platen is radiated into the product. The reservoir behind the platen is easy to insulate and this insulation remains in place with no hinderance to inspection or maintenance. Further, since the heat is controlled in zones corresponding to the need profile of the formulation, there is no wasteful input of energy into the product.

The reduced thin film leakage loss at the perimeter is easy to collect and recirculate.

Because of the difficulty in calculating comparative data, we have collected data from operating lines. To compare heat losses, we have data from comparable double belt and fluid film lines. The operating conditions for both units were the same: 50 feet (15.24 meters) long line producing 4 feet (1.22 meters) wide panel at 50 ft./min (15.24 meters/min.) and a 160°F (71°C) skin temperature. The heat input into the double belt line was 333,000 BTU/hr. (84,000 Kg calories/hour) and into the fluid film line was 121,000 BTU/hr. (30,500 Kg calories/hr.). This the fluid film line operates with a 64% saving of heat input.

At a working pressure of 3 psi (0.21 Kg/Sq.cm) in a 50 foot (15.24 meters) long line, a 4 foot (1.22 meters) wide panel is subjected to a total belt load of 86,400 lbs. (39,273 Kgms.).

With a coefficient of friction of 0.001 for the roller supported belts assuming the use of lubricated roller bearings, the total belt pull is 86.4 lbs. (39 Kgms.), requiring a 15 HP drive for each belt at a 50 ft./min. (15.24 meters/min.) production speed.



$$\begin{aligned}
 U &= \frac{1}{\frac{1}{h_1} \times 2} \\
 &= \frac{1}{1.34} \times 2 \\
 &= 2.7
 \end{aligned}$$

U = heat transfer coefficient
h = transfer coefficient of panel skin surface
2 = transfer gain due to velocity of Process Film

Advantage of Process Tunnel over conventional Double Belt is $\frac{2.7}{.435} = 6.2$

Figure 4.

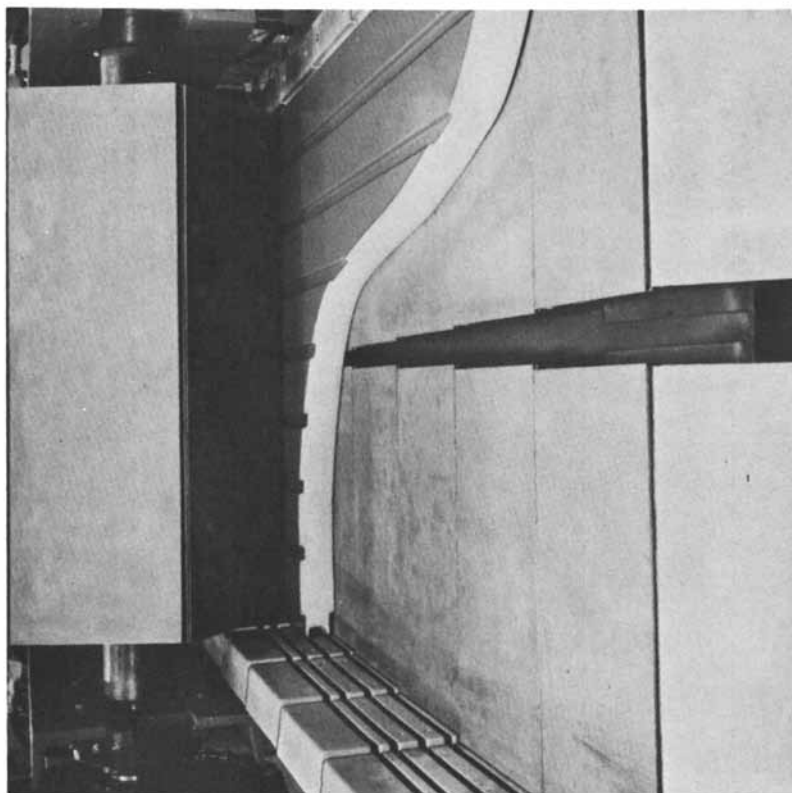


Figure 5. Edgemold Foamboarder center seam of split bottom belt is tight in the process zone. The belts diverge at the discharge end to free panel from the side restraint blocks.

In the fluid film process, where the panel floats in a enveloping film of air, very little force is needed to move the panel.

Higher Temperatures

Some formulations, such as isocyanurates, require or benefit from temperatures higher than normally possible in double belt lines. An operating temperature of 350°F (82°C) has been necessary for some formulations. Production temperatures can be achieved within 60 minutes. The difficulty in meeting this requirement on a double belt line results from the much less efficient heat transfer and the excessive heat losses. A further problem on double belt lines has been the accelerated wear of bearings at higher temperatures as explained later under the topic that follows.

Maintenance

Maintenance requirements of the tunnel are minimal because of the elimination of moving parts. The troublesome and frequent lubrication of rollers and bearings is completely eliminated. This is a fortunate improvement since the high temperatures shorten the life of lubricants and the high pressure load on the rollers cause bearing breakdown and wears grooves in the supporting tracks. Proper lubrication practice calls for removal of spent grease and replacement. The replacement schedule depends primarily on speed, hours of operations and temperature. This renewal period is halved for each 25°F (14°C) increase in temperature. For example, a lubricant life of 1000 work hours at 150°F (66°C) is reduced to 500 hours at 175°F (79°C) and only 250 hours at 200°F (93°C). Failure to observe a proper schedule on double belt units has resulted not only in destruction of bearings and rollers but also damage to the belt slats, the tracks and drive sprockets and a costly shutdown of the line.

Quieter

As operating speeds get higher the metal to metal contact of rollers and track add considerably to the plant noise level. Since quietness is recognized as a desired and mandatory condition of the workplace, the silent operation of the fluid film system is another of its many important advantages.

Safer

An ominous safety hazard is present on double belt lines at the entry throat formed by the two conveyors. Its location in the area of greatest activity - paper entry, paper folding, chemical laydown and distribution is a constant hazard to workers

in the area. This is particularly so if an operator attempts to adjust a paper wrinkle or a faulty fold. Or he might grab for an object which had fallen on the lower paper and was about to enter double belt and cause considerable damage to the belts or to itself. Further down the line, hazard is greatly reduced, but some is present because of the exposed edges of the moving belts, particularly at points where they pass by stationery supports and braces at the three moving levels at the panel level and at the top and bottom idle return levels.

The fluid film process has no moving parts in the pressure zone.

Compact

The overall thickness of a fluid film section when set for a 5 inch (127 mm) thick panel is only 24 inches (610 mm). This includes 2 inches of insulation on top and bottom exposed surfaces of the line. The resulting installation is only waist high permitting easy visibility and communication across the line.

Interchangeable With Double Belts

The fluid film processor can match any size, speed, formulation capability, temperature, pressure, energy use, control, and duty capability of a double belt conveyor for the production of cellular panel produced of urethane, cyanurate or phenolic and two flexible skins. It will easily fit into the same space and as a replacement may then offer the capability of higher speeds, higher densities, greater accuracy, smoother surface and greater core material versatility. In addition, its quietness safety and reduced maintenance make the replacement a welcome change.

In review it appears that the new fluid film process offers insulation panel manufacturers and chemical companies an opportunity to increase output, raise quality, enter new markets and reduce costs at a time when improved insulation offers the best immediate relief from rising costs and uncertain supplies of fuel.

New experiments with the fluid film process are continuing and new technical data is still being developed at the time of writing this paper. Some of this data, if appropriate will be added at the conference.

RECEIVED May 1, 1981.

The Role of Release Agents in Urethane Molding

DAVID B. COX

Chem-Trend Incorporated, 3205 East Grand River, Howell, MI 48843

Background. The process of molding urethane products requires the use of a mold release agent in order to prevent the adhesive bonding of isocyanates to the mold. Without a release agent, the reaction of isocyanate with active hydrogens on the mold surface would produce such strong chemical bonds that the molded part could not be removed intact. This is reason enough for considering release agents an important element of molded urethane production, but release alone is usually not enough. The release agent must often produce, or permit production of, a desired surface. The release agent must also not introduce (ideally) other problems, such as excessive buildup on the mold or problems with painting or glueing the part. The purpose of this paper is to present a brief review of the state of the art in urethane mold releases, with some comments on the chemical and physical nature of successful products, and some further comments on future possibilities.

Scientific publications on the topic of urethane mold release are nearly nonexistent. There is no coherent body of basic research publication. The patent literature is illustrated by a few entries in a review of release agents published in 1972 (1).

The fact that a release agent is needed for molding urethanes is a problem, if only because production would be simpler without the need. Once one accepts the reality of the need, one can arrive at four options for providing release. These are: 1) a permanent release coating on the mold, 2) an internal release agent added to the reaction mixture, 3) a combination of a permanent base coat with an occasionally renewable top coat, and 4) a renewable release coat applied every cycle or every few cycles. The options are listed in order of desirability from a production point of view. Option 4 is in fact what nearly everyone uses, by necessity. Once Option 4 is accepted, it is reassuring to know that excellent release agents are available which can provide smooth, automatic production. On the other hand, achieving that smoothness, and keeping it,

0097-6156/81/0172-0565\$05.00/0

© 1981 American Chemical Society

requires a careful matching of production variables to release agent formula.

These generalities will be illustrated through a discussion of the release agent technology in two different and important types of molded urethane product. These are automotive seat foams and RIM urethanes. Before that discussion, however, it seems useful to discuss why Options 1, 2, and 3 for releasing urethanes have not been successful so far.

Permanent Coatings. The usual first candidates one thinks of are materials with low surface energy, such as perfluoropolymers or silicones. In fact, these materials are normally successful at first try. Even sheet polyethylene may be successful at first. The limitation appears when a large number of multiple releases is required. If one wishes to use a mold for making a thousand parts or more, one finds that the "permanent," low-energy surfaces begin to fail in release, usually long before one thousand parts have been molded. How soon the failure occurs depends on the urethane type, the composition of the surface, and the manner in which it was coated on the mold, but the mechanism involves a gradual alteration of the original surface. Spotwise adherence of the urethane begins, probably due to deposition of urethane components in microscopic depressions in the surface. Subsequent contact with fresh urethane allows chemical bonding to the deposited material, and the area tends to grow rapidly.

Internal Release Agents. Incorporation of a release agent in the urethane mix would at least remove the need for a separate pre-molding process step. Once again, it can be shown that internal release agents do work to some extent. The drawbacks, nevertheless, are severe enough to outweigh the advantages. The internal release must be mixed into the urethane, but it can only act at the surface of the part, so the mass that must be used is partly wasted unless it can either migrate rapidly to the surface at the right time or else contribute some other useful property to the urethane. At the least, the internal release should not make the bulk properties of the urethane part less satisfactory. In practice, so far, internal release agents have typically been found to fail after the molding of ten or twenty parts because they cannot protect the mold surface against urethane buildup deposits. They also may continue to migrate to the surface after the part is made, causing problems with painting or surface appearance. The basic idea is attractive enough that there will be continuing pressure to find a way around the problems, but for the immediate future, use of internal release agents is likely to be quite limited.

Permanent Base Coat and Renewable Top Coat. This concept has an advantage (over renewing the release coat each cycle)

only when the top coat is required at infrequent intervals. Therefore, the problems tend to be like those of the simple permanent coat option. Nevertheless, some experimentation is going on with this concept. With careful matching of production cycle needs and release agent properties, there is some promise to the concept.

Discussion of Current Technology

Automobile Seat Foams. Let us start by considering how auto seats are manufactured, which will define the performance requirements for the mold release agent used. The typical production machine is a carousel with a large number of molds being moved through a cycle with the following steps: spraying and drying of mold release, pouring of urethane, curing of the foam, and demolding. This cycle is over-simplified but contains the major steps from the release agent point of view. The basic requirements for the mold release agent are that it be in a form for easy application to the mold in the correct amount (usually sprayed), that it dry to form a film before the time of urethane pour, that it resist penetration of the urethane to the mold surface, and that it provide easy and complete release at the time of demold. There are usually additional demands made, which include production of a desired surface. Some companies prefer a closed or "skin" surface. Others require an open cell surface. At the least, the surface should be free of collapsed foam areas. Other secondary, but important, considerations are effects of the evaporating solvent on air quality and fire hazard. Buildup of either mold release agent or urethane on the mold is a problem in that it requires stopping production for cleaning, so minimum buildup is desirable. On the other hand, the effect of buildup on the dimensions or cosmetics of the part surface may not be critical.

Historically, the successful mold release agents used for seat foam have been based on waxes. The first seat foams were so-called one-shot, or "hot" foams. The term "hot" usually meant a cure temperature between 200°F and 300°F. This in turn meant that the mold surface temperature at demold was both hot enough to melt most waxes, and that it was also hot enough to evaporate water. Therefore, it was possible to use a release agent applied with either a high flash point mineral spirits or with water as a carrier. It is possible to make dispersions of waxes in mineral spirits by dissolving the wax mixture in hot solvent and cooling in a manner to precipitate the waxes in a particle size range of about one micron average. Such dispersions can be sprayed to produce a thin, continuous film when dried. In order to use water as a carrier solvent, it is necessary to emulsify the wax mixture in the melted state, and then cool the emulsion to produce a dispersion of solid wax particles. Once again, these can be produced in a particle size

range of one micron or smaller, so that a thin sprayed film can be deposited.

In the 1970's, there had been a strong trend toward use of High Resilient (HR) foams, which are cured at a lower temperature than hot foam. The original attempts were called "cold-cure" foams, but for various reasons, the surviving foam systems have come to have a range of cure temperatures from about 110°F to 170°F. The main significance of this drop in temperature from the hot foam range is that use of water-dispersed release agents was not practical at first. In fact, in some cases, high flash mineral spirits have been replaced with lower flash types, which is more hazardous, or by chlorinated solvents, which is more expensive and which causes some odor problem. The possibility for use of water dispersions is getting renewed attention because of the rising cost of petroleum-based solvent and because of air pollution control laws. There is no doubt that water-dispersed release agents can be successfully developed and used, but their use may require some special efforts to handle the problem of evaporation of water from the sprayed film at system temperatures. That is, foam producers may have to install air blow-off devices, use radiant heaters, or some such energy-using device.

RIM Urethanes. The use of Reaction Injection Molding for producing urethane parts is growing, particularly in auto parts such as bumpers and fascia. There are many potential and actual uses for RIM, including rigid housings for office equipment and instruments. One of the economic attractions of RIM in autos is that, if parts can be made rapidly enough, the cost for molds and machinery can be held low enough for overall competition with stamped steel. Cycle times have now been brought down to a few minutes, and the need to apply and dry a mold release film in each cycle has become relatively more of a time limit. On the other hand, a major need for auto parts is a Class A surface finish. This must be produced no matter what else, so keeping the mold surface smooth and blemish-free is mandatory. Internal mold release agents have not been able to prevent buildup for enough cycles before cleaning is necessary, and they also fail to give adequate release within a few cycles, probably for the same reason. Therefore, external mold release agents are still necessary at present. In addition to the surface finish requirement, the release agent must still do its primary release function very well. RIM urethanes tend to be less aggressive and adhesive than seat foam urethanes, in part because they react so rapidly that much of the isocyanate is gone by the time they contact the mold surface, but there are still problems. Sometimes the part shape is complex, as in the case of grillwork on an auto front fascia. The part must release easily at those locations where there is sliding motion between finished part and the mold surface. Another problem may occur in the gate and runner areas

because the urethane is injected very rapidly; it can actually abrade or erode away a release film. RIM molds are typically at temperatures of 165°-180°F at the time of spraying mold release agent, so the choice of carrier solvent is similar to that of HR type seat foam. Both aqueous and non-aqueous solvent systems are in use, usually depending on the chemistry of the active ingredients of the release agent. Some successful RIM release agents are based on waxes, and these are usually carried in mineral spirits or other non-aqueous, non-polar solvents. Other formulas are based on amphiphatic soap-like ingredients, which can be carried by water. In these formulas, the evaporation of water is usually promoted by inclusion of low molecular weight alcohols. Water-based release agents can be easier to remove from the part surface when cleaning is critical, but wax-solvent release agents are also successful with proper cleaning.

Formulations and Mechanisms. The above discussion has set forth some of the details which must be considered in selection and use of mold release agents for urethanes, although there are also many special problems which have not been covered. In this section, the discussion is directed to some probable elements of the mechanism of function. Mold release technology, like many others, has developed in advance of the detailed basic scientific understanding. Nevertheless, progress is being made, and more science is emerging from the art.

One may divide the requirements for a mold release agent into two aspects. The first is prevention of contact between the urethane and the mold surface, and the second is the release itself. If we consider the first requirement, it seems logical to suppose that at minimum, one must have a continuous film, or at least one with gaps which are very small so that the urethane cannot wet well enough to get into them. Next, it appears that the film must usually be a solid in nature. Success can be achieved in some cases with films of liquid silicone, for example, but liquid films have not been at all adequate for seat foam, and not good enough for RIM. The film should probably not be highly soluble in urethane components, at least at the temperatures encountered. Many attempts have been made to create release agent films in which some components play an active chemical role. That is, the principle was that an active chemical ingredient reacted with isocyanates to make sure they reacted in the film and not at the mold surface itself. Such attempts have not usually been successful. On the other hand, some experiments to determine the reactivity of TDI with waxes and other ingredients used in successful release agents has shown that a reaction takes place in some cases. One may summarize by saying that chemical reactivity is not necessary, but may be present.

The problem of producing a film that is continuous, very thin (to minimize cost and buildup), and impervious to urethane has been solved in most cases by use of waxes. There are many

wax-like materials to choose from, including petroleum-based paraffin and microcrystalline types, other natural waxes from vegetable, animal, and mineral sources, and synthetic waxes such as polyethylenes. Most will not work by themselves. It has been necessary to make mixtures, use special additives, and otherwise modify the basic properties. There is not any useful generalization here except to say that it is frequently necessary to tailor-make release agents to match a particular set of urethane producing requirements. This is often due to the need to combine special requirements such as a particular surface character with a particular temperature range of cure, and so forth. Some reasons why this is so may be seen by considering the second function, namely the release itself.

Let us examine the case of hot cure seat foam as one example of how the release itself is accomplished. At the time of pouring of the foam, a mold is typically at a temperature of about 95° to 110°F., so that a wax-based film is a solid. During the early moments of the foam rise, the film is probably still solid, but the exotherm of the foam plus the imposed heat from the curing ovens gradually increases the temperature of the release film. By the time of demolding, the system is above 200°F., and the wax film has melted. Presumably, the isocyanate content of the surface of the foam has declined to zero or near it, so the foam can no longer be adhesive. Then, the act of demolding is a simple peeling of the foam away from a liquid film, with resulting low force. The actual picture may not be that simple. For example, it is possible to get extremely easy release from solvent-carried release agents, but in general, the release ease from water-based release agents has not been as good. It is complete, but the actual force may be higher. The reasons are not fully understood yet.

In the case of HR foam, RIM, and many other urethane types which are cured at temperatures under 200°F., the release film is normally not melted at the time of demold. The mechanism of release could, in principle, involve several possibilities. The urethane part could adhere to the release film, with the release occurring between the mold surface and the release film. The urethane could fail to wet the release film, and therefore never adhere to it. Or the release film could break in such a way that some part stayed with the mold and some transferred to the urethane part surface. In fact, one can find examples of all three mechanisms. The knowledge necessary to elucidate more of the details of these mechanisms, and the expected greater ability to control the function through chemical formulation are now being gathered through a basic research approach.

Figures 1-4 illustrate some evidence for the third mechanism just listed, in which the release film fails cohesively. The photographs were taken from a scanning electron microscope. The specimens were produced as follows. Figure 1 is the top surface of a freshly sprayed and dried release film. It shows that the

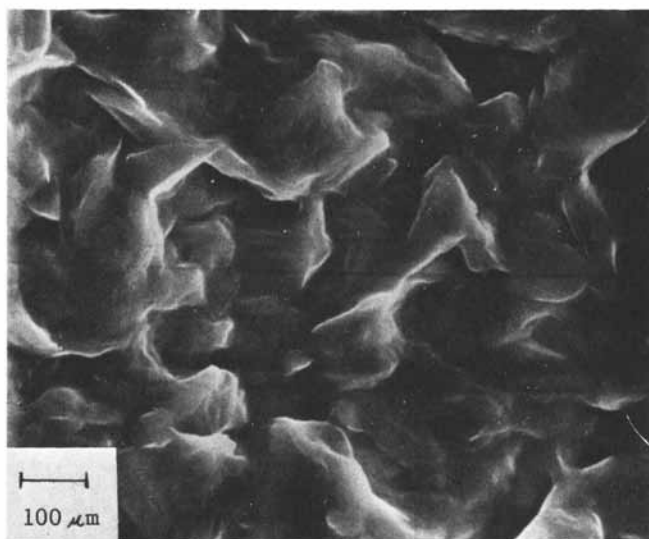


Figure 1. Undisturbed surface of mold release film.

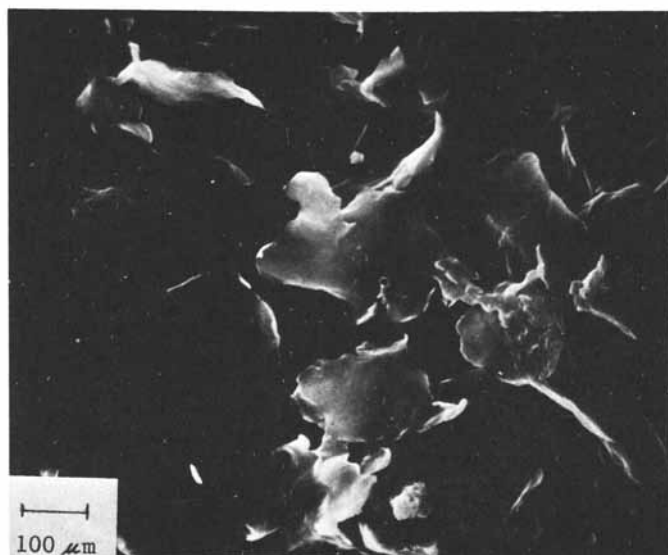


Figure 2. Surface of film remaining on the mold after demolding of HR urethane foam.

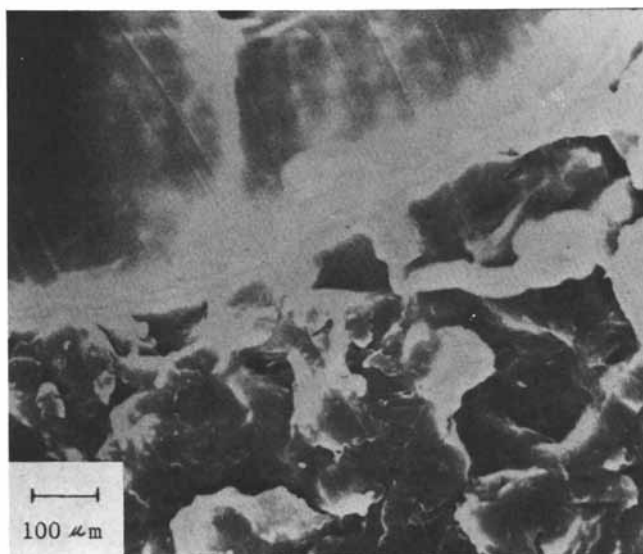


Figure 3. Surface of film transferred to the urethane foam surface after demolding.

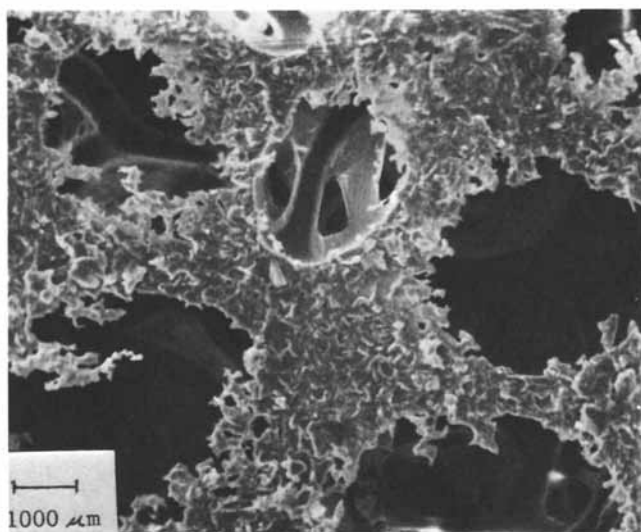


Figure 4. Same surface as in Figure 3, at lower magnification, showing underlying urethane cell structure.

release agent contained solid wax particles which still give a structure to the film, including a relatively rough surface. HR foam was then poured and cured on a specimen of the film, followed by demolding. Figure 2 is the surface of the mold, and Figure 3 is the surface of the foam, both at the same magnification as Figure 1. The texture is the same, as one would expect from a failure within the film. Figure 4 is the same specimen as Figure 3, but at smaller magnification. In this view, one can see the underlying cell structure of the urethane to which the wax from the mold release film has adhered.

Future Trends

Molded urethane technology in the immediate future should not be limited by mold release considerations, but the role of the mold release in new systems should be considered early in the plans. Regulations for air quality control and worker safety are expected to create a continuing shift to water-based mold releases, or at least some means of greatly reducing the amount of solvent evaporated. Some progress seems likely in use of semi-permanent release coatings which can be renewed by periodic application of a top coat.

Acknowledgement: The knowledge expressed in this paper contains contributions from the work of C. Peer Lorentzen, Steen Tamstorf, Kenneth C. Rennells, G. Clarke Borgeson, and Roberto Torres.

Literature Cited

1. McDonald, M., Ed. "Release Agents"; Noyes Data Corp., Park Ridge, N.J., 1972.

RECEIVED April 30, 1981.

INDEX

A

- Absence of heat loss, fluid film transfer system 560-563
- Accelerated aging 300
- Acid number 444, 446, 460
- Activation effect 214*f*
- Activation energy(ies) 421*t*
- calculation, for dynamic mechanical transitions 347
- soft segment glass transition 349*f*
- Adhesives
- comparison of hard and soft segments 358
- construction 65
- Halthane 73-series 344-353
- isocyanate vs. phenolic, in bonding particle 66*t*
- polymeric MDI 59
- polyurethane, dynamic, mechanical, and thermal properties 343-362
- polyurethane, preparation 335
- solventless 505-517
- synthetic, value and projections 58*t*
- urethane
- transportation industry 67-68
- U.S. use 58*t*
- used to bond foundry sands, advantages 60*t*
- used to bond foundry sands, improvement 63*t*
- Aerosol propellants 120
- Aged modulus of rupture 306
- vs. nominal density for aspen waferboard 308*f*
- Air quality control 573
- Alcohols, catalysis of isocyanate reaction 393-402
- Allophanate, formation 129, 287
- Aluminum castings 63*t*, 64
- Ames test 533
- Amine catalyzed phase II elastomers, properties 545*t*
- Amine, coordination to isocyanate 393
- Anisotropic expansion 133
- Antifirction rollers 554
- Antishrink efficiency, definition 270
- Antishrink efficiency of methyl isocyanate-treated Southern pine 273*f*
- Arrhenius plot of rate constants of thermal *cis-trans* isomerization of azochromophore 232*f*
- Arrhenius plot, reduced, for the isomerization of azoaromatic chromophores 224*f*
- Articulating patellas, polyurethane 493
- Aspen waferboard 304
- internal bond vs. nominal density 308*f*
- with Mondur E-441 binder 307*f*
- ASTM analysis 476
- ASTM urethane coatings 506
- Automobile seat foams 566, 567-568
- Automotive application for TPU
- elastomers 246
- Automotive castings, change 64*t*
- Azochromophore 226
- cis-trans* isomerization
- kinetics 228
- photochemical 228
- rate constants 228
- thermal, first order plot 31*f*
- single-phase polyurethane in hard segments 235-236
- two-phase polyurethanes in hard segments 233-234
- two-phase polyurethanes in soft segments 228-233

B

- Backbone elements 510-512
- structure variation 510*t*, 511*t*, 513*t*
- Baking temperatures 521
- BB drop test 133
- BDO extender 155
- Bedding, foam consumption 29
- Bedding, use of flexible foam 29
- Benzyl alcohols, reactivity with phenyl isocyanate 404
- Bifunctional monomers, synthesis 519
- Binder level 300
- effect on mixed hardwood flake-board properties 302*t*
- Binders and adhesives, urethane 57-86
- Biocompatibility 492-493, 498
- Biodegradable polymers 471
- Biodegradation, ASTM recommended procedure 472-473
- Biodegradation of polyurethanes 475*t*
- by *Aspergillus fumigatus* 482*t*, 485*t*

- Biodegradation of polyurethanes
(continued)
- by *Cryptococcus laurentii* 483*t*, 486*t*
 - derived from polycaprolactonediolols 471-487
 - by *Fusarium solanii* 478*t*, 484*t*
- Biomechanical compliance 501
- Biomedical polyurethane development 489-503
- Biurets, formation 287
- Bis cyclic ureas 521
- Block copolymers 343, 489
- Blocked aliphatic diisocyanates 519
- Blowing agents 95
- Blowing reaction 129
- Bond formation, isocyanate with wood, evidence 266, 267*f*
- Bonding, isocyanate, chemistry 286-288
- Bonding of isocyanates to wood 263-284
- Brabender plasticorder 466
- Bronchial asthmatic reactivity to isocyanate 89
- Bronchial asthmatic response 90
- Brown-rot fungus (*Gloeophyllum trabeum*) 275
- Building codes, model 114-116
- Bumpers 568
- Butanediol-capped MDI, molecular conformation 193*f*
- C**
- Calculation of theoretical nitrogen content of hydroxyl groups in Southern pine 279*t*, 280
- Calculation of adjusted MOR 300
- Capped polyols 330
- analysis data 329*t*
- Capping hydroxyl groups 324
- Carbamate(s) 285
- linkages 522
- Carbamic acid formation 120
- Carbamic acid conversion to polyureas 130
- Carbon dioxide evolution 134
- from A compared with gel profile, rate 140*f*
 - from A compared with rise profile, rate 140*f*
 - comparison with rate of foam rise .. 140*f*
 - from reacting foam 138*f*
 - water-blown urethane 141*f*
- Carboxylation of lignin 330
- kraft 314
- Carboxylation of ligninsulfonates 314
- Carpet underlay, foam consumption .. 30*t*
- Carrier solvent 567
- Cartilage, viscoelastic and hydrophilic properties 493*t*
- Cast elastomers 419-431
- composition and properties 427*t*
 - polyurethane 429*t*
 - effect of temperature on physical properties 426
 - preparation 420
- Castings, aluminum 63*t*, 64
- Catalysis
- by cobalt compounds 398*f*
 - effect on reactivity of phenol benzyl alcohol and ethyl alcohol with phenyl isocyanate 415*t*
 - isocyanate-hydroxyl reaction by acid 448*t*
 - isocyanate reaction(s)
 - with alcohols 393-402
 - by DBTDL, effect of triphenylphosphine 401*f*
 - with protonic substrates 205-217
 - polyurethane formation
 - complexation between reagents 206-210
 - consequences of the proposed reaction mechanism 210-213
 - explanation of experimental results 213-215
 - nucleophilic attack 212
 - orbital considerations 213-215
 - via tertiary amines and organometallic compounds 205-217
- Catalyst(s) 537*t*
- BF₃ · OEt₂ 197
 - comparison in the reaction of phenol and benzyl alcohol with phenyl isocyanate 412*t*
 - complex formation 397
 - content 512-515
 - effect of stannous octoate 458*t*
 - and initiator concentrations 319*t*
 - Nafion perfluorosulfonic acid resin 198
 - type, effect on compressive strength build-up for urethane binders 61*f*
- Catalytic species, configuration 397
- Catalyzed polymerization 456-458
- Cell opening 133-134, 136-139
- CFC (see Chlorofluorocarbon)
- Chain
- extender(s) 426, 523, 536*t*
 - effects, ethylene glycol 454
 - dissimilar, effect on TPU elastomers 256*t*
 - hardness build-up, effect 254*t*
 - structure 254
 - for polyurethane elastomers 182, 220
 - for urethane elastomers, aromatic diol 533-551
 - extension of α -di(hydroxy)polyisobutylene with tolylene diisocyanate 388*t*

- Chain (*continued*)
 extension of polyisobutylene diols .. 385
 length, effect 492
 segment organization 227f
 Characterization of polyurethane
 networks 373-381
 Chemical composition of softwood
 cell wall 264f
 Chemical ionization mass
 spectrum for EO:THF 2:3 crown .. 200f
 spectrum for EO:THF 3:2 crown .. 200f
 spectroscopy for EO/THF polym-
 erization, crown ethers
 identified 199f
 Chemistry of isocyanate bonding .. 286-288
 Chlorofluorocarbon 11 96, 118
 Chlorofluorocarbon 12 96
 Chlorofluorocarbon(s) 95
 advantages 96
 blown rigid polyurethane foams 113
 regulation, energy consequences 98
 Cigarette smoldering standards 104
 Classification, polyurethane based on
 RNCO 508t
 Classification of urethane coatings 506-516
 Comparison of HER with HEQ 535
 Complexation between reagents,
 catalysis of polyurethane
 formation 206-210
 Compression set 524
 Coat, permanent base and renewable
 top 566-567
 Coatings, solventless 505-517
 Coatings, urethane 330
 classification 506-516
 Cobalt compounds, in catalysis of
 phenyl isocyanate-butanol 308f
 Coefficient of friction 560
 Cold box process 63
 schematic layout of equipment 62f
 Comparison of hard and soft seg-
 ments in adhesives 358
 Complex formation between DBTDL
 and DABCO catalyst 397
 Complex formation, NMR studies 397
 Compounding ingredients, classes 515
 Configuration of catalytic species 397
 Conformational analysis of
 poly(MDI-BDO) 184-187
 Construction adhesives 65
 Construction, flammability
 variables 105-106
 Consumption, foam
 bedding 29
 carpet underlay 30t
 furniture 29t
 Coordination complex, tin 399
 Copolyether glycols, comparison of
 PTMEG and EO/THF 201f
 Copolymers, lignin-maleic anhydride,
 formulas and maleic acid
 content 316t
 Copolymer, ratio to propylene oxide,
 influence on polyols 314
 Copolymerization
 degree 314
 EO and THF, gas chromatograms 198
 ethylene oxide and tetrahydro-
 furan 197-202
 Coreactive polyurethanes 507
 Correlation coefficients 306
 Cotton linters vs. urethane inter-
 mediates 31f
 Coupling constant, effect of added
 TEDA 398f
 Cross-link 287
 Cross-linking 129
 agent quadrol 351f
 concept of polymeric MDI-wood
 matrix 288f
 Crown ethers identified by chemical
 ionization mass spectroscopy for
 EO/THF polymerization 199f
 Crystallization of elastomers 544
 Curing
 agent formulations 345t
 of coatings 521
 endotherm 356f
 mechanisms 60
 rate with Desmodur PI-1520A 20 .. 292
 Curtius rearrangement 321
 Cutting pattern for test specimens 294f
 Cyclic ureas 519
trans-Cyclohexane-1,4-diisocyanate,
 reactivity studies and cast
 elastomers 419-431
 Cyclotrimerization 421, 426
- D**
- Dacron velour-silicone rubber
 implants 501
 Damping coefficient 494
 measurement 496f, 499f
 DBTDL as catalyst 410
 1-Decanol
 polymerization, shortstopped
 with 462-465
 shortstop effect 464t
 Degree of substitution, calculation 280
 Degree of substitution of hydroxyl
 groups in holocellulose in methyl
 isocyanate-treated Southern pine 281t
 Degree of swelling 376
 calculation 375
 polyurethane networks 377f

Demand for polyurethane	
Japan/Far East	21 <i>t</i>
Latin American	13-15, 14 <i>t</i>
Middle East/Africa/E.	
Europe	17-20, 21 <i>t</i>
outlook, worldwide	14 <i>t</i>
U.S./Canada	11-13, 14 <i>t</i>
Western Europe	21 <i>t</i>
Density gradient	304
Density, mean as a function of time	176 <i>f</i>
Desmodur PU-1520A 20 binder, red	
oak flakeboard with	293 <i>f</i>
Diamine curing agents	533
Differential scanning calorimetric (DSC)	150
curve(s)	
cooling, TPU elastomers	253 <i>f</i>
polymers	368
total heat generated during polyurethane formulation	152 <i>f</i>
urethane reaction formulation	152 <i>f</i>
data	347
kinetic analysis	151-153
measurement of heat released during urethane polymerization	154 <i>f</i>
model polymers	370 <i>f</i>
results of physical blending of hard and soft segments	367 <i>f</i>
traces	389, 390 <i>f</i>
73-series Halthanes	350 <i>f</i>
87- and 88-series Halthanes	356 <i>f</i>
use	363
Difunctional monomers, stability	519
Diisocyanate(s)	
deficiency	465
masked aliphatic	519-522
reaction rates	421 <i>t</i>
trimerization reaction	425 <i>f</i>
Dilute solution viscosity	443
Dimensional stability	
calculation	269
methyl isocyanate modified Southern pine as a function of weight percent gain	272 <i>t</i>
mixed hardwood flakeboard	298 <i>t</i>
from isocyanate reacted with Southern pine	269-274, 271 <i>t</i>
Diol crosslinkers, comparison	523-531
Dispersion of waxes	567
Dissolution processes	311
Distribution of bonded isocyanates in cell wall components	276
Distribution of nitrogen in methyl isocyanate-treated Southern pine	277 <i>t</i> , 279 <i>t</i>
DMCHA as catalyst	410
DOE, Building Energy Performance Standards (B.E.P.S.)	53-54
DOE, Residential Conservation Service (R.C.S.) program	53
Domain formation, kinetics, quenching from melt, TPU elastomers	250, 252
Double belt system	560
Drilled disc, cross-section	500 <i>f</i>
Dry method	321
DSC (see Differential scanning calorimetric)	150
DSV value	449
Dynamic extrusion rheometer T ₂ value	444
Dynamic mechanical spectrum of Halthane 73-14	348 <i>f</i>
Dynamic mechanical spectrum of Halthane 88-2	357 <i>f</i>
E	
Economic analysis of lignin-derived polyols	330, 334 <i>t</i>
Eczematous dermatitis from TDI	90
Elastomers	
cast	426-431
composition and properties	427 <i>t</i>
polyurethane	429 <i>t</i>
effect of temperature on physical properties	426
preparation	420
castable urethane, comparison of diol crosslinkers	523-531
chain organization	435 <i>f</i>
data from PPG and PTMG polyols	247 <i>t</i>
green strength results of phase I polyester-based	542 <i>t</i>
green strength results of phase I polyether-based	541 <i>t</i>
nonautomotive applications	83
phase IV processing studies	550 <i>t</i>
physical properties	530 <i>t</i>
polymer morphology	247
polyurethane	
chain extenders	182, 220
formation	226
phase separation	179
definition	226
preparation	149, 182-184, 523
properties	219
stereochemistry of MDI unit	180
structure of hard segments in MDI/diol/PTMA	179-195
structure of segmented	227 <i>f</i>
two-phase synthesis	219-220
chain extension with HER	534
preparation	244-246, 534-544
properties	
amine catalyzed phase II	545 <i>t</i>
organometal catalyzed phase II	546-547
phase I polyester-based	540 <i>t</i>

- Elastomers (*continued*)
 properties (*continued*)
 phase III polyester-based 549*t*
 phase III polyether-based 548*t*
 prepared from polyester-MDI 526*t*–527*t*
 prepared from polyether-MDI 528*t*–529*t*
 polyether-based 539*t*
 RIM polyurethane 69
 stress properties 428*t*, 430*t*
 study of melt polymerization 433–470
 test methods 246, 538
 thermoplastic, polyurethane, formation 433
 TPU
 automotive application 246
 DSC cooling curves 253*f*
 effect of
 chain extender on hardness 254*t*
 dissimilar chain extenders 256*t*
 hardness build-up 250
 NCO/OH ratio on hardness
 build-up for polymer made from tipped PPG polyol 251*f*
 segment length 252
 kinetics of domain formation on quenching from melt 250
 urethane, aromatic diol chain extender 533–551
 urethane, comparison of properties 524
 uses, U.S./Canada 12
 vulcanization 373
 Elbow joint replacement 494–498
 Electron micrograph of HR urethane foam 128*f*
 Electron micrographs of radially split Southern pine, treated with methyl isocyanate 274*f*
 Elemental analysis of model type A intermediates 325*t*
 Elemental analysis of model type C intermediates 327*t*
 Enzymatic degradation 474
 Ethyl alcohol, reactivity, with phenyl isocyanate 413*t*, 415*t*
 Ethylene glycol chain extender effects 454
 Evolution of carbon dioxide from reacting foam 138*f*
 Extended formulation, definition 155
- F**
- Fabric, flammability variables 105–106
 Fascia 568
 Fascia applications, major ingredients of RIM elastomeric polyurethanes 72*t*
- Films
 of liquid silicone 569
 percent moisture absorption 492*t*
 polyurethane, x-ray diffraction patterns 188*f*
 Fire risk, urethane foams 111
 Fischer, Karl, titration 130
 Flake moisture content 300, 304
 effect on mixed hardwood flake-board properties 305*t*
 Flammability
 market changes due to insulation 55
 standards 106–109, 110*f*
 urethane foam 101–112
 considerations 103*f*
 variables
 construction and fabric 105–106
 ignition source 104–105
 occupancy 105
 Flame retardant, definition 104
 Flame spread 114
 rating 114
 Flange/stem ratio 501
 Flexible urethane foam, bedding segment 29
 Flory–Rehner equation 376
 Flow mechanics of polyurethane foam formation 167–178
 Fluid film
 process
 application 553–564
 accuracy of thickness 558
 cross section 555*f*
 features 556
 heat transfer 558
 line 557*f*
 speed 556
 lower energy use 558
 smooth surface 558
 standard 558
 section, compactness 564
 transfer formula 560, 561*f*
 transfer system
 absence of heat loss 560–563
 double belt interchangeability 564
 safety 363–364
 silent operation 563
 Fluidyne system 133
 Fluorocarbons, energy extenders of polyurethane foams 95–99
 Foam(s)
 apparatus for measurement of viscous forces 170*f*
 automobile seat 567–568
 blown, EPA vs. chlorofluoro-carbon 119–120
 consumption, in bedding 29*t*, 30
 consumption, carpet underlay 30*t*
 core panels, manufacture 553–564

Foam(s) (<i>continued</i>)	Foam(s) (<i>continued</i>)
experimental procedure for measurement of viscous forces 169	viscosity 133, 136
flexible urethane	Foaming pressure 133
reaction sequence model 127-147	Formation
total market 25-26	polyurethane 506-507
use	elastomers 226
automotive formulation	thermoplastic 433
for 169-171	foams, rigid 313
in carpet underlay 30	foams, lignin in 312
U.S./Canada 11	isocyanurate 426
flow, experimental results 172 <i>f</i>	urea 426
flow, as a function of time	urethane 426
apparent viscosity 177 <i>f</i>	Formulas of lignins and lignin-maleic
mean density 176 <i>f</i>	anhydride copolymers 316 <i>t</i>
pressure profile 174 <i>f</i>	Formulation
pressure gradient 174 <i>f</i>	DSC curve of urethane reaction 152 <i>f</i>
volumetric flowrate 176 <i>f</i>	HR foam, absorbance measured as
as a fluid medium 168-178	a function of time 131 <i>f</i>
formulations, infrared spectra 141 <i>f</i> , 143 <i>f</i>	polyurethane, DCS curve, total
high resilient (HR)	heat generated 152 <i>f</i>
electron micrograph of formation 128 <i>f</i>	urethane, calculation of degree of
surface of foam 572 <i>f</i>	reaction when phase separation
surface of mold 571 <i>f</i>	occurs 162
IR analysis 129	Foundry binders 59-68
laboratory, procedure for	shakeout 63
making 130-135	Free volume theory 221
polyester urethane 4 <i>f</i>	Functional groups reacted at phase
polystyrene 96	separation 164 <i>t</i>
polyurethane 507	Functional moieties 512, 514 <i>t</i>
fluorocarbons as energy	Functionality data of model type C
extenders 95-99	intermediates 327 <i>t</i>
formation, flow mechanics 167-178	Fungal degradation of polymers 473
furnishings market 25-32	Furnishings markets, polyurethane
lignin in formation 312	foam in 25-32
preparation 335	Furniture, foam consumption 29 <i>t</i>
properties, comparison 331 <i>t</i>	
rigid polyurethane 286	
effect of regulatory actions on	
marketing 113-121	
formation 313	
insulating 96	
uses in U.S./Canada 12	
rise	
and evolution of carbon dioxide,	
comparison 140 <i>f</i>	
physical description 136	
profile 133	
rate for formulation B 138 <i>f</i>	
testing, future 106	
urethane	
energy efficiency 98	
flammability 101-112	
considerations 103 <i>f</i>	
flexible, total market 25-26	
fire risk 111	
IR spectrum of water-blown 135 <i>f</i>	
synthesis 127	
UFAC standards, impact on	
business 109	
	G
	Gas
	chromatograms of copolymerization of EO and THF 198
	chromatograph for EO:THF
	crowns 199 <i>f</i>
	cure process 63
	Gel permeation chromatography 481
	Gel profile 133
	formulation A, B, and HR 137 <i>f</i>
	rate of evolution of carbon dioxide
	from A compared with 140
	reaction sequence model 145 <i>f</i>
	Gelling reaction 129
	Gibbs free energies 375
	Glass transition 360
	hard segments 347
	temperature 357 <i>f</i>
	GPC analysis 476
	Green strength results of phase I
	elastomers 541 <i>t</i> , 541 <i>t</i>
	Growth rate of polyether flexible
	urethane foam 27 <i>f</i> , 28 <i>f</i>
	Growth rating 476

- H**
- Half-life of fluorocarbon 96
- Halthane(s) 343
- 73-14, dynamic mechanical spectrum 348f
- 73-series
- adhesive 344-353
- soft segment behavior 344-347
- hard segment behavior 347-353
- differential scanning calorimeter traces 350f
- transition temperatures 352t
- thermogravimetric analysis curves 354f
- 88-2, dynamic mechanical spectrum 357f
- 87- and 88-series
- adhesives 353-358
- soft segment behavior 353
- hard segment behavior 353-358
- differential scanning calorimeter traces 356f
- storage moduli 355f
- thermogravimetric analysis curves 359f
- transition temperatures 358t
- Hard segments 343, 434
- adhesives, prepolymer and curing agent formulations 345t
- amorphous 365
- behavior of Halthane 87- and 88-series adhesives 353-358
- behavior of Halthane 73-series adhesive 347-353
- chemical components of thermoplastic polyurethanes 245f
- structure 244, 245f
- chromomorphic molecular structure in single phase polyurethane 236f
- compatibility rules 365
- concentration, effect on modulus 360
- glass transition 350f
- in MDI/diol/PTMA polyurethane elastomers, structure 179-195
- physical blending 367f
- polyester urethanes, molecular structure 229f
- photochromic 234f
- sequence lengths 164t
- UV absorption spectra of polyurethane with photochromic 234f
- Hardness build-up
- effect of chain extender 254t
- effect of NCO/OH ratio 250
- effect on TPU elastomers 250
- index values for polymers 252t
- HDI-capped polyols 329t
- Health considerations for isocyanates 87-93
- Heart assist balloon pumps 490
- Heat loss absence, fluid film transfer system 560-563
- Heat sink/radiation loss 560
- Heating cost, average monthly, Consumer Energy Index 49t
- Hemiarthroplasty 494
- Hemodialysis 490
- HER
- comparison with HEQ, phase III 535, 543
- determination of optimum properties with phase II 535, 543
- polyurethane chain extender, phase I 534-543
- specifications 534
- High pressure liquid chromatography (HPLC) 473
- High resilient (HR) foams 568
- surface of foam 572f
- surface of mold 571f
- Hindered base 386
- Histological results 493
- Histological section showing vigorous tissue ingrowth 500f
- Hofmann degradation 419
- Holocellulose 268, 277
- Hot foams 567
- cure seat 570
- Housing demand in U.S., average annual projected 65t
- HPLC 473
- Hydrazide pathway 324, 336
- reaction scheme 323f
- Hydrazinolysis of ester 321
- Hydroboration/alkaline oxidation 386
- Hydrogen bonding, van der Waals forces 449
- Hydrolysis of isocyanate 129
- Hydrophilic properties of cartilage 493t
- Hydroxyl
- containing polymers 263
- groups in holocellulose, degree of substitution in methyl isocyanate-treated Southern pine 281t
- groups in Southern pine, theoretical nitrogen content 279t
- I**
- Ignition, open flame 104
- Ignition source, flammability variables 104-105
- Impact test 498
- Improvement of urethane adhesives used to bond foundry sands 63t

- Insulation
 commercial/industrial 50-51
 cumulative market 52-53
 farm building 52
 flammability 55
 markets 50-55
 isocyanates and polyurethanes 49-55
 metal building 52
 residential 51
 rigid polyurethane foam, effect of
 regulatory actions on mar-
 keting 113-121
 toxicity 55
- Industry structure, flexible urethane
 foam 25
- Inifers 383
- Initiator and catalyst concentrations 319*t*
- Injection moldability 249-250
- Injection molding, influence of
 NCO/OH ratios 249-250
- Instrumental, definition 130
- Insurance services office 116-117
- Interaction parameter 375
- Internal bond
 vs. nominal density for aspen
 waferboard 308*f*
 vs. press time for red oak flake-
 board 296*f*
 relationships 292
 and thickness swell vs. percentage
 Mondur MR for mixed hard-
 wood flakeboards 303*f*
- Internal release agents 566
- IR
 analysis 130, 134-135
 data of model type A intermediates 325*t*
 measurements 139
 spectrum(a)
 dibutyltindilaurate 209*f*
 methyl isocyanate-treated
 Southern pine 266, 267*f*
 isocyanate formation 326*f*, 328*f*
 triethylamine 209*f*
 spectrometry 510
- Irganox 1010 antioxidant 454
 structure 449
- Isocyanate(s)
 abbreviations 87*t*
 analyses of shortstopped polymers 464*t*
 analysis during melt polymeriza-
 tions 451*t*
 binders, history of development 289-290
 wood binders, disadvantages 290
 binders for wood composite
 boards 285-309
 testing 292
 boards, durability 300
 bond formation with wood,
 evidence 267*f*
- Isocyanate(s) (*continued*)
 bonded, distribution in cell wall
 components 276
 bonding chemistry 286-288
 bonding to wood 263-284
 bronchial asthmatic reactivity 89
 concentrations 89
 content, measurement 444
 formation, IR spectra 326*f*, 328*f*
 functional group 507
 functionality 324
 health considerations 87-93
 -hydroxyl reaction kinetics 149
 insulation markets 49-55
 methyl, reaction with Southern
 pine, volume changes 269*t*
 methyl-treated Southern pine
 antishrink efficiency 273*f*
 degree of substitution of hydroxyl
 groups in holocellulose 281*t*
 distribution of nitrogen 277*t*
 dimensional stability as a func-
 tion of weight percent gain 272*t*
 nitrogen in partially delignified
 holocellulose samples 278*f*
 whole wood basis 279*t*
 IR spectra 267*f*
 scanning electron micrographs 274*f*
 soil block test 276*t*
 -metal complexation 208
 -metal interaction 211*f*
 OSHA LTV 120
 vs. phenolic adhesives in bonding
 particle board 66*t*
 vs. phenolic resin 292, 297
 reaction, catalysis with
 alcohols 393-402
 reactions
 with Southern pine, reaction and
 dimensional stability 271*t*
 with Southern pine, volume
 changes 270*t*
 with wood 266
 -tin complex 394*f*
 treated southern pine inoculated
 with *Gloeophyllum trabeum*,
 soil block test 275*t*
 treated southern pine, resistance
 to attack by microorganisms 275
- Isocyanurate(s) 511*t*, 563
- Isocyanurates, formation 287, 426
- Isoeugenol-malic anhydride
 copolymer 324
- cis-trans* Isomerization of azochromo-
 phore
 Arrhenius plot of rate constants
 of thermal 232*f*
 first order plot, thermal 231*f*
 kinetics 228

- cis-trans* Isomerization of polymer
 film, UV absorption spectra 222f
- Isomerization of aromatic azochromophore affected by
 position in backbone of polyurethane 228, 233, 235
 morphology of the polymer
 matrix 228, 233, 235
 segmental mobility 228, 233, 235
 Isotopic labeling with C-14 373
- K**
- Kinetic studies of reactions of
 PPDT and CHDT 420-426
- K factor 54
- Kinetic(s)
 of domain formation on quenching
 from melt, TPU elastomers 250
 experiments 395
 of isocyanate-hydroxyl reaction 149
 of *cis-trans* isomerization,
 azochromophore 228
 parameters for polymerization of
 extended and unextended
 urethane formulations 156t
 phenol-formaldehyde inter-
 mediates 403
 photoisomerization of aromatic
 azochromophore 228
- Kraft lignin 330
 carboxylation 314
- L**
- Labeling, UFAC 108
- Law of Mass Action 461
- Leakage of hot air 560
- Lignin 277, 311-312
 based polyurethanes, procedure for
 preparation 330
 block copolymers 243
 carboxylation 330
 copolymer, ratio to propylene
 oxide 318t
 -derived
 polyols 313-321
 economic analysis 334t
 economic considerations 330
 polyisocyanates and polyure-
 thanes 311-328
 polyisocyanates 321-324
 polyurethanes 324-330
 disadvantages 313
 formulas and maleic acid contents 316t
 formation of polyurethane foams 312
 model compounds 322f
 oxyalkylation 335
 utilization approach 313
- Ligninsulfonates, carboxylation 314
- Liquefaction during oxyalkylation 321
- Liquid films 569
- Lopez-Serrano equations 164
- Loss modulus(i) 348f, 357f
 of Halthane 73-14 and 73-19 351f
- Lubrication and wear, in vitro
 study 493-494
- Lyophilization 473
- M**
- Macrocyclic(s)
 EO/THF, mechanism for formation 201f
 oligomers 197
 ureas, difunctional, ring opening 521
 ureas, difunctional, synthesis 520
- Maintenance requirements of the
 process tunnel 563
- Maleic acid contents of lignins and
 lignin-maleic anhydride
 copolymers 316t
- Market impact, polyurethane replace-
 ment for steel 83
- Markets, worldwide polyurethane 9-23
- Mastication of polymer 466, 469
- Mastication of thermoplastic urethane 467f
- MDI 374
 prepolymers 523
 quasipolymer 74
 structure 346
 supply/demand 84t
- MDI-butanediol fragment, minimum
 energy conformations 191t
- MDI-DPG 368
- MDI-EDO fragment, minimum
 energy conformations 191t
- MDI-PDO fragment, minimum
 energy conformations 191t
- Measurement of kinetics 404
- Mechanical properties 492-493
 elastomers 538
 phase I 539t, 540t
 polyurethane adhesives 343-362
- Mechanical testing of polyurethanes .. 493
- Mechanism
 olefin polymerization 383
 release 570
 tin-amine synergism 393-402
 carboxylate 400
 urethane formation catalyzed by
 organometallic compound 214f
- Melt polymerization 445f, 447f, 450f,
 453f, 455f, 457f, 459f, 463f, 467f
 study 433-470
- Melting points of model type A
 intermediates 325t
- Metal replacement opportunities 69-86
- Metallic catalyst 512

- Methanol-capped MDI
 conformation 181f
 structure 181f
 projection 181f
- Methyl isocyanate-treated Southern pine
 distribution of nitrogen 277t, 279t
 IR spectra 267f
 nitrogen in partially delignified holocellulose samples from 278f
 soil block test 276t
- Microbial degradation 471
- Monthly heating cost, average, Consumer Energy Index 49t
- MR boards, durability 300
- Multiphase description 512
- N**
- NCO/OH ratio 422
 effect on hardness build-up 250, 251f
 influence on injection molding 249-250
- Networks, polyurethane
 characterization 373-381
 swelling 378t
 degree 377f
 stress relaxation 378f, 379t
- Network synthesis 374
- Nitrogen
 content, theoretical, of hydroxyl groups in Southern pine 279t
 effect on hyphal development 480f
 in partially delignified holocellulose samples from methyl isocyanate-treated Southern pine 278f
- NMR 510, 520
 chemical shift 399
 studies 393
 complex formation 397
- Nominal density vs. aged modulus of rupture for aspen waferboard 308f
- Nominal density vs. internal bond for aspen waferboard 308f
- Nonresinous compounding ingredients 515
- Number average functionality 385, 386t
- O**
- Occupancy, flammability variables 105
- Occupancy percentages, use of urethane foam 103f
- Occupational exposure to TDI 89
- Octahedral complex 397
- Olefin polymerization, mechanism 383
- Open cell surface 567
- Organometal catalyzed phase II elastomers, properties 546t-547t
- Organotin catalysts 412t
- Orthopedic implant applications 489-503
- OSHA TLV for exposure to TDI and MDI 90
- OSHA LTV, isocyanate 120
- Oxyalkylated wood 312
- Oxyalkylation reaction of a carboxylated kraft lignin 317f
- Oxyethylene
 content 248
 group content, effect on stability of TPU elastomer 248t
 group content of polyol, dependence of stability 249t
- P**
- Panel
 characteristics, mixed hardwood flakeboard 297, 299t
 characteristics, red oak flakeboard 291t
 density 304
- Particleboard binder 286
- Permanent coatings 566
- Percutaneous
 device, factors affecting 501
 implantable devices and molds 499f
 implant experiment 498
- Phase
 development during polymerization of polyurethanes 158-165
 mixing in urethane polymers 363-372
 separation 162, 389
 degree 363
 fraction of functional groups reacted at 164t
 in urethane formulations, calculation of degree of reaction 162
 polyurethane elastomers 179
 during polyurethane polymerization 163f
 polyurethane elastomers, definition 226
- PHD polyols 78
- Phenapan-V-100-Iso-Spanplatte 289
- Phenol benzyl alcohol, reactivity with phenyl isocyanate 415t
- Phenol, reactivity with phenyl isocyanate 413t, 414t
- Phenolic
 vs. isocyanate adhesives in bonding particle board 66t
 vs. isocyanate resin 292, 297
 resins 60, 65
 -urethane polymers, model studies 403-417
- Phenyl isocyanate, effect of catalysts on reactivity with phenyl benzyl alcohol 415t
- Phenyl isocyanate, effect of substitution on reactivity with model benzyl alcohols 411t

- p*-Phenylene diisocyanate, reactivity studies and cast elastomers 419-431
- Photochemical *cis-trans* isomerization of azochromophore 228
- Photochromic probe, two-phase system vs. single phase system 226
- Photochromism
 azobenzene 220
 probes to study structure and segmental mobility of polyester urethanes 219-238
 definition 220
cis-trans isomerization kinetics of glassy polymers 223f
 in polymer matrices 220-225
 in polyurethanes 226-227
- Physical
 blending of polymers 368
 properties of elastomers 530t
 properties of polyols 314, 320t
 testing of elastomer 523
- Plasticorder 438
 mixing chamber 439
 removable sigma blade rotors 440
- Polyesters, properties of phase I elastomers 540t
- Polyesters, properties of phase III elastomers 549t
- Polyether
 glycols, formation 197
 glycols from tetrahydrofuran and ethylene oxide 197-202
 macroglycol 153
 polyols 507
 properties of phase III elastomers .. 548t
- Poly(MDI-BDO), conformational analysis 184-187
- Poly(MDI-BDO), projection of conformation 186f
- Poly(MDI-butanediol), projection of structure 183f
- Poly(MDI-EDO), effect of chemical structure on crystalline order 187-195
- Poly(MDI-EDO), predicted conformation 194f
- Poly(MDI-PDO)
 conformations 192f
 effect of chemical structure on crystalline order 187-195
 energy map for conformations 189
- Polyaddition reaction 226
- Polyadipate polyglycols 507
- Polycaprolactonediois, biodegradation of polyurethanes derived from 471-487
- Polyisobutylene diols
 chain extension 385
 and polyurethanes 383-391
 telechelic, synthesis 385-389
- Polyisocyanates, lignin-derived 311-328
- Polyisocyanates from polymeric lignins, reaction pathways 321
- Polymer(s)
 (2.0) ratio, catalyzed by stannous octoate 458
 (3.0) ratio, catalyzed by stannous octoate 456-458
 (3.0) ratio, effect of urethane group concentration 452-454
 compatibility of hard segment in soft segment 365
 data 454t, 456t, 466t
 from high acid number polyester glycol 446t
 from low acid number polyester glycol 448t, 452t
 DSC curves 368
 degradation 353, 358
 film, UV absorption spectra 230f
 films, percent moisture absorption .. 492t
 formation 433-434
 hydrophilicity 490
 hydroxyl-containing 263
 mastication 466-468
 matrices, photochromism in 220-225
 networks, swelling behavior 374
 phenolic urethane, model studies 403-417
 physical blending 368
 preparation from MDI and polyols 364
 properties, effect of phase 363
 reversible dissociation 436
 solubility 443
 structure 434-436
 telechelic 383
 TMA curves 368
 urethane
 block, experimental procedure for preparation 150-151
 block, kinetics of formation and phase development 149-166
 phase mixing 363-372
 viscosity 441
- Polymeric MDI 66t, 285, 511t
 adhesives 59
 advantages 290
 structure of monomer 285
 -wood matrix, cross-linking concept 288f
- Polymerization(s) 129
 (2.0) ratio polymers 444
 (3.0) ratio polymers 452
 change in onset and completion of low temperature transition ... 161f
- EO/THF, crown ethers identified by chemical ionization mass spectroscopy 199f
- of extended and unextended urethane formulations, kinetic parameters 156t

Polymerization(s) (<i>continued</i>)	
kinetics of polyurethane formula- tions	153-158
low-temperature glass relaxation, change as a function of conversion	160f
melt, procedure	442-443
melt, study	433-470
olefin, mechanism	383
of polycaprolactonediol with 1,6- hexamethylene diisocyanate	476-477
polyurethane	
effect of soft segment content on point of phase separation	163f
formulations, catalyst depend- ence of rate constants	157f
phase development	158-165
reactor	441-442
and ancillary equipment	439
shortstopped with 1-decanol	462-465
shortstopped with 1-propanol	458-462
variables	437t, 438t
urethane, DSC measurement of heat released during	154f
viscosity-time-temperature relations	444, 445f, 447f, 450f, 453f, 455f, 457f, 459f
Polyols	59, 420
capped, analysis data	329t
capped lignin-derived	328f
capping	336
characteristics	314
component of thermoplastic poly- urethanes, structure	245f
dependence of stability on oxy- ethylene group content	249t
formation pathways, reaction scheme	315f
functionality in relation to method of preparation	318t, 319t
influenced by the ratio of copolymer to propylene oxide	314
lignin-derived	311-338
economic analysis	334t
molecular weight, branching reactions	251f
molecular weight, effect	
injection moldability	249-250
low-temperature and elevated- temperature properties	247-248
oxyethylene group content on stability of TPU elastomer	248t
processing stability	248
physical properties	320t
supply, industry	85t
structural configuration	410
viscosity, color and solubility	320t
Polyurea hard segment adhesives, prepolymer and curing agent formulations	345t
Polyurethane(s)	312-313
biodegradation	475t
definition	506
insulation markets	49-55
lignin-derived	311-328
polyisobutylene based	383-391
PUR-SMC	81-82
SMC	81-82
synthesis	386-389
Porous interface	501
Potential energy curve of alcohol- isocyanate-metal ternary com- plex	211f
Preparation	
elastomers	244-246
model	364
polymer from MDI and polyols	364
polyol functionality in relation to method	318t, 319t
polyurethane elastomers	149
Prepolymer(s)	536t
73-series, formulation	345t
Prereacted polyurethanes	507
Press temperature	306
Press time	297, 304
effect on mixed hardwood flake- board properties	305t
vs. internal bonds for red oak flakeboard	296f
vs. modulus of rupture for red oak flakeboard	296f
Pressure-temperature diagram for an oxyalkylation reaction	317f
Price index, petroleum and gasoline	35f
Procedure for red oak flakeboard	290
Process Tunnel	553
maintenance requirements	563
Processing	
parameters for standard panels, mixed hardwood flakeboard	299t
problems	533
stability, polyol molecular weight, effect	248
Production	
flexible urethane foam	26
isocyanates	87t
temperatures	563
world, polyurethane chemicals	6f
1-Propanol, shortstop	460
effect	461t
Property values, average, for control mixed hardwood panels	301t
Propylene oxide, ratio to copolymer, influence on polyols	314
Propylene oxide, ratio to lignin copolymer	318t
Prosthesis	494
Prosthetic replacement	492
Psychological problems from iso- cyanates	90

- PU-SMC (Baypreg), physical properties, compared to competitive materials 82*t*
- PUR-SMC, polyurethane 81-82
- Q**
- Quadrol, cross-linking agent 351*f*
- Quality factor, calculation 494
- R**
- R value 113
- representations 117-119
- Radiation from belt 560
- Rate(s)
- constant(s)
- as a function of temperature and catalyst level for BDO extended system 158
- phenyl isocyanate-alcohol reactions 207*t*
- of thermal *cis-trans* isomerization of azochromophore, Arrhenius plot 232*f*
- of evolution of carbon dioxide from A compared with gel profile 140*f*
- of evolution of carbon dioxide from A compared with rise profile 140*f*
- reactions of diisocyanates 422
- ring opening 520
- Rating schedule, commercial fire 116
- Reaction(s)
- blowing 129
- between diisocyanates and *n*-butanol, second order plot 423*f*
- diisocyanates and water, second order plot 424*f*
- gelling 129
- injection molding 149, 568
- isocyanate with urethane 129
- rates of catalyzed diisocyanate reactions 421*t*
- scheme of polyol formation pathways 315*f*
- sequence model for flexible urethane foam 127-147
- sequence model summarized by rise and gel profiles 145*f*
- Reactivity
- of model phenols and benzyl alcohols with phenyl isocyanate 404
- model phenols with phenyl isocyanate, effect of substitution 409*t*
- phenol benzyl alcohol and ethyl alcohol with phenyl isocyanate, effect of catalysts 415*t*
- phenol with phenyl isocyanate, effect of solvents 414*t*
- Rearrangement of alcohol and isocyanate, transition structure during 211*f*
- Red oak flakeboard 290-297
- constants for all panels 291*t*
- with Desmodur PU-1520A 20 binder 293*f*
- panel characteristics 291*t*
- procedure 290
- thickness swell 298*f*
- variable levels 292
- Relaxation time of the azochromophore, WLF-plot 225*f*
- Release
- agent(s)
- mold, performance requirements 567
- internal 566
- in urethane molding 565-573
- film, mold, undisturbed surface 571*f*
- options
- internal agents 565-566
- permanent coating 565-566
- permanent base coat and renewable top coat 565-566
- Regression equations 306
- Resin content, polyurethane 515
- Resin level 306
- Regulatory action on CFCs 97
- Resilience 524
- Resistance to attack by microorganisms, isocyanate treated Southern pine 275
- Resocinol formaldehyde resins 66
- Respiratory irritancy 90
- Retrofit potential of insulation 51
- Reverse cosmosis 490
- RIM
- elastomeric polyurethanes, major ingredients for fascia applications 72*t*
- fascia 69-74
- market 73*f*
- polyurethane elastomers 69-74
- release agents 569
- urethanes 566, 568-569
- urethane materials 43
- uses 568
- Ring opening of difunctional macrocyclic ureas 521
- RMS (Rheometric Mechanical Spectrometer) 344
- RRIM (reinforced RIM) 74-81
- market for automotive front fenders 80*f*
- polymers, physical properties 76*t*, 77*t*, 79*t*
- Rubbers, polyurethane 388
- S**
- Scanning electron microscope 570
- Scott Tensile Tester 444
- Second order plot for reaction between diisocyanates and *n*-butanol 423*f*

Second order plot of reaction of diisocyanates and water	424f	Solvents, effect on reactivity of phenol with phenyl isocyanate	414t
Secondary relaxation	348f	Stability dependence on oxyethylene group content of polyol	249t
Segment(s), hard (<i>see</i> Hard segments)		Stability of TPU elastomer, effect of oxyethylene group content	248t
Segment length, effect on TPU elastomers	252	Standard, federal, cigarette and mattress	107f
Segments, soft (<i>see</i> Soft segments)		Standards, flammability	107f, 110f
Shakeout, foundry binders	63	Stannous octoate	456-458
Shear rate	441	catalyst effect	458t
Shear storage of Halthane 73-14 and 73-19	351f	Stereochemistry of the MDI unit	180
Sheathing potential of insulation	52	Steric hindrance	449
Shore hardness	523	Storage moduli of 87- and 88-series Halthanes	355f
Shortstop effect of 1-decanol	464t	Storage modulus	357f
Shortstop effect of 1-propanol	461t	Strength properties of paper strips	333t
Shortstopped polymerizations	458-466	Stress	
Shortstopping a polyester urethane chain by terminal urethane formation	460	properties of elastomers	428t, 430t
Silicones	566	relaxation	374, 376
Simplified inifer mechanism	387f	calculation	376
Single-phase polyurethane containing chromophoric hard segments, molecular structure	236f	swollen polyurethane net-works	378f, 379t
Sodium azide	324	-strain	523
pathway	336	values	444
reaction scheme	322f	Structural configuration of polyols	410
Soft segment(s)	343, 434	Structure	
amorphous	365	of hard segment chemical components of thermoplastic polyurethanes	244, 245f
azochromophore of two-phase polyurethanes	228-233	molecular	
behavior of Halthane 73-series adhesive	344-347	hard segments of polyester urethanes	229f
behavior of Halthane 87- and 88-series adhesives	353	photochromic soft and hard segments of polyester urethane	234f
compatibility rules	365	a single phase polyurethane containing chromophoric hard segments	236f
glass transition	347, 348f, 350f, 355f, 356f	soft segments of polyester urethanes	229f
activation energy	349f	polyol component of thermoplastic polyurethanes	245f
physical blending	267f	PPG-type polyols	245f
polyester urethanes, molecular structure	229f	Substitution, effect on reactivity of model benzyl alcohols with phenyl isocyanate	411t
photochromic	234f	Substitution, effect on reactivity of model phenols with phenyl isocyanate	409t
polyisobutylene	389	Swelling	
Softwood cell wall, chemical composition	264f	behavior of polymer networks	374
Softwood, three-dimensional view	265f	degree	376
Soil block test of isocyanate-treated Southern pine	275t	degree, calculation	375
inoculated with <i>Gloeophyllum trabeum</i>	275t	measurements	373
Soil block test of methyl isocyanate-treated Southern pine	276t	polyurethane networks	378t
Solubility parameter	376	Synergism	
Solubility, polymer	443	amine-tin carboxylate, mechanism	400
Solution method	321	effect of metal coordination number	397
Solvation effect	416	effects	205
Solvents, effect on the kinetics of phenol-phenyl isocyanate reaction	410		

- Synergism (*continued*)
 measurement 395
 tin-amine, mechanism 393-402
- Synthesis
 of difunctional macrocyclic ureas .. 520
 and modification of polymers 490
 network 374
 polyisobutylene-based diols and
 polyurethanes 384*f*
 telechelic polyisobutylene diol ... 385-389
 two-phase, of polyurethane
 elastomers 219
- System design 507-510
 one component 509*t*
 two component 509*t*
- T**
- TDI, reactivity with waxes 569
 Tear resistance 523
 Ternary complex of tin-alcohol-
 isocyanate 394*f*
 Tertiary amines 393, 512
 catalysts 412*t*
 effect on reactivity of phenol and
 ethyl alcohol with phenyl
 isocyanate 413*t*
 Test methods for elastomers 246, 538
 Testing of mixed hardwood flakeboard 297
 Tetrafunctional quadrol, effects on
 mechanical properties 353
 Tetrahedral complexes 397
 Tetralin dicarboxylic acid 324
 Thermal dissociation of polyurethane 251*f*
 Thermal *cis-trans* isomerization 228
 Thermal properties of polyurethane
 adhesives 343-362
 Thermogravimetric analysis curves of
 73-series Halthanes 354*f*
 Thermogravimetric analysis curves of
 87- and 88-series Halthanes 359*f*
 Thermoplastic polyurethanes
 derived from polyglycols 243-257
 hard segment chemical components 245*f*
 high cost 243
 preparation 243
 structure 245*f*
 hard segment chemical com-
 ponents 244, 245*f*
 polyol component 245*f*
 variation in hardness 243
- Thickness swell
 and internal bond vs. percentage
 Mondur MR for mixed hard-
 wood flakeboards 303*f*
 measurements 300
 red oak flakeboard 298*f*
 values 297
 Tin carboxylates 393
- Tin coordination complex 399
 Tin-isocyanate complex 394
 Tipped PPG polyols, preparation 244
 Tissue necrosis 498
 TLV for exposure to TDI and MDI,
 OSHA 90
 TMA curves of polymers 368
 model 371*f*
 Torque level 468
 Torque values 441
 Toluene diisocyanate, chain
 extension 388*t*
 Toxicity of insulation 55
 Transition temperatures of 73-series
 Halthanes 352*t*
 Transition temperatures of 87- and
 88-series Halthanes 358*t*
 Transportation industry, urethane
 adhesives 67-68
 Triethylene diamine 535
 Trimerization reaction of diisocyanate 425*f*
 Triphenylphosphine
 effect on catalysis 401*f*
 effect on rate of tin-amine
 catalyzed reaction 401*f*
 -DBTDL combination 399
 Tunnel test 114
- U**
- Ultrafiltration 490
 Urea formation 422, 426
 Ureas, substituted, absorbance due to 144*f*
 Urethane
 equilibrium constant 434
 formation 426
 equation 434
 and ureas, relative absorbance
 due to 143*f*, 144*f*
- Use(s) (of)
 auto, of plastics and urethanes 37*f*
 auto, of urethane foam and
 elastomers 38*f*
 automotive
 future market 40-48
 present market 36-40
 for polyurethanes 33-48
 RIM, bumpers and facia 71*t*
 average
 of major components of high
 modulus RIM elastomers .. 80*t*
 per car of plastics 39*f*
 RIM facia polyurethane 72*t*
 DSC in studying polymer
 morphology 363
 elastomer in U.S./Canada 12
 flexible urethane foam 32*t*
 carpet underlay 30
 bedding 29

